

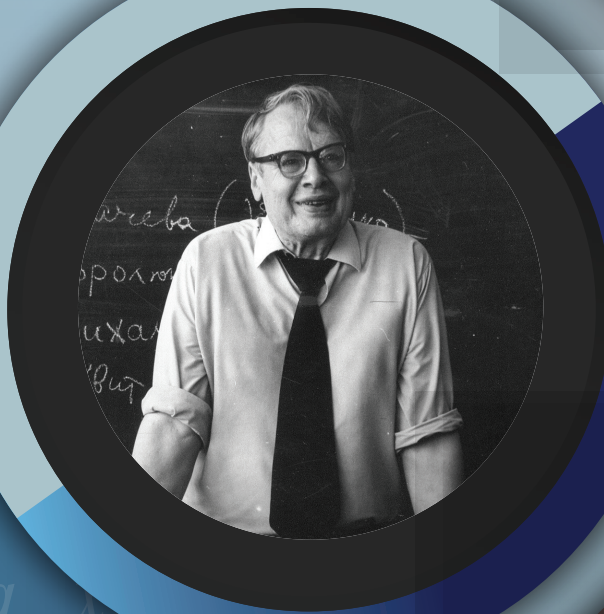
RTA

ISSN 1932-2321

JOURNAL IS REGISTERED
IN THE LIBRARY OF THE
U.S. CONGRESS

RELIABILITY:
THEORY & APPLICATIONS

INTERNATIONAL
GROUP ON
RELIABILITY



GNEDENKO FORUM PUBLICATIONS

#1

(67) VOL.17
MARCH
2022

SAN DIEGO

RELIABILITY

RISK ANALYSIS

MAINTENANCE

SAFETY

ISSN 1932-2321

© "Reliability: Theory & Applications", 2006, 2007, 2009-2022

© " Reliability & Risk Analysis: Theory & Applications", 2008

© I.A. Ushakov

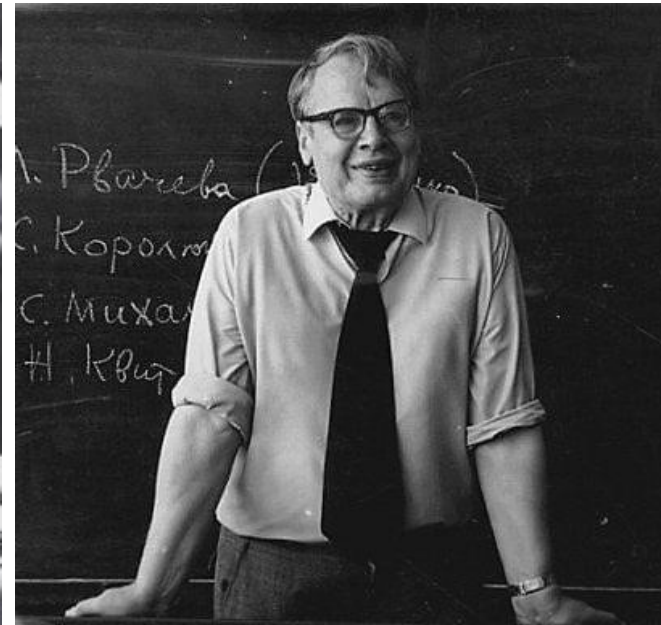
© A.V. Bochkov, 2006-2022

© Kristina Ushakov, Cover Design, 2022

<http://www.gnedenko.net/Journal/index.htm>

All rights are reserved

The reference to the magazine "Reliability: Theory & Applications"
at partial use of materials is obligatory.



RELIABILITY: THEORY & APPLICATIONS

Vol.17 No.1 (67),
March 2022

San Diego
2022

Editorial Board

Editor-in-Chief

Rykov, Vladimir (Russia)
Doctor of Sci, Professor, Department of Applied Mathematics & Computer Modeling, Gubkin Russian State Oil & Gas University, Leninsky Prospect, 65, 119991 Moscow, Russia.
e-mail: vladimir_rykov@mail.ru

Managing Editors

Bochkov, Alexander (Russia)
Doctor of Technical Sciences, Deputy Head of the Scientific and Technical Complex JSC NIIAS, Scientific-Research and Design Institute Informatization, Automation and Communication in Railway Transport, Moscow, Russia, 107078, Orlikov pereulok, 5, building 1
e-mail: a.bochkov@gmail.com

Gnedenko, Ekaterina (USA)
PhD, Lecturer Department of Economics Boston University, Boston 02215, USA
e-mail: gnedenko@bu.edu

Deputy Editors

Dimitrov, Boyan (USA)
Ph.D., Dr. of Math. Sci., Professor of Probability and Statistics, Associate Professor of Mathematics (Probability and Statistics), GMI Engineering and Management Inst. (now Kettering)
e-mail: bdimitro@kettering.edu

Gnedenko, Dmitry (Russia)
Doctor of Sci., Assos. Professor, Department of Probability, Faculty of Mechanics and Mathematics, Moscow State University, Moscow, 119899, Russia
e-mail: dmitry@gnedenko.com

Krishnamoorthy, Achyutha (India)
M.Sc. (Mathematics), PhD (Probability, Stochastic Processes & Operations Research), Professor Emeritus, Department of Mathematics, Cochin University of Science & Technology, Kochi-682022, INDIA.
e-mail: achyuthacusat@gmail.com

Recchia, Charles H. (USA)
PhD, Senior Member IEEE Chair, Boston IEEE Reliability Chapter A Joint Chapter with New Hampshire and Providence, Advisory Committee, IEEE Reliability Society
e-mail: charles.recchia@macom.com

Shybinsky Igor (Russia)
Doctor of Sci., Professor, Division manager, VNIIS (Russian Scientific and Research Institute of Informatics, Automatics and Communications), expert of the Scientific Council under Security Council of the Russia
e-mail: igor-shubinsky@yandex.ru

Yastrebenetsky, Mikhail (Ukraine)
Doctor of Sci., Professor. State Scientific and Technical Center for Nuclear and Radiation Safety (SSTC NRS), 53, Chernishevskaya str., of.2, 61002, Kharkov, Ukraine
e-mail: ma_yastrebenetsky@sstc.com.ua

Associate Editors

Aliyev, Vugar (Azerbaijan)
Doctor of Sci., Professor, Chief Researcher of the Institute of Physics of the National Academy of Sciences of Azerbaijan, Director of the AMIR Technical Services Company
e-mail: prof.vugar.aliyev@gmail.com

Balakrishnan, Narayanaswamy (Canada)
Professor of Statistics, Department of Mathematics and Statistics, McMaster University
e-mail: bala@mcmaster.ca

Carrion García, Andrés (Spain)
Professor Titular de Universidad, Director of the Center for Quality and Change Management, Universidad Politécnica de Valencia, Spain
e-mail: acarrion@eio.upv.es

Chakravarthy, Srinivas (USA)
Ph.D., Professor of Industrial Engineering & Statistics, Departments of Industrial and Manufacturing Engineering & Mathematics, Kettering University (formerly GMI-EMI) 1700, University Avenue, Flint, MI48504
e-mail: schakrav@kettering.edu

Cui, Lirong (China)
PhD, Professor, School of Management & Economics, Beijing Institute of Technology, Beijing, P. R. China (Zip:100081)
e-mail: lirongcui@bit.edu.cn

Finkelstein, Maxim (SAR)

Doctor of Sci., Distinguished Professor in Statistics/Mathematical Statistics at the UFS. Visiting researcher at Max Planck Institute for Demographic Research, Rostock, Germany and Visiting research professor (from 2014) at the ITMO University, St Petersburg, Russia
e-mail: FinkelM@ufs.ac.za

Kaminsky, Mark (USA)

PhD, principal reliability engineer at the NASA Goddard Space Flight Center
e-mail: mkaminskiy@hotmail.com

Krivtsov, Vasiliy (USA)

PhD. Director of Reliability Analytics at the Ford Motor Company. Associate Professor of Reliability Engineering at the University of Maryland (USA)
e-mail: VKrivtso@Ford.com_krivtsov@umd.edu

Lemeshko Boris (Russia)

Doctor of Sci., Professor, Novosibirsk State Technical University, Professor of Theoretical and Applied Informatics Department
e-mail: Lemeshko@ami.nstu.ru

Lesnykh, Valery (Russia)

Doctor of Sci. Director of Risk Analysis Center, 20-8, Staraya Basmannaya str., Moscow, Russia, 105066, LLC "NIIGAZECONOMIKA" (Economics and Management Science in Gas Industry Research Institute)
e-mail: vvlesnykh@gmail.com

Levitin, Gregory (Israel)

PhD, The Israel Electric Corporation Ltd. Planning, Development & Technology Division. Reliability & Equipment Department, Engineer-Expert; OR and Artificial Intelligence applications in Power Engineering, Reliability.
e-mail: levitin@iec.co.il

Limnios, Nikolaos (France)

Professor, Université de Technologie de Compiègne, Laboratoire de Mathématiques, Appliquées Centre de Recherches de Royallieu, BP 20529, 60205 COMPIEGNE CEDEX, France
e-mail: Nikolaos.Limnios@utc.fr

Papic, Ljubisha (Serbia)

PhD, Professor, Head of the Department of Industrial and Systems Engineering Faculty of Technical Sciences Cacak, University of Kragujevac, Director and Founder the Research Center of Dependability and Quality Management (DQM Research Center), Prijedor, Serbia
e-mail: dqmcenter@mts.rs

Ram, Mangey (India)

Professor, Department of Mathematics, Computer Science and Engineering, Graphic Era (Deemed to be University), Dehradun, India. Visiting Professor, Institute of Advanced Manufacturing Technologies, Peter the Great St. Petersburg Polytechnic University, Saint Petersburg, Russia.
e-mail: mangeyram@gmail.comq

Zio, Enrico (Italy)

PhD, Full Professor, Direttore della Scuola di Dottorato del Politecnico di Milano, Italy.
e-mail: Enrico.Zio@polimi.it

e-Journal *Reliability: Theory & Applications* publishes papers, reviews, memoirs, and bibliographical materials on Reliability, Quality Control, Safety, Survivability and Maintenance.

Theoretical papers have to contain new problems, finger practical applications and should not be overloaded with clumsy formal solutions.

Priority is given to descriptions of case studies.

General requirements for presented papers

1. Papers have to be presented in English in MS Word or LaTeX format.
2. The total volume of the paper (with illustrations) can be up to 15 pages.
3. A presented paper has to be spell-checked.
4. For those whose language is not English, we kindly recommend using professional linguistic proofs before sending a paper to the journal.

The manuscripts complying with the scope of journal and accepted by the Editor are registered and sent for external review. The reviewed articles are emailed back to the authors for revision and improvement.

The decision to accept or reject a manuscript is made by the Editor considering the referees' opinion and taking into account scientific importance and novelty of the presented materials. Manuscripts are published in the author's edition. The Editorial Board are not responsible for possible typos in the original text. The Editor has the right to change the paper title and make editorial corrections.

The authors keep all rights and after the publication can use their materials (re-publish it or present at conferences).

Publication in this e-Journal is equal to publication in other International scientific journals.

Papers directed by Members of the Editorial Boards are accepted without referring. The Editor has the right to change the paper title and make editorial corrections.

The authors keep all rights and after the publication can use their materials (re-publish it or present at conferences).

Send your papers to Alexander Bochkov, e-mail: a.bochkov@gmail.com

Table of Contents

Inferences on Stress Strength Reliability in Multicomponent System for Type I Generalized Half-Logistic Distribution 18

Phillip Oluwatobi Awodutire, Thomas Xavier, Joby K. Jose

This article deals with inferences on stress strength reliability in a multicomponent system for Type I generalized half-logistic distribution. It is assumed that the strength and stress components are independently distributed. In this work, we develop some statistical properties of the type I generalized half-logistic distribution. Furthermore, the expression for stress strength reliability for a multicomponent setup was obtained and studied. Two methods to estimate the multicomponent stress-strength reliability -maximum likelihood and Bayesian estimation were employed. The Bayes estimates of the multicomponent stress strength reliability are obtained under squared error loss function and using gamma priors for the parameters. Simulation studies were conducted to assess the efficiency of the methods. The importance of this model was studied by applying it to a real life data set.

A New Mixed Poisson Distribution for Over-dispersed Count Data: Theory and Applications 33

Ramajeyam Tharshan, Pushpakanthie Wijekoon

In this paper, an alternative mixed Poisson distribution is proposed by amalgamating Poisson distribution and a modification of the Quasi Lindley distribution. Some fundamental structural properties of the new distribution, namely the shape of the distribution and moments and related measures, are explored. It was noted that the new distribution to be either unimodal or bimodal, and over-dispersed. Further, it has a tendency to accommodate various right tail behaviors and variance-to-mean ratios. Its unknown parameter estimation by using the maximum likelihood estimation method is examined by a simulation study based on the asymptotic theory. Finally, two real-world data sets are used to illustrate the flexibility and potentiality of the new distribution.

A Novel Approach for Constructing Distributions with an Example of the Rayleigh Distribution 52

Aijaz Ahmad, Muzamil Jallal, Afaq Ahmad

In this paper, we describe a novel technique for creating distributions based on logarithmic functions, which we referred the Log Exponentiated Transformation (LET). The LET technique is then applied to Rayleigh distributions, resulting in a new distribution known as the Log Exponentiated Rayleigh distribution (LERD). Several distributional properties of the formulated distribution have been discussed. The expressions for ageing properties have been derived and discussed explicitly. The behaviour of the pdf, cdf and hazard rate function has been illustrated through different graphs. The parameters are estimated through the technique of MLE. A simulation analysis was conducted to measure the effectiveness of all estimators. Eventually the versatility and the efficacy of the formulated distribution have been examined through real life data set.

A New Reliability Model and Applications 65

M. Manoharan, P. Kavya

The Lomax or Pareto Type II distribution has a wide range of applications in many areas including reliability and life testing. In this paper, we modify the Lomax distribution using KM transformation to enhance the applicability of the Lomax distribution. The distribution introduced using KM transformation is parsimonious in parameter. Substituting the cumulative distribution function (cdf) of the Lomax distribution in KM transformation provides a new modified Lomax distribution. The behavior of hazard rate function is studied graphically and also theoretically using Glacer method. Its analytical properties are derived and parameters are estimated using maximum likelihood estimation method. We consider two real data sets to show the flexibility of the proposed model. The model proposed in this paper provides a better fit to the data sets compared to other well-known distributions given in this study.

A New Life Time Distribution: Burr III Modified Weibull Distribution and its Application in Burn in Process 76

Deepthy G S, Nicy Sebastian

In burn-in analysis, models with a bathtub-shaped hazard rate and a bimodal density function are inevitable. This work focusses on a new five parameter distribution called Burr III Modified Weibull distribution which can be used to design burn-in procedures and preventative maintenance for incurable devices. The statistical properties such as quantile function, hazard rate function and order statistics have been discussed. The model parameters are estimated using the maximum likelihood estimation technique, and the performance of the proposed model is evaluated using the simulation technique. Finally, a real data set is presented to demonstrate the model 's utility and its application in the burn-in process.

Analysis of Some Proposed Replacement Policies 87

Tijjani A. Waziri, Bashir M. Yakasai, Rahama S. Abdullahi

This paper is coming up with an age replacement cost model under the standard age replacement policy (SARP) for some multi-unit systems. Furthermore, some two other age replacement cost models will be constructed for the multi-unit systems under some proposed policies (policy A and policy B). For simple illustration of the proposed age replacement cost models under SARP, policy A and policy B, numerical example was provided, and the result obtained will be beneficial to engineers, maintenance managers and plant management, in selecting and applying the optimal preventive maintenance policies.

Effect of Preprocessing in Human Emotion Analysis Using Social Media Status Dataset 104

Komal Anadkat, Hiteishi Diwanji, Shahid Modasiya

Emotion analysis using social media text is the emerging research area now a day. It helps the researcher to recognize the emotional state of the users and identify mental health-relevant problems like depression or anxiety, which may lead to suicide if not cured. The social media platforms like WhatsApp, Facebook, Instagram, etc. are widely used as these applications provide an affordable and reliable medium for transferring data, sharing thoughts, and even for routine informal communication. Social media status is normally analyzed to recognize the mood, emotion, thought process, or mental state of the individual as people generally share status for what they feel. On the other hand, pre-processing is the crucial step for any kind of text data analysis. In this paper, the social media status dataset is first pre-processed using various methods, given for feature extraction and classification purpose. For the machine learning approach, we have used count vectors and TF-IDF techniques for extracting the different features of the data. Using count vector feature extraction accuracy achieved by pre-processed data is 68.90%, 69.33%, 70.59%, 64.95%, 69.33% for naïve Bayes, LDA, Random forest, SGD and MLP respectively. Similarly, using TF-IDF feature extraction accuracy achieved by pre-processed data is 65.76%, 69.96%, 68.49%, 65.96%, 70.80% for naïve Bayes, LDA, Random forest, SGD and MLP respectively. The experimental results show that pre-processing helps to improve the accuracy of the classifier and CNN outperforms the traditional approach and achieves 79% accuracy

A Two Non-Identical Unit Parallel System With Priority in Repair and Correlated Life Times 113

Pradeep Chaudhary, Anika Sharma

The paper analyses a two non-identical unit parallel system in respect of various measures of system effectiveness by using regenerative point techniques. It has been considered that the life times of both the units are correlated random variables and a single repairman is always available with the system to repair a failed unit.

Stochastic Analysis of a Repairable System of Non-Identical Units With Priority and Conditional Failure of Repairman 123

Naveen Kumar, S.C. Malik, N. Nandal

Here, we describe the stochastic analysis of a repairable system consisting of two non-identical units called the main unit and the other is a duplicate unit. The units have direct complete failure from the operative state. A single repairman has been engaged to carry out the repair activities that can be failed while performing his jobs with the main unit. The repairman does repair activities of the duplicate unit without any problem. Priority for operation and repair to the duplicate unit is given over the main unit. The repairman performs with full efficiency after getting treatment. The distribution for failure rates of the units has been considered as negative exponential while arbitrary distributions have been taken for repair and treatment rates. The use of semi-Markov process and regenerative point technique has been made to study the probabilistic behavior of the system in different possible transition states. The reliability characteristics of the system model have been examined numerically and graphically for particular values of the parameters. The profit of the system has also been analyzed for some fixed values of the repair and other maintenance costs.

The Reliability Performance of the Exponential Inverted Marshall-Olkin-G Family of Distributions: Non-Bayesian Properties and Applications 134

Joseph Thomas Eghwerido, Eferhonore Efe-Eyefia

This article introduces a class of generator for enhancing the performance, productivity and flexibility of statistical distributions called the exponential Inverted Marshall-Olkin-G (EMA-G) distribution. The characteristics of the new class of generator were obtained and examined. Some special models of the proposed model were investigated. The Bernstein function of the EMA-G model was also obtained in a closed form. The maximum likelihood method was adopted to obtain the parameters estimate of the formulated EMA-G distribution model. The flexibility, productivity, tractability, applicability, and viability of the new contemporary class of distribution were examined by Monte Carlo simulation. A two real life data sets were used to illustrate the empirical performance and flexibility, productivity, tractability of the generator. The up-to-the-minute outcomes of the new generator indicated that the EMA-G density gives a better fit compared to some existing statistical generators in literature using their goodness-of-fit.

Optimization of a Feedback Working Vacation Queue With Reverse Balking and Reverse Reneging..... 154

K. Jyothsna, P. Vijaya Laxmi, P. Vijaya Kumar

This paper analyzes a steady-state finite buffer M/M/1 feedback queue with reverse balking, reverse reneging and multiple working vacations. The concept of reverse balking and reverse reneging evolves from investment businesses wherein more the number of customers associated with a firm less the probability of balking of a customer and similar is the case of reverse reneging. Furthermore, if a customer is dissatisfied with the service provided, he or she may chose to rejoin the queue as a feedback customer. The server exits for working vacations whenever the system becomes empty instead of staying idle in the system. Vacation times and service times during working vacations are all independent random variables following exponential distribution. The model 's steady-state system length distributions are calculated using the matrix approach. Some performance characteristics and cost optimization using ant colony optimization (ACO) are presented. Sensitivity analysis is performed using numerical results which are shown in the form of tables and graphs.

Analysis of the Primary Factors Affecting the Most Fatal Aviation Accidents: A Machine Learning Approach..... 164

Tuzun Tolga İnan - Neslihan Gokmen İnan

The safety concept is primarily examined in this study considering the most fatal accidents in aviation history with human, technical, and sabotage/terrorism factors. Although the aviation industry was started with the first engine flight in 1903, the safety concept has been examined since the beginning of the 1950s. However, the safety concept was firstly examined with technical factors, in the late 1970s, human factors have started to analyze. Despite these primary causes, there have other factors which could have an impact on accidents. So, the purpose of the study is to determine the affecting factors of the most fatal 100 accidents including aircraft type, distance, flight phase, primary cause, number of total passengers, and time period by classifying survivor/non-survivor passengers. Logistic regression and discriminant analysis are used as multivariate statistical analyses to compare with the machine learning approaches in terms of showing the algorithms' robustness. Machine learning techniques have better performance than multivariate statistical methods in terms of accuracy (0.910), false-positive rate (0.084), and false-negative rate (0.118). In conclusion, flight phase, primary cause, and total passenger numbers are found as the most important factors according to machine learning and multivariate statistical models for classifying the accidents' survivor/non-survivor passengers.

Statistical Properties and Application of a Transformed Lifetime Distribution: Inverse Muth Distribution..... 178

Agni Saroj, Prashant K. Sonker, Mukesh Kumar

In this paper, we have proposed a transformed distribution called inverse Muth (IM) distribution. The expressions for probability density function (pdf), cumulative distribution function (cdf), reliability and hazard function of this distribution are well defined. The statistical properties such as, quantile function, moments, skewness and kurtosis are derived. The methods of estimation such as maximum likelihood estimation (MLE) and maximum product spacing estimation (MPSE) are used to estimate the parameters. The IM distribution is positively skewed and its behavior of hazard rate is upside-down bathtub (UBT) shape. The important finding of the study is that the moments of IM distribution do not exist. A real dataset (the active repair time for airborne communication transceiver) used for application purpose, after taking a natural extension of IM distribution. It is expected that the proposed model would be used as a life time model in field of reliability and its applicability.

Hybrid Deep Resnet With Inception Model for Optical Character Recognition in Gujarati Language Short Title: Optical Character Recognition in Gujarati Language 194

Sanket B. Suthar, Amit R. Thakkar

In the Optical Character Recognition (OCR) system, achieving high recognition performance is important. OCR and visual perception are affected by the inclined characters in each language. Deep learning methods play an important role in the OCR field, which can outperform humans with higher recognition performance. So, in this research, a hybrid deep learning technique is applied to recognize the Gujarati language characters. Initially, Gujarati characters collected from different sources are pre-processed using different techniques. Adaptive Weiner Filter (AWF) is used for noise removal, Binarization, and contrast enhancement is done by Contrast Limited Adaptive Histogram Equalization (CLAHE) method. Finally, a hybrid deep ResNet with Inception model (GoogleNet) is suggested to perform character recognition in the Gujarati language. This hybrid architecture also performs feature extraction tasks, considered a major task in OCR. Python tool is utilized to illustrate the proposed methodology and solve the mathematical model. Scanned documents containing Gujarati characters are engaged to evaluate the robustness of the proposed methodology. Using various performance parameters, the influence of the proposed methodology is examined and its results compared with various deep learning algorithms.

Reliability Analysis and Profit Optimization of Briquette Machine by Considering Neglected Faults 210

Divesh Garg, Reena Garg

Sustainable energy plays a significant role in socio-economic advancement by raising the standard of living of all human beings. Briquetting is the process of compaction of biomass residues into solid fuels in order to increase the effectiveness of thermal capacity, combustion rate, calorific value to name a few. In this paper, we consider not only the occurrence of minor/ major faults but also the other neglected faults such as abnormal sound, overheating of the motor unit, vibration, etc. Such neglected faults may not affect the working of the system at a time but their ignorance may convert into major faults in the future. An ordinary repairman can easily rectify all machine faults except some major faults for which an expert repairman is required. Moreover, we analyse the availability of the system and optimize system profit by using the Artificial Bee Colony optimization algorithm. Furthermore, a graphical study of these parameters is presented.

A New Method for Generating Distributions with an Application to Weibull Distribution..... 223

M. A. Lone, I. H. Dar, T. R. Jan

In the literature of probability theory, it has been noticed that the classical probability distributions do not furnish an ample fit and fail to model the real-life data with a non-monotonic hazard rate behaviour. To overcome this limitation, researchers are working in the refinement of these distributions. In this paper, a new method has been presented to add an extra parameter to a family of distributions for more flexibility and potentiality. We have specialized this method to two-parametric Weibull distribution. A comprehensive mathematical treatment of the new distribution is provided. We provide closed-form expressions for the density, cumulative distribution, reliability function, hazard rate function, the r -th moment, moment generating function, and also the order statistics. Moreover, we discussed mean residual life time, stress strength reliability and maximum likelihood estimation. The adequacy of the proposed distribution is supported by using two real lifetime data sets as well as simulated data.

Skip-Lot Sampling Plan of Type Sksp-T With Group Acceptance Sampling Plan as Reference Plan Under Burr-Type Xii Distribution 240

S. Suganya, K. Pradeepa Veerakumari

This paper clearly assigns skip-lot sampling plan of type SkSP-T with Group Acceptance sampling plan is designing and Burr type XII distribution is applied to determine the lifetime of the product. The new proposed plan parameters are determined by using the two-point method on the Operating Characteristics curve together with consistent producer and consumer risks are specified. Tables are simulated for various parametric values of SkSP-T, Group acceptance sampling plan and Burr type XII distribution. Skip-lot sampling plan of type SkSP-T is also compared with Group acceptance single sampling plan and skip-lot sampling plan of type SkSP-2 with group acceptance sampling plan using Burr type XII distribution. Further, the efficiency of the proposed plan is discussed. Numerical illustration and examples are given to justify the efficiency of the proposed plan.

Some Properties and Different Estimation Methods for Inverse A() Distribution with an Application to Tongue Cancer Data..... 251

Shreya Bhunia, Proloy Banerjee

The inverted distribution is the distribution of the reciprocal of a random variable that follows a specified distribution. Here, a new one parameter inverse A() distribution has been introduced, which is the reciprocal of the A() distribution. An account of mathematical and statistical properties of the new distribution such as survival characteristics, quantile functions, mode, order statistics, ageing intensity function and stochastic ordering have been derived and discussed. Furthermore, from the frequentist view point we discussed several estimation approaches including maximum likelihood method, method of maximum product of spacings, ordinary and weighted least square methods, Cram/er-Von-Mises estimation and Anderson-Darling estimation methods. These methods are compared for both small and large samples by performing an extensive numerical simulation. The flexibility of the new lifetime distribution is demonstrated by modeling a tongue cancer data. The result indicates the superiority for proposed model compared to some popular competing ones.

Safety at Work: A Complex or an Exceedingly Simple Matter?..... 267

Rodrigo F. S. Gomes, Leandro Gauss, Fabio Sartori Piran, Daniel Pacheco Lacerda

This paper uses the concept of inherent simplicity stemming from the Theory of Constraints to explain whether safety at work is a complex or an exceedingly simple matter. In this context, the study seeks to explore the causalities that govern safety at work, identifying its constructs and presenting logic propositions based on the theory-building blocks: classification, correlation, and causal consistency. To support the research, a dataset composed of 46 work-related accident investigation reports from an elevator industry in Latin America was carefully analyzed using association rules. Moreover, direct observations grounded on inductive reasoning were used to speculate plausible causes concerning the effect of work-related accidents. The research strategy followed common strategies of theory building to reach common sense: theory-to-practice and practice-to-theory. As a result, a conceptual proposition is postulated based on the reasoning that safety at work is governed by very few constructs, and that its complexity is explained through the two elements from inherent simplicity: degrees of freedom (interdependencies between constructs) and harmony (conflicts resolution within the work environment). From the practitioners' perspective, the study also offers directions towards safety improvements at the organizational level by considering the impact of the interdependencies between constructs in safety at work.

Gumbel Marshall-Olkin Lomax: A new distribution for reliability modelling..... 288

Elebe E. Nwezza, Uchenna U. Uwadi, C.K. Acha, Christian Osagie

A new distribution for modeling the two approaches (physical and actuarial) of reliability problems is introduced. The statistical properties including the moments, mode, quantile function are derived. Some reliability measures including the mean residual life and hazard rate are derived. An alternative measure for total time of test (TTT) for evaluation of the interfailure times is derived. The unknown parameters of the new distribution are estimated using the maximum likelihood approach. Furthermore, the asymptotic consistency of the estimated parameters is evaluated through a simulation study. Two real-life datasets were used to illustrate the applicability of the new distribution and comparison with already existing distributions.

A Novel Transformation: Based on Inverse Trigonometric Lindley Distribution 303

D. Kumar, P. K. Chaurasia, P. Kumar, A. Chaurasia

As we see that the present era is directly depending upon various kinds of machines. In other words, we can say that we are fully surrounded by machines. Machines are assembled with many components and each component has its own importance. For proper functioning of a machine, these components should be up to date. Therefore, for smooth functioning, we have to make replacement of the component before its failure. In this present paper, we propose a new transformation which is purely based on inverse trigonometry with lindley distribution for the first time and so, named "Inverse Trigonometric Lindley Distribution". It find its various properties like survival function, hazard rate function, moments, conditional moments, order statistics, entropy measurement etc. Maximum likelihood estimator have also considered for estimation of parameter. To know the paternal behavior of the model, different real datasets have been considered. To understand the behavior of estimators at the long run, simulation study is being performed in detail.

Study on Acceptance Sampling Plan for Truncate Life Tests Based on Percentiles Using Gompertz Frechet Distribution..... 316

S.J Ayalakshmi, S. Vijilamery

In this paper, Acceptance Sampling approaches useful for minimizing the cost and time of the submitted lots. In this busy world expect the Quality assurance and reliability of the product is very high. So, use the truncated life tests in acceptance sampling plan. Time truncated life tests in sampling plan are used to certain reach a decision on the product. Therefore, Gompertz Frechet Distribution is considered as model for a life time random variable when the lifetime test is truncated at pre-determined time. The operating characteristic functions of the sampling plans and Producers risk is also discussed. The results are illustrated by an example.

Explicit Time Dependent Solution of a Twostate Retrial Queueing Model with Heterogenous Servers 325

Neelam Singla, Sonia Kalra

In this paper, two-dimensional state retrial queueing system with two non - identical parallel servers is considered. Incoming calls (primary calls) arrive at the server according to a Poisson process. Repeating calls also follows the same fashion. Service times of two servers follow exponential distribution with different rates. An incoming call that finds the servers busy, joins an orbit and retries after some random amount of time. Time dependent probabilities of exact number of arrivals and exact number of departures at when the servers are free or when one server is busy or when both servers are busy are derived for the system. Finally busy period distribution obtained to illustrate the system dynamics.

A Discrete Analogue of Teissier Distribution: Properties and Classical Estimation with Application to Count Data..... 340

Bhupendra Singh, Varun Agiwal, Amit Singh Nayal, Abhishek Tyagi

This article presents a novel discrete distribution with a single parameter, called the discrete Teissier distribution. It is noted that this model, with one parameter, offers a high degree of fitting flexibility as it is capable of modelling equi-, over-, and under-dispersed, positive and negative skewed, and increasing failure rate datasets. In this article, we have explored its numerous essential distributional features such as recurrence relation, moments, generating function, index of dispersion, coefficient of variation, entropy, survival and hazard rate functions, mean residual life and mean past life functions, stress-strength reliability, order statistics, and infinite divisibility. The classical point estimators have been developed using the method of maximum likelihood, method of moment, and least-squares estimation, whilst an interval estimation based on Fisher ' s information has also been presented. Finally, the applicability of the suggested discrete model has been demonstrated using two complete real datasets.

Costs of Age Replacement under Accelerated Life Testing with Censored Information 356

Intekhab Alam, Mohd Asif Intezar, Lalit Kumar Sharma, Mohammad Tariq Intezar, Aqsa Irfan

Accelerated life testing (ALTg) helps manufacturers to predict the various costs associated with the product under the warranty policy. The main aim of undertaking ALTg is the extended time of today's manufactured goods, the small-time among design and make public, and the difficulty of analysis of items that are continuously used in ordinary environments. Hence ALTg is used to offer quick information about the life distribution of products. We describe how to propose and analyze the accelerated life testing plans to develop the excellence and reliability of the item for consumption. We also focus on finding the expected cost rate and the expected total cost for age replacement in the prorated rebate warranty plan. The problem is studied using constant stress, under the hypothesis that the life spans of the units follow the Gompertz distribution (GD) for predicting the cost of age replacement in the warranty plan. The asymptotic variance and covariance matrix, confidence intervals for parameters, and respective errors are also obtained. A simulation study is carried out to show the statistical properties of distribution parameters.

Selection of Life Test Sampling Inspection Plans for Continuous Production 371

R. Vijayaraghavana, A. Pavithrab

Reliability sampling is the methodology often used in manufacturing industries for making decision about the disposition of lots of finished products based on the information generated from a life test. Such a methodology can be applied effectively for isolated lots as well as for a continuous stream of lots through the life tests to ensure control over the quality characteristics that are mainly related to the functioning of the manufacturing items in time. Sampling inspection plans for isolated lots are classified under lot-by-lot inspection procedures. Cumulative results plans are classified under the sampling inspection for continuous production, which results in continuous stream of lots. This paper presents the notion of life tests for cumulative results plans with a particular reference to chain sampling inspection plans when the lots are formulated from a continuous stream of production. The operating characteristic (OC) function of chain sampling plans for life tests is presented as a measure of performance when the lifetime random variable follows an exponential distribution. A procedure for designing the proposed plans indexed by two points on the characteristic curve for providing protection to the producer and consumer is discussed with illustrations. Tables yielding the parameters of the optimum plans are also provided.

Critical Path Intervals of Intuitionistic Triangular Fuzzy Numbers Using Maximum Edge Distance Method 382

S. Priyadharshini, G. Deepa

We live in a contemporary world where successful project management strategies are complex to manipulate the projects for project managers and decision-makers. It is essential to pinpoint strategies so that managers can accomplish projects and polish off them within a predetermined period of time and resource restraint. This research assists us to detect the critical path in an acyclic network in terms of intuitionistic triangular fuzzy numbers, we have proposed the "maximum edge distance" method. Forward and backward algorithms are designed to find the optimal path for the proposed method. Numerical examples are also illustrated for the same. Verification is done using the path length ranking technique. Simulation results are included by the use of the C program and MATLAB. Finally, the comparison is made with the traditional forward and backward pass (existing method) technique to point out the conclusion.

Sentiment Analysis Performance and Reliability Evaluation Using an XLNet-based Deep Learning Approach..... 391

Dhaval Bhoi, Amit Thakkar

Online reviews are now a global form of communication between consumers and E-commerce companies. When it comes to making day-to-day decisions, customers rely heavily on the availability of internet reviews, as well as their trustworthiness and performance. Due to the unique qualities of user reviews, customers are finding it increasingly difficult to define and examining the authenticity and reliability of sentiment evaluations. These sentiment classifications for user reviews can aid in understanding user feelings, review dependability, and customer perceptions of movie items. Deep Learning is a strong technique for learning several layers of data representations or features. When compared to traditional machine learning approaches, deep learning techniques yield better results. To assess, analyze, and weight the usefulness of each review comment, we employed the XLNet Deep Learning Model Approach on balanced movie review dataset. Experimental result demonstrates that the proposed deep learning model achieves higher performance evaluation than those of other classifiers.

Sharma-Mittal Entropy Properties on Generalized (k) Record Values..... 398

Jerin Paul, P. Yageen Thomas

In this paper, we derive Sharma-Mittal entropy of generalized (k) record values and analyse some of its important properties. We establish some bounds for the Sharma-Mittal entropy of generalized (k) record values. We generate a characterization result based on the properties of Sharma-Mittal entropy of generalized (k) record values for the exponential distribution. We further establish some distribution-free properties of Sharma-Mittal divergence information between the distribution of a generalized (k) record value and the parent distribution. We extend the concept of Sharma-Mittal entropy to the concomitants of generalized (k) record values arising from a Farlie-Gumbel-Morgenstern (FGM) bivariate distribution. Also, we consider residual Sharma-Mittal Entropy and used it to describe some properties of generalized (k) record values.

The New Mixed Erlang Distribution: A Flexible Distribution for Modeling Lifetime Data..... 411

Therrar Kadri, Souad Kadri, Seifedine Kadry, Khaled Smaili

We introduce a new mixed distribution of the Erlang distribution that is generated from the convolution of the Extension Exponential distribution denoted by the Mixed Erlang distribution (ME). We derive an exact closed expression of the probability density function which is used to obtain closed expressions of the cumulative function, reliability function, hazard function, moment generating function and kth moment. The method of maximum likelihood and method of moments is used for estimating the model parameters. Two applications to real data sets are given to illustrate the potentiality of this distribution.

**Construction of Life Test Sampling Inspection Plans
by Attributes Based on Marshall – Olkin Extended
Exponential Distribution 421**

R. Vijayaraghavan, A. Pavithra

A life test is a random experiment conducted on the manufactured items such as electrical and electronic components for estimating their life time based on the inspection of randomly sampled items. Life time of the items is a random variable which follows a specific continuous-type distribution, called the lifetime distribution. Reliability sampling, which is one among the classifications of product control, deals with inspection procedures for sentencing one or more lots or batches of items submitted for inspection. In this paper, the concept of sampling plans for life tests involving two samples is introduced under the assumption that the life time random variable is modeled by Marshall - Olkin extended exponential distribution. A procedure is developed for designing the optimum plan with minimum sample sizes when two points on the desired operating characteristic curve are prescribed to ensure protection to the producer and the consumer.

**A Comparative study of outlier detection of Yamuna
River Delhi India by Classical Statistics and Statistical Quality Control..... 430**

Mohammad Ahmad, Ahteshamul Haq, Abdul Kalam, Sayed Kifayat Shah

Water quality control aids in preventing pollution, public health, and the preservation and improvement of the biological integrity of water bodies. Water quality involves many variables and observations, some of which are outside of the acceptable range. An observation that apart from the rest of the data or looks diverge from other observation of the sample in which it occurs. In this paper, we proposed two methodologies for detecting outliers for the Yamuna River water quality data with three variables Chemical Oxygen Demand (COD), Bio-chemical Demand Oxygen (BOD) and PH, at three different locations did comparison of these two methodologies. These two methodologies are based on Descriptive Statistics and Statistical Process Control (SPC). A few outliers are present in the data. The outcome shows how far the outlier detection method has progressed and better knowledge of the various outlier methodologies and provide a clear path for future outlier detection methods for researchers.

Inferences on Stress Strength Reliability in Multicomponent System for Type I Generalized Half-Logistic Distribution

PHILLIP OLUWATOBI AWODUTIRE¹

Thomas Xavier²

Joby K. Jose³

•

Department of Mathematical Sciences, University of Africa¹

Department of Statistics, Kannur University^{2,3}

phillip.awodutire@gmail.com¹

thomasmxavier@gmail.com²

jobyk@kannuruniv.ac.in³

Abstract

This article deals with inferences on stress strength reliability in a multicomponent system for Type I generalized half-logistic distribution. It is assumed that the strength and stress components are independently distributed. In this work, we develop some statistical properties of the type I generalized half-logistic distribution. Furthermore, the expression for stress strength reliability for a multicomponent setup was obtained and studied. Two methods to estimate the multicomponent stress-strength reliability - maximum likelihood and Bayesian estimation were employed. The Bayes estimates of the multicomponent stress strength reliability are obtained under squared error loss function and using gamma priors for the parameters. Simulation studies were conducted to assess the efficiency of the methods. The importance of this model was studied by applying it to a real life data set.

Keywords: Type I generalized half-logistic distribution; multicomponent system; stress strength reliability; beta function.

1. INTRODUCTION

Researchers and statisticians have paid a lot of attention to stress-strength reliability. Their vast range of applications includes industries ranging from transportation and communications to medicine and healthcare. If the system's strength is higher than the stress it is subjected to, it is called trustworthy. Random stress is given to an appliance, Y , and the strength is X then a measure of the reliability of a system is given by $R = Pr\{X > Y\}$. There has been a great deal of effort done on estimating R using various X and Y distributions and estimate methodologies. Kotz *et al.* (2003) provide an overview of the applications and theories in this field. Raqab *et al.* (2008) and Kundu and Raqab (2009) found R where X and Y are independent three-parameter generalized exponential and three-parameter Weibull random variables, respectively. Kundu and Raqab (2013) have calculated the stress-strength reliability for a three-parameter generalized Rayleigh distribution. Using the phase-type distribution and a discrete distribution, Jose *et al.* (2020) calculated stress-strength reliability and Jose and Drisya (2020) evaluated time-dependent reliability using the phase-type distribution, respectively.

The development of multicomponent stress-strength reliability has also received considerable attention. For example, consider a system with k statistically independent and identically

distributed strength components subjected to a shared load. When $s(1 \leq s \leq k)$ or more components concurrently survive, this multicomponent stress-strength system is activated. This was initially explored by Bhattacharya and Johnson (1974). A wide range of industrial and military applications can benefit from such systems. When $s = k$ and $s = 1$ respectively, the following system corresponds to series and parallel. Using a panel of k identical solar cells, Johnson (1988) showed that this set-up may be used in practice to ensure that the mission's power requirements are met even if only s of the cells are in use at any one time. Some cells may be unable to function properly due to severe temperatures, and this extreme temperature may be a factor in a cell's strength. Dey *et al.* (2016) used this model to estimate the multicomponent stress-strength reliability for the Kumaraswamy distribution, among many other practical uses. An example of a log-logistic distribution of strength and stress was studied by Rao and Kantam (2010). The dependability of multicomponent stress-strength models was calculated by assuming generalized exponential and Burr XII distributions for the components in Kizilaslan and Nadar (2015), Rao (2012), and Rao *et al.* (2014).

Olapade developed the type I generalized half-logistic model, which is shown below (2014). A generalized version of the half-logistic distribution suggested by Balakrishnan, the distribution is used in this case (Balakrishnan, 1985). If a random variable X has the density function $f(x)$ of the type I generalized half-logistic (TIGHL) distribution, it is said to have the type I generalized half-logistic (TIGHL) distribution if

$$f(x) = \frac{b2^b}{\sigma} \frac{e^{\frac{x}{\sigma}}}{\left(1 + e^{\frac{x}{\sigma}}\right)^{b+1}}; 0 \leq x < \infty, b > 0, \sigma > 0 \quad (1)$$

and $f(x) = 0$ elsewhere with cumulative distribution function as

$$F(x) = 1 - \left(\frac{2}{1 + e^{\frac{x}{\sigma}}}\right)^b \quad (2)$$

where σ and b are the scale and shape parameters, respectively. Jose and Manoharan's approach is a particular case of the model in (1) (Jose and Manoharan, 2016). This model's dependability qualities haven't been well studied in the literature, which prompted us to investigate them and come up with clearer formulations. In addition to Bello *et al.* (2017), Awodutire and Awodutire *et al.* (2020a) and others, the type I generalized half-logistic model has been further generalized. According to Jose *et al.* (2019) the stress-strength reliability of Kumaraswamy half-logistic distribution was analyzed. Furthermore, a power-transformed half-logistic distribution was used to estimate stress-strength reliability in single and multicomponent system (Xavier and Jose, 2020a, 2020b).

The following is the article's flow: The type-I generalized half-logistic model's dependability features are discussed in Section 2. Under a multicomponent arrangement, the calculation of the distribution's strength stress reliability is discussed in Section 3. Maximum likelihood estimates and Bayesian estimates are developed. Gamma priors are used for Bayesian estimation under the squared error loss function. In Section 4, characteristics were tested in a series of computer simulations. In the same section, a real-world dataset is used to demonstrate the model's capabilities. Section 5 is the final conclusions of the paper.

2. RELIABILITY PROPERTIES

Olapade(2014) had studied some properties of the Type I generalized half logistic distribution. In this section, more research is carried out in order to derive precise formulations for a number of dependability characteristics. Moment generating function, mean failure time, mean residual life function, and Renyi and Shannon entropies are among the properties that are further studied.

2.1. Moment generating function

The moment generating function can be obtained as

$$M_x(t) = E(e^{tx}) = \frac{b2^b}{\sigma} \int_0^\infty e^{tx} \frac{e^{\frac{x}{\sigma}}}{\left(1 + e^{\frac{x}{\sigma}}\right)^{b+1}} dx$$

Now consider the transformation $\frac{1}{\left(1 + e^{\frac{x}{\sigma}}\right)} = u$, then

$$\begin{aligned} M_x(t) = E(e^{tx}) &= b2^b \int_0^1 u^{b-t\sigma-1} (1-u)^{t\sigma} du \\ &= 2^b \frac{\Gamma(b-t\sigma)\Gamma(t\sigma+1)}{\Gamma(b)}; \Re(b-t\sigma) > 0 \end{aligned} \tag{3}$$

where $\Gamma(\cdot)$ is called the gamma function defined as $\Gamma(a) = \int_0^\infty x^{a-1} e^{-x} dx; \Re(a) > 0$.

2.2. Mean Time to Failure Function

Then we can have mean time to failure (MTTF) or $E(X)$ as $E(X) = \frac{d}{dt} M_x(t)|_{t=0}$

$$\begin{aligned} E(X) &= 2^b \frac{\Gamma(b-t\sigma)\Gamma(t\sigma+1)}{\Gamma(b)} [\sigma\psi(b-t\sigma) + \sigma\psi(t\sigma+1)]|_{t=0} \\ &= 2^b \sigma [\psi(b) + \psi(1)] \end{aligned} \tag{4}$$

Here $\psi(\cdot)$ called the digamma function is the logarithmic derivative of the gamma function, that is $\psi(\cdot) = \frac{\Gamma'(\cdot)}{\Gamma(\cdot)}$.

2.3. Mean residual life function

The mean residual life function for a non-negative continuous random variable X is defined as $\eta(x) = E(X - x | X > x)$ and can be obtained by

$$\begin{aligned} \eta(x) &= \frac{1}{S(x)} \int_x^\infty S(y) dy \\ &= \frac{\left(1 + e^{\frac{x}{\sigma}}\right)^b}{2^b} 2^b \int_x^\infty \frac{1}{\left(1 + e^{\frac{y}{\sigma}}\right)^b} dy \end{aligned}$$

Now consider the transformation $\frac{1}{\left(1 + e^{\frac{y}{\sigma}}\right)} = u$, then

$$\begin{aligned} \eta(x) &= \sigma \left(1 + e^{\frac{x}{\sigma}}\right)^b \int_0^{\frac{1}{1+e^{\frac{x}{\sigma}}}} \frac{u^{b-1}}{1-u} du \\ &= \sigma \left(1 + e^{\frac{x}{\sigma}}\right)^b \sum_{k=0}^\infty \frac{(1)_k}{k!} \int_0^{\frac{1}{1+e^{\frac{x}{\sigma}}}} u^{b+k-1} du \\ &= \sigma \left(1 + e^{\frac{x}{\sigma}}\right)^b \sum_{k=0}^\infty \frac{(1)_k}{(b+k)k!} \left(\frac{1}{1+e^{\frac{x}{\sigma}}}\right)^{b+k} \\ &= \frac{\sigma}{b} \sum_{k=0}^\infty \frac{(1)_k (b)_k}{(b+1)_k k!} \left(\frac{1}{1+e^{\frac{x}{\sigma}}}\right)^k \\ &= \frac{\sigma}{b} {}_2F_1\left(1, b; b+1; \frac{1}{1+e^{\frac{x}{\sigma}}}\right) \end{aligned} \tag{5}$$

where $(t)_m = t(t+1)\dots(t+m-1)$ and ${}_pF_q(z)$ is the generalized hypergeometric function. The generalized hypergeometric function ${}_pF_q(z)$ is defined as

$${}_pF_q(a_1, \dots, a_p; b_1, \dots, b_q; z) = \sum_{k=0}^{\infty} \frac{(a_1)_k \dots (a_p)_k}{(b_1)_k \dots (b_q)_k} \frac{z^k}{k!}$$

where $b_j \neq 0, -1, -2, \dots; i = 1, 2, \dots, p; j = 1, 2, \dots, q$. The convergence conditions and other details are available from books on special functions, see for example Mathai and Haubold (2008).

2.4. Renyi and Shannon entropies

The entropy of a random variable X is a measure of variation of the uncertainty. Renyi entropy is defined as $I_r(\gamma) = \frac{1}{1-\gamma} \ln \left\{ \int_{\mathcal{R}} f^\gamma(x) dx \right\}$, where $\gamma > 0$ and $\gamma \neq 1$.

$$\begin{aligned} I_r(\gamma) &= \frac{1}{1-\gamma} \ln \left[\frac{b^\gamma 2^{\gamma b}}{\sigma^\gamma} \int_0^\infty \frac{e^{\frac{\gamma x}{\sigma}}}{\left(1 + e^{\frac{x}{\sigma}}\right)^{\gamma(b+1)}} dx \right] \\ &= \frac{1}{1-\gamma} \ln \left[\frac{b^\gamma 2^{\gamma b}}{\sigma^\gamma} \int_0^1 u^{\gamma b-1} (1-u)^{\gamma-1} du \right] \\ &= \frac{1}{1-\gamma} \ln \left[\left(\frac{b2^b}{\sigma}\right)^\gamma B(\gamma b, \gamma) \right]; \gamma > 0, \gamma \neq 1 \end{aligned} \tag{6}$$

The Shannon entropy is defined as $E[-\ln f(x)]$ and can be obtained as

$$E[-\ln f(x)] = -E[\ln b + b \ln 2 - \ln \sigma] - E\left[\frac{x}{\sigma}\right] + (b+1)E\left[\ln\left(1 + e^{\frac{x}{\sigma}}\right)\right]$$

Now

$$\begin{aligned} E\left[\frac{x}{\sigma}\right] &= 2^b(\psi(b) - \psi(1)) \\ E\left[\ln\left(1 + e^{\frac{x}{\sigma}}\right)\right] &= \frac{b(b+1)2^b}{\sigma} \int_0^\infty \frac{e^{\frac{x}{\sigma}} \ln\left(1 + e^{\frac{x}{\sigma}}\right)}{\left(1 + e^{\frac{x}{\sigma}}\right)^{b+1}} dx \\ &= b(b+1)2^b \int_0^1 u^{b-1} \ln\left(\frac{1}{u}\right) du \\ &= \frac{(b+1)2^b}{b} \end{aligned}$$

Hence, the Shannon entropy reduces to

$$E[-\ln f(x)] = -[\ln b + b \ln 2 - \ln \sigma] + 2^b(\psi(b) - \psi(1)) + \frac{(b+1)2^b}{b} \tag{7}$$

3. MULTICOMPONENT STRENGTH STRESS RELIABILITY

The stress-strength reliability of a system is defined as the chance that the system will continue to work effectively until the strength surpasses the stress. When the system is placed to use and subjected to a random stress, the system's strength changes as a result of the manufacturing variability and unpredictable circumstances. Material, production technique, humidity, temperature, and other variables may all be exploited to create manufacturing variations and unpredictability in products. There are several studies in the literature that have attempted to estimate the multicomponent stress-strength reliability for different statistical distributions.

Reliability of multicomponent stress strength is established by Bhattacharyya and Johnson (1974) as

$$\begin{aligned}
 R_{s,k} &= Pr \{ \text{at least } s \text{ of } (X_1, X_2, \dots, X_k) \text{ exceed } Y \} \\
 &= \sum_{i=s}^k \binom{k}{i} \int_0^\infty [1 - F(y)]^i [F(y)]^{k-i} dG(y)
 \end{aligned} \tag{8}$$

where $X_1, X_2, X_3, \dots, X_k$ are independently distributed with the cumulative distribution function $F(x)$ and are subjected to common random stress Y with cumulative distribution function $G(y)$. Let X_1, X_2, \dots, X_k be iid with $TIGHL(q, \sigma)$ and $Y \sim TIGHL(b, \sigma)$ be independently distributed. Thus, by putting equations (1) and (2) into (8), we can derive the multicomponent system's stress strength reliability using the type I generalized half logistic distribution as

$$R_{s,k} = \frac{b2^b}{\sigma} \sum_{i=s}^k \binom{k}{i} \int_0^\infty \left(\frac{2}{1 + e^{\frac{x}{\sigma}}} \right)^{qi} \left(1 - \left(\frac{2}{1 + e^{\frac{x}{\sigma}}} \right)^q \right)^{k-i} \frac{e^{\frac{x}{\sigma}}}{(1 + e^{\frac{x}{\sigma}})^{b+1}} dx$$

Let $t = \left(\frac{2}{1 + e^{\frac{x}{\sigma}}} \right)^q$ then $dt = -\frac{q2^q e^{\frac{x}{\sigma}}}{\sigma(1 + e^{\frac{x}{\sigma}})^{q+1}} dx$ and when $x \rightarrow 0, t \rightarrow 1$ and when $x \rightarrow \infty, t \rightarrow 0$.

$$\begin{aligned}
 R_{s,k} &= \frac{b}{q} \sum_{i=s}^k \binom{k}{i} \int_0^1 t^i [1 - t]^{k-i} t^{\frac{b}{q}} dt \\
 &= \frac{b}{q} \sum_{i=s}^k \binom{k}{i} \int_0^1 t^{\frac{b}{q} + i} [1 - t]^{k-i} dt \\
 &= \delta \sum_{i=s}^k \binom{k}{i} B(\delta + i + 1, k - i + 1)
 \end{aligned} \tag{9}$$

where $\delta = \frac{b}{q}$ and $B(\cdot)$ is the beta function defined as $B(x, y) = \int_0^1 t^{x-1} (1 - t)^{y-1} dt$; $\Re(x) > 0, \Re(y) > 0$.

As special case, consider X_1, X_2, \dots, X_k are connected in parallel, then $s = 1$ and $R_{s,k}$ will be

$$R_{1,k} = \delta \sum_{i=1}^k \binom{k}{i} B(\delta + i + 1, k - i + 1) \tag{10}$$

Consider X_1, X_2, \dots, X_k are connected in series, then $s = k$ and $R_{k,k}$ will be

$$R_{k,k} = \delta \sum_{i=k}^k \binom{k}{i} B(\delta + i + 1, k - i + 1) = \frac{\delta}{\delta + k + 1} \tag{11}$$

3.1. Maximum Likelihood Estimation of $R_{s,k}$

Consider two random samples of size m and n , respectively, drawn from the variables strength, X , and stress, Y , each of which follows a type I generalized half-logistic distribution with shape parameters q and b , respectively, and a common scale parameter σ , then the log-likelihood function of the observed data is as follows:

$$\begin{aligned}
 l &= m(\ln q + q \ln 2 - \ln \sigma) + n(\ln b + b \ln 2 - \ln \sigma) + \sum_{i=1}^m \frac{x_i}{\sigma} + \sum_{j=1}^n \frac{y_j}{\sigma} \\
 &- (q + 1) \sum_{i=1}^m \ln(1 + e^{\frac{x_i}{\sigma}}) - (b + 1) \sum_{j=1}^n \ln(1 + e^{\frac{y_j}{\sigma}})
 \end{aligned}$$

$$\frac{\partial l}{\partial q} = \frac{m}{q} + m \ln 2 - \sum_{i=1}^m \ln(1 + e^{\frac{x_i}{\sigma}}) \Rightarrow \hat{q} = \frac{m}{\sum_{i=1}^m \ln(1 + e^{\frac{x_i}{\sigma}}) - m \ln 2} \quad (12)$$

$$\frac{\partial l}{\partial b} = \frac{n}{q} + n \ln 2 - \sum_{j=1}^n \ln(1 + e^{\frac{y_j}{\sigma}}) \Rightarrow \hat{b} = \frac{n}{\sum_{j=1}^n \ln(1 + e^{\frac{y_j}{\sigma}}) - n \ln 2} \quad (13)$$

$$\begin{aligned} \frac{\partial l}{\partial \sigma} &= (q+1) \sum_{i=1}^m \frac{x_i e^{\frac{x_i}{\sigma}}}{\sigma^2 (1 + e^{\frac{x_i}{\sigma}})} + (b+1) \sum_{j=1}^n \frac{y_j e^{\frac{y_j}{\sigma}}}{\sigma^2 (1 + e^{\frac{y_j}{\sigma}})} \\ &- \frac{1}{\sigma^2} \left(\sum_{i=1}^m x_i + \sum_{j=1}^n y_j \right) - \frac{(m+n)}{\sigma} \end{aligned} \quad (14)$$

$\hat{\sigma}$ can be obtained by iteratively solving the equation $\frac{\partial l}{\partial \sigma} = 0$. Given the estimates, the MLE of $R_{s,k}$ becomes

$$\hat{R}_{s,k} = \hat{\delta} \sum_{i=s}^k \binom{k}{i} B(\hat{\delta} + i + 1, k - i + 1) \quad (15)$$

The asymptotic variance of the estimate of $R_{s,k}$ as defined by Rao (1973) is

$$AVar(\hat{R}_{s,k}) = Var(\hat{q}) \left(\frac{\partial R_{s,k}}{\partial q} \right)^2 + Var(\hat{b}) \left(\frac{\partial R_{s,k}}{\partial b} \right)^2 \quad (16)$$

where

$$\begin{aligned} Var(\hat{q}) &= E \left[-\frac{\partial^2 l}{\partial q^2} \right]^{-1} = \frac{q^2}{m} \\ Var(\hat{b}) &= E \left[-\frac{\partial^2 l}{\partial b^2} \right]^{-1} = \frac{b^2}{n} \end{aligned}$$

$$\frac{\partial R_{s,k}}{\partial q} = -\frac{R_{s,k}}{q} + \frac{\delta^2}{q} \sum_{i=s}^k \binom{k}{i} B(\delta + i + 1, k - i + 1) \{ \psi(\delta + k + 2) - \psi(\delta + i + 1) \}$$

$$\frac{\partial R_{s,k}}{\partial b} = \frac{R_{s,k}}{b} + \frac{\delta}{b} \sum_{i=s}^k \binom{k}{i} B(\delta + i + 1, k - i + 1) \{ \psi(\delta + i + 1) - \psi(\delta + k + 2) \}$$

Then the asymptotic 95% confidence interval for the system reliability, $R_{s,k}$ can be obtained as $R_{s,k} \mp 1.96 \sqrt{AVar(\hat{R}_{s,k})}$.

3.2. Bayes estimation of $R_{s,k}$

Parameters are assumed to be constants in the conventional estimate technique. For example, the parameters in the model may not be constant over the entire testing time, therefore they must be handled as random variables. The prior distribution of the parameters may be utilized as information on the uncertainty associated with them in Bayesian estimation, which is a method for overcoming this. This section is devoted to estimating $R_{s,k}$ by use of a Bayesian approach. Here, we assume that the parameters q, b and σ have gamma prior distributions with $(c_i, d_i), i=1, 2, 3$ correspondingly. Assume random variable Z has parameters (c_i, d_i) with the following gamma density is

$$h(z) = \frac{d_i^{c_i}}{\Gamma(c_i)} z^{c_i-1} e^{-zd_i}; \quad 0 \leq z < \infty, c_i > 0, d_i > 0, i=1, 2, 3$$

and $h(z) = 0$ elsewhere. The joint prior of b, q and σ can be written as

$$\pi(b, q, \sigma) \propto q^{c_1-1} b^{c_2-1} \sigma^{c_3-1} e^{-d_1 q - d_2 b - d_3 \sigma} \quad (17)$$

On the basis of the squared error loss function, it was possible to generate Bayes estimates of $R_{s,k}$ when the likelihood function and the prior posterior distribution of the parameters q, b and σ are combined and the following result is obtained:

$$\begin{aligned} \pi_0^*(\sigma|b, q, \text{data}) &\propto \sigma^{c_3-m-n-1} e^{\frac{1}{\sigma}(\sum_{r=1}^m x_r + \sum_{s=1}^n y_s) - d_3 \sigma} \\ &\times \prod_{r=1}^m \left(1 + e^{\frac{x_r}{\sigma}}\right)^{-(q+1)} \prod_{s=1}^n \left(1 + e^{\frac{y_s}{\sigma}}\right)^{-(b+1)} \\ \pi_1^*(q|\sigma, \text{data}) &\propto \text{Gamma} \left(m + c_1, d_1 - m \ln 2 + \sum_{r=1}^m \ln \left(1 + e^{\frac{x_r}{\sigma}}\right) \right) \\ \pi_2^*(b|\sigma, \text{data}) &\propto \text{Gamma} \left(n + c_2, d_2 - n \ln 2 + \sum_{s=1}^n \ln \left(1 + e^{\frac{y_s}{\sigma}}\right) \right) \end{aligned}$$

Any well-known distribution cannot be reduced to the posterior distribution of σ . Random samples are generated using the Markov chain Monte Carlo (MCMC) method because posterior distributions cannot be reduced into closed forms. It is possible to estimate the posterior density functions if they are unimodal and generally symmetric; for details, see Gelman *et al* (2003). When a previous is log-concave, then a posterior is similarly log-concave, according to Kundu (2008) Metropolis-Hasting and the normal proposal distribution will be utilized to generate random samples from posterior distributions of σ . Bayesian $R_{s,k}$ estimation is given in the following manner:

Step 1: Set the initial values σ^0 and $i = 1$. Let $\gamma = \sigma^{i-1}$.

Step 2: Generate q from $\text{Gamma} \left(m + c_1, d_1 - m \ln 2 + \sum_{r=1}^m \ln \left(1 + e^{\frac{x_r}{\sigma}}\right) \right)$.

Step 3: Generate b from $\text{Gamma} \left(n + c_2, d_2 - n \ln 2 + \sum_{s=1}^n \ln \left(1 + e^{\frac{y_s}{\sigma}}\right) \right)$.

Step 4: Using the proposal density $h(\sigma) \equiv N(\sigma^{i-1}, 1), \sigma > 0$, generate σ^i from $\pi_0^*(\sigma|b^{i-1}, q^{i-1}, \text{data})$ using step 5.

Step 5: From the proposal density, generate a sample, τ . Generate U from Uniform (0, 1) and if $U \leq \min \left\{ 1, \frac{\pi_0^*(\tau)h(\gamma)}{\pi_0^*(\gamma)h(\tau)} \right\}$, accept τ and set $\sigma^i = \tau$.

Step 6: Compute $R_{s,k}^i$ and set i to $i + 1$.

Step 7: Repeat steps 2 to 6, K times and obtain the Bayesian estimates of q, b, σ and $R_{s,k}$ as $\frac{\sum_{i=1}^K q^i}{K}, \frac{\sum_{i=1}^K b^i}{K}, \frac{\sum_{i=1}^K \sigma^i}{K}$ and $\frac{\sum_{i=1}^K R_{s,k}^i}{K}$ respectively.

The method of Chen and Shao (1999) can be used to construct the $100(1 - \alpha)\%$ high posterior density (HPD) credible interval of $R_{s,k}$.

4. SIMULATION STUDY AND DATA ANALYSIS

Here, we compare the performances of $R_{s,k}$ for different sample sizes. Random samples of sizes 15, 20, 30, 40, and 50 with 1000 replications each from the strength and stress populations were generated for $(q, b) = \{(3.5, 1.0), (2.5, 1.0), (1.5, 1.0), (1.0, 1.5), (1.0, 2.5), (1.0, 3.5)\}$ respectively. The value of σ was fixed at 2 for all simulation results. The ML estimators of \hat{q} and \hat{b} were then substituted to obtain the estimate for $R_{s,k}$ with $(s, k) = \{(1, 3), (2, 4)\}$. The bias, MSE, and asymptotic confidence intervals of the MLE of $R_{s,k}$ are presented in Table 1. The MSE values decrease as the sample size increases for both (s, k) which verifies the consistency property of the MLE of $R_{s,k}$.

Table 1: Bias and MSE for MLE of $R_{s,k}$

(q, b)	n	$R_{1,3}$	$\hat{R}_{1,3}$	Bias(e-5)	MSE	ACI	$R_{2,4}$	$\hat{R}_{2,4}$	Bias(e-5)	MSE	ACI
(3.5,1)	10	0.180797101	0.180796973	-0.01280	0.00200	(0.09312,0.26847)	0.150567959	0.150567848	-0.01110	0.00115	(0.08385,0.21728)
	20	0.180797069	0.180797069	-0.00320	0.00149	(0.10496,0.25663)		0.150567931	-0.00280	0.00086	(0.09286,0.20826)
	30	0.180797039	0.180797039	-0.00620	0.00099	(0.11898,0.24260)		0.150567905	-0.00540	0.00057	(0.10354,0.19758)
	40	0.180797055	0.180797055	-0.00460	0.00074	(0.12731,0.23427)		0.1505679195	0.00039	0.00043	(0.10988,0.19124)
	50	0.180797055	0.180797055	-0.00460	0.00059	(0.13299,0.22860)		0.1505679190	-0.00400	0.00034	(0.11420,0.18693)
(2.5,1)	10	0.237967914	0.237967743	-0.01710	0.00324	(0.12631,0.34962)	0.200831848	0.200831695	-0.01530	0.0019	(0.11488,0.28677)
	20	0.2379678833	0.2379678833	-0.00307	0.00241	(0.14139,0.33453)		0.2008318202	-0.00278	0.00143	(0.12651,0.27514)
	30	0.2379679029	0.2379679029	-0.00111	0.00161	(0.15927,0.31666)		0.2008318376	-0.00104	0.00095	(0.14028,0.26137)
	40	0.2379678962	0.2379678962	-0.00074	0.00158	(0.16988,0.30604)		0.2008318316	-0.00084	0.00071	(0.14845,0.25320)
	50	0.2379679	0.2379679	-0.00014	0.00096	(0.17711,0.29882)		0.2008318	-0.00480	0.00057	(0.15402,0.24764)
(1.5,1)	10	0.347402597	0.347402677	0.00800	0.00615	(0.19358,0.50122)	0.300993125	0.300993199	0.00740	0.00397	(0.17744,0.42453)
	20	0.3474025377	0.3474025377	-0.00593	0.00460	(0.21439,0.48040)		0.3009930684	-0.00566	0.00296	(0.19419,0.40779)
	30	0.347402578	0.347402578	-0.00190	0.00305	(0.23905,0.45575)		0.300993106	-0.00190	0.00196	(0.21402,0.38796)
	40	0.347402670	0.347402670	-0.00108	0.00228	(0.25367,0.44112)		0.300993192	-0.00108	0.00147	(0.22577,0.37620)
	50	0.347402511	0.347402511	0.00129	0.00182	(0.26363,0.43116)		0.300993044	0.00129	0.00117	(0.23377,0.36820)
(1,1.5)	10	0.558441558	0.558441470	-0.00088	0.01379	(0.32821,0.78866)	0.510489510	0.510489417	0.00133	0.0120	(0.29563,0.72534)
	20	0.5584416232	0.5584416232	0.00065	0.01031	(0.35941,0.75746)		0.5104895784	0.00068	0.00898	(0.32471,0.69626)
	30	0.5584415802	0.5584415802	0.00022	0.00683	(0.39635,0.72052)		0.5104895333	0.00023	0.00596	(0.35916,0.66181)
	40	0.558441478	0.558441478	-0.00084	0.00511	(0.41826,0.69862)		0.510489426	0.00068	0.00446	(0.37959,0.64138)
	50	0.558441653	0.558441653	0.00095	0.00408	(0.43316,0.68371)		0.510489610	0.00100	0.00356	(0.39350,0.62747)
(1,2.5)	10	0.687645688	0.687645901	0.00213	0.02103	(0.40335,0.97193)	0.650349650	0.650349888	0.00238	0.02266	(0.35524,0.94545)
	20	0.687645726	0.687645726	0.00038	0.01573	(0.44182,0.93347)		0.650349694	0.00044	0.01696	(0.39505,0.90564)
	30	0.6876457020	0.6876457020	0.00014	0.01043	(0.48738,0.88790)		0.650349664	0.00016	0.01127	(0.44222,0.85847)
	40	0.6876457103	0.6876457103	0.00022	0.00781	(0.51441,0.86087)		0.6503496757	0.00025	0.00844	(0.47025,0.83044)
	50	0.687645700	0.687645700	0.00012	0.00623	(0.53282,0.84246)		0.6503497	0.00050	0.00674	(0.48934,0.81134)
(1,3.5)	10	0.76037296	0.760373130	0.01700	0.02690	(0.43886,1.08188)	0.73273002	0.73273021	0.01900	0.03229	(0.38051,1.08494)
	20	0.7603730025	0.7603730025	0.00425	0.02013	(0.48228,1.03846)		0.7327300634	0.00434	0.02418	(0.42791,1.03754)
	30	0.760373041	0.760373041	0.00441	0.01337	(0.53373,0.98701)		0.732730108	0.00880	0.01609	(0.48411,0.98134)
	40	0.7603730198	0.7603730198	0.00598	0.01000	(0.56428,0.95646)		0.7327300833	0.00633	0.01205	(0.51753,0.94792)
	50	0.7603730206	0.7603730206	0.00606	0.00799	(0.58509,0.93565)		0.7327300842	0.00642	0.00963	(0.54031,0.92514)

Table 2: Bias, Risk and HPDCI for Bayes estimate of $R_{s,k}$ under prior 1

$(q, b,)$	(m, n)	$R_{1,3}$	$\hat{R}_{1,3}$	Bias	MSE	ACI	$R_{2,4}$	$\hat{R}_{2,4}$	Bias	MSE	ACI
(3.5, 1)	(15, 15)	0.1808	0.2063	0.0255	0.0040	(0.1122, 0.3301)	0.1506	0.1749	0.0243	0.0034	(0.0897, 0.2960)
	(20, 20)		0.2052	0.0244	0.0033	(0.1156, 0.3190)		0.1693	0.0187	0.0025	(0.0967, 0.2766)
	(30, 30)		0.1908	0.0100	0.0017	(0.1225, 0.2740)		0.1618	0.0112	0.0012	(0.1046, 0.2390)
	(40, 40)		0.1869	0.0061	0.0012	(0.1289, 0.2625)		0.1595	0.0089	0.0010	(0.1067, 0.2267)
	(50, 50)		0.1886	0.0078	0.0010	(0.1328, 0.2552)		0.1575	0.0069	0.0007	(0.1096, 0.2153)
(2.5, 1)	(15, 15)	0.2380	0.2690	0.0311	0.0057	(0.1549, 0.4209)	0.2008	0.2259	0.0251	0.0044	(0.1224, 0.3634)
	(20, 20)		0.2578	0.0198	0.0039	(0.1582, 0.3791)		0.2195	0.0187	0.0035	(0.1318, 0.3480)
	(30, 30)		0.2520	0.0141	0.0026	(0.1671, 0.3542)		0.2108	0.0100	0.0019	(0.1401, 0.3016)
	(40, 40)		0.2479	0.0100	0.0020	(0.1669, 0.3366)		0.2108	0.0100	0.0016	(0.1439, 0.29954)
	(50, 50)		0.2464	0.0084	0.0014	(0.1811, 0.3232)		0.2106	0.0098	0.0012	(0.1534, 0.2774)
(1.5, 1)	(15, 15)	0.3474	0.3704	0.0230	0.0076	(0.2203, 0.5473)	0.3010	0.3229	0.0219	0.0074	(0.1846, 0.5010)
	(20, 20)		0.3656	0.0182	0.0057	(0.2314, 0.5150)		0.3217	0.0207	0.0056	(0.1975, 0.4827)
	(30, 30)		0.3593	0.0119	0.0038	(0.2460, 0.4843)		0.3114	0.0104	0.0037	(0.2077, 0.4390)
	(40, 40)		0.3553	0.0079	0.0028	(0.2584, 0.4639)		0.3107	0.0097	0.0027	(0.2155, 0.4171)
	(50, 50)		0.3582	0.0108	0.0023	(0.2675, 0.4565)		0.3090	0.0080	0.0020	(0.2305, 0.4017)
(1, 1.5)	(15, 15)	0.5584	0.5653	0.0069	0.0085	(0.3754, 0.7398)	0.5105	0.5254	0.0149	0.0093	(0.3387, 0.7152)
	(20, 20)		0.5667	0.0083	0.0066	(0.4072, 0.7224)		0.5171	0.0067	0.0071	(0.3499, 0.6851)
	(30, 30)		0.5653	0.0068	0.0043	(0.4384, 0.6904)		0.5164	0.0060	0.0049	(0.3810, 0.6521)
	(40, 40)		0.5608	0.0024	0.0033	(0.4429, 0.6680)		0.5142	0.0037	0.0039	(0.3935, 0.6389)
	(50, 50)		0.5620	0.0036	0.0025	(0.4631, 0.6562)		0.5144	0.0039	0.0031	(0.4063, 0.6213)
(1, 2.5)	(15, 15)	0.6876	0.6867	-0.0009	0.0064	(0.5090, 0.8277)	0.6503	0.6475	-0.0028	0.0078	(0.4519, 0.8012)
	(20, 20)		0.6889	0.0012	0.0048	(0.5392, 0.8047)		0.6461	-0.0042	0.0061	(0.4865, 0.7896)
	(30, 30)		0.6860	-0.0017	0.0034	(0.5634, 0.7917)		0.6532	0.0029	0.0040	(0.5240, 0.7653)
	(40, 40)		0.6845	-0.0031	0.0026	(0.5813, 0.7786)		0.6506	0.0003	0.0033	(0.5352, 0.7556)
	(50, 50)		0.6882	0.0005	0.0021	(0.5929, 0.7748)		0.6495	-0.0008	0.0027	(0.5469, 0.7446)
(1, 3.5)	(15, 15)	0.7604	0.7578	-0.0025	0.0046	(0.6086, 0.8808)	0.7327	0.7242	-0.0085	0.0062	(0.5492, 0.8564)
	(20, 20)		0.7532	-0.0071	0.0038	(0.6198, 0.8610)		0.7250	-0.0078	0.0046	(0.5709, 0.8369)
	(30, 30)		0.7579	-0.0024	0.0026	(0.6410, 0.8441)		0.7365	0.0038	0.0033	(0.6137, 0.8373)
	(40, 40)		0.7612	0.0008	0.0018	(0.6722, 0.8354)		0.7323	-0.0004	0.0023	(0.6298, 0.8216)
	(50, 50)		0.7546	-0.0058	0.0017	(0.6672, 0.8267)		0.7300	-0.0027	0.0020	(0.6388, 0.8117)

Table 3: Bias, Risk and HPDCI for Bayes estimate of $R_{s,k}$ under prior 2

$(q, b,)$	(m, n)	$R_{1,3}$	$\hat{R}_{1,3}$	Bias	MSE	ACI	$R_{2,4}$	$\hat{R}_{2,4}$	Bias	MSE	ACI
(3.5, 1)	(15, 15)	0.1808	0.2329	0.0521	0.0069	(0.1259, 0.3698)	0.1506	0.2029	0.0523	0.0064	(0.1025, 0.3363)
	(20, 20)		0.2218	0.0410	0.0047	(0.1252, 0.3406)		0.1842	0.0337	0.0034	(0.1008, 0.2876)
	(30, 30)		0.2072	0.0264	0.0025	(0.1328, 0.2998)		0.1785	0.0283	0.0023	(0.1142, 0.2586)
	(40, 40)		0.2044	0.0237	0.0020	(0.1370, 0.2845)		0.1695	0.0189	0.0014	(0.1100, 0.2375)
	(50, 50)		0.2006	0.0198	0.0014	(0.1441, 0.2715)		0.1627	0.0121	0.0008	(0.1163, 0.2230)
(2.5, 1)	(15, 15)	0.2380	0.2995	0.0615	0.0096	(0.1637, 0.4635)	0.2009	0.2632	0.0624	0.0096	(0.1397, 0.4275)
	(20, 20)		0.2777	0.0397	0.0054	(0.1660, 0.4109)		0.2321	0.0312	0.0043	(0.1347, 0.3694)
	(30, 30)		0.2746	0.0366	0.0042	(0.1843, 0.3973)		0.2309	0.0300	0.0031	(0.1494, 0.3300)
	(40, 40)		0.2599	0.0219	0.0024	(0.1843, 0.3550)		0.2199	0.0191	0.0018	(0.1537, 0.3018)
	(50, 50)		0.2556	0.0177	0.0018	(0.1863, 0.3335)		0.2191	0.0183	0.0016	(0.1554, 0.2953)
(1.5, 1)	(15, 15)	0.3474	0.4127	0.0653	0.0120	(0.2599, 0.5983)	0.3010	0.3657	0.0647	0.0113	(0.2146, 0.5522)
	(20, 20)		0.3846	0.0371	0.0073	(0.2498, 0.5392)		0.3422	0.0412	0.0076	(0.2017, 0.5048)
	(30, 30)		0.3771	0.0297	0.0049	(0.2622, 0.5094)		0.3281	0.0271	0.0044	(0.2238, 0.4586)
	(40, 40)		0.3652	0.0178	0.0031	(0.2627, 0.4722)		0.3209	0.0199	0.0029	(0.2312, 0.4255)
	(50, 50)		0.3614	0.0140	0.0025	(0.2705, 0.4636)		0.3155	0.0145	0.0022	(0.2321, 0.4091)
(1, 1.5)	(15, 15)	0.5584	0.5897	0.0312	0.0094	(0.3988, 0.7579)	0.5105	0.5459	0.0354	0.0103	(0.3564, 0.7243)
	(20, 20)		0.5845	0.0260	0.0066	(0.4366, 0.7249)		0.5393	0.0288	0.0075	(0.3816, 0.6390)
	(30, 30)		0.5736	0.0152	0.0040	(0.4472, 0.6888)		0.5314	0.0209	0.0051	(0.3987, 0.6637)
	(40, 40)		0.5726	0.0142	0.0035	(0.4570, 0.6815)		0.5258	0.0154	0.0037	(0.4068, 0.6412)
	(50, 50)		0.5690	0.0106	0.0025	(0.4675, 0.6601)		0.5243	0.0138	0.0033	(0.4137, 0.6393)
(1, 2.5)	(15, 15)	0.6876	0.7008	0.0131	0.0061	(0.5438, 0.8389)	0.6503	0.6675	0.0172	0.0076	(0.4918, 0.8174)
	(20, 20)		0.7012	0.0136	0.0048	(0.5517, 0.8227)		0.6718	0.0214	0.0061	(0.5107, 0.8027)
	(30, 30)		0.6966	0.0090	0.0036	(0.5774, 0.8078)		0.6634	0.0130	0.0045	(0.5211, 0.7788)
	(40, 40)		0.6965	0.0088	0.0026	(0.5899, 0.7912)		0.6578	0.0075	0.0030	(0.5463, 0.7563)
	(50, 50)		0.6929	0.0053	0.0021	(0.5990, 0.7755)		0.6576	0.0072	0.0026	(0.5558, 0.7556)
(1, 3.5)	(15, 15)	0.7604	0.7662	0.0059	0.0043	(0.6170, 0.8781)	0.7327	0.7471	0.0143	0.0058	(0.5757, 0.8656)
	(20, 20)		0.7666	0.0062	0.0038	(0.6263, 0.8746)		0.7380	0.0053	0.0045	(0.6015, 0.8555)
	(30, 30)		0.7686	0.0082	0.0024	(0.6662, 0.8529)		0.7389	0.0062	0.0031	(0.6158, 0.8368)
	(40, 40)		0.7659	0.0055	0.0018	(0.6674, 0.8383)		0.7351	0.0024	0.0026	(0.6248, 0.8269)
	(50, 50)		0.7589	-0.0014	0.0015	(0.6723, 0.8258)		0.7368	0.0041	0.0020	(0.6384, 0.8180)

The Bayesian estimates were derived using the MCMC technique with two priors. The Bayesian estimates were derived using the MCMC technique with two priors. Prior 1: $(c_1, d_1) = (1, 0.5)$, $(c_2, d_2) = (2, 0.5)$, $(c_3, d_3) = (1, 1)$ and Prior 2: $(c_1, d_1) = (1, 1.5)$, $(c_2, d_2) = (2.5, 0.5)$, $(c_3, d_3) = (1, 1)$ (2,1). We ran the MCMC chains with a variety of beginning values and generated a total of 10000 iterations. The first 9000 iterations were deleted to reduce the distribution's initial influence. This is referred to as burn-in. Tables 2 and 3 show the bias, Bayes risk, and HPD confidence ranges for $R_{s,k}$ estimations. With increasing sample size, the risk and interval lengths are seen to decrease. We ran the MCMC chains with a variety of beginning values and generated a total of 10000 iterations. The first 9000 iterations were deleted to reduce the distribution's initial influence. This is referred to as burn-in. Tables 2 and 3 show the bias, Bayes risk, and HPD confidence ranges for $R_{s,k}$ estimations. With increasing sample size, the risk and interval lengths are seen to decrease.

4.1. Data analysis

In this part, a real-world dataset is examined to demonstrate how the produced conclusions may be used. Al-Mutairi et al. (2013) and Rao (2014) considered the dataset, the amount of time (in minutes) that clients had to wait before being served. As an example, suppose bank A has five service points, say X_1, X_2, \dots, X_5 , while bank B has one service point, say Y with $m = 100$ and $n = 60$ as the sample sizes, respectively. For your convenience, the dataset is displayed here.

Data X: 0.8,0.8,1.3,1.5,1.8,1.9,1.9,2.1,2.6,2.7,2.9,3.1,3.2,3.3,3.5,3.6,4.0,4.1,4.2, 4.2,4.3,4.3,4.4,4.4, 4.6,4.7,4.7,4.8,4.9,4.9,5.0,5.3,5.5,5.7,5.7,6.1,6.2,6.2,6.2,6.3, 6.7,6.9,7.1,7.1,7.1,7.1,7.4,7.6,7.7,8.0, 8.2,8.6,8.6,8.6,8.8,8.8,8.9,8.9,9.5,9.6,9.7,9.8,10.7,10.9,11.0,11.0,11.1,11.2,11.2,11.5,11.9,12.4,12.5, 12.9,13.0,13.1,13.3,13.6,13.7,13.9,14.1,15.4,15.4,17.3,17.3,18.1,18.2,18.4,18.9,19.0,19.9,20.6,21.3, 21.4,21.9,23.0,27.0,31.6,33.1,38.5

Data Y: 0.1,0.2,0.3,0.7,0.9,1.1,1.2,1.8,1.9,2.0,2.2,2.3,2.3,2.3,2.5,2.6,2.7,2.7,2.9,3.1,3.1,3.2,3.4,3.4, 3.5,3.9,4.0,4.2,4.5,4.7,5.3,5.6,5.6,6.2,6.3,6.6,6.8,7.3,7.5,7.7,7.7,8.0,8.0,8.5,8.5,8.7,9.5,10.7,10.9,11.0, 12.1,12.3,12.8,12.9,13.2,13.7,14.5,16.0,16.5,28.0

In order to match the datasets, we used the Type I generalized half-logistic distribution, and it can be shown that the model fits the data quite well. q and σ have MLE values of 0.41 and 3.33 for Data X. The MLEs of b and σ for Data Y are 0.69 and 3.33. Table 4 contains the results of the KS-test as well as the relevant p -values. Figure 1 shows a histogram of the fit, which shows how well the model fits. The values $s = 5$ and $k = 5$ are used for example reasons only, which means that the service points in Bank A are connected in a series fashion. A series connection of the service points might be read as consumers offering services for all five of the service points that are now accessible. The estimate of $R_{5,5}$ is obtained as 0.2160 with a 95 percent asymptotic confidence range of (0.1580,0.2740).

Table 4: Goodness for fit for data set

	Shape parameter	Scale parameter	K-S Statistic	p -value
Data X	0.41	3.33	0.1136	0.1513
Data Y	0.69	3.33	0.0728	0.9083

The MCMC technique under two priors was used to produce the Bayesian estimates in this case. Preliminary estimates for the following priors are used:

Prior 1: $(c_1, d_1) = (2, 1)$, $(c_2, d_2) = (2, 1)$, $(c_3, d_3) = (0.5, 0.5)$, and

Prior 2: $(c_1, d_1) = (1, 0.5)$, $(c_2, d_2) = (2, 0.5)$, $(c_3, d_3) = (1, 1)$.

We ran the MCMC chains and generated 20000 iterations, the first 10000 iterations of the distribution were removed in order to reduce the initial influence of the distribution. In order to break the

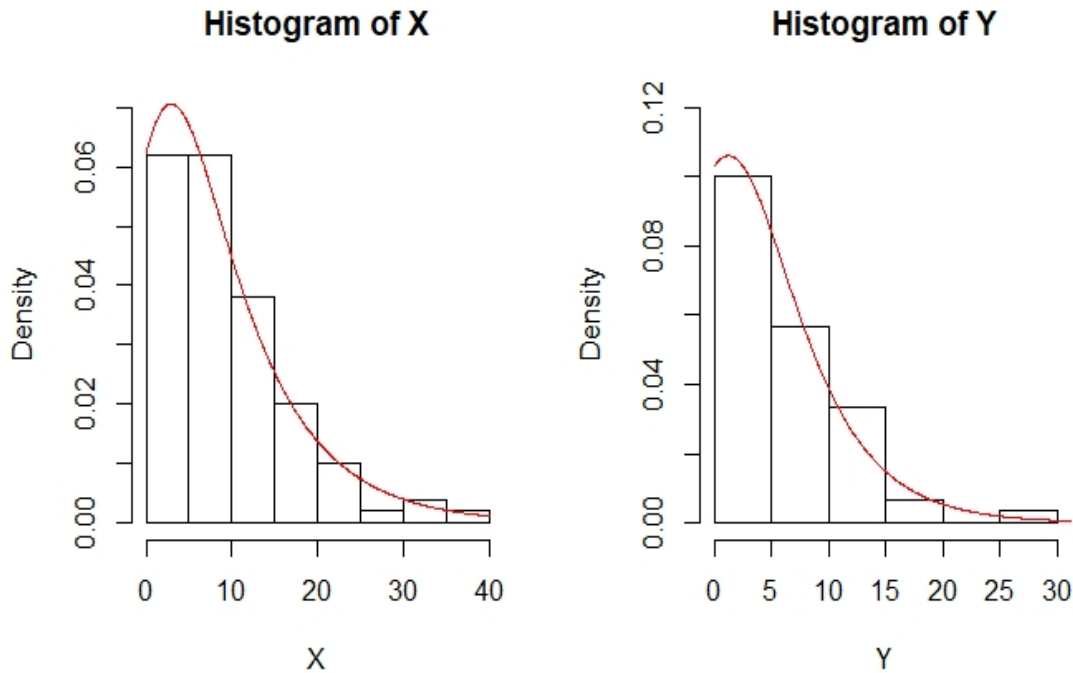


Figure 1: The fitted density for X and Y

reliance among the produced samples, we select a sample every tenth one. This results in a final chain of 1000 samples. According to the preceding condition, the multicomponent stress-strength reliability is derived as $\hat{R}_{5,5} = 0.2189$ with 95 percent credible interval as (0.1660,0.2766). Figure 2 shows the trace plot of and histogram of the $R_{s,k}$ values. Prior 2 yields the multicomponent stress-strength reliability as $\hat{R}_{5,5} = 0.2192$ with 95 percent credible interval as (0.1701,0.2760). Figure 3 depicts a trace plot and histogram of the $R_{s,k}$ values.

5. CONCLUSIONS

Using the Type I generalized half-logistic model, we may derive explicit formulas for several of the model's dependability features. Additional point and interval estimates of the multicomponent stress strength reliability, $R_{s,k}$ where the strength of its constituents and the stress applied to it are statistically independent and follow a Type I generalized half-logistic distribution are presented. The maximum likelihood estimates and Bayesian estimates under the squared error loss function are generated. The results of the simulations indicate that the estimations were compatible with one another. Furthermore, as the sample size was increased, the length of the confidence interval shrank as a result of this. As an example of how the proposed conclusions can be put into practice, a real-life scenario is explored.

FUNDING STATEMENT

This manuscript is funded by Digiteknologian TKI-ymparisto project A74338 (ERDF, Regional Council of Pohjois-Savo).

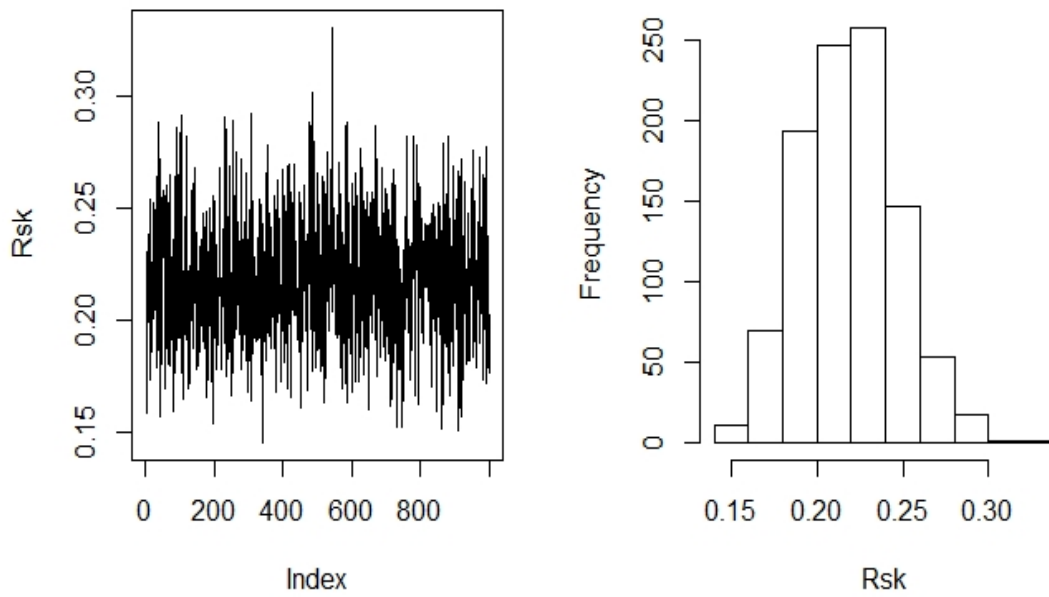


Figure 2: Trace plot and histogram of $R_{s,k}$ values under prior 1

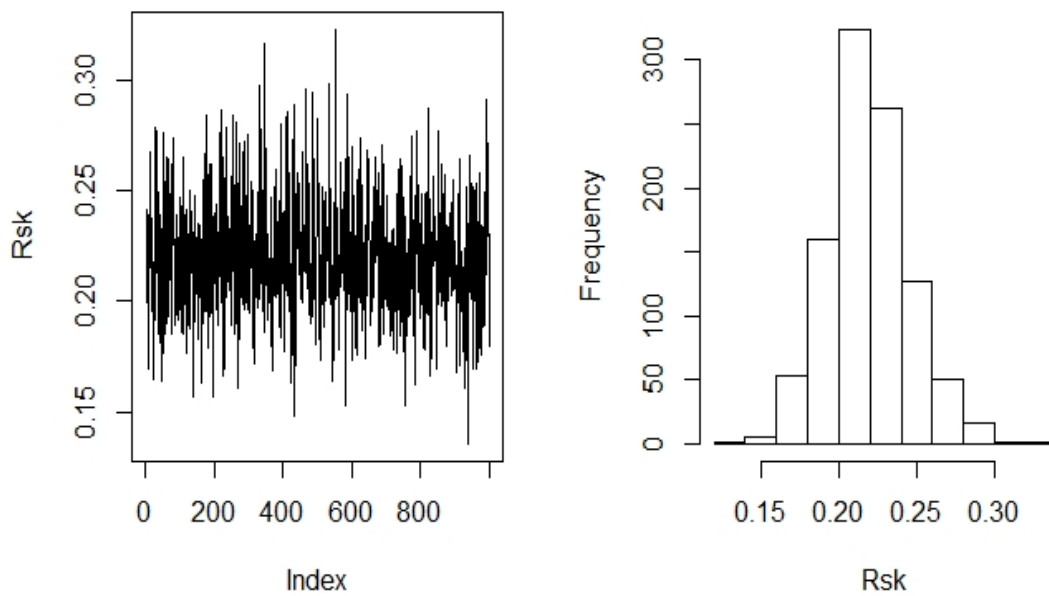


Figure 3: Trace plot and histogram of $R_{s,k}$ values under prior 2

REFERENCES

- [1] Al-Mutairi, D.K., Ghitany, M.E., Kundu, D. (2013), Inferences on stress-strength reliability from Lindley distributions, *Communications in Statistics - Theory and Methods*, 42(8): 1464-1475.

- [2] Awodutire, P. O, Nduka, E. C, Ijomah, M. A. (2020), Lehmann Type II Generalized Half Logistic Distribution: Properties and Application. *Mathematical Theory and Modeling*, 10(2):103-115.
- [3] Awodutire, P. O., Nduka, E. C., Ijomah, M. A. (2020), The Beta Type I Generalized Half Logistic Distribution: Properties and Application. *Asian Journal of Probability and Statistics*, 6(2), 27-41.
- [4] Balakrishnan, N. (1985). Order statistics from the half logistic distribution. *Journal of Statistical Computation and Simulation*, 20, 287-309.
- [5] Bhattacharyya, G. K., Johnson, R. A. (1974). Estimation of reliability in multicomponent stress strength model, *Journal of American Statistical Association* 69:966–970.
- [6] Bello, O. A., Sule, I., Awodutire, P.O., Olapade, A.K.(2018). A Study of Five Parameter Type I Generalized Half Logistic Distribution. *Pure and Applied Mathematics Journal*, 6(6), 177-181.
- [7] Chen, Ming-Hui, Shao, Qi-Man (1999), Monte Carlo Estimation of Bayesian Credible and HPD Intervals, *Journal of Computational and Graphical Statistics*, 8 (1), 69-92.
- [8] Dey, S., Mazucheli, J. and Anis, M. (2017), Estimation of reliability of multicomponent stress-strength for a Kumaraswamy distribution, *Communications in Statistics-Theory and Methods*, 46(4):1560-1572.
- [9] Gelman A., Carlin J. B., Stern H. S. and Rubin D. B. (2003), *Bayesian Data Analysis*. 2nd edition, Chapman Hall, London, U.K..
- [10] Johnson, R. A. (1988), 3 Stress-strength models for reliability, *Handbook of Statistics*, 7:27-54.
- [11] Jose, J. K., Manoharan, M. (2016). Beta half-logistic distribution - A new probability model for lifetime data. *Journal of Statistics and Management Systems*, 9:587-604.
- [12] Jose, J. K., Xavier, Thomas and Drisya, M. (2019), Estimation Of Stress-Strength Reliability Using Kumaraswamy half-logistic distribution, *Journal of Probability and Statistical Science*, 17(2):141-154.
- [13] Jose, J. K. and Drisya, M. (2020), Time-dependent stress–strength reliability models based on phase type distribution, *Computational Statistics*, DOI: 10.1007/s00180-020-00991-3.
- [14] Jose, J. K., Drisya, M., Manoharan, M. (2020), Estimation of stress-strength reliability using discrete phase type distribution, *Communication in Statistics- Theory and Methods*, DOI: 10.1080/03610926.2020.1749663.
- [15] Kizilaslan, F. and Nadar, M. (2015), Classical and bayesian estimation of reliability in multicomponent stress-strength model based on weibull distribution, *Revista Colombiana de Estadística* 38(2):467-484.
- [16] Kotz, S., Lumelskii, Y., and Pensky, M. (2003), *The stress-strength model and its generalizations*, World Scientific Publishing.
- [17] Kundu, D. (2008). Bayesian Inference and Life Testing Plan for Weibull Distribution in Presence of Progressive Censoring. *Technometrics* 50(2): 144-154.
- [18] Kundu, D., Raqab, M. Z. (2009). Estimation of $R = P(Y < X)$ for three-parameter Weibull distribution. *Statistics and Probability Letters* 79:1839–1846.
- [19] Kundu, D. and Raqab, M. Z. (2013). Estimation of $R = P(Y < X)$ for three-parameter generalized Rayleigh distribution. *Journal of Statistical Computation and Simulation*, 85:725 - 739.
- [20] Mathai, A. M., Haubould, H. J. (2008). *Special Function for Applied Scientists*, New York: Springer-Verlag.
- [21] Olapade, A. K. (2014). The Type I Generalized Half Logistic Distribution, *JIRSS*, 13(1),69-82.
- [22] Rao, C. R. (1973), *Linear Statistical Inference and its Applications*, New Delhi, Wiley Eastern.
- [23] Rao, G. S., Kantam, R. R. L., (2010). Estimation of reliability in multicomponent stress-strength model: log-logistic distribution, *Journal of Applied Statistical Science* 3(2):75-84.
- [24] Rao, G. S. (2012), Estimation of reliability in multicomponent stress-strength model based on generalized exponential distribution, *Revista Colombiana de Estadística*, 35(1):67-76.
- [25] Rao, G. S., Aslam, M., Kundu, D. (2014), Burr type XII distribution parametric estimation and estimation of reliability in multicomponent stress-strength model, *Communication in Statistics-Theory and Methods*, 44(23):4953-4961.
- [26] Rao, G. S. (2015), Estimation of stress-strength reliability from truncated type-I generalised logistic distribution, *International Journal of Mathematics in Operational Research*, 7(4), 372-382.

- [27] Raqab, M. Z., Madi, M. T., Kundu, D. (2008). Estimation of $P(Y < X)$ for the three-parameter generalized exponential distribution, *Communication in Statistics. Theory and Methods*, 37(18):2854–2864.
- [28] Xavier T. and Jose, J. K., (2020). A study of stress-strength reliability using a generalization of power transformed half-logistic distribution, *Communications in Statistics - Theory and Methods*, DOI: 10.1080/03610926.2020.1716250.
- [29] Xavier T. and Jose J. K., (2020). Estimation of reliability in a multicomponent stress-strength model based on power transformed half-logistic distribution, *International Journal of Reliability, Quality and Safety Engineering*, DOI: 10.1142/S0218539321500091.

A New Mixed Poisson Distribution for Over-dispersed Count Data: Theory and Applications

RAMAJEYAM THARSHAN

•

Postgraduate Institute of Science, University of Peradeniya, Peradeniya, Sri Lanka
Department of Mathematics and Statistics, University of Jaffna, Jaffna, Sri Lanka
tharshan10684@gmail.com

PUSHPAKANTHIE WIJEKOON

•

Department of Statistics and Computer Science, University of Peradeniya, Peradeniya, Sri Lanka
pushpaw@pdn.ac.lk

Abstract

In this paper, an alternative mixed Poisson distribution is proposed by amalgamating Poisson distribution and a modification of the Quasi Lindley distribution. Some fundamental structural properties of the new distribution, namely the shape of the distribution and moments and related measures, are explored. It was noted that the new distribution to be either unimodal or bimodal, and over-dispersed. Further, it has a tendency to accommodate various right tail behaviors and variance-to-mean ratios. Its unknown parameter estimation by using the maximum likelihood estimation method is examined by a simulation study based on the asymptotic theory. Finally, two real-world data sets are used to illustrate the flexibility and potentiality of the new distribution.

Keywords: over-dispersion, mixed Poisson distribution, Lindley distribution, Quasi Lindley distribution, goodness of fit.

1. INTRODUCTION

Most of the real-world applications, especially, reliability, actuarial, biomedical, engineering, ecological sciences, and among others, the variable of interest is in the form of count data. The Poisson distribution is a standard tool to model the count data if the empirical and theoretical properties satisfy the related underline assumptions. A random variable X is said to have a Poisson distribution with parameter λ if both the $E(X)$ and $Var(X)$ of the distribution equal to the parameter λ . This property is commonly known as equidispersion. Even though its probability mass function (pmf) is very flexible to compute its probabilities, in some real-world applications the Poisson distribution fails to match empirical observations. Here the variance of the observed data exceeds the theoretical variance. This phenomenon is explained as over-dispersion or variation inflation (Greenwood and Yule, 1920). The over-dispersion occurs by the failure of the basic assumptions of the Poisson distribution. The reasons might be by phenomena of the clustered structure of the population or population is heterogeneous, and heavy right tail that cannot accommodate by the Poisson distribution (McCullagh et al., 1989; Ridout et al., 1998). The heterogeneity of a population is determined by the Poisson parameter λ which differs individual to individual, and then the $Var(X) = \tau E(X)$; ($\tau > 1$), where τ is called the index of dispersion.

The mixed Poisson distributions are well-known flexible modeling methods to explain the

heterogeneity of the Poisson parameter as well as heavy right tail behaviors (Feller,1943; Shaked, 1980). The mixed Poisson distribution is a resultant distribution or unconditional distribution by assuming that the Poisson parameter is a random variable that has as a parameterized distribution P . The distribution P and its parameter vector Θ are called prior distribution and hyperparameter, respectively. Then, the resultant distribution of the random variable X can be expressed mathematically in the following form

$$f_X(x) = \int_0^\infty f_{X|\Lambda}(x|\lambda)f_\Lambda^P(\lambda)d\lambda, \quad (1)$$

where $X|\Lambda$ has a Poisson distribution with parameter λ as

$$f_{X|\Lambda}(x|\lambda) = \frac{e^{-\lambda}\lambda^x}{x!}, \quad x = 0, 1, 2, \dots, \lambda > 0, \quad (2)$$

Λ is the random variable of the Poisson parameter λ , and $f_\Lambda^P(\lambda)$ is the density function of the assumed continuous distribution P to the Poisson parameter λ . Hence, the random variable X has the same support of $X|\Lambda$ with parameter(s) of the prior distribution. Further, Lynch (1988) showed that the form of the mixing distribution has ascendancy over to the form of the resultant mixed distribution.

In literature, researchers assumed the standard lifetime distributions to model the Poisson parameter λ as a classical approach. Greenwood and Yule (1920) used the gamma distribution, and the resultant distribution is negative binomial (NBD). Johnson et al., (1992) assumed the exponential distribution to model the Poisson parameter, and the resultant distribution is geometric distribution (GD). Even though NBD and GD are computationally flexible pmfs, they are not befitting distributions for a higher value of τ and long right tail. In this context, researchers have assumed several modifications of the standard lifetime distributions for the Poisson parameter. They were modified to have more flexibility in their shapes and failure rate criteria than the standard lifetime distributions. Confluent Hypergeometric series, Gamma product ratio, Generalized gamma, Shifted gamma, Inverse gamma, and Modified Bessel of the 3rd kind are used by Bhattacharya (1967), Irwin (1975), Albrecht (1984), Ruohonen (1988), Willmot (1993), and Ong and Muthaloo (1995), respectively to model the Poisson parameter. The pmfs of such distributions are derived through the recursive formulas or Laplace transform technique, or by using the special mathematical functions. Hence, computing the probabilities of such distributions is complicated and they are limited in practice.

The Lindley distribution (LD) is one of the life time distributions introduced by Lindley (1958) having the density function

$$f_\Lambda(\lambda) = \frac{\theta^2}{1+\theta}(1+\lambda)e^{-\theta\lambda}, \quad \lambda > 0, \theta > 0, \quad (3)$$

where θ is the shape parameter, and Λ is the respective random variable. Equation (3) presents a two-component mixture of two different continuous distributions namely exponential (θ) and gamma ($2, \theta$) distributions with the mixing proportion, $p = \frac{\theta}{1+\theta}$. Sankaran (1970) introduced the one-parameter discrete Poisson-Lindley distribution (PLD) by combining the Poisson and LD. Its pmf is given as

$$f_X(x) = \frac{\theta^2(x+\theta+2)}{(\theta+1)^{x+3}}, \quad x = 0, 1, 2, \dots, \theta > 0. \quad (4)$$

Note that the pmf of the PLD is an explicit form. Then, obtaining its probabilities is computationally flexible. However, the PLD flexibility is limited to fit various types of the over-dispersed count data sets since it has only one parameter. Then, as an alternative to PLD, Bhati et al. (2015) have obtained the Generalized Poisson-Lindley distribution (GPLD), where the Poisson parameter is distributed to Two-parameter Lindley distribution (Shanker et al., 2013b); Wongrin

and Bodhisuwan (2016) introduced Poisson-generalized Lindley distribution (PGLD), which was obtained by mixing the Poisson distribution with the generalized Lindley distribution (Elbatal et al., 2013); Grine et al. (2017) have obtained the Quasi-Poisson distribution (PQLD) by modeling Poisson parameter to Quasi Lindley distribution (Shanker et al., 2013a). Table 1 summarizes the mixing proportions, mixing components, and parameters of the above continuous distributions that have been used to model the Poisson parameter. We can see that the mixing proportions of the Two-parameter Lindley and generalized Lindley distributions are incorporated with the scale parameter, θ of the mixing components. Further, the shape parameter of the mixing component gamma ($2, \theta$) is fixed with value 2 for the Two-parameter Lindley and the Quasi Lindley distributions. These settings of such mixing distributions may limit the flexibility of the above-mentioned Poisson mixtures to fit well for the various types of the right tail heaviness and τ for an over-dispersed count data (Tharshan and Wijekoon, 2020 a b).

Table 1: *Mixing proportions, mixing components, and parameters of some modified-Lindley distributions.*

Distribution	Mixing proportion	Mixing components	Parameters	
			shape	scale
Two-parameter Lindley	$\frac{\theta}{\theta + \alpha}$	exponential (θ) , gamma ($2, \theta$)	θ, α	
Generalized Lindley	$\frac{\theta}{1 + \theta}$	gamma (α, θ) , gamma (β, θ)	θ, α, β	
Quasi Lindley	$\frac{\alpha}{\alpha + 1}$	exponential (θ) , gamma ($2, \theta$)	θ	α

The main contribution of this paper is to propose an alternative mixed Poisson distribution for over-dispersed count data to address the above issues. It is obtained by mixing the Poisson distribution and the Modification of the Quasi Lindley distribution (MQLD) (Tharshan and Wijekoon, 2021). The density function of the MQLD(θ, α, δ) is given as

$$f_{\Lambda}(\lambda; \theta, \alpha, \delta) = \frac{\theta e^{-\theta \lambda}}{(\alpha^3 + 1)\Gamma(\delta)} \left(\Gamma(\delta) \alpha^3 + (\theta \lambda)^{\delta-1} \right); \lambda > 0, \theta > 0, \alpha^3 > -1, \delta > 0, \quad (5)$$

where α , and δ are shape parameters, θ is a scale parameter, and Λ is the respective random variable. Equation (5) presents the mixture of two non-identical distributions, exponential (θ) , and gamma (δ, θ) with the mixing proportion, $p = \frac{\alpha^3}{\alpha^3 + 1}$. We can clearly observe that its mixing proportion p does not incorporate with scale parameter, θ of the mixing components. Further, the shape parameter of the mixing component gamma distribution, δ is not fixed with a value. The authors have shown that these settings of the MQLD provide the capability to capture the various ranges of right tail heaviness measured by excess kurtosis (kurtosis -3), horizontal symmetry measured by skewness, and heterogeneity measured by Fano factor (variance-to-mean ratio) by setting its parameter values. Further, its density function can be either unimodal or bimodal.

The remaining part of this paper is organized as follows: In section 2, we introduce the PMQLD with its explicit forms of the probability mass and distribution functions. Its fundamental structural properties are discussed in section 3. The simulation of its random variables and parameter estimations are discussed in section 4. Finally, a simulation study is done to examine the performance of parameter estimation by using the maximum likelihood estimation method, and some real-world examples are taken to show the applicability of the proposed model by comparing it with some other existing Poisson mixtures, NBD, GD, PLD, GPLD, PQLD, PGLD.

2. FORMULATION OF THE NEW MIXED POISSON DISTRIBUTION

In this section, we introduce the new mixed Poisson distribution with its pmf and cumulative distribution function (cdf).

Let the random variable X represent the total counts of a specific experiment with mean λ . Then, the traditional distribution to calculate probabilities of such outcomes is the Poisson distribution. The PMQLD is obtained by mixing the Poisson and MQLD (Tharshan and Wijekoon, 2021) for over-dispersed count data. The following theorem gives the pmf of the PMQLD.

Theorem 1. Let $X|\Lambda$ is a random variable that follow the Poisson distribution with parameter λ , abbreviated as $X|\Lambda \sim \text{Poisson}(\lambda)$ and the Poisson parameter $\Lambda \sim \text{MQLD}(\theta, \alpha, \delta)$. Then, the pmf of the PMQLD is defined as

$$f_X(x) = \frac{\theta \left(\Gamma(\delta) \Gamma(x+1) \alpha^3 (1+\theta)^{\delta-1} + \theta^{\delta-1} \Gamma(x+\delta) \right)}{x! (\alpha^3 + 1) (1+\theta)^{x+\delta} \Gamma(\delta)}, x = 0, 1, 2, \dots, \theta > 0, \delta > 0, \alpha^3 > -1. \quad (6)$$

Proof. Since $X|\Lambda \sim \text{Poisson}(\lambda)$ and $\Lambda \sim \text{MQLD}(\theta, \alpha, \delta)$, the unconditional distribution of X can be obtained by substituting equations (2) and (5) in equation (1) as below

$$\begin{aligned} f(X) &= \int_0^\infty \frac{e^{-\lambda} \lambda^x}{x!} \frac{\theta e^{-\theta \lambda}}{(\alpha^3 + 1) \Gamma(\delta)} \left(\Gamma(\delta) \alpha^3 + (\theta \lambda)^{\delta-1} \right) d\lambda \\ &= \frac{\theta}{x! (\alpha^3 + 1) \Gamma(\delta)} \left(\Gamma(\delta) \alpha^3 \int_0^\infty e^{-\lambda(1+\theta)} \lambda^x d\lambda + \theta^{\delta-1} \int_0^\infty \lambda^{x+\delta-1} e^{-\lambda(1+\theta)} d\lambda \right) \\ &= \frac{\theta}{x! (\alpha^3 + 1) \Gamma(\delta)} \left(\frac{\Gamma(\delta) \alpha^3 \Gamma(x+1)}{(1+\theta)^{x+1}} + \frac{\theta^{\delta-1} \Gamma(x+\delta)}{(1+\theta)^{x+\delta}} \right) \\ &= \frac{\theta}{x! (\alpha^3 + 1) \Gamma(\delta) (1+\theta)^{x+\delta}} \left((1+\theta)^{\delta-1} \Gamma(\delta) \alpha^3 \Gamma(x+1) + \theta^{\delta-1} \Gamma(x+\delta) \right). \end{aligned}$$

■

Remarks:

1. Equation (6) presents a two-component mixture of $\text{GD}(\frac{\theta}{1+\theta})$ and $\text{NBD}(\delta, \frac{1}{1+\theta})$ with the mixing proportion $p = \frac{\alpha^3}{\alpha^3+1}$.
2. For $\alpha \rightarrow 0$, the PMQLD reduces to the $\text{NBD}(\delta, \frac{1}{1+\theta})$.
3. For $\alpha \rightarrow \infty$, the PMQLD reduces to the $\text{GD}(\frac{\theta}{1+\theta})$.

The right tail behaviors of the PMQLD for different values of θ, α , and δ are illustrated in Figure 1. For fixed α and δ , it is clear that the distribution's right tail approaches to zero at a faster rate when θ increases. For fixed θ and δ , and when α is increasing, the distribution's right tail approaches to zero at a slower rate when compared with the changes of θ . Further, for fixed θ and α , and when δ is increasing, the distribution captures more right tail. From Figure 2, we may note that the PMQLD may be a bimodal distribution when parameter value δ is very different (higher value) from the parameter values of θ and α .

The corresponding cumulative distribution function of PMQLD is given as

$$F_X(x) = \sum_{t=0}^x f(x)$$

$$= \frac{\delta(1+\theta)^{\delta-1}\Gamma(\delta)\alpha^3\Gamma(x+1)((1+\theta)^{x+1}-1) + \theta^\delta\Gamma(x+\delta+1)_2F_1(1, x+\delta+1; \delta+1; \frac{\theta}{1+\theta})}{(\alpha^3+1)\Gamma(\delta)x!\delta(1+\theta)^{x+\delta+1}} \quad (7)$$

$$, x = 0, 1, 2, \dots, \theta > 0, \delta > 0, \alpha^3 > -1,$$

where ${}_2F_1(c, d; r; w)$ is the Gaussian hypergeometric function defined as

$${}_2F_1(c, d; r; w) = \sum_{i=0}^{\infty} \frac{(c)_i(d)_i w^i}{(r)_i i!},$$

which is a special case of the generalized hypergeometric function given by the expression

$${}_aF_b(p_1, p_2, \dots, p_a; q_1, q_2, \dots, q_b; w) = \sum_{i=0}^{\infty} \frac{(p_1)_i \dots (p_a)_i w^i}{(q_1)_i \dots (q_b)_i i!},$$

and $(p)_i = \frac{\Gamma(p+i)}{\Gamma(p)} = p(p+1)\dots(p+i-1)$ is the Pochhammer symbol.

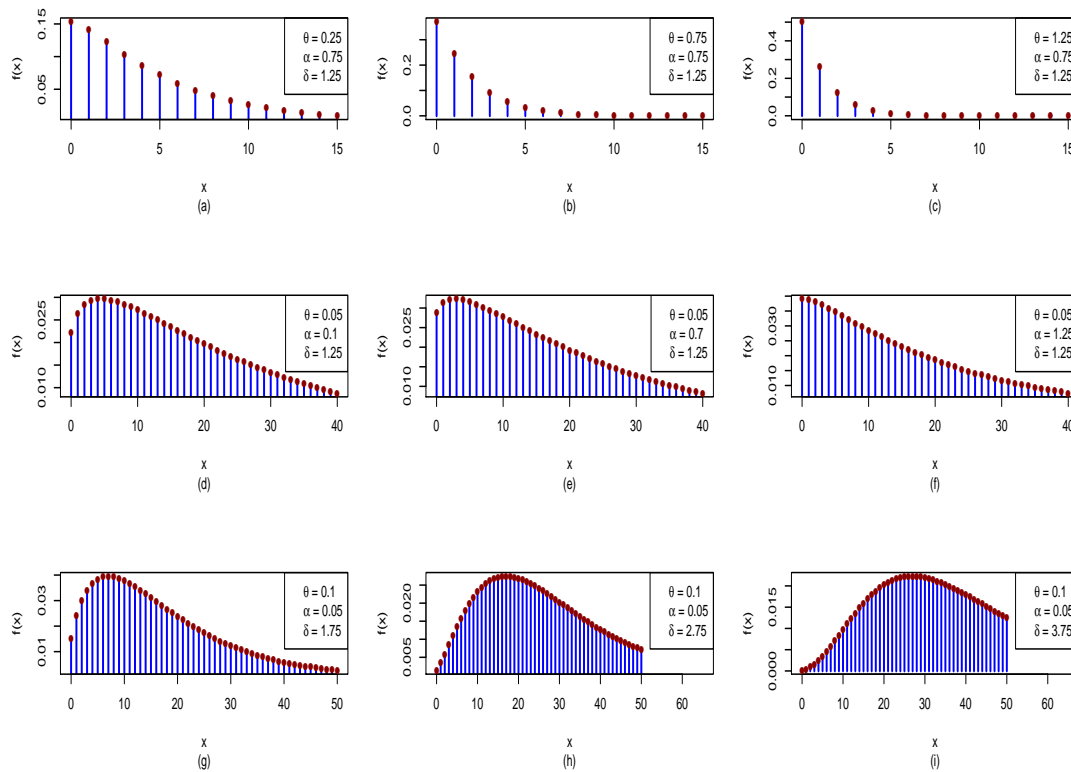


Figure 1: The probability mass function of the PMQLD at different parameter values of θ, α , and δ

3. STATISTICAL PROPERTIES OF PMQLD

In this section, we present some important statistical properties of the PMQLD such as the shape of the distribution, moments and related measures, probability and moment generating functions, and quantile function.

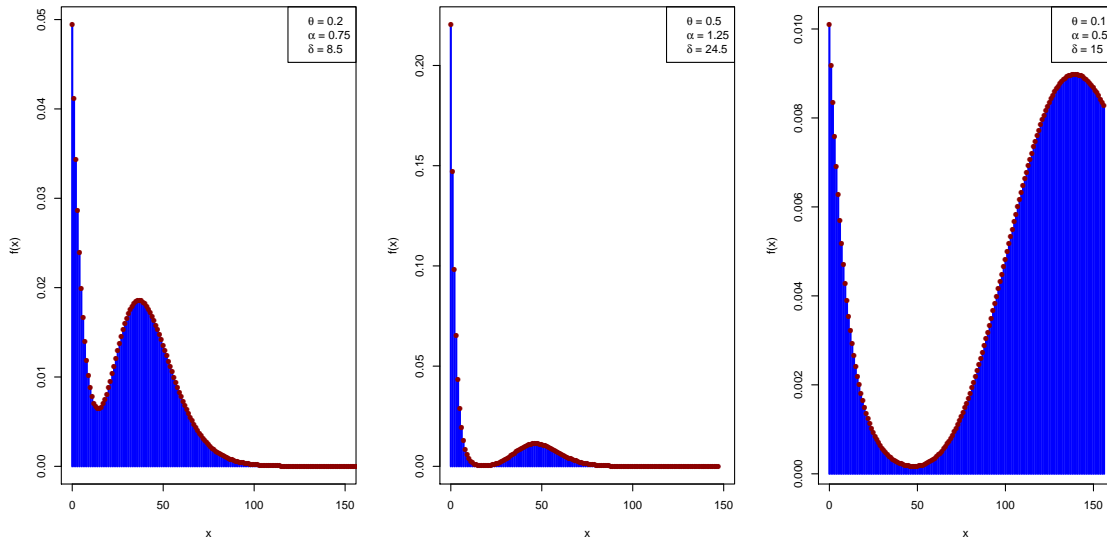


Figure 2: Some bimodal distributions of the PMQLD

3.1. Shape of the distribution

From (6) we can easily derive $f(0) = \frac{\theta((1+\theta)^{\delta-1}\alpha^3 + \theta^{\delta-1})}{(\alpha^3+1)(1+\theta)^\delta}$, and $\lim_{x \rightarrow \infty} f(x) = 0$.

The recurrence relation for probabilities is given by

$$\frac{f(x+1)}{f(x)} = \frac{A}{(x+1)(1+\theta)B}; \quad x = 0, 1, 2, \dots, \quad (8)$$

where $A = (1+\theta)^{\delta-1}\Gamma(\delta)\alpha^3\Gamma(x+2) + \theta^{\delta-1}(x+\delta)\Gamma(x+\delta)$, and

$$B = (1+\theta)^{\delta-1}\Gamma(\delta)\alpha^3\Gamma(x+1) + \theta^{\delta-1}\Gamma(x+\delta).$$

The PMQLD(θ, α, δ) has a log-concave probability mass function when

$$\begin{aligned} \Delta\eta(x) &= \frac{f(x+1)}{f(x)} - \frac{f(x+2)}{f(x+1)} > 0, \forall x \text{ (Gupta et al., 1997)} \\ \Rightarrow &\frac{(x+2)A^2}{(x+1)\left((1+\theta)^{\delta-1}\Gamma(\delta)\alpha^3\Gamma(x+3) + \theta^{\delta-1}\Gamma(x+\delta+2)\right)B} > 1. \end{aligned}$$

Under this condition, the distribution represents a unimodal distribution. Further, by using (8), it can be shown that

- (i) For $(1+\theta)^{\delta-1}\alpha^3 + \theta^{\delta-1}\delta < (1+\theta)((1+\theta)^{\delta-1}\alpha^3 + \theta^{\delta-1})$, equation (6) has unique mode at $X = 0$.
- (ii) Equation (6) has a unique mode at $X = x_0$, for

$$\frac{(1+\theta)^{\delta-1}\Gamma(\delta)\alpha^3\Gamma(x_0+2) + \theta^{\delta-1}(x_0+\delta)\Gamma(x_0+\delta)}{(x_0+1)(1+\theta)\left((1+\theta)^{\delta-1}\Gamma(\delta)\alpha^3\Gamma(x_0+1) + \theta^{\delta-1}\Gamma(x_0+\delta)\right)} < 1,$$

and

$$\frac{(1 + \theta)^{\delta-1}\Gamma(\delta)\alpha^3\Gamma(x_0) + \theta^{\delta-1}\Gamma(x_0 + \delta - 1)}{x_0(1 + \theta)\left((1 + \theta)^{\delta-1}\Gamma(\delta)\alpha^3\Gamma(x_0 + 1) + \theta^{\delta-1}\Gamma(x_0 + \delta)\right)} < 1.$$

(iii) Equation (6) has two modes at $X = x_0$ and $X = x_0 + 1$, for

$$\begin{aligned} & (1 + \theta)^{\delta-1}\Gamma(\delta)\alpha^3\Gamma(x_0 + 2) + \theta^{\delta-1}(x_0 + \delta)\Gamma(x_0 + \delta) \\ &= (x_0 + 1)(1 + \theta)\left((1 + \theta)^{\delta-1}\Gamma(\delta)\alpha^3\Gamma(x_0 + 1) + \theta^{\delta-1}\Gamma(x_0 + \delta)\right). \end{aligned}$$

The above facts are also shown in Figures 1 and 2 at different parameter settings.

Further, the PMQLD(θ, α, δ) has a log-convex probability mass function when $\Delta\eta(x) \leq 0$:

$$\Rightarrow \frac{(x + 2)A^2}{(x + 1)\left((1 + \theta)^{\delta-1}\Gamma(\delta)\alpha^3\Gamma(x + 3) + \theta^{\delta-1}\Gamma(x + \delta + 2)\right)B} \leq 1.$$

3.2. Survival and hazard rate functions

The survival/reliability function is associated with the probability of a system that will survive beyond a specified time. The survival function of the PMQLD is defined as

$$S(x) = 1 - F(x) = 1 - \frac{\beta_1 + \theta^\delta\Gamma(x + \delta + 1)_2F_1(1, x + \delta + 1; \delta + 1; \frac{\theta}{1+\theta})}{\beta_2} \quad (9)$$

where $\beta_1 = \delta(1 + \theta)^{\delta-1}\Gamma(\delta)\alpha^3\Gamma(x + 1)((1 + \theta)^{x+1} - 1)$ and $\beta_2 = (\alpha^3 + 1)\Gamma(\delta)x!\delta(1 + \theta)^{x+\delta+1}$. The hazard rate function (hrf) is the instantaneous failure rate. The hrf of the PMQLD is defined as

$$\begin{aligned} h(x) &= \lim_{\Delta x \rightarrow 0} \frac{P(x < X < x + \Delta x | X > x)}{\Delta x} \\ &= \frac{f(x)}{S(x)} = \frac{\delta\theta(1 + \theta)\left((1 + \theta)^{\delta-1}\Gamma(\delta)\alpha^3\Gamma(x + 1) + \theta^{\delta-1}\Gamma(x + \delta)\right)}{\beta_1 - (\beta_2 + \theta^\delta\Gamma(x + \delta + 1)_2F_1(1, x + \delta + 1; \delta + 1; \frac{\theta}{1+\theta}))}. \end{aligned} \quad (10)$$

Figure 3 provides an illustration of the possible shapes of the PMQLD's hazard rate function at different shape parameter values. According to these illustrations, it is clear that the proposed model has the capability to model the bathtub, monotonic increasing, and decreasing failure rate shapes.

3.3. Moments and related measures

The central tendency, horizontal symmetry, tail heaviness, and dispersion are important characteristics of a distribution. These characteristics can be studied by using the moments. The following theorem provides the r^{th} factorial moment of the PMQLD.

Theorem 2. Let $X \sim \text{PMQLD}(\theta, \alpha, \delta)$, then the r^{th} factorial moment of X is given as

$$\mu'_{(r)} = \frac{\Gamma(\delta)\Gamma(r + 1)\alpha^3 + \Gamma(\delta + r)}{(\alpha^3 + 1)\Gamma(\delta)\theta^r}. \quad (11)$$

Proof.

$$\mu'_{(r)} = E(\Pi_{i=0}^{r-1}(X - i))$$

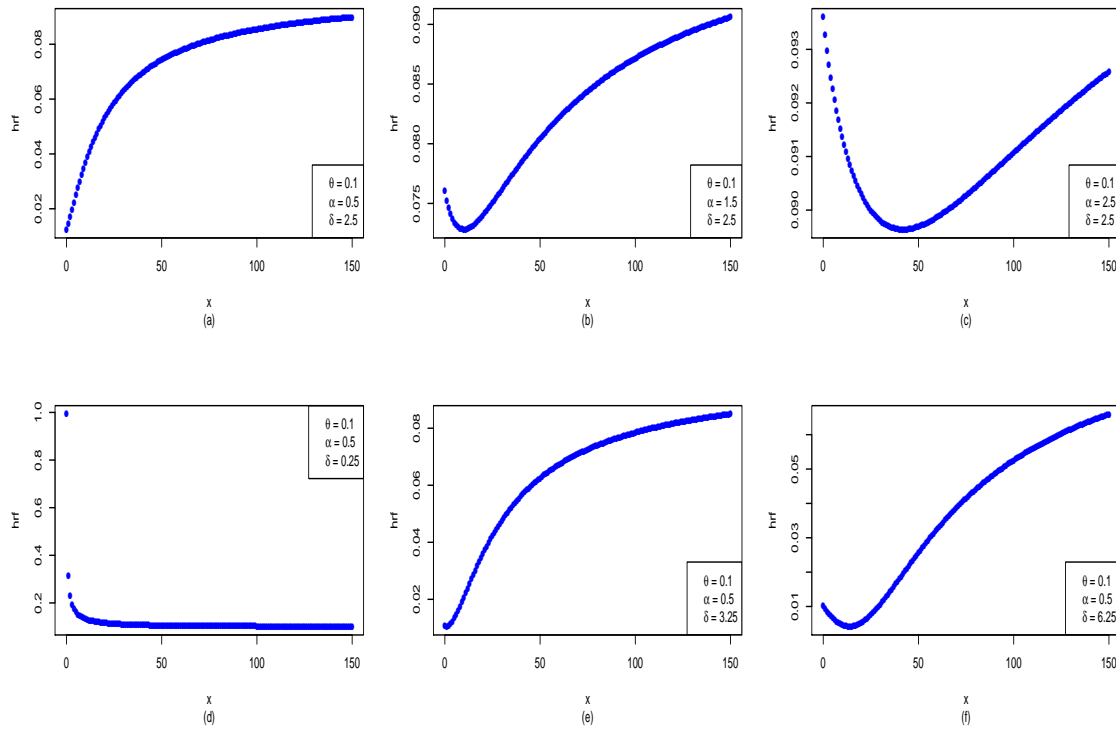


Figure 3: The hazard rate function at different values of α , and δ

$$\begin{aligned}
 &= \sum_{x=0}^{\infty} x^{(r)} \int_0^{\infty} \frac{e^{-\lambda} \lambda^x}{x!} \frac{\theta e^{-\theta \lambda}}{(\alpha^3 + 1)\Gamma(\delta)} \left(\Gamma(\delta) \alpha^3 + (\theta \lambda)^{\delta-1} \right) d\lambda \\
 &= \int_0^{\infty} \lambda^r \frac{\theta e^{-\theta \lambda}}{(\alpha^3 + 1)\Gamma(\delta)} \left(\Gamma(\delta) \alpha^3 + (\theta \lambda)^{\delta-1} \right) d\lambda \\
 &= \frac{\theta}{(\alpha^3 + 1)\Gamma(\delta)} \left(\frac{\Gamma(\delta) \alpha^3 \Gamma(r+1)}{\theta^{r+1}} + \frac{\Gamma(\delta+r)}{\theta^{r+1}} \right) \\
 &= \frac{\Gamma(\delta) \Gamma(r+1) \alpha^3 + \Gamma(\delta+r)}{(\alpha^3 + 1)\Gamma(\delta) \theta^r}.
 \end{aligned}$$

Then, the first four raw moments of X can be derived by the following relationship

$$\mu'_r = E(x^r) = \sum_{i=0}^r S(r,i) \mu'_{(i)} ; r = 1, 2, \dots,$$

where $S(r,i)$ is the Stirling numbers of the second kind, and it is defined as

$$S(r,i) = \frac{1}{i!} \sum_{j=0}^i (-1)^{i-j} \binom{i}{j} j^r, \quad 0 < i < r.$$

Let

$$\kappa_1 = \alpha^3 + \delta, \quad \kappa_2 = 2\alpha^3 + \delta(\delta + 1), \quad \kappa_3 = 6\alpha^3 + \delta(\delta + 1)(\delta + 2), \quad \kappa_4 = 24\alpha^3 + \delta(\delta + 1)(\delta + 2)(\delta + 3).$$

Then,

$$\mu'_1 = \frac{\kappa_1}{(\alpha^3 + 1)\theta} = \mu, \mu'_2 = \frac{\theta\kappa_1 + \kappa_2}{(\alpha^3 + 1)\theta^2}, \mu'_3 = \frac{\theta^2\kappa_1 + 3\theta\kappa_2 + \kappa_3}{(\alpha^3 + 1)\theta^3}, \mu'_4 = \frac{\theta^3\kappa_1 + 7\theta^2\kappa_2 + 6\theta\kappa_3 + \kappa_4}{(\alpha^3 + 1)\theta^4}.$$

Further, the r^{th} -order moments about the mean can be obtained by using the relationship between moments about the mean and moments about the origin, i.e.

$$\mu_r = E \left[(Y - \mu)^r \right] = \sum_{i=0}^r \binom{r}{i} (-1)^{r-i} \mu'_i \mu^{r-i}; \quad r = 1, 2, \dots$$

Therefore, the variance of X, σ^2 and index of dispersion, γ_1 are derived as

$$\sigma^2 = \mu_2 = \frac{\alpha^6(1 + \theta) + \alpha^3(2 + \theta + \delta(\theta + \delta - 1)) + \delta(\theta + 1)}{(\alpha^3 + 1)^2\theta^2} = \mu + \mu^2 \left(\frac{\alpha^3(\alpha^3 + 2 + \delta(\delta - 1)) + \delta}{(\alpha^3 + \delta)^2} \right),$$

and

$$\gamma_1 = \frac{\mu_2}{\mu^2} = 1 + \frac{\alpha^3(\alpha^3 + 2 + \delta(\delta - 1)) + \delta}{(\alpha^3 + 1)(\alpha^3 + \delta)\theta},$$

respectively. It is clear that the $\gamma_1 > 1$. Then, the PMQLD is an over-dispersed distribution. Since the mathematical expressions of μ_3 and μ_4 are very long, we present the graphical presentations of the skewness ($\gamma_2 = \frac{\mu_3}{(\mu_2)^{3/2}}$) and kurtosis ($\gamma_3 = \frac{\mu_4}{\mu_2^2}$) of the PMQLD in Figure 5. The surface plots in Figures 4, and 5 show some possible values of the index of dispersion, skewness, and kurtosis that can be accommodated by the PMQLD at different settings of the parameters. Hence, these plots indicate that the PMQLD (θ, α, δ) has the capability to accommodate various ranges of the index of dispersion, skewness, and kurtosis at different sets of parameters for over-dispersed count data.

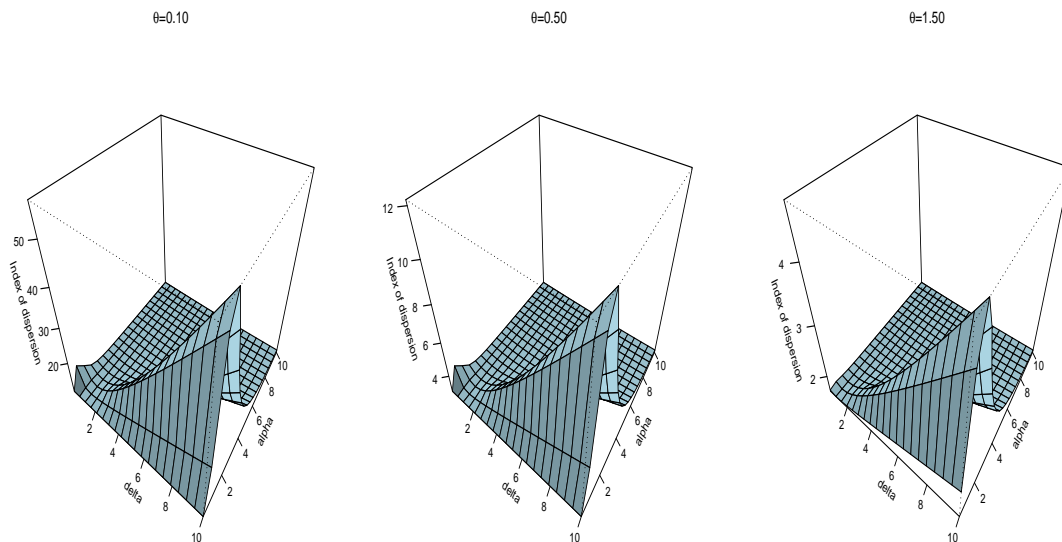


Figure 4: Surface plots for the index of dispersion at different values of θ, α , and δ

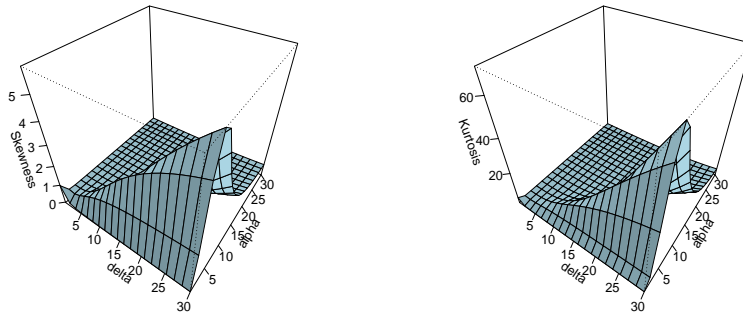


Figure 5: Surface plots for the skewness and kurtosis functions at different values of θ , and α

3.4. Probability and moment generating functions

The characteristics of a probability distribution are directly associated with its probability generating function (pgf) and the moment generating function (mgf). The following theorem provides the pgf of the PMQLD.

Theorem 3. The pgf, $G(t) = E(t^X)$, $X \sim \text{PMQLD}(\theta, \alpha, \delta)$ is given as

$$G(t) = \frac{\theta(\alpha^3(1-t+\theta)^{\delta-1} + \theta^{\delta-1})}{(\alpha^3 + 1)(1-t+\theta)^\delta}, t \in \mathbb{R}. \quad (12)$$

Proof.

$$\begin{aligned} G(t) &= E(t^X) \\ &= \sum_{x=0}^{\infty} t^x \int_0^{\infty} \frac{e^{-\lambda} \lambda^x}{x!} \frac{\theta e^{-\theta\lambda}}{(\alpha^3 + 1)\Gamma(\delta)} \left(\Gamma(\delta)\alpha^3 + (\theta\lambda)^{\delta-1} \right) d\lambda \\ &= \int_0^{\infty} e^{-\lambda(1-t)} \frac{\theta e^{-\theta\lambda}}{(\alpha^3 + 1)\Gamma(\delta)} \left(\Gamma(\delta)\alpha^3 + (\theta\lambda)^{\delta-1} \right) d\lambda \\ &= \frac{\theta}{(\alpha^3 + 1)\Gamma(\delta)} \left(\Gamma(\delta)\alpha^3 \int_0^{\infty} e^{-\lambda(1-t+\theta)} d\lambda + \theta^{\delta-1} \int_0^{\infty} e^{-\lambda(1-t+\theta)} \lambda^{\delta-1} d\lambda \right) \\ &= \frac{\theta(\alpha^3(1-t+\theta)^{\delta-1} + \theta^{\delta-1})}{(\alpha^3 + 1)(1-t+\theta)^\delta}. \end{aligned}$$

■

The mgf can be obtained effortlessly from pgf by using the relationship $G(e^t) = E(e^{tX}) = M_X(t)$, and given as

$$M_X(t) = \frac{\theta(\alpha^3(1-e^t+\theta)^{\delta-1} + \theta^{\delta-1})}{(\alpha^3 + 1)(1-e^t+\theta)^\delta}, t \in \mathbb{R}. \quad (13)$$

3.5. Quantile function

The quantile function is a useful function to estimate the quantiles. Let us define the quantiles for random variable $X \sim \text{PMQLD}(\theta, \alpha, \delta)$. The u^{th} quantile can be derived by solving $F(x_u) = u$ for $x_u, 0 < u < 1$. Then, the u^{th} quantile function of the PMQLD is given as

$$\beta_1(x_u) + \theta^\delta \Gamma(x_u + \delta + 1) {}_2F_1(1, x_u + \delta + 1; \delta + 1; \frac{\theta}{1+\theta}) - u\beta_2(x_u) = 0, \quad 0 < u < 1, \quad (14)$$

where $\beta_1(x_u) = \delta(1 + \theta)^{\delta-1}\Gamma(\delta)\alpha^3\Gamma(x_u + 1)((1 + \theta)^{x_u+1} - 1)$ and $\beta_2(x_u) = (\alpha^3 + 1)\Gamma(\delta)x_u!\delta(1 + \theta)^{x_u+\delta+1}$.

Since equation (14) is not a closed-form in x_u , the estimates of the quantiles can be evaluated by using any numerical method. Further, the first three quartiles can be calculated by substituting $u = 0.25, 0.50$, and 0.75 in equation (14) and solving the respective equations.

4. SIMULATION AND PARAMETER ESTIMATION

4.1. Simulation of the random variables

Here, we provide two different algorithms to simulate the random variables x_1, x_2, \dots, x_n from the PMQLD(θ, α, δ) with size n based on the inverse transform method.

The first algorithm is obtained by considering the mixing of the PMQLD. Since $X|\Lambda \sim \text{Poisson}(\lambda)$ and $\Lambda \sim \text{MQLD}(\theta, \alpha, \delta)$, the first algorithm is obtained as follows

Algorithm I:

- i Simulate the random variables, $u_i \sim \text{uniform}(0, 1)$; $i = 1, 2, \dots, n$.
- ii Solve the non-linear equation for λ_i : $\Gamma(\delta)(1 + \alpha^3(1 - e^{-\theta\lambda_i})) - \Gamma(\delta, \theta\lambda_i) - u_i(\alpha^3 + 1)\Gamma(\delta) = 0$ to simulate the random variables, $\lambda_i \sim \text{MQLD}(\theta, \alpha, \delta)$; $i = 1, 2, \dots, n$.
- iii Simulate x_i from Poisson (λ_i); $i = 1, 2, \dots, n$.

The second algorithm is obtained from the quantile function of PMQLD discussed in subsection 3.5, and the steps are as follows

Algorithm II:

- i Simulate the random variables, $u_i \sim \text{uniform}(0, 1)$; $i = 1, 2, \dots, n$.
- ii Solve the non-linear equation for $[x_{u_i}]$: $\beta_1(x_{u_i}) + \theta^\delta\Gamma(x_{u_i} + \delta + 1)_2F_1(1, x_{u_i} + \delta + 1; \delta + 1; \frac{\theta}{1+\theta}) - u_i\beta_2(x_{u_i}) = 0$, where $\beta_1(x_{u_i})$ and $\beta_2(x_{u_i})$ are defined as in section 3.6. $[\cdot]$ denotes the integer part.

4.2. Parameter estimation of PMQLD

In this subsection, we discuss the parameter estimation of the PMQLD by using the method of moment estimation and the maximum likelihood estimation method.

4.2.1 Method of moment estimation (MME)

Given a random samples x_1, x_2, \dots, x_n with size n from the PMQLD(θ, α, δ), the method of moment estimators of θ, α , and δ , abbreviated as $\hat{\theta}_{MME}, \hat{\alpha}_{MME}$, and $\hat{\delta}_{MME}$, can be evaluated by equating

the raw-moments, say μ'_r , to the sample moments, say $\frac{\sum_{i=1}^n x_i^r}{n}, r = 1, 2, 3$, i.e. we need to find the solutions of the following system of non-linear equations:

$$n\kappa_1 - (\alpha^3 + 1)\theta \sum_{i=1}^n x_i = 0; \quad n(\theta\kappa_1 + \kappa_2) - (\alpha^3 + 1)\theta^2 \sum_{i=1}^n x_i^2 = 0;$$

$$n(\theta^2\kappa_1 + 3\kappa_2 + \kappa_3) - (\alpha^3 + 1)\theta^3 \sum_{i=1}^n x_i^3 = 0,$$

where κ_1, κ_2 , and κ_3 are defined in subsection 3.3. It is clear that these equations are not a closed form. However, the solutions can be derived by using a numerical method.

4.2.2 Maximum likelihood estimation (MLE)

Given a random samples x_1, x_2, \dots, x_n with size n from the PMQLD(θ, α, δ), the likelihood function of the i^{th} sample value x_i is given as

$$L(\theta, \alpha, \delta | x) = \frac{\theta}{x_i!(\alpha^3 + 1)(1 + \theta)^{x_i + \delta} \Gamma(\delta)} \left(\Gamma(\delta) \Gamma(x_i + 1) \alpha^3 (1 + \theta)^{\delta - 1} + \theta^{\delta - 1} \Gamma(x_i + \delta) \right).$$

Then, the log-likelihood function is given as

$$\begin{aligned} \log(L(\theta, \alpha, \delta | x_i)) &= l(\theta, \alpha, \delta | x) \\ &= n \left(\log(\theta) - \log(\alpha^3 + 1) - \log(\Gamma(\delta)) \right) + \sum_{i=1}^n \log \left(\Gamma(\delta) \Gamma(x_i + 1) \alpha^3 (1 + \theta)^{\delta - 1} + \theta^{\delta - 1} \Gamma(x_i + \delta) \right) \\ &\quad - \log(x_i!) - (x_i + \delta) \log(1 + \theta). \end{aligned} \tag{15}$$

The score functions are

$$\begin{aligned} \frac{\partial l(\theta, \alpha, \delta | x)}{\partial \theta} &= \frac{n}{\theta} + \sum_{i=1}^n \frac{\Gamma(\delta) \Gamma(x_i + 1) \alpha^3 (\delta - 1) (1 + \theta)^{\delta - 2} + \Gamma(x_i + \delta) (\delta - 1) \theta^{\delta - 2}}{\Gamma(\delta) \Gamma(x_i + 1) \alpha^3 (1 + \theta)^{\delta - 1} + \theta^{\delta - 1} \Gamma(x_i + \delta)} - \sum_{i=1}^n \frac{x_i + \delta}{1 + \theta}, \\ \frac{\partial l(\theta, \alpha, \delta | x)}{\partial \alpha} &= \sum_{i=1}^n \frac{3\alpha^2 \Gamma(\delta) \Gamma(x_i + 1) (1 + \theta)^{\delta - 1}}{\Gamma(\delta) \Gamma(x_i + 1) \alpha^3 (1 + \theta)^{\delta - 1} + \theta^{\delta - 1} \Gamma(x_i + \delta)} - \frac{3n\alpha^2}{\alpha^3 + 1} \end{aligned}$$

and

$$\begin{aligned} \frac{\partial l(\theta, \alpha, \delta | x)}{\partial \delta} &= \sum_{i=1}^n \frac{\Gamma(x_i + 1) \alpha^3 (\Gamma(\delta) (1 + \theta)^{\delta - 1} \log(1 + \theta) + (1 + \theta)^{\delta - 1} \Gamma(\delta) \psi(\delta)) + \Gamma(x_i + \delta) \theta^{\delta - 1} (\log(\theta) + \psi(x_i + \delta))}{\Gamma(\delta) \Gamma(x_i + 1) \alpha^3 (1 + \theta)^{\delta - 1} + \theta^{\delta - 1} \Gamma(x_i + \delta)} \\ &\quad - n(\log(1 + \theta) + \psi(\delta)), \end{aligned}$$

where $\psi(a) = \frac{\partial}{\partial a} \log \Gamma(a) = \frac{\Gamma'(a)}{\Gamma(a)}$. By setting the score functions equal to zero, the maximum likelihood estimators of θ, α , and δ , abbreviated as $\hat{\theta}_{MLE}, \hat{\alpha}_{MLE}$, and $\hat{\delta}_{MLE}$ can be derived. These systems of non-linear equations can be solved by a numerical method. Here, the solutions of the parameter estimates will be obtained by using the *optim* function in the R package *stats*.

The asymptotic confidence intervals for the parameters θ, α , and δ are derived by the asymptotic theory. The estimators are asymptotic three-variate normal with mean (θ, α, δ) and the observed information matrix

$$I(\theta, \alpha, \delta) = \begin{pmatrix} -\frac{\partial^2 l(\theta, \alpha, \delta | x)}{\partial \theta^2} & -\frac{\partial^2 l(\theta, \alpha, \delta | x)}{\partial \theta \partial \alpha} & -\frac{\partial^2 l(\theta, \alpha, \delta | x)}{\partial \theta \partial \delta} \\ -\frac{\partial^2 l(\theta, \alpha, \delta | x)}{\partial \alpha \partial \theta} & -\frac{\partial^2 l(\theta, \alpha, \delta | x)}{\partial \alpha^2} & -\frac{\partial^2 l(\theta, \alpha, \delta | x)}{\partial \alpha \partial \delta} \\ -\frac{\partial^2 l(\theta, \alpha, \delta | x)}{\partial \delta \partial \theta} & -\frac{\partial^2 l(\theta, \alpha, \delta | x)}{\partial \delta \partial \alpha} & -\frac{\partial^2 l(\theta, \alpha, \delta | x)}{\partial \delta^2} \end{pmatrix}$$

at $\theta = \hat{\theta}_{MLE}, \alpha = \hat{\alpha}_{MLE}$, and $\delta = \hat{\delta}_{MLE}$, i.e. $(\hat{\theta}_{MLE}, \hat{\alpha}_{MLE}, \hat{\delta}_{MLE}) \sim N_3((\theta, \alpha, \delta), I^{-1}(\theta, \alpha, \delta))$. The second order partial derivatives of the log-likelihood function are given in Appendix.

Therefore, a $(1 - a)100\%$ confidence interval for the parameters θ, α , and δ are given by

$$\theta_{MLE} \pm z_{a/2} \sqrt{Var(\hat{\theta}_{MLE})}, \quad \hat{\alpha}_{MLE} \pm z_{a/2} \sqrt{Var(\hat{\alpha}_{MLE})}, \quad \hat{\delta}_{MLE} \pm z_{a/2} \sqrt{Var(\hat{\delta}_{MLE})},$$

wherein, the $Var(\hat{\theta}_{MLE}), Var(\hat{\alpha}_{MLE})$, and $Var(\hat{\delta}_{MLE})$ are the variance of $\hat{\theta}_{MLE}, \hat{\alpha}_{MLE}$, and $\hat{\delta}_{MLE}$, respectively, and can be derived by diagonal elements of $I^{-1}(\theta, \alpha, \delta)$ and $z_{a/2}$ is the critical value at a level of significance.

5. MONTE CARLO SIMULATION STUDY AND REAL-WORLD APPLICATION

This section is devoted to discuss the simulation study and the applicability of PMQLD.

5.1. Monte Carlo simulation study

Here, we examine the accuracy of the MLE method in the unknown parameter estimation of the PMQLD with respect to sample size n . The second algorithm given in subsection 4.1 is used to simulate the random variables from the PMQLD. The sample sizes are taken as 60, 100, 200, and 300, and the simulation study is repeated 1000 times. The study is designed as follows

- (i) Simulate 1000 samples of size n .
- (ii) Compute the maximum likelihood estimates for the 1000 samples, say $(\hat{\theta}_i, \hat{\alpha}_i, \hat{\delta}_i), i = 1, 2, \dots, 1000$.
- (iii) Compute the average MLEs, biases, and mean square errors (MSEs) by using the following equations

$$\hat{s}(n) = \frac{1}{1000} \sum_{i=1}^{1000} \hat{s}_i, \quad bias_s(n) = \frac{1}{1000} \sum_{i=1}^{1000} (\hat{s}_i - s), \quad \text{and} \quad MSE_s(n) = \frac{1}{1000} \sum_{i=1}^{1000} (\hat{s}_i - s)^2,$$

for $s = \theta, \alpha, \delta$, and $n = 60, 100, 200, 300$.

Tables 2 to 5 represent the average MLEs, biases, and MSEs (in parentheses) of θ, α , and δ for different values of θ, α , and δ which are $\theta = 0.1, 0.3; \alpha = 0.25, 0.50, 0.75$; and $\delta = 2.50, 3.50, 4.50$. Note that the biases and MSEs decrease as n increases for all parameters. Then, MLE method verifies the asymptotic property for all parameter estimates, and the parameters θ, α , and δ are over estimated. Further, while the estimation of θ is good for small value of θ , the estimation of α does not show a good estimation for small value of α based on average biases and MSEs. However, there is no particular pattern for estimation of δ .

Table 2: Performance of MLE method for the PMQLD($\theta = 0.10, \alpha = 0.50, \delta$)

	$n = 60$		$n = 100$		$n = 200$		$n = 300$	
	MLE	Bias(MSE)	MLE	Bias(MSE)	MLE	Bias(MSE)	MLE	Bias(MSE)
$\delta = 2.50$								
θ	0.1151	0.0152(0.0014)	0.1086	0.0086(0.0007)	0.1067	0.0067(0.0002)	0.1009	0.0009(0.0001)
α	0.7519	0.2519(0.0691)	0.7482	0.2482(0.0648)	0.7290	0.2290(0.0557)	0.7195	0.2195(0.0494)
δ	3.0685	0.5685(1.0107)	3.0545	0.5545 (0.9155)	2.8466	0.3466(0.3078)	2.8358	0.3358(0.2186)
$\delta = 3.50$								
θ	0.1101	0.0101(0.0010)	0.1051	0.0051(0.0006)	0.1044	0.0044(0.0002)	0.1029	0.0029(0.0001)
α	0.6733	0.1733(0.0348)	0.6662	0.1662(0.0317)	0.6684	0.1684(0.0300)	0.6509	0.1509(0.0259)
δ	3.8991	0.3991(0.9110)	3.8494	0.3494(0.8928)	3.6791	0.1791(0.2898)	3.6010	0.1010(0.0887)
$\delta = 4.50$								
θ	0.1087	0.0087(0.0009)	0.1054	0.0054(0.0006)	0.1037	0.0037(0.0002)	0.1029	0.0021(0.0001)
α	0.6299	0.1299(0.0213)	0.6268	0.1268(0.0191)	0.6217	0.1217(0.0161)	0.6192	0.1192(0.0156)
δ	4.8664	0.3664(1.3188)	4.7506	0.2506(1.1957)	4.6354	0.1354(0.3871)	4.5805	0.0805(0.0122)

Table 3: Performance of MLE method for PMQLD($\theta = 0.30, \alpha = 0.50, \delta$)

	$n = 60$		$n = 100$		$n = 200$		$n = 300$	
	MLE	Bias(MSE)	MLE	Bias(MSE)	MLE	Bias(MSE)	MLE	Bias(MSE)
$\delta = 2.50$								
θ	0.3791	0.0790 (0.0242)	0.3635	0.0635(0.0215)	0.3378	0.0378 (0.0075)	0.3367	0.0367(0.0039)
α	0.8392	0.3392 (0.1199)	0.8243	0.3243(0.1109)	0.7956	0.2956 (0.0933)	0.7503	0.2503(0.0853)
δ	3.6229	1.1229(3.5560)	3.4672	0.9672(2.9115)	3.1876	0.6876(1.2228)	3.1509	0.6509 (0.7488)
$\delta = 3.50$								
θ	0.3839	0.0839 (0.0245)	0.3710	0.0710(0.0216)	0.3275	0.0275(0.0042)	0.3207	0.0207(0.0018)
α	0.7493	0.2493 (0.0698)	0.7215	0.2215(0.0543)	0.7170	0.2170(0.0487)	0.6983	0.1983(0.0457)
δ	4.3284	0.8284(2.5256)	4.1190	0.6190(1.9316)	3.7680	0.2680(0.4910)	3.7393	0.2393(0.2547)
$\delta = 4.50$								
θ	0.3638	0.0638 (0.0210)	0.3484	0.0484(0.0118)	0.3143	0.0143(0.0033)	0.3117	0.0117(0.0016)
α	0.6784	0.1784 (0.0373)	0.6703	0.1703(0.0330)	0.6658	0.1658(0.0299)	0.6578	0.1578(0.0277)
δ	5.1958	0.6958(3.0589)	4.9240	0.4240(2.0855)	4.6154	0.1154(0.6430)	4.6713	0.1713(0.2667)

Table 4: Performance of MLE method for PMQLD($\theta = 0.10, \alpha, \delta = 2.50$)

	$n = 60$		$n = 100$		$n = 200$		$n = 300$	
	MLE	Bias(MSE)	MLE	Bias(MSE)	MLE	Bias(MSE)	MLE	Bias(MSE)
$\alpha = 0.25$								
θ	0.1128	0.0128(0.0014)	0.1079	0.0079(0.0007)	0.1080	0.0080(0.0002)	0.1027	0.0027 (0.0001)
α	0.7109	0.4609(0.2184)	0.7034	0.4534(0.2088)	0.6957	0.4457(0.2000)	0.6804	0.4304 (0.1888)
δ	3.0685	0.5685(1.0447)	3.0085	0.5085(0.7195)	2.9490	0.4490(0.3138)	2.8473	0.3473 (0.1865)
$\alpha = 0.75$								
θ	0.1351	0.0351(0.0065)	0.1217	0.0217(0.0017)	0.1203	0.0203(0.0023)	0.1156	0.0156(0.0004)
α	0.8487	0.0987(0.0167)	0.8414	0.0914(0.0135)	0.8318	0.0818(0.0095)	0.8190	0.0690(0.0081)
δ	3.1905	0.6905(2.0102)	3.1765	0.6765(1.4733)	3.0104	0.5104(0.7818)	2.8781	0.3781(0.3592)

Table 5: Performance of MLE method for PMQLD($\theta = 0.30, \alpha, \delta = 2.50$)

	$n = 60$		$n = 100$		$n = 200$		$n = 300$	
	MLE	Bias(MSE)	MLE	Bias(MSE)	MLE	Bias(MSE)	MLE	Bias(MSE)
$\alpha = 0.25$								
θ	0.3998	0.0998(0.0329)	0.3805	0.0805(0.0240)	0.3482	0.0482(0.0060)	0.3336	0.0336(0.0030)
α	0.7823	0.5323(0.2928)	0.7795	0.5295(0.2873)	0.7611	0.5111(0.2636)	0.7437	0.4937(0.2508)
δ	3.5545	1.0545(2.7164)	3.4774	0.9774(2.2678)	3.1584	0.6584(0.7994)	3.0583	0.5583(0.5396)
$\alpha = 0.75$								
θ	0.3773	0.0773(0.0621)	0.3566	0.0566(0.0506)	0.3275	0.0275(0.0267)	0.3097	0.0097(0.0225)
α	0.8962	0.1462(0.0280)	0.8889	0.1389(0.0221)	0.8693	0.1193(0.0186)	0.8475	0.0975(0.0175)
δ	2.9598	0.4598(4.7991)	2.8278	0.3278(4.4320)	2.6089	0.1089(2.7618)	2.5723	0.0723(2.4811)

5.2. Real-world applications

In this subsection, we discuss the real-world applications of the proposed mixed Poisson distribution. Two data sets are considered to illustrate whether the proposed distribution is well fitted compared to some other existing competing Poisson mixtures. The best-fitted distribution was selected based on the negative log-likelihood ($-2\log L$), Akaike Information Criterion (AIC), and chi-square goodness of fit statistic. The unknown parameters of the models are estimated by using the MLE method. Tables 6 and 7 summarize all these statistical measures for each data set, and the standard errors of the parameter estimates are reported in parentheses.

The first data set contains the epileptic seizure counts (Chakraborty, 2010). The sample index dispersion (τ) of this data set is 1.867. Since τ value is greater than one, the distribution of

this data set is clearly over-dispersed. Also, the skewness and excess kurtosis for this example are 1.239 and 1.680, respectively, which show that the distribution of the data set is positively skewed and leptokurtic. This data set was used to fit the PMQLD, GD, NBD, PLD, GPLD, PQLD, and PGLD. Table 6 presents the estimates of the parameters of distributions and the goodness of fit test. Of all eight distributions, the PMQLD performs well based on the smallest AIC value of 1191.83 and the smallest chi-square value (χ^2) of 2.93 (p-value=0.71).

The second data set represents the number of roots produced by 270 micro-propagated shoots of the columnar apple cultivar Trajan (Ridout et al., 1998). This is a bimodal data set for which the sample index dispersion, skewness, and excess kurtosis are 3.077, 0.182, and -1.056, respectively. These values indicate that the distribution of the data set is extremely over-dispersed, mild positively skewed, and platykurtic. This data set was also used to fit the same distributions that we used for the first example. Table 7 summarizes the results of parameter estimations and the goodness of fit test. The results show that the PMQLD having AIC=1350.20, $\chi^2 = 11.75$, p-value=0.47 outperforms clearly than other distributions.

Figure 6 illustrates how the expected values of the proposed distribution adhere with the observed value for the data sets. We can see that the observed values of the first and second data sets are very close to the expected values of the PMQLD, and the observed values of the third data set are very close to the expected values of the ZMPQLD.

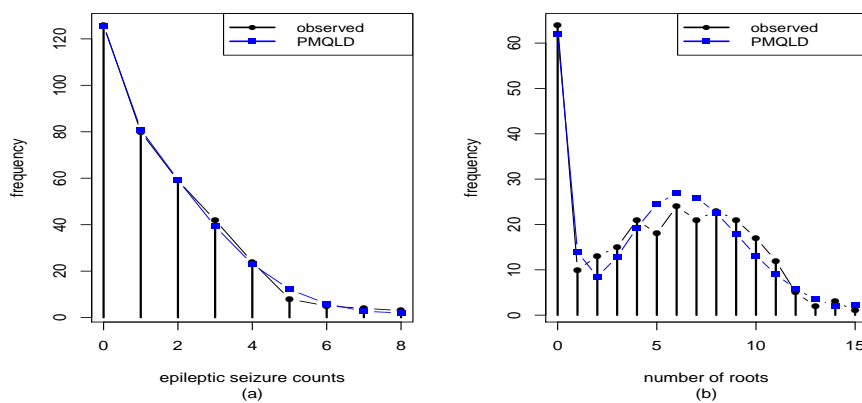


Figure 6: Performance of PMQLD for the real-data sets

Table 6. Epileptic seizure counts

Counts	Observed	Expected						
		GD	NBD	PLD	GPLD	PQLD	PGLD	PMQLD
0	126	137.95	120.22	128.72	121.93	121.82	122.85	125.65
1	80	83.73	93.00	87.14	90.92	90.95	90.08	80.98
2	59	50.82	59.18	55.26	58.72	58.76	57.85	59.30
3	42	30.85	34.94	33.63	35.20	35.23	35.20	39.25
4	24	18.72	19.84	19.89	20.16	20.17	20.53	22.99
5	8	11.37	10.99	11.52	11.20	11.20	11.54	12.17
6	5	6.90	5.98	6.57	6.08	6.08	6.27	5.94
7	4	4.19	3.22	3.70	3.25	3.25	3.31	2.72
8	3	6.47	3.63	4.57	3.54	3.54	3.37	2.00
Total	351	351	351	351	351	351	351	351
		$\hat{\theta} = 0.65$ (0.04)	$\hat{\beta} = 1.00$ (0.19)	$\hat{\theta} = 0.97$ (0.05)	$\hat{\theta} = 1.11$ (0.13)	$\hat{\theta} = 1.12$ (0.13)	$\hat{\theta} = 1.57$ (0.66)	$\hat{\theta} = 2.70$ (1.26)
MLE			$\hat{\alpha} = 1.55$ (0.28)		$\hat{\alpha} = 2.76$ (2.76)	$\hat{\alpha} = 0.38$ (0.33)	$\hat{\alpha} = 1.49$ (0.57)	$\hat{\alpha} = 0.82$ (0.07)
							$\hat{\beta} = 3.89$ (2.38)	$\hat{\delta} = 5.89$ (2.83)
χ^2		11.42	5.67	5.84	4.85	4.86	4.66	2.93
p-value		0.12	0.46	0.56	0.56	0.56	0.46	0.71
$-2\log L$		1196.79	1189.88	1190.36	1188.96	1188.96	1188.54	1185.83
AIC		1198.79	1193.88	1192.36	1192.96	1192.96	1194.54	1191.83

Table 7. Number of roots

Counts	Observed	Expected						
		GD	NBD	PLD	GPLD	PQLD	PGLD	PMQLD
0	64	44.62	36.87	31.09	35.46	35.45	82.81	61.93
1	10	37.25	36.05	32.94	34.00	33.99	17.81	13.92
2	13	31.09	32.16	31.79	31.19	31.19	15.31	8.47
3	15	25.95	27.77	29.06	27.78	27.77	16.46	12.85
4	21	21.66	23.58	25.63	24.20	24.20	17.53	19.30
5	18	18.08	19.83	22.04	20.74	20.74	17.70	24.53
6	24	15.09	16.56	18.60	17.55	17.55	16.95	26.85
7	21	12.60	13.76	15.48	14.69	14.69	15.53	25.94
8	23	10.52	11.39	12.73	12.20	12.20	13.70	22.55
9	21	8.78	9.40	10.37	10.05	10.05	11.72	17.90
10	17	7.33	7.74	8.39	8.23	8.24	9.76	13.13
11	12	6.12	6.37	6.74	6.71	6.71	7.96	8.99
12	5	5.11	5.23	5.38	5.44	5.45	6.36	5.78
13	2	4.26	4.28	4.27	4.40	4.40	5.01	3.52
14	3	3.56	3.51	3.38	3.54	3.54	3.88	2.03
≥ 15	1	17.98	15.50	12.11	13.82	13.83	11.51	2.31
Total	270	270	270	270	270	270	270	270
		$\hat{\theta} = 0.12$ (0.01)	$\hat{\beta} = 0.24$ (0.03)	$\hat{\theta} = 0.35$ (0.02)	$\hat{\theta} = 0.37$ (0.03)	$\hat{\theta} = 0.32$ (0.03)	$\hat{\theta} = 0.59$ (0.08)	$\hat{\theta} = 4.23$ (1.36)
MLE			$\hat{\alpha} = 1.21$ (0.16)		$\hat{\alpha} = 0.47$ (0.26)	$\hat{\alpha} = 0.68$ (0.27)	$\hat{\alpha} = 0.22$ (0.12)	$\hat{\alpha} = 0.73$ (0.04)
							$\hat{\beta} = 4.25$ (0.66)	$\hat{\delta} = 29.34$ (9.28)
χ^2		121.92	120.76	117.44	110.58	110.58	46.72	11.74
p-value		0.00	0.00	0.00	0.00	0.00	0.00	0.466
$-2\log L$		1464.90	1462.63	1454.10	1451.45	1451.45	1384.21	1344.20
AIC		1466.90	1466.63	1456.10	1455.45	1455.45	1390.21	1350.20

6. CONCLUSION

This paper proposes an alternative mixed Poisson distribution to model the over-dispersed count data. Explicit expressions of the pmf, hazard rate function, moments, mean, variance, skewness, and kurtosis were derived for the proposed distribution. Its pmf possesses to be either unimodal or bimodal, and hazard rate function presents monotonic increasing, decreasing, and bathtub shapes. The kurtosis and the variance-to-mean ratio functions of the new distribution indicate that

the distribution can capture various ranges of right tail weights as well as the index of dispersions. Further, its structural properties show that the new distribution is much more flexible than its predecessors, negative binomial, geometric, and Poisson-Lindley distributions. The maximum likelihood method was employed to estimate the parameters of the distribution, and the observed information matrix has also been derived. The proposed distribution and some other competing Poisson mixtures have been fitted to two real-world data sets. The results show that the proposed distribution could provide a better fit than a set of common Poisson mixtures considered in these applications.

Acknowledgement

We thank the Postgraduate Institute of Science, University of Peradeniya, Sri Lanka for providing all facilities to do this research.

REFERENCES

- [1] Albrecht, P. (1984). Laplace Transforms, Mellin Transforms and Mixed Poisson Processes. *Scandinavian Actuarial Journal*, 11: 58-64. <https://doi.org/10.1080/03461238.1984.10413753>
- [2] Bhati, D., Sastry, D. V. S., and Qadri, P. Z. (2015). A New Generalized Poisson Lindley Distribution, applications and Properties. *Austrian Journal of Statistics*, 44: 35-51. <https://doi.org/10.17713/ajs.v44i4.54>
- [3] Bhattacharya, S. K. (1967). A Result in Accident Proneness. *Biometrika*, 54: 324-325. <https://doi.org/10.1093/biomet/54.1-2.324>
- [4] Cameron, A. C. and Trivedi, P. K. *Regression Analysis of Count Data*, (2nd Ed.) Cambridge University Press, New York, USA, 2013. <https://doi.org/10.1017/CBO9781139013567>
- [5] Chakraborty, S. (2010). On Some Distributional Properties of the Family of Weighted Generalized Poisson Distribution. *Communications in Statistics - Theory and Methods*, 39: 2767-2788. <https://doi.org/10.1080/03610920903129141>
- [6] Elbatal, I., Merovci, F., and Elgarhy, M. (2013). A new generalized Lindley distribution, *Mathematical Theory and Modeling*, 3: 30-47.
- [7] Feller, W. (1943). On a Generalized Class of Contagious Distributions. *Annals of Mathematical Statistics*, 14: 389-400. <https://www.jstor.org/stable/2235926>
- [8] Greenwood, M. and Yule, G. U. (1920). An inquiry into the nature of frequency distributions representative of multiple happenings with particular reference to the occurrence of multiple attacks of disease or of repeated accidents, *Journal of the Royal Statistical Society*, 83: 255-279. <https://www.jstor.org/stable/2341080>
- [9] Grine, R. and Zeghdoudi, H. (2017). On Poisson quasi-Lindley distribution and its applications. *J. of Modern Applied Statistical Methods*, 16: 403-417.
- [10] Irwin, J. (1975). The Generalized Waring Distribution Parts I, II, III. *Journal of the Royal Statistical Society A*, 138: 18-31 (Part I), 204-227 (Part II), 374-384 (Part III).
- [11] Johnson, N. L., Kotz, S., and Kemp, A. W. *Univariate Discrete Distributions*, (2nd Ed.) John Wiley and Sons, New York, USA, 1992.
- [12] Lindley, D. V. (1958). Fiducial Distributions and Bayes' Theorem. *Journal of the Royal Statistical Society*, 20: 102-107. <https://www.jstor.org/stable/2983909>
- [13] Lynch, J. (1988). Mixtures, Generalized Convexity and Balayages, *Scandinavian Journal of Statistics*, 15: 203-210.
- [14] McCullagh, P. and Nelder, J. *Generalized Linear Models*, (2nd Ed.) Chapman and Hall, New York, USA, 1989.
- [15] Ong, S.H. and Muthaloo, S. (1995). A Class of Discrete Distributions Suited to Fitting Very Long Tailed Data. *Communication in Statistics-Simulation and Computation*, 24: 929-945. <https://doi.org/10.1080/03610919508813285>
- [16] Ridout, M., Demktrio, C. G. B., and Hinde, J. (1998). Models for count data with many zeros, Invited paper presented at the Nineteenth International Biometric Conference, Capetown, South Africa.

- [17] Ruohonen, M. (1988). A Model for the Claim Number Process. *ASTIN Bulletin*, 18: 57-68. <https://doi.org/10.2143/AST.18.1.2014960>
- [18] Sankaran, M. (1970). The discrete Poisson-Lindley distribution, *Biometrics*, 26: 145-149. <https://www.jstor.org/stable/2529053>
- [19] Shaked, M. (1980). On Mixtures from Exponential Families, *Journal of the Royal Statistical Society B*, 42: 192-198. <https://doi.org/10.1111/j.2517-6161.1980.tb01118.x>
- [20] Shanker, R. and Mishra, A. (2013a). A Quasi Lindley Distribution. *African Journal of Mathematics and Computer Science Research*, 6: 64-71.
- [21] Shanker, R., Sharma, S., and Shanker, R. (2013b). A Two-Parameter Lindley Distribution for Modeling Waiting and Survival Times Data. *Applied Mathematics*, 4: 363-368.
- [22] Tharshan, R. and Wijekoon, P. (2020a). Location Based Generalized Akash Distribution: Properties and Applications, *Open Journal of Statistics*, 10: 163-187.
- [23] Tharshan, R. and Wijekoon, P. (2020b). A comparison study on a new five-parameter generalized Lindley distribution with its sub-models. *Statistics in Transition new Series*, 21: 89-117. <https://doi.org/10.21307/stattrans-2020-015>
- [24] Tharshan, R. and Wijekoon, P. (2021). A modification of the Quasi Lindley distribution. *Open Journal of Statistics*, 11: 369-392.
- [25] Willmot, G. E. (1993). On Recursive Evaluation of Mixed Poisson Probabilities and Related Quantities, *Scandinavian Actuarial Journal*, 18: 114-133.
- [26] Wongrin, W. and Bodhisuwan, W. (2016). The Poisson-generalised Lindley distribution and its applications, *Songklanarin J.Sci. Technol*, 38: 645-66.

Appendix: Elements of the observed information matrix, $I(\theta, \alpha, \delta)$ defined in subsection 4.2.1:

Let us define $T_1, T_2, T_3, T_4, T_5, T_6, T_7, T_8, T_9, T_{10}, T_{11}, T_{12}, T_{13}$ and T_{14} as follows

$$T_1 = \Gamma(\delta)\Gamma(x_i + 1)\alpha^3(\delta - 1)(1 + \theta)^{\delta-2} + \Gamma(x_i + \delta)(\delta - 1)\theta^{\delta-2},$$

$$T_2 = \Gamma(\delta)\Gamma(x_i + 1)\alpha^3(1 + \theta)^{\delta-1} + \theta^{\delta-1}\Gamma(x_i + \delta),$$

$$T_3 = 3\alpha^2\Gamma(\delta)\Gamma(x_i + 1)(1 + \theta)^{\delta-1},$$

$$T_4 = \Gamma(x_i + 1)\alpha^3(\Gamma(\delta)(1 + \theta)^{\delta-1}\log(1 + \theta) + (1 + \theta)^{\delta-1}\Gamma(\delta)\psi(\delta)) + \Gamma(x_i + \delta)\theta^{\delta-1}(\log(\theta) + \psi(x_i + \delta)),$$

$$T_5 = \Gamma(\delta)\Gamma(x_i + 1)\alpha^3(1 + \theta)^{\delta-3} + \Gamma(x_i + \delta)\theta^{\delta-3},$$

$$T_6 = \Gamma(\delta)\Gamma(x_i + 1)\alpha^3(1 + \theta)^{\delta-2} + \Gamma(x_i + \delta)\theta^{\delta-2},$$

$$T_7 = \log(1 + \theta)(\Gamma(\delta)(1 + \theta)^{\delta-1}\log(1 + \theta) + (1 + \theta)^{\delta-1}\Gamma(\delta)\psi(\delta))$$

$$T_8 = (1 + \theta)^{\delta-1}(\Gamma(\delta)\psi_1(\delta) + (\psi(\delta))^2\Gamma(\delta)) + \Gamma(\delta)\psi(\delta)(1 + \theta)^{\delta-1}\log(1 + \theta),$$

$$T_9 = \Gamma(x_i + \delta)\theta^{\delta-1}\log(\theta) + \theta^{\delta-1}\Gamma(x_i + \delta)\psi(x_i + \delta),$$

$$T_{10} = \Gamma(x_i + \delta)\theta^{\delta-1}\psi_1(x_i + \delta),$$

$$T_{11} = \Gamma(x_i + 1)\alpha^3(\Gamma(\delta)(1 + \theta)^{\delta-1}\log(1 + \theta) + (1 + \theta)^{\delta-1}\Gamma(\delta)\psi(\delta)),$$

$$T_{12} = \theta^{\delta-1}\Gamma(x_i + \delta)\psi(x_i + \delta) + \Gamma(x_i + \delta)\theta^{\delta-1}\log(\theta),$$

$$T_{13} = \Gamma(\delta)((1 + \theta)^{\delta-2} + \log(1 + \theta)(\delta - 1)(1 + \theta)^{\delta-2}) + (\delta - 1)(1 + \theta)^{\delta-2}\Gamma(\delta)\psi(\delta),$$

and

$$T_{14} = (\log(\theta) + \psi(x_i + \delta))\Gamma(x_i + \delta)(\delta - 1)\theta^{\delta-2}.$$

Then, the second order partial derivatives of the log-likelihood function are as follows

$$\begin{aligned} \frac{\partial^2 l(\theta, \alpha, \delta | x)}{\partial \theta^2} &= \frac{-n}{\theta^2} + \sum_{i=1}^n \frac{x_i + \delta}{(1 + \theta)^2} + \sum_{i=1}^n \frac{T_2(\delta - 1)(\delta - 2)T_5 - T_1(\delta - 1)T_6}{T_2^2}, \\ \frac{\partial^2 l(\theta, \alpha, \delta | x)}{\partial \alpha^2} &= \sum_{i=1}^n \frac{T_2(6\alpha\Gamma(\delta)\Gamma(x_i + 1)(1 + \theta)^{\delta-1}) - T_3(3\alpha^2\Gamma(\delta)\Gamma(x_i + 1)(1 + \theta)^{\delta-1})}{T_2^2} - \frac{3n\alpha(2(\alpha^2 + 1) - 3\alpha^3)}{(\alpha^3 + 1)^2}, \\ \frac{\partial^2 l(\theta, \alpha, \delta | x)}{\partial \delta^2} &= \sum_{i=1}^n \frac{T_2(\Gamma(x_i + 1)\alpha^3(T_7 + T_8) + (\log(\theta) + \psi(x_i + \delta))T_9 + T_{10}) - T_4(T_{11} + T_{12})}{T_2^2} - n\psi_1(\delta), \\ \frac{\partial^2 l(\theta, \alpha, \delta | x)}{\partial \theta \partial \alpha} &= \sum_{i=1}^n \frac{T_2(3\alpha^2\Gamma(\delta)\Gamma(x_i + 1)(\delta - 1)(1 + \theta)^{\delta-1}) - T_1T_3}{T_1^2}, \\ \frac{\partial^2 l(\theta, \alpha, \delta | x)}{\partial \delta \partial \alpha} &= \sum_{i=1}^n \frac{T_2(3\alpha^2\Gamma(x_i + 1)(\Gamma(\delta)(1 + \theta)^{\delta-1}\log(1 + \theta) + (1 + \theta)^{\delta-1}\Gamma(\delta)\psi(\delta))) - T_4T_3}{T_2^2}, \end{aligned}$$

and

$$\frac{\partial^2 l(\theta, \alpha, \delta | x)}{\partial \delta \partial \theta} = \sum_{i=1}^n \frac{T_2(\Gamma(x_i + 1)\alpha^3T_{13} + \Gamma(x_i + \delta)\theta^{\delta-2} + T_{14}) - T_4T_1}{T_2^2} - \frac{n}{1 + \theta},$$

where $\psi_1(s)$ is the trigamma function and defined as $\psi_1(s) = \frac{d^2}{ds^2} \log(\Gamma(s)) = \sum_{i=1}^n \frac{1}{(s + k)^2}$.

A novel approach for constructing distributions with an example of the Rayleigh distribution

Aijaz Ahmad¹, Muzamil jallal² and Afaq Ahmad³

^{1,2}Department of Mathematics, Bhagwant University, Ajmer, India
³Department of Mathematical Science, IUST, Awantipora, Kashmir
Email: ¹ahmadaijaz4488@gmail.com, Email: ²muzamiljallal@gmail.com
Email: ³baderaafaq@gmail.com

Abstract

In this paper, we describe a novel technique for creating distributions based on logarithmic functions, which we referred the Log Exponentiated Transformation (LET). The LET technique is then applied to Rayleigh distributions, resulting in a new distribution known as the Log Exponentiated Rayleigh distribution (LERD). Several distributional properties of the formulated distribution have been discussed. The expressions for ageing properties have been derived and discussed explicitly. The behaviour of the pdf, cdf and hazard rate function has been illustrated through different graphs. The parameters are estimated through the technique of MLE. A simulation analysis was conducted to measure the effectiveness of all estimators. Eventually the versatility and the efficacy of the formulated distribution have been examined through real life data set.

Keywords: Log Exponentiated Transformation, Rayleigh distribution, Moments, reliability measures, maximum likelihood function.

Mathematics subject classification: 60-XX, 62-XX, 11-KXX.

I. Introduction

The adoption of an efficient statistical model is critical in a variety of practical analyses. This is especially inconvenient for specific data studies, because the typically employed distributional models are inadequate for producing a plausible fit. Several approaches, such as the generation of families of adaptable distributions, have been presented in recent times. Most of them attempt to increase the effectiveness of a baseline distribution by utilising diverse mathematical expansion approaches. As a result, the related models may incorporate some extra characteristics that provide sufficient flexibility to examine real-life data in many areas of study, such as reliability, survival analysis, computer science, finance, biological research, medicine, and so on. Academics have recently been concerned with developing new techniques for creating new families of distributions so that real data can be adequately analysed and explored. Among them are Marshall and Olkin [9], Eugene et al.[4], Mudholkar et al. [11], Nadrajah and Kotz [12], Alzaatreh et al. [2], Mahdavi and Kundu [9], Ijaz et al. [8], Anwar Hassan et al.[3]. Based on the argumentation stated above, we suggest a novel family of distributions that adds versatility to the provided family and entitles it Log Exponentiated Transformation (LET). We give a thorough explanation of its fundamental mathematical characteristics, and subsequently employ the Rayleigh distribution as an application.

II. Log Exponentiated Transformation (LET)

This section demonstrates a novel generating family of probability distributions termed as log Exponentiated transformation, abbreviated as LET. If X is a continuous random variable, then the cumulative distribution function (cdf) of the log Exponentiated transformation is described as

$$F(x; \zeta, \theta) = 1 - \log(e + \bar{e}(G(x; \zeta))^\theta) \quad ; x \in \mathfrak{R}, \theta, \zeta > 0 \quad (1)$$

Where $G(x; \zeta)$ denotes the cdf of baseline distribution and $\frac{d(G(x; \zeta))}{dx} = g(x; \zeta)$.

The associated probability density function (pdf) is described as

$$f(x; \zeta, \theta) = \frac{(e-1)\theta g(x; \zeta)(G(x; \zeta))^{\theta-1}}{e + \bar{e}(G(x; \zeta))^\theta} \quad ; x \in \mathfrak{R}, \theta, \zeta > 0 \quad (2)$$

The survival function $s(x; \zeta, \theta)$, hazard rate function $h(x; \zeta, \theta)$ and cumulative hazard rate function $H(x; \zeta, \theta)$ are stated as respectively

$$\begin{aligned} s(x; \zeta, \theta) &= \log(e + \bar{e}(G(x; \zeta))^\theta) \\ h(x; \zeta, \theta) &= \frac{(e-1)\theta g(x; \zeta)(G(x; \zeta))^{\theta-1}}{(e + \bar{e}G^\theta(x; \zeta))(\log(e + \bar{e}(G(x; \zeta))^\theta))} \\ H(x; \zeta, \theta) &= -\log(\log(e + \bar{e}(G(x; \zeta))^\theta)) \end{aligned}$$

III. Mixture Form

This section provides an expression for the mixture form of the probability density function. Equation (2) can be written as

$$\begin{aligned} f(x; \zeta, \theta) &= (e-1)\theta g(x; \zeta)G^{\theta-1}(x; \zeta)(e + \bar{e}(G(x; \zeta))^\theta)^{-1} \\ &= \frac{(e-1)}{e}\theta g(x; \zeta)G^{\theta-1}(x; \zeta)\left(1 + \frac{\bar{e}}{e}(G(x; \zeta))^\theta\right)^{-1} \end{aligned} \quad (3)$$

We know that $(1+z)^{-1} = \sum_{p=0}^{\infty} (-1)^p z^p \quad ; |z| < 1$, using it in equation (3), we have

$$f(x; \zeta, \theta) = \frac{(e-1)}{e}\theta g(x; \zeta)(G(x; \zeta))^{\theta-1} \sum_{p=0}^{\infty} (-1)^p \left(\frac{\bar{e}}{e}\right)^p (G(x; \zeta))^{p\theta}$$

After simplification, we obtain the mixture form of pdf as

$$f(x; \zeta, \theta) = \sum_{p=0}^{\infty} (-1)^{p+1} \left(\frac{\bar{e}}{e}\right)^{p+1} \theta g(x; \zeta)(G(x; \zeta))^{(p+1)\theta-1} \quad (4)$$

IV. Log Exponentiated Rayleigh Distribution with properties

The Rayleigh distribution, named after the Lord Rayleigh, is a continuous probability distribution. Due to its wide range of applications, researchers have extended Rayleigh distribution for instance Exponentiated Rayleigh distribution by Voda [13], Weibull-Rayleigh distribution by Faton Merovci et al.[5], transmuted generalized Rayleigh distribution by Faton Merovci [6], Topp-Leone Rayleigh distribution with application by Fatoki O [7] and inverse Weibull Rayleigh distribution by Aijaz et al. [1]. The probability density function (pdf) of Rayleigh distribution with scale parameter α is defined by

$$g(x; \alpha) = \alpha x e^{-\frac{\alpha}{2}x^2} \quad ; x > 0, \alpha > 0 \quad (5)$$

The related cumulative distribution function (cdf) is given by

$$G(x; \alpha) = 1 - e^{-\frac{\alpha}{2}x^2}; x > 0, \alpha > 0 \quad (6)$$

The cumulative distribution function (cdf) of the formulated distribution can be obtained by substituting the value of equation (6) in equation (1), which follows

$$F(x; \alpha, \theta) = 1 - \log \left(e + \bar{e} \left(1 - e^{-\frac{\alpha}{2}x^2} \right)^\theta \right); x > 0, \alpha, \theta > 0 \quad (7)$$

The related probability density function is stated as

$$f(x; \alpha, \theta) = \frac{\alpha \theta (e-1) x e^{-\frac{\alpha}{2}x^2} \left(1 - e^{-\frac{\alpha}{2}x^2} \right)^{\theta-1}}{e + \bar{e} \left(1 - e^{-\frac{\alpha}{2}x^2} \right)^\theta}; x > 0, \alpha, \theta > 0 \quad (8)$$

Equation (8) may be stated in mixture form by substituting equations (5) and (6) in equation (4).

$$f(x; \alpha, \theta) = \sum_{p=0}^{\infty} (-1)^{p+1} \left(\frac{\bar{e}}{e} \right)^{p+1} \alpha \theta x e^{-\frac{\alpha}{2}x^2} \left(1 - e^{-\frac{\alpha}{2}x^2} \right)^{(p+1)\theta-1} \quad (9)$$

Since $(1-z)^{b-1} = \sum_{q=0}^{\infty} (-1)^q \binom{b-1}{q} z^q$; $|z| < 1$, using it in equation (9), we have

$$\begin{aligned} f(x; \alpha, \theta) &= \sum_{p=0}^{\infty} \sum_{q=0}^{\infty} (-1)^{p+q} \binom{(p+1)\theta-1}{q} \left(\frac{\bar{e}}{e} \right)^{p+1} \alpha \theta x e^{-\frac{\alpha(q+1)}{2}x^2} \\ &= \sum_{p=0}^{\infty} \sum_{q=0}^{\infty} \delta_{p,q} \alpha x e^{-\frac{\alpha(q+1)}{2}x^2} \end{aligned} \quad (10)$$

Where

$$\delta_{p,q} = (-1)^{p+q} \binom{(p+1)\theta-1}{q} \left(\frac{\bar{e}}{e} \right)^{p+1} \theta$$

Figures (1.1), (1.2), (1.3), and (1.4) depict several probable pdf and cdf layouts of LERD for distinct parameter selections.

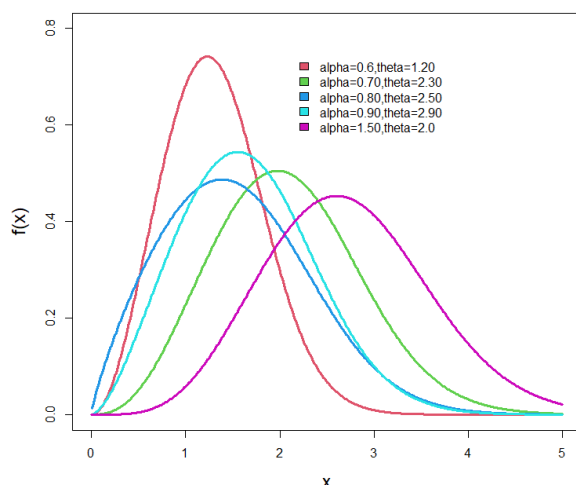


Figure 1.1: pdf of LERD under different values to parameters

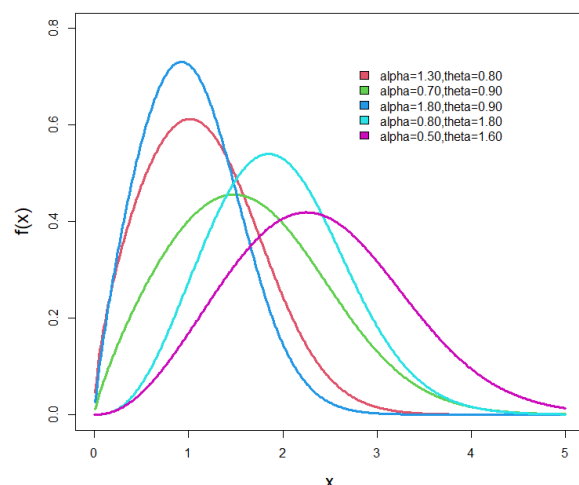


Figure 1.2: pdf of LERD under different values to parameters

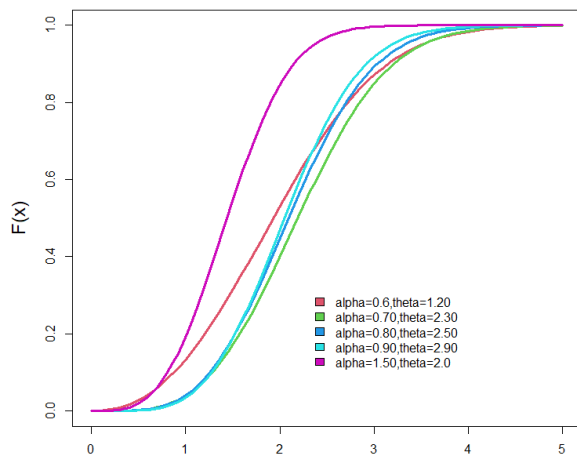


Figure 1.3: cdf of LERD under x different values to parameters

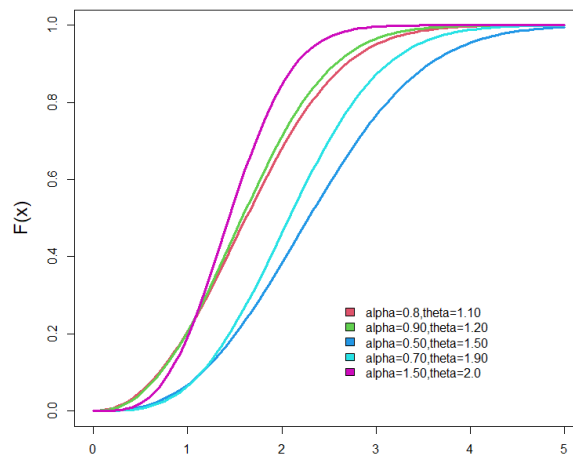


Figure 1.4: cdf of LERD under x different values to parameters

V. Mathematical Properties of LER Distribution

I. Moments of LER Distribution

Let suppose X denotes random variable follows LERD. Then r^{th} moment denoted by μ_r , is given as

$$\mu_r' = E(X^r) = \int_0^{\infty} x^r f(x; \alpha, \theta) dx$$

Using equation (10), we have

$$\begin{aligned} \mu_r' &= \int_0^{\infty} x^r \sum_{p=0}^{\infty} \sum_{q=0}^{\infty} \delta_{p,q} \alpha x e^{-\frac{\alpha(q+1)}{2}x^2} dx \\ &= \sum_{p=0}^{\infty} \sum_{q=0}^{\infty} \delta_{p,q} \alpha \int_0^{\infty} x^{r+1} e^{-\frac{\alpha(q+1)}{2}x^2} dx \end{aligned}$$

Making substitution $\frac{\alpha}{2}(q+1)x^2 = z$, so that $0 < z < \infty$, we have

$$\mu_r' = \sum_{p=0}^{\infty} \sum_{q=0}^{\infty} \delta_{p,q} \left(\frac{2}{\alpha(q+1)} \right)^{\frac{r}{2}} \frac{1}{(q+1)} \int_0^{\infty} z^{\frac{r}{2}} e^{-z} dz$$

After solving the integral, we get

$$\mu_r' = \sum_{p=0}^{\infty} \sum_{q=0}^{\infty} \delta_{p,q} \frac{\alpha}{2} \left(\frac{2}{\alpha(q+1)} \right)^{\frac{r}{2}+1} \Gamma\left(\frac{r}{2}+1\right)$$

II. Moment Generating Function of LER Distribution

Let X be a random variable follows LERD. Then the moment generating function of the distribution denoted by $M_X(t)$ is given

$$M_X(t) = E(e^{tx}) = \int_0^{\infty} e^{tx} f(x; \alpha, \theta) dx$$

Using Taylor's series

$$\begin{aligned}
 &= \int_0^{\infty} \left(1 + tx + \frac{(tx)^2}{2!} + \frac{(tx)^3}{3!} + \dots \right) f(x; \alpha, \theta) dx \\
 &= \sum_{r=0}^{\infty} \frac{t^r}{r!} \int_0^{\infty} x^r f(x; \alpha, \theta) dx \\
 &= \sum_{r=0}^{\infty} \frac{t^r}{r!} E(X^r) \\
 M_X(t) &= \sum_{p=0}^{\infty} \sum_{q=0}^{\infty} \sum_{r=0}^{\infty} \frac{t^r}{r!} \delta_{p,q} \frac{\alpha}{2} \left(\frac{2}{\alpha(q+1)} \right)^{\frac{r}{2}+1} \Gamma\left(\frac{r}{2}+1\right)
 \end{aligned}$$

III. Quantile Function of LER Distribution

The quantile function of any distribution may be described as follows:

$$Q(u) = X_q = F^{-1}(u)$$

Where $Q(u)$ denotes the quantile function of $F(x)$ for $u \in (0,1)$.

Let us suppose

$$F(x) = 1 - \log \left(e + e \left(1 - e^{-\frac{\alpha}{2}x^2} \right) \right) = u \tag{11}$$

After simplifying equation (11), we obtain quantile function of LER distribution as

$$Q(u) = X_q = \left[-\frac{2}{\lambda} \log \left(1 - \left(\frac{e^{1-u} - e}{e} \right)^{\frac{1}{\theta}} \right) \right]^{\frac{1}{2}}$$

VI. Mean Deviation From Mean and Median of LER Distribution

The entirety of deviations is apparently a measure of amount of dispersion in a population. Let X be a random variable from LER distribution with mean μ . Then the mean deviation from mean is defined as.

$$\begin{aligned}
 D(\mu) &= E(|X - \mu|) \\
 &= \int_0^{\infty} |X - \mu| f(x) dx \\
 &= 2\mu F(\mu) - 2 \int_0^{\mu} xf(x) dx
 \end{aligned} \tag{12}$$

Now

$$\int_0^{\mu} xf(x) dx = \sum_{p=0}^{\infty} \sum_{q=0}^{\infty} \delta_{p,q} \alpha \int_0^{\mu} x^2 e^{-\frac{\alpha(q+1)}{2}x^2} dx$$

Making substitution $\frac{\alpha(q+1)}{2} = z$ so that $0 < z < \frac{\alpha(q+1)}{2} \mu^2$, we have

$$\int_0^{\mu} xf(x)dx = \sum_{p=0}^{\infty} \sum_{q=0}^{\infty} \delta_{p,q} \left(\frac{2}{\alpha(q+1)} \right)^{\frac{1}{2}} \left(\frac{1}{q+1} \right)^{\frac{1}{2}} \int_0^{\frac{\alpha(q+1)\mu^2}{2}} z^{\frac{1}{2}} e^{-z} dz$$

After solving the integral, we have

$$\int_0^{\mu} xf(x)dx = \sum_{p=0}^{\infty} \sum_{q=0}^{\infty} \delta_{p,q} \left(\frac{2}{\alpha(q+1)} \right)^{\frac{1}{2}} \left(\frac{1}{q+1} \right)^{\frac{1}{2}} \gamma \left(\frac{3}{2}, \frac{\alpha(q+1)\mu^2}{2} \right) \quad (13)$$

Substituting value of equation (7) and (13) in equation (12), we get

$$D(\mu) = 2\mu \left[1 - \log \left(e + \bar{e} \left(1 - e^{-\frac{\alpha}{2}\mu^2} \right) \right) \right] - 2 \sum_{p=0}^{\infty} \sum_{q=0}^{\infty} \delta_{p,q} \left(\frac{2}{\alpha(q+1)} \right)^{\frac{1}{2}} \left(\frac{1}{q+1} \right)^{\frac{1}{2}} \gamma \left(\frac{3}{2}, \frac{\alpha(q+1)\mu^2}{2} \right)$$

Let X be a random variable from LER distribution with median M . Then the mean deviation from median is defined as.

$$D(M) = E(|X - M|) = \int_0^{\infty} |X - M| f(x) dx = \mu - 2 \int_0^M xf(x) dx \quad (14)$$

Now

$$\int_0^M xf(x) dx = \sum_{p=0}^{\infty} \sum_{q=0}^{\infty} \delta_{p,q} \alpha \int_0^M x^2 e^{-\frac{\alpha(q+1)}{2}x^2} dx$$

Making substitution $\frac{\alpha(q+1)}{2} = z$ so that $0 < z < \frac{\alpha(q+1)}{2} M^2$, we have

$$\int_0^M xf(x) dx = \sum_{p=0}^{\infty} \sum_{q=0}^{\infty} \delta_{p,q} \left(\frac{2}{\alpha(q+1)} \right)^{\frac{1}{2}} \left(\frac{1}{q+1} \right)^{\frac{1}{2}} \int_0^{\frac{\alpha(q+1)M^2}{2}} z^{\frac{1}{2}} e^{-z} dz$$

After solving the integral, we have

$$\int_0^M xf(x) dx = \sum_{p=0}^{\infty} \sum_{q=0}^{\infty} \delta_{p,q} \left(\frac{2}{\alpha(q+1)} \right)^{\frac{1}{2}} \left(\frac{1}{q+1} \right)^{\frac{1}{2}} \gamma \left(\frac{3}{2}, \frac{\alpha(q+1)M^2}{2} \right) \quad (15)$$

Substituting value of equation (15) in equation (14), we get

$$D(M) = \mu - 2 \sum_{p=0}^{\infty} \sum_{q=0}^{\infty} \delta_{p,q} \left(\frac{2}{\alpha(q+1)} \right)^{\frac{1}{2}} \left(\frac{1}{q+1} \right)^{\frac{1}{2}} \gamma \left(\frac{3}{2}, \frac{\alpha(q+1)M^2}{2} \right)$$

VII. Ageing Properties of LER Distribution

Suppose X be a continuous random variable with cdf $F(x), x \geq 0$. Then its reliability function which is also known survival function is stated as

$$S(x) = p_r(X > x) = \int_x^{\infty} f(x) dx = 1 - F(x)$$

Therefore, the survival function for LER distribution is given as

$$\begin{aligned} S(x, \alpha, \theta) &= 1 - F(x, \alpha, \theta) \\ &= \log \left(e + \bar{e} \left(1 - e^{-\frac{\alpha}{2}x^2} \right) \right) \end{aligned} \quad (16)$$

The hazard rate function of a random variable x is given as

$$h(x, \alpha, \theta) = \frac{f(x, \alpha, \theta)}{S(x, \alpha, \theta)} \quad (17)$$

Using equation (8) and (16) in equation (17), we have

$$h(x, \alpha, \theta) = \frac{\alpha \theta (e-1) x e^{-\frac{\alpha}{2} x^2} \left(1 - e^{-\frac{\alpha}{2} x^2}\right)^{\theta-1}}{\left(e + \bar{e} \left(1 - e^{-\frac{\alpha}{2} x^2}\right)^\theta\right) \left(\log \left(e + \bar{e} \left(1 - e^{-\frac{\alpha}{2} x^2}\right)^\theta\right)\right)}$$

Figures (1.5) and (1.6) depict several probable hazard rate function layouts of LERD for distinct parameter selections.

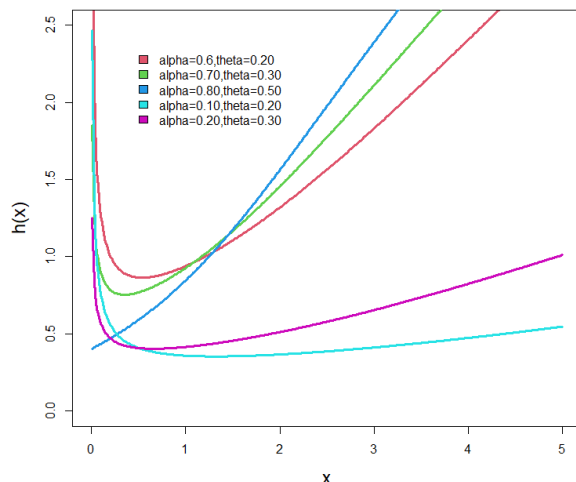


Figure 1.5. hrf of LERD under different values to parameters

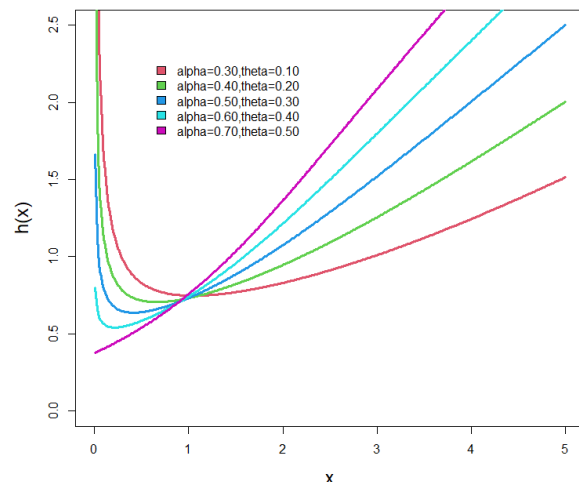


Figure 1.6. hrf of LERD under different values to parameters

The cumulative hazard rate function of a continuous random variable x is defined as

$$H(x, \alpha, \theta) = -\log[\bar{F}(x; \alpha, \theta)] \quad (18)$$

Using equation (16) in equation (18), we obtain the cumulative hazard rate function of LER distribution

$$H(x, \alpha, \theta) = -\log \left[\log \left(e + \bar{e} \left(1 - e^{-\frac{\alpha}{2} x^2} \right)^\theta \right) \right]$$

VIII. Renyi Entropy of LER Distribution

If X denotes a continuous random variable having probability density function $f(x)$. Then Renyi entropy is stated as

$$T_R(\delta) = \frac{1}{1-\delta} \log \left\{ \int_0^\infty f^\delta(x) dx \right\}, \text{ where } \delta > 0 \text{ and } \delta \neq 1$$

Thus, the Renyi entropy of LER distribution is given as

$$\begin{aligned} T_R(\delta) &= \frac{1}{1-\delta} \log \left\{ \int_0^\infty \left(\frac{(e-1)\theta g(x; \zeta) (G(x; \zeta))^{\theta-1}}{e + \bar{e} (G(x; \zeta))^\theta} \right)^\delta dx \right\} \\ &= \frac{1}{1-\delta} \log \left\{ (e-1)^\delta e^{-\delta} \theta^\delta \int_0^\infty (g(x; \zeta))^\delta (G(x; \zeta))^{(\theta-1)\delta} \left(1 + \frac{\bar{e}}{e} (G(x; \zeta))^\theta \right)^{-\delta} dx \right\} \end{aligned} \quad (19)$$

Since $(1+z)^{-b} = \sum_{p=0}^{\infty} (-1)^p \binom{b+p-1}{p} z^p$; $|z| < 1$, using it in equation (19), we have

$$\begin{aligned} T_R(\delta) &= \frac{1}{1-\delta} \log \left\{ (e-1)^\delta e^{-\delta} \theta^\delta \int_0^\infty (g(x; \zeta))^\delta (G(x; \zeta))^{\theta-1} \sum_{p=0}^{\infty} (-1)^p \binom{p+\delta-1}{p} \left(\frac{\bar{e}}{e}\right)^p (G(x; \zeta))^{p\theta} dx \right\} \\ &= \frac{1}{1-\delta} \log \left\{ \sum_{p=0}^{\infty} (-1)^{p+\delta} \binom{p+\delta-1}{p} \left(\frac{\bar{e}}{e}\right)^{p+\delta} \theta^\delta \int_0^\infty (g(x; \zeta))^\delta (G(x; \zeta))^{\theta(p+\delta)-\delta} dx \right\} \end{aligned}$$

Using equation (5) and (6), we have

$$T_R(\delta) = \frac{1}{1-\delta} \log \left\{ \sum_{p=0}^{\infty} (-1)^{p+\delta} \binom{p+\delta-1}{p} \left(\frac{\bar{e}}{e}\right)^{p+\delta} \theta^\delta \int_0^\infty \left(\alpha x e^{-\frac{\alpha}{2}x^2} \right)^\delta \left(1 - e^{-\frac{\alpha}{2}x^2} \right)^{\theta(p+\delta)-\delta} dx \right\} \quad (20)$$

Since $(1-z)^b = \sum_{q=0}^{\infty} (-1)^q \binom{b}{q} z^q$; $|z| < 1$, using it in equation (20), we have

$$\begin{aligned} T_R(\delta) &= \frac{1}{1-\delta} \log \left\{ \sum_{p=0}^{\infty} \sum_{q=0}^{\infty} (-1)^{p+q+\delta} \binom{p+\delta-1}{p} \binom{\theta(p+\delta)-\delta}{q} \left(\frac{\bar{e}}{e}\right)^{p+\delta} \theta^\delta \alpha^\delta \int_0^\infty x^\delta e^{-\frac{\alpha(q+\delta)}{2}x^2} dx \right\} \\ &= \frac{1}{1-\delta} \log \left\{ \sum_{p=0}^{\infty} \sum_{q=0}^{\infty} \omega_{p,q} \int_0^\infty x^\delta e^{-\frac{\alpha(q+\delta)}{2}x^2} dx \right\} \end{aligned}$$

Where

$$\omega_{p,q} = (-1)^{p+q+\delta} \binom{p+\delta-1}{p} \binom{\theta(p+\delta)-\delta}{q} \left(\frac{\bar{e}}{e}\right)^{p+\delta} \theta^\delta \alpha^\delta$$

Making substitution $\frac{\alpha(q+\delta)}{2}x^2 = z$ so that $0 < z < \infty$, we have

$$T_R(\delta) = \frac{1}{1-\delta} \log \left\{ \sum_{p=0}^{\infty} \sum_{q=0}^{\infty} \omega_{p,q} \frac{2^{\frac{\delta-1}{2}}}{(\alpha(q+\delta))^{\frac{\delta+1}{2}}} \int_0^\infty z^{\frac{\delta+1}{2}-1} e^{-z} dz \right\}$$

After solving the integral, we get

$$T_R(\delta) = \frac{1}{1-\delta} \log \left\{ \sum_{p=0}^{\infty} \sum_{q=0}^{\infty} \omega_{p,q} \frac{2^{\frac{\delta-1}{2}}}{(\alpha(q+\delta))^{\frac{\delta+1}{2}}} \Gamma\left(\frac{\delta+1}{2}\right) \right\}$$

IX. Maximum Likelihood Estimation of LER Distribution

Let X_1, X_2, \dots, X_n be a random sample of size n from LERD then its likelihood function is given by

$$\begin{aligned} l &= \prod_{i=1}^n f(y_i, \alpha, \theta) \\ &= \prod_{i=1}^n \frac{\alpha \theta (e-1) x e^{-\frac{\alpha}{2}x^2} \left(1 - e^{-\frac{\alpha}{2}x^2} \right)^{\theta-1}}{e + \bar{e} \left(1 - e^{-\frac{\alpha}{2}x^2} \right)^\theta} \end{aligned}$$

The log likelihood function is given as

$$\begin{aligned} \log l = n \log \alpha + n \log \theta + n \log(e-1) - \frac{\alpha}{2} \sum_{i=1}^n x_i + \sum_{i=1}^n \log(x_i) \\ + (\theta-1) \sum_{i=1}^n \log \left(1 - e^{-\frac{\alpha}{2} x_i^2} \right) - \sum_{i=1}^n \log \left(e + \bar{e} \left(1 - e^{-\frac{\alpha}{2} x_i^2} \right)^\theta \right) \end{aligned} \quad (21)$$

Differentiate equation (21), partially with respect parameters, we have

$$\frac{\partial \log l}{\partial \alpha} = \frac{n}{\alpha} - \frac{1}{2} \sum_{i=1}^n x_i + \alpha(\theta-1) \sum_{i=1}^n \frac{x e^{-\frac{\alpha}{2} x_i^2}}{1 - e^{-\frac{\alpha}{2} x_i^2}} - \alpha \theta \sum_{i=1}^n \frac{\left(1 - e^{-\frac{\alpha}{2} x_i^2} \right)^{\theta-1} x e^{-\frac{\alpha}{2} x_i^2}}{e + \bar{e} \left(1 - e^{-\frac{\alpha}{2} x_i^2} \right)^\theta} \quad (22)$$

$$\frac{\partial \log l}{\partial \theta} = \frac{n}{\theta} + \sum_{i=1}^n \log \left(1 - e^{-\frac{\alpha}{2} x_i^2} \right) + \bar{e} \sum_{i=1}^n \frac{\left(1 - e^{-\frac{\alpha}{2} x_i^2} \right)^\theta \log \left(1 - e^{-\frac{\alpha}{2} x_i^2} \right)}{e + \bar{e} \left(1 - e^{-\frac{\alpha}{2} x_i^2} \right)^\theta} \quad (23)$$

The equations (22) and (23) are non-linear equations and hence cannot be expressed in compact form. Therefore to solve these equations explicitly for α and θ is difficult. So we can apply iterative methods such as Newton–Raphson method, secant method, Regula-falsi method etc. The MLE of the parameters denoted as $\hat{\zeta}(\hat{\alpha}, \hat{\theta})$ of $\zeta(\alpha, \theta)$ can be obtained by using the above methods.

For interval estimation and hypothesis tests on the model parameters, an information matrix is required. The 2 by 2 observed matrix is

$$I(\zeta) = \begin{bmatrix} E \left(\frac{\partial^2 \log l}{\partial \alpha^2} \right) & E \left(\frac{\partial^2 \log l}{\partial \alpha \partial \theta} \right) \\ E \left(\frac{\partial^2 \log l}{\partial \theta \partial \alpha} \right) & E \left(\frac{\partial^2 \log l}{\partial \theta^2} \right) \end{bmatrix}$$

The elements of above information matrix can obtain by differentiating equations(22)and (23) again partially. Under standard regularity conditions when $n \rightarrow \infty$ the distribution of $\hat{\zeta}$ can be approximated by a multivariate normal $N(0, I(\hat{\zeta})^{-1})$ distribution to construct approximate confidence interval for the parameters.

Hence the approximate $100(1-\psi)\%$ confidence interval for α, θ and λ are respectively given by

$$\hat{\alpha} \pm Z_{\frac{\psi}{2}} \sqrt{I_{\alpha\alpha}^{-1}(\hat{\zeta})} \quad \text{and} \quad \hat{\theta} \pm Z_{\frac{\psi}{2}} \sqrt{I_{\theta\theta}^{-1}(\hat{\zeta})}$$

Where $Z_{\frac{\psi}{2}}$ denotes the ζ^{th} percentile of the standard normal distribution.

X. Simulation Analyses

In this segment, a Monte Carlo simulation analysis was performed using R software to evaluate the consistency of the MLE's. This analysis was performed 500 times using sample sizes of n=30, 50, 150, 250,350 and 450 and various parameter combinations (0.5, 0.7) and (0.7, 0.5) created from LERD. In each case, the bias, variance, and mean square errors (MSEs) were calculated. Table 10.1 shows the simulation findings. In particular, we see that, pursuant to the theory, the MSEs and bias decrease as sample size increases.

Table 1: Average bias, variance and MSEs of 500 simulations of LERD for different parameter combinations.

Sample Size n	parameters	$\alpha = 0.5, \theta = 0.7$			$\alpha = 0.7, \theta = 0.5$		
		Bias	Variance	MSE	Bias	Variance	MSE
30	α	0.04106	0.01906	0.02075	0.06495	0.04404	0.04826
	θ	0.08050	0.05995	0.06643	0.04658	0.02140	0.02357
50	α	0.01797	0.00826	0.00858	0.03166	0.02274	0.02375
	θ	0.03925	0.02402	0.02556	0.02152	0.01128	0.01175
150	α	0.01085	0.00321	0.00333	0.01693	0.00608	0.00637
	θ	0.01481	0.00729	0.00751	0.01100	0.00305	0.00317
250	α	0.00280	0.00186	0.00187	0.00456	0.00366	0.00368
	θ	0.00702	0.00401	0.00406	0.00280	0.00169	0.00170
350	α	0.00219	0.00102	0.00102	0.00461	0.00271	0.00273
	θ	0.00175	0.00232	0.00232	0.00296	0.00123	0.00124
450	α	0.00309	0.00088	0.00089	-0.0002	0.00200	0.00200
	θ	0.00311	0.00222	0.00223	0.00188	0.00102	0.00103

XI. Data Analysis

This section assesses the effectiveness of the stated distribution using real-world data. We fitted the LER distribution to many other models for comparative purposes, including Weibull distribution (WD), Exponentiated exponential distribution (EED), Frechet distribution (FD), inverse Burr distribution (IBD), Rayleigh distribution (RD) and exponential distribution (EXD).

We will use certain measures to evaluate which of the competitive models is the strongest, including AIC (Akaike Information Criterion), CAIC (Consistent Akaike Information Criterion), BIC (Bayesian Information Criterion) and HQIC (Hannan-Quinn Information Criterion). Such criteria can be represented mathematically by

$$AIC = 2k - 2 \ln l \quad CAIC = \frac{2kn}{n-k-1} - 2 \ln l$$

$$BIC = k \ln n - 2 \ln l \quad \text{and} \quad HQIC = 2k \ln(\ln(n)) - 2 \ln l$$

We compute Anderson-Darling (A^*), Cramer-Von Misses (W^*), Kolmogorov-Smirnov Statistic, and P-value in addition to the aforementioned goodness of measures. The model with the lowest value of these indicators and the greatest p-value is considered the best among the competing models.

Data Set: The data set was originally reported by Bader and Priest (1982), on failure stresses (in GPa) of 65 single carbon fibres of lengths 50 mm, respectively. The data set is given as follows
 1.339,1.434,1.549,1.574,1.589,1.613,1.746,1.753,1.764,1.807,1.812,1.84,1.852,1.852,1.862,1.864,1.931,1.952,1.974,2.019,2.051,2.055,2.058,2.088,2.125,2.162,2.171,2.172,2.18,2.194,2.211,2.27,2.272,2.28,2.299,2.308,2.335,2.349,2.356,2.386,2.39,2.41,2.43,2.458,2.471,2.497,2.514,2.558,2.577,2.593,2.601,2.604,2.62,2.633,2.67,2.682,2.699,2.705,2.735,2.785,3.02,3.042, 3.116, 3.174.

Table 2: The for data set

Min	Q ₁	Med.	Mean	Q ₃	Kurt.	Skew.	Max
1.339	1.914	2.271	2.241	2.563	2.5270	0.0419	3.174

descriptive statistics

Table 3: *The ML Estimates for data set*

Model	ML Estimates		Standard Error	
	$\hat{\alpha}$	$\hat{\theta}$	$\hat{\alpha}$	$\hat{\theta}$
LERD	1.3473	12.660	0.1356	3.7652
WD	0.0059	5.8363	0.0022	0.4026
EED	2.3310	115.52	0.2045	46.011
FD	1.9940	4.9923	0.0530	0.4439
RD	0.3849	0.0481
IBD	5.0822	34.299	0.4311	9.5300
EXD	0.4462	0.0557

(standard error in parenthesis)

Table 4: *Comparison criterion and goodness of fit statistics for data set*

Model	$-2\log l$	AIC	CAIC	BIC	HQIC
LERD	69.712	73.712	73.909	78.030	75.413
WD	70.756	74.756	74.952	79.073	76.457
EED	76.657	80.657	80.853	84.974	82.358
FD	86.443	90.443	90.642	94.761	92.144
RD	149.168	151.16	151.23	153.32	152.01
IBD	85.506	89.506	89.702	93.824	91.207
EXD	231.29	233.29	233.35	235.45	234.14

Table 5: *Other goodness of fit statistics criterion for data set*

Model	W*	A*	K-S value	p-value
LERD	0.04714	0.2987	0.0670	0.9357
WD	0.0590	0.3836	0.0787	0.9181
EED	0.1173	0.7114	0.1006	0.5363
FD	0.2547	1.5484	0.1221	0.2949
RD	0.0834	0.3266	0.3501	3.054e-07
IBD	0.2428	1.4748	0.1186	0.3288
EXD	0.04735	0.3986	0.4677	1.374e-12

Fig. 1.7 :Estimated pdf's of the fitted models for data set

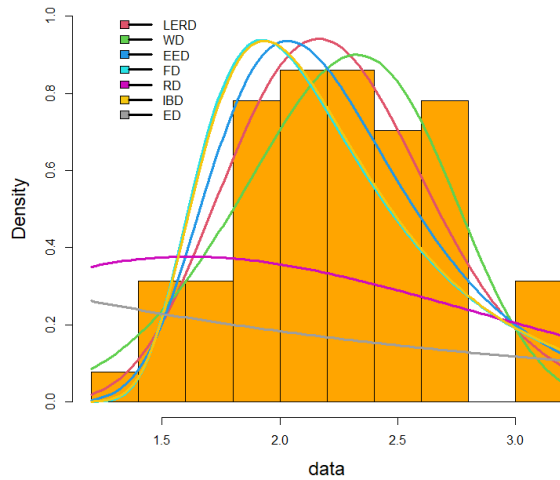
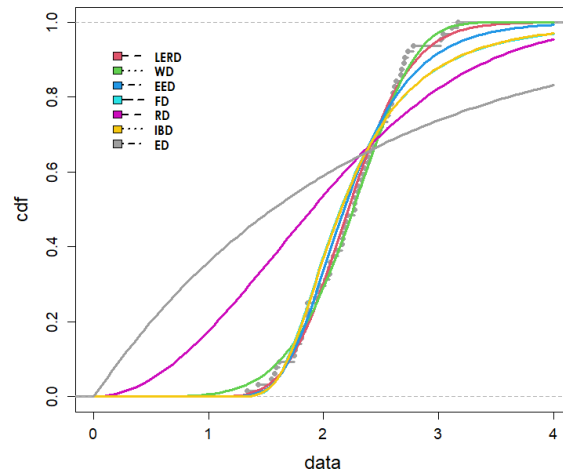


Fig 1.8 Empirical cdf versus fitted cdf's for data set



XII. Conclusions

In this study, a novel technique known as log exponentiated transformation (LET) is suggested. As an illustration, the Rayleigh distribution is employed as the baseline distribution, and a novel two-parameter log exponentiated Rayleigh distribution (LERD) which proved more flexible has been studied. Several mathematical aspects of the newly developed distribution are deduced and analysed. The MLE approach is used to acquire the parameters. From table 8.3 and 8.6 it is evident that the formulated distribution outranks than compared ones.

References

- [1] Aijaz, A., Qurat Ul-Ain, S., Rajnee, T and Afaq, A. (2021). Inverse Weibull-Rayleigh distribution: characterization with application related cancer data. RT&A 16(4), 364-382.
- [2] Alzaatreh, A., Lee, C., and Famoye, F., and Ghosh, I. (2016). The generalized Cauchy family of distributions with applications. Journal of statistical distributions and applications, 3(1), 1-16.
- [3] Anwar, H., Dar, I.H. and Lone., M.A. (2021). A novel family of generating distributions based on trigonometric function with an application to exponential distribution. Journal of scientific research, 65(5), 173-179.
- [4] Eugene N, Lee C and Famoye F (2002). Beta-normal distribution and its applications. Communication in statistics- theory and methods, 31, 497-512.
- [5] Fatou, M., and Ibrahim, E. (2015). Weibull-Rayleigh distribution theory and applications. Applied mathematics and information sciences an international journal, vol 9(5), 1-11.
- [6] Fatou, M., (2014). Transmuted generalized Rayleigh distribution. Journal of statistics applications and probability, 3(1), 9-20.
- [7] Fatoki, O.(2019). The Topp-Leone Rayleigh distribution with application. American journal of mathematics and statistics, 9(6), 215-220.
- [8] Ijaz, M., Asim, S. M., Farooq, M., Khan, S.A., and Manzoor, S. (2020). A gull alpha power Weibull distribution with applications to real and simulated data. Plos one, 15(6), e0233080.

- [9] Mahdavi, A. and Kundu, D. (2017). A new method for generating distributions with an application to exponential distribution. *Communication in statistics-theory and methods*, 46(13), 6543-6557.
- [10] Marshall, A. W and Olkin, I. (1997). A new method for adding a parameter to a family of distributions with applications to exponential and Weibull families. *Biometrika*, 84(3), 641-652.
- [11] Mudholkar, G. S., Srivastava, D. k. and Friemer, k. (1995). The exponentiated Weibull family: a reanalysis of the bus-motor failure data, *Technometrics*, 37(4), 436-445.
- [12] Nadrajah, S and Kotz, K. (2006). The exponentiated type distributions. *Acta applicandae mathematicae*, 92(2), 97-111.
- [13] Voda, V.G. (1976). Inferential procedures on generalized Rayleigh variate. *Applications of mathematics*, 21, 395-412.

A New Reliability Model and Applications

MANOHARAN M. AND KAVYA P.



University of Calicut
manumavila@gmail.com, kavyapnair90@gmail.com

Abstract

The Lomax or Pareto Type II distribution has a wide range of applications in many areas including reliability and life testing. In this paper, we modify the Lomax distribution using KM transformation to enhance the applicability of the Lomax distribution. The distribution introduced using KM transformation is parsimonious in parameter. Substituting the cumulative distribution function (cdf) of the Lomax distribution in KM transformation provides a new modified Lomax distribution. The behavior of hazard rate function is studied graphically and also theoretically using Glacer method. Its analytical properties are derived and parameters are estimated using maximum likelihood estimation method. We consider two real data sets to show the flexibility of the proposed model. The model proposed in this paper provides a better fit to the data sets compared to other well-known distributions given in this study.

Keywords: Parsimonious model Lifetime KM transformation Lomax distribution Decreasing failure rate.

1. INTRODUCTION

The Lomax distribution has wide applications in many fields like economics, actuarial science, and so on. The Lomax distribution is also called Pareto Type II distribution. The distribution was introduced by Lomax [13] and it is a heavy-tailed distribution. It has also been useful in reliability and life testing problems in engineering and survival analysis as an alternative distribution [9], [11]. The Lomax distribution shows decreasing failure rate. Modified and extended versions of the Lomax distribution have been studied; examples include the weighted Lomax distribution [11], exponential Lomax distribution [7], exponentiated Lomax distribution [19], gamma Lomax distribution [5], transmuted Lomax distribution [3], Poisson Lomax distribution [2], McDonald Lomax distribution [12], Weibull Lomax distribution [21], power Lomax distribution [18], Kumaraswamy-Generalized Lomax distribution [20], Gompertz-Lomax distribution [16], and DUS-Lomax distribution [6]. Besides, estimation of the parameters of Lomax distribution under general progressive censoring has been considered by Al-Zahrani and Al-Sobhi [1].

The principal objective of the study is to introduce a modified Lomax distribution which is parsimonious in parameter and enhance the application of the Lomax distribution in reliability theory and survival analysis. We try to improve the properties of the Lomax distribution as a useful lifetime model.

We organize the paper as follows: In Section 2, we introduce a new life distribution using the Lomax distribution as the baseline distribution in the KM transformation. We then discuss the analytical characteristics of the new distribution in Section 3. In Section 4, we establish the ordering of the new distribution. In section 5, the parametric estimation for the new distribution is studied. We carry out an analysis using a real-life data set to illustrate the model's flexibility in Section 6. In section 7, we summarize the conclusions and outline our future works.

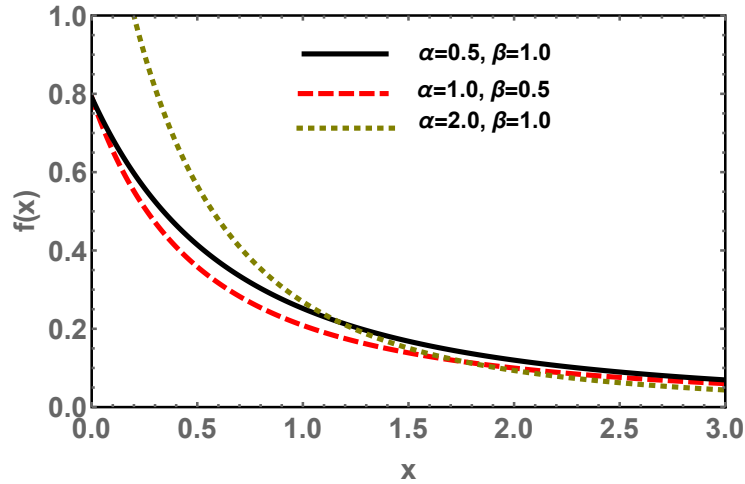


Figure 1: Probability density plot

2. THE MODIFIED LOMAX MODEL

In this paper we have modified the Lomax distribution with cumulative distribution function (cdf)

$$G(x) = 1 - (1 + \beta x)^{-\alpha}, \quad x > 0, \quad \alpha, \beta > 0, \quad (1)$$

using KM (Kavya and Manoharan) transformation introduced by Kavya and Manoharan [10]. Let X be a random variable with cdf $G(x)$ and probability density function (pdf) $g(x)$ of some baseline distribution. Then the cdf $F(x)$ of new distribution is defined as,

$$F(x) = \frac{e}{e-1} [1 - e^{-G(x)}]. \quad (2)$$

Here we introduce a new distribution by substituting the cdf of Lomax distribution (1) in (2). The cdf and pdf of the new distribution are respectively obtained as

$$F(x) = \frac{e}{e-1} [1 - e^{-(1 - (1 + \beta x)^{-\alpha})}], \quad x > 0, \quad \alpha, \beta > 0, \quad (3)$$

$$f(x) = \frac{\alpha\beta(1 + \beta x)^{-(\alpha+1)}e^{(1 + \beta x)^{-\alpha}}}{e-1}, \quad x > 0, \quad \alpha, \beta > 0, \quad (4)$$

$$(5)$$

The graphical representation of pdf is given in Fig. 1 for different values of parameters. In the whole paper we used the software MATHEMATICA [23] for plotting the graphs.

3. HAZARD RATE FUNCTION OF THE MODEL

The hazard function is defined as

$$h(x) = \frac{f(x)}{1 - F(x)} \quad (6)$$

The hazard function of the proposed model is obtained as

$$h(x) = \frac{\alpha\beta(1 + \beta x)^{-(\alpha+1)}e^{(1 + \beta x)^{-\alpha}}}{e^{(1 + \beta x)^{-\alpha}} - 1} \quad (7)$$

The shape of the hazard rate function is given in Fig. 2.

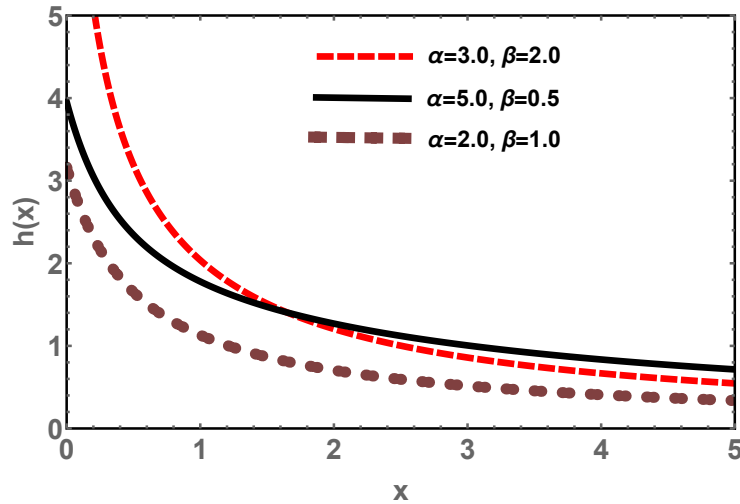


Figure 2: Hazard rate plot

3.1. Theoretical explanation of the shape of the hazard rate function

We follow Glaser [8] for theoretical explanation of the shape of the hazard rate. Suppose $f(t)$ is the pdf of some distribution and $f'(t)$ is the first derivative of $f(t)$. Then

$$v(t) = \frac{-f'(t)}{f(t)}$$

For our proposed distribution

$$v(x) = \beta \left[\alpha + (\alpha + 1)(1 + \beta x)^{-1} \right]$$

and

$$v'(x) = -\beta^2(\alpha + 1)(1 + \beta x)^{-2} \tag{8}$$

based on Glaser [8] we get a result from Equation (8):

$v'(x) < 0$ for all $x > 0$ when $\alpha \geq 0$. Then the distribution has decreasing failure rate (DFR).

4. SOME ANALYTICAL CHARACTERISTICS

Here we discuss some of the analytical characteristics of our proposed distribution.

4.1. Moments

The moments of a random variable, if they exist, are useful for estimating measures of central tendency, dispersion, and shapes. The r^{th} raw moments of the proposed distribution is

$$E(X^r) = \frac{\alpha\beta}{e-1} \int_0^\infty x^r (1 + \beta x)^{-(\alpha+1)} e^{(1+\beta x)^{-\alpha}} dx.$$

After transformation, we get,

$$E(X^r) = \frac{1}{\beta^r(e-1)} \int_0^1 (1 - u^{\frac{1}{\alpha}})^r u^{-\frac{r}{\alpha}} e^u du,$$

applying binomial expansion, then

$$E(X^r) = \frac{1}{\beta^r(e-1)} \sum_{i=0}^\infty (-1)^i \binom{r}{i} \int_0^1 u^{\frac{1}{\alpha}(i-r)} e^u du.$$

Expanding exponential term, and we get the r^{th} raw moment as

$$E(X^r) = \frac{1}{\beta^r(e-1)} \sum_{i=0}^{\infty} \frac{(-1)^i}{j!} \binom{r}{i} \frac{\alpha}{\alpha j + \alpha - r + i}.$$

4.2. Moment generating function

The moment generating function of the proposed distribution is

$$M_X(t) = \frac{\alpha}{(e-1)} \sum_{m=0}^{\infty} \sum_{n=0}^{\infty} \frac{1}{m! n!} \frac{t^m}{\beta^m} \frac{(n\alpha + \alpha - 2)!}{(n + \alpha)!} \quad (9)$$

4.3. Characteristic function

The characteristic function of the proposed distribution is obtained as

$$\phi_X(t) = \frac{\alpha}{(e-1)} \sum_{m=0}^{\infty} \sum_{n=0}^{\infty} \frac{1}{m! n!} \frac{(it)^m}{\beta^m} \frac{(n\alpha + \alpha - 2)!}{(n + \alpha)!} \quad (10)$$

where $i = \sqrt{-1}$.

4.4. Quantile function

The quantile function is useful when generating random observations from a distribution. It can also be utilized in estimating measures of shapes (skewness and kurtosis) when the moments of the random variable do not exist. The p^{th} quantile function of the proposed distribution is obtained as

$$Q(p) = \frac{1}{\beta} \left[\left(1 + \log\left(1 - \frac{p(e-1)}{e}\right) \right)^{\frac{1}{\alpha}} - 1 \right] \quad (11)$$

We can easily find the first, second and third quartile functions after substituting $p = \frac{1}{4}, \frac{1}{2},$ and $\frac{3}{4}$ in Equation (11).

4.5. Order statistic

Order statistics are important for estimating summary statistics such as the minimum, maximum, and range of a data set. They are also used in quality control testing and reliability to forecast failure of future items based on the times of few early failures. Let X_1, X_2, \dots, X_n be a random sample of size n from the proposed distribution and $X_{(1)}, X_{(2)}, \dots, X_{(n)}$ denote the corresponding order statistics. The pdf of the r^{th} order statistic $f_r(x)$ is given by

$$f_r(x) = \frac{n!}{(r-1)!(n-r)!} F^{r-1}(x) [1 - F(x)]^{n-r} f(x),$$

and the pdf of the r^{th} order statistic of our proposed model is obtained as

$$f_r(x) = \frac{n!}{(r-1)!(n-r)!} \frac{\alpha\beta}{(e-1)^n} \sum_{i=0}^{\infty} \sum_{j=0}^{\infty} \sum_{k=0}^{\infty} \frac{(-1)^{i+j}}{j!k!} \binom{r-1}{j} [i(1 - (1 + \beta x)^{-\alpha})]^j (1 + \beta x)^{-(\alpha k + \alpha + 1)} \left(e^{(1 + \beta x)^{-\alpha}} - 1 \right)^{n-r} \quad (12)$$

Substitute $r = 1$ and $r = n$ in Equation (12), we get the pdf of the smallest and the largest order statistics respectively.

The cdf of the r^{th} order statistic is

$$F_r(x) = \sum_{j=r}^n \binom{n}{j} F^j(x) [1 - F(x)]^{n-j},$$

and the cdf $F_r(x)$ of r^{th} order statistic of the new distribution is obtained by using the Equation (3) as,

$$F_r(x) = \sum_{j=r}^n \binom{n}{j} \frac{e^j}{(e-1)^n} \sum_{i=0}^{\infty} \sum_{k=0}^{\infty} \frac{(-1)^{i+k}}{k!} \binom{j}{i} [j(1 - (1 + \beta x)^{-\alpha})]^k (e^{(1+\beta x)^{-\alpha}} - 1)^{n-j}. \quad (13)$$

The cdf of $X_{(1)}$ and $X_{(n)}$ are obtained by putting $r = 1$ and $r = n$ respectively in Equation (13).

5. ORDERING

Stochastic ordering of positive continuous random variables is an important tool for judging the comparative behavior. There are different types of stochastic orderings that are useful in ordering random variables in terms of different properties. Here we consider four different stochastic orders, namely, the usual, the hazard rate, the mean residual life, and likelihood ratio order for KM-Lomax random variables. If X and Y are two random variables with cumulative distribution functions F_X and F_Y , respectively, then X is said to be smaller than Y in the

- stochastic order ($X \leq_{st} Y$) if $F_X(x) \geq F_Y(x)$ for all x
- hazard rate order ($X \leq_{hr} Y$) if $h_X(x) \geq h_Y(x)$ for all x
- mean residual life order ($X \leq_{mrl} Y$) if $m_X(x) \geq m_Y(x)$ for all x
- likelihood ratio order ($X \leq_{lr} Y$) if $\frac{f_X(x)}{f_Y(x)}$ decreases in x

The implication between the ordering is $X \leq_{lr} Y \Rightarrow X \leq_{hr} Y \Rightarrow X \leq_{mrl} Y \Rightarrow X \leq_{st} Y$. The KM-Lomax distribution is ordered with respect to the strongest "likelihood ratio" ordering as shown in the following theorem. It shows the flexibility of the proposed distribution.

Theorem 1. Let $X \sim \text{KML}(\alpha_1, \beta_1)$ and $Y \sim \text{KML}(\alpha_2, \beta_2)$ if $\alpha_1 = \alpha_2 = \alpha$ and $\beta_1 \geq \beta_2$ and if $\beta_1 = \beta_2 = \beta$ and $\alpha_1 \geq \alpha_2$, then $X \leq_{lr} Y$, $X \leq_{hr} Y$, $X \leq_{mrl} Y$ and $X \leq_{st} Y$.

Proof. The likelihood ratio is

$$\frac{f_X(x)}{f_Y(x)} = \frac{\alpha_1 \beta_1 (1 + \beta_1 x)^{-(\alpha_1+1)} e^{(1+\beta_1 x)^{-\alpha_1}}}{\alpha_2 \beta_2 (1 + \beta_2 x)^{-(\alpha_2+1)} e^{(1+\beta_2 x)^{-\alpha_2}}} \quad (14)$$

and

$$\begin{aligned} \log \frac{f_X(x)}{f_Y(x)} &= \log \alpha_1 + \log \beta_1 - (\alpha_1 + 1) \log(1 + \beta_1 x) + (1 + \beta_1 x)^{-\alpha_1} \\ &\quad - \log \alpha_2 - \log \beta_2 + (\alpha_2 + 1) \log(1 + \beta_2 x) - (1 + \beta_2 x)^{-\alpha_2} \end{aligned}$$

thus,

$$\begin{aligned} \frac{d}{dx} \log \frac{f_X(x)}{f_Y(x)} &= -(\alpha_1 + 1) \frac{\beta_1}{1 + \beta_1 x} - \alpha_1 \beta_1 (1 + \beta_1 x)^{-(\alpha_1+1)} \\ &\quad + (\alpha_2 + 1) \frac{\beta_2}{1 + \beta_2 x} + \alpha_2 \beta_2 (1 + \beta_2 x)^{-(\alpha_2+1)} \end{aligned} \quad (15)$$

1. Case I: $\alpha_1 = \alpha_2 = \alpha$, $\beta_1 \geq \beta_2$

$$\frac{d}{dx} \log \frac{f_X(x)}{f_Y(x)} \leq 0 \Rightarrow X \leq_{lr} Y \text{ hence } X \leq_{hr} Y, X \leq_{mrl} Y \text{ and } X \leq_{st} Y.$$

2. Case II: $\beta_1 = \beta_2 = \beta$, $\alpha_1 \geq \alpha_2$

$$\frac{d}{dx} \log \frac{f_X(x)}{f_Y(x)} \leq 0 \Rightarrow X \leq_{lr} Y \text{ hence } X \leq_{hr} Y, X \leq_{mrl} Y \text{ and } X \leq_{st} Y.$$

■

6. ESTIMATION OF THE PARAMETERS OF THE MODEL

In this section we estimate the parameters involved in the distribution using maximum likelihood estimation method. This is one of the most popular methods used for estimation. The likelihood function is defined as,

$$L(x; \lambda) = \prod_{i=1}^n f(x_i, \lambda)$$

In our distribution,

$$L(x; \alpha, \beta) = \left(\frac{\alpha\beta}{e-1} \right)^n \prod_{i=0}^n (1 + \beta x_i)^{-(\alpha+1)} e^{\sum_{i=0}^n (1 + \beta x_i)^{-\alpha}}.$$

The log-likelihood function of the distribution is given by,

$$\log L(x; \alpha, \beta) = -n \log(e-1) + n \log \alpha + n \log \beta - (\alpha+1) \sum_{i=1}^n \log(1 + \beta x_i) + \sum_{i=1}^n (1 + \beta x_i)^{-\alpha}.$$

We proceed as follows. First we find partial derivatives of the log-likelihood function with respect to the parameters α and β . The partial derivatives are

$$\frac{\partial \log L}{\partial \alpha} = \frac{n}{\alpha} - \sum_{i=1}^n \log(1 + \beta x_i) + \sum_{i=1}^n \log(1 + \beta x_i)^{-\alpha} \log(1 + \beta x_i),$$

and

$$\frac{\partial \log L}{\partial \beta} = \frac{n}{\beta} - (\alpha+1) \sum_{i=1}^n \frac{x_i}{1 + \beta x_i} - \alpha \sum_{i=1}^n x_i (1 + \beta x_i)^{-(\alpha+1)}.$$

Two non-linear equations can be obtained by equating these partial derivatives to zero, the solutions for which provide the maximum likelihood estimates of the parameters. The Newton-Raphson method can be used to solve this equation with the help of the available statistical packages. We use R [17] language for finding the numerical solution of the non-linear system of equations.

7. APPLICATION

In this section we are showing the flexibility of the proposed distribution using two real-life data sets. The first data set is the uncensored data set corresponding to intervals in days between 109 successive coal-mining disasters in Great Britain, for the period 1875-1951, published by Maguire et al. [15] and the data set is given in Table 1. The second data set is of Wheaton River obtained from Choulakian and Stephens [4] and presented in Table 2.

We use AIC (Akaike Information Criterion), BIC (Bayesian Information Criterion), HQC (Hannan-Quinn Information Criterion) and K-S (Kolmogorov-Smirnov) test value for the comparison. The distribution which shows minimum AIC, BIC, HQC and K-S test value is the sign of a better fit for the data set. The AIC, BIC and HQC are defined as

$$AIC = -2 \log(\hat{L}) + 2m,$$

$$BIC = -2 \log(\hat{L}) + m \log(n),$$

and

$$HQC = -2 \log(\hat{L}) + 2m \log(\log(n)),$$

where n is the sample size, m is the number of parameters, and \hat{L} is the maximum value of the likelihood function for the considered distribution. Here R [17] language is used for all the computation. We compare the proposed distribution with the following distributions,

Table 1: Flood Level Data.

1	4	4	7	11	13	15	15	17	18	19	19
20	20	22	23	28	29	31	32	36	37	47	48
49	50	54	54	55	59	59	61	61	66	72	72
75	78	78	81	93	96	99	108	113	114	120	120
120	123	124	129	131	137	145	151	156	171	176	182
188	189	195	203	208	215	217	217	217	224	228	233
255	271	275	275	275	286	291	312	312	312	315	326
326	329	330	336	338	345	348	354	361	364	369	378
390	457	467	498	517	566	644	745	871	1312	1357	1613
1630											

Table 2: Wheaton River Data.

1.7	2.2	14.4	1.1	0.4	20.6	5.3	0.7	1.9	13.0
12.0	9.3	1.4	18.7	8.5	25.5	11.6	14.1	22.1	1.1
2.5	14.4	1.7	37.6	0.6	2.2	39.0	0.3	15.0	11.0
7.3	22.9	1.7	0.1	1.1	0.6	9.0	1.7	7.0	20.1
0.4	2.8	14.1	9.9	10.4	10.7	30.0	3.6	5.6	30.8
13.3	4.2	25.5	3.4	11.9	21.5	27.6	36.4	2.7	64.0
1.5	2.5	27.4	1.0	27.1	20.2	16.8	5.3	9.7	27.5
2.5	27.0								

1. DUS-Lomax distribution Deepthi and Chacko [6] with cdf,

$$F(x) = \frac{1}{(e-1)} \left[e^{(1-(1+\theta x)^{-\alpha})} - 1 \right], \quad x > 0, \alpha, \theta > 0$$

2. Lomax distribution Lomax [13] with cdf,

$$F(x) = 1 - (1 + \theta x)^{-\alpha}, \quad x > 0, \alpha, \theta > 0$$

3. KM-Exponential (KME) distribution Kavya and Manoharan [10] with cdf,

$$F(x) = \frac{e}{e-1} [1 - e^{-(1-e^{-\lambda x})}], \quad x > 0, \lambda > 0$$

4. KM-Weibul (KMW) distribution Kavya and Manoharan [10] with cdf,

$$F(x) = \frac{e}{e-1} [1 - e^{-(1-e^{-(x\beta)^\alpha})}], \quad x > 0, \alpha, \beta > 0$$

5. Weibull distribution Weibull [22] with cdf,

$$F(x) = 1 - e^{-(\beta x)^\alpha}, \quad x > 0, \alpha, \beta > 0$$

The values of AIC, BIC, HQC and K-S test for distributions based on the first data set are given in Table 3.

From Table 2, we can see that the new model shows the lowest AIC, BIC and HQC values among all the distributions considered here. The K-S test value of Lomax distribution is smaller than KM-Lomax distribution. In general we can say that our proposed model shows better fit to the data compared to other distributions given in this study. The plot of empirical cdf along with other cdf of the distributions for the first data set is given in Fig. 3. for a better understanding of

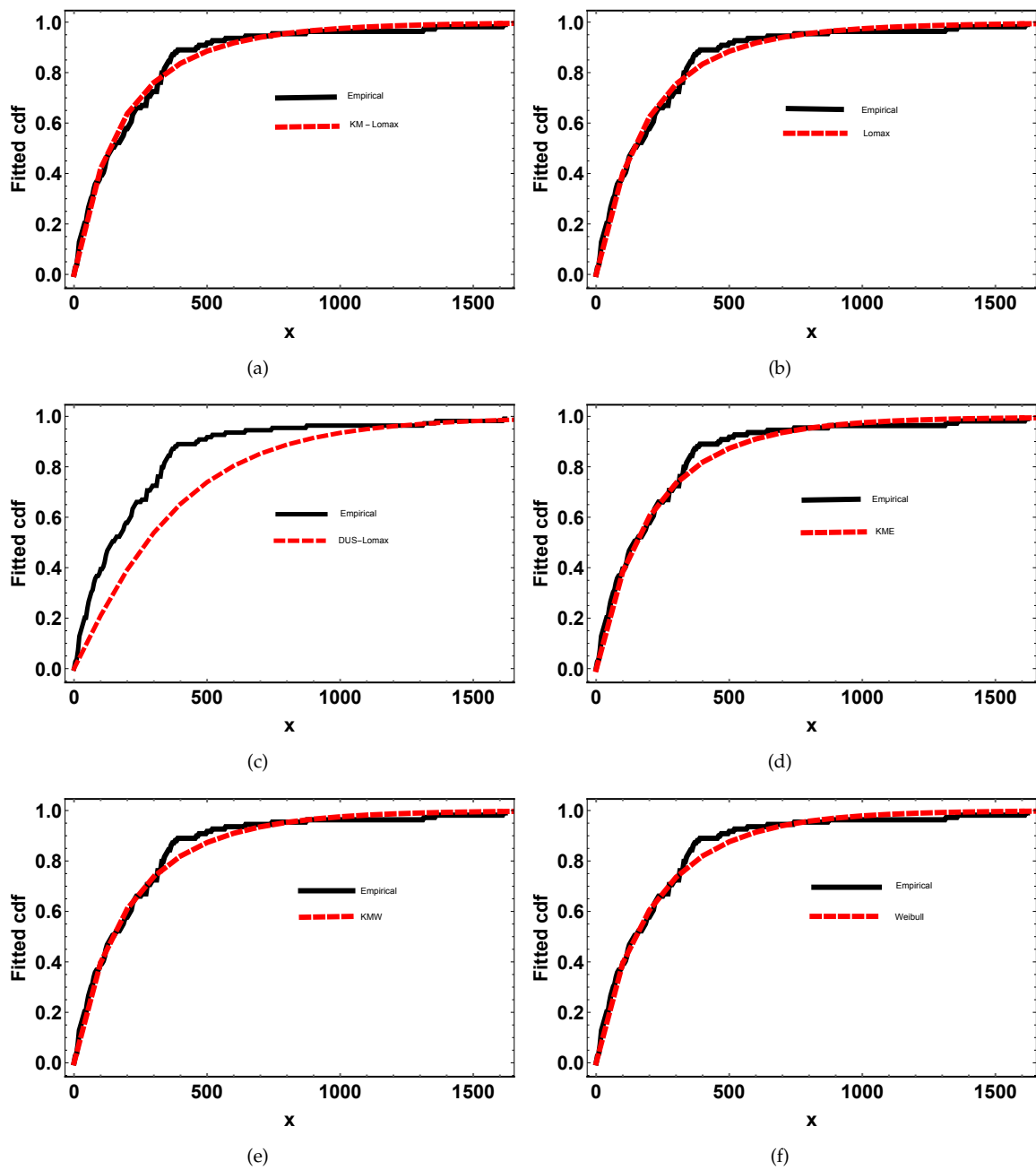


Figure 3: Comparison plot for the first data set.

the result. Compared to the distributions mentioned in Mahdavi [14] for this particular data set, the proposed model gives better result.

The comparison table of the considered models for the second data set is given in Table 4.

Based on the AIC, BIC and HQC values, we can conclude that the proposed model gives the best fit to the data set compared to other Lomax, KM family and Weibull distributions considered here. The K-S test value of the KMW distribution is slightly lower than the KM-Lomax distribution. The empirical and fitted cdf plot of distributions considered for the comparison for the second data set is given in Fig. 4.

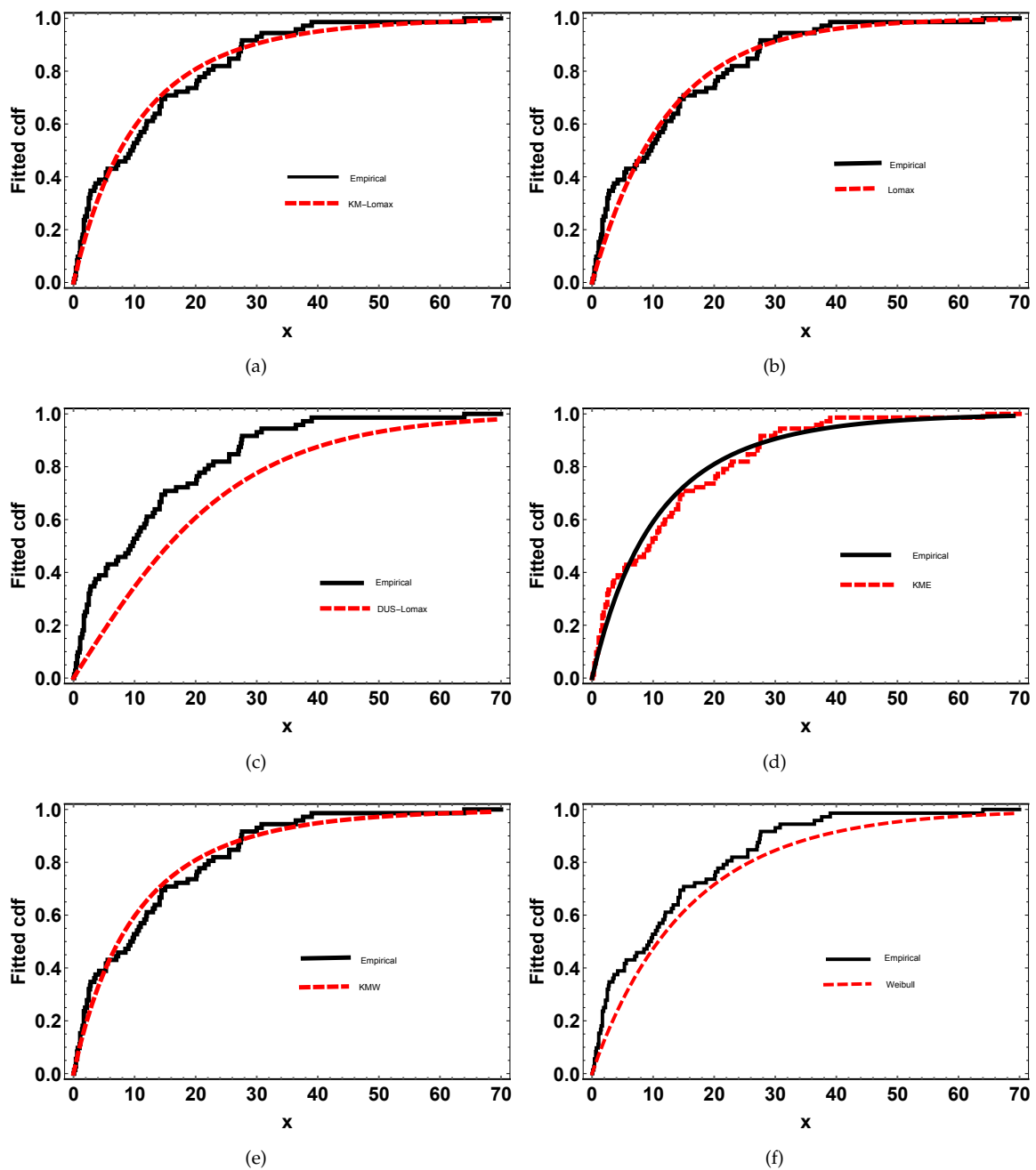


Figure 4: Comparison plot for the second data set.

8. CONCLUSIONS

In the present work, we introduce a new modified Lomax distribution using KM transformation. The main advantage of the new model is that which is parsimonious in parameter. So we can use the model more conveniently. The behavior of the hazard rate function is studied and the shape of the hazard function is shown both graphically and theoretically. Some of properties of the new model like moments, mgf, characteristic function, quantile function and order statistics are derived. stochastic ordering of the KM Lomax distribution is discussed and established the condition for the stronger mode of ordering viz likelihood ratio. We consider two real data sets to

Table 3: Maximum likelihood (ML) estimates, K-S test value, AIC, BIC, and HQC of the fitted models.

Model	ML estimates	K-S value	AIC	BIC	HQC
KM-Lomax	$\hat{\alpha} = 9.4097, \hat{\beta} = 0.0004$	0.0720	1040.647	1046.03	1042.83
DUS-Lomax	$\hat{\alpha} = 9.4008, \hat{\theta} = 0.0004$	0.2703	1187.936	1193.319	1190.119
Lomax	$\hat{\alpha} = 4.9251, \hat{\theta} = 0.0011$	0.0642	1405.426	1410.809	1407.609
KME	$\hat{\lambda} = 0.0033$	0.0761	1404.864	1407.555	1405.955
KMW	$\hat{\alpha} = 0.9685, \hat{\beta} = 0.0033$	0.0772	1406.654	1412.037	1408.837
Weibull	$\hat{\alpha} = 0.8848, \hat{\beta} = 0.0046$	0.0784	1407.545	1412.927	1409.728

Table 4: Maximum likelihood (ML) estimates, K-S test value, AIC, BIC, and HQC of the fitted models.

Model	ML estimates	K-S value	AIC	BIC	HQC
KM-Lomax	$\hat{\alpha} = 243.7254, \hat{\beta} = 0.000258$	0.11	286.6547	291.2081	288.4674
DUS-Lomax	$\hat{\alpha} = 251.4388, \hat{\theta} = 0.00025$	0.24	364.0633	368.6166	365.876
Lomax	$\hat{\alpha} = 80.7719, \hat{\theta} = 0.00102$	0.14	508.2621	512.8155	510.0748
KME	$\hat{\lambda} = 0.0632$	0.11	506.025	508.3017	506.9313
KMW	$\hat{\alpha} = 0.9722, \hat{\beta} = 0.0633$	0.10	507.9317	512.4851	509.7444
Weibull	$\hat{\alpha} = 0.9012, \hat{\beta} = 0.08597$	0.11	506.9973	511.5506	508.81

show the suitability of the model. The proposed model shows better fit to the data sets compared to other models in the literature. We can conclude that the proposed model can be used as a useful lifetime model for decreasing failure rate.

REFERENCES

- [1] Al-Zahrani, B., Al-Sobhi, M. (2013). On parameters estimation of Lomax distribution under general progressive censoring. *Journal of Quality and Reliability Engineering*, vol. 2013, Article ID 431541.
- [2] Al-Zahrani, B., Sagor, H. (2014). The Poisson-Lomax distribution. *Revista Colombiana de Estadística*, vol. 37, no. 1, pp. 225-245.
- [3] Ashour, S. K., Eltehiwy, M. A. (2013). Transmuted lomax distribution. *American Journal of Applied Mathematics and Statistics*, vol. 1, no. 6, pp. 121-127.
- [4] Choulakian, V., Stephens, M. A. (2001). Goodness-of-fit for the generalized Pareto distribution. *Technometrics*, 43:478-484.
- [5] Cordeiro, G.M., Ortega, E.M.M., Popovi'c, B. V. (2015). The gamma-Lomax distribution. *Journal of Statistical Computation and Simulation*, vol. 85, no. 2, pp. 305-319.
- [6] Deepthi, K. S., Chacko, V. M. (2020). An upside-down bathtub-shaped failure rate model using a dus transformation of lomax distribution. *Stochastic Models in Reliability Engineering*, 1st Edition, CRC Press.
- [7] El-Bassiouny, A. H., Abdo, N. F., Shahen, H. S. (2015). Exponential lomax distribution. *International Journal of Computer Applications*, vol. 121, no. 13, pp. 24-29.
- [8] Glaser, R. E. (1980). Bathtub and related failure rate characterizations. *Journal of American Statistical Association*, 75:667-672.
- [9] Hassan, A., Al-Ghamdi, A. (2009). Optimum step stress accelerated life testing for Lomax distribution. *Journal of Applied Sciences Research*, vol. 5, pp. 2153-2164.
- [10] Kavya, P., Manoharan, M. (2021). Some parsimonious models for lifetimes and applications. *Journal of Statistical Computation and Simulation*, vol. 91, no. 18, 3693-3708.
- [11] Kilany, N.M. (2016). Weighted Lomax distribution. *SpringerPlus*, vol. 5, no. 1, article no. 1862.

- [12] Lemonte, A. J., Cordeiro, G. M. (2013). An extended Lomax distribution *A Journal of Theoretical and Applied Statistics*, vol. 47, no. 4, pp. 800-816.
- [13] Lomax, K. S. (1954). Business failures: another example of the analysis of failure data. *Journal of the American Statistical Association*, vol. 49, no. 268, pp. 847-852.
- [14] Mahdavi, A., Kundu, D. (2016): A new method for generating distributions with an application to exponential distribution. *Communications in Statistics - Theory and Methods*
- [15] Maguire, B. A., Pearson, E., and Wynn, A. (1952). The time intervals between industrial accidents. *Biometrika*, 168-180.
- [16] Oguntunde, P. E., Khaleel, M. A., Ahmed, M. T., Adejumo, A. O., Odetunmbi, O. A. (2017). A new generalization of the lomax distribution with increasing, decreasing, and constant failure rate. *Modelling and Simulation in Engineering*, Volume 2017, Article ID 6043169.
- [17] R Core Team (2019). R: A language and environment for statistical computing. R Foundation for Statistical Computing, Vienna, Austria.
- [18] Rady, E.-H. A., Hassanein, W. A., Elhaddad, T. A. (2016). The power Lomax distribution with an application to bladder cancer data. *SpringerPlus*, vol. 5, 1838 pages.
- [19] Salem, H. M. (2014). The exponentiated lomax distribution: different estimation methods. *American Journal of Applied Mathematics and Statistics*, vol. 2, no. 6, pp. 364-368.
- [20] Shams, T. M. (2013). The kumaraswamy-generalized lomax distribution. *Middle-East Journal of Scientific Research*, 17 (5): 641-646.
- [21] Tahir, M. H., Cordeiro, G. M., Mansoor, M., Zubair, M. (2015). The weibull-lomax distribution: properties and applications. *Hacetatepe Journal of Mathematics and Statistics*, vol. 44, no. 2, pp. 461-480.
- [22] Weibull, W. (1951). A statistical distribution function of wide applicability. *Journal of Applied Mechanics*, 293-297.
- [23] Wolfram Research, Inc. (2016). Mathematica, Version 11.0. Champaign, Illinois.

A New Life Time Distribution: Burr III Modified Weibull Distribution And Its Application in Burn in Process

DEEPTHY G S¹, NICY SEBASTIAN¹



¹Department of Statistics, St. Thomas College (Autonomous) Thrissur, Kerala - 680 001 (India)
deepthygs@gmail.com,nicycms@gmail.com

Abstract

In burn-in analysis, models with a bathtub-shaped hazard rate and a bimodal density function are inevitable. This work focusses on a new five parameter distribution called Burr III Modified Weibull distribution which can be used to design burn-in procedures and preventative maintenance for incurable devices. The statistical properties such as quantile function, hazard rate function and order statistics have been discussed. The model parameters are estimated using the maximum likelihood estimation technique, and the performance of the proposed model is evaluated using the simulation technique. Finally, a real data set is presented to demonstrate the model's utility and its application in the burn-in process.

Keywords: Burr III distribution, Modified Weibull distribution, maximum likelihood estimation.

1. INTRODUCTION

In lifetime analysis, one is often interested to know about the reasons for the failure of a system or component. The different ways through which a system or product may fail is known as competing risk. Some normal reasons for the failures are material defects, imperfection of manufacturing process, wear out processes etc. Here comes the importance of burn-in process in reliability. Burn-in is an important technique for detecting and eliminating early fault, thereby increasing system reliability. It is used to find the defective units before they reach the customers. Items that survive burn-in period ensure the product quality. Burn-in must have a high failure rate in the early stages of life in order to be successful. This characteristic is mainly found in a class of life time distributions with bathtub-shaped failure rates. In the modelling of the lifetime of a system, distributions with bathtub-shaped failure rates are preferred. The bathtub curve has three phases: an infant mortality phase (decreasing failure rate), a normal life phase (constant failure rate), and a wear-out phase (increasing failure rate). The necessary condition in distribution of lifetime of system is bathtub hazard rate and sufficient condition is bimodal density function. That is, a model with bathtub hazard rate function and a bimodal density function allows designing burn-in procedures and preventive maintenance of malfunctioning devices. The goal of this study is to create a new reliability distribution that meets both the necessary and sufficient conditions of the lifetime of system. The important works related to this are reliability enhancement through optimal burn-in by Way K [22], a new model in relation to burn-in of components and its consequences are discussed by Mølltoft [8], the burn-in problems by Lawrence [12] and Chandrasekaran [5]. Park [17] learned about the impact of burn-in on the average residual life.

In reliability analysis, lifetime distributions has an importance because of its ability to explain the nature of data and its properties. For analysing lifetime data, one often consider Weibull distribution. But one of the disadvantage of Weibull distribution is that it possess only monotone hazard rates not non-monotone hazard rates. Hence it cannot be used in the case of lifetime data possessing bathtub hazard rates. To overcome this problem, several new models were

proposed such as three parameter modified Weibull distribution introduced by Lai et al. [11], a four-parameter generalisation of the Weibull distribution that can simulate a bathtubshaped hazard rate function by Carrasco et al. [4], a modification is given to weibull distribution which exhibit non monotone behavior by Sarhan et al. [19], beta modified Weibull distribution introduced by Silva et al. [20], extended flexible Weibull distribution by Bebbington et.al. [1]. Khan [15] introduced another flexible distribution called modified beta Weibull distribution etc. Among which modified Weibull proposed by Lai et al. [11] seems to be more flexible than other proposed ones. Another important life time distribution that we consider in our study is Burr III distribution. In 1942, Burr introduced twelve types of cumulative distribution function based on the Pearson system of distributions among which Burr XII and Burr III are commonly used. The Burr type III distribution is used in a variety of domains, including survival and reliability research, forestry, and environmental studies etc. BurrIII is the inverse of BurrXII distribution. Burr III distribution is also known as dagum distribution studies on the wealth of distribution [6] and as kappa distribution in the meteorological literature [14]. Many modification of Burr III have been already intoduced such as Burr and Cislak [3], Johnson et al. [9] etc. This distribution has a wide range of applications in statistical modelling, including forestry by Gove et al. [7], meteorological field Mielke [14] and actuarial literature Kleiber [10] etc.

Using the concept of competing risk model, a new five parameter distribution called Burr III Modified Weibull (BIIIMW) is proposed in this paper. If we model lifetime of units subjecting to two risk as series system, then the life time of the observed unit is the minimum of the individual potential lifetimes associated with each risk (see [23]). That is the realibility function of the BIIIMW model is the product of the reliability function of Burr III and Modified Weibull distribution. This model exhibits both bathtub hazard function and bimodal density function, which are commonly present when dealing with survival and lifetime data, and it can also be utilised in burn-in procedures.

The cumulative distribution function (cdf) of the modified Weibull (MW) distribution proposed by Lai is given by,

$$F_{MW}(x; \alpha, \beta, \lambda) = 1 - e^{-\alpha x^\beta e^{\lambda x}}; x \geq 0, \alpha > 0, \beta > 0, \lambda \geq 0. \quad (1)$$

where α is the scale parameter, β is the shape parameter and λ is the accelerating factor in the time of imperfection and a factor of fragility in the individual's survival as time increases. The cumulative distribution (cdf) of the Burr III distribution is given by,

$$G_B(x; c, k) = (1 + x^{-c})^{-k}; x \geq 0, k > 0, c > 0. \quad (2)$$

where c and k are shape parameters.

2. PROPOSED DISTRIBUTION

The concept of competing risk model is used to create the new Burr III Modified Weibull distribution (BIIIMW). Realibility function of the model is the product of reliability functions of Burr III and Modified Weibull distributions. The realibility function, cumulative distribution function and probability density function of the Burr III modified Weibull distribution (BIIIMW) are respectively given by,

$$\begin{aligned} r(x, c, k, \alpha, \beta, \lambda) &= e^{-\alpha x^\beta e^{\lambda x}} \left(1 - (1 + x^{-c})^{-k}\right) \quad x \geq 0, c > 0, k > 0, \alpha > 0, \beta > 0, \lambda \geq 0, \\ F(x, c, k, \alpha, \beta, \lambda) &= 1 - e^{-\alpha x^\beta e^{\lambda x}} \left(1 - (1 + x^{-c})^{-k}\right), \quad x \geq 0, c > 0, k > 0, \alpha > 0, \beta > 0, \lambda \geq 0 \end{aligned} \quad (3)$$

and

$$f(x, c, k, \alpha, \beta, \lambda) = \begin{cases} e^{-\alpha x^\beta e^{\lambda x}} \left[c k x^{-c-1} (1 + x^{-c})^{-k-1} + \left(1 - (1 + x^{-c})^{-k} \right) \alpha x^{\beta-1} e^{\lambda x} (\beta + \lambda x) \right], & \text{for } x \geq 0, c > 0, k > 0, \alpha > 0, \beta > 0, \lambda \geq 0. \\ 0, & \text{otherwise.} \end{cases} \quad (4)$$

Where α is the scale parameter. β, c, k are the shape parameters and λ is the accelerating factor in the imperfection time and a factor of fragility increases.

Plot of the density function of BIIMW distribution is given in Figure 1. The figures shows that

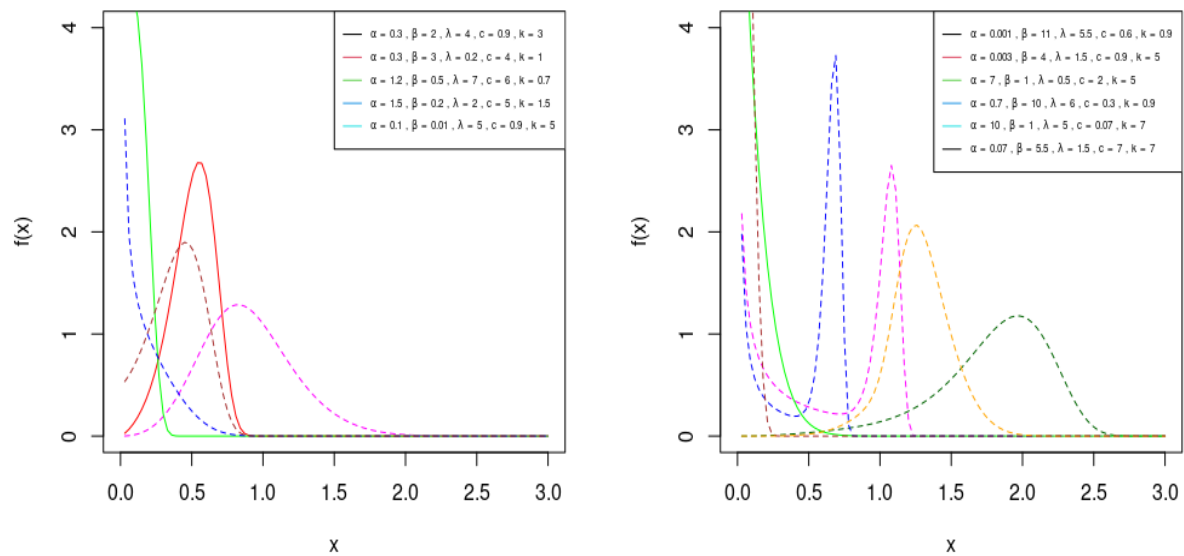


Figure 1: Probability density functions of the BIIMW distribution for different parameteric values.

the the BIIMW distribution can be decreasing, positively skewed, negatively skewed, unimodal and bimodal for selected values of parameters.

The particular case of the BIIMW distribution is included in Table 1.

Table 1: Special cases of BIIMW distribution

Parameters	Distribution
$\alpha = 0$	BurrIII
$c=1, \alpha = 0$	Inverse Lomax
$\lambda = 0$	BurrIII-Weibull
$\lambda = 0, \beta = 1$	BurrIII-Exponential
$\lambda = 0, \beta = 2$	BurrIII-Rayleigh
$c=1$	Inverse Lomax-Modified Weibull
$c=1, \lambda=0, \beta=1$	Inverse Lomax-Exponential

3. RELIABILITY ANALYSIS

The hazard and reverse hazard function of the BIIMW distribution is obtained respectively, as follows

$$h(x) = \frac{ckx^{-c-1}(1+x^{-c})^{-k-1} + (1 - (1+x^{-c})^{-k})\alpha x^{\beta-1}e^{\lambda x}(\beta + \lambda x)}{(1 - (1+x^{-c})^{-k})} \quad (5)$$

and

$$t(x) = \frac{e^{-\alpha x^{\beta}}e^{\lambda x} [ckx^{-c-1}(1+x^{-c})^{-k-1} + (1 - (1+x^{-c})^{-k})\alpha x^{\beta-1}e^{\lambda x}(\beta + \lambda x)]}{1 - [e^{-\alpha x^{\beta}}e^{\lambda x} (1 - (1+x^{-c})^{-k})]}. \quad (6)$$

Plot of the hazard function for selected values of BIIMW parameters are shown in Figure (2). The shape of the hazard function shows that BIIMW distribution can accommodate both monotone and non monotone behavior such as monotonically decreasing, monotonically increasing, unimodal and bathtub shapes for different values of the parameters, which are more likely to be meet when dealing with survival and lifetime data.

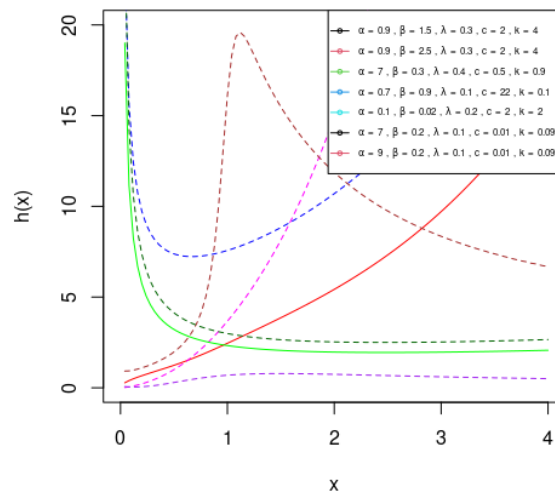


Figure 2: Plot for hazard rate functions of BIIMW distribution.

4. THE STATISTICAL PROPERTIES

In this section, some statistical properties of BIIMW distribution such as quantile function and order statistics are discussed.

4.1. Quantile Function

The quantile function of the BIIMW distribution is obtained by solving the non-linear equation, that is $F_{BIIMW}(x) = u, 0 \leq u \leq 1$.

$$1 - e^{-\alpha x^{\beta}}e^{\lambda x} (1 - (1+x^{-c})^{-k}) = u,$$

$$e^{-\alpha x^{\beta}}e^{\lambda x} (1 - (1+x^{-c})^{-k}) = 1 - u.$$

Taking logarithm on both sides we have,

$$\log \left(1 - (1 + x^{-c})^{-k} \right) - \alpha x^\beta e^{\lambda x} - \log(1 - u) = 0. \tag{7}$$

The quantile values of the BIIMW distribution can be obtained by solving the equation (7) using numerical methods, where u denotes a uniformly distributed random variable on the interval [0,1]. Table 2 describe the quantile values of BIIMW distribution for certain given parameter values.

Table 2: BIIMW quantile values for selected parameters

u	(c,k,α,β,λ)				
	(3,2,0.7,0.4,2)	(3,2,1,2,2)	(0.7,1,0.5,2,4)	(1,0.5,3,4,3)	(0.7,0.4,0.4,0.6,0.8)
0.1	0.00844	0.25199	0.04266	0.01010	0.000244
0.2	0.04566	0.33641	0.12545	0.04167	0.00274
0.3	0.10799	0.39880	0.22052	0.09871	0.01134
0.4	0.18256	0.45172	0.30147	0.18620	0.03183
0.5	0.26241	0.50027	0.36646	0.28989	0.07354
0.6	0.34600	0.54755	0.42171	0.37356	0.15240
0.7	0.43513	0.59646	0.47254	0.43637	0.29609
0.8	0.53557	0.65143	0.52404	0.49053	0.55078
0.9	0.66521	0.72343	0.58525	0.54787	0.99652

4.2. Order Statistics

Order statistics have a wide application in realibility. Let X_1, X_2, \dots, X_n be a simple random sample from BIIMW distribution with cdf and pdf given in (3) and (4), respectively. Let $X_{(1)} \leq X_{(2)} \leq \dots \leq X_{(n)}$ denote the order statistics. Then the pdf of i^{th} order statistc is given by,

$$f_{X_i}(x) = \frac{n!f(x)}{(i-1)!(n-i)!} [F(x)]^{i-1} [1-F(x)]^{n-i}.$$

$$f_{X_i}(x) = \frac{n!}{(i-1)!(n-i)!} e^{-\alpha x^\beta e^{\lambda x}} [ckx^{-c-1} (1+x^{-c})^{-k-1} + (1 - (1+x^{-c})^{-k}) \alpha x^{\beta-1} e^{\lambda x} (\beta + \lambda x)] \\ * \left[1 - e^{-\alpha x^\beta e^{\lambda x}} (1 - (1+x^{-c})^{-k}) \right]^{i-1} * \left[e^{-\alpha x^\beta e^{\lambda x}} (1 - (1+x^{-c})^{-k}) \right]^{n-i}.$$

The pdf of 1^{st} order statistic X_1 is given by,

$$f_{X_1}(x) = ne^{-\alpha x^\beta e^{\lambda x}} [ckx^{-c-1} (1+x^{-c})^{-k-1} + (1 - (1+x^{-c})^{-k}) \alpha x^{\beta-1} e^{\lambda x} (\beta + \lambda x)] \\ * \left[e^{-\alpha x^\beta e^{\lambda x}} (1 - (1+x^{-c})^{-k}) \right]^{n-1}.$$

The pdf of n^{th} order statistic X_n is given by,

$$f_{X_n}(x) = ne^{-\alpha x^\beta e^{\lambda x}} [ckx^{-c-1} (1+x^{-c})^{-k-1} + (1 - (1+x^{-c})^{-k}) \alpha x^{\beta-1} e^{\lambda x} (\beta + \lambda x)] \\ * \left[1 - e^{-\alpha x^\beta e^{\lambda x}} (1 - (1+x^{-c})^{-k}) \right]^{n-1}.$$

5. MAXIMUM LIKELIHOOD ESTIMATION

In this section, we consider the estimation of unknown parameters of BIIMW model using maximum lilelihood estimation technique. Let x_1, x_2, \dots, x_n be a random sample from BIIMW

distribution having parameters $\Delta=(c, k, \alpha, \beta, \lambda)^T$ then the log likelihood function is given by,

$$l(x; c, k, \alpha, \beta, \lambda) = \sum_{i=1}^n \ln (f(x_i, c, k, \alpha, \beta, \lambda)). \quad (8)$$

The log likelihood of a single observation x of X is given by,

$$l(x; c, k, \alpha, \beta, \lambda) = -\alpha x^\beta e^{\lambda x} + \ln \left[c k x^{-c-1} (1+x^{-c})^{-k-1} + \left(1 - (1+x^{-c})^{-k}\right) \alpha x^{\beta-1} e^{\lambda x} (\beta + \lambda x) \right]. \quad (9)$$

The first order derivatives of the log-likelihood function with respect to the parameters $\Delta=(c, k, \alpha, \beta, \lambda)^T$ is given by,

$$\frac{\partial l}{\partial \alpha} = \frac{\left[1 - (1+x^{-c})^{-k}\right] (\lambda x^\beta e^{\lambda x} + \beta x^{\beta-1} e^{\lambda x})}{c k x^{-c-1} (1+x^{-c})^{-k-1} + \left[1 - (1+x^{-c})^{-k}\right] (\alpha \lambda x^\beta e^{\lambda x} + \alpha \beta x^{\beta-1} e^{\lambda x})} - x^\beta e^{\lambda x}. \quad (10)$$

$$\frac{\partial l}{\partial \beta} = \frac{\left[1 - (1+x^{-c})^{-k}\right] (\alpha e^{\lambda x} (x^{\beta-1} \ln(x) \beta + x^{\beta-1}) + \alpha \lambda x^\beta e^{\lambda x} \ln(x))}{c k x^{-c-1} (1+x^{-c})^{-k-1} + \left[1 - (1+x^{-c})^{-k}\right] (\alpha \lambda x^\beta e^{\lambda x} + \alpha \beta x^{\beta-1} e^{\lambda x})} - \alpha x^\beta e^{\lambda x} \ln(x). \quad (11)$$

$$\frac{\partial l}{\partial \lambda} = \frac{\left[1 - (1+x^{-c})^{-k}\right] (\alpha x^\beta (x \lambda e^{x \lambda} + e^{x \lambda}) + \alpha \beta x^\beta e^{x \lambda})}{c k x^{-c-1} (1+x^{-c})^{-k-1} + \left[1 - (1+x^{-c})^{-k}\right] (\alpha \lambda x^\beta e^{\lambda x} + \alpha \beta x^{\beta-1} e^{\lambda x})} - \alpha x^{\beta+1} e^{x \lambda}. \quad (12)$$

$$\frac{\partial l}{\partial c} = \frac{k \left(-x^{-c-1} \ln(x) (1+x^{-c})^{-k-1} c + c(k+1) x^{-2c-1} \ln(x) (1+x^{-c})^{-k-2} + x^{-c-1} (1+x^{-c})^{-k-1}\right) - A}{c k x^{-c-1} (1+x^{-c})^{-k-1} + \left[1 - (1+x^{-c})^{-k}\right] (\alpha \lambda x^\beta e^{\lambda x} + \alpha \beta x^{\beta-1} e^{\lambda x})}. \quad (13)$$

where,

$$A = \frac{k (\alpha \lambda x^\beta e^{\lambda x} + \alpha \beta x^{\beta-1} e^{\lambda x}) \ln(x) (1+x^{-c})^{-k-1}}{x^c}.$$

$$\frac{\partial l}{\partial k} = \frac{c x^{-c-1} B + (\alpha \lambda x^\beta e^{\lambda x} + \alpha \beta x^{\beta-1} e^{\lambda x}) \ln(1+x^{-c}) (1+x^{-c})^{-k}}{c k x^{-c-1} (1+x^{-c})^{-k-1} + \left[1 - (1+x^{-c})^{-k}\right] (\alpha \lambda x^\beta e^{\lambda x} + \alpha \beta x^{\beta-1} e^{\lambda x})}, \quad (14)$$

where $B = (1+x^{-c})^{-k-1} [1 - \ln(1+x^{-c}) k]$.

The total log-likelihood function of BIIMW distribution based on a random sample of size n (x_1, x_2, \dots, x_n) is given by $l(\Delta)=\sum_{i=1}^n l_i(\Delta)$ where $l_i(\Delta)$ ($i=1, 2, \dots, n$) is the log-likelihood of i^{th} observation. By setting the above partial derivatives to zero, the solution will yield the maximum likelihood estimators of \hat{c} , \hat{k} , $\hat{\alpha}$, $\hat{\beta}$ and $\hat{\lambda}$. These equations can be solved by using Newton-Raphson method. All the second order derivatives are exist for BIIMW distribution. Then the observed information matrix is given by,

$$V^{-1} = -E \begin{pmatrix} V_{cc} & V_{ck} & V_{c\alpha} & V_{c\beta} & V_{c\lambda} \\ V_{kc} & V_{kk} & V_{k\alpha} & V_{k\beta} & V_{k\lambda} \\ V_{\alpha c} & V_{\alpha k} & V_{\alpha\alpha} & V_{\alpha\beta} & V_{\alpha\lambda} \\ V_{\beta c} & V_{\beta k} & V_{\beta\alpha} & V_{\beta\beta} & V_{\beta\lambda} \\ V_{\lambda c} & V_{\lambda k} & V_{\lambda\alpha} & V_{\lambda\beta} & V_{\lambda\lambda} \end{pmatrix}^{-1}. \quad (15)$$

Here V_{jj} , $j=c, k, \alpha, \beta, \lambda$ denotes the second order derivatives of log-likelihood function with respect to the parameters and $E(\cdot)$ denotes the expected value. The asymptotic variance and co-variances of these maximum likelihood estimators for \hat{c} , \hat{k} , $\hat{\alpha}$, $\hat{\beta}$ and $\hat{\lambda}$ can be obtained by solving this observed information matrix. From (15), the $100(1-\zeta)\%$ confidence intervals for the parameters are approximately given as follows,

$$\hat{c} \pm Z_{\zeta/2} \sqrt{\hat{V}_{cc}}, \hat{k} \pm Z_{\zeta/2} \sqrt{\hat{V}_{kk}}, \hat{\alpha} \pm Z_{\zeta/2} \sqrt{\hat{V}_{\alpha\alpha}}, \hat{\beta} \pm Z_{\zeta/2} \sqrt{\hat{V}_{\beta\beta}}, \hat{\lambda} \pm Z_{\zeta/2} \sqrt{\hat{V}_{\lambda\lambda}}.$$

where $Z_{\zeta/2}$ is the upper ζ^{th} percentile of the standard normal distribution.

6. SIMULATION AND DATA ANALYSIS

In this section, we consider the simulation of BIIMW distribution. Parameters are estimated by using optim CG method in R. We simulate 1000 samples for the true parameters values I : $c = 8.5, k = 6, \alpha = 2, \beta = 5, \lambda = 0.8$ and II: $c=2, k=9, \alpha=0.5, \beta=9, \lambda=1.5$. Table 3 lists the means of the MLE estimates, bias and RMSE. From the table, it is obvious that as the sample size grows, estimates approach the true value of the parameter, whereas bias and RMSE decrease as expected.

Table 3: Simulation Results: Mean Estimates, Bias and MSE of BIIMW distriburion.

Sample Size	Parameter	I			II		
		Mean	Bias	RMSE	Mean	Bias	RMSE
n=200	c	7.8901	-0.6098	0.7106	2.0048	0.0048	0.0070
	k	7.6779	1.6779	1.8808	9.0031	0.0031	0.0036
	α	2.2418	0.2418	1.5350	0.2244	-0.2755	0.2783
	β	7.7369	2.7369	2.9288	9.9856	0.9856	1.0549
	λ	0.3435	0.2435	0.866	2.3495	0.8495	0.8946
n=500	c	7.9066	-0.5933	0.6594	2.0045	0.0045	0.0059
	k	7.6698	1.6698	1.7860	9.0028	0.0028	0.0032
	α	1.8931	-0.1068	1.094	0.2281	-0.2734	0.2780
	β	7.6866	2.6866	2.786	9.9638	0.9667	0.9752
	λ	0.3193	0.2193	0.6565	2.3398	0.8398	0.8577
n=800	c	8.0117	-0.4882	0.568	2.0042	0.0042	0.0052
	k	7.3521	1.3521	1.5066	9.0025	0.0025	0.0026
	α	1.9233	-0.0766	0.3474	0.2286	-0.2712	0.2751
	β	7.6809	2.6809	2.7521	9.9581	0.9581	0.9925
	λ	0.3089	0.2089	0.4682	2.3216	0.8276	0.8396

6.1. Data Analysis

We evaluate a data set in this part to demonstrate the importance and flexibility of the BIIMW distribution and comparison is done with other well known distributions such as Burr III, modified Weibull, inverse Lomax, exponentiated Weibull and Rayleigh(BIII, MW, IL, EW, R). The data is obtained from Sylwia ([21]) on the lifetime of a certain device (30 device).

Data set : 0.0094, 0.05, 0.4064, 4.6307, 5.1741, 5.8808, 6.3348,7.1645, 7.2316, 8.2604, 9.2662, 9.3812, 9.5223, 9.8783, 9.9346, 10.0192, 10.4077,10.4791, 11.076, 11.325, 11.5284, 11.9226, 12.0294, 12.074, 12.1835, 12.3549, 12.5381, 12.8049, 13.4615, 13.853.

The estimated values of the parameters, Akaike Information Criterion, Bayesian Information Criterion are presented. Also presented Kolmogorov-Smirnov(KS) (its p value), Cramer-Von Mises(W) and Anderson-Darling (A) statistic for hypothesis test. Goodness of fit is performed to test whether the proposed model fits better to the real data sets. In general, the distribution with smallest values of these statistics better fits for the data. Table 4 list the MLE's of model parameters of BIIMW, BIII, MW, EW, IL, R and the statistics values of W, A and KS.

Table 4: Goodness of fit of Dataset

Model	Estimates		W	A	KS	P value	AIC	BIC
	Parameters	Estimates						
BIIMW	c	2.693	0.076	0.585	0.124	0.692	156.0103	180.0223
	k	1920.256						
	α	0.0202						
	β	0.2089						
	λ	0.3164						
BIII	c	0.6941	1.295	6.373	0.367	0.00038	231.1692	240.774
MW	k	2.564	0.118	1.258	0.154	0.428	233.1692	247.5763
	α	3.797						
	λ	0.021						
EW	β	0.0001	6.200	1.250	0.348	0.0009	213.734	223.339
	α	0.396						
IL	β	4.658	1.046	5.277	0.357	0.0006	215.5066	225.1113
	α	0.9301						
R	β	8.432	0.456	3.652	0.257	0.030	213.5066	218.3089
	α	6.935						

From the table 4, it is clear that BIIMW distribution has the smallest values for these statistics, hence the proposed model is regarded as the better one. The variance-covariance matrix after substituting the unknown parameters of the MLE's in (15), we get,

$$\begin{pmatrix} 0.00560 & -0.012635 & -0.000049 & 0.001199 & 0.00162 \\ -0.01263 & 0.71116 & 0.00062 & -0.08420 & -0.00695 \\ -0.00004 & 0.00062 & 0.00001 & -0.00428 & 0.00018 \\ 0.00119 & -0.08420 & -0.00428 & 1.56465 & -0.14485 \\ 0.00162 & -0.00695 & 0.00018 & -0.14485 & 0.02210 \end{pmatrix}$$

and the corresponding 95% confidence interval is given by $c \in (2.693 \pm 1.96 * 0.0748)$, $k \in (1920.256 \pm 1.96 * 0.8433)$, $\alpha \in (0.0202 \pm 1.96 * 0.0031)$, $\beta \in (0.2089 \pm 1.96 * 1.2508)$ and $\lambda \in (0.3164 \pm 1.96 * 0.1486)$. Plot of the fitted densities, histogram of the data and pp plot of the real data set is shown in figure (3).

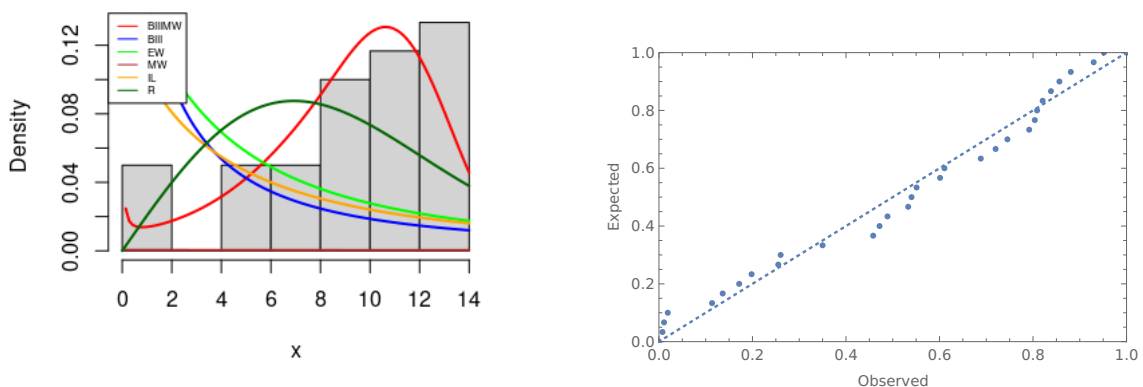


Figure 3: (a) Plot of the estimated pdfs over the histogram and (b) PP plot of the BIIMW model for dataset.

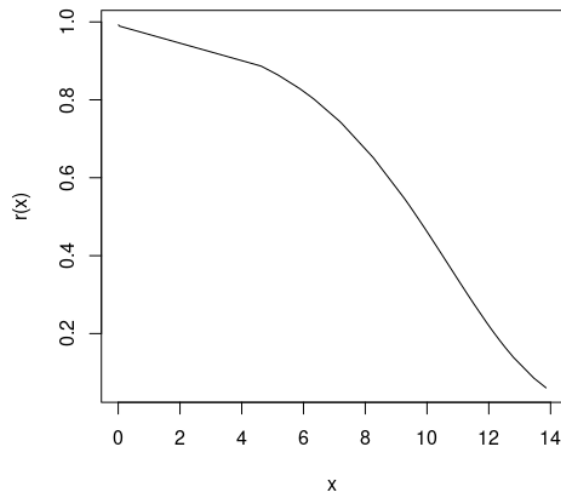


Figure 4: Survival plot of BIIMW distribution with the estimated parameter values.

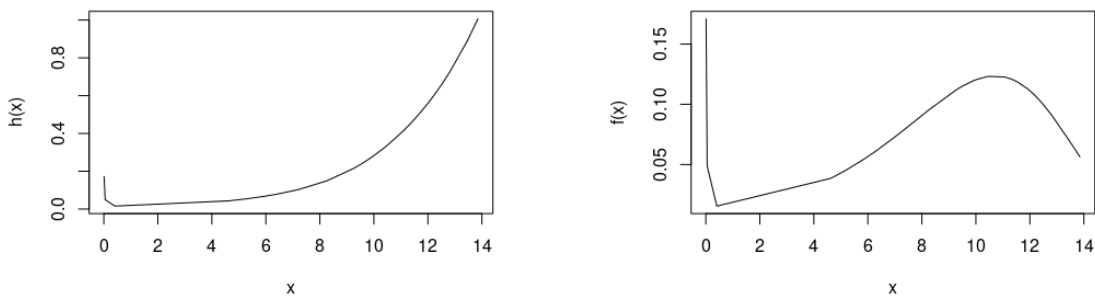


Figure 5: (a) The expected parameter values for the BIIMW distribution hazard rate function (b) The BIIMW density function for the estimated parameter values.

Figure (4) describe the survival plot of BIIMW distribution. Figure (5) gives a clear picture that the model satisfy both the necessary and sufficient condition of the distribution of lifetime of system (both bathtub hazard rate and bimodal density function). The hazard rate function reaches minimum at time, $x=0.05$ (time period till which the system may undergo breakdown at the beginning of its use itself), followed by normal life till $x=4.5$ and thereafter exhibit an increasing failure rate (wear-out process of the system). Also from figure (5b) it is evident that the density function attains maximum at time $x=0.05$ and $x=10.5$. From the results, it is clear that the model can be used for modelling burn-in procedures.

7. CONCLUSION

In this paper, we introduce the Burr III-Modified Weibull (BIIMW) distribution, a new five-parameter lifetime distribution. This distribution can be used to represent both monotone and non-monotone hazard rates in lifetime data. The statistical properties such as quantile function, hazard rate function and order statistics are presented. The performance of the new BIIMW

distribution is performed by using simulation study. Finally, flexibility and applicability of this model is illustrated by a real data set. From the data analysis, it is obvious that the proposed model is highly desirable in the modeling of the lifetime of system. The model satisfy both the necessary and sufficient condition of the distribution of lifetime of system. The proposed method can be used to successfully plan a burn-in process and preventive maintenance of inoperable devices.

REFERENCES

- [1] Bebbington, Mark., Chin-Diew Lai. and Ricardas Zitikis. (2007). A flexible Weibull extension, *Reliability Engineering and System Safety*, 92, pp. 719-726.
- [2] Burr, I. W. (1942). Cumulative frequency functions. *The Annals of Mathematical Statistics*, 13(2), pp. 215-232.
- [3] Burr, I. W. and Cislak, P. J. (1968). On a general system of distributions: I. its curve shaped characteristics, II . the sample median. *Journal of the American Statistical Association*, 63, pp. 627-635.
- [4] Carrasco, J. M. F., Ortega, E. M. M. and Cordeiro, G. M. (2008). A generalized modified Weibull distribution for lifetime modeling. *Computational Statistics and Data Analysis*. 53(2), pp. 450-462.
- [5] Chandrasekaran, R. (1977). Optimal policies for burn-in procedures. *Opsearch*, 4, pp. 149-160.
- [6] Dagum, C. A. (1977). New model of personal income distribution: specification and estimation. *Economic Applique*, 30(3), pp. 413-437.
- [7] Gove, J. H., Ducey, M. J., Leak, W. B., and Zhang, L. (2008). Rotated sigmoid structures in managed uneven-aged northern hardwood stands: a look at the Burr Type III distribution. *Forestry*, 81(2), pp. 161-176.
- [8] Mølltoft, J. (1983). Behind The Bathtub – Curve a New Model and Its Consequences, *Microelectronics and Reliability*. 23(3),pp 489-500 .
- [9] Johnson, N. L., Kot, S. and Balakrishnan, N. (1995). Continuous Univariate Distributions, *John Wiley and Sons, New York, USA*, 2nd edition.
- [10] Kleiber, C. and Kotz, S. (2003). Statistical size distribution in economics and actuarial sciences. New York, John Wiley and Sons.
- [11] Lai, C. D., Xie, M., and Murthy, D. N. P. (2003). A modified Weibull distribution. *IEEE Trans. Reliab*, 52, pp. 33-37.
- [12] Lawrence, M. J. (1966). An investigation of the burn-in problem. *Technometrics*, 8(1), pp. 61-71.
- [13] Meeker, W. Q. and Escobar, L. A. (1998). Statistical Methods for Reliability Data, New York, Wiley.
- [14] Mielke, P. W. (1973). Another family of distributions for describing and analyzing precipitation data. *J. Appl. Meterol*, 12, pp. 275-280.
- [15] Khan, M. N. (2015). The modified beta Weibull distribution, *Journal of Mathematics and Statistics*, 44 , pp. 1553-1568.
- [16] Oluyede, B. O., Huang, S. and Yang, T. (2015). A new class of generalized modified weibull distribution with applications. *Austrian Journal of Statistics*, 44, pp. 45-68.
- [17] Park, K. S. (1985). Effect of burn-in on mean residual life. *IEEE Transactions on Reliability*, 34(5), pp. 522-523.
- [18] Pham, H. and Lai, C. D. (2007). On recent generalizations of the weibull distribution. *IEEE Transaction on Reliability*, 56, pp. 454-458.
- [19] Sarhan, A. M. and Zaindin, M. (2009). Modified Weibull distribution. *APPS Appl. Sci*. 11, pp. 123-136.
- [20] Silva, G. O., Ortega, E. M. M. and Cordeiro, G. M. (2010). The Beta Modified Weibull Distribution. *Lifetime Data Anaysis*, 16, pp. 409-430.
- [21] Sylwia, K. B. (2007). Makeham's Generalised Distribution. *Computational Methods In Science and Technology*, 13, pp. 113-120.
- [22] Way, K. (1984). Reliability Enhancement Through Optimal Burn-In. *IEEE Trans. Reliab*, 33(2).

- [23] Yanez, S., Escobar, L. A. and Gonzalez N. (2014). Characteristics of two Competing Risks Models with Weibull Distributed Risks. *Mathematicas*, 38(148), pp. 298-311.
- [24] Zwillinger, D. and Jeffrey, A. (2014). Table of Integrals, Series and Products. *Academic Press-Elsevier*, USA, 7th edition.

Analysis of Some Proposed Replacement Policies

Tijjani A. Waziri

•

School of Continuing Education, Bayero University, Kano, Nigeria
tijjanaw@gmail.com

Bashir M. Yakasai

•

Department of Mathematical Sciences, Bayero University, Kano, Nigeria
bashiryakasai119@gmail.com

Rahama S. Abdullahi

•

School of Continuing Education, Bayero University, Kano, Nigeria
rahamasani1996@gmail.com

Abstract

This paper is coming up with an age replacement cost model under the standard age replacement policy (SARP) for some multi-unit systems. Furthermore, some two other age replacement cost models will be constructed for the multi-unit systems under some proposed policies (policy A and policy B). For simple illustration of the proposed age replacement cost models under SARP, policy A and policy B, numerical example was provided, and the result obtained will be beneficial to engineers, maintenance managers and plant management, in selecting and applying the optimal preventive maintenance policies.

Keywords: failure rate, proposed policies, multi-unit systems

I. Introduction

Multi-components systems deteriorate and subsequently fail due to age and usage. To reduce the occurrence of system failures, management of organizations are always interested in selecting and implementing the optimal preventive replacement policy for normal system operation. Furthermore, in describing the reliability of a multi-unit system, it is necessary to specify how the units of the system are connected and provide the rule of the operation. The simplest form of the system configuration is the series configuration. Designing systems in parallel configuration is done with the intention to improve systems reliability. In most practical situations, a combination of both series and parallel configurations is inevitable.

Enogwe *et al.* [1] used the distribution of the probability of failure times and come up with a replacement model for items that fails un-notice. Fallahnezhad and Najafian [2] investigated the number of spare parts and installations for a unit and parallel systems, so as cut down the average

cost per unit time. Gertsbakh [3] described and presented some vital preventive maintenance models for some multi-component systems. Huang and Wang [4] constructed a time-replacement model for multistate systems, which can be used to determine the optimal time to replace the entire system, and this proposed approach provides further insight into the relationship between preventive maintenance policy setting and long-term system benefits. Jain *et al.* [5] developed Markov model for a multi-component system which is subjected to two types of failures, which are hardware failure and human error. Jain and Gupta [6] presented a preventive replacement model for a repairable system with multiple vacation and imperfect coverage. Lim *et al.* [7] presented some characteristics of some age substitution policies. Liu *et al.* [8] come up with mathematical models of uncertain reliability of some multi-component systems. Malki *et al.* [9] studied some age replacement policies of a parallel system with stochastic dependency. Murthy and Hwang [10] discussed that, the failures can be reduced through effective maintenance actions, and such maintenance actions can occur either at discrete time instants or continuously over time. Nakagawa [11] presented age replacement model for series and parallel system based on standard age replacement policy. Nakagawa *et al.* [12] presented the advantages of some proposed replacement policies. In an approach for analyzing the behavior of an industrial system under the cost free warranty policy, Niwas and Garg [13] developed a mathematical model of a system based on the Markov process, they also derived various parameters such as reliability, mean time to system failure, availability and expected profit for the system. Safaei *et al.* [14] studied the optimal preventive maintenance action for a system based on some conditions. Sudheesh *et al.* [15] studied age replacement model in discrete approach. Tsoukalas and Agrafiotis [16] presented a new replacement policy warrant for a system with correlated failure and usage time. Waziri and Yusuf [17] constructed an age replacement cost model for a parallel-series system based on some proposed policies, where they investigated the characteristics of the proposed policies. In trying to extending the optimal replacement time of multi-unit systems, Waziri *et al.* [18] come up with some proposed age replacement cost models involving discounting rate and minimal repair for a series system. Waziri [19] presented a discounted age replacement model for a unit based on discrete time. Wu *et al.* [20] proposed a new replacement policy and established corresponding replacement models for a deteriorating repairable system with multiple vacations of one repairman. Xie *et al.* [21] assessed the effects of safety barriers on the prevention of cascading failures. Zhao *et al.* [22] collected some recent results on age replacement policies and proposed some modified age replacement policies, such as optimal age replacement policy for a parallel system with a random number of units.

The literature review presented in this paper did not captured a way or strategy of extending the optimal replacement time of a multi-component system. This paper will proposed some proposed replacement cost models under some policies, so as to see the possibility of extending the optimal replacement time of some four multi-component systems, and this will be achieved through the following objectives:

1. By constructing age replacement cost model for series and parallel systems under the standard age replacement policy (SARP).
2. By constructing age replacement cost models for series and parallel systems under two proposed policies (policy A and policy B).
3. By providing a numerical example for simple illustration of the constructed replacement cost models.

II. Methods

Reliability measures namely reliability function and failure rates are used to obtain the expressions of replacement cost models for four systems under the standard age replacement policy (SARP) and under proposed two policies (policy A and policy B). A numerical example was given so to assess the three replacement policies.

III. Notations

- $r_i(t)$: Level I failure rate of unit D_i , for $i = 1, 2, 3, 4, 5, 6$.
- $r_i^*(t)$: Level II failure rate of unit D_i , for $i = 1, 2, 3, 4, 5, 6$.
- $R_i^*(t)$: Reliability function of Level II failure of unit B_i , for $i = 1, 2, 3, 4, 5, 6$.
- *SARP*: Standard age replacement policy.
- $R_{S_i}^*(t)$: Reliability function of system S_i due to Level II failure, for $i = 1, 2, 3, 4$.
- $CS_i(T)$: Cost rate of system S_i under SARP, for $i = 1, 2, 3, 4$.
- $CYS_i(T)$: Cost rate of system S_i under policy A, for $i = 1, 2, 3, 4$.
- $CZ(T)$: Cost rate of system S_i under policy B, for $i = 1, 2, 3, 4$.
- $X_{S_i}^*$: Optimal replacement time of system S_i under SARP, for $i = 1, 2, 3, 4$.
- $Y_{S_i}^*$: Optimal replacement time of system S_i under policy A, for $i = 1, 2, 3, 4$.
- $Z_{S_i}^*$: Optimal replacement time of system S_i under policy B, for $i = 1, 2, 3, 4$.
- C_{ir} : Cost of unplanned replacement of failed D_i due to Level II failure, for $i = 1, 2, 3, 4, 5, 6$.
- C_{im} : Cost of minimal repair of failed D_i due to Level II failure, for $i = 1, 2, 3, 4, 5, 6$.
- C_{sp} : Cost of planned replacement of system S_i at planned replacement time T, for $i = 1, 2, 3, 4$.
- C_{sr} : Cost of un-planned replacement of system S_i due to Level II failure, for $i = 1, 2, 3, 4$.

IV. Description of the Systems

Consider six units D_1, D_2, D_3, D_4, D_5 and D_6 , arranged in four different configurations, so as to formed four different systems, which are series-parallel system (S_1), series-parallel system (S_2), parallel-series system (S_3) and parallel-series system (S_4). All the six units are subjected to Level I and Level II failures, such that, Level I failure is repairable one, while the Level II failure is non-repairable failure. Since all the six units are subjected to Level I and Level II failures, then, this implies that, all the four systems are also subjected to Level I and Level II failures. See the Figure 1, Figure 2, Figure 3 and Figure 4 as the diagram of the four systems (S_1, S_2, S_3 and S_4).

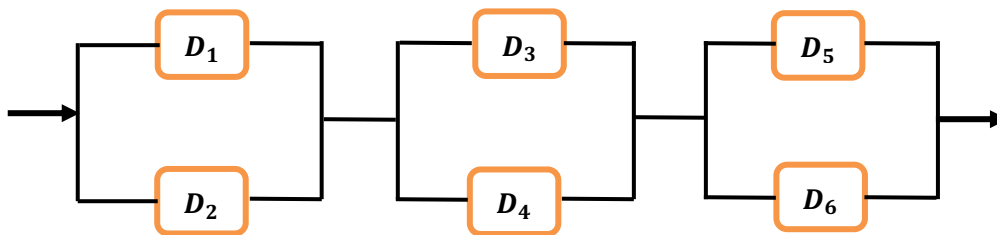


Figure 1: Reliability block diagram of system S_1

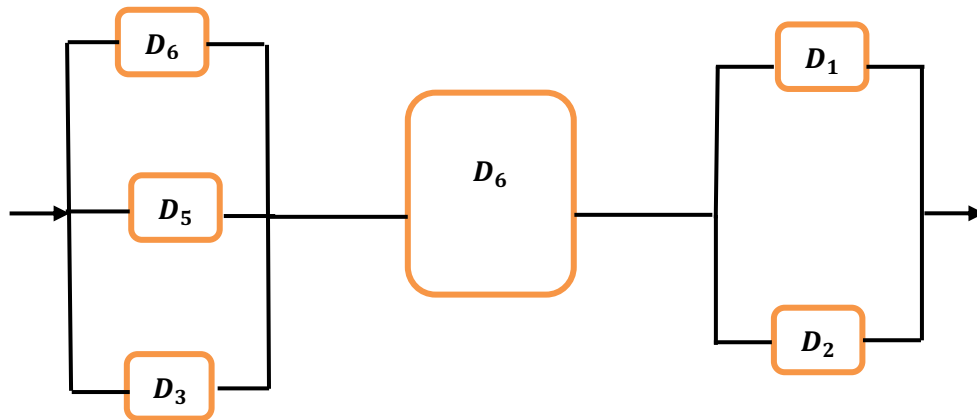


Figure 2: Reliability block diagram of system S_2

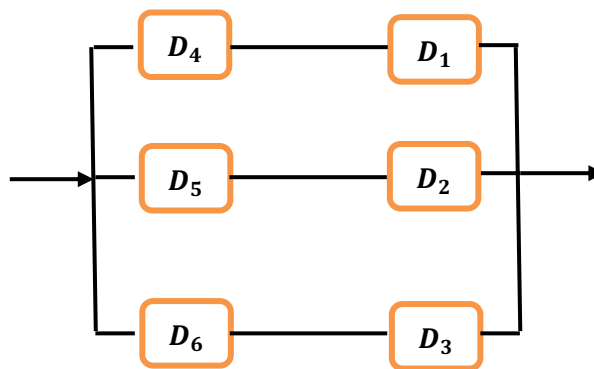


Figure 3: Reliability block diagram of system S_3

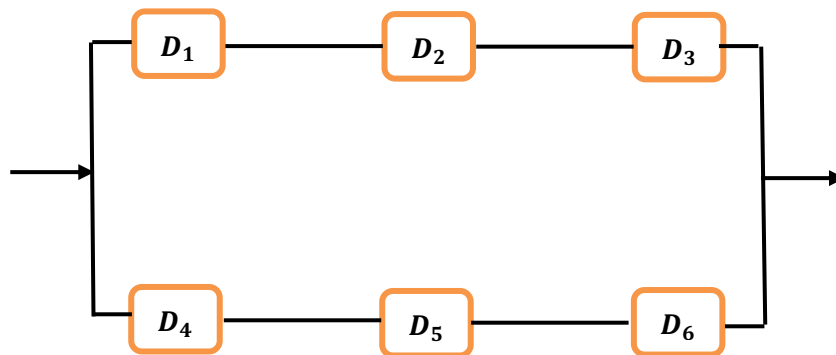


Figure 4: Reliability block diagram of system S_4

V. Replacement Cost Models Under SARP

Some Assumptions for SARP:

1. If a system fails due to Level I failure, then the system is minimally repaired.
2. If a system fails due to Level II failure, then the whole system replaced completely with new one.
3. Both the two levels of failures (Level I and Level II) of the six units arrives according to non-homogeneous Poisson process.
4. Rate of Level I failure of the six units follows the order: $r_1(t) \geq r_3(t) \geq r_5(t) \geq r_2(t) \geq r_4(t) \geq r_6(t)$.
5. Rate of Level II failure of the six units follows the order: $r_1^*(t) \geq r_3^*(t) \geq r_5^*(t) \geq r_2^*(t) \geq r_4^*(t) \geq r_6^*(t)$.
6. The cost of repair and replacement follows the order: $C_{im} < C_{Sp} < C_{Sr}$, for $i = 1, 2, 3, 4, 5, 6$.
7. A system is replaced at a planned time $T(T > 0)$ or at Level II failure, whichever occurs first.
8. The cost of planned replacement of a system is less than the cost of un-planned replacement.
9. The cost of repair of a failed unit is less than the cost of replacement of a unit.
10. All costs are positive numbers.

From the assumptions above, the probability that system S_1 will be replaced at planned replacement time T , before Level II failure occurs, is

$$R_{S_1}^*(T) = (1 - \prod_{i=1}^2(1 - R_i^*(T))) \times (1 - \prod_{i=1}^2(1 - R_i^*(T))) \times (1 - \prod_{i=1}^2(1 - R_i^*(T))). \quad (1)$$

From the assumptions above, the probability that system S_2 will be replaced at planned replacement time T , before Level II failure occurs, is

$$R_{S_2}^*(T) = (1 - \prod_{i=1}^2(1 - R_i^*(T))) \times (1 - \prod_{i=1}^3(1 - R_i^*(T))) \times R_6^*(T). \quad (2)$$

From the assumptions above, the probability that system S_3 will be replaced at planned replacement time T , before Level II failure occurs, is

$$R_{S_3}^*(T) = 1 - (1 - R_3^*(T)R_6^*(T)) \times (1 - R_2^*(T)R_5^*(T)) \times (1 - R_1^*(T)R_4^*(T)). \quad (3)$$

From the assumptions above, the probability that system S_4 will be replaced at planned replacement time T , before Level II failure occurs, is

$$R_{S_4}^*(T) = 1 - (1 - R_1^*(T)R_2^*(T)R_3^*(T)) \times (1 - R_4^*(T)R_5^*(T)R_6^*(T)). \quad (4)$$

The mean time of systems S_1, S_2, S_3 and S_4 under SARP, is

$$\int_0^T R_{S_i}^*(t)dt, \text{ for } i = 1, 2, 3, 4. \quad (5)$$

The cost of un-planned replacement (failure due to Level II failure) of S_1 and S_2 in one replacement cycle under SARP, is

$$C_{sr}(1 - R_{S_i}^*(T)), \text{ for } i = 1, 2, 3, 4. \quad (6)$$

The cost of planned replacement at time T of S_1, S_2, S_3 and S_4 in one replacement cycle under

SARS, is

$$C_{sp}R_{Si}^*(T), \text{ for } i = 1, 2, 3, 4. \quad (7)$$

The cost of minimal repair of components D_1, D_2, D_3, D_4, D_5 and D_6 due to Level I failure in one replacement cycle under SARP, is

$$J(T) = \int_0^T C_{1m}r_1(t)R_{S1}^*(t)dt + \int_0^T C_{2m}r_2(t)R_{S1}^*(t)dt + \int_0^T C_{3m}r_3(t)R_{S1}^*(t)dt \\ + \int_0^T C_{4m}r_4(t)R_{S1}^*(t)dt + \int_0^T C_{4m}r_5(t)R_{S1}^*(t)dt + \int_0^T C_{5m}r_6(t)R_{S1}^*(t)dt. \quad (8)$$

Using equations (5), (6), (7) and (8), the replacement cost rate of systems S_1, S_2, S_3 and S_4 under SARP is

$$CS_i(T) = \frac{C_{sr}(1 - R_{Si}^*(T)) + C_{sp}R_{Si}^*(T) + \int_0^T J(t)R_{Si}^*(t)dt}{\int_0^T R_{Si}^*(t)dt}, \quad i = 1, 2, 3, 4, \quad (9)$$

where

$$J(t) = C_{1m}r_1(t) + C_{2m}r_2(t) + C_{3m}r_3(t) + C_{4m}r_4(t) + C_{5m}r_5(t) + C_{6m}r_6(t). \quad (10)$$

Noting that, $CS_i(T)$ for $i = 1, 2, 3, 4$, is adopted as an objective function of an optimization problem, and the main goal is to obtain an optimal replacement time T_{Si}^* that minimizes $CS_i(T)$, for $i = 1, 2, 3, 4$.

VI. Replacement Cost Models Under Policy A

From assumption 4, observe that, Level II failure of units D_1, D_3 and D_5 is higher than that of units D_2, D_4 or D_6 . Policy A is a preventive maintenance policy, in which the un-planned replacement of a system, which depends on the failure of units D_1, D_3 and D_5 due to Level II. Noting that, the reliability function of a system due to policy A, depends on the location of units D_1, D_3 and D_5 in a system. But when any of the units D_2, D_4 or D_6 fails due to Level II failure, the failed unit is replace completely with new one and allow the system to continue operating from where it stopped.

Under policy A, we have the following descriptions:

1. System S_1 : the system is replace completely with new one when at least one of the components D_1, D_3 or D_5 fails due to Level II failure. Now, the probability that system S_1 will be replaced at planned replacement time T , before Level II failure occurs due to policy A, is

$$R_{S1}^{a*}(T) = R_1^*(T)R_3^*(T)R_5^*(T). \quad (11)$$

2. System S_2 : the system is replace completely with new one when all the three units D_1, D_3 and D_5 fails due to Level II failure. Now, the probability that system S_2 will be replaced at planned replacement time T , before Level II failure occurs due to policy A, is

$$R_{S2}^{a*}(T) = R_1^*(T)(1 - (1 - R_3^*(T))(1 - R_5^*(T))). \quad (12)$$

3. System S_3 : the system is replace completely with new one when at least one of the units D_1, D_3 or D_5 fails due to Level II failure. Now, the probability that system S_3 will be replaced at planned replacement time T , before Level II failure occurs due to policy A, is

$$R_{S_3}^{a*}(T) = (1 - (1 - R_1^*(T))(1 - R_3^*(T))(1 - R_5^*(T))) . \quad (13)$$

4. System S_4 : the system is replace completely with new one when any of the combination fails: D_1 and D_5 , or D_3 and D_5 fails. Now, the probability that system S_3 will be replaced at planned replacement time T , before Level II failure occurs due to policy A, is

$$R_{S_4}^{a*}(T) = 1 - (1 - R_1^*(T)R_3^*(T))(1 - R_5^*(T)) . \quad (14)$$

The mean time of systems of S_1, S_2, S_3 and S_4 in one replacement cycle under policy A, is

$$\int_0^T R_{S_i}^{a*}(t)dt , \text{ for } i = 1, 2, 3, 4 . \quad (15)$$

The cost of un-planned replacement (failure due to Level II failure) of S_1, S_2, S_3 and S_4 in one replacement cycle under policy A, is

$$C_{sr}(1 - R_{S_i}^{a*}(T)), \text{ for } i = 1, 2, 3, 4 . \quad (16)$$

The cost of planned replacement at time T of S_1, S_2, S_3 and S_4 in one replacement cycle under policy A, is

$$C_{sp}R_{S_i}^{a*}(T), \text{ for } i = 1, 2, 3, 4 . \quad (17)$$

The cost of minimal repair of components D_1, D_2, D_3, D_4, D_5 and D_6 due to Level I failure in one replacement cycle under policy A, is

$$\int_0^T C_{1m}r_1(t)R_{S_i}^{a*}(t)dt + \int_0^T C_{2m}r_2(t)R_{S_i}^{a*}(t)dt + \int_0^T C_{3m}r_3(t)R_{S_i}^{a*}(t)dt \\ + \int_0^T C_{4m}r_4(t)R_{S_i}^{a*}(t)dt + \int_0^T C_{4m}r_5(t)R_{S_i}^{a*}(t)dt + \int_0^T C_{5m}r_6(t)R_{S_i}^{a*}(t)dt . \quad (18)$$

The cost of replacement of components D_2, D_4 and D_6 due to Level II failure in one replacement cycle under policy A, is

$$\int_0^T C_{2r}r_2^*(t)R_{S_i}^{a*}(t)dt + \int_0^T C_{4r}r_4^*(t)R_{S_i}^{a*}(t)dt + \int_0^T C_{6r}r_6^*(t)R_{S_i}^{a*}(t)dt . \quad (19)$$

Using equations (15), (16), (17), (18) and (19), the replacement cost rate of S_1, S_2, S_3 and S_4 under policy A, is

$$CYS_i(T) = \frac{C_{sr}(1 - R_{S_i}^{a*}(T)) + C_{sp}R_{S_i}^{a*}(T) + \int_0^T K(t)R_{S_i}^{a*}(t)dt + \int_0^T L(t)R_{S_i}^{a*}(t)dt}{\int_0^T R_{S_i}^{a*}(t)dt}, \text{ for } i = 1, 2, 3, 4 \quad (20)$$

where

$$K(t) = C_{1m}r_1(t) + C_{2m}r_2(t) + C_{3m}r_3(t) + C_{4m}r_4(t) + C_{5m}r_5(t) + C_{6m}r_6(t), \quad (21)$$

and

$$L(t) = C_{2r}r_2^*(t) + C_{4r}r_4^*(t) + C_{6r}r_6^*(t) . \quad (22)$$

Noting that, $CYS_i(T)$ for $i = 1, 2, 3, 4$, is adopted as an objective function of an optimization problem, and the main goal is to obtain an optimal replacement time $Y_{S_i}^*$ that minimizes $CYS_i(T)$, for $i = 1, 2, 3, 4$.

VII. Replacement Cost Models Under Policy B

Observe from assumption 4, that Level II failure of units D_2 , D_4 and D_6 is lower than that of units D_1 , D_3 or D_5 . Policy B is a preventive maintenance policy, in which the un-planned replacement of a whole system depends on the failure of units D_2 , D_4 and D_6 due to Level II. Noting that, the reliability function of a system due to policy B, depends on the location of units D_2 , D_4 and D_6 in a system. But when any of the units D_1 , D_3 or D_5 fails due to Level II failure, the failed unit is replace completely with new one and allow the system to continue operating from where it stopped.

Under policy B, we have the following descriptions:

1. System S_1 : the system is replace completely with new one when at least one of the units D_2, D_4 or D_6 fails due to Level II failure. Now, the probability that system S_1 will be replaced at planned replacement time T , before Level II failure occurs due to policy B, is

$$R_{S_1}^{b*}(T) = R_2^*(T)R_4^*(T)R_6^*(T). \quad (23)$$

2. System S_2 : the system is replace completely with new one when all the three units D_2, D_4 or D_6 fails due to Level II failure. Now, the probability that system S_2 will be replaced at planned replacement time T , before Level II failure occurs due to policy B, is

$$R_{S_2}^{b*}(T) = R_2^*(T)R_4^*(T)R_6^*(T). \quad (24)$$

3. System S_3 : the system is replace completely with new one when at least one of the components D_2, D_4 or D_6 fails due to Level II failure. Now, the probability that system S_3 will be replaced at planned replacement time T , before Level II failure occurs due to policy B, is

$$R_{S_3}^{b*}(T) = 1 - (1 - R_2^*(T))(1 - R_4^*(T))(1 - R_6^*(T)). \quad (25)$$

4. System S_4 : the system is replace completely with new one when any of the combination fails: D_4 and D_2 , or D_6 and D_2 fails. Now, the probability that system S_3 will be replaced at planned replacement time T , before Level II failure occurs due to policy B, is

$$R_{S_4}^{b*}(T) = 1 - (1 - R_4^*(T)R_6^*(T))(1 - R_2^*(T)). \quad (26)$$

The mean time of systems of S_1, S_2, S_3 and S_4 in one replacement cycle under policy B, is

$$\int_0^T R_{S_i}^{b*}(t) dt, \text{ for } i = 1, 2, 3, 4. \quad (27)$$

The cost of un-planned replacement (failure due to Level II failure) of S_1, S_2, S_3 and S_4 in one replacement cycle under policy B, is

$$C_{sr} \left(1 - R_{S_i}^{b*}(T) \right), \text{ for } i = 1, 2, 3, 4. \quad (28)$$

The cost of planned replacement at time T of S_1, S_2, S_3 and S_4 in one replacement cycle under policy B, is

$$C_{sp} R_{S_i}^{b*}(T), \text{ for } i = 1, 2, 3, 4. \quad (29)$$

The cost of minimal repair of components D_1, D_2, D_3, D_4, D_5 and D_6 due to Level I failure in one replacement cycle under policy B, is

$$\int_0^T C_{1m}r_1(t)R_{Si}^{b*}(t)dt + \int_0^T C_{2m}r_2(t)R_{Si}^{b*}(t)dt + \int_0^T C_{3m}r_3(t)R_{Si}^{b*}(t)dt + \int_0^T C_{4m}r_4(t)R_{Si}^{b*}(t)dt + \int_0^T C_{4m}r_5(t)R_{Si}^{b*}(t)dt + \int_0^T C_{5m}r_6(t)R_{Si}^{b*}(t)dt . \quad (30)$$

The cost of replacement of components D_1, D_3 and D_5 due to Level II failure in one replacement cycle under policy B, is

$$\int_0^T C_{1r}r_1^*(t)R_{Si}^{b*}(t)dt + \int_0^T C_{3r}r_3^*(t)R_{Si}^{b*}(t)dt + \int_0^T C_{5r}r_5^*(t)R_{Si}^{b*}(t)dt. \quad (31)$$

Using equations (27), (28), (29), (30) and (31), the replacement cost rate of systems S_1, S_2, S_3 and S_4 under policy B, is

$$CZS_i(T) = \frac{C_{sr}(1-R_{Si}^{b*}(T)) + C_{sp}R_{Si}^{b*}(T) + \int_0^T M(t)R_{Si}^{b*}(t)dt + \int_0^T N(t)R_{Si}^{b*}(t)dt}{\int_0^T R_{Si}^{b*}(t)dt}, \text{ for } i = 1, 2, 3, 4, \quad (32)$$

where

$$M(t) = C_{1m}r_1(t) + C_{2m}r_2(t) + C_{3m}r_3(t) + C_{4m}r_4(t) + C_{5m}r_5(t) + C_{6m}r_6(t), \quad (33)$$

and

$$N(t) = C_{1r}r_1^*(t) + C_{3r}r_3^*(t) + C_{5r}r_5^*(t) . \quad (34)$$

Noting that, $CZS_i(T)$ for $i = 1, 2, 3, 4$, is adopted as an objective function of an optimization problem, and the main goal is to obtain an optimal replacement time Z_{Si}^* that minimizes $CZS_i(T)$, for $i = 1, 2, 3, 4$.

VIII. Numerical Example

To illustrate the characteristics of the constructed replacement cost models under SARP, policies A and B. Let the time of Level I failure for the six units follows Weibull distribution:

$$r_i(t) = \lambda_i \alpha_i t^{\alpha_i-1}, \text{ for } i = 1, 2, 3, 4, 5, 6, \quad (35)$$

where $\alpha_i > 1$ and $t \geq 0$.

Also, let the time of Level II failure for the six units follows Weibull distribution:

$$r_i^*(t) = \lambda_i^* \alpha_i^* t^{\alpha_i^*-1}, \text{ for } i = 1, 2, 3, 4, 5, 6, \quad (36)$$

where $\alpha_i > 1$ and $t \geq 0$.

Let the set of parameters and cost of repair and replacement be used throughout this particular example:

1. $\alpha_1 = 4, \alpha_2 = 3, \alpha_3 = 3, \alpha_4 = 3, \alpha_5 = 4$ and $\alpha_6 = 2$.
2. $\lambda_1 = 0.03, \lambda_2 = 0.002, \lambda_3 = 0.03, \lambda_4 = 0.001, \lambda_5 = 0.001$ and $\lambda_6 = 0.001$.

3. $\alpha_1^* = 4, \alpha_2^* = 3.5, \alpha_3^* = 4, \alpha_4^* = 3.5, \alpha_5^* = 4,$ and $\alpha_6^* = 3.5$.
4. $\lambda_1^* = 0.00033, \lambda_2^* = 0.00025, \lambda_3^* = 0.00030, \lambda_4^* = 0.00023, \lambda_5^* = 0.00025$ and $\lambda_6^* = 0.0002$.
5. $C_{sr} = 70, C_{sp} = 50$ and $C_{im} = 0.5,$ for $i = 1, 2, 3, 4, 5, 6$.

By substituting the parameters in equations (35) and (36), the following equations (Level I and Level II failures) below are obtained as follows:

$$r_1(t) = 0.12t^3. \tag{37}$$

$$r_2(t) = 0.06t. \tag{38}$$

$$r_3(t) = 0.09t^2. \tag{39}$$

$$r_4(t) = 0.003t^2. \tag{40}$$

$$r_5(t) = 0.004t^3. \tag{41}$$

$$r_6(t) = 0.002t. \tag{42}$$

$$r_1^*(t) = 0.00132t^3. \tag{43}$$

$$r_2^*(t) = 0.000875t^{2.5}. \tag{44}$$

$$r_3^*(t) = 0.00012t^3. \tag{45}$$

$$r_4^*(t) = 0.000805t^{2.5}. \tag{46}$$

$$r_5^*(t) = 0.001t^3. \tag{47}$$

$$r_6^*(t) = 0.0007t^{2.5}. \tag{48}$$

Tables 1, 2 and 3 below are obtained, by substituting the assumed cost of replacement/repair and rates of Level I and Level II failures obtained above (equations (37) to (48)) in the replacement cost models constructed above (equations (9), (20) and (32)), so as to determine the optimal replacement times of the four systems.

Table 1. Results obtained from evaluating the replacement cost rates of systems S_1, S_2, S_3 and S_4 under SARP.

T	$CS_1(T)$	$CS_2(T)$	$CS_3(T)$	$CS_4(T)$
1	240.04	240.09	240.04	240.03
2	120.16	120.43	120.16	120.11
3	80.42	81.14	80.37	80.41
4	61.06	62.38	60.75	61.61
5	50.68	52.48	49.65	53.17
6	46.28	48.04	44.23	52.86
7	46.64	48.13	44.70	59.29
8	53.74	52.16	51.31	67.98
9	61.01	58.01	60.74	72.17
10	63.97	58.91	64.89	74.11
11	70.03	61.84	65.31	76.16
12	73.92	68.98	67.87	78.97

Table 2. Results obtained from evaluating the replacement cost rates of systems S_1, S_2, S_3 and S_4 under policy A.

T	$CYS_1(T)$	$CYS_2(T)$	$CYS_3(T)$	$CYS_4(T)$
1	240.78	240.65	240.57	240.57
2	122.87	121.82	121.18	121.19
3	87.58	84.10	81.96	82.03
4	76.01	68.08	62.89	63.41
5	76.62	62.52	52.13	54.13
6	83.71	64.18	46.27	51.36
7	89.44	70.76	44.88	53.95
8	90.24	77.06	48.34	59.77
9	92.73	77.01	55.49	64.92
10	94.99	73.65	61.79	66.28
11	95.45	76.44	62.77	67.90
12	98.00	79.00	65.57	69.72

Table 3. Results obtained from evaluating the replacement cost rates of systems S_1, S_2, S_3 and S_4 under policy B.

T	$CZS_1(T)$	$CZS_2(T)$	$CZS_3(T)$	$CZS_4(T)$
1	240.80	243.3	240.64	240.64
2	122.54	125.04	121.62	121.63
3	85.61	88.11	83.11	83.13
4	70.10	72.6	65.11	65.20
5	63.97	66.47	55.61	55.94
6	62.95	65.45	50.64	51.48
7	64.67	67.17	49.55	50.22
8	67.21	69.71	48.55	51.27
9	68.67	71.17	50.20	53.79
10	70.74	73.24	53.05	56.80
11	74.46	76.96	56.43	59.10
12	76.97	79.47	59.34	59.61

Table 4. The optimal replacement times of systems S_1, S_2, S_3 and S_4 under SARP, policy A and policy B from tables 1, 2 and 3.

System	Under SARP	Under policy A	Under policy B
S_1	$X_{S1}^* = 6.00$	$Y_{S1}^* = 4.00$	$Z_{S1}^* = 6.00$
S_2	$X_{S2}^* = 6.00$	$Y_{S2}^* = 5.00$	$Z_{S2}^* = 6.00$
S_3	$X_{S3}^* = 6.00$	$Y_{S3}^* = 7.00$	$Z_{S3}^* = 8.00$
S_4	$X_{S4}^* = 6.00$	$Y_{S4}^* = 6.00$	$Z_{S4}^* = 7.00$

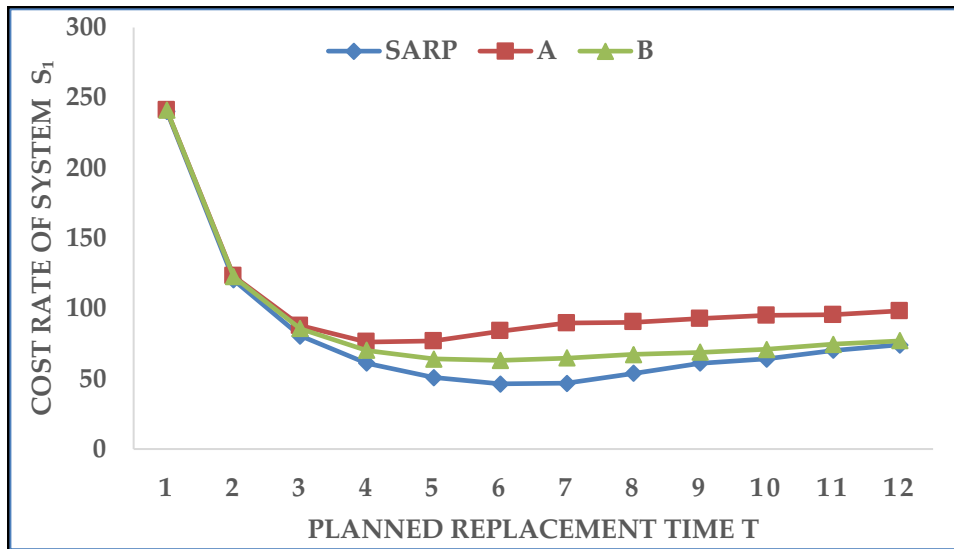


Figure 5: The plot of cost rates of system S_1 under SARP, policy A and policy B against planned replacement time T.

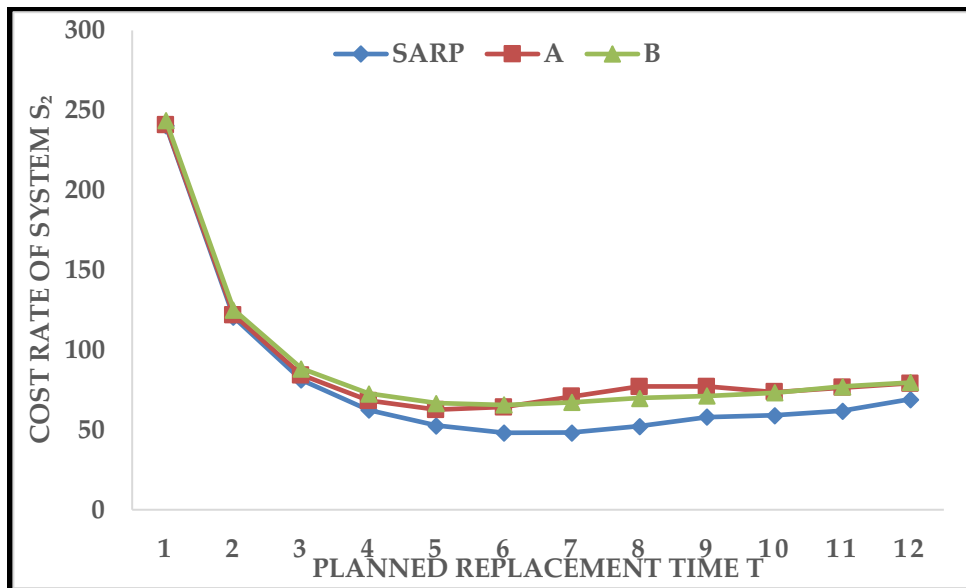


Figure 6: The plot of cost rates of system S_2 under SARP, policy A and policy B against planned replacement time T.

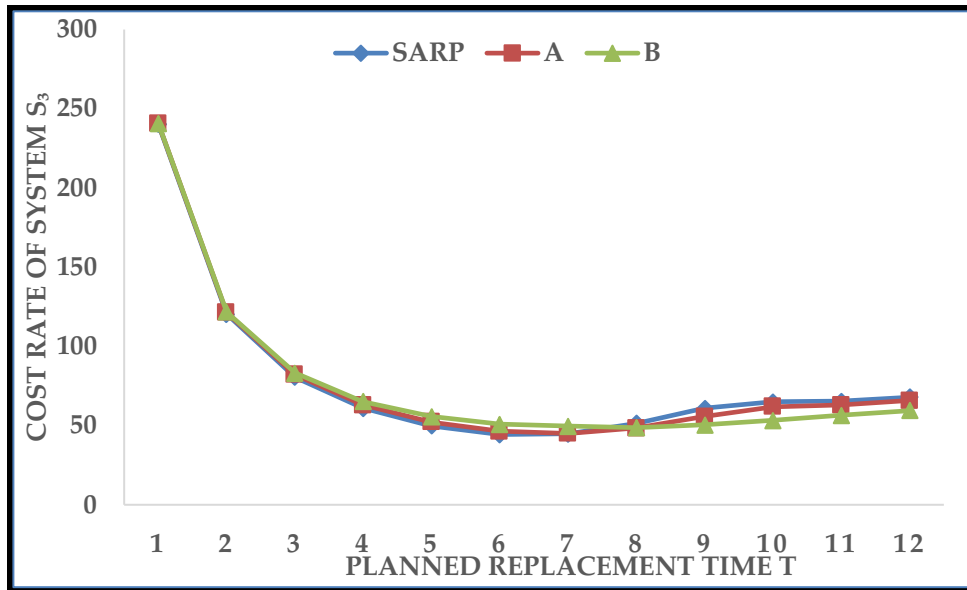


Figure 7: The plot of cost rates of system S_3 under SARP, policy A and policy B against planned replacement time T .

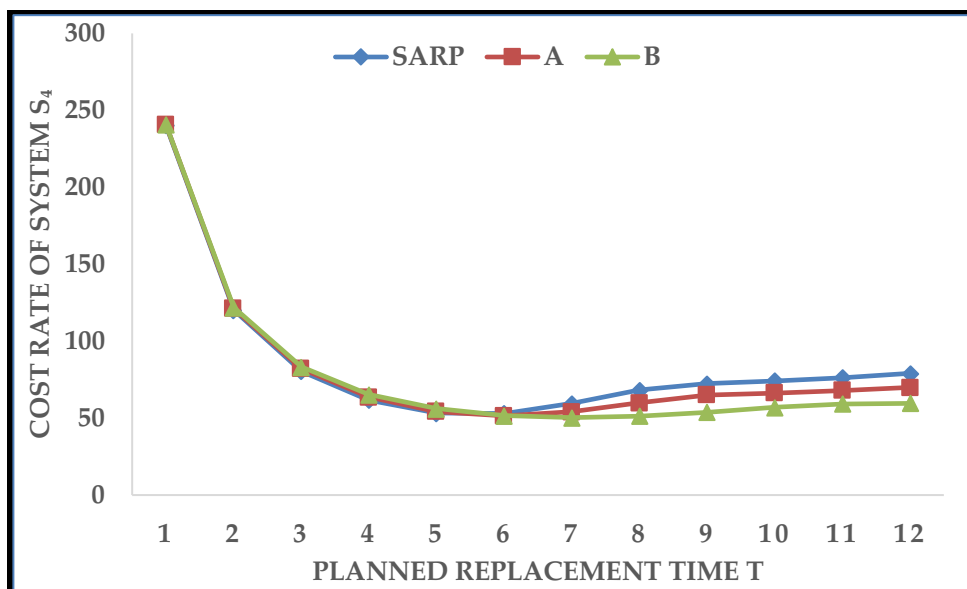


Figure 8: The plot of cost rates of system S_4 under SARP, policy A and policy B against planned replacement time T .

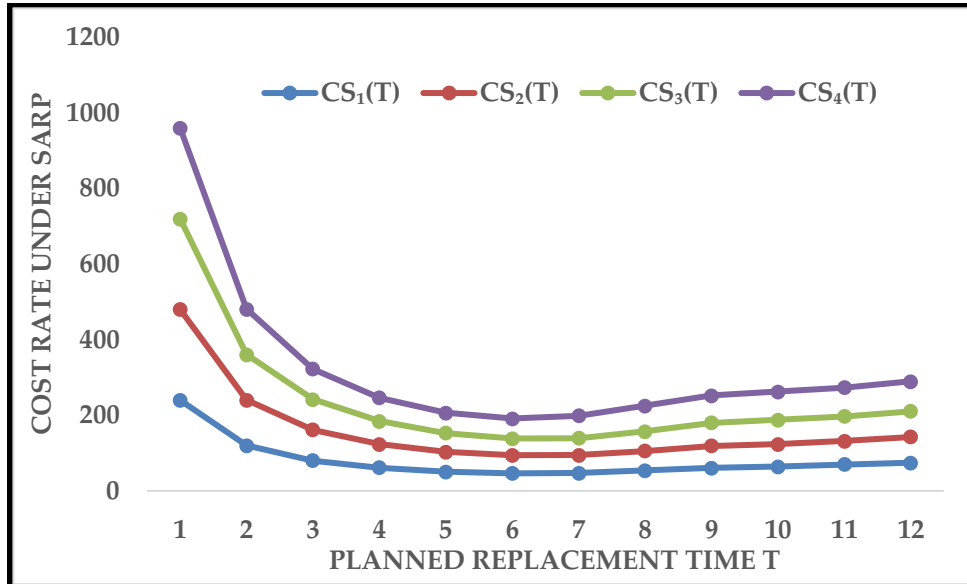


Figure 9 : The plot of cost rates of the four systems under SARP against planned replacement time T.

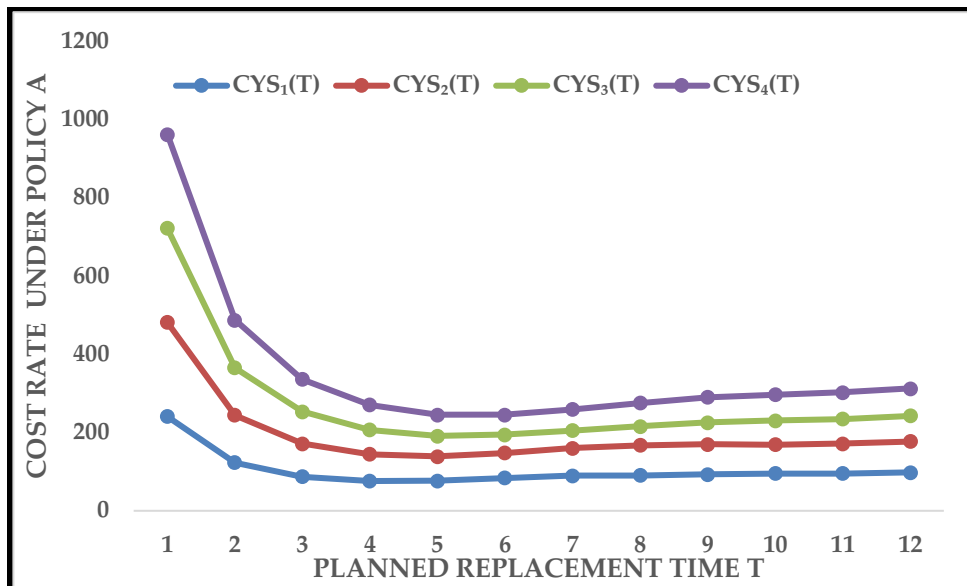


Figure 10 : The plot of cost rates of the four systems under SARP against planned replacement time T.

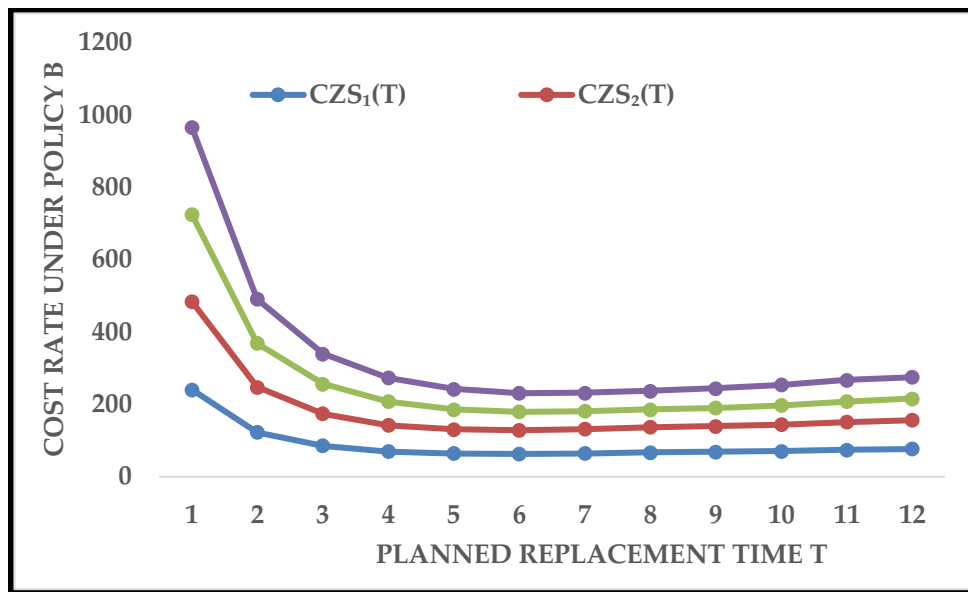


Figure 11 : The plot of cost rates of the four systems under SARP against planned replacement time T.

Some observations from the results obtained are as follows

1. From Table 4, observe that, optimal replacement time of systems S_3 and S_4 under policy B is higher than that of SARP and policy A.
2. From Table 4, observe that, optimal replacement time of systems S_1 and S_2 under SARP and policy B are the same.
3. From Table 4, observe that, optimal replacement time of all the four systems under SARP are the same.
4. From Figure 5, observe that:

$$CS_1(T) \leq CZS_1(T) \leq CYS_1(T). \quad (49)$$

5. From Figure 6, observe that:

$$CS_2(T) \leq CZS_2(T) \leq CYS_2(T). \quad (50)$$

6. From Figure 7, observe that:

$$CZS_3(T) \leq CYS_3(T) \leq CS_3(T). \quad (51)$$

7. From Figure 8, observe that:

$$CZS_4(T) \leq CYS_4(T) \leq CS_4(T). \quad (52)$$

8. From Figure 9, observe that:

$$CS_1(T) \leq CS_2(T) \leq CS_3(T) \leq CS_4(T). \quad (53)$$

9. From Figure 10, observe that:

$$CYS_1(T) \leq CYS_2(T) \leq CYS_3(T) \leq CYS_4(T). \quad (54)$$

10. From Figure 11, observe that:

$$CZS_1(T) \leq CZS_2(T) \leq CZS_3(T) \leq CZS_4(T). \quad (55)$$

IX. Discussion of Results Obtained

From the results obtained, we have the following observations:

1. It can be seen that, the optimal replacement time of the parallel - series systems (S_3 and S_4) under policy B, is higher than that of SARP and policy A. Furthermore, the results also showed that, the cost rates of the parallel - series systems (S_3 and S_4) under policy B is lower than that of SARP and policy A. With these reasons, preventive maintenance of the parallel - series systems under policy B is optimal when compared to preventive maintenance of parallel - series systems under SARP and policy A.
2. It can be seen that, the optimal replacement time of series - parallel systems (S_1 and S_2) under SARP and policy B are the same or very closed. While, the cost rates of the series - parallel systems (S_1 and S_2) under SARP is lower than that of under policies A and B. With these reasons, preventive maintenance of the series-parallel systems under SARP is optimal when compared to preventive maintenance of the series-parallel systems under policies A and B.

Hence, from the observations above, we suggest maintenance managers and plant management to adopt policy B as an optimal preventive policy of maintaining multi-unit systems which are in parallel-series configuration. While for systems with series-parallel configuration, SARP should be adopted as an optimal preventive replacement policy.

X. Conclusion

In trying to come up with some modifications and extension of the age replacement policy, this paper presented some proposed age replacement cost models for multi-unit systems under standard age replacement policy (SARP), policy A and policy B. The results obtained, showed that, preventive replacement of parallel-series systems under policy B is optimal when compared to SARP and policy A. While, preventive replacement of series-parallel systems under SARP is optimal when compared to policies A and B. Thus, the results is beneficial to maintenance managers, in selecting the optimal preventive replacement policy. All the replacement cost models and the results presented in this paper are vital to engineers, maintenance managers and plant management for proper maintenance analysis, decision and safety for multi-unit systems.

References

- [1] Enogwe, S. U., Oruh, B. I. and Ekpenyong E. J. (2018). A modified replacement model for items that fail suddenly with variable replacement costs. *American Journal of Operations Research*, 8:457–473.
- [2] Fallahnezhad, M. S. and Najafian, E. (2017). A model of preventive maintenance for parallel, series and single item replacement systems based on statistical analysis. *Communications in Statistics-Simulation and Computation*, 46:5846–5859.
- [3] Gertsbakh, I. Reliability Theory with Applications to Preventive Maintenance. *Springer-Verlag*, London Limited, 2002.
- [4] Huang, C. H. and Wang, C. H. (2019). A time-replacement policy for multistate systems with aging components under maintenance, from a Component Perspective. *Mathematical Problems in*

Engineering, <https://doi.org/10.1155/2019/9651489>.

[5] Jain, M., Agrawal, S. C. and Rani, S. (2010). Availability analysis of embedded computer System with two types of failure and common cause failure. *Journal of International Academy of Physical Sciences*, 14(4): 439–448.

[6] Jain, M. and Gupta, R. (2013). Optimal replacement policy for a repairable system with multiple vacations and imperfect fault coverage. *Computers and Industrial Engineering*, 66: 710–719.

[7] Lim, J. H., Qu, J. and Zuo, J. M. (2016). Age replacement policy based on imperfect repair with random probability. *Reliability Engineering and System Safety*, 149: 24–33.

[8] Liu, Y., Ma, Y., Qu, Z. and Li, X. (2018). Reliability mathematical models of repairable Systems with uncertain lifetimes and repair time. *IEEE*, 6: 71285–71295.

[9] Malki, Z., Ait, D. A. and Ouali, M. S. (2015). Age replacement policies for two-component systems with stochastic dependence. *Journal of Quality in Maintenance Engineering*, 20(3):346–357.

[10] Murthy, D. N. P. and Hwang, M. C. (2007). Optimal discrete and continuous maintenance policy for a complex unreliable machine. *International Journal of Systems Science*, 6(1):35–52.

[11] Nakagawa, T. Maintenance Theory of Reliability: *Springer-Verlag*, London Limited, 2005.

[12] Nakagawa, T., Chen, M. and Zhao, X. (2018). Note on history of age replacement policies. *International Journal of Mathematical, Engineering and Management Sciences*, 3(2): 151–161.

[13] Niwas, R. and Garg, H. (2018). An approach for analyzing the reliability and profit of an industrial system based on the cost free warranty policy. *J Braz Soc Mech Sci Eng*, 40(5): 5. 10.1007/s40430-018-1167-8.

[14] Safaei, F., Ahmadi, J., and Balakrishnan, N. (2018). A repair and replacement policy for systems based on probability and mean of profits. *Reliability Engineering and System Safety*, 183: 143–152.

[15] Sudheesh, K. K., Asha, G. and Krishna, K. M. J. (2019). On the mean time to failure of an age replacement model in discrete time. *Communications in Statistics - Theory and Methods*, 50 (11): 2569–2585.

[16] Tsoukalas, M. Z. and Agrafiotis, G. K. (2013). A new replacement warranty policy indexed by the product's correlated failure and usage time. *Computers and Industrial Engineering*, 66:203–211.

[17] Waziri, T. A. and Yusuf, I. (2020). On age replacement policy of system involving minimal repair. *Reliability Theory and Application*, 4(59): 54–62.

[18] Waziri, T. A., Yakasai, B. M. and Yusuf, I. (2019). On Some Discounted Replacement Models of a Series System. *Life Cycle Reliability and Safety Engineering*, doi.org/10.1007/s41872-019-00101-3.

[19] Waziri, T. A. (2021). On discounted discrete scheduled replacement model. *Annals of Optimization Theory and Practice*, 4(2): 69–82.

[20] Wu, W., Song, J., Jiang, K. and Li, H. (2021). Optimal replacement policy based on the effective age of the system for a deteriorating repairable system with multiple vacations. *Journal of Quality in Maintenance Engineering*, <https://doi.org/10.1108/JQME-06-2014-0036>.

[21] Xie, L., Lundteigen, M. A. and Liu, Y. (2020). Reliability and barrier assessment of series-parallel systems subject to cascading failures. *Journal of Risk and Reliability*, 00(0): 1–15.

[22] Zhao, X., Al-Khalifa, N. K., Hamouda, A. M. and Nakagawa, T. (2017). Age replacement models: a summary of new perspectives and methods. *Reliability Engineering and System Safety*, 161: 95–105.

EFFECT OF PREPROCESSING IN HUMAN EMOTION ANALYSIS USING SOCIAL MEDIA STATUS DATASET

Komal Anadkat¹, Dr. Hiteishi Diwanji², Dr. Shahid Modasiya³



¹Ph.D. Scholar, Information Technology department, Gujarat Technological University, Ahmedabad, India. komalanadkat@gecg28.ac.in

² Associate Professor, Information Technology department, L.D. College of Engineering, Ahmedabad, India. hiteishi.diwanji@gmail.com

³Assistant Professor, Electronics & Communication department, G.E.C., Gandhinagar, Gandhinagar, India. shahid@gecg28.ac.in

Abstract

Emotion analysis using social media text is the emerging research area now a day. It helps the researcher to recognize the emotional state of the users and identify mental health-relevant problems like depression or anxiety, which may lead to suicide if not cured. The social media platforms like WhatsApp, Facebook, Instagram, etc. are widely used as these applications provide an affordable and reliable medium for transferring data, sharing thoughts, and even for routine informal communication. Social media status is normally analyzed to recognize the mood, emotion, thought process, or mental state of the individual as people generally share status for what they feel. On the other hand, pre-processing is the crucial step for any kind of text data analysis. In this paper, the social media status dataset is first pre-processed using various methods, given for feature extraction and classification purpose. For the machine learning approach, we have used count vectors and TF-IDF techniques for extracting the different features of the data. Using count vector feature extraction accuracy achieved by pre-processed data is 68.90%, 69.33%, 70.59%, 64.95%, 69.33% for naïve Bayes, LDA, Random forest, SGD and MLP respectively. Similarly, using TF-IDF feature extraction accuracy achieved by pre-processed data is 65.76%, 69.96%, 68.49%, 65.96%, 70.80% for naïve Bayes, LDA, Random forest, SGD and MLP respectively. The experimental results show that pre-processing helps to improve the accuracy of the classifier and CNN outperforms the traditional approach and achieves 79% accuracy.

Keywords: Pre-processing, Emotion analysis, Feature extraction, classifiers, Count Vectors, TF-IDF

I. Introduction

Emotions are defined as psychological conditions caused by neurophysiological changes, associated with thoughts and feelings of happiness or dislike. The advent of internet technology and communication makes them a great platform for people to express their feelings and ideas. If a person is having positive emotions like happiness, it can help to improve the health and work efficiency of a person [1]. On the other side, constant negative emotions like sadness and anger can cause major physical or mental disorders Persistent negative emotions can cause psychological issues like depression, which in some cases can lead to suicide. Nowadays people are using social media platforms to share their moods and feelings. Many popular applications like Twitter, WhatsApp, Facebook etc. are not only used to share static forwarded messages or multimedia contents but

also used to express feelings and emotions. To provide such insight, machine learning strategies may provide some unique features that can help explore unique patterns hidden in online communication and process them to reveal emotions like happy, sad, anger, surprise, or disgust. In addition, there is a growing body of literature on the role of social media concerning the structure of social networks such as broken relationships, mental illness smoking and drinking, sexual abuse, and suicidal thoughts among users of social media.

Many social media applications like WhatsApp, Facebook, Instagram etc. has a feature called status or story. The WhatsApp messenger started in 2009 with the purpose of instant communication and transfer of information. People use to share an image, video, text, GIFs in the status of WhatsApp which disappears automatically after 24 hours of uploading. To predict the mood or emotion of the person, WhatsApp status or Facebook story data can be very useful as people use it to post on the status what they usually feel. WhatsApp users are very careful about what they post as their status because their contacts will make meanings from their posts. People are sensitive to WhatsApp profile status; this implies there is a lot of significance attached to it. This phenomenon shows that users are sensitive, alert, and mindful of WhatsApp profile statuses.

In this paper, we have observed that social media status can be used to classify emotions effectively. For extracting meaningful information from the textual status data, the essential step is data preprocessing [5][2]. We used count vectors and TF-IDF feature extraction methods and report experimental results with different machine learning classifiers with the effect of different preprocessing methods. At last, we demonstrated the results of CNN on the same dataset. Our main contributions are, first we have developed a system that could find the emotion label like happy, sad, and anger for any piece of text, especially status and stories on social media with their probability for each emotion using its textual features, Preprocessing techniques, and various machine learning and deep learning algorithms. Second, we were able to achieve an accuracy of around 79% using a CNN classifier with a dataset available on Kaggle and last we Show the effect of pre-processing techniques on the final accuracy of the model.

II. Existing Research

Since the last decade, many researchers are working in the area of emotion analysis and classification using social media datasets. The main goal of emotion classification is to identify the specific text and decide the relevant emotion in a different category.

In [3], the authors have proposed a novel hybrid approach to determine the sentiment hidden in the individual tweet. They have also shown the effectiveness of the pre-processing using different methods like slang/abbreviations and lemmatization and correct and stop words removal. In [4], the authors conducted an extended comparison of sentiment polarity classification methods for Twitter text. Furthermore, they proceeded to the inclusion of a combination of classifiers in the compared set and the aggregation and use of several manually annotated tweets for the evaluation of the methods. In [9], the authors have worked on the Spanish language for the mobile phone and Mexican presidential elections relevant tweets .they proposed parameter settings for SVM, naïve bays, and decision trees. They used n-gram as a feature extraction method and presented results for positive, negative, and neutral classes. Wiebe et al. [5] has manually annotated the emotions, opinions, and sentiments of a sentence, which are taken from news articles. Sana Shahid [7], the author has analyzed the popular social media platform WhatsApp and concluded that it helps in building aimed to explore that WhatsApp helps in building the interpersonal relationship and used by Professionals for meeting business goals .he also analyzed the usage pattern and kind of conversation users made by observing the frequency and composition of users. Church, K. et al [6], have compared SMS to MIM and give the reason for the success of WhatsApp. They conclude that

SMS is more private, formal, and more reliable and WhatsApp messages are more social, informal, and conversational. Yeboah and Ewur [8], authors have analyzed the performance of students in Ghana and conclude that WhatsApp can help in making communication easy and fast. In [11], The Lexicon-based methods have experimented for the instant messaging system as it uses sentiment expression keywords from the corpus and uses this to classify the emotions in different categories. The proposed method first identifies the emotion-relevant content in the text using keywords. After this to detect the emotional meaning of the text, they extracted syntactic features. Other functions like gestures, postures can be used to help the users to communicate with individual users. Aman et al. [12] have proposed a novel classification method that is based on emotional intensity knowledge. The author has achieved around 66% of accuracy rate for the blog corpus emotion classification task. Alm et al. [13], proposed an SVM-based text sentiment prediction method combined with SNoW (sparse network of winnows) architecture. In this approach, 22 fairy tales of Grimm's are taken as the input dataset. These fairy tales are divided into six emotion categories named happy, sad, fearful, angry, disgusted, surprised by selecting 30 features such as the first sentence of the story and specific connectives. Then the author has compared the result of the proposed method SVM + SNoW with existing well-known approaches and achieved 69.37% accuracy.

However, many researchers have done lots of work in the field of emotion classification and sentiment analysis using various social media datasets. But after a thorough investigation of the related literature, we came up with the conclusion that still there is a scope in the field of emotion classification using social media status. Hence, we present the effect of pre-processing in emotion analysis, and a report on experiment results demonstrating that feature selection and representation can affect the classification performance positively.

II. Proposed Methodology

The ultimate goal of this paper is to evaluate the effect of pre-processing methods for emotion classification for social media status datasets. Several pre-processing techniques are available but we have applied some of them like cleaning Html tags, converting to lower, removing special characters and stopping words, and performing stemming and evaluating the effectiveness of these methods for different classifiers. Figure. 1 shows the flow for analyzing the emotions using social media status. In this paper, Emotion analysis has been performed by two different approaches. One is using the traditional machine learning methods, which extract the hand-crafted features from the data using TF-IDF and Count Vector methods. The other is using the deep learning methods, which don't require manual extraction of features.

I. Dataset Description

The input dataset is available on Kaggle (<https://www.kaggle.com/sankha1998/emotion>). It has social media status collected by scraping from different sources. The dataset contains a textual status for three basic emotions happy, sad, and angry. The .csv file for each emotion category has two columns for status and relevant sentiment respectively.

II. Preprocessing Techniques

Preprocessing is the basic mandatory step for any kind of classification problem. It tries to clean the data by removing noise and preparing suitable data for the machine-learning model. We have applied the following methods to convert raw data into a suitable form.

- Cleaning Html tag: - Unstructured text contains a lot of noise, especially here, we use

techniques like web or screen scraping.

- Converting to lower: - Converting all data to lowercase helps in the process of pre-processing.
- Remove special characters:-Special characters and symbols are usually non-alphanumeric characters, which add to the extra noise in unstructured text.
- Remove stop words: - Words that have little or no significance, especially when constructing meaningful features from the text, are known as stop words. Typically, these can be articles, conjunctions, prepositions, and so on. Some examples of stop words are a, an, the, and the like.
- Perform stemming: - Word stems are also known as the base form of a word, and we can Create new words by attaching affixes to them in a process known as inflection. The reverse process of obtaining the base form of a word from its inflected form is known as stemming. Stemming helps us in standardizing words to their base or root stem, irrespective of their inflections.

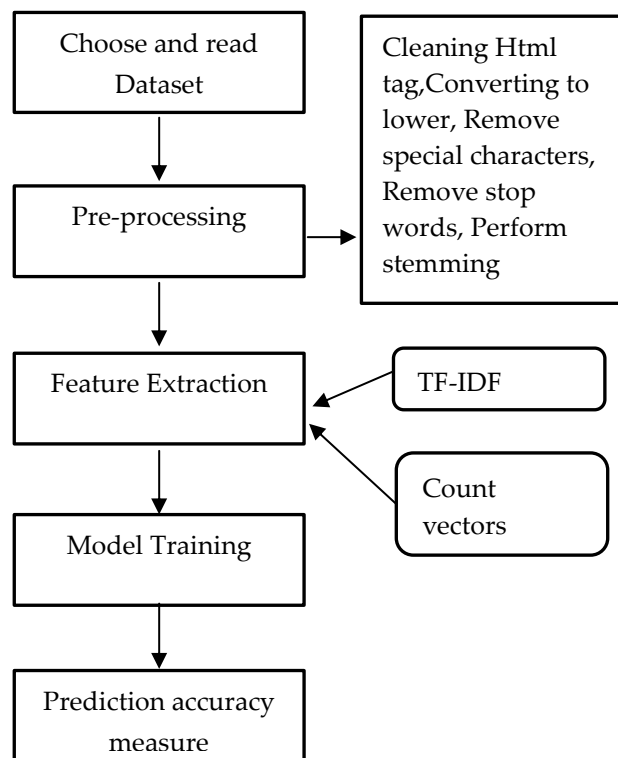


Figure 1: Work Flow basic of emotion analysis

III. Feature Extraction

The preprocessed data is high-dimensional and unstructured. So different data is structured in different ways, which makes it difficult for the different classifiers to work on these data. The process to reduce the dimensionality of these kinds of data and extract the useful features from the text is known as feature extraction.

- TF-IDF: - Term frequency and inverse document frequency method is normally used for information retrieval from text purposes. It shows the relevance of particular term is in the

document.[10] It converts simple words into vectors and assigns weights to not relevant words. We have used it as a feature extraction method to determine which terms in a document are most distinguishing for that document.

- Count Vector:-This method counts the number of occurrences of each word that appears in the particular document and makes a vector to store the result of it.

IV. Classifiers

The ultimate goal for emotion recognition is to classify the input into relevant emotion classes like happy, sad, or anger. Many classification models are available for this purpose. We have chosen some well-known classifiers, named Naïve Bayes, Linear Discriminant Analysis (LDA), Random Forest (RF), Multi-Layer Perceptron, SGD, and CNN to evaluate their performance depending on the preprocessing method applied to the input dataset.

Each classifier has its own merits and demerits, so as per the input data and require the appropriate classifier can be chosen. The naïve Bayes algorithms are widely used for text classification purpose because it is efficient even though the dataset size is less and resources are scarce. LDA works well for the linear classification of data as it has good generalization ability. Random forest and MLP work well if data is high-dimensional. CNN is the updated version of a simple neural network, as it tries to make the network less complex by sharing weights and making a local connection. As shown in figure:-2, we have sequentially implemented the deep model, layer by layer. To add the layers we have used add () function. In the out model, we have a total of three dense layers and two Dropout layers as shown in the figure:-2 Activation function has a dominant effect on the performance of the network. We have used ReLu in our network as it works normally effectively with the neural network. Finally, we compiled our model by using 'adam' as out optimizer, 'accuracy' as a metric, and 'categorical_crossentropy' for our loss function.

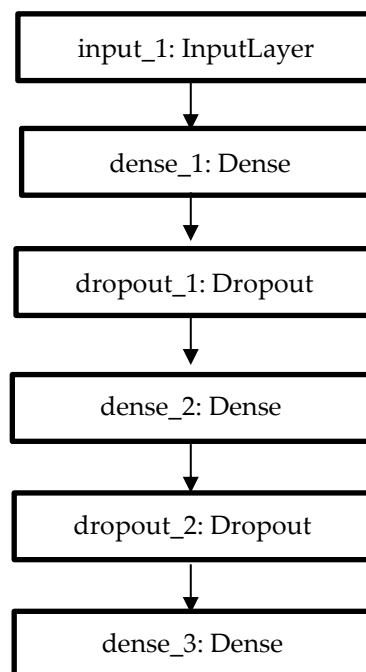


Figure 2: Deep architecture for emotion classification

IV. Experimental Results and Discussion

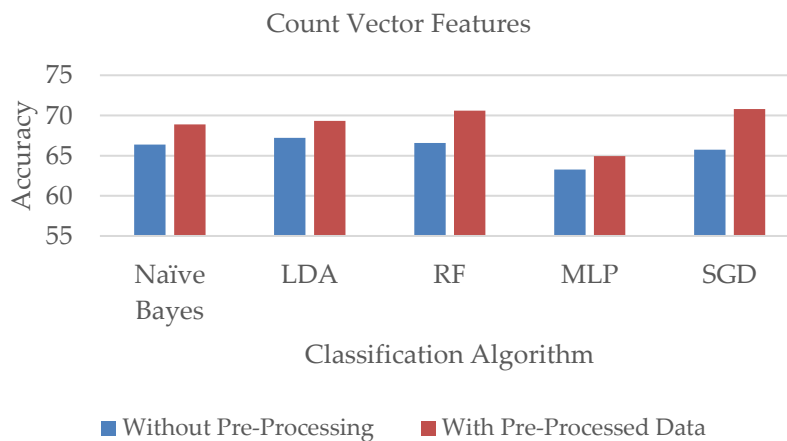
We have performed various Pre-processing techniques on the dataset as mentioned in the previous section and will show the results in this section. We have tried Count vector and TF-IDF feature extraction methods and will show the results. Then, will show the results obtained from deep neural networks.

I. Count Vector Feature Experiments

First, we have used Count Vector Features with different classifiers named Naïve Bayes, LDA, Random Forest, Multilayer Perceptron, and SGD. As shown in the table:-1 the result shows that maximum accuracy can be achieved by using a random forest classifier which is 70.59% by applying pre-processing which is 4% higher than without applying pre-processing techniques.

Table 1: Performance Comparison of Count vector features

Classifier	Accuracy(%) without Pre-processing	Accuracy(%) with Pre-processed data
Naïve Bayes	66.38	68.90
LDA	67.23	69.33
RF	66.59	70.59
MLP	63.27	64.95
SGD	65.75	69.33



II. TF-IDF Feature Experiments

Now, we tried TF-IDF Features with different classifiers named Naïve Bayes, LDA, Random Forest, Multilayer Perceptron, and SGD. As shown in the table:-2 The result shows that maximum accuracy can be achieved by using SGD which is 70.80% by applying pre-processing which is 5% higher than without applying pre-processing techniques. Here, Random forest gives good results without pre-processing which is 67.43%.

Table 2: Performance Comparison of TF-IDF features

Classifier	Accuracy(%) without Pre-processing	Accuracy(%) with Pre-processed data
Naïve Bayes	63.44	65.76
LDA	65.96	69.96
RF	67.43	68.49
MLP	63.44	65.96
SGD	65.75	70.80

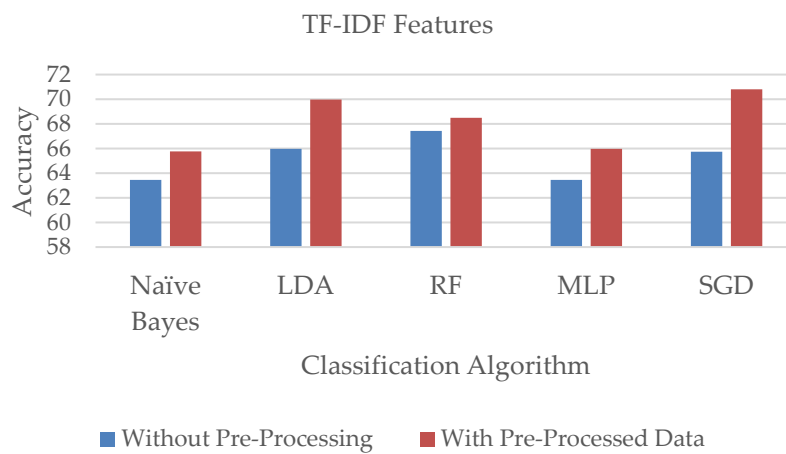


Figure 4: Effect of pre-processing on different classifiers for TF-IDF features

III. CNN Based Experiments

CNN architecture we have used is already explained in section III. As given in table 3, we have achieved 79% validation accuracy by implementing this model for all three emotion categories. Figure: - 5 shows the confusion metrics for happy, sad, and angry emotions. It clearly shows that the deep model achieves almost 9% higher accuracy than manual feature extractions.

Table 3: Class-wise Precision, F1-score, and support

	Precision	Recall	F1-score	support
Angry	0.79	0.87	0.83	237
Happy	0.79	0.75	0.77	228
Sad	0.79	0.75	0.77	208
Accuracy	NA	NA	0.79	673
Macro avg	0.79	0.79	0.79	673
Weighted avg	0.79	0.79	0.79	673

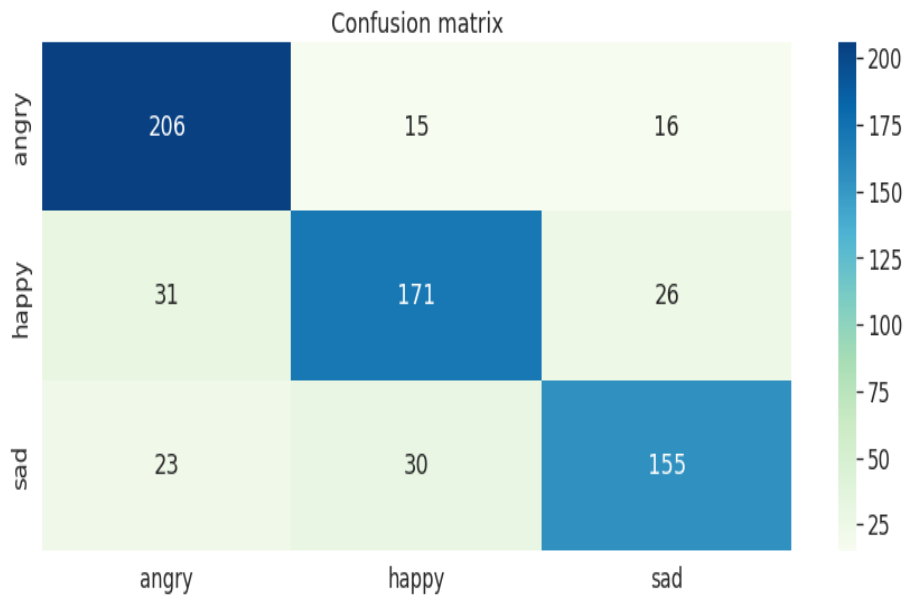


Figure 5: Confusion Matrix for different emotions

V. Conclusion and Future Work

Even though detail research has been done in the area of analyzing social media text for emotion detection, still it faces many problems like poor accuracy when applied to real-life data. For making classification tasks efficient, pre-processing and feature extraction should be performed properly on the raw dataset. We applied different preprocessing techniques to the dataset of social media status and evaluated the performance of five different machine-learning classifiers and CNN for deep learning classification. Our experimental results concluded that the appropriate pre-processing methods could effectively improve the efficiency of the classifiers by around 4-5%. By the traditional approach, the highest accuracy has been achieved by SGD classifiers which is 70.59% for count vector features whereas the highest accuracy has been achieved by random forest classifiers which is 70.80% for TF-IDF features. For the deep learning approach, CNN achieved 79% accuracy for classifying the emotions in three different categories which is almost 9% higher than the traditional approach. However, this work can be further extended by incorporating the different pre-processing methods to find the optimal settings. In future, these results can be cross verified on other wide and real-world datasets of social media status for emotion classification.

References

- [1] Akrivi Krouska, Christos Troussas and Maria Virvou (2016).The effect of preprocessing techniques on Twitter Sentiment Analysis.*7th International Conference on Information, Intelligence, Systems & Applications (IISA)*.
- [2] Lin Shu, Jinyan Xie, Mingyue Yang, Ziyi Li, Zhenqi Li, Dan Liao, Xiangmin Xu, and Xinyi Yang(2018). A Review of Emotion Recognition Using Physiological Signals., *sensors*.
- [3] F. H. Khan, S. Bashir, and U. Qamar(2014). TOM: Twitter opinion mining framework using hybrid classification scheme. *Decision Support Systems*. 57(1), 245-257, 2014.
- [4] E. Psomakelis, K. Tserpes, D. Anagnostopoulos, T. Varvarigou(2014). Comparing methods for twitter sentiment analysis.*KDIR 2014 - Proceedings of the Int. Conf. on Knowledge Discovery and Information Retrieval*, 225-232.
- [5] Janyce Wiebe, Theresa Wilson, and Claire Cardie (2005).Annotating expressions of

opinions and emotions in language. *Language resources and evaluation*. 39(2-3):165–210, 2005.

[6] Church, K., de Oliveira(2013). What's Up with Whatsapp: Comparing Mobile Instant Messaging Behaviors with Traditional SMS .In: *Proceedings of the 15th International Conference on Human-computer Interaction with Mobile Devices and Services*, 352–361.

[7] Sana Shahid (2018). Content Analysis of Whatsapp Conversations: An Analytical Study to Evaluate the Effectiveness of Whatsapp Application in Karachi. *International Journal of Media, Journalism and Mass Communications (IJMJMC)*. Volume 4, Issue 1, 2018, 14-26 ISSN 2454-9479.

[8] Rice, D. R. and Zorn, C. (2013).Corpus-Based Dictionaries for Sentiment Analysis of Specialized Vocabularies. *Proceedings of NDATAAD*, 1–17.

[9] G. Sidorov, S. Miranda-Jiménez, F. Viveros-Jiménez, and J. Gordon (2012). Empirical study of machine learning based approach for opinion mining in tweets. *11th Mexican International Conference on Artificial Intelligence, MICAI*.

[10] Zach CHASE, Nicolas Genain, and Orren Karniol-Tambour (2013). Learning Multi-Label Topic Classification of News Articles. *Semantic scholar*.

[11] Ma Chunling, Osherenko A, Prendinger H, et al (2005). A chat system based on emotion estimation from text and embodied conversational messengers. *Proc of the 4th Int Conf on Active Media Technology. Piscataway, NJ: IEEE*, 546-548.

[12] Aman S, Szpakowicz S. Identifying expressions of emotion in text (2007). Proc of the 10t Int Conf on Text, Speech and Dialogue. *Berlin: Springer*, 196-205.

[13] Alm C, Roth D, Sproat R.(2005). Emotions from text: Machine learning for text-based emotion Prediction. *Proc of the 2nd Conf on Human Language Technology and on Empirical Methods in Natural Language Processing. New York: ACM*, 579-586.

A TWO NON-IDENTICAL UNIT PARALLEL SYSTEM WITH PRIORITY IN REPAIR AND CORRELATED LIFE TIMES

Pradeep Chaudhary, Anika Sharma

•

Department of Statistics
Ch. Charan Singh University, Meerut – 250004 (India)
E-mail: pc25jan@gmail.com; ash27sharma@gmail.com

Abstract

The paper analyses a two non-identical unit parallel system in respect of various measures of system effectiveness by using regenerative point techniques. It has been considered that the life times of both the units are correlated random variables and a single repairman is always available with the system to repair a failed unit.

Keywords: Transition probabilities, mean sojourn time, bi-variate exponential distribution, reliability, MTSF, availability, expected busy period of repairman, net expected profit.

I. Introduction

Various authors including Sridharan & Kalyani (2002), Mokaddis & Sherbeny (2008) in the field of reliability theory have been analyzed two unit parallel system models under different sets of assumptions using regenerative point technique. Some of the authors using the concept of giving the priority to one of the unit in repair and compare to other, Malik et al. (2010), Kumar et al. (2018, 2021) developed a reliability model for a system of non-identical units parallel system with priority to repair. In all these systems models it is assumed that the lifetimes are uncorrelated random variables, but in practical situations this seems to be unrealistic because in many cases there may be some sort of correlation between the lifetimes of operating units. Singh & Poonia (2019) introduced the concept of correlation between failure and their times in the analysis of a single server two unit cold standby system. Later various papers including those by Gupta et al. (2010) have been analyzed the correlated failure and repair time distribution of a unit.

Gupta and co-workers [2008,2018] analyzed two unit parallel and standby system models under different sets of assumptions by taking the failure and repair times as correlated random variables having their joint distribution as bivariate exponential. They have considered only single type of failure in an operating unit. Some authors including [1999, 2013] analyzed two-unit parallel system models by taking the joint distribution of life times of the units working in parallel as bivariate exponential. They have also considered the single type of failure in an operating unit.

In the present paper we analyze a two non-identical unit parallel system model with priority in repair and correlated life times of the units working in parallel having their joint distribution as

bivariate exponential distribution with different parameters as the form of the joint p.d.f. given below.

$$f(x_1, x_2) = \alpha_1 \alpha_2 (1-r) e^{-\alpha_1 x_1 - \alpha_2 x_2} I_0(2\sqrt{\alpha_1 \alpha_2 r x_1 x_2}); \quad x_1, x_2, \alpha_1, \alpha_2 > 0; \quad 0 \leq r < 1$$

Where, $I_0 = \sum_{k=0}^{\infty} \frac{(z/2)^{2k}}{(k!)^2}$

is the modified Bessel function of type-I and order zero.

By using regenerative point technique, the following measures of system effectiveness are obtained-

- i. Transition probabilities and mean sojourn times in various states.
- ii. Reliability and mean time to system failure (MTSF).
- iii. Point-wise and steady-state availabilities of the system as well as expected up time of the system during time interval (0, t).
- iv. Expected busy period of repairman in the repair of unit-1 and unit-2 during time interval (0, t).
- v. Net expected profit earned by the system in time interval (0, t).

II. System Description and Assumptions

1. The system consists of two non-identical units (unit-1 and unit-2). Initially, both the units work in parallel configuration.
2. Each unit of the system has two possible modes-Normal (N) and total failure (F).
3. The first unit gets priority in repair.
4. System failure occurs when both the units stop functioning.
5. A single repairman is always available with the system to repair a totally failed unit and repair discipline is first come, first served (FCFS).
6. If during the repair of a failed unit the other unit also fails, then the later failed unit waits for repair until the repair of the earlier failed unit is completed.
7. The repair times of both the units are uncorrelated random variables, each having a general distribution with different parameters.
8. Each repaired unit works as good as new.
9. The joint distribution of lifetimes (failure times) of both the units is taken to be bivariate exponential having a joint density function of the form ,

$$f(x_1, x_2) = \alpha_1 \alpha_2 (1-r) e^{-\alpha_1 x_1 - \alpha_2 x_2} I_0(2\sqrt{\alpha_1 \alpha_2 r x_1 x_2}); \quad x_1, x_2, \alpha_1, \alpha_2 > 0; \quad 0 \leq r < 1$$

Where, $I_0 = \sum_{k=0}^{\infty} \frac{(z/2)^{2k}}{(k!)^2}$

10. The arrival time distribution of repairman is general.

III. Notations and States of the System

We define the following symbols for generating the various states of the system-

- N_{10}, N_{20} : Unit-1 and unit-2 is in N-mode and operative in parallel.
 F_{1r}, F_{2r} : Unit-1 and unit-2 is in F-mode and under repair.
 F_{2w} : Unit-2 is in F-mode and under waiting for repair.
 F_{1r}^1 : First unit is in failure mode and its repair is continued from state S_1 .

Considering the above symbols in view of assumptions stated in section-2, the possible states of the system are shown in the transition diagram represented by **Figure. 1**. It is to be noted that the epochs of transitions into the state S_1 from S_2 are non-regenerative, whereas all the other entrance epochs into the states of the systems are regenerative.

The other notations used are defined as follows:

- E : Set of regenerative states.
- $X_i (i = 1, 2)$: Random variables denoting the failure time of unit-1 N-mode and unit-2 respectively for $(i=1, 2)$
- $f(x_1, x_2)$: Joint probability density function of $x_i; i = 1, 2$
 $= \alpha_1 \alpha_2 (1-r) e^{-\alpha_1 x_1 - \alpha_2 x_2} I_0(2\sqrt{\alpha_1 \alpha_2 r x_1 x_2})$
; $x_1, x_2, \alpha_1, \alpha_2 > 0; 0 \leq r < 1$

$$\text{Where, } I_0(2\sqrt{\alpha_1 \alpha_2 r x_1 x_2}) = \sum_{k=0}^{\infty} \frac{(\alpha_1 \alpha_2 r x_1 x_2)^k}{(k!)^2}$$

- $g_i(x)$: Marginal p.d.f. of $X_i = x$
 $= \alpha_i (1-r) e^{-\alpha_i (1-r)x}; x > 0, \alpha > 0$
- $K_i(\bullet | X)$: Conditional p.d.f. of $X_i | X_j = x; i \neq j, j = 1, 2$
- $k_1(x_1 | X_2 = x_2)$: Conditional p.d.f. of $X_1 | X_2 = x$
 $= \alpha_1 e^{-(\alpha_1 x_1 + \alpha_2 r x)} I_0(2\sqrt{\alpha_1 \alpha_2 r x_1 x})$
- $k_2(x_2 | X_1 = x_1)$: Conditional p.d.f. of $X_2 | X_1 = x$
 $= \alpha_2 e^{-(\alpha_2 x_2 + \alpha_1 r x)} I_0(2\sqrt{\alpha_1 \alpha_2 r x x_2})$
- $g_i(\bullet), G_i(\bullet); i = 1, 2$: The repair time probability distribution function and cumulative distribution function of x_i
- $g_{ij}(\bullet), g_{ij}^{(k)}(\bullet)$: P.d.f. of transition time from state S_i to S_j and S_i to S_j via S_k .
- $p_{ij}(\bullet), p_{ij}^{(k)}(\bullet)$: Steady-state transition probabilities from state S_i to S_j and S_i to S_j via S_k .
- $p_{ijx}(\bullet), p_{ijx}^{(k)}(\bullet)$: Steady-state transition probabilities from state S_i to S_j and S_i to S_j via S_k when it is known that the unit has worked for time x before its failure.
- β_1 : Repair time of failed unit-2
- $*$: Symbol for Laplace Transform i.e. $g_{ij}^*(s) = \int e^{-st} q_{ij}(t) dt$
- \sim : Symbol for Laplace Stieltjes Transform i.e. $\mathcal{Q}_{ij}^{\sim}(s) = \int e^{-st} dQ_{ij}(t)$
- \odot : Symbol for ordinary convolution i.e.

$$A(t) \odot B(t) = \int_0^t A(u) B(t-u) du$$

†The limits of integration are 0 to ∞ whenever they are not mentioned.

TRANSITION DIAGRAM

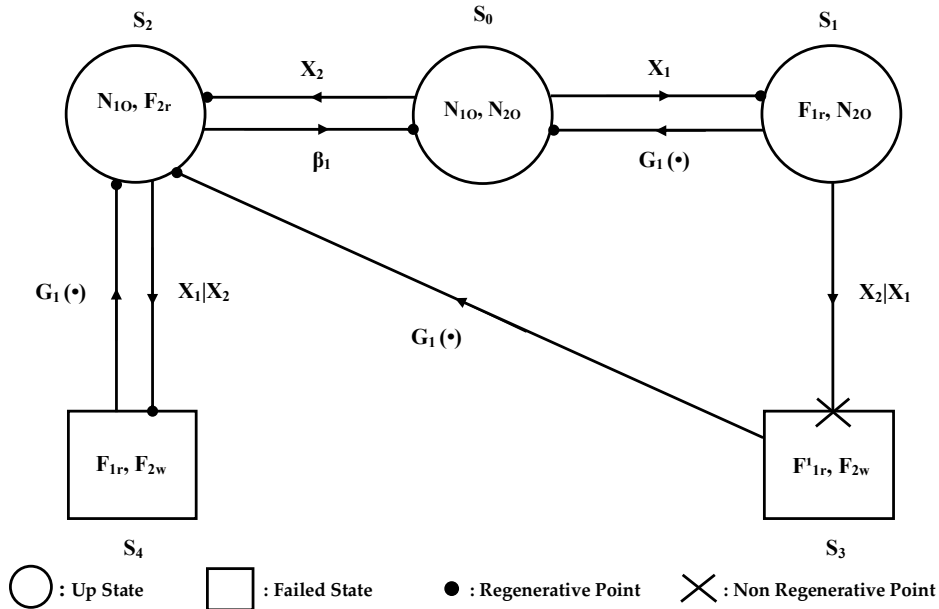


Figure.1

IV. Transition Probabilities and Sojourn Times

Let $X(t)$ be the state of the system at epoch t , then $\{X(t); t \geq 0\}$ constitutes a continuous parametric Markov-Chain with state space $E = \{S_0$ to $S_4\}$. The various measures of system effectiveness are obtained in terms of steady-state transition probabilities and mean sojourn times in various states. First we obtain the direct conditional and unconditional transition probabilities in terms of

$$\alpha'_1 = \frac{\alpha_1}{\alpha_1 + \beta_1}, \quad \alpha'_2 = \frac{\alpha_2}{\alpha_2 + \theta_1}$$

as follows-

$$p_{01} = \int \alpha_1 (1-r) e^{-\alpha_1(1-r)t} e^{-\alpha_2(1-r)t} dt = \frac{\alpha_1}{\alpha_1 + \alpha_2}$$

$$p_{02} = \int \alpha_2 (1-r) e^{-\alpha_2(1-r)t} e^{-\alpha_1(1-r)t} dt = \frac{\alpha_2}{\alpha_1 + \alpha_2}$$

$$p_{42} = \int dG_1(t) = 1$$

$$\begin{aligned} p_{10|x} &= \int dG_1(t) \bar{K}_2(t|x) = \int_0^\infty dG_1(t) \int_u^\infty \alpha_2 e^{-(\alpha_2 y + \alpha_1 r x)} I_0(2\sqrt{\alpha_1 \alpha_2 r x y}) dy \\ &= \int_0^\infty dG_1(t) \left(\int_u^\infty \alpha_2 e^{-(\alpha_2 y + \alpha_1 r x)} \sum_{j=0}^\infty \frac{(\alpha_1 \alpha_2 r x y)^j}{(j!)^2} \right) du \\ &= \alpha_2 e^{-\alpha_1 r x} \sum_{j=0}^\infty \frac{(\alpha_1 \alpha_2 r x)^j}{(j!)^2} \left(\int_0^\infty e^{-\alpha_2 y} y^j [\bar{G}_1(y)] dy \right) \end{aligned}$$

Similarly,

$$p_{20|x} = 1 - \alpha_1' e^{-\alpha_2 r x (1 - \alpha_1')}, \quad p_{24|x} = \alpha_1' e^{-\alpha_2 r x (1 - \alpha_1')}$$

$$p_{12}^{(3)} = 1 - \left[\alpha_2 e^{-\alpha_1 r x} \sum_{j=0}^{\infty} \frac{(\alpha_1 \alpha_2 r x)^j}{(j!)^2} \left(\int_0^{\infty} e^{-\alpha_2 y} y^j [\bar{G}_1(y)] dy \right) \right]$$

The unconditional transition probabilities with correlation coefficient from some of the above conditional transition probabilities can be obtained as follows:

$$p_{10} = \int p_{10|x} g_1(x) dx$$

$$= \alpha_1 (1-r) \int e^{-\alpha_1 (1-r)x} \alpha_2 e^{-\alpha_1 r x} \sum_{j=0}^{\infty} \frac{(\alpha_1 \alpha_2 r x)^j}{(j!)^2} \left(\int_0^{\infty} e^{-\alpha_2 y} y^j [\bar{G}_1(y)] dy \right) dx$$

Similarly,

$$p_{20} = 1 - \frac{\alpha_1' (1-r)}{(1 - \alpha_1' r)}, \quad p_{24} = \frac{\alpha_1' (1-r)}{(1 - \alpha_1' r)}$$

$$p_{12}^{(3)} = \alpha_1 (1-r) \int e^{-\alpha_1 (1-r)x} \left(1 - \left[\alpha_2 e^{-\alpha_1 r x} \sum_{j=0}^{\infty} \frac{(\alpha_1 \alpha_2 r x)^j}{(j!)^2} \left(\int_0^{\infty} e^{-\alpha_2 y} y^j [\bar{G}_1(y)] dy \right) \right] \right) dx$$

It can be easily verified that,

$$p_{01} + p_{02} = 1, \quad p_{10} + p_{12}^{(3)} = 1, \quad p_{42} = 1, \quad p_{20} + p_{24} = 1 \tag{1-4}$$

V. Mean Sojourn Time

The mean sojourn time ψ_i in state S_i is defined as the expected time taken by the system in state S_i before transiting into any other state. If random variable U_i denotes the sojourn time in state S_i then,

$$\psi_i = \int P[U_i > t] dt$$

Therefore, its values for various regenerative states are as follows-

$$\psi_0 = \int e^{-\alpha_1 (1-r)t} e^{-\alpha_2 (1-r)t} dt = \frac{1}{(\alpha_1 + \alpha_2)(1-r)} \tag{5}$$

$$\psi_{1|x} = \int \bar{G}_1(t) \bar{K}_2(t|x) dt = \alpha_2 e^{-\alpha_1 r x} \sum_{j=0}^{\infty} \frac{(\alpha_1 \alpha_2 r x)^j}{(j!)^2} \left(\int_0^{\infty} e^{-\alpha_2 y} y^j \left(\int_0^y \bar{G}_1(t) dt \right) dy \right)$$

So that,

$$\psi_1 = \int \psi_{1|x} g_1(x) dx$$

$$= \int \psi_{1|x} \alpha_1 (1-r) e^{-\alpha_1 (1-r)x} dx$$

$$= \alpha_1 \alpha_2 (1-r) \sum_{j=0}^{\infty} \frac{(\alpha_1 \alpha_2 r)^j}{(j!)^2} \left[\left(\int_0^{\infty} e^{-\alpha_2 y} y^j \left(\int_0^y \bar{G}_1(t) dt \right) dy \right) \left(\int_0^{\infty} e^{-\alpha_1 r x} e^{-\alpha_1 (1-r)x} x^j dx \right) \right] \tag{6}$$

$$= \int e^{-\alpha_2 (1-r)t} \bar{G}_1(t) dt$$

$$\psi_{2|x} = \frac{1}{\beta_1} \left[1 - \alpha_1' e^{-\alpha_2 r x (1 - \alpha_1')} \right]$$

So that,

$$\psi_2 = \frac{1}{\beta_1} \left[1 - \frac{\alpha_1' (1-r)}{(1 - \alpha_1' r)} \right] \tag{7}$$

$$\psi_4 = \int \bar{G}_1(t) dt \tag{8}$$

VI. Analysis of Characteristics

I. Reliability and MTSF

Let $R_i(t)$ be the probability that the system operates during $(0, t)$ given that at $t=0$ system starts from $S_i \in E$. To obtain it we assume the failed states S_2 and S_4 as absorbing. By simple probabilistic arguments, the value of $R_0(t)$ in terms of its Laplace Transform (L.T.) is given by

$$R_0^*(s) = \frac{Z_0^* + q_{01}^* Z_1^* + q_{02}^* Z_2^*}{1 - q_{01}^* q_{10}^* - q_{02}^* q_{20}^*} \quad (9)$$

We have omitted the argument's from $q_{ij}^*(s)$ and $Z_i^*(s)$ for brevity. $Z_i^*(s); i = 0, 1, 2$ are the L. T. of

$$Z_0(t) = e^{-(\alpha_1 + \alpha_2)(1-r)t}, \quad Z_1(t) = \bar{G}_1(t), \quad Z_2(t) = e^{-\beta_1 t}$$

Taking the Inverse Laplace Transform of (9), one can get the reliability of the system when system initially starts from state S_0 .

The MTSF is given by,

$$E(T_0) = \int R_0(t) dt = \lim_{s \rightarrow 0} R_0^*(s) = \frac{\Psi_0 + p_{01}\Psi_1 + p_{02}\Psi_2}{1 - p_{01}p_{10} - p_{02}p_{20}} \quad (10)$$

II. Availability Analysis

Let $A_i(t)$ be the probability that the system is up at epoch t , when initially it starts operation from state $S_i \in E$. Using the regenerative point technique and the tools of Laplace transform, one can obtain the value of $A_0(t)$ in terms of its Laplace transforms i.e. $A_0^*(s)$ given as follows-

$$A_0^*(s) = \frac{N_1(s)}{D_1(s)} \quad (11)$$

Where,

$$N_1(s) = Z_0^* [1 - q_{24}^* q_{42}^*] + Z_1^* q_{01}^* [1 - q_{24}^* q_{42}^*] + Z_2^* [q_{01}^* q_{12}^{(3)*} + q_{02}^*]$$

and

$$D_1(s) = 1 - q_{24}^* q_{42}^* - q_{10}^* q_{01}^* (1 - q_{24}^* q_{42}^*) - q_{20}^* (q_{01}^* q_{12}^{(3)*} + q_{02}^*) \quad (12)$$

Where, $Z_i(t), i=0,1,2$ are same as given in section VI(I).

The steady-state availability of the system is given by

$$A_0 = \lim_{t \rightarrow \infty} A_0(t) = \lim_{s \rightarrow 0} s A_0^*(s) \quad (13)$$

We observe that

$$D_1(0) = 0$$

Therefore, by using L. Hospital's rule the steady state availability is given by

$$A_0 = \lim_{s \rightarrow 0} \frac{N_1(s)}{D_1(s)} = \frac{N_1}{D_1} \quad (14)$$

Where,

$$N_1 = \Psi_0 [1 - p_{24}p_{42}] + \Psi_1 p_{01} [1 - p_{24}p_{42}] + \Psi_2 [p_{01}p_{12}^{(3)} + p_{02}]$$

and

$$D_1 = \Psi_0 p_{20} + \Psi_1 p_{01} p_{20} + \Psi_2 (1 - p_{10} p_{01}) + \Psi_4 p_{24} (1 - p_{10} p_{01}) \quad (15)$$

The expected up time of the system in interval $(0, t)$ is given by

$$\mu_{up}(t) = \int_0^t A_0(u) du$$

So that, $\mu_{up}^*(s) = \frac{A_0^*(s)}{s}$ (16)

III. Busy Period Analysis

Let $B_1^1(t)$ and $B_1^2(t)$ be the respective probabilities that the repairman is busy in the repair of unit-1 failed due to first repair with priority of unit-1 and unit-2 failed due to second repair at epoch t , when initially the system starts operation from state $S_i \in E$. Using the regenerative point technique and the tools of L. T., one can obtain the values of above two probabilities in terms of their L. T. i.e. $B_1^{1*}(s)$ and $B_1^{2*}(s)$ as follows-

$$B_1^{1*}(s) = \frac{N_2(s)}{D_1(s)}, \quad B_1^{2*}(s) = \frac{N_3(s)}{D_1(s)} \quad (17-18)$$

Where,

$$N_2(s) = (Z_1^* + q_{13}^* Z_3^*) q_{01}^* (1 - q_{42}^* q_{24}^*) - Z_4^* (q_{01}^* q_{12}^{(3)*} q_{24}^* + q_{02}^* q_{24}^*)$$

and

$$N_3(s) = Z_2^* (q_{01}^* q_{12}^{(3)*} + q_{02}^*)$$

and $D_1(s)$ is same as defined by the expression (12) of section VI(II).

The steady state results for the above two probabilities are given by-

$$B_0^1 = \lim_{s \rightarrow 0} s B_0^{1*}(s) = N_2 \setminus D_1^1 \quad \text{and} \quad B_0^2 = \lim_{s \rightarrow 0} s B_0^{2*}(s) = N_3 \setminus D_1^1 \quad (19-20)$$

Where,

$$N_2(0) = (\psi_1 + p_{13}\psi_3) p_{01} (1 - p_{42}p_{24}) - \psi_4 (p_{01}p_{12}^{(3)} p_{24} + p_{02}p_{24}) \quad (21)$$

$$N_3(0) = \psi_2 (p_{01}p_{12}^{(3)} + p_{02}) \quad (22)$$

and D_1^1 is same as given in the expression (15) of section VI(II).

The expected busy period in repair of unit-1 failed due to first repair with priority of unit-1 and unit-2 failed due to second repair during time interval $(0, t)$ are respectively given by-

$$\mu_b^1(t) = \int_0^t B_0^1(u) du, \quad \text{and} \quad \mu_b^2(t) = \int_0^t B_0^2(u) du$$

So that,

$$\mu_b^{1*}(s) = \frac{B_0^{1*}(s)}{s} \quad \text{and} \quad \mu_b^{2*}(s) = \frac{B_0^{2*}(s)}{s} \quad (23-24)$$

IV. Profit Function Analysis

The net expected total cost incurred in time interval $(0, t)$ is given by

$$P(t) = \text{Expected total revenue in } (0, t) - \text{Expected cost of repair in } (0, t) \\
= K_0 \mu_{up}(t) - K_1 \mu_b^1(t) - K_2 \mu_b^2(t) \quad (25)$$

Where, K_0 is the revenue per-unit up time by the system during its operation. K_1 and K_2 are the amounts paid to the repairman per-unit of time when the system is busy in repair of unit-1 failed due to first repair with priority of unit-1 and unit-2 failed due to second repair respectively.

The expected total profit incurred in unit interval of time is $P = K_0A_0 - K_1B_0^1 - K_2B_0^2$

VII. Particular Case

Let, $\bar{G}_1(y) = e^{-\theta_1 y}$

In view of above, the changed values of transition probabilities and mean sojourn times.

$$p_{10|x} = \alpha_2 e^{-\alpha_1 r x} \sum_{j=0}^{\infty} \frac{(\alpha_1 \alpha_2 r x)^j}{(j!)^2} \left(\int_0^{\infty} e^{-\alpha_2 y} y^j [\bar{G}_1(y)] dy \right) = \alpha_2' e^{-\alpha_1 r x (1 - \alpha_2')}$$

$$p_{12|x}^{(3)} = 1 - \alpha_2' e^{-\alpha_1 r x (1 - \alpha_2')}, \quad p_{10} = \frac{\alpha_2' (1 - r)}{(1 - \alpha_2' r)}, \quad p_{12}^{(3)} = 1 - \frac{\alpha_2' (1 - r)}{(1 - \alpha_2' r)}$$

$$\psi_1 = \frac{1}{\theta_1 + \alpha_2 (1 - r)}, \quad \psi_4 = \frac{1}{\theta_1}$$

VIII. Graphical Study of Behaviour and Conclusions

For a more clear view of the behaviour of system characteristics with respect to the various parameters involved, we plot curves for **MTSF** and **profit function** in **Fig. 2** and **Fig. 3** w.r.t. α_1 for three different values of correlation coefficient $\alpha_2 = 0.1, 0.5, 0.9$ and two different values of repair parameter $r = 0.25, 0.6$ while the other parameters are $\beta_1 = 0.085, \theta_1 = 0.6$. It is clearly observed from **Fig. 2** that **MTSF** increases uniformly as the value of α_2 and r increase and it decrease with the increase in α_1 . Further, to achieve **MTSF** at least 17 units we conclude for smooth curves that the values of α_1 must be less than **0.13, 0.23** and **0.45** respectively for $\alpha_2 = 0.1, 0.5, 0.9$ when $r = 0.6$. Whereas from dotted curves we conclude that the values of α_1 must be less than **0.12, 0.14** and **0.31** for $\alpha_2 = 0.1, 0.5, 0.9$ when $r = 0.25$.

Similarly, **Fig.3** reveals the variations in **profit (P)** with respect to α_1 for three different values of $\alpha_2 = 0.3, 0.6, 0.9$ and two different values of $r = 0.3, 0.6$, when the values of other parameters $\beta_1 = 0.95, \theta_1 = 0.09, K_0 = 200, K_1 = 95$ and $K_2 = 175$. Here also the same trends in respect of α_1, α_2 and r are observed in case of **MTSF**. Moreover, we conclude from the smooth curves that the system is profitable only if α_1 is less than **0.22, 0.42** and **0.66** respectively for $\alpha_2 = 0.3, 0.6, 0.9$ when $r = 0.6$. From dotted curves, we conclude that the system is profitable only if α_1 is less than **0.19, 0.3** and **0.5** respectively for $\alpha_2 = 0.3, 0.6, 0.9$ when $r = 0.3$.

Behaviour of **MTSF** w.r.t. α_1 for different values of α_2 and r

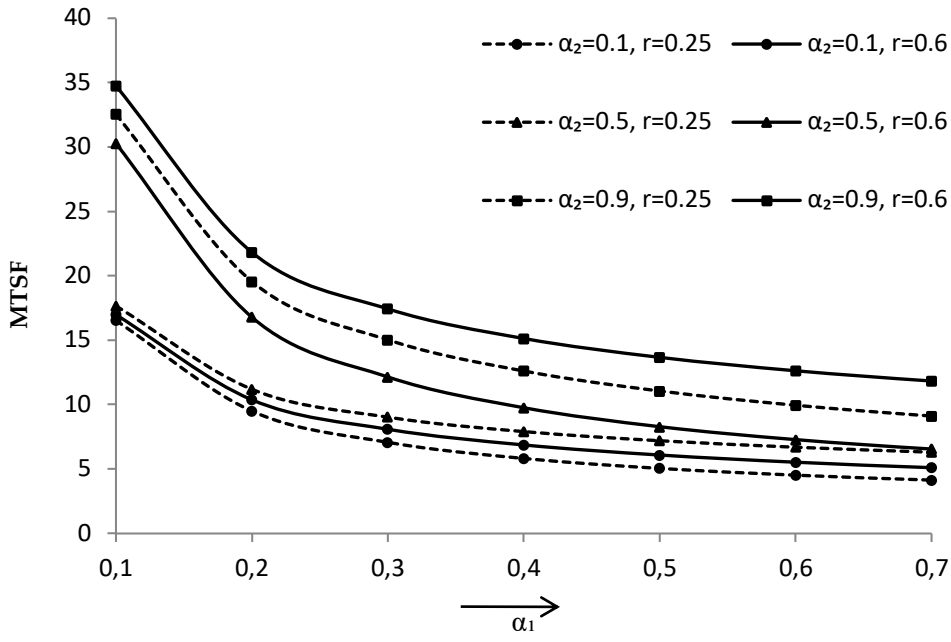


Figure.2
 Behaviour of PROFIT (P) w.r.t. α_1 for different values of α_2 and r

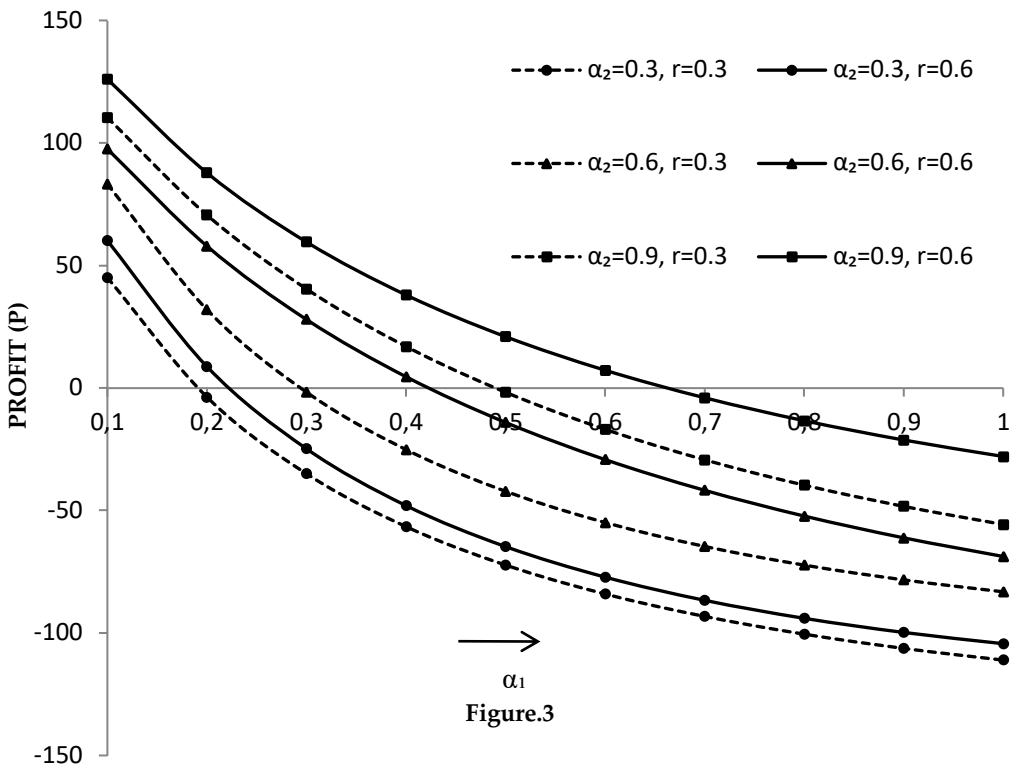


Figure.3

References

- [1] Gupta, R. and Vaishali (2018). A two non-identical unit parallel system with correlated failure and repair times of repair. *International Journal of Agricultural and Statistical Sciences*, 14(2): 721-730.
- [2] Gupta, R., Kishan, R. and Kumar, P. (1999). A two-non-identical unit parallel system with correlated lifetimes. *International Journal of Systems Science*, 30(10):1123-1129.
- [3] Gupta, R., Goel, C.K. and Tomer, A. (2010). Analysis of a two standby system with correlated failure and repair and random appearance and disappearance of repairman. *Journal of Reliability and Statistical Studies*, 3(1):53-61.
- [4] Gupta, R., Mahi, M. and Sharma, V. (2008). A two component two unit standby system with correlated failure and repair times. *Journal of Statistics and Management Systems*, 11(1):77-90.
- [5] Gupta, R., Sharma, P. K. and Shivakar (2013). A two-unit active redundant system with two physical conditions of repairman and correlated life times. *Journal of Ravishankar University*, 24(26):40-51.
- [6] Kumar, A., Saini, M. and Devi, K. (2021). Stochastic modeling of a non-identical redundant system with priority in repair activities. *Thailand Statistician*, 19(1):154-161.
- [7] Kumar, A., Saini, M. and Devi, K. (2018). Stochastic modeling of a non-identical redundant system with priority, preventive maintenance and weibull failure and repair distributions. *Life Cycle Reliability and Safety Engineering*, 7(2):61-70.
- [8] Mokaddis, G.S. and Sherbeny, M.S.EI. (2008). A dissimilar two unit parallel system with common-cause failure and preventive maintenance. *The Journal of Mathematics and Computer Science*, 19(2):153-167.
- [9] Malik, S.C., Bhardwaj, R.K. and Grewal, A.S. (2010). Probabilistic analysis of a system of two non-identical parallel units with priority to repair subject to inspection. *Journal of Reliability and Statistical Studies*, 3(1):1-11.
- [10] Singh, V.V. and Poonia, P.K. (2019). Probabilistic assessment of two unit parallel system with correlated lifetime under inspection using regenerative point technique. *International Journal of Reliability, Risk and Safety*, 2(1):5-14.
- [11] Sridharan, V. and Kalyani, T.V. (2002). Stochastic analysis of a non-identical two unit parallel system with common-cause failure GERT technique. *International Journal of Information and Management Science*, 13(1):49-57.

STOCHASTIC ANALYSIS OF A REPAIRABLE SYSTEM OF NON-IDENTICAL UNITS WITH PRIORITY AND CONDITIONAL FAILURE OF REPAIRMAN

Naveen Kumar¹, S.C. Malik², N. Nandal*

•

¹Department of Mathematics, SGT University, Gurugram

²Department of Statistics, M.D. University, Rohtak

naveenkadian78@gmail.com

sc_malik@rediffmail.com

nsinghnandal@gmail.com

Abstract

Here, we describe the stochastic analysis of a repairable system consisting two non-identical units called the main unit and the other is a duplicate unit. The units have direct complete failure from the operative state. A single repairman has been engaged to carry out the repair activities that can be failed while performing his jobs with the main unit. The repairman does repair activities of the duplicate unit without any problem. Priority for operation and repair to the duplicate unit is given over the main unit. The repairman performs with full efficiency after getting treatment. The distribution for failure rates of the units has been considered as negative exponential while arbitrary distributions have been taken for repair and treatment rates. The use of semi-Markov process and regenerative point technique has been made to study the probabilistic behavior of the system in different possible transition states. The reliability characteristics of the system model have been examined numerically and graphically for particular values of the parameters. The profit of the system has also been analyzed for some fixed values of the repair and other maintenance costs.

Keywords: System of Non-identical Units, Priority, Conditional Failure of Repairman and Stochastic Analysis

I. Introduction

Over the years the researchers in the field of the reliability have been struggling to identify the best possible structure of the components and the techniques which can be used to improve the performance of repairable systems. As a result of which some reliability improve techniques for the repairable systems have been emerged as the provision of redundancy, priority in repair discipline and configuration of the components such as series, parallel, series-parallel, parallel-series, k-out-of-n and other mixed mode structures. The technique of cold standby redundancy with different repair policies has been used most frequently during stochastic modeling of repairable systems. Subramanian and Natarajan [10] developed an N-Unit standby redundant system with R repair facilities. Cao and Wu [2] discussed a cold standby system of two unit with replaceable repair facility. Smith [9] highlighted the concept of regenerative stochastic processes. On the other hand, the objective of the manufacturers is not only to produce the systems with considerable reliability but also to launch the products in markets with optimal balance between reliability and the production costs. To cope with this situation it becomes necessary to use systems

with non-identical units and appropriate repair facilities. The systems with non-identical units have also been studied in the past considering the ideas of priority in repair discipline. Kadyan et al. [4] discussed the stochastic modeling of a system of non-identical units with priority in different mode of failures. Salah and EL-Sherbeny [8] described a two unit non-identical parallel system subject to preventive maintenance and repairs. Kumar et al. [5] analyzed profit of a warm standby non-identical unit system with single server. Kadyan et al. [7] developed system models using the concept of priority. In the field of reliability research it is a common practice that the repair facility called server or repairman cannot fail while performing its assignments i.e. the jobs related to maintenance, repair of the faults and any other precautionary needs of the systems. This assumption on repair facility seems to be unrealistic when repair activities perturb due to the reasons which cause the failure of the service facility or any other catastrophic failure. Chen and Wang [3] analyzed a retrial machine repair problem with warm standbys and a single server with N-policy. Kumar and Nandal [6] developed a system of two non-identical units with conditional failure of repairman. Anuradha et al. [1] analyzed a 1-out-of-2: G System with Priority to Repair and Conditional Failure of Service Facility.

In view of the above observations and facts, the purpose of the present paper is to analyze stochastically a repairable system of non-identical units with the concept of priority and conditional failure of the repairman. The system has one main unit which is initially operative and the other unit is considered as duplicate in cold standby redundancy. The units have direct complete failure from the operative state. A single repairman is engaged to carry out the repair activities that can be failed while performing his jobs with the main unit. The repairman does repair activities of the duplicate unit without any problem. Priority for operation and repair to the duplicate unit is given over the main unit. The repairman performs with full efficiency after getting treatment. The distribution for failure rates of the units has been considered as negative exponential while arbitrary distributions have been taken for repair and treatment rates. The use of semi-Markov process and regenerative point technique has been made to study the probabilistic behavior of the system in different possible transition states. The reliability characteristics of the system model such as MTSF, availability, busy period of the server due to repair of the main and duplicate units, expected number of repairs of the units, expected number of the treatments given to the repairman and finally the profit function have been examined numerically and graphically for particular values of the parameters. The profit of the system has also been analyzed for some fixed values of the repair and other maintenance costs.

II. System Description

1. The system comprises of two non-identical units; one main unit which is initially operative and the other unit is considered as duplicate in cold standby redundancy.
2. The duplicate unit becomes operative after the failure of main unit.
3. A single repairman is engaged to carry out the repair activities that can be failed while performing his jobs with the main unit.
4. The repaired unit works as good as new.
5. Priority for operation and repair to the duplicate unit is given over the main unit.
6. The distribution for failure rates of the units has been considered as negative exponential while arbitrary distributions have been taken for repair and treatment rates

The state transition diagram shown in the figure 1 as:

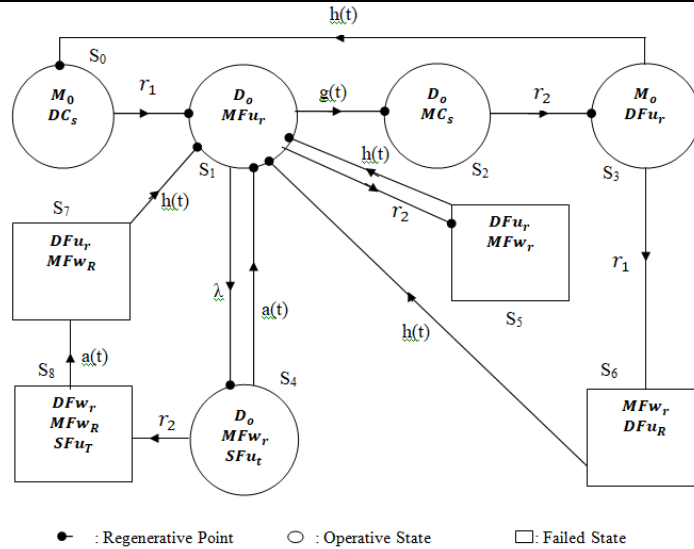


Figure 1: State Transition Diagram

a) Notations and Abbreviations

- O Operative state
- Failed State
- Regenerative point
- λ Failure rate of the repairman
- M_0 Main unit is Operative and in normal mode
- D_{CS} Duplicate unit is in cold standby
- r_1 Failure rate of the main unit
- r_2 Failure rate of the duplicate unit
- $g(t)/G(t)$ pdf/cdf of the main unit repair time
- $h(t)/H(t)$ pdf/cdf of the duplicate unit repair time
- $a(t)/A(t)$ pdf/cdf of the treatment time of the repairman
- MF_{ur}/MF_{UR} Main unit failed under repair /continuously under repair from previous state
- DF_{ur}/DF_{UR} Duplicate unit failed under repair/continuously under repair from previous state
- MW_{ur}/MW_{UR} Main unit waiting for repair /continuously waiting for repair from previous state
- DW_{ur}/DW_{UR} Duplicate unit waiting for repair/continuously waiting for repair from previous state
- SF_{ur}/SF_{UR} Repairman failed under treatment/continuously under treatment from previous state
- q_{ij}/Q_{ij} pdf/cdf of transition from regenerative state (or non-regenerative state) S_i or to a failed state S_j without visiting any regenerative state in $(0,t]$
- m_{ij} Mean sojourn time (μ_i) in state S_i when system transits directly to state S_j so that $\mu_i = \sum_j m_{ij}$ and $m_{ij} = \int_0^\infty t dQ_{ij}(t) = -q'_{ij}(0)$
- μ_i The mean sojourn time in state S_i
- $M_i(t)$ Probability that the system up initially in state $S_i \in E$ is up at time t without visiting to any regenerative state
- $W_i(t)$ Probability that the repairman is busy in the state S_i up to time t without making any transition to any other regenerative state or returning to the same state via one or more non regenerative states
- $\phi_i(t)$ cdf of the first passage time from regenerative state S_i to a failed state
- $A_i(t)$ Probability that the system is in upstate at instant t given that the system entered regenerative state S_i at t = 0
- $B_i(t)$ Probability that the repairman is busy at instant t given that the system entered regenerative

	state S_i at $t = 0$
$RM_i(t)$	Expected number of repair of the main unit given to the repairman in $(0, t]$ such that the system entered regenerative state S_i at $t = 0$
$RD_i(t)$	Expected number of repair of the duplicate unit given to the repairman in $(0, t]$ such that the system entered regenerative state S_i at $t = 0$
$TR_i(t)$	Expected number of Treatment given to the repairman in $(0, t]$ such that the system entered regenerative state S_i at $t = 0$
⊗	Symbol for Stieltjes convolution
⊙	Symbol for Laplace convolution
*/**	Symbol for Laplace Transform/ Laplace Stieltjes Transform
P	Profit function of the system
K_0	Revenue per unit to the system
K_1	Cost per unit for which repairman is busy to repair the main unit.
K_2	Cost per unit for which repairman is busy to repair the duplicate unit.
K_3	Cost per unit for repair of main unit
K_4	Cost per unit for repair of duplicate unit
K_5	Cost per unit treatment given to the repairman
TP	Transition Probabilities
MSTs	Mean Sojourn Times
MTSF	Mean Time to System Failure
LT	Laplace Transform
LST	Laplace Stieltjes Transform
LIT	Laplace Inverse Transform
s-MP	semi-Markov Process
RPT	Regenerative Point Technique

III. Reliability Measures of the System

a) Transition Probabilities

Simple probabilistic considerations yield the following expression for the non-zero elements $p_{ij} = \lim_{t \rightarrow \infty} Q_{ij}(t) = \int_0^\infty q_{ij}(t)dt$ as:

$$\begin{aligned}
 dQ_{01}(t) &= r_1 e^{-r_1 t} dt, & dQ_{12}(t) &= g(t) e^{-(r_2 + \lambda)t} dt, & dQ_{14}(t) &= \lambda e^{-(r_2 + \lambda)t} \overline{G}(t) dt, \\
 dQ_{15}(t) &= r_2 e^{-(r_2 + \lambda)t} \overline{G}(t) dt, & dQ_{23}(t) &= r_2 e^{-r_2 t} dt, & dQ_{30}(t) &= h(t) e^{-r_1 t} dt, \\
 dQ_{36}(t) &= r_1 e^{-r_1 t} \overline{H}(t) dt, & dQ_{41}(t) &= a(t) e^{-r_2 t} dt, & dQ_{48}(t) &= r_2 e^{-r_2 t} \overline{A}(t) dt \\
 dQ_{51}(t) &= h(t) dt, & dQ_{61}(t) &= h(t) dt, & dQ_{71}(t) &= h(t) dt, & dQ_{87}(t) &= a(t) dt
 \end{aligned}$$

By taking $t \rightarrow \infty$ of the above expressions using $p_{ij} = Q_{ij}(\infty) = \int_0^\infty q_{ij}(t)dt$, we get

$$\begin{aligned}
 p_{01} &= 1, p_{12} = g^*(r_2 + \lambda), p_{14} = \frac{\lambda}{(r_2 + \lambda)} [1 - g^*(r_2 + \lambda)], p_{15} = \frac{r_2}{(r_2 + \lambda)} [1 - g^*(r_2 + \lambda)], \\
 p_{23} &= 1, p_{30} = h^*(r_1), p_{36} = [1 - h^*(r_1)], p_{41} = a^*(r_2), p_{48} = [1 - a^*(r_2)], \\
 p_{51} &= h^*(0), p_{71} = h^*(0), p_{61} = h^*(0), p_{87} = a^*(0)
 \end{aligned}$$

It is verified that:

$$p_{01} = p_{12} + p_{14} + p_{15} = p_{30} + p_{36} = p_{41} + p_{48} = p_{51} = p_{61} = p_{71} = p_{87} = 1$$

b) Mean Sojourn Times

The expected time taken by the system in a particular state before transiting to any other state is known as mean sojourn time or mean survival time in the state. If T_i be the sojourn time in the

state i , then the mean sojourn time in the state i is

$$\begin{aligned} \mu_i &= \int_0^\infty Pr(T_i > t) dt \text{ or } \mu_i = \sum_j m_{ij} \text{ But } m_{ij} = -\frac{d}{ds} [Q_{ij}^{**}(s)]_{s=0} \\ \mu_0 &= m_{00}, \mu_1 = m_{12} + m_{14} + m_{15}, \mu_2 = m_{23} \\ \mu_3 &= m_{30} + m_{36}, \mu_4 = m_{41} + m_{48} \\ \mu_3' &= m_{30} + m_{31.6}, \mu_4' = m_{41} + m_{41.87} \end{aligned}$$

c) Reliability and MTSF

Let $\phi_i(t)$ be the c.d.f. of first passage time from regenerative state S_i to a failed state. Regarding the failed state as absorbing state, we have following recursive relations for $\phi_i(t)$:

$$\phi_i(t) = \sum_j Q_{ij}(t) \otimes \phi_j(t) + \sum_k Q_{ik}(t) \tag{1}$$

where S_j is an un-failed regenerative state to which the given regenerative state S_i can transit and S_k is a failed state to which the state S_i can transit directly. Thus, the following equations are obtained by using (1) as:

$$\begin{aligned} \phi_0(t) &= Q_{01}(t) \otimes \phi_1(t) \\ \phi_1(t) &= Q_{12}(t) \otimes \phi_2(t) + Q_{14}(t) \otimes \phi_4(t) + Q_{15}(t) \\ \phi_2(t) &= Q_{23}(t) \otimes \phi_3(t) \\ \phi_3(t) &= Q_{30}(t) \otimes \phi_0(t) + Q_{36}(t) \\ \phi_4(t) &= Q_{41}(t) \otimes \phi_1(t) + Q_{48}(t) \end{aligned}$$

Taking LST of above relations to obtain $\phi_0^{**}(s)$ using this, we have

$$R^*(s) = \frac{1 - \phi_0^{**}(s)}{s}$$

Taking LIT of $R^*(s)$, we can obtain the reliability $R(t)$ of the system model. The MTSF is given by

$$MTSF = \lim_{n \rightarrow 0} R^*(s) = \frac{N_1}{D_1}$$

where,

$$\begin{aligned} N_1 &= \mu_0(p_{12} + p_{15} + p_{14}p_{48}) + \mu_1 + \mu_2p_{12} + \mu_3p_{12} + \mu_4p_{14} \\ D_1 &= (1 - p_{12}p_{30} - p_{14}p_{41}) \end{aligned}$$

d) Steady State Availability

Let $A_i(t)$ be the probability that the system is in up-state at epoch 't' given that the computer system entered regenerative state S_i at $t = 0$. The recursive relations for $A_i(t)$ are given as

$$A_i(t) = M_i(t) + \sum_j q_{ij}^{(n)}(t) \odot A_j(t) \tag{2}$$

where S_j is any successive regenerative state to which the regenerative state S_i can transit through n transitions. Thus, the following equations are obtained by using (2) as:

$$\begin{aligned} A_0(t) &= M_0(t) + q_{01} \odot A_1(t) \\ A_1(t) &= M_1(t) + q_{12}(t) \odot A_2(t) + q_{14}(t) \odot A_4(t) + q_{15}(t) \odot A_5(t) \\ A_2(t) &= M_2(t) + q_{23} \odot A_3(t) \\ A_3(t) &= M_3(t) + q_{30}(t) \odot A_0(t) + q_{31.6}(t) \odot A_1(t) \\ A_4(t) &= M_4(t) + q_{41}(t) \odot A_1(t) + q_{41.87}(t) \odot A_1(t) \\ A_5(t) &= q_{51}(t) \odot A_1(t) \end{aligned}$$

where

$$M_0(t) = e^{-r_1 t}, M_1(t) = e^{-(r_2 + \lambda)t} \overline{G}(t), M_2(t) = e^{-r_2 t}, M_4(t) = e^{-r_2 t} \overline{A}(t), M_3(t) = e^{-r_1 t} \overline{H}(t)$$

Taking L.T of above expressions and calculate the value of $A_0^*(s)$, we have

$$A_0 = \lim_{t \rightarrow \infty} A_0(t) = \lim_{s \rightarrow 0} s A_0^*(s) = \frac{N_2}{D_2}$$

where,

$$\begin{aligned} N_2 &= \mu_0 - \mu_0 p_{12} p_{36} - \mu_0 p_{14} - \mu_0 p_{15} + \mu_1 + \mu_2 p_{12} + \mu_3 p_{12} - \mu_4 p_{14} \\ D_2 &= \mu_0 p_{12} p_{30} + \mu_1 + \mu_2 p_{12} + \mu_3 p_{12} + \mu_4 p_{14} + \mu_5 p_{15} \end{aligned}$$

e) Busy Period of the Repairman Due to Repairs

Let $B_i^R(t)$ be the probability that server is busy in repairing the unit at epoch 't' given that the system entered state S_i at $t = 0$. The recursive relations for $B_i^R(t)$ are given as:

$$B_i^R(t) = W_i^R(t) + \sum_j q_{ij}^{(n)}(t) \odot B_j^H(t) \tag{3}$$

where S_j is any successive regenerative state to which the regenerative state S_i can transit through n transitions. Thus, the following equations are obtained by using (3) as:

i) Repair of Main Unit

$$\begin{aligned} B_0^M(t) &= q_{01} \odot B_1^M(t) \\ B_1^M(t) &= W_1(t) + q_{12}(t) \odot B_2^M(t) + q_{11.5}(t) \odot B_1^M(t) + q_{14}(t) \odot B_4^M(t) \\ B_2^M(t) &= q_{23} \odot B_3^M(t) \\ B_3^M(t) &= q_{30}(t) \odot B_0^M(t) + q_{31.6}(t) \odot B_1^M(t) \\ B_4^M(t) &= q_{41}(t) \odot B_1^M(t) + q_{41.87}(t) \odot B_1^M(t) \\ B_5^M(t) &= q_{51} \odot B_1^M(t) \end{aligned}$$

where

$$W_1(t) = e^{-(r_2 + \lambda)t} \overline{G(t)}$$

Taking L.T. of above expressions and calculate the value of $B_0^*(s)$, we have

$$B_0^M = \lim_{s \rightarrow 0} s B_0^*(s) = \frac{N_3}{D_2}$$

Where, $N_3 = \mu_1$ and D_2 is already defined.

ii) Repair of Duplicate unit

$$\begin{aligned} B_0^D(t) &= q_{01} \odot B_1^D(t) \\ B_1^D(t) &= q_{10}(t) \odot B_0^D(t) + q_{14}(t) \odot B_4^D(t) + q_{11.5}(t) \odot B_1^D(t) \\ B_2^D(t) &= q_{23} \odot B_3^D(t) \\ B_3^D(t) &= W_3(t) + q_{30}(t) \odot B_0^D(t) + q_{31.6}(t) \odot B_1^D(t) \\ B_4^D(t) &= q_{41}(t) \odot B_1^D(t) + q_{41.87}(t) \odot B_1^D(t) \\ B_5^D(t) &= W_5(t) + q_{51} \odot B_1^D(t) \end{aligned}$$

where

$$\begin{aligned} W_3(t) &= e^{-(r_1)t} \overline{H(t)} + [r_1 e^{r_1 t} \odot 1] \overline{H(t)} \\ W_5(t) &= \overline{H(t)}, \end{aligned}$$

Taking L.T. of above expressions and calculate the value of $B_0^*(s)$, we have

$$B_0^D = \lim_{s \rightarrow 0} s B_0^*(s) = \frac{N_{3D}}{D_2}$$

where, $N_{3D} = W_3^*(0)p_{12}$ and D_2 is already defined.

f) Expected Number of Repairs of the Main Unit

Let $R_i^M(t)$ be the expected number of repairs of the unit by the repairman in $(0, t]$ such that the system entered regenerative state i at $t = 0$. The recursive relation for $R_i^M(t)$ are given as:

$$R_i^M(t) = \sum_j Q_{ij}^{(n)}(t) \mathcal{S}[\delta_j + R_i^M(t)] \tag{4}$$

Where j is any regenerative state to which the given regenerative state i transits and $\delta_j = 1$ if j is the regenerative state where the repairman does job afresh, otherwise, $\delta_j = 0$. Thus, the following equations are obtained by using (4) as:

$$\begin{aligned} R_0^M(t) &= Q_{01} \otimes R_1^M(t) \\ R_1^M(t) &= Q_{12}(t) \otimes [1 + R_2^M(t)] + Q_{14}(t) \otimes R_4^M(t) + Q_{11.5}(t) \otimes R_1^M(t) \\ R_2^M(t) &= Q_{23} \otimes R_3^M(t) \\ R_3^M(t) &= Q_{30}(t) \otimes R_0^M(t) + Q_{31.6}(t) \otimes R_1^M(t) \\ R_4^M(t) &= Q_{41}(t) \otimes R_1^M(t) + Q_{41.87}(t) \otimes R_1^M(t) \\ R_5^M(t) &= Q_{51} \otimes R_1^M(t) \end{aligned}$$

Taking L.S.T. of above expressions and calculating for $R_0^*(s)$, we have

$$R_0^M = \lim_{s \rightarrow 0} s \overline{R_0^M}(s), = \frac{N_4}{D_2}$$

where, $N_4 = p_{12}$ and D_2 is already defined.

g) Expected Number of Repairs of the Duplicate Unit

Let $R_i^D(t)$ be the expected number of repairs of the unit by the repairman in $(0, t]$ such that the system entered regenerative state i at $t = 0$. The recursive relation for $R_i^D(t)$ are given as:

$$R_i^D(t) = \sum_j Q_{i,j}^{(n)}(t) \otimes [\delta_j + R_i^D(t)] \quad (5)$$

Where j is any regenerative state to which the given regenerative state i transits and $\delta_j = 1$ if j is the regenerative state where the repairman does job afresh, otherwise, $\delta_j = 0$. Thus, the following equations are obtained by using (5) as:

$$\begin{aligned} R_0^D(t) &= Q_{01} \otimes R_1^D(t) \\ R_1^D(t) &= Q_{12}(t) \otimes R_2^D(t) + Q_{14}(t) \otimes R_4^D(t) + Q_{11.5}(t) \otimes R_1^D(t) \\ R_2^D(t) &= Q_{20} \otimes R_3^D(t) \\ R_3^D(t) &= Q_{30}(t) \otimes [1 + R_0^D(t)] + Q_{31.6}(t) \otimes [1 + R_1^D(t)] \\ R_4^D(t) &= Q_{41}(t) \otimes R_1^D(t) + Q_{41.87}(t) \otimes [1 + R_1^D(t)] \\ R_5^D(t) &= Q_{51} \otimes [1 + R_1^D(t)] \end{aligned}$$

Taking L.S.T. of above expressions and calculating for $\overline{R_0^D}(s)$, we have

$$R_0^D = \lim_{s \rightarrow 0} s \overline{R_0^D}(s) = \frac{N_5}{D_2}$$

where, $N_5 = p_{12}$ and D_2 is already defined.

h) Expected Number of Treatment Given to the Repairman

Let $T_i^R(t)$ be the expected number of repairs of the unit by the repairman in $(0, t]$ such that the system entered regenerative state i at $t = 0$. The recursive relation for $T_i^R(t)$ are given as:

$$T_i^R(t) = \sum_j Q_{i,j}^{(n)}(t) \otimes [\delta_j + T_i^R(t)] \quad (6)$$

Where j is any regenerative state to which the given regenerative state i transits and $\delta_j = 1$ if j is the regenerative state where the repairman does job afresh, otherwise, $\delta_j = 0$. Thus, the following equations are obtained by using (6) as:

$$\begin{aligned} T_0^R(t) &= Q_{01} \otimes T_1^R(t) \\ T_1^R(t) &= Q_{12}(t) \otimes T_2^R(t) + Q_{14}(t) \otimes T_4^R(t) + Q_{11.5}(t) \otimes T_1^R(t) \\ T_2^R(t) &= Q_{23} \otimes T_3^R(t) \\ T_3^R(t) &= Q_{30}(t) \otimes T_0^R(t) + Q_{31.6}(t) \otimes T_1^R(t) \\ T_4^R(t) &= Q_{41}(t) \otimes [1 + T_1^R(t)] + Q_{41.87}(t) \otimes [1 + T_1^R(t)] \\ T_5^R(t) &= Q_{51} \otimes T_1^R(t) \end{aligned}$$

Taking L.S.T. of above expressions and calculating for $\overline{T_0^R}(s)$, we have

$$T_0^R = \lim_{s \rightarrow 0} s \overline{T_0^R}(s) = \frac{N_6}{D_2}$$

where, $N_6 = p_{14}$ and D_2 is already defined.

IV Profit Analysis

The following expression can be used to obtain Profit of the system model:

$$P_A = K_0 A_0 - K_1 B_0^M(t) - K_2 B_0^D(t) - K_3 R_0^M(t) - K_4 R_0^D(t) - K_5 T_0^R(t) \quad (7)$$

V. Particular Cases

Let us take

$$g(t) = \alpha e^{-at}, h(t) = \beta e^{-bt}, a(t) = \gamma e^{-\gamma t},$$

$$p_{12} = \frac{\alpha}{(\alpha+\lambda+r_2)}, p_{15} = \frac{r_2}{(\alpha+\lambda+r_2)}, p_{14} = \frac{\lambda}{(\alpha+\lambda+r_2)}, p_{41} = \frac{\gamma}{(\gamma+r_2)}, p_{48} = \frac{r_2}{(\gamma+r_2)}, p_{30} = \frac{\beta}{(\beta+r_1)}, p_{36} = \frac{r_1}{(\beta+r_1)}$$

$$\mu_0 = \frac{1}{r_1}, \mu_1 = \frac{1}{(\alpha+\lambda+r_2)}, \mu_2 = \frac{1}{r_2}, \mu_3 = \frac{1}{(\beta+r_2)}, \mu_4 = \frac{1}{(\gamma+r_2)}, \mu_5 = \frac{1}{\beta}, \mu_4' = \frac{r_2}{(\gamma+r_2)} \left[\frac{1}{\beta} + \frac{1}{\beta} \right], \mu_3' = \frac{1}{\beta} \left(\frac{r_1}{(\beta+r_1)} \right),$$

$$MTSF = \frac{N_1}{D_1}, \text{Availability} = \frac{N_2}{D_2}$$

$$\text{Busy period of the repairman (B)} = \frac{N_3}{D_2}$$

$$\text{Expected number of repairs of main unit (R}_{M0}) = \frac{N_5}{D_2}$$

$$\text{Expected number of repairs of duplicate unit (R}_{D0}) = \frac{N_4}{D_2}$$

$$\text{Expected number of Treatment given to the Repairman (T}_{R0}) = \frac{N_6}{D_2}$$

where,

$$N_1 = \frac{1}{r_1} \left[\frac{\alpha}{(\alpha+\lambda+r_2)} + \frac{r_2}{(\alpha+\lambda+r_2)} + \frac{\lambda}{(\alpha+\lambda+r_2)(\gamma+r_2)} \right] + \frac{1}{(\alpha+\lambda+r_2)} + \frac{1}{r_2} \frac{\alpha}{(\alpha+\lambda+r_2)} + \frac{1}{(\beta+r_2)} \frac{\alpha}{(\alpha+\lambda+r_2)} + \frac{\lambda}{(\alpha+\lambda+r_2)(\gamma+r_2)}$$

$$D_1 = 1 - \frac{\alpha}{(\alpha+\lambda+r_2)} \frac{\beta}{(\beta+r_1)} - \frac{\lambda \gamma}{(\alpha+\lambda+r_2)(\gamma+r_2)}$$

$$N_2 = \frac{1}{r_1} - \frac{r_1}{(\beta+r_1)} \frac{1}{r_1} \frac{\alpha}{(\alpha+\lambda+r_2)} - \frac{1}{r_1} \frac{\lambda}{(\alpha+\lambda+r_2)} - \frac{1}{r_1} \frac{r_2}{(\alpha+\lambda+r_2)} + \frac{1}{(\alpha+\lambda+r_2)} + \frac{1}{r_2} \frac{\alpha}{(\alpha+\lambda+r_2)} + \frac{\alpha}{(\alpha+\lambda+r_2)} \frac{1}{(\beta+r_1)} - \frac{1}{(\alpha+\lambda+r_2)(\gamma+r_2)}$$

$$N_3 = \frac{1}{(\alpha+\lambda+r_2)}, N_{3D} = \frac{\alpha}{(\alpha+\lambda+r_2)}, N_4 = \frac{\alpha}{(\alpha+\lambda+r_2)}, N_5 = \frac{\alpha}{(\alpha+\lambda+r_2)}, N_6 = \frac{\lambda}{(\alpha+\lambda+r_2)}$$

$$D_2' = \frac{1}{(\alpha+\lambda+r_2)} + \frac{1}{r_1} \frac{\alpha}{(\alpha+\lambda+r_2)} \frac{\beta}{(\beta+r_1)} + \frac{1}{r_2} \frac{\alpha}{(\alpha+\lambda+r_2)} + \frac{1}{\beta} \frac{\alpha}{(\alpha+\lambda+r_2)} \frac{r_1}{(\beta+r_1)} + \frac{r_2}{(\gamma+r_2)} \frac{\lambda}{(\alpha+\lambda+r_2)} \left[\frac{1}{\gamma} + \frac{1}{\beta} \right] + \frac{1}{\beta} \frac{r_2}{(\alpha+\lambda+r_2)}$$

VI. Graphical Presentation

The graphical representation of MTSF, availability and profit function has been shown in figures 2,3 and 4 respectively to check their behavior with respect to the values of the parameters associated with failure and repair rates. From Figure 2, it is observed that the MTSF of the system decreases when failure rate of main unit is increased from 0.01 to 0.1. Also, MTSF increases with an increase in repair rate of main unit, duplicate unit and treatment rate of the repairman.

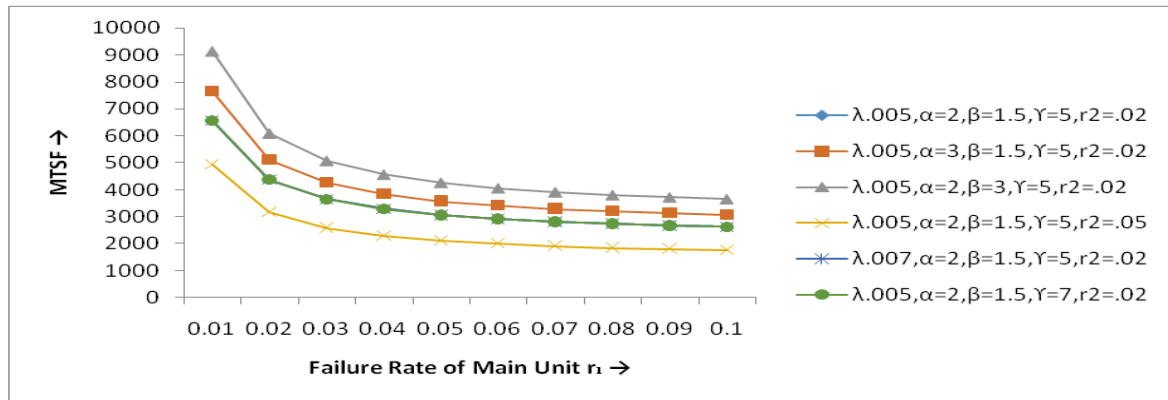


Figure 2: MTSF Vs Failure Rate of Main Unit

From Figure 3, it is clearly seen that the availability of the system decreases rapidly with increase of failure rate of main unit. Also, availability of the system increases with an increase in repair rate of main unit, duplicate unit and treatment rate of the repairman.

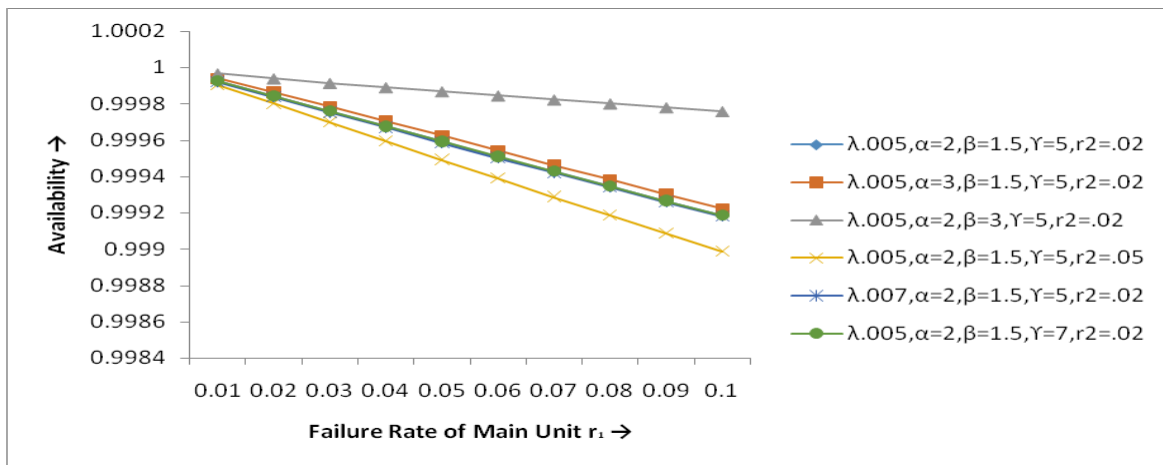


Figure 3: Availability Vs Failure Rate of Main Unit

From Figure 4, it is observed that the profit decreases when failure rate of the main unit increases. Also, the profit of the system increases with an increase in repair rate of main unit, duplicate unit and treatment rate of the repairman.

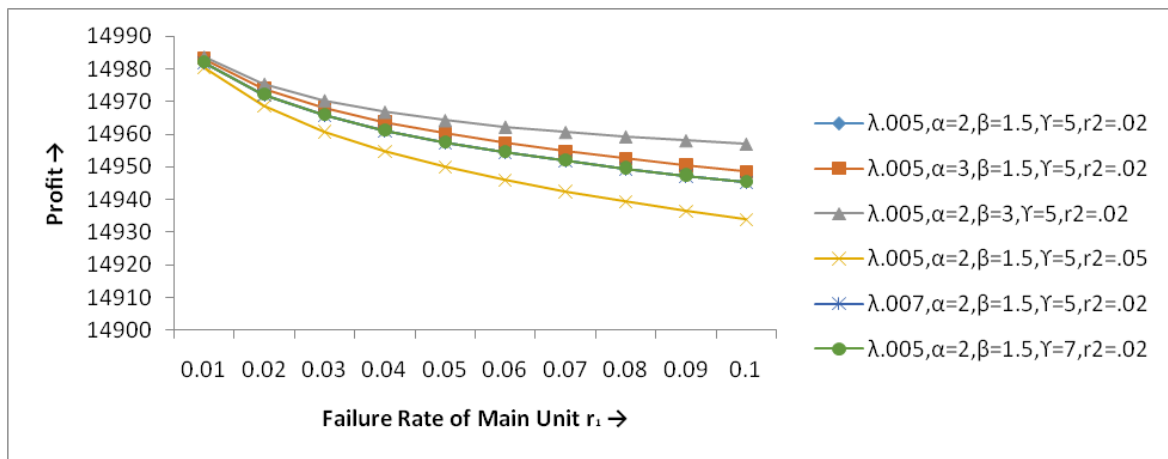


Figure 4: Profit Vs Failure Rate of Main Unit

VII. Conclusion

The idea of priority for repair and operation of the duplicate unit has been used to determine reliability characteristics of a stochastic model developed for a system of non-identical units with failure of repairman. The failure of repairman is called conditional failure as it fails only during the repair of the main unit. In this study reliability measures such as MTSF, availability and profit function are obtained and their behavior is shown respectively figures: Figure 2, Figure 3 and Figure 4. It is observed that MTSF, availability and profit function decline when failure rate increases. On the other hand, these measures increase with the increase of repair rate of main unit, duplicate unit and treatment rate of the repairman. Further, the study reveals that profit of the system model can be increased by increasing the repair rate of the duplicate unit.

VIII. Application

The oxygen supply system which is shown in figure 5 can be considered as a direct application of the present study. An acute shortage of medical oxygen and oxygen cylinders has been observed during COVID-19 pandemic situation everywhere throughout the World. The oxygen therapy was in dire need for the survival of patients during this pandemic. The scarcity of oxygen cylinders has also pushed up the demand for oxygen concentrators. Today, oxygen concentrators are in great demand after devices for oxygen therapy in home isolation. Therefore, the present study has been designed to analyze the oxygen supply system comprises oxygen concentrator as a main unit and the oxygen cylinder as its duplication. In case of electricity failure, it becomes necessary to give priority for operation and repair of the oxygen cylinder to cover the risk. Thus, it is a non-identical system of two units in which the concepts of priority and the failure of repairman have been considered to examine some important reliability characteristics so that the users of the oxygen supply system may take appropriate decision to minimize the risk.

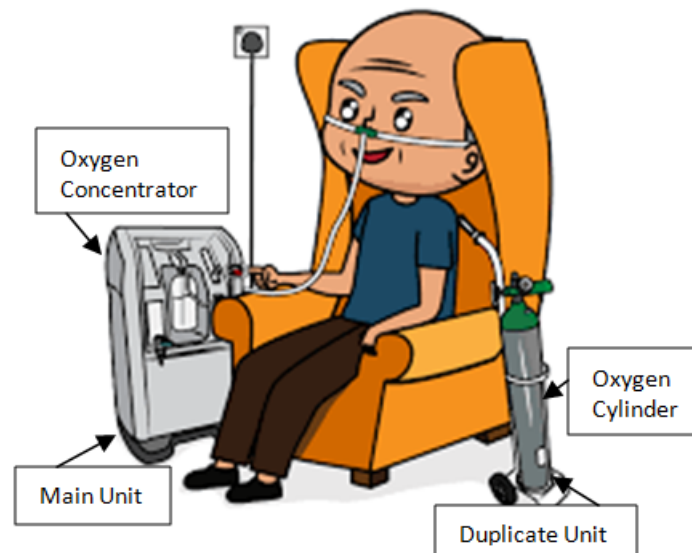


Figure 5: *Oxygen Supply System*

References

- [1] Anuradha, Malik, S.C. and Jha, P.C. (2021). Profit analysis of a 1-out-of-2: G system with priority to repair and conditional failure of service facility. *International Journal of Statistics and Reliability Engineering*, 8(2): 264-271.
- [2] Cao, J. and Yanhong, W. (1989). Reliability of a two unit cold standby system with replaceable repair facility. *Microelectron. Reliab.*, 29(2):145 -150.
- [3] Chen, W.L. and Wang, K.H. (2018). Reliability analysis of a retrial machine repair problem with warm standbys and a single server with N-policy. *Reliability Engineering & System Safety*, 180: 476-486.
- [4] Kadyan, M.S., Chander, S. and Grewal, A.S. (2004). Stochastic analysis of non-identical units reliability models with priority and different modes of failure. *Decision and Mathematical Sciences*, 9(1-3):59 – 82.
- [5] Kumar, A., Pawar, D. and Malik, S.C. (2019). Profit analysis of a warm standby non-identical unit system with single server performing in normal/abnormal environment. *Life Cycle*

Reliability and Safety Engineering, 8:219–226.

- [6] Kumar, N. and Nandal, N. (2020). Stochastic modeling of a system of two non-identical units with priority for operation and repair to main unit subject to conditional failure of repairman. *International Journal of Statistics and Reliability Engineering*, 7(1):114-122.
- [7] Kadyan, S., Barak, M.S. and Gitanjali (2020). Stochastic analysis of a non-identical repairable system of three units with priority for operation and simultaneous working of cold standby units. *International Journal of Statistics and Reliability Engineering*, 7(2):269–274.
- [8] Salah and Sherbeny, E.L. (2012). Stochastic analysis of a two non-identical unit parallel system with different types of failures subject to preventive maintenance and repairs. *Mathematical Problems in Engineering*, 2013:1-10.
- [9] Smith W.L. *Regenerative Stochastic Processes*, Proceeding Royal Society, London, 1955.
- [10] Subramanian, R. and Natarajan, R. (1982). An N-Unit Standby Redundant System with R Repair Facilities and Preventive Maintenance. *Microelectronics Reliability*, 22 (3):367 – 377.

The Reliability Performance of the Exponential Inverted Marshall-Olkin-G Family of Distributions: Non-Bayesian Properties and Applications

JOSEPH THOMAS EGHWERIDO AND EFERHONORE EFE-EYEFIA

Department of Statistics, Federal University of Petroleum Resources Effurun, Delta State, Nigeria

School of Mathematics, Cardiff University, UK

eghwerido.joseph@fupre.edu.ng

efe-eyefiae@cardiff.ac.uk

Abstract

This article introduces a class of generator for enhancing the performance, productivity and flexibility of statistical distributions called the exponential Inverted Marshall-Olkin-G (EMA-G) distribution. The characteristics of the new class of generator were obtained and examined. Some special models of the proposed model were investigated. The Bernstein function of the EMA-G model was also obtained in a closed form. The maximum likelihood method was adopted to obtain the parameters estimate of the formulated EMA-G distribution model. The flexibility, productivity, tractability, applicability and viability of the new contemporary class of distribution were examined by Monte Carlo simulation. A two real life data sets was used to illustrate the empirical performance and flexibility, productivity, tractability of the generator. The up-to-the-minute outcomes of the new generator indicated that the EMA-G density gives a better fit compare to some existing statistical generators in literature using their goodness-of-fit.

Keywords: Bernstein function, Exponential distribution, Generating function, Generator, Marshall-Olkin characterization, Vehicle fatalities.

1. INTRODUCTION

Statistical distributions have unraveled the behaviour, characteristics and nature of life time processes. However, these scenarios depend on the flexibility, productivity, performance and tractability of the underlying probability used in analysing these processes. Hence, the performance, productiveness and flexibility can be enhanced either by adding a new parameter or compounding the probability density function (pdf) involved. One of such methods for high productivity is using the T-X family approach called exponential Inverted Marshall-Olkin generator(EMA-G) distribution. This method negates the exponentiated method in existing literature by using the T-X approach in developing the underlying exponential generator.

Despite the emerging statistical generators in literature, newer generators are still being proposed to improve productivity and performance of lifetimes scenarios. However, many models have been proposed in literature. These include the works of [3] who proposed the Gompertz-G model. [17] proposed the logistic-X generator. [8] proposed the Weibull-G generator. [9] proposed the Kumaraswamy-G generator. [10] proposed the alpha power Marshall-Olkin-G generator. [11] proposed the transmuted alpha power-G generator. [14] proposed the alpha power transformation method of adding a new parameter. The beta transmuted-H generator was proposed in [1]. Kumaraswamy Marshall-Olkin generator was proposed in [2]. [4] proposed the transmuted Weibull-G generator. The transmuted odd log-logistic-G generator was proposed in [5]. [6] proposed the log-gamma family of distributions. The exponentiated generalized-G Poisson generator was proposed in [7]. [12] proposed the bivariate Gumbel-G generator. [16] proposed the Topp Leone odd Lindley-G generator. Marshall-Olkin generalized-G generator

was proposed in [20]. The transmuted Topp-Leone-G generator was proposed in [18]. Burr-X generator was proposed in [19]. Of most important is the works of [13] who proposed the exponentiated generalized Marshall-Olkin distribution. However, the exponentiated family of distribution is contrary and different from the EMA-G family of distributions.

Thus, [15] proposed a one parameter model for adding a contemporary parameter with a pdf $g(t) = \frac{dG}{dt}$ such that $G(t)$ is associated cdf for a random variable t . Then, its pdf can be expressed as

$$g(t) = \frac{\beta m(t)}{[1 - \bar{\beta} \bar{M}(t)]^2} \quad \text{for } \beta > 1, \quad (1)$$

with a tilt parameter $\bar{\beta} = (1 - \beta)$ and $\bar{M}(t) = 1 - M(t)$. The cumulative distribution function (cdf) that corresponds to Equation (1) is expressed as

$$G(t) = \frac{M(t)}{[1 - \bar{\beta} \bar{M}(t)]} \quad \text{for } \beta > 1. \quad (2)$$

Redefining (1) and (2), we have the inverted Marshall-Olkin cdf and pdf as

$$M(t) = \frac{\beta G(t)}{(1 - \bar{\beta} G(t))}. \quad (3)$$

and

$$m(t) = \beta^{-1} g(t) (1 - \bar{\beta} M(t))^2 \quad \text{for } \beta > 1, \quad (4)$$

where $g(t)$ and $G(t)$ are the parents pdf and cdf.

However, using the T-X characterization proposed by [3], the pdf of the exponential-G can be expressed as

$$g(t) = \alpha f(t) \bar{F}(t)^{\alpha-1} \quad \text{for } \alpha > 0. \quad (5)$$

The cdf that corresponds to Equation (3) is expressed as

$$G(t) = 1 - \bar{F}(t)^\alpha \quad \text{for } \alpha > 0. \quad (6)$$

The study introduces a generator for enhancing the performance and flexibility of distribution with a better goodness-of-fit to real life data. The EMA-G model was applied to the Weibull, Burrxii and Frechet distributions in a bid to investigate their performance and flexibility with glass fibers data obtained from the UK National Physical Laboratory, breaking stress of carbon fiber data and data from the Highway Traffic Safety Administration of accidents fatality rate in the United States real life data (Vehicle fatalities in South Caroline for 2012, www.fars.nhtsa.dot.gov/states). It is also motivated as a result of inefficiency in researched existing literature in distribution theory and some results obtained from Weibull Frechet, Gompertz Weibull, Gompertz Burrxii, transmuted Gompertz, Gompertz Frechet, Kumaraswamy Frechet models and to mention but for a few.

The aim of this study is to introduce a new class of generator called the exponential Marshall-Olkin-G (EMA-G) distribution using both the T-X and Marshall-Olkin characterizations that is different from the exponentiated generalized Marshall-Olkin of [13].

2. THE EMA-G METHOD

Let $g(t)$ and $G(t)$ be the pdf and cdf of the Marshall-Olkin distribution respectively for a random variable $T \in \mathfrak{R}$. Then, the pdf of the new class of generator is defined as

$$f(t) = \alpha \beta^\alpha \frac{m(t) [1 - M(t)]^{\alpha-1}}{[\beta + (1 - \beta) M(t)]^{\alpha+1}}, \quad \alpha > 0 \quad \beta > 1, \quad (7)$$

with a baseline cdf and pdf given as $M(t)$ and $m(t)$ respectively. The cdf of Equation (5) is defined as

$$F(t) = 1 - \left[\frac{\beta(1 - M(t))}{\beta + (1 - \beta) M(t)} \right]^\alpha, \quad \alpha > 0 \quad \beta > 1. \quad (8)$$

However, when $\beta = 1, \alpha > 0$, we obtained the exponential-G family of distribution. Also, when $\beta > 1, \alpha = 0$, we obtained the usual Marshall-Olkin transformation of adding a one parameter.

The survival rate, hazard rate, cumulative hazard rate, odd and reversed hazard rate functions of the EMA-G distribution can be expressed respectively as

$$S(t) = \left[\frac{\beta(1 - M(t))}{\beta + (1 - \beta)M(t)} \right]^\alpha,$$

$$h(t) = \frac{\alpha m(t)}{\left[1 - M(t) \right] \left[\beta + (1 - \beta)M(t) \right]},$$

$$H(t) = -\alpha \left[\log(\beta(1 - M(t))) - \log(\beta + (1 - \beta)M(t)) \right],$$

$$O(t) = \frac{1 - \left[\frac{\beta(1 - M(t))}{\beta + (1 - \beta)M(t)} \right]^\alpha}{\left[\frac{\beta(1 - M(t))}{\beta + (1 - \beta)M(t)} \right]^\alpha},$$

and

$$r(t) = \frac{\alpha \beta^\alpha \frac{m(t)[1 - M(t)]^{\alpha-1}}{[\beta + (1 - \beta)M(t)]^{\alpha+1}}}{1 - \left[\frac{\beta(1 - M(t))}{\beta + (1 - \beta)M(t)} \right]^\alpha}.$$

The quantile function t_u for a given EMA-G density when $u \in (0, 1)$ is defined as

$$t_u = M^{-1} \beta (1 - (1 - u)^{\frac{1}{\alpha}}) (\beta + (1 - u)^{\frac{1}{\alpha}} (1 - \beta))^{-1}. \tag{9}$$

The skewness and kurtosis of the EAP-G density can be obtained respectively as

$$SK(t_u) = \frac{t_{0.25} + t_{0.75} - 2t_{0.5}}{t_{0.75} - t_{0.25}},$$

$$KU(t_u) = \frac{t_{0.875} + t_{0.125} - t_{0.625} - t_{0.375}}{t_{0.75} - t_{0.25}}.$$

The performance of the skewness and kurtosis of the EMA-G models are given in Table 1 with the skewness as (SK), kurtosis denoted as (KU), 25th percent as (Q_1), the median as (M), and the 75th percent as (Q_3) for some EMA-G models. The data set were generated with the quantile function given in Equation (7) with different parameter values cases. The simulation sub-model are Weibull, Burrxii and Frechet. The results of the simulation show that increase in parameter estimates increases the skewness and kurtosis and decreases the median and the quarters for Weibull, Burrxii and Frechet models. However, increase in parameter estimate increases the quarters in Weibull, Frechet and Burrxii models. The EMA-G Burrxii model is left skewed. Otherwise right skewed and the parameter values increases. The kurtosis increases as parameter increases.

Table 1: Results for goodness-of-fit with skewness, kurtosis, first quantile, median and third quantile for different paramet values cases for the EMA-G models

Distribution	Parameter				SK	KU	Q ₁	M	Q ₃
	α	β	λ	μ					
Weibull	0.5	1.0	0.5		0.5675	1.6591	0.6620	3.8436	15.3745
		1.5	1.0		0.2136	0.4911	0.8109	1.8325	3.4094
		2.0	2.0	0.5	0.0258	0.0631	1.0384	1.5536	2.0962
		3.5	3.0		-0.0584	-0.0987	1.3414	1.7297	2.0751
		5.0	5.0		-0.1064	-0.1864	1.5269	1.7783	1.9814
		10.0	8.0		-0.1474	-0.2556	1.7290	1.8931	2.0150
	1.5	1.0	0.5		0.5675	1.6591	0.1324	0.7687	3.0748
		1.5	1.0		0.2136	0.4911	0.1621	0.3665	0.6818
		2.0	2.0	2.5	0.0258	0.0631	0.2076	0.3107	0.4192
		3.5	3.0		-0.0584	-0.0987	0.2682	0.3459	0.4150
		5.0	5.0		-0.1064	-0.1864	0.3053	0.3556	0.3962
		10.0	8.0		-0.1474	-0.2556	0.3458	0.3786	0.4030
	2.5	1.0	0.5		0.5675	1.6591	0.0662	0.3843	1.5374
		1.5	1.0		0.2136	0.4911	0.0810	0.1832	0.3409
		2.0	2.0	5.0	0.0258	0.0631	0.1038	0.1553	0.2096
		3.5	3.0		-0.0584	-0.0987	0.1341	0.1729	0.2075
		5.0	5.0		-0.1064	-0.1864	0.1526	0.1778	0.1981
		10.0	8.0		-0.1474	-0.2556	0.1729	0.1893	0.2015
Burrxii	0.5	1.0	0.5		0.9932	257.8495	4.6677	225.00	65025
		1.5	1.0		0.8000	5.1096	0.2500	2.2500	20.25
		2.0	2.0	0.5	0.5992	1.9455	0.0208	0.1240	0.5358
		3.5	3.0		0.5141	1.4381	0.0111	0.0579	0.2035
		5.0	5.0		0.4690	1.2171	0.0028	0.0138	0.0442
		10.0	8.0		0.4122	1.0082	0.0015	0.0070	0.0201
	1.5	1.0	0.5		0.5922	2.6458	1.3608	2.9541	9.1752
		1.5	1.0		0.2162	0.5446	0.7578	1.1760	1.8250
		2.0	2.0	2.5	0.0621	0.1398	0.4609	0.6587	0.8827
		3.5	3.0		0.0099	0.0311	0.4072	0.5656	0.7273
		5.0	5.0		-0.0182	-0.0243	0.3093	0.4247	0.5360
		10.0	8.0		-0.0487	-0.0799	0.2753	0.3711	0.4580
	2.5	1.0	0.5		0.4070	1.2491	1.1665	1.7187	3.0290
		1.5	1.0		0.1094	0.2515	0.8705	1.0844	1.3509
		2.0	2.0	5.0	-0.0182	-0.0287	0.6789	0.8116	0.9395
		3.5	3.0		-0.0617	-0.1093	0.6381	0.7521	0.8528
		5.0	5.0		-0.0859	-0.1521	0.5562	0.6517	0.7321
		10.0	8.0		-0.1112	-0.1945	0.5246	0.6091	0.6767
Frechet	0.5	1.0	0.5		0.9109	16.6310	0.7316	6.0414	120.0417
		1.5	1.0		0.7497	4.5117	0.8285	3.8322	24.8331
		2.0	2.0	0.5	0.6019	2.3041	0.9609	3.1910	12.1653
		3.5	3.0		0.5644	1.9297	1.6578	5.4552	19.0959
		5.0	5.0		0.5134	1.5901	2.2939	6.8833	21.1601
		10.0	8.0		0.5063	1.5110	4.6143	14.4425	44.4367

Table 1 – Continued from previous page

Distribution	Parameter				SK	KU	Q ₁	M	Q ₃
	α	β	λ	μ					
1.5	1.0	0.5			0.4075	1.2536	0.5395	0.8230	1.4963
	1.5	1.0			0.2640	0.6746	0.9630	1.3082	1.9011
	2.0	2.0	2.5		0.1796	0.4158	1.7272	2.1958	2.8697
	3.5	3.0			0.1465	0.3277	2.6644	3.3811	4.3439
	5.0	5.0			0.1214	0.2635	4.2785	5.3301	6.6723
	10.0	8.0			0.1052	0.2254	7.1662	9.0032	11.2725
2.5	1.0	0.5			0.2934	0.7643	0.5194	0.6414	0.8649
	1.5	1.0			0.1826	0.4294	0.9813	1.1437	1.3788
	2.0	2.0	5.0		0.1174	0.2589	1.8586	2.0956	2.3957
	3.5	3.0			0.0862	0.1864	2.8272	3.1848	3.6099
	5.0	5.0			0.0663	0.1405	4.6252	5.1624	5.7759
	10.0	8.0			0.0490	0.1042	7.5716	8.4868	9.4963

In Table 1, increase in parameter decreases the skewness, kurtosis and the quartiles with EMA-GWb model.

Theorem 1. The EMA-G density behaviour can be examined by investigating the characteristics of $f(t)$, $W'(t)$ and $W''(t)$; where $W(t) = \ln f(t)$.

Proof. Given that $W(t) = \ln f(t)$, then

$$W(t) = \alpha \log \beta + \log \alpha + \log m(t) + (\alpha - 1) \log(1 - M(t)) - (\alpha + 1) \log(\beta + (1 - \beta)M(t)).$$

Thus,

$$W'(t) = \frac{m'(t)}{m(t)} - \frac{(\alpha - 1)m(t)}{1 - M(t)} - (\alpha + 1) \frac{(1 - \beta)m(t)}{\beta + (1 - \beta)M(t)}.$$

However, $F(t)$ is monotonically decreasing for all t if $W' < 0$ for all t . The mode is obtained when W'' for α, β . More so, if $f(t)''$ changes sign from negative to positive and to negative and again positive as t increases viz-a-viz, then, the pdf of the EMA-G distribution will be bimodal. ■

3. SPECIAL MODELS

Some examples of the EMA-G family of distributions will be investigated for various parameter cases. This is to enable us examine the model performance, flexibility and the goodness-of-fit. The models examined include the Weibull (Wb), Frechet (F) and Burrxii (Br) distributions.

3.1. The EMA-GWb distribution

Let T be a random variable with the pdf and cdf (for $t \geq 0$), say $m(t) = \lambda\mu^\lambda t^{\lambda-1} \exp(-(\mu t)^\lambda)$ and $M(t) = 1 - \exp(-(\mu t)^\lambda)$ respectively, (for $\mu > 0, \lambda > 0$) of the Weibull density function. Then, the pdf, cdf and hazard rate function of the EMA-GWb distribution for are expressed respectively as

$$f(t) = \alpha\beta^\alpha \frac{\lambda\mu^\lambda t^{\lambda-1} \exp(-(\mu t)^\lambda) [\exp(-(\mu t)^\lambda)]^{\alpha-1}}{[\beta + (1 - \beta)(1 - \exp(-(\mu t)^\lambda))]^{\alpha+1}}, \quad \alpha > 0 \quad \beta > 1, \quad (10)$$

The corresponding cdf is defined as

$$F(t) = 1 - \left[\frac{\beta \exp(-(\mu t)^\lambda)}{\beta + (1 - \beta)(1 - \exp(-(\mu t)^\lambda))} \right]^\alpha, \quad \alpha > 0 \quad \beta > 1, \quad (11)$$

and

$$h(t) = \frac{\alpha \lambda \mu^\lambda t^{\lambda-1} \exp(-(\mu t)^\lambda)}{\left[\exp(-(\mu t)^\lambda) \right] \left[\beta + (1 - \beta)(1 - \exp(-(\mu t)^\lambda)) \right]} \quad (12)$$

Figure 1 shows the density functions for the EMA-GWb density for selected values of parameters α, β, λ and μ . The plot in Figure 1 shows that the EMA-GWb density could be increasing, decreasing or skewed depending on the values of the parameters.

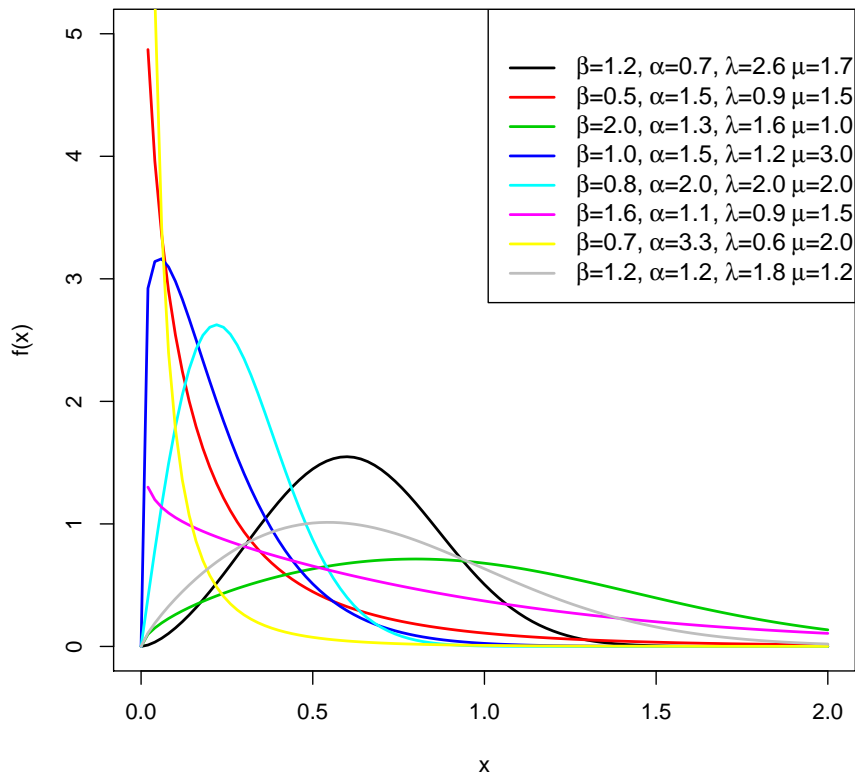


Figure 1: The plots of the EMA-GWb model for some parameter values cases

3.2. The EMA-GBr distribution

Let the pdf and cdf say (for $\lambda > 0, \mu > 0$) of the Burrxii density be $m(t) = \lambda \mu t^{\mu-1} (1 + t^\mu)^{-(\lambda+1)}$ and $M(t) = 1 - (1 + t^\mu)^{-\lambda}$, respectively. Then, the pdf, cdf and hazard rate function of the EMA-GBr density are expressed respectively as

$$f(t) = \alpha \beta^\alpha \frac{\lambda \mu t^{\mu-1} (1 + t^\mu)^{-(\lambda+1)} [(1 + t^\mu)^{-\lambda}]^{\alpha-1}}{[\beta + (1 - \beta)(1 - (1 + t^\mu)^{-\lambda})]^{\alpha+1}}, \quad \alpha > 0 \quad \beta > 1, \quad (13)$$

The corresponding cdf is defined as

$$F(t) = 1 - \left[\frac{\beta((1 + t^\mu)^{-\lambda})}{\beta + (1 - \beta)(1 - (1 + t^\mu)^{-\lambda})} \right]^\alpha, \quad \alpha > 0 \quad \beta > 1, \quad (14)$$

and

$$h(t) = \frac{\alpha \lambda \mu t^{\mu-1} (1+t^\mu)^{-(\lambda+1)}}{\left[(1+t^\mu)^{-\lambda} \right] \left[\beta + (1-\beta)M(t) \right]}. \quad (15)$$

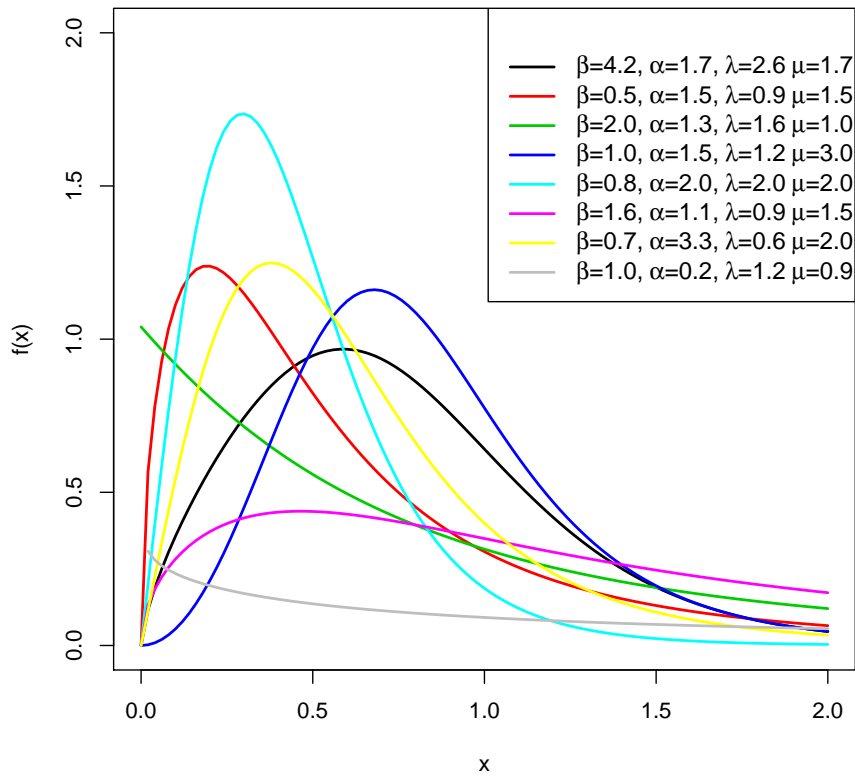


Figure 2: The plots of the EMA-GBr model for some parameter values cases

Figure 2 shows the EMA-GBr density plot for selected values of parameters α, β, λ and μ . The plot shows that the EMA-GBr density is increasing and decreasing.

3.3. The EMA-GF distribution

Let the pdf of the Frechet is expressed as $m(t) = \mu \lambda^\mu t^{-\mu-1} e^{-(\frac{\lambda}{t})^\mu}$ and the cdf as $M(t) = e^{-(\frac{\lambda}{t})^\mu}$ for positive parameters λ and μ . Then the pdf, cdf and hazard rate function of the EMA-GFr model $\alpha \in \mathfrak{R} - \{1\}$ are expressed respectively as

$$f(t) = \alpha \beta^\alpha \frac{\mu \lambda^\mu t^{-\mu-1} e^{-(\frac{\lambda}{t})^\mu} [1 - e^{-(\frac{\lambda}{t})^\mu}]^{\alpha-1}}{[\beta + (1-\beta)e^{-(\frac{\lambda}{t})^\mu}]^{\alpha+1}}, \quad \alpha > 0 \quad \beta > 1, \quad (16)$$

The corresponding cdf is defined as

$$F(t) = 1 - \left[\frac{\beta(1 - e^{-(\frac{\lambda}{t})^\mu})}{\beta + (1-\beta)e^{-(\frac{\lambda}{t})^\mu}} \right]^\alpha, \quad \alpha > 0 \quad \beta > 1, \quad (17)$$

and

$$h(t) = \frac{\alpha \mu \lambda^\mu t^{-\mu-1} e^{-\left(\frac{\lambda}{t}\right)^\mu}}{\left[1 - e^{-\left(\frac{\lambda}{t}\right)^\mu}\right] \left[\beta + (1 - \beta)e^{-\left(\frac{\lambda}{t}\right)^\mu}\right]} \quad (18)$$

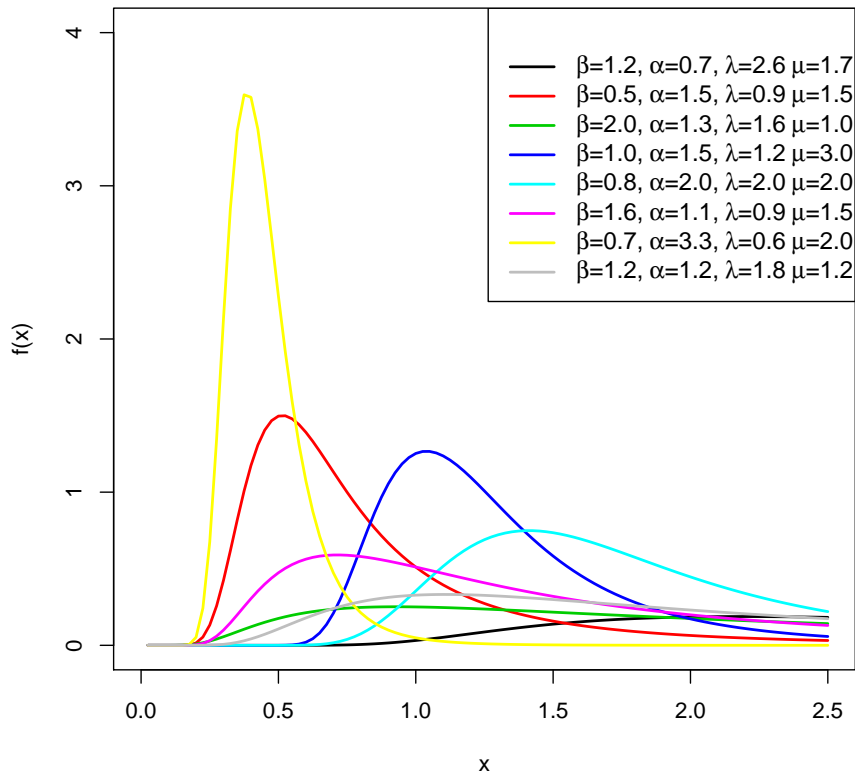


Figure 3: The plots of the EMA-GF model for some parameter values cases

Figure 3 shows the density functions for selected values of parameters β, α, λ and μ . The density plot shows that the EMA-GFr distribution can be increasing, decreasing or unimodal and skewed to the left.

4. STATISTICAL USEFUL REPRESENTATION

A useful representation of the EMA-G family of distributions will be derived in this section. The representation is used to study the statistical characteristics of the EMA-G distribution. This representation will help to simplify the properties of the proposed EMA-G model. However, for $\tau > 0$, $(a - b)^\tau = \sum_{\eta=0}^{\tau} (-1)^\eta \binom{\tau}{\eta} a^{\tau-\eta} b^\eta$. Thus, the pdf and cdf of the EMA-G density can be defined respectively as

$$f(t) = \sum_{r=0}^{\infty} \sum_{\eta=0}^{\alpha-1} \alpha (-1)^{\eta+r} \binom{\alpha-1}{\eta} \binom{\alpha+r}{r} \beta^{-r-1} (1-\beta)^r m(t) M^{\eta+r}(t) \quad (19)$$

and

$$F(t) = 1 - \sum_{r=0}^{\infty} \sum_{\eta=0}^{\alpha} (-1)^{\eta+r} \binom{\alpha}{\eta} \binom{\alpha+r-1}{r} \beta^{-r} (1-\beta)^r M^{\eta+r}(t). \quad (20)$$

5. STATISTICAL PROPERTIES OF THE EMA-G DISTRIBUTION

This section investigated the statistical properties of the EMA-G family of distributions. These properties include the moments, generating function, entropies, probability weighted moment, moments of the residual and reversed residual lives and order statistics.

5.1. The moments of the EMA-G distribution

The k^{th} moment of the EMA-G density with random variable T for is expressed as

$$\begin{aligned} \mu'_k &= \sum_{r=0}^{\infty} \sum_{\eta=0}^{\alpha-1} Avio_{r,\eta} \int_0^{\infty} t^k m(t) M^{\eta+r}(t) dt \\ &= \sum_{r=0}^{\infty} \sum_{\eta=0}^{\alpha-1} Avio_{r,\eta} D_t, \end{aligned} \tag{21}$$

where

$$Avio_{r,\eta} = \alpha(-1)^{\eta+r} \binom{\alpha-1}{\eta} \binom{\alpha+r}{r} \beta^{-r-1} (1-\beta)^r, \quad D_t = \int_0^{\infty} t^k m(t) M^{\eta+r}(t) dt.$$

The mean of Equation (21) is obtained when $k = 1$. The central moment of the random variable T , say μ_ψ and the cumulants (Ko_ψ) of the random variable T can be obtained respectively as

$$\mu_\psi = \sum_{v=0}^{\psi} (-1)^v \binom{\psi}{v} \mu_1^v \mu'_{\psi-r}, \tag{22}$$

and

$$Ko_\psi = \mu'_\psi - \sum_{v=0}^{\psi-1} \binom{\psi-1}{v-1} K_r \mu'_{\psi-r}, \tag{23}$$

with $Ko_1 = \mu'_1$.

The d^{th} incomplete moment for, say $\rho_d(s)$ of the EAP-G density can be obtained as

$$\begin{aligned} \rho_d(s) &= \sum_{r=0}^{\infty} \sum_{\eta=0}^{\alpha-1} Avio_{r,\eta} \int_0^s t^s m(t) M^{\eta+r}(t) dt \\ &= \sum_{r=0}^{\infty} \sum_{\eta=0}^{\alpha-1} Avio_{r,\eta} D_s, \end{aligned} \tag{24}$$

where

$$D_s = \int_0^s t^s m(t) M^{\eta+r}(t) dt.$$

However, the Bonferroni and Lorenz curve can be obtained respectively as

$$B(p) = \frac{\rho_1(t_p)}{p\mu'_1},$$

and

$$L(p) = \frac{\rho_1(t_p)}{\mu'_1},$$

where t_p is evaluated numerically from the quantile function in Equation (8) for probability p

More so, the mean deviation about the median, say M of T can be obtained as

$$\delta_M = \int_0^{\infty} |T - M| f(t) dt = \mu'_1 - \rho_1(M).$$

Also, the mean deviation about the mean of random variable T can be expressed

$$\delta_\mu = \int_0^{\infty} |T - \mu'_1| f(t) dt = 2\mu'_1 F(\mu'_1) - \rho_1\mu'_1,$$

with $\mu'_1 = E[T]$ and $F(\mu'_1)$ evaluated numerically from Equation (6).

5.2. Probability weighted moments (PWM)

The estimate of the estimators of the parameters and the quantiles of the generalized distributions can be derived using the PWMs of the EMA-G density. The (s, r) th PWM of T , say for $s \geq 0, r \geq 1$ is given as

$$\begin{aligned} PWM_{r,s} &= \int_0^\infty t^r f(t) F(t)^s dt \\ &= \sum_{r=0}^\infty \sum_{\eta}^{\alpha} B_{r,\eta} Avio_{r,\eta} \int_0^\infty t^s m(t) M^{(\eta+r)(\phi+1)}(t) dt \\ &= \sum_{r=0}^\infty \sum_{\eta}^{\alpha} B_{r,\eta} Avio_{r,\eta} Qp_s \end{aligned} \tag{25}$$

where

$$B_{r,\eta} = (-1)^{\eta+r} \binom{\alpha}{\eta} \binom{\alpha+r-1}{r} \beta^{-r} (1-\beta)^r, \quad Qp = \int_0^\infty t^s m(t) M^{(\eta+r)(\phi+1)}(t) dt.$$

5.3. Generating function

The probability generating function of EMA-G density function of a random variable T is expressed as

$$\begin{aligned} M(x) &= \sum_{\delta=0}^\infty \frac{(\log x)^\delta}{\delta!} \int_1^\infty t^\delta f(t) dt \quad \text{for } |x| > 1, \quad t > 0 \\ &= \sum_{\delta=0}^\infty \sum_{r=0}^\infty \sum_{\eta=0}^{\alpha-1} \frac{(\log x)^\delta}{\delta!} Avio_{r,\eta} L_\delta, \end{aligned} \tag{26}$$

where

$$L_\delta = \int_1^\infty t^\delta m(t) M^{\eta+r}(t) dt.$$

More so, the moment generating function of the random variable T is given as

$$M_T(x) = \sum_{r=0}^\infty \sum_{\eta=0}^{\alpha-1} Avio_{r,\eta} R_\psi \tag{27}$$

where

$$R_\psi = \int_0^\infty e^{tx} m(t) M^{(\eta+r)(\phi+1)}(t) dt.$$

5.4. Moments of the residual life and reversed residual life

The η^{th} moment of the residual life, say $b_\eta(x) = E[(T-x)^\eta | T > x]$ for $\eta = 1, \dots$ uniquely determines $M(t)$ (see [?]). However, the η^{th} moment of the residual life is given as

$$m_\eta(x) = \frac{1}{1-F(x)} \sum_{r=0}^\infty \sum_{\eta=0}^{\alpha-1} \sum_{p=0}^{\eta} (-1)^{\eta-p} x^{\eta-p} \binom{\eta}{p} Avio_{r,\eta} \zeta_p, \tag{28}$$

where

$$\zeta_p = \int_x^\infty t^p m(t) M^{\eta+r}(t) dt.$$

Similarly, the η^{th} moment of the reversed residual life, say $M_\eta(t) = E[(x-T)^\eta | T \leq x]$ for $\eta > 0$, and $\eta = \dots$ uniquely determines $F(t)$ is given as

$$M_\eta(x) = \frac{1}{F(x)} \sum_{r=0}^\infty \sum_{\eta=0}^{\alpha-1} \sum_{u=0}^{\eta} (-1)^{\eta-u} x^{\eta-u} \binom{\eta}{u} Avio_{r,\eta} \vartheta_u, \tag{29}$$

where

$$\vartheta_u = \int_0^x t^u m(t) M^{\eta+r}(t) dt.$$

5.5. Order statistics

Let T_1, T_2, \dots, T_η is a random sample of size η from the $f(t)$ distribution and $T_{(1)}, T_{(2)}, \dots, T_{(\eta)}$ be the corresponding order statistics. Then, the probability density function of the k^{th} order statistic $T_{(k)}$, say $f_k(t)$ is given as

$$f_k(t) = \frac{\eta!}{(k-1)!(\eta-k)!} \left[1 - \left[\frac{\beta(1-M(t))}{\beta+(1-\beta)M(t)} \right]^\alpha \right]^{k-1} \left[\left[\frac{\beta(1-M(t))}{\beta+(1-\beta)M(t)} \right]^\alpha \right]^{\eta-k} \times \alpha \beta^\alpha \frac{m(t)[1-M(t)]^{\alpha-1}}{[\beta+(1-\beta)M(t)]^{\alpha+1}}. \tag{30}$$

The minimum order statistics is obtained when $k = 1$, while that of the maximum order statistics is obtained when $k = n$.

5.6. Entropies

The Renyi entropy of the EMA-G random variable T measures the variation of the uncertainty is given as

$$Ren_\delta = \frac{1}{1-\delta} \log \sum_{r=0}^{\infty} \sum_{\eta=0}^{\delta(\alpha-1)} \alpha^\delta (-1)^{\eta+r} \binom{\delta(\alpha-1)}{\eta} \binom{\delta(\alpha+1)+r-1}{r} \beta^{-r-1} (1-\beta)^r Q_{Ren}, \tag{31}$$

where $Q_{Ren} = \int_{-\infty}^{\infty} m^\delta(t) M^{\eta+r}(t) dt$. $\delta > 0, \delta \neq 1$.

The δ entropy $D_\delta(T)$ for $\delta > 0, \delta \neq 1$ is expressed as

$$D_\delta = \frac{1}{1-\delta} \log \left[1 - \sum_{r=0}^{\infty} \sum_{\eta=0}^{\delta(\alpha-1)} \alpha^\delta (-1)^{\eta+r} \binom{\delta(\alpha-1)}{\eta} \binom{\delta(\alpha+1)+r-1}{r} \beta^{-r-1} (1-\beta)^r \right]. \tag{32}$$

6. ESTIMATION

In this section, we shall examine the Bernstein function and maximum likelihood estimation of the EMA-G density. The maximum likelihood estimators of the model performance will be investigated in terms of their means, biases, variance and mean squared errors using the Monte Carlo simulation method. However, real life applications were also provided to examine the flexibility, performance and potential of the EMA-G density.

6.1. The Bernstein estimation

The Bernstein polynomials were developed as a probabilistic proof of the Weierstrass Approximation Theorem (WAT) for continuous function say, $f(t)$ on the closed interval $[a, b]$ is defined in [?] as

$$B_\varphi(t, f) = \sum_{\phi=1}^{\varphi} f\left(a + \frac{\phi-1}{\varphi-1}(b-a)\right) \alpha \beta^\alpha \frac{m(t)[1-M(t)]^{\alpha-1}}{[\beta+(1-\beta)M(t)]^{\alpha+1}}, \tag{33}$$

which converges to the true function, i.e. $\|B_\varphi(t, f) - f(t)\|_\infty \equiv \sup_{y \leq t \leq z} |B_\varphi(t, f) - f(t)| \rightarrow 0$, as $\varphi \rightarrow \infty$.

However, for $a = 0, b = 1$, and re-scaling Equation (33), we have the pdf of EAP-G model as

$$f_\varphi(t) = \frac{\sum_{\phi=1}^{\varphi} f\left(\frac{\phi-1}{\varphi-1}\right) \alpha \beta^\alpha \frac{m(t)[1-M(t)]^{\alpha-1}}{[\beta+(1-\beta)M(t)]^{\alpha+1}}}{\sum_{\phi=1}^{\varphi} f\left(\frac{\phi-1}{\varphi-1}\right)}. \tag{34}$$

6.2. Maximum likelihood estimation

The maximum likelihood method is used to obtain the parameters estimates of the EMA-G density. Let $\mathbf{t} = (t_1, t_2, t_2, \dots, t_{\eta-1}, t_{\eta})$ be a random sample from the EMA-G density with unknown parameter vector ε . Then, the log-likelihood function ℓ of the EMA-G can be expressed as

$$\begin{aligned} \ell = & \eta \log \alpha + \eta \alpha \log \beta + \sum_{i=1}^{\eta} \log m(t) + (\alpha - 1) \sum_{i=1}^{\eta} \log(1 - M(t)) \\ & - (\alpha + 1) \sum_{i=1}^{\eta} \log(\beta + (1 - \beta)M(t)). \end{aligned} \tag{35}$$

The partial derivative of Equation (35) with respect to parameters $\alpha, \beta, \varepsilon$ and equating to zero gives

$$\frac{\partial \ell}{\partial \alpha} = \frac{1}{\eta} + \eta \log \beta + \sum_{i=1}^{\eta} \log(1 - M(t)) - \sum_{i=1}^{\eta} \log(\beta + (1 - \beta)M(t)) = 0, \tag{36}$$

$$\frac{\partial \ell}{\partial \beta} = \frac{\eta \alpha}{\beta} - (\alpha + 1) \sum_{i=1}^{\eta} \frac{1 - M(t)}{\beta + (1 - \beta)M(t)} = 0, \tag{37}$$

and

$$\frac{\partial \ell}{\partial \varepsilon} = \sum_{i=1}^{\eta} \frac{m'_{\varepsilon}(t)}{m(t)} - (\alpha - 1) \sum_{i=1}^{\eta} \frac{m(t)}{1 - M(t)} + \frac{(\alpha + 1)(1 - \beta)m(t)}{\beta + (1 - \beta)M(t)} = 0. \tag{38}$$

The unknown parameters estimate can be obtained by solving the nonlinear Equations in (36), (37) and (38) numerically using the Newton-Raphson algorithm in R, Matlap, Maple and Mathematica.

6.3. Simulations study

In order to examine performance of the EMA-G density, a Monte Carlo simulation is performed and examined. The distributions considered include the Burrxii (Br), Frechet (F) and Weibull (Wb) distributions.

The simulation study is carried out using n sample size by computing their mean estimates (MEs), biases, variance and means squared errors (MSEs) of the maximum likelihood estimate MLEs ($\beta, \alpha, \lambda, \mu$) using Equation (7). The random samples used are 5, 10, 30, 50, 100, 150, 200, 300, 400, and 500. The simulation was performed using ($\hat{\beta} = 1.0, \hat{\alpha} = 1.0, \hat{\lambda} = 1.5, \hat{\mu} = 1.5$). The bias is estimated by (for $Q = \alpha, \beta, \lambda, \mu$)

$$\hat{Bias}_Q = \frac{1}{5000} \sum_{\rho=1}^{5000} (\hat{Q}_{\rho} - Q).$$

Also, the MSE is obtained as

$$\hat{MSE}_U = \frac{1}{5000} \sum_{\rho=1}^{5000} (\hat{Q}_{\rho} - Q)^2.$$

The results of the simulation is shown in Table 2. The results indicate that increase in sample sizes decreases the mean, bias, variance and MSE and tends to zero.

7. REAL LIFE DATA APPLICATION

This section investigated the empirical flexibility and performance of the EMA-G model with a three real life data set. The test statistics of the EMA-GBr was also compared with the Kumaraswamy Burr-XII (KBur), beta Burrxii (BBur), transmuted Burr-XII, lognormal Burr-XII

Table 2: Monte Carlo simulation results for parameter estimates

Distribution	n	ME	Bias	Variance	MSE
Weibull	05	1.18, 1.28, 2.07, 1.99	0.78, 0.28, 0.57, 0.30	1.53, 2.02, 2.43, 1.41	1.56, 2.11, 0.76, 1.50
	10	1.26, 1.09, 1.82, 1.54	0.46, 0.09, 0.32, 0.14	1.09, 1.29, 1.20, 1.04	1.16, 1.30, 0.31, 1.07
	30	1.12, 0.96, 1.65, 1.49	0.32, -0.03, 0.15, 0.05	0.57, 0.48, 1.07, 0.46	0.67, 0.49, 0.09, 0.46
	50	1.02, 0.13, 0.61, 1.48	0.32, -0.06, 0.11, 0.02	0.39, 0.31, 0.24, 0.29	0.49, 0.31, 0.06, 0.29
	100	0.68, 0.09, 0.58, 1.47	0.32, -0.09, 0.08, 0.01	0.24, 0.17, 0.09, 0.18	0.35, 0.18, 0.03, 0.18
	150	0.45, 0.08, 0.57, 0.50	0.32, -0.11, 0.07, -0.01	0.18, 0.12, 0.07, 0.12	0.28, 0.13, 0.02, 0.12
	200	0.12, 0.07, 0.57, 0.51	0.31, -0.12, 0.07, -0.01	0.14, 0.09, 0.07, 0.09	0.24, 0.11, 0.01, 0.09
	300	0.02, 0.07, 0.56, 0.51	0.32, -0.12, 0.06, -0.01	0.11, 0.06, 0.06, 0.07	0.21, 0.08, 0.01, 0.07
	400	0.02, 0.07, 0.55, 0.51	0.32, -0.12, 0.05, -0.01	0.09, 0.05, 0.01, 0.05	0.20, 0.07, 0.01, 0.05
	500	0.02, 0.07, 0.55, 0.51	0.32, -0.12, 0.05, -0.01	0.08, 0.04, 0.01, 0.04	0.18, 0.06, 0.01, 0.04
Burrxii	05	1.65, 1.30, 2.18, 0.95	0.65, 0.30, 0.68, -0.54	2.06, 3.38, 0.95, 2.15	2.50, 3.48, 1.42, 2.45
	10	1.62, 1.22, 1.85, 1.15	0.62, 0.22, 0.35, 0.34	1.71, 2.56, 0.32, 1.60	2.10, 2.61, 0.45, 1.72
	30	1.53, 1.08, 1.64, 1.34	0.53, 0.08, 0.14, 0.15	0.80, 0.87, 0.09, 0.75	1.09, 0.88, 0.11, 0.78
	50	0.48, 1.02, 0.60, 0.57	0.48, 0.02, 0.10, 0.12	0.54, 0.57, 0.06, 0.51	0.78, 0.57, 0.07, 0.53
	100	0.44, 0.96, 0.57, 0.41	0.44, -0.03, 0.07, 0.08	0.31, 0.28, 0.03, 0.27	0.34, 0.28, 0.03, 0.28
	150	0.42, 0.94, 0.05, 0.34	0.42, -0.05, 0.05, 0.05	0.21, 0.18, 0.02, 0.17	0.29, 0.19, 0.02, 0.17
	200	0.41, 0.93, 0.05, 0.14	0.41, -0.06, 0.05, 0.05	0.17, 0.14, 0.01, 0.13	0.14, 0.15, 0.01, 0.14
	300	0.41, 0.92, 0.04, 0.08	0.41, -0.07, 0.04, 0.04	0.12, 0.10, 0.01, 0.09	0.09, 0.10, 0.01, 0.09
	400	0.01, 0.92, 0.04, 0.06	0.41, -0.07, 0.04, 0.03	0.10, 0.08, 0.01, 0.07	0.07, 0.09, 0.01, 0.07
	500	0.01, 0.92, 0.03, 0.01	0.41, -0.07, 0.03, 0.02	0.08, 0.06, 0.01, 0.05	0.05, 0.07, 0.01, 0.05
Frechet	05	1.97, 1.33, 1.75, 1.04	0.97, 0.33, 1.25, -0.45	3.21, 5.96, 0.13, 3.19	4.16, 6.07, 0.19, 3.40
	10	1.94, 1.40, 1.63, 1.09	0.94, 0.40, 0.13, 0.40	2.75, 4.74, 0.05, 2.86	3.63, 4.90, 0.07, 3.03
	30	1.72, 1.23, 1.54, 1.25	0.72, 0.23, 0.04, 0.24	1.07, 1.69, 0.01, 1.09	1.60, 1.75, 0.02, 1.15
	50	0.64, 1.15, 0.53, 0.81	0.64, 0.15, 0.03, 0.18	0.61, 0.92, 0.01, 0.59	1.02, 0.95, 0.01, 0.62
	100	0.12, 1.02, 0.51, 0.69	0.52, 0.02, 0.01, 0.10	0.22, 0.30, 0.01, 0.25	0.49, 0.30, 0.01, 0.26
	150	0.08, 0.98, 0.51, 0.51	0.48, -0.01, 0.01, 0.08	0.13, 0.19, 0.01, 0.18	0.37, 0.19, 0.01, 0.18
	200	0.07, 0.96, 0.51, 0.42	0.47, -0.03, 0.01, 0.07	0.08, 0.12, 0.01, 0.13	0.31, 0.12, 0.00, 0.13
	300	0.05, 0.94, 0.51, 0.22	0.45, -0.05, 0.01, 0.07	0.05, 0.07, 0.00, 0.09	0.26, 0.07, 0.00, 0.09
	400	0.04, 0.93, 0.51, 0.13	0.44, -0.06, 0.01, 0.06	0.04, 0.05, 0.00, 0.06	0.24, 0.05, 0.00, 0.06
	500	0.04, 0.93, 0.51, 0.03	0.44, -0.06, 0.01, 0.06	0.03, 0.04, 0.00, 0.05	0.23, 0.04, 0.00, 0.05

(LogBur) and Gompertz Burrxii distributions. More so, the goodness-of-fit of the EMA-GWb was compared with Gompertz Weibull (GW), alpha power Weibull (APW), transmuted Weibull (TW), Kumaraswamy Weibull and alpha power inverted Weibull (APIW) distributions. Also, the goodness-f-fit of the EMA-GF distribution is compared with the transmuted Marshall-Olkin Frechet (TMFr), Weibull Frechet (WFr), Kumaraswamy Frechet (KFr), exponentiated Frechet (EFr), and Marshall-Olkin Frechet (MFr) distributions. Finally, the goodness-of-fit of the EMA-G models are compared with Exponentiated shifted exponential (ESE), Kumaraswamy Frechet (KFr), gamma extended Frechet (GaFr), Generalized Lindley (GL) , beta Frechet (BFr), Alpha power inverted exponential (APIE) distribution, and the Generalized inverted generalized exponential (GIGE) distributions using the Akaike Information Criteria (AIC), Consistent Akaike Information Criteria (CAIC), Bayesian Information Criteria (BIC), Hannan and Quinn Information Criteria (HQIC), Anderson Darling (A), and Cramer-von Mises (W) test statistics.

The first data as used in [?], [?], [?], [?], [?], [?] [10], and [?] consist of 63 workers at the UK National Physical Laboratory observations of strength of 1.5cm glass fibers in [?]. The results of the test statistics are shown in Table 3.

Table 3: The statistics rating of the EMA-G distribution with glass fibres dataset with standard errors in parentheses

Distribution	Parameter MLEs	AIC	CAIC	BIC	HQIC	W	A
EMA-GBr	$\hat{\alpha} = 4.15(3.04)$	35.89	36.58	44.46	39.26	0.19	1.06
	$\hat{\beta} = 197.58(131.80)$						
	$\hat{\lambda} = 1.93(0.76)$						

Table 3 – Continued from previous page

Distribution	Parameter MLEs	AIC	CAIC	BIC	HQIC	W	A
	$\hat{\mu} = 3.99(1.14)$						
GBur	$\hat{\alpha} = 15.09(69.05)$ $\hat{\beta} = 36.95(98.24)$ $\hat{a} = 2.06(0.64)$ $\hat{b} = 0.65(0.69)$	37.00	36.70	44.58	39.38	0.17	1.00
KBur	$\hat{a} = 15.52(7.31)$ $\hat{b} = 132.22(145.98)$ $\hat{\alpha} = 1.36(0.57)$ $\hat{\beta} = 1.03(0.30)$	47.20	47.89	55.78	50.57	0.42	2.29
BBur	$\hat{\alpha} = 15.09(69.05)$ $\hat{\beta} = 36.95(98.24)$ $\hat{a} = 2.06(0.64)$ $\hat{b} = 0.65(0.69)$	67.34	68.03	76.00	70.80	0.71	3.86
TBur	$\hat{\alpha} = -0.92(0.11)$ $\hat{\beta} = 0.58(0.14)$ $\hat{\lambda} = 5.80(1.22)$	85.37	85.77	91.80	87.90	0.98	5.33
LoGBur	$\hat{\alpha} = 87.39(260.09)$ $\hat{\beta} = 10.04(13.70)$ $\hat{a} = 10.04(13.71)$ $\hat{b} = 0.37(0.59)$	305.08	305.49	315.49	309.30	32.11	197.6
EMA-GF	$\hat{\alpha} = 23.43(19.43)$ $\hat{\beta} = 0.01(0.01)$ $\hat{\lambda} = 0.73(0.08)$ $\hat{\mu} = 23.52(11.09)$	31.85	32.53	36.84	33.64	0.21	1.32
WFr	$\hat{\alpha} = 0.40(0.81)$ $\hat{\beta} = 0.30(0.30)$ $\hat{a} = 1.49(4.77)$ $\hat{b} = 16.85(20.48)$	38.80	39.48	47.38	42.17	0.25	1.36
KFr	$\hat{\alpha} = 2.12(4.56)$ $\hat{\beta} = 0.74(0.07)$ $\hat{a} = 5.51(7.98)$ $\hat{b} = 857.35(153.94)$	47.63	48.31	56.18	52.84	0.31	0.57
EFr	$\hat{\alpha} = 7.82(2.95)$ $\hat{\beta} = 1.01(0.14)$ $\hat{\mu} = 132.83(116.64)$	50.50	50.70	56.70	52.80	0.31	0.58
TMFr	$\hat{\alpha} = 0.66(0.06)$ $\hat{\beta} = 0.16(0.34)$ $\hat{a} = 6.88(0.61)$ $\hat{b} = 376.27(246.84)$	56.51	57.11	65.10	59.81	0.16	1.29
MFr	$\hat{\beta} = 0.17(0.045)$ $\hat{\gamma} = 6.48(0.56)$ $\hat{\mu} = 161.612(91.50)$	57.11	57.51	63.51	59.61	0.22	2.80
EMA-GW	$\hat{\alpha} = 1.18(0.72)$ $\hat{\beta} = 21.83(6.98)$ $\hat{\lambda} = 0.91(0.25)$ $\hat{\mu} = 2.98(1.22)$	31.98	32.67	40.55	35.35	0.09	0.56
KW	$\hat{\alpha} = 0.55(0.01)$ $\hat{\beta} = 0.23(0.01)$ $\hat{a} = 0.74(0.01)$	35.413	36.11	43.99	38.79	0.16	0.87

Table 3 – Continued from previous page

Distribution	Parameter MLEs	AIC	CAIC	BIC	HQIC	W	A
	$\hat{b} = 7.10(0.01)$						
TW	$\hat{\alpha} = -0.51(0.28)$ $\hat{\beta} = 0.66(0.04)$ $\hat{\lambda} = 5.17(0.68)$	36.69	37.38	45.26	40.06	0.22	1.13
APW	$\hat{\alpha} = 6.57(8.04)$ $\hat{\beta} = 0.16(0.10)$ $\hat{\lambda} = 4.74(0.82)$	38.19	38.59	44.62	40.72	0.18	0.97
GW	$\hat{\alpha} = 0.23(0.82)$ $\hat{\beta} = 0.01(0.05)$ $\hat{a} = 0.80(0.52)$ $\hat{b} = 5.62(0.51)$	38.38	39.07	46.95	41.75	0.24	1.29
APIW	$\hat{\alpha} = 61.03(48.15)$ $\hat{\beta} = 0.79(0.17)$ $\hat{\lambda} = 3.82(0.30)$	82.59	83.00	89.02	85.13	0.99	5.30

Figures 4 and 5 shows the empirical densities and cdfs with the glass fiber data set for some models. The quantile-quantile plots of some of the models for glass data are shown in Figure 6. However, the plots of the EMA-G models performed favourably when compared to some existing models.

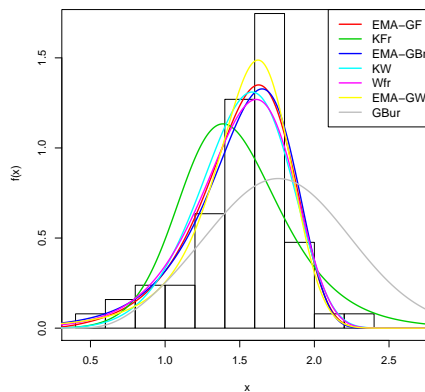


Figure 4: EMA-G density empirical pdf plots for glass fiber data

The second data consist of data set obtained from the National Highway Traffic Safety Administration on fatal accidents that occur on roads in the United States. The data represent the number of vehicle fatalities for 39 counties in South Carolina for 2012 (www-fars.nhtsa.dot.gov/States) as used in [?]. The test statistics are shown in Table 4. Figures 7 and 8 show the empirical density and cdf of the EMA-G model.

Table 4: The statistics rating of the EMA-G distribution with vehicle fatalities dataset with standard errors in parentheses

Distribution	Parameter MLEs	AIC	CAIC	BIC	HQIC	W	A
EMA-GWb	$\hat{\alpha} = 0.13(0.04)$ $\hat{\beta} = 3.89(2.85)$ $\hat{\lambda} = 0.41(0.04)$ $\hat{\mu} = 1.02(0.04)$	314.12	315.29	320.77	316.50	0.03	0.26

Table 4 – *Continued from previous page*

Distribution	Parameter MLEs	AIC	CAIC	BIC	HQIC	W	A
BW	$\hat{\alpha} = 2.45(2.13)$ $\hat{\beta} = 1.33(0.01)$ $\hat{a} = 0.80(0.16)$ $\hat{b} = 12.90(0.01)$	315.56	316.74	322.22	317.95	0.14	0.47
APW	$\hat{\alpha} = 0.01(0.02)$ $\hat{\beta} = 0.01(0.01)$ $\hat{\lambda} = 1.33(0.22)$	316.15	316.84	321.14	317.94	0.15	0.50
TW	$\hat{\alpha} = 0.43(0.51)$ $\hat{\beta} = 0.04(0.02)$ $\hat{\lambda} = 1.34(0.17)$	316.41	317.09	321.40	318.20	0.09	0.87
GW	$\hat{\alpha} = 0.01(0.01)$ $\hat{\beta} = 4.73(2.46)$ $\hat{a} = 0.28(0.58)$ $\hat{b} = 0.19(0.04)$	318.15	319.32	324.80	320.53	0.13	0.80
APIW	$\hat{\alpha} = 69.69(107.78)$ $\hat{\beta} = 4.25(1.88)$ $\hat{\lambda} = 1.25(0.14)$	319.74	320.43	324.73	321.53	0.12	0.73
EMA-GBr	$\hat{\alpha} = 3.22(3.75)$ $\hat{\beta} = 145.95(112.32)$ $\hat{\lambda} = 0.40(0.86)$ $\hat{\mu} = 3.33(6.82)$	314.43	315.61	321.08	316.82	0.03	0.25
KUBur	$\hat{a} = 26.04(53.60)$ $\hat{b} = 63.01(0.55)$ $\hat{\alpha} = 1.77(2.57)$ $\hat{\beta} = 0.23(0.18)$	324.87	326.05	331.52	327.26	0.04	0.85
BBur	$\hat{\alpha} = 90.30(214.17)$ $\hat{\beta} = 78.59(223.29)$ $\hat{a} = 0.81(1.90)$ $\hat{b} = 0.18(0.24)$	326.24	327.42	332.89	328.63	0.05	0.85
LoGBur	$\hat{\alpha} = 57.63(133.08)$ $\hat{\beta} = 33.79(52.95)$ $\hat{a} = 1.65(2.58)$ $\hat{b} = 0.23(0.31)$	326.13	327.31	332.79	328.52	0.77	0.92
EMA-GF	$\hat{\alpha} = 0.01(0.02)$ $\hat{\beta} = 2.51(2.23)$ $\hat{\lambda} = 0.98(0.98)$ $\hat{\mu} = 0.54(0.27)$	290.95	291.37	301.37	295.16	0.01	0.02
WFr	$\hat{\alpha} = 4.24(6.48)$ $\hat{\beta} = 60.30(65.46)$ $\hat{\lambda} = 1.28(0.37)$ $\hat{\mu} = 2.20(01.72)$	311.27	312.44	317.92	313.65	0.03	0.26
KFr	$\hat{\alpha} = 5.52(0.00)$ $\hat{\beta} = 78.42(71.71)$ $\hat{a} = 0.26(0.05)$ $\hat{b} = 8.09(0.00)$	314.44	315.62	321.10	316.83	0.03	0.24

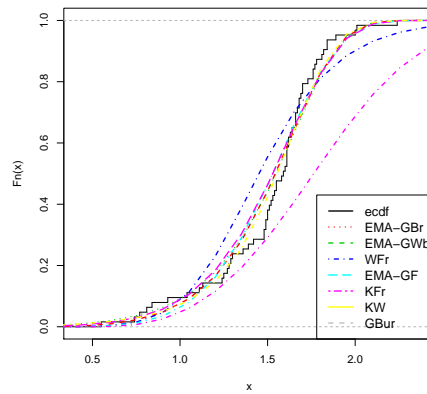


Figure 5: EMA-G density empirical cdf plots for glass fiber data

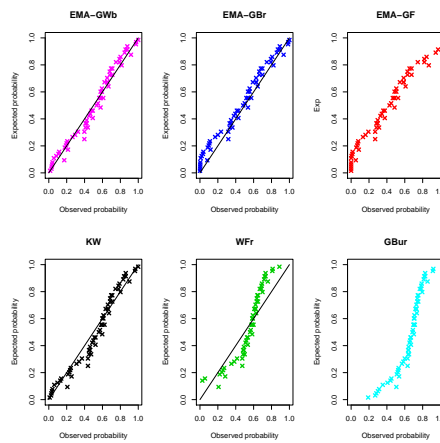


Figure 6: EMA-G density Q-Q plots for glass data

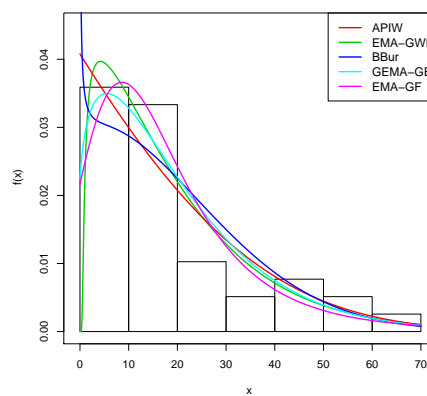


Figure 7: EMA-G density empirical cdf plots for vehicle fatalities data

7.1. Discussion

Two real life data sets were used to examine the performance of the EMA-G models. However, a model is said to perform better than another if its value of the lowest Akaike Information Criteria

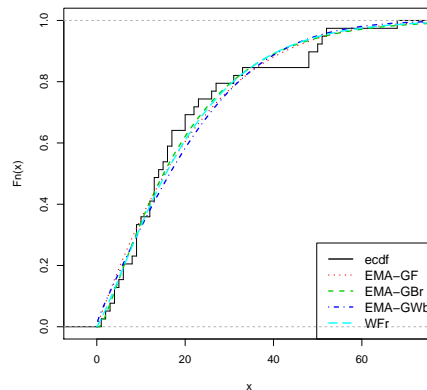


Figure 8: EMA-G density empirical cdf plots for vehicle fatalities data

(AIC) is the smallest. However, in the real data cases investigated, the EMA-G distributions have the lowest AIC value in glass fibres data and vehicle fatalities data respectively. Hence, it is said to be better for these data sets under consideration and competes favourably with other existing model for the data used.

8. CONCLUSION

This study introduces a new class of generator called EMA-G distribution in probability theory. This generator extends the performance of some existing generators like the Gompertz, Weibull, Frechet generators. Basic characteristics of the EMA-G distribution were examined. The EMA-G generator was expressed as a linear form of the baseline distribution. The entropy and PWMs of the proposed distribution were derived. The unknown parameters of the EMA-G density were obtained by maximum likelihood. A simulation study of the EMA-G model was illustrated using the Monte Carlo method. The simulation shows that the shape of the proposed distribution could be skewed, unimodal, increasing or decreasing (depending on the value of the parameters cases). The new distribution was applied to a real life data. It shows that the EMA-G distribution performed better than some existing models in literature like APIE, APIW, GW, TW, APW, KW, BBur, KBur, LoGBur, TMFr, TGGz, TGz, KGz, WFr, TMFr, EFr, and MFr.

REFERENCES

- [1] Afify, A. Z., Yousof, H. M., and Nadarajah, S. (2017). The beta transmuted-H family of distributions: properties and applications. *Statistics and its Inference*, 10:505–520.
- [2] Alizadeh, M., Tahir, M. H., Cordeiro, G. M., Mansoor, M., Zubair, M., and Hamedani, G. G. (2015). The Kumaraswamy Marshal-Olkin family of distributions. *Journal of the Egyptian Mathematical Society*, 23(3):546–557.
- [3] Alizadeh, M., Cordeiro, G. M., Pinho, L. G. B., and Ghosh, I. (2017). The Gompertz-G family of distributions. *Journal of Statistical Theory and Practice*, 11(1):179 – 207.
- [4] Alizadeh, M., Rasekhi, M., Yousof, H. M., and Hamedani, G. G. (2018). The transmuted Weibull-G family of distributions. *Hacettepe Journal of Mathematics and Statistics*, 47(6): 1–20.
- [5] Alizadeh, M., Yousof, H. M., Jahanshahiz, S. M. A., Najibi, S. M., and Hamedani, G. G. (2020). The transmuted odd log-logistic-G family of distributions. *Journal of Statistics and Management systems*, doi:10.1080/09720510.2019.1685228.
- [6] Amini, M., Mir-Mostafaei, S. M. T. K., and Ahmadi, J. (2014). Log-gamma- generated families of distributions. *Statistics*, 48(4): 1–20.

- [7] Aryal, G. R. and Yousof, H. M. (2017). The exponentiated generalized-G poisson family of distributions. *Economic Quality Control*, 32(1):1–17.
- [8] Bourguignon, B. M., Silva, R., and Cordeiro, G. M. (2014). The Weibull-G family of probability distributions. *Journal of Data Science*, 12: 53–68.
- [9] Cordeiro, G. M. and de Castro, M. (2011). A new family of generalized distributions. *Journal of Statistical Computation and Simulation*, 81(7): 883–898.
- [10] Eghwerido, J. T., Oguntunde, P. E., and Agu, F. I. (2021). The alpha power Marshall-olkin-G distribution: properties, and applications. *Sankhya A - The Indian Journal of Statistics*, <https://doi.org/10.1007/s13171-020-00235-y>.
- [11] Eghwerido, J. T., Zelibe, S. C., and Efe-Eyefia, E. (2020c). The transmuted alpha power-G family of distributions. *Journal of Statistics and Management Systems*, <https://doi.org/10.1080/09720510.2020.1794528>.
- [12] Eliwa, M. S. and El-Morshedy, M. (2018). Bivariate Gumbel-G family of distributions: statistical properties, bayesian and non-bayesian estimation with application. *Annals of Data Science*, doi/10.1007/s40745-018-00190-4.
- [13] Handique, L. and Chakraborty, S. and de Andrade, T. A. (2019). The Exponentiated Generalized Marshall-Olkin Family of Distribution: Its Properties and Applications. *Annals of Data Science*, 6(3): 391–411.
- [14] Mahdavi, A. and Kundu, D. (2017). A new method for generating distributions with an application to exponential distribution. *Communications in Statistics - Theory and Methods*, 46(13): 6543–6557.
- [15] Marshall, A. W. and Olkin, I. (1997). A new method for adding a parameter to a family of distributions with application to the exponential and Weibull families. *Biometrika*, 84: 641–652.
- [16] Reyad, H., Alizadeh, M., Jamal, F., and Othman, S. (2018). The Topp Leone odd Lindley-G family of distributions: Properties and applications. *Journal of Statistics and Management Systems*, 21(7):1273–1297.
- [17] Tahir, M. H., Cordeiro, G. M., Alzaatreh, A., Mansoor, M., and Zubair, M. (2016). The logistic-X family of distributions and its applications. *Communications in Statistics-Theory and Methods*, 45(24): 7326–7348.
- [18] Yousof, H. M., Alizadeh, M., Jahanshahiand, S. M. A., Ramires, T. G., Ghosh, I., and Hamedani, G. G. (2017). The transmuted Topp-Leone-G family of distributions: theory, characterizations and applications. *Journal of Data Science*, 15: 6723–740.
- [19] Yousof, H. M., Afify, A. Z., Hamedani, G. G., and Aryal, G. (2017a). The Burr-X generator of distributions for lifetime data. *Journal of Statistical Theory and Applications*, 16:288–305.
- [20] Yousof, H. M., Afify, A. Z., Alizadeh, M., Nadarajah, S., Aryal, G. R., and Hamedani, G. G. (2018). The Marshall-Olkin generalized-G family of distributions with applications. *Statistica*, 78(3): 273–295.

APPENDIX

ABBREVIATIONS

A = Anderson Darling
AIC = Akaike Information Criteria
APIE = Alpha power inverted exponential
APIW = alpha power inverted Weibull
APW = alpha power Weibull
BBur = beta Burrxii
BFr = beta Frechet
BIC = Bayesian Information Criteria
CAIC = Consistent Akaike Information Criteria
EFr = exponentiated Frechet

EMA-G = Exponential Marshall-Olkin-G
EMA-GBr = Exponential Marshall-Olkin-G Burrxii
EMA-GF = Exponential Marshall-Olkin-G Frechet
EMA-GWb = Exponential Marshall-Olkin-G Weibull
ESE = Exponentiated shifted exponential
GaFr = gamma extended Frechet
GBur = Gompertz Burrxii
GIGE = Generalized inverted generalized exponential
GL = Generalized Lindley
GW = Gompertz Weibull
HQIC = Hannan and Quinn Information Criteria
KBur = Kumaraswamy Burrxii
KFr = Kumaraswamy Frechet
KWb = Kumaraswamy Weibull
LogBur = lognormal Burrxii
MFr = Marshall-Olkin Frechet
TBur = transmuted Burrxii
TMFr = Marshall-Olkin Frechet
TW = transmuted Weibull
W = Cramer-von Mises
WFr = Weibull Frechet
UK = United Kingdom

OPTIMIZATION OF A FEEDBACK WORKING VACATION QUEUE WITH REVERSE BALKING AND REVERSE RENEGING

K. JYOTHSNA^{1,*}, P. VIJAYA LAXMI², P. VIJAYA KUMAR³

^{1,*}Department of Basic Sciences and Humanities, Vignan's Institute of Engineering for Women,

Visakhapatnam, Andhra Pradesh, India.

mail2jyothsnak@yahoo.co.in, drjyothsnak1984@gmail.com

²Department of Applied Mathematics, Andhra University,

Visakhapatnam, Andhra Pradesh, India.

vijayalaxmiau@gmail.com

³Department of Mathematics, GITAM (Deemed to be University),

Visakhapatnam, Andhra Pradesh, India.

vprathi@gitam.edu

Abstract

This paper analyzes a steady-state finite buffer M/M/1 feedback queue with reverse balking, reverse reneging and multiple working vacations. The concept of reverse balking and reverse reneging evolves from investment businesses wherein more the number of customers associated with a firm less the probability of balking of a customer and similar is the case of reverse reneging. Furthermore, if a customer is dissatisfied with the service provided, he or she may chose to rejoin the queue as a feedback customer. The server exits for working vacations whenever the system becomes empty instead of staying idle in the system. Vacation times and service times during working vacations are all independent random variables following exponential distribution. The model's steady-state system length distributions are calculated using the matrix approach. Some performance characteristics and cost optimization using ant colony optimization (ACO) are presented. Sensitivity analysis is performed using numerical results which are shown in the form of tables and graphs.

Keywords: reverse balking, reverse reneging, feedback, multiple working vacations, ACO

1. INTRODUCTION

Queueing models with server vacations have been actively researched and successfully used in manufacturing and production systems, service systems, communication systems, and other fields over the last three decades. Working vacations (WV) are a form of vacation policy established by Servi and Finn [13] wherein the server can provide service at a reduced rate rather than shutting down altogether during the vacation period. Wu and Takagi [16] and Baba [2] extended the M/M/1/WV queue to M/G/1 and GI/M/1 queues with working vacations, respectively. Krishnamoorthy and Sreenivasan [8] analyzed an M/M/2 queue with one of the two servers in working vacations. A survey on WV queues has been presented by Chandrasekaran et al. [4].

There is a growing trend to examine queueing systems from an economic perspective in order to address customers' unhappiness with waiting and desire for service. Customer impatience has a damaging influence on businesses since it causes them to lose potential consumers, which has a negative impact on the entire company. Balking and reneging are two queueing concepts that are commonly used to depict customer impatience. In balking, if a customer sees a large

queue ahead of him, he may resist at joining the queueing system. In the case of renegeing, the customer joins the queue, waits for his service, and then departs the system without receiving service if the wait time exceeds his expectations. The situation of impatient customers in a server vacation period was investigated by Altman and Yechiali [1]. Yue, Yue and Xu [17] analyzed the single server queueing systems with customer impatience and WV. A Markovian queueing system with balking, renegeing and WV has been studied by Vijaya Laxmi et al. [15].

In the above mentioned queueing models, the size of the system or the length of the queue influences balking and renegeing. The larger the system, the more balking occurs, and the same is true with renegeing. However, in the case of investment enterprizes, the number of customers with a certain firm becomes an intriguing and appealing feature for potential investors. As a result, the likelihood of joining such a company is high. In this scenario, the larger the system size, the greater the number of consumers who join it. As a result, when the system size is high, the chance of balking is low which is referred to as "reverse balking". Furthermore, having a large number of investors with an investment firm instils trust in investors and helps them to complete the term of their policies/bonds. That instance, when a firm has a big number of investing consumers, waiting customers will have more patience. When seen as a queueing system, it is obvious that as the queue becomes longer, fewer consumers would renege, a phenomenon known as "reverse renegeing". Jain et al. [7] first incorporated the concept of reverse balking in queueing theory. Kumar and Som [10] developed the concept of reverse renegeing and incorporated into an M/M/1 queueing system with reverse balking. A heterogeneous two server queue with reverse balking and renegeing has been studied by Bouchentouf and Messabihi [3].

In queueing theory, feedback refers to a dissatisfied client rejoining the queue owing to poor service quality. Rework is another example of a queue with feedback in industrial processes. Tackacs [14] studied a single server queue with feedback to determine the stationary process for the queue size. Shanthakumaran and Thangaraj [12] considered a single server feedback queue with impatient customers. An M/M/1 feedback queueing model with retention of renegeed customers and balking has been studied by Kumar and Sharma [9]. Kumar et al. [11] developed an M/M/1/N feedback queueing system with reverse balking.

To the best of our knowledge, the impatient attitude of customers in the reverse view has not been explored in working vacations queues. Therefore, we intend to embed reverse balking and reverse renegeing in a feedback WV queue. In this article, we explore a finite buffer feedback WV queue in which customers may balk or renege owing to impatience in the reverse notion. The inter-arrival times, service times during regular service period, during WV period and vacation times are presumed to be exponentially distributed. The matrix form solution of the steady-state probabilities is found by putting the steady-state equations in block matrix form. The model's performance metrics, cost analysis using ACO are obtained. Tables and graphs have been used to demonstrate certain numerical findings.

The rest of the paper is laid out as follows. The queueing model is described in Section 2, followed by the steady-state equations and their solution in Section 3. In Section 4, we offer different model performance metrics as well as a cost model. Section 5 contains the sensitivity analysis followed by conclusions in Section 6.

2. MODEL DESCRIPTION

Consider an M/M/1/N feedback queueing system with reverse balking, reverse renegeing and WV. According to a Poisson process with an arrival rate λ , customers arrive one at a time. When the system is unoccupied, a new customer has a probability q of joining the system and a $p = (1 - q)$ probability of not joining. When there are i customers ahead of him in the system, let b_i indicate the probability that the customer will join the queue or balk with probability $1 - b_i$. Furthermore, we assume that $b_0 = q$ and $b_N = 0$. The assumption of reverse balking has been incorporated with $b_{i+1} > b_i$, $1 \leq i \leq N - 1$.

After joining the queue each customer will wait a certain length of time which is exponentially distributed with mean $1/\alpha$. When there are i customers in the system, the average rate of

reverse renegeing of a customer is given by $(N - (i - 1))\alpha, , 1 \leq i \leq N$.

If a customer receives service and finds it unsatisfactory, it can return to the system as a feedback customer with a probability q_1 or depart with a probability $p_1 = 1 - q_1$.

A single server serves the customers on a first-come first-served basis with a service rate that follows an exponential distribution with mean $1/\mu$. When the system gets empty, the server takes WV. If there are waiting customers in the line after a vacation expires, the server resumes regular service; otherwise, he departs for another WV. During the vacation time, the server stays active and provides service at a different service rate to the arriving customers. This type of working vacation is called multiple working vacations (MWV).

The vacation times and service times during WV are assumed to follow Poisson distribution with parameter ϕ and η , respectively. The inter-arrival times, vacation times, service times during regular service and during working vacation are mutually independent.

3. ANALYSIS OF THE MODEL

In this section, the Markov process is used to build the steady-state probability equations and the matrix technique is adopted to determine steady-state probabilities. Let $\pi_{0,i}, 0 \leq i \leq N$, be the probability that the server is on WV when there are i customers in the system, and $\pi_{1,i}, 1 \leq i \leq N$, be the probability that there are i customers in the system while the server is in regular service period. The steady-state equations are derived using the Markov process as:

$$\lambda b_0 \pi_{0,0} = u_1 \pi_{0,1} + v_1 \pi_{1,1}, \tag{1}$$

$$z_i \pi_{0,i} = \lambda b_{i-1} \pi_{0,i-1} + u_{i+1} \pi_{0,i+1}, 1 \leq i \leq N - 1, \tag{2}$$

$$z_N \pi_{0,N} = \lambda b_{N-1} \pi_{0,N-1}, \tag{3}$$

$$t_1 \pi_{1,1} = v_2 \pi_{1,2} + \phi \pi_{0,1}, \tag{4}$$

$$t_i \pi_{1,i} = \lambda b_{i-1} \pi_{1,i-1} + v_{i+1} \pi_{1,i+1} + \phi \pi_{0,i}, 2 \leq i \leq N - 1, \tag{5}$$

$$v_N \pi_{1,N} = \lambda b_{N-1} \pi_{1,N-1} + \phi \pi_{0,N}, \tag{6}$$

where for $1 \leq i \leq N, u_i = \eta p_1 + (N - i + 1)\alpha; v_i = \mu p_1 + (N - i + 1)\alpha; z_i = \lambda b_i + \phi + u_i; t_i = \lambda b_i + v_i$.

3.1. Matrix solution

In this subsection, the steady-state probabilities $\pi_{j,i}, j = 0, 1; j \leq i \leq N$, are obtained by solving the system of equations (1) to (6) using matrices.

Let $\Pi = (\Pi_0, \Pi_1)$ be the steady-state probability vector, where $\Pi_0 = (\pi_{0,0}, \pi_{0,1}, \pi_{0,2}, \dots, \pi_{0,N})$ and $\Pi_1 = (\pi_{1,1}, \pi_{1,2}, \dots, \pi_{1,N})$. The equations (1) to (6) can be written in matrix form as

$$\Pi Q = \mathbf{0}, \tag{7}$$

$$\Pi \mathbf{e} = 1, \tag{8}$$

where \mathbf{e} is a column vector with each component equal to unity and the Markov process's transition rate matrix \mathbf{Q} has the block form:

$$\mathbf{Q} = \begin{pmatrix} \mathbf{A}_{vv} & \mathbf{A}_{vb} \\ \mathbf{A}_{bv} & \mathbf{A}_{bb} \end{pmatrix}.$$

The elements of the matrices $\mathbf{A}_{vv}, \mathbf{A}_{vb}, \mathbf{A}_{bv}$ and \mathbf{A}_{bb} are given by

$$\mathbf{A}_{vv} = \begin{cases} -\lambda b_0 & , \text{ if } i = j = 1, \\ \lambda b_{i-1} & , \text{ if } i = j - 1, j \geq 2, \\ u_{i-1} & , \text{ if } i = j + 1, \\ -z_{i-1} & , \text{ if } i = j, j \geq 2, \\ 0 & , \text{ otherwise} \end{cases}$$

$$\mathbf{A}_{vb} = \begin{cases} \phi, & \text{if } i = j + 1, \\ 0, & \text{otherwise} \end{cases}$$

$$\mathbf{A}_{bv} = \begin{cases} v_1, & \text{if } i = j = 1, \\ 0, & \text{otherwise} \end{cases}$$

$$\mathbf{A}_{bb} = \begin{cases} -t_i, & \text{if } i = j, \\ \lambda b_i, & \text{if } i = j - 1, j \geq 2, \\ v_i, & \text{if } i = j + 1, \\ 0, & \text{otherwise.} \end{cases}$$

\mathbf{A}_{vb} is a $(N + 1) \times N$ matrix, \mathbf{A}_{bv} is a $N \times (N + 1)$ matrix, \mathbf{A}_{vv} and \mathbf{A}_{bb} are square matrices of orders $N + 1$ and N , respectively.

Based on the partition $\mathbf{\Pi} = (\mathbf{\Pi}_0, \mathbf{\Pi}_1)$, equations (7) and (8) can be written as:

$$\mathbf{\Pi}_0 \mathbf{A}_{vv} + \mathbf{\Pi}_1 \mathbf{A}_{bv} = \mathbf{0}, \quad (9)$$

$$\mathbf{\Pi}_0 \mathbf{A}_{vb} + \mathbf{\Pi}_1 \mathbf{A}_{bb} = \mathbf{0}, \quad (10)$$

$$\mathbf{\Pi}_0 \mathbf{e}_0 + \mathbf{\Pi}_1 \mathbf{e}_1 = \mathbf{1}, \quad (11)$$

where $\mathbf{e}_0, \mathbf{e}_1$ are column vectors of order $N + 1$ and N , respectively, with each component as 1. From (9), we have

$$\mathbf{\Pi}_0 = -\mathbf{\Pi}_1 \mathbf{A}_{bv} \mathbf{A}_{vv}^{-1}. \quad (12)$$

Using (12) in (10) and (11), we get

$$\mathbf{\Pi}_1 \left(\mathbf{I} - \mathbf{A}_{bv} \mathbf{A}_{vv}^{-1} \mathbf{A}_{vb} \mathbf{A}_{bb}^{-1} \right) = \mathbf{0}, \quad (13)$$

$$\mathbf{\Pi}_1 \left(\mathbf{e}_1 - \mathbf{A}_{bv} \mathbf{A}_{vv}^{-1} \mathbf{e}_0 \right) = \mathbf{1}. \quad (14)$$

The matrices \mathbf{A}_{bv} and \mathbf{A}_{vb} can be written as

$$\mathbf{A}_{bv} = \begin{pmatrix} v_1 & \mathbf{O}_1 \\ \mathbf{O}_2 & \mathbf{O}_3 \end{pmatrix}_{N \times (N+1)}, \quad \mathbf{A}_{vb} = \phi \begin{pmatrix} \mathbf{O}_1 \\ \mathbf{I}_{N \times N} \end{pmatrix}_{(N+1) \times N},$$

where $\mathbf{O}_1, \mathbf{O}_2$ and \mathbf{O}_3 are zero matrices of order $1 \times N, (N - 1) \times 1$ and $(N - 1) \times N$, respectively. Let $\mathbf{A}_{vv}^{-1} = [a_{i,j}]_{(N+1) \times (N+1)}$ and \mathbf{w} denote the first row of \mathbf{A}_{vv}^{-1} , i.e., $\mathbf{w} = (a_{11}, a_{12}, \dots, a_{1,N+1})$, then

$$\mathbf{A}_{bv} \mathbf{A}_{vv}^{-1} = \begin{pmatrix} v_1 \mathbf{w} \\ \mathbf{O}_4 \end{pmatrix}_{N \times (N+1)}, \quad (15)$$

where \mathbf{O}_4 is a zero matrix of order $(N - 1) \times (N + 1)$.

Now,

$$\mathbf{A}_{vb} \mathbf{A}_{bb}^{-1} = \phi \begin{pmatrix} \mathbf{O}_1 \\ \mathbf{A}_{bb}^{-1} \end{pmatrix}. \quad (16)$$

From (15) and (16), we have

$$\mathbf{A}_{bv} \mathbf{A}_{vv}^{-1} \mathbf{A}_{vb} \mathbf{A}_{bb}^{-1} = v_1 \phi \begin{pmatrix} \mathbf{w}_0 \mathbf{A}_{bb}^{-1} \\ \mathbf{O}_3 \end{pmatrix}, \quad (17)$$

where $\mathbf{w}_0 = (a_{12}, a_{13}, \dots, a_{1,N+1})$.

Let us partition $\mathbf{\Pi}_1$ as $[\pi_{1,1}, \widetilde{\mathbf{\Pi}}_1]$ where $\widetilde{\mathbf{\Pi}}_1 = [\pi_{1,i}, 2 \leq i \leq N]_{1 \times (N-1)}$. From (13) and (17), we have

$$[\pi_{1,1}, \widetilde{\mathbf{\Pi}}_1] = [\pi_{1,1}, \widetilde{\mathbf{\Pi}}_1] \begin{pmatrix} v_1 \phi \mathbf{w}_0 \mathbf{A}_{bb}^{-1} \\ \mathbf{O}_3 \end{pmatrix}.$$

Hence, the system length probabilities of regular service period are given by

$$\pi_{1,i} = \pi_{1,1} v_1 \phi \mathbf{w}_0 \mathbf{A}_{bb}^{-1} \epsilon_i, 1 \leq i \leq N,$$

where ϵ_i is a column vector whose i^{th} component is unity and the remaining components are zero. From (12) and (15), the system length probabilities of server being in WV are given by

$$[\pi_{0,0}, \pi_{0,1}, \dots, \pi_{0,N}] = -[\pi_{1,1}, \widetilde{\Pi}_1] \begin{pmatrix} v_1 \mathbf{w} \\ \mathbf{O}_4 \end{pmatrix}.$$

Hence,

$$\pi_{0,i} = -\pi_{1,1} v_1 \mathbf{w} \epsilon_{i+1}, 0 \leq i \leq N.$$

Using the normalization condition $\sum_{j=0}^1 \sum_{i=j}^N \pi_{j,i} = 1$, the only unknown $\pi_{1,1}$ is obtained as

$$\pi_{1,1} = \left(v_1 \phi \sum_{i=1}^N \mathbf{w}_0 \mathbf{A}_{bb}^{-1} \epsilon_i - v_1 \sum_{i=0}^N \mathbf{w} \epsilon_{i+1} \right)^{-1}.$$

This completes the evaluation of steady-state probabilities.

4. PERFORMANCE MEASURES

Once the steady-state probabilities are determined, several model performance measures may be calculated. The average number of customers in the system (l_s), the probability that the server is busy with regular service (p_b) and the probability that the server is in WV (p_{wv}) are given by

$$l_s = \sum_{i=1}^N i (\pi_{0,i} + \pi_{1,i}) ; p_b = \sum_{i=1}^N \pi_{1,i} ; p_{wv} = \sum_{i=0}^N \pi_{0,i}.$$

The average reverse balking rate (br), the average reverse reneging rate (rr) and the average rate of loosing a customer due to impatience (lr) are obtained as

$$br = \sum_{i=0}^N \lambda (1 - b_i) \pi_{0,i} + \sum_{i=1}^N \lambda (1 - b_i) \pi_{1,i} ; rr = \sum_{i=1}^N \alpha (N - i + 1) (\pi_{0,i} + \pi_{1,i}) ; lr = br + rr.$$

4.1. Cost model

The total expected cost function per unit time is formulated in this subsection with service rates as the decision variables. Our goal is to figure out the best service rates that minimize the total expected cost function. The cost parameters are assumed to be:

- C_{l_s} – holding cost per unit time,
- C_{l_r} – cost incurred when a customer is lost due to impatience,
- C_{μ} – cost per service during regular service period,
- C_{η} – cost per service during WV period,
- $C_{f\mu}$ – cost per service for a feedback customer during regular service period,
- $C_{f\eta}$ – cost per service for a feedback customer during WV period.

The total expected cost (tec) is defined as:

$$tec = C_{l_s} l_s + C_{l_r} lr + \mu (C_{\mu} + q_1 C_{f\mu}) + \eta (C_{\eta} + q_1 C_{f\eta}).$$

Analytical optimization of the aforementioned cost model is a tedious job due to the complexity of the cost function. As a result, we have used the ACO developed by Colorni et al. [5] and Dorigo et al. [6] to find the best values for μ and η . A brief algorithm of ACO is given below:

Algorithm for ACO

Step 1: Consider a suitable number of ants in the colony (B). Assume a set of permissible discrete values for each of the n design variables x_{ij} as $x_{i1}, x_{i2}, \dots, x_{ip}$ ($i = 1, 2, \dots, n$). Assume equal amounts of pheromone $\tau_{ij}^{(1)}$ initially along all the arcs. The superscript to τ_{ij} denotes the iteration number. For simplicity, $\tau_{ij}^{(1)}$ is assumed to be 1. Set the iteration number $l = 1$.

Step 2: (a) Compute the probabilities (p_{ij}) of selecting the arc x_{ij} as

$$p_{ij}^{(l)} = \frac{\tau_{ij}^{(l)} D_{ij}^{(\beta)}}{\sum_{m=1}^p [\tau_{im}^{(l)} D_{im}^{(\beta)}]}; \quad i = 1, 2, \dots, n; \quad j = 1, 2, \dots, p,$$

where τ_{ij} is a pheromone amount between arc i and arc j , D_{ij} is a reciprocal of the distance between arc i and arc j , β is the parameter that allow a user control on the relative importance of trail versus visibility.

(b) The specific path (or discrete values) chosen by the k^{th} ant can be determined using random numbers generated in the range (0, 1). For this, we find the cumulative probability ranges associated with different paths based on the probabilities given by above equation. The specific path chosen by ant k will be determined using the roulette-wheel selection process in step 3(a).

Step 3: (a) Generate B random numbers r_1, r_2, \dots, r_B in the range (0, 1), one for each ant. Determine the discrete value or path assumed by ant k for variable i as the one for which the cumulative probability range (found in step 2 (b)) includes the value r_i .

(b) Repeat step 3 (a) for all design variables $i = 1, 2, \dots, n$.

(c) Evaluate the objective function values corresponding to the complete paths (design vectors $X^{(k)}$ or values of x_{ij} chosen for all design variables $i = 1, 2, \dots, n$ by ant k , $k = 1, 2, \dots, B$):

$$f_k = f(X^{(k)}); \quad k = 1, 2, \dots, B.$$

Determine the best and worst paths among the B paths chosen by different ants as follows:

$$f_{best} = \min_{k=1,2,\dots,B} f_k, \quad f_{worst} = \max_{k=1,2,\dots,B} f_k.$$

Step 4: Test for the convergence of the process. The process is assumed to have converged if all the B ants take the same best path. If convergence is not achieved, assume that all the ants return home and start again in search of food. Set the new iteration number as $l = l + 1$, and update the pheromone on different arcs as

$$\tau_{ij} = \tau_{ij}^{(old)} + \sum_k \Delta\tau_{ij}^{(k)},$$

where $\tau_{ij}^{(old)}$ denotes the pheromone amount of the previous iteration left after evaporation, $\Delta\tau_{ij}^{(k)}$ is the amount of pheromone deposited on arc i and arc j by the best ant k and are taken as

$$\tau_{ij}^{(old)} = (1 - \rho)\tau_{ij},$$

$$\Delta\tau_{ij}^{(k)} = \begin{cases} \frac{\zeta f_{best}}{f_{worst}}; & \text{if } (i, j) \in \text{global best tour,} \\ 0; & \text{otherwise,} \end{cases}$$

where $\rho \in (0, 1]$ is the evaporation rate (also known as the pheromone decay factor) and ζ is the parameter used to control the scale of the global updating of the pheromone. With the new values of τ_{ij} , go to step 2. Steps 2, 3, and 4 are repeated until the process converges. In some cases, the iterative process may be stopped after completing a prespecified maximum number of iterations (l_{max}).

The complexity of the algorithm is $O(l\varrho^2B)$ where l is the number of iterations, ϱ is the number of nodes and B is the number of ants.

Table 1: Various performance measures of the model for different λ and q_1

	$\lambda=1.0$		$\lambda=1.7$		$\lambda=2.4$	
	$q_1 = 0.6$	$q_1 = 0.2$	$q_1 = 0.6$	$q_1 = 0.2$	$q_1 = 0.6$	$q_1 = 0.2$
l_s	0.038536	0.027681	0.092328	0.052341	0.407215	0.094482
p_b	0.002170	0.001060	0.006109	0.002123	0.036461	0.004367
p_{wv}	0.997830	0.998930	0.993891	0.997876	0.963538	0.995632
br	0.947901	0.948532	1.606110	1.610020	2.237570	2.266750
rr	0.034617	0.025827	0.061203	0.044884	0.092589	0.065255
lr	0.982518	0.974359	1.667310	1.654901	2.330160	2.332010

Table 2: Effect of α on the performance measures

	$\alpha = 0.5$	$\alpha = 1.0$	$\alpha = 1.5$
l_s	0.015341	0.008061	0.005467
p_b	0.000244	0.000071	0.000033
p_{wv}	0.999756	0.999929	0.999966
br	1.613650	1.614230	1.614530
rr	0.073773	0.079008	0.080914
lr	1.687420	1.693310	1.695440

5. SENSITIVITY ANALYSIS

In this section, tables and graphs have been used to display certain numerical results. We fix the capacity of the system as $N = 10$ and the balking function is taken as $b_i = i/N, 1 \leq i \leq N - 1, b_N = 0$. The various parameters of the model are chosen to be $\lambda = 1.7, \mu = 2.0, \eta = 1.2, \phi = 0.1, q = 0.05, \alpha = 0.1, q_1 = 0.3$, unless they are considered as variables or their values are mentioned in the respective tables and figures. For employing the ACO, we have arbitrarily chosen the following: $n = 2, B = 3, \rho = 40, l = 100, \beta = 0.5, \zeta = 2, \rho = 0.5$ and the distances between the arcs are obtained using the *RandomReal* function of *Mathematica* software.

Table 1 shows the model's performance metrics for various values of λ and q_1 . All the performance measures, with the exception of p_{wv} and br , drop as q_1 lowers, whereas p_{wv} and br rise as q_1 decreases for fixed λ . Further, increase in λ results in a drop in p_{wv} , whereas increase in λ results in the increase of the remaining performance metrics.

Table 2 shows the influence of α on the model's performance measures. With the rise of α , a rising trend can be noticed in p_{wv}, br, rr and lr while a declining trend can be found in l_s and p_b .

Figure 1 shows the influence of μ on the server's state probabilities for various values of the vacation parameter (ϕ). The picture illustrates that when μ grows, the probability of the server being busy with regular service (p_b) decreases while the probability of the server being on vacation (p_{wv}) increases. Furthermore, as the vacation parameter (ϕ) is increased, p_b grows while p_{wv} decreases for any μ .

The impact of λ on the average number of customers in the system (l_s) in models with and without reverse balking and reverse reneging is shown in Figure 2. From the graph, one may observe that in either of the models l_s increases with the increase of the arrival rate λ . Further, the queue lengths are lower in models with reverse balking and reverse reneging when compared to models without reverse balking and reverse reneging.

Figure 3 displays the effect of service rates μ and η on the average rate of losing a customer (lr). With the increase of both μ and η , the average rate of losing a customer decreases. We can carefully setup the service rates μ and η in the system in order to ensure the minimum average rate of losing a customer due to impatience.

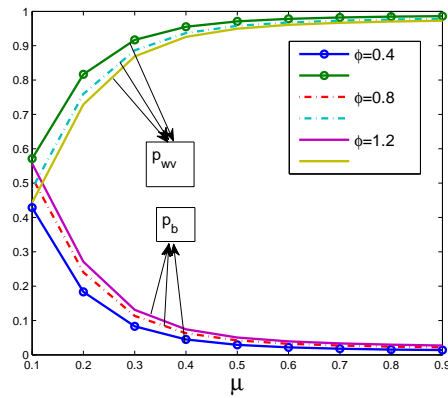


Figure 1: μ versus p_{wv} and p_b

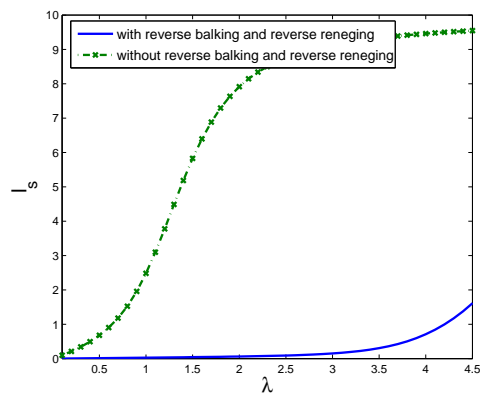


Figure 2: Impact of λ on l_s

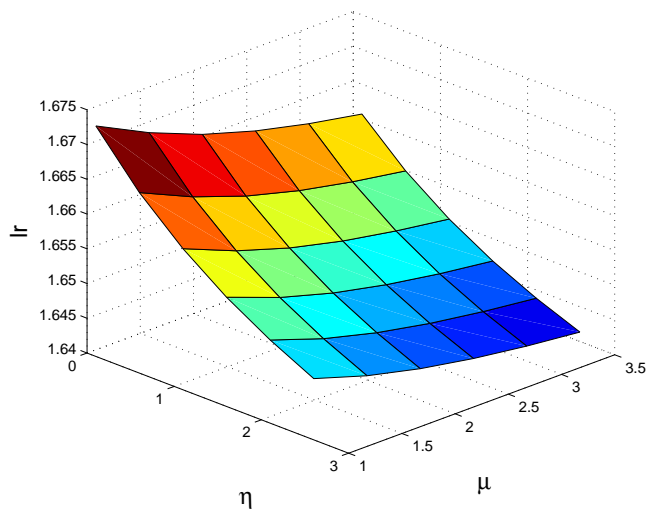


Figure 3: Effect of μ and η on l_r

Table 3: Optimum service rates and the corresponding minimum *tec*.

	ϕ	0.06	0.08	0.1
Case 1	(μ^*, η^*)	(0.606627, 0.393620)	(0.648424, 0.295251)	(0.679539, 0.213562)
	<i>tec</i> *	65.9207	65.3714	64.7454
Case 2	(μ^*, η^*)	(0.613050, 0.539007)	(0.656637, 0.446063)	(0.689743, 0.366756)
	<i>tec</i> *	70.8644	70.5699	70.1348
Case 3	(μ^*, η^*)	(0.608498, 0.390333)	(0.650509, 0.291586)	(0.681784, 0.209613)
	, <i>tec</i> *	57.5689	57.0077	56.3712
Case 4	(μ^*, η^*)	(0.557353, 0.457533)	(0.597739, 0.360028)	(0.628019, 0.278463)
	<i>tec</i> *	68.8265	68.4826	68.0101
Case 5	(μ^*, η^*)	(0.695438, 0.199822)	(0.737154, 0.101221)	(0.768531, 0.018769)
	<i>tec</i> *	67.9667	66.7260	65.5257
Case 6	(μ^*, η^*)	(0.590782, 0.413392)	(0.632152, 0.315211)	(0.662999, 0.233546)
	<i>tec</i> *	66.8187	66.3317	65.7522
Case 7	(μ^*, η^*)	(0.622554, 0.356552)	(0.664430, 0.257807)	(0.695557, 0.175969)
	<i>tec</i> *	66.3707	65.703	64.9789

Table 4: Optimum service rates and the corresponding model characteristics for various model parameters

		(μ^*, η^*)	<i>tec</i> *	l_s	p_b	p_{wv}	lr
$\lambda =$	1.5	(0.560865, 0.053717)	53.0653	0.291992	0.027470	0.972530	1.486520
	2.0	(0.856029, 0.449138)	82.0273	0.355744	0.032820	0.967180	1.955930
	2.5	(1.145080, 0.832582)	110.272	0.415343	0.037775	0.962225	2.421721
$q_1 =$	0.1	(0.533546, 0.289963)	55.1871	0.231776	0.021178	0.978822	1.672162
	0.2	(0.597385, 0.258192)	59.5429	0.269601	0.024895	0.975105	1.673490
	0.3	(0.679539, 0.213562)	64.7454	0.318140	0.029674	0.970325	1.674791
$\alpha =$	0.04	(1.021179, 0.862099)	91.8238	0.332031	0.034453	0.965547	1.625062
	0.08	(0.782366, 0.436608)	73.5377	0.320756	0.030862	0.969137	1.659655
	0.12	(0.572881, 0.022225)	81.3452	0.304472	0.027703	0.972297	1.687794

Table 3 presents the optimum values of the service rates (μ^*, η^*) that minimize the total expected cost (*tec*) for different values of ϕ and for the following cost values:

Case 1: $C_{ls} = 40, C_{lr} = 15, C_{\mu} = 25, C_{\eta} = 20, C_{f\mu} = 22, C_{f\eta} = 18,$

Case 2: $C_{ls} = 60, C_{lr} = 15, C_{\mu} = 25, C_{\eta} = 20, C_{f\mu} = 22, C_{f\eta} = 18,$

Case 3: $C_{ls} = 40, C_{lr} = 10, C_{\mu} = 25, C_{\eta} = 20, C_{f\mu} = 22, C_{f\eta} = 18,$

Case 4: $C_{ls} = 40, C_{lr} = 15, C_{\mu} = 30, C_{\eta} = 20, C_{f\mu} = 22, C_{f\eta} = 18,$

Case 5: $C_{ls} = 40, C_{lr} = 15, C_{\mu} = 25, C_{\eta} = 27, C_{f\mu} = 22, C_{f\eta} = 18,$

Case 6: $C_{ls} = 40, C_{lr} = 15, C_{\mu} = 25, C_{\eta} = 20, C_{f\mu} = 27, C_{f\eta} = 18,$

Case 7: $C_{ls} = 40, C_{lr} = 15, C_{\mu} = 25, C_{\eta} = 20, C_{f\mu} = 22, C_{f\eta} = 22.$

One may observe from the table that for any set of cost values with the increase of ϕ, μ^* increases while *tec** and η^* decrease.

The values of the service rates that minimize the total expected cost are presented in Table 4 along with the corresponding performance metrics for λ, q_1, α and the cost values in Case 1. It is clear from the table that an increase in λ or q_1 results in the increase of μ^*, tec^*, l_s, p_b and lr while p_{wv} decreases with λ or q_1 . One may note that η^* increases with λ and decreases with q_1 . On the otherhand increase in α leads to the decrease of all the values except p_{wv} and lr .

6. CONCLUSIONS

We investigated a Markovian feedback queue with reverse balking, reverse reneging, and working vacations in this study. Using the matrix technique, we have obtained the steady-state probabilities. Different performance measures, cost analysis using ACO and numerical findings in the form of tables and graphs are sketched out to show the influence of the system parameters. The provided approach has the potential to be utilized in a variety of investment business areas, including insurance, mutual funds, banking and so on. The current model may be expanded to a renewal input feedback queue with working vacations under reverse balking and reverse reneging in future.

REFERENCES

- [1] Altman, E. and Yechiali, U. (2006). Analysis of customers' impatience in queues with server vacation. *Queueing Systems*, 52(4):261–279.
- [2] Baba, Y. (2005). Analysis of a GI/M/1 queue with multiple working vacations. *Operations Research Letters*, 33(2):201-209.
- [3] Bouchentouf, A. A. and Messabihi, A. (2017) . Heterogeneous two-server queueing system with reverse balking and reneging. *Opsearch*, 55(2):251-267.
- [4] Chandrasekaran, V. M., Indhira, K., Saravananarajan, M. C. and Rajadurai, P. (2016). A survey on working vacation queueing models. *International Journal of Pure and Applied Mathematics*, 106(6):33-41.
- [5] Colorni, A., Dorigo, M. and Maniezzo, V. (1991). Distributed optimization by ant colonies. Proceedings of ECAL'91 European Conference on Artificial Life, Elsevier Publishing, 134–142.
- [6] Dorigo, M., Maniezzo, V. and Colorni, A. (1996). The ant system: Optimization by a colony of cooperating agents, *IEEE Transactions on Systems, Man, and Cybernetics–Part B*, 26:29–41.
- [7] Jain, N. K., Kumar, R. and Som, B. K. (2014). An M/M/1/N queueing system with reverse balking. *American Journal of Operational Research*, 4(2):17-20.
- [8] Krishnamoorthy, A. and Sreenivasan, C. (2012). An M/M/2 queueing system with heterogeneous servers including one with working vacation. *International Journal of Stochastic Analysis*, Article ID 145867, 16 pages.
- [9] Kumar, R. and Sharma, S. K. (2013). M/M/1 feedback queueing models with retention of reneged customers and balking, *American Journal of Operational Research*, 3(A):1-6.
- [10] Kumar, R. and Som, B. K. (2014). An M/M/1/N queueing system with reverse balking and reverse reneging. *Advanced Modeling and Optimization*, 16(2):339-353.
- [11] Kumar, R., Som, B. K. and Jain, S. (2015). An M/M/1/N feedback queueing system with reverse balking. *Journal of Reliability and Statistical Studies*, 8(1):31-38.
- [12] Santhakumaran, A. and Thangaraj, V. (2000). A single server queue with impatient and feedback customers. *International Journal of Information and Management Sciences*, 11(3):57-70.
- [13] Servi, L. D. and Finn, S. G. (2002). M/M/1 queue with working vacations (M/M/1/WV). *Performance Evaluation*, 50:41-52.
- [14] Takacs, L. (1963). A single server queue with feedback, *The Bell System Technical Journal*, 42(2):134-149.
- [15] Vijaya Laxmi, P., Goswami, V. and Jyothisna, K. (2013). Analysis of finite buffer Markovian queue with balking, reneging and working vacations. *International Journal of Strategic Decision Sciences*, 4(1):1-24.
- [16] Wu, D. and Takagi, H. (2006). M/G/1 queue with multiple working vacations, *Performance Evaluation*, 63(7):654-681.
- [17] Yue, D., Yue, W. and Xu, G. (2012). Analysis of customer's impatience in an M/M/1 queue with working vacations, *Journal of Industrial and Management Optimization*, 8(4):895-908.

ANALYSIS OF THE PRIMARY FACTORS AFFECTING THE MOST FATAL AVIATION ACCIDENTS: A MACHINE LEARNING APPROACH

Tüzün Tolga İnan - Neslihan Gökmen İnan

•
Bahcesehir University
tuzuntolga.inan@sad.bau.edu.tr

•
Istanbul Technical University
ngokmen@itu.edu.tr

Abstract

The safety concept is primarily examined in this study considering the most fatal accidents in aviation history with human, technical, and sabotage/terrorism factors. Although the aviation industry was started with the first engine flight in 1903, the safety concept has been examined since the beginning of the 1950s. However, the safety concept was firstly examined with technical factors, in the late 1970s, human factors have started to analyze. Despite these primary causes, there have other factors which could have an impact on accidents. So, the purpose of the study is to determine the affecting factors of the most fatal 100 accidents including aircraft type, distance, flight phase, primary cause, number of total passengers, and time period by classifying survivor/non-survivor passengers. Logistic regression and discriminant analysis are used as multivariate statistical analyses to compare with the machine learning approaches in terms of showing the algorithms' robustness. Machine learning techniques have better performance than multivariate statistical methods in terms of accuracy (0.910), false-positive rate (0.084), and false-negative rate (0.118). In conclusion, flight phase, primary cause, and total passenger numbers are found as the most important factors according to machine learning and multivariate statistical models for classifying the accidents' survivor/non-survivor passengers.

Keywords: machine learning; primary causes; fatal aviation accidents; classification of survivor/non-survivor passengers; multivariate statistical analysis.

I. Introduction

Aviation safety specialists and researchers have determined that aircraft accidents (fatal) and incidents (non-fatal) are almost caused by a sequence of events, each one which is consolidated with several cause factors. Hence, the cause of accidents and incidents has lots of perspectives. The international admitted descriptions in the status of the aircraft accident and/or incident investigations are classified below [1]:

- Causes are activities, failures, cases, situations, or combinations therefrom which lead to an accident and/or incident.

- Accidents are cases related to the aircraft operation that people board an aircraft about the purpose of flight till the time all people have disembarked, which ends in one or more cases below:

- Fatally or seriously injured of a person.
- Continuing damage or structural failure of the aircraft that negatively influences the mechanical structure, performance, and flight characteristics of the aircraft. These issues would generally need grand maintenance and overhaul of the influenced component.
- If the aircraft is missed or entirely unattainable.

- Furthermore, incidents are defined as cases, and they differ from accidents related to the aircraft operation which influence or could affect operational safety [1].

The safety of aviation is constructed on reactive examinations of previous accidents and the introduction of reformative strategies to prevent the repetition related to this kind of incident. For this reason, according to the development in worldwide air traffic, civil aviation research has operated by the requirement to guarantee safety [2]. Although the safety of aviation was presented by the Civil Aeronautics Authority in 1938, it developed with a substantial trend later in the 1990s [3]. Oster, et al. [4] emphasized that the worldwide air transportation accident and/or incident ratio was one accident and/or incident in each 1.6 million flights with a development trend of 42% since 2000. This ratio shows that the positive evaluation of safety is related to the consequence of the ultra-safe civil aviation industry. This situation is specifically appropriate for leaders and managers in a civil aviation industry liable for providing and enhancing ultra-safe performance, however, meanwhile directing the demand for strategic business purposes [5]. The safety of civil aviation relies on the operation process of all elements in the system that unluckily can not be performed risk-free. It is mostly known that human factors can be the causes. These factors are included in aviation accidents. The researches have conventionally intensified related to the errors of flight crew personnel and air traffic controllers. A growing number of maintenance and examination errors have increased the requirement of research and studies related to human factors [6].

Besides safety, the primary problem behind the application of aviation security is related to the ideal distribution of limited resources for the purpose of decreasing the possibility of a judgment. This judgment has two significant purposes. The first purpose is related to resources dedicated to defense operations of any kind (including aviation security) that do not straight improve economic prosperity (rather such operations serving to prohibit possible declines in prosperity). When it is needed to compel consume sources, it is significant to preserve the decline of existing investment in capital funds. These sources are related to technology, production, and expenditure of commodities and services. Secondly, given a finalized income distributed to the common service of domestic protection, the sources used for aviation security demonstrating a decrease in resources available to preserve non-aviation purposes. Furthermore, the source distribution problem is complicated for strategic decisions such as; security risks, and native disastrous risks in aviation. For instance, if it is decided to distribute more sources to guarantee buildings are earthquake-proof, this does not alter the possibility of an earthquake happening. Although, if it is allocated comparatively more sources to one aviation security measure, it is being anticipated to implement the reaction of terrorists and potential preventions about the possibilities of attack modes [7].

Besides security, aviation safety is a crucial term and the investigation of accidents plays a

significant role in the risk management concept. This concept is very important to prohibit aviation accidents. The safety of aviation is a key issue for survival, prestige, an international reputation, and passenger trustworthiness in airlines. In the previous years, air transportation in the aviation industry has developed immensely, and the safety condition has also evolved importantly [8]. Furthermore, the investigation process of safety in risk management is harder to analyze human error than to detect the effects of the failures in mechanical structure in aircraft accidents. In civil aviation, specialists of the human factors have primarily given attention to bio-psychological perspectives like physical characteristics, cognitive operations, visual abilities, and decision-making [9].

In addition to the safety of aviation, the development in the safety of flight has a fundamental objective in all phases of the aviation industry. To prevent and decrease risks in aviation, the rules of flight safety are significant to evaluate measures that are accepted globally. The sustainability of the effort with cooperation between stakeholders of the aviation industry is related to the decreasing trend in aviation fatalities (the accidents which ended with death) which have decreased since the publication of the ICAO Safety Management System (SMS) Document 9859. In addition to the fatalities, the accident rates have also shown a decreasing trend [10]. For instance, in Japan between the years of 1974 and 2010, the crashes of aircraft excluding Self-Defence Forces have happened an average of more than 10 times a year. This accident rate has been quite high although Japan's economy has been at a good level as a member of G8 countries. Besides Japan, after 2010 with the usage of the Safety Management System (SMS), the accident rates have entered a downward trend. The level of gross domestic product (GDP) has importance in the aviation industry covers the aircraft usage that became widespread and popular module of transportation for all citizens regardless of whether poor or rich. Presently, billions of citizen's national and international travel are actualized by aircraft. Though the increasing demand for air transportation, the number of accidents has a decreasing trend for the last 40 years. This is because aircraft accidents have been prevented efficiently with the aid of advanced technological innovations in the aviation industry [11].

To analyze the issue of human factors, the safety of aviation has altered from being reactive to being proactive applying safety management systems (SMS). Therefore, Brown, et al. [12] specified that every accident is stemmed from an unsuccessful organization. Because of this situation, airlines should comprise the issues which cover the organization and management issues in their SMS to direct air safety in a universal aspect [13]. Although, the base reasons for accidents are generally constituted of many complicated, and connected concepts inside the organizational level. These connected concepts include organizational management structure and management issues are explained with the description of latent factors. These factors have become progressively significant, however, little significance has been given to describing what composes a powerful SMS and the connections between the issues in an SMS [14].

Furthermore, the safety of aviation is an important term related to providing the protection of airlines' and air companies' reputation, passenger reliance, and brand image at the international level. In the last years, air transportation in the civil aviation industry has expanded dramatically, and the safety concept has also expanded immensely too. Despite this increased level, the accident rate of air transportation has decreased day by day at the global level. It can be understood that civil aviation safety has increased the attention of the public on the global level like the accidents rate of air Transportation with the amendments in safety regulations. So, it can be understood from this definition that the accident rates in general aviation have not decreased, so the new safety regulations have not been effective. Except for general aviation, civil aviation accident rates tend to decline significantly despite the increasing number of flights [8].

In light of these explanations, the most fatal 100 aviation accidents are analyzed with different variables to provide a detailed justification for all-time aviation accidents. The purpose of the study is to determine the affecting factors including aircraft type, distance, flight phase, primary cause, the number of total passengers, and time period of the most 100 fatal accidents by classifying survivor/non-survivor with the machine learning approach. In the machine learning approach, the aircraft type is examined in three classifications named Boeing, Airbus, and other brands. Distance is examined in three classifications named short-haul (0-3 hour flights), medium-haul (3-6 hour flights), and long-haul (6 and/or more hour flights). The flight phase is examined in three classifications named flight, landing, and take-off. The primary cause of the accident is examined in three classifications named human factor, technical, and terrorism/sabotage. The number of total passengers is examined in two classifications named affected, non-affected passengers from the fatal accident. The time period is examined in four classifications named between 06-12, 12-18, 18-24, and 24-06. In section 2, the prior studies that cover machine learning is explained, and also defined the history of safety concept in aviation accidents. Afterward, in section 3, it is defined the significant terms used in aviation accidents. Finally, in section 4, the methodology of the study is completed with the usage of machine learning and multivariate statistical modeling. The study is ended with a general evaluation by adding a recommendation to future studies in the conclusion part.

II. Literature Review

In the aviation concept, the volume of air transportation traffic grows rapidly worldwide, and civil aviation safety becomes a stunning problem in many countries. The accidents in civil aviation may conclude in human injury or even death. Human injury or even death affects the prestige and the economic status of the air transportation industry in a country [15]. Especially in the last 10 years that started from the year 2010 (with the publishment of ICAO Document 9859), aviation safety was placed in a widespread concept. So, this widespread concept has preliminarily estimated the accidents rates in aviation safety with influencing factors such as:

a. The assessment of safety concept in aviation: This concept has focused on the assessment process of safety concept from lots of perspectives such as; safety target level [16], identification system needs [17], safety supervisor performance in aviation [18], evaluating the safety concept in a changing industry in aviation [5], the evaluation of risk in aviation [19], and the climate of safety culture [20].

b. The factors that affected the safety of aviation: These factors have focused on impressive factors such as; the passengers' perception about to seat exit door [21], training of passengers in aviation safety [22], threats, human factors with errors related to the flight phases [23], the grand amendments in organizational structure related to the human factor [24], the behaviors of personnel with the relationship between safety management system (SMS) [25], the severe weather conditions especially in the winter season related to the time period and the flight distances [26], and the personal usage of electronic devices [27].

The present literature principally analyzes static assessment of safety in aviation, and determination of the affected elements, however, the efficiency of aviation safety, and the airline's performance have not been measured. The efficiency of safety in aviation is described to assess the causes of the safety inputs rely on the vital safety performance of airlines [8]. Safety is the most important concept related to the operation process of all activities in aviation. In the last years, the

widespread development of SMS has affected the operation of safety performance including new missions and defiances for protecting potential accidents. SMS describes the measurable performance of the consequences. The development of the SMS system has also related to the expectancies in design that meet the recent regulator necessities [28]. The safety performance indicators (SPIs) are applied to examine the safety risks which are known. These indicators determine the safety risks which are emerged to specify all required corrective actions. The Federal Aviation Administration (FAA) that is operated the regulations in the United States publishes reports about the performance indicators and responsibilities every year [29]. Moreover, the safety air navigation of the European Organisation (Eurocontrol) has published yearly performance reports related to the evaluation of air traffic management (ATM) in Europe [30].

In addition to these reports, there have three basic concepts related to safety thinking in aviation as described by ICAO and added to the post-SMS era. After the year 2010 with the Safety Management System (SMS) Document 9859, the post-SMS era was put into practice. There has a need for extra motivation to determine the changes in accident rates clearly to link with those concepts. Defining these concepts could provide to list and distinguish complex efforts to manage safety. These are classified as human factors, organizational factors, and technical factors. Matching the efforts with the results of the analysis about accident rates undoubtedly is expected to reveal the rights and the wrongs in the efforts to answer real-world safety management requirements. Nonetheless, the information set may not explain the efficiency of each implementation since each organization could have different safety management considerations or focuses. Another significant deficiency in matching has new developments in Safety-II that are related to the post-SMS era since no substantial practice could have been observed yet [31].

In addition to the Safety-II concept, the primarily related machine learning studies that can be covered under the aviation concept are examined. Firstly, Burnett and Si [32] were concerned about the application process connected the number of machine learning techniques to provide classification models. These models are aimed to estimate situations about the probable increment of aviation accidents including accidents, and incidents. One of the purposes of this study is to take into account the factors which cover type ratings related to profession, last experiences about flights, and particular weather conditions which act in the severity of the injuries in aviation accidents.

Secondly, Ayres, et al. [33] examined five sets of models. The first three are classified in landing overruns, veer-offs, and undershoots; the other two one classify in takeoff veer-offs, and overruns. Each set comprised the frequency models of accident and incident by adding location and consequence models. Thirdly, Goode [34] examined the anxiety about the aviation community that schedules of the pilots can lead to fatigue by increasing the chance of an aviation accident. This study tried out to show the empirical connection between schedules of the pilots and accidents in aviation.

Fourthly, Lee, et al. [35] examined the machine learning application to develop the reveal risk factors during the flight phase with the causal chains. This study's purpose aims to predict the application of machine learning capability against the isolation of crucial parameters (and potency causal factors) leading to safety-related causes from the inside stages classified as unimportant, unconnected, or tangentially unified ones. The fifth and the last study that was prepared by Dangut, et al. [36] examined an approach to hybrid machine learning which mix native language working techniques and group learning for estimating unusual failure of an aircraft component.

In this study, the primary causes of the accidents are classified into three factors. These are; human, technical, and terrorism/sabotage. The organizational factors are added to the term of the

human factor due to its connection. Technical factors are related to maintenance failures in the operation process of aircraft, and terrorism/sabotage is related to unlawful control of the aircraft. The primary definitions of the accidents are interpreted from the knowledge taken from the Bureau of Aircraft Accident Archives [37]. Because of the potential severities about the primary consequences of accidents, the concept of safety has generally been taken into account as a term that has the greatest significance in the air transport industry [38]. The application of machine learning is used to classify most fatal accidents' survivor/non-survivor. The classification is included the factors such as; aircraft (A/C) type, the time period of the accident, total passenger and/or affected people, flight phase, the duration of the flight, probable cause, and primary definitions.

III. Methodology

In this study, to figure out potential factors in aircraft type, distance, flight phase, primary cause, the number of total passenger and time period play an important role in evaluating survivor and non-survivor of the most 100 fatal accidents, various statistical and machine learning (ML) algorithms are used. In multivariate statistical analysis, the most 100 fatal accident datasets are examined by means of discriminant analysis and logistic regression models with the variable selection method with the cross-validation. Unlike the classical statistical techniques, to estimate the non-linear models that is able to provide more accurate classification performance in terms of evaluating survivor and non-survivor, machine learning (ML) methods are utilized. ML can be defined as an algorithm that can learn from its experience. Three types of learning procedures in ML are supervised, unsupervised, reinforcement learning. Supervised learning algorithms are handled in this study. In this learning methods, there is prior information on the output which is categorized. Artificial Neural Networks (ANNs) and Decision Trees (DTs) are utilized in this study.

Dimension reduction of feature vector have importance to tune the model complexity according to the statistical learning theory [39; 40]. There are many approaches for dimension reduction of feature matrix. For instance, forward selection, backward elimination, stepwise selections or some transformation techniques as Principal Component Analysis (PCA) are the feature selection methods in literature. In this study, ML algorithms are utilized with k-fold and leave-one-out cross validation and PCA based variable selection. Principal component analysis provides the weights needed to obtain the new feature that explains the variation best in the dataset. This new variable having weights, is called the 1st principal component. Moreover, to tune the complexity of model automatically, the cross-validation methods such as k-fold and leave-one-out are used.

In analysis, to determine the best independent variables and their importance on the most 100 fatal accidents' survivor, firstly ANN and DT models were trained with PCA. Before starting the analysis, firstly the dataset is normalized, and then the cross-validation type is chosen as k-fold or leave-one-out. Min-max normalization procedure is utilized to train the models with PCA's components as inputs. Min-max normalization formula is given as follows [41]:

$$x_i^* = \frac{x_i - \min(x_i)}{\max(x_i) - \min(x_i)}, \quad i = 1, 2, \dots, 100$$

DT Classifiers use the Classification and Regression Tree (CART) model, which comprises a univariate binary decision hierarchy. The 'Tree' begins with the "root," and consists of nodes, branches, and leaf nodes. Internal node expresses as a binary test on a unique variable, with branches demonstrating the consequence of the test, however, each leaf node shows class labels. CART starts

by choosing the best variable for dividing the data into two groups at the root such that each branch is as homogeneous as probable, and this dividing process is repeated in a recursive manner for each branch. Ongoing ‘purity’ calculations are implemented to specify which of the (remaining) properties are best to divide. The Gini index is used at CART. The nodes are divided according to the smallest Gini index. CART recursively enlarges the tree from the root node and then prunes back the large tree [42].

In training of DTs, to obtain the robust models using the variable selection procedure, various kernels in them such as complex, medium and simple are used. The other ML technique is used in this study is ANN are created by inspiration of human brain. The brain is formed by a very huge number of neurons. The interconnection between the neurons is provided by synapses. Perceptrons are used to model ANNs’ neurons, that consists of inputs or outputs. Inputs are related with a synaptic weight, and in the simplest form output a value equal to the sum of the weighted inputs. In other words, activation or transfer function can be applied by a perceptron, like a linear, sigmoid and, hyperbolic tangent function. ANNs include hidden layers which have conduct a connection between an input layer and an output layer. The basic approach used to train networks is backpropagation [43; 32; 44]. To train ANNs with the stopping criteria of MSE or cross-entropy, there are different gradient-based algorithms: Scaled Conjugant Gradient (SCG), Gradient Descent with Momentum (GDwM) and Levenberg Marquardt (LM) [45]. The framework for accidents’ survivor/non-survivor classification can be seen in Figure 1.

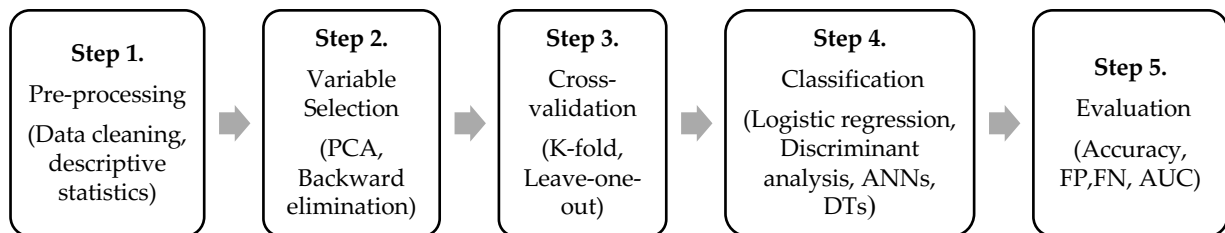


Figure 1: Flowchart of the methodology

I. Sample of Data

Determined as one of the three types of safety concept with its cultural structure, the human factor approach (including organizational factor) includes the identification of the conditions which assist safe behaviors at whole phases of the organization. Consolidating this approach inside the organization level of the companies as a robust factor has been already developed severely in the technical and management concepts [46]. The second type of safety culture includes the technical factors which provide continuous and sustainable qualities of an experience that covers the current time period which includes their physical condition. They usually include the parameters that direct the experiences which belong to the specific degrees of sensorial details such as navigation and the related systems [14]. The third and the last type of safety culture includes the factor of terrorism/sabotage which covers the intentional intervention of aircraft during the flight phase. The meaning of sabotage is diversified from abduction because, in aviation, terrorism is accepted as hijacking which is generally defined as aircraft hijacking and/or unlawful control (intervention) of the aircraft [47]. In the classification of most fatal accidents, only the cause of one accident is diversified from terrorism and/or sabotage because the cause of this accident covers the intentional and/or deliberate action of the pilot which defines as only sabotage. The distribution of these features is given in Table 1. 44% of the accidents were caused by Boeing type aircraft. 28% of the accidents

are caused by long haul flights and the 36% of the accidents are occurred in landing phase. 32% of the accidents are occurred at 6-12 time period. 65% of the accidents are caused by human factor and the percentage of survivor is 22%. The average number of total passengers is 200.6+65.1.

Table 1: *The distribution of the features*

		N	%
Type of aircraft	Airbus	15	15.0
	Boeing	44	44.0
	Other	41	41.0
Distance	Short Haul	50	50.0
	Medium Haul	22	22.0
	Long Haul	28	28.0
Phase of flight	Flight	33	33.0
	Landing	36	36.0
	Take-Off	31	31.0
Time Period	6-12	32	32.0
	12-18	27	27.0
	18-24	24	24.0
	24-06	17	17.0
Primary cause	Human factor	65	65.0
	Technical	25	25.0
	Terror/Sabotage	10	10.0
Survivor	Non-survivor	78	78.0
	Survivor	22	22.0
		Mean±SD	Med (Min-Max)
The number of total passengers		200.6±65.1	173 (133-524)

SD= Standard Deviation, Med= Median, Min= Minimum, Max= Maximum

Dataset that is used in learning phase includes totally the most fatal 100 accidents. As seen from Table 2, this dataset includes 6 variables, that are thought to affect being a survivor. Within the scope of supervised learning, the model training procedure comprise of two types variables: dependent and independent or output and input. The output variable is taken as survivor and non-survivor. The inputs are type of aircraft, distance, phase of flight, primary cause, the number of total passengers, time period.

Table 2. *Dependent and independent variables*

Independent Variables	
Type of aircraft (1:airbus, 2:boeing, 3:other)	Primary cause (1:Human factor, 2:Technical, 3:Terror/Sabotage)
Distance (1:short haul, 2:medium haul, 3:long haul)	The number of total passengers
Phase of flight (1:flight, 2:landing, 3:take-off)	Time period (1: 6-12, 2:12-18, 3:18-24, 4:24-06)
Dependent Variable	
Survivor (0/1)	

IV. Findings

I. Model Estimation

The analysis considers various multivariate statistical and machine learning methods to predict robust models that provide high classification accuracy and low false positive/negative rates for determining survivor and non-survivor on the most 100 fatal accidents. During the model estimation, all the methods are trained by k-fold, leave-one-out cross validation and PCA feature

selection procedures. The learning algorithms are written in MATLAB 2020a. The model outcomes of all the multivariate statistical and machine learning methods are given as follows.

I.I. Logistic regression and discriminant analysis

This part of the study includes the results of logistic regression and discriminant analysis to show the contribution of independent variables on the survivor/non-survivor classification of the most 100 accidents. The backward Wald variable selection with k-fold and leave-one-out procedures are used to estimate logistic regression models. Particularly, AUC, accuracy ratio, false positive and false positive rates are used to assess the performances of estimated models. The results of the logistic regression and discriminant analysis are given in Table 3.

Table 3. *The performances of Logistic Regression and Discriminant models*

Method	Models	#Input	NSV	AUC	Acc.	FP	FN	Selected Variables
Logistic Regression	Model 1 Backward No cross-val.	6	3	0.580	0.780	0.064	0.773	The number of total passengers, Phase of flight, Primary cause
	Model 2 Backward with 10-fold	6	3	0.560	0.770	0.064	0.818	The number of total passengers, Phase of flight, Primary cause
	Model 3 Backward with Leave-one-out	6	3	0.560	0.770	0.064	0.818	The number of total passengers, Phase of flight, Primary cause
Discriminant	Model 4 (K-fold)	6	3	0.690	0.720	0.054	0.568	The number of total passengers, Phase of flight, Primary cause
	Model 5 (Leave-one-out)	6	3	0.670	0.710	0.070	0.581	The number of total passengers, Phase of flight, Primary cause

NSV = Number of selected features; Acc=Accuracy Ratio, FP=False Positive; FN=False Negative

The selected variables in all 5 models are found statistically significant ($p < 0.05$), and the first 3 logistic regression models are also suitable interpretations according to Hosmer-Lemeshow test statistics ($p > 0.05$). As can be seen from results, the assumption of equality of variance-covariance matrices is provided (Box-M, $p < 0.001$) and the selected variables are found significant (Wilks' Lambda $p < 0.001$) in discriminant analysis. Table 4 shows that all the 5 models consist of the number of total passengers, Phase of flight, Primary cause. All the 5 models' accuracies are found above $>70\%$. The first logistic regression model (M1) has the highest accuracy (0.780) in addition to the low FP (0.064) and FN (0.773).

Table 4. *Odds ratios of independent variables*

	The number of total passengers	Phase of flight (landing)	Phase of flight (take-off)	Primary cause (technical)	Primary cause (terror/sabotage)
OR	1.014	6.479	9.674	0.103	0.000
(p)	(0.003)	(0.049)	(0.022)	(0.016)	(0.998)

The odds ratios and p values of the logistic regression model with selected variables are given in Table 5. The number of total passengers is increasing the survivors 1.014 times more than non-survivor. The accidents that have landing phase is increased survivors 6.479 times more than flight phase. The accidents that have take-off is increased survivors 9.674 times more than flight. The accidents which are occurred from technical primary cause is decreased survivors 9.709 (1/0.103) times more than human factor.

I.II. ANNs and DTs' estimation results with PCA dimension reduction

In machine learning approach, the variable selection procedure runs automatically during training ANNs and DTs. Before the training part, initial tunings are set. Classification accuracies, false positive and false negative ratios over training, test and overall datasets are used to choose the models having best performance at the end of the training and variable selection phase.

During the variable selection, the PCA is used to reduce dimensions and PCA results shows that 6 parameters are adjusted 3 dimensions having 69.5% variance explanation rate. The first dimension is included the number of total passengers and primary cause which is called capability component (C1), the second dimension is included distance and time period which is called geographical component (C2) and the third dimension is included type of aircraft which is called qualification component (C3). The normalized component scores obtained from PCA are taken as input variables in ANNs and DTs. According to ANNs and DTs' results, the best estimated models are given with accuracy ratios, false positive and false negative rates to measure performance in Table 5. Table 5 shows that the models have better performance than logistic regression and discriminant models by considering all the performance criteria. Particularly, when we evaluate the machine learning methods in themselves the best models with selected variables with PCA have higher performance to the full models with all the independent variables according to most of the performance measurements as well.

Table 5. *The classification performance of the ANN and SVM models*

Methods	Procedure	#Input	AUC	Acc.	FP	FN	Selected Variables
ANNs (trainlm, mse)	Feature Selection with PCA	3	0.870	0.880	0.116	0.142	C1, C2, C3
	Full Model	6	0.866	0.841	0.020	0.643	All variables in Table 2
DTs (complex tree)	Feature Selection with PCA	3	0.900	0.910	0.084	0.118	C1, C2, C3
	Full Model	6	0.820	0.870	0.078	0.304	All variables in Table 2

To reveal the importance of independent variables on survivor and non-survivor, the ANN model with estimated weights is used. Independent variables' normalized importance over the best full model is given in Fig. 2. According to Figure 2, the top 3 variables above 50% normalized importance are primary cause, the number of total passenger and the phase of flight which is supporting the logistic regression and discriminant models.

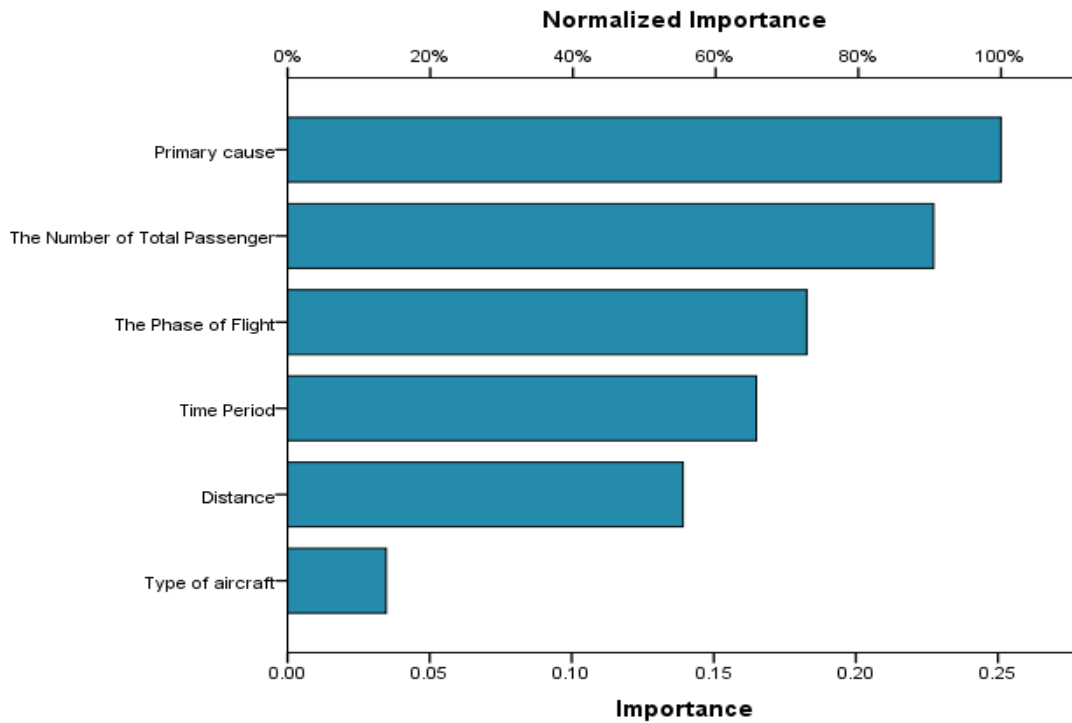


Figure 2: Normalized importance of independent features

V. Discussion and Conclusion

In this study, the causes of aircraft accidents which comprised the most fatal 100 ones are classified with six variables. The variables are; aircraft type, distance, flight phase, primary cause, the number of total passengers, and time period. These are used to classify survivor/non-survivor passengers. In the literature review, the primary causes of the accidents are defined with three factors named human factor, technical, and terrorism/sabotage to define the concept of safety and how the safety concept is affected the most fatal accidents.

When it is examined the three primary causes about the effect of safety on the most fatal accidents, 10 of the most fatal aviation 100 accidents are related to terrorism/sabotage factors. However, the all-time terrorism/sabotage effect in all fatal accidents was approximately equal to %5. 65 of 100 of the most fatal aviation accidents are related to the human factor. However, the all-time human factor effect in all fatal accidents was approximately equal to %70. 25 of 100 of the most fatal aviation accidents are related to technical ones, this ratio is nearly the same as the all-time technical effect in all fatal accidents which was approximately equal to %25. When it was examined the total percentages, it is understood that except for the %5 percent difference related to human factor and terrorism/sabotage, the revealed percentages are similar to all-time aviation accidents' history numbers [48].

The findings are supported that the human factor is increased the survivors 9.709 times more than the technical factor. So, the accidents are occurred by technical factors are more hazardous and difficult to recover. Furthermore, the phase of flight has decreased the survivors 6.479 times more than the phase of landing, and 9.674 times more than the phase of take-off. Finally, the 1 unit change in the total number of passengers has increased the number of survivors 1.014 times. According to machine learning results, these parameters are found above 50% importance. These algorithms integrated with PCA have better performance than multivariate statistical models. So, it can be said

that the dimensions obtained from PCA called capability, geographical, and qualification have a significant impact on the survivor status.

So, the analysis of the most fatal 100 accidents can be a reference to determine the causes of all-time aviation accidents with the selected variables. Future studies can be analyzed the all-time aviation accidents by segmenting their flight phases with their flight types by determining danger levels. Also, this research can be continued with much more comprehensive accident datasets, and utilize various hybrid ML approaches in order to make a more detailed analysis.

Acknowledgement

The authors declare that there are no potential conflicts of interest with respect to the research, authorship, and/or publication of this article.

Conflict of Interest

The authors declare no conflict of interest.

Author Contributions

Corresponding Author Tüzün Tolga İNAN: Data curation, Conceptualization, Investigation, Writing, Original draft preparation, Reviewing and Editing, Supervision, Resources
Second Author Neslihan GÖKMEN İNAN: Methodology, Validation, Software, Formal analysis, Visualization.

References

- [1] International Civil Aviation Organization (ICAO). International Standards and Recommended Practices: Aircraft Accident and Incident Investigation. Annex 13 to the Convention on International Civil Aviation, 8th ed. Montreal, Canada: ICAO, 1994.
- [2] Singh, V., Sharma, S. K., Chadha, I., and Singh, T. (2019). Investigating the moderating effects of multi group on safety performance: The case of civil aviation. *Case studies on transport policy*, 7(2): 477-488. <https://doi.org/10.1016/j.cstp.2019.01.002>
- [3] Harizi, R., Belhaiza, M. A., and Harizi, B. (2013). A cliometric analysis of the explanatory factors of the air crashes in the world (1950–2008). *Journal of Transportation Safety & Security*, 5(2): 165-185 <https://doi.org/10.1080/19439962.2012.749968>
- [4] Oster Jr, C. V., Strong, J. S., and Zorn, C. K. (2013). Analyzing aviation safety: Problems, challenges, opportunities. *Research in transportation economics*, 43(1): 148-164 <https://doi.org/10.1016/j.retrec.2012.12.001>
- [5] Lofquist, E. A. (2010). The art of measuring nothing: The paradox of measuring safety in a changing civil aviation industry using traditional safety metrics. *Safety Science*, 48(10): 1520-1529 <https://doi.org/10.1016/j.ssci.2010.05.006>
- [6] Gramopadhye, A. K., and Drury, C. G.: Human factors in aviation maintenance: how we got to where we are, 2000. [https://doi.org/10.1016/S0169-8141\(99\)00062-1](https://doi.org/10.1016/S0169-8141(99)00062-1)
- [7] Gillen, D., and Morrison, W. G. (2015). Aviation security: Costing, pricing, finance and performance. *Journal of Air Transport Management*, 48: 1-12 <https://doi.org/10.1016/j.jairtraman.2014.12.005>
- [8] Cui, Q., and Li, Y. (2015). The change trend and influencing factors of civil aviation safety efficiency: the case of Chinese airline companies. *Safety science*, 75: 56-63 <https://doi.org/10.1016/j.ssci.2015.01.015>
- [9] Hawkins, F. H., and Orlady, H. W.: Human Factors in Flight. 2nd, 1987.
- [10] Huang, C. (2020). Further Improving General Aviation Flight Safety: Analysis of Aircraft

Accidents During Takeoff. *The Collegiate Aviation Review International*, 38(1)

[11] Iwadare, K., and Oyama, T. (2015). Statistical Data Analyses on Aircraft Accidents in Japan: Occurrences, Causes and Countermeasures. *American Journal of Operations Research*, 5(03): 222 <https://doi.org/10.4236/ajor.2015.53018>

[12] Brown, K. A., Willis, P. G., and Prussia, G. E. (2000). Predicting safe employee behavior in the steel industry: development and test of a sociotechnical model. *Journal of Operations Management*, 18: 445-465

[13] McDonald, N., Corrigan, S., Daly, C., and Cromie, S. (2000). Safety management systems and safety culture in aircraft maintenance organizations. *Safety Science*, 34: 151-176

[14] Santos-Reyes, J., and Beard, A. (2002). Assessing safety management systems. *Journal of Loss Prevention in the Process Industries*, 15: 77-95

[15] Shyur, H. J. (2008). A quantitative model for aviation safety risk assessment. *Computers & Industrial Engineering*, 54(1): 34-44 <https://doi.org/10.1016/j.cie.2007.06.032>

[16] Li, D. B., Xu, X. H., and Li, X. (2009). Target level of safety for Chinese airspace. *Safety Science*, 47(3): 421-424 <https://doi.org/10.1016/j.ssci.2008.06.005>

[17] Persing, I., and Ng, V. *Semi-supervised cause identification from aviation safety reports*. In Proceedings of the Joint Conference of the 47th Annual Meeting of the ACL and the 4th International Joint Conference on Natural Language Processing of the AFNLP (pp. 843-851), 2009, August.

[18] Chen, F. *Fuzzy comprehensive evaluation of civil aviation safety supervisor*. In 2010 International Conference on Multimedia Communications (pp. 45-48), IEEE, 2010, August. <https://doi.org/10.1109/MEDIACOM.2010.17>

[19] Brooker, P. (2011). Experts, Bayesian Belief Networks, rare events and aviation risk estimates. *Safety Science*, 49(8-9): 1142-1155 <https://doi.org/10.1016/j.ssci.2011.03.006>

[20] O'Connor, P., O'Dea, A., Kennedy, Q., and Buttrey, S. E. (2011). Measuring safety climate in aviation: A review and recommendations for the future. *Safety Science*, 49(2): 128-138 <https://doi.org/10.1016/j.ssci.2010.10.001>

[21] Chang, Y. H., and Liao, M. Y. (2008). Air passenger perceptions on exit row seating and flight safety education. *Safety science*, 46(10): 1459-1468 <https://doi.org/10.1016/j.ssci.2007.11.006>

[22] Chang, Y. H., and Liao, M. Y. (2009). The effect of aviation safety education on passenger cabin safety awareness. *Safety science*, 47(10): 1337-1345 <https://doi.org/10.1016/j.ssci.2009.02.001>

[23] Chen, C. C., Chen, J., and Lin, P. C. (2009). Identification of significant threats and errors affecting aviation safety in Taiwan using the analytical hierarchy process. *Journal of Air Transport Management*, 15(5): 261-263 <https://doi.org/10.1016/j.jairtraman.2009.01.002>

[24] Herrera, I. A., Nordskog, A. O., Myhre, G., and Halvorsen, K. (2009). Aviation safety and maintenance under major organizational changes, investigating non-existing accidents. *Accident Analysis & Prevention*, 41(6): 1155-1163 <https://doi.org/10.1016/j.aap.2008.06.007>

[25] Remawi, H., Bates, P., and Dix, I. (2011). The relationship between the implementation of a Safety Management System and the attitudes of employees towards unsafe acts in aviation. *Safety Science*, 49(5): 625-632 <https://doi.org/10.1016/j.ssci.2010.09.014>

[26] Mäkelä, A., Saltikoff, E., Julkunen, J., Juga, I., Gregow, E., and Niemelä, S. (2013). Cold-season thunderstorms in Finland and their effect on aviation safety. *Bulletin of the American Meteorological Society*, 94(6): 847-858

[27] Molesworth, B. R., and Burgess, M. (2013). Improving intelligibility at a safety critical point: In flight cabin safety. *Safety science*, 51(1): 11-16 <https://doi.org/10.1016/j.ssci.2012.06.006>

[28] International Civil Aviation Organization (ICAO). *Safety Management Manual (SMM)*. International Civil Aviation Organization, 2013.

[29] Federal Aviation Administration (FAA).: Fiscal Year 2014 Performance and Accountability Report (Dec., 2014), 2014.

- [30] Eurocontrol Performance Review Commission (EPRC).: Performance Review Report-An Assessment of Air Traffic Management in Europe during the Calendar Year 2013, 2014.
- [31] International Civil Aviation Organization (ICAO). Safety Management Manual (SMM) (Doc 9859).
<https://www.icao.int/safety/safetymanagement/documents/doc.9859.3rd%20edition.alltext.en.pdf>, 2020. Accessed 19 Dec 2020
- [32] Burnett, R. A., and Si, D. *Prediction of injuries and fatalities in aviation accidents through machine learning*. In Proceedings of the International Conference on Compute and Data Analysis (pp. 60-68), 2017, May. <https://doi.org/10.1145/3093241.3093288>
- [33] Ayres Jr, M., Shirazi, H., Carvalho, R., Hall, J., Speir, R., Arambula, E., ... and Pitfield, D. (2013). Modelling the location and consequences of aircraft accidents. *Safety science*, 51(1): 178-186 <https://doi.org/10.1016/j.ssci.2012.05.012>
- [34] Goode, J. H. (2003). Are pilots at risk of accidents due to fatigue?. *Journal of safety research*, 34(3): 309-313 [https://doi.org/10.1016/S0022-4375\(03\)00033-1](https://doi.org/10.1016/S0022-4375(03)00033-1)
- [35] Lee, H., Madar, S., Sairam, S., Puranik, T. G., Payan, A. P., Kirby, M., ... and Mavris, D. N. (2020). Critical Parameter Identification for Safety Events in Commercial Aviation Using Machine Learning. *Aerospace*, 7(6): 73
- [36] Dangut, M. D., Skaf, Z., and Jennions, I. K. *An integrated machine learning model for aircraft components rare failure prognostics with log-based dataset*. ISA transactions, 2021. <https://doi.org/10.1016/j.isatra.2020.05.001>
- [37] Bureau of Aircraft Accident Archives. <https://www.baaa-acro.com/crash-archives>, 2021. Accessed 06 May 2021.
- [38] Janic, M. (2000). An assessment of risk and safety in civil aviation. *Journal of Air Transport Management*, 6(1): 43-50 [https://doi.org/10.1016/S0969-6997\(99\)00021-6](https://doi.org/10.1016/S0969-6997(99)00021-6)
- [39] Bozdogan, H. (2000). Akaike's information criterion and recent developments in information complexity. *J. Math. Psychol.*, 44(1): 62-91 <https://doi.org/10.1006/jmps.1999.1277>
- [40] Kocadagli, O., and Langari, R. (2017). Classification of EEG signals for epileptic seizures using hybrid artificial neural networks based wavelet transforms and fuzzy relations. *Expert Syst. Appl.*, 88: 419-434 doi: 10.1016/j.eswa.2017.07.020
- [41] İnan, T. T., and Gokmen, N. (2021). The Determination of the Factors Affecting Air Transportation Passenger Numbers. *International Journal of Aviation, Aeronautics, and Aerospace*, 8(1) <https://doi.org/10.15394/ijaaa.2021.1553>
- [42] Chong, M. M., Abraham A., and Paprzycki, M. (2005). Traffic accident analysis using machine learning paradigms. *Informatica*, 29(1): 89-98
- [43] Alpaydin, E. *Introduction to Machine Learning (3rd ed.)*. The MIT Press, 2014.
- [44] MATLAB R. https://www.mathworks.com/products/new_products/release2020a.html, 2020a. Accessed 30 July 2021
- [45] Kocadagli, O. (2015). A Novel Hybrid Learning Algorithm For Full Bayesian Approach of Artificial Neural Networks. *Applied Soft Computing, Elsevier*, 35: 52-65 <https://doi.org/10.1016/j.asoc.2015.06.003>
- [46] Institute for an Industrial Safety Culture (ICSI). <https://www.icsi-eu.org/en/human-organizational-factors>, 2021. Accessed 07 May 2021.
- [47] Security and Facilitation. <https://www.icao.int/Security/Pages/default.aspx>, 2020. Accessed 21 December 2020.
- [48] Plane Crash Info Causes of Fatal Accidents by Decade. planecrashinfo.com/cause.htm, 2021. Accessed July 01 2020.

STATISTICAL PROPERTIES AND APPLICATION OF A TRANSFORMED LIFETIME DISTRIBUTION: INVERSE MUTH DISTRIBUTION

AGNI SAROJ¹, PRASHANT K. SONKER² AND MUKESH KUMAR^{*3}

^{1,2}Department of Statistics, Banaras Hindu University, Varanasi, 221005, India.

³Department of Statistics, MMV, Banaras Hindu University, Varanasi 221005, India.

E-mail: ¹agni.saroj4@bhu.ac.in, ²prashant.s4@bhu.ac.in, ^{*3}mukesh.mmv@bhu.ac.in

*Corresponding Author

Abstract

In this paper, we have proposed a transformed distribution called inverse Muth (IM) distribution. The expressions for probability density function (pdf), cumulative distribution function (cdf), reliability and hazard function of this distribution are well defined. The statistical properties such as, quantile function, moments, skewness and kurtosis are derived. The methods of estimation such as maximum likelihood estimation (MLE) and maximum product spacing estimation (MPSE) are used to estimate the parameters. The IM distribution is positively skewed and its behavior of hazard rate is upside-down bathtub (UBT) shape. The important finding of the study is that the moments of IM distribution do not exist. A real dataset (the active repair time for airborne communication transceiver) used for application purpose, after taking a natural extension of IM distribution. It is expected that the proposed model would be used as a life time model in field of reliability and its applicability.

Keywords: Inverse Muth distribution, quantile function, maximum likelihood estimation, maximum product spacing estimation, real data analysis.

1. INTRODUCTION

In the statistical literature, there are lots of distribution exist, which are very useful in various fields of science with its applicability. The application of statistical distributions gives the well explanation about the probabilistic behavior of random phenomenon and plays an important role to analyze the different types of data from various fields.

In the field of reliability, the various lifetime distributions derived which are preferred in reliability analyses or lifetime investigation see Martz & Waller [1], and the behavior of failure rate observed to be as increasing, decreasing and bathtub shape. Some distributions (Maxwell, normal, Gompertz, etc.) are having only increasing failure rate whereas Gamma, Weibull and other distributions gives increasing, decreasing as well as constant failure rate. In many situations failure rate increases consistently, after reaching the peak, it starts to decrease which is discussed in Bennett [2], Langlands et. al. [3]. Such type of failure rate is named as UBT failure rate given in Sharma et. al. [4]. Muth distribution is defined on a continuous random variable and introduced by Muth [5] in 1977 for reliability analysis. Let us consider that a random variable Y follow Muth distribution with the shape parameter α and its pdf is defined as

$$f(y; \alpha) = \begin{cases} (e^{\alpha y} - \alpha) \cdot \exp \left\{ \alpha y - \frac{1}{\alpha} (e^{\alpha y} - 1) \right\} & y > 0, \quad \alpha \in (0, 1] \\ 0 & \text{otherwise} \end{cases} \quad (1)$$

The cdf is given by,

$$F(y; \alpha) = 1 - \exp \left\{ \alpha y - \frac{1}{\alpha} \cdot (e^{\alpha y} - 1) \right\} \quad y > 0, \quad \alpha \in (0, 1] \quad (2)$$

It has mainly focused on strictly positive memory in Muth [5]. The basic statistical properties of Muth distribution are discussed by Jodra et. al. [6]. The reliability function and hazard function are given by respectively

$$R(t) = P[Y \geq t] = \exp \left\{ \alpha t - \frac{1}{\alpha} \cdot (e^{\alpha t} - 1) \right\} \quad t > 0, \quad \alpha \in (0, 1] \quad (3)$$

$$h(t) = \frac{f(t)}{R(t)} = \frac{(e^{\alpha t} - \alpha) \cdot \exp \left\{ \alpha t - \frac{1}{\alpha} (e^{\alpha t} - 1) \right\}}{\exp \left\{ \alpha t - \frac{1}{\alpha} \cdot (e^{\alpha t} - 1) \right\}} \quad t > 0, \quad \alpha \in (0, 1] \quad (4)$$

At different values of parameter α pdf, cdf, reliability and hazard functions are plotted in Figure 1.

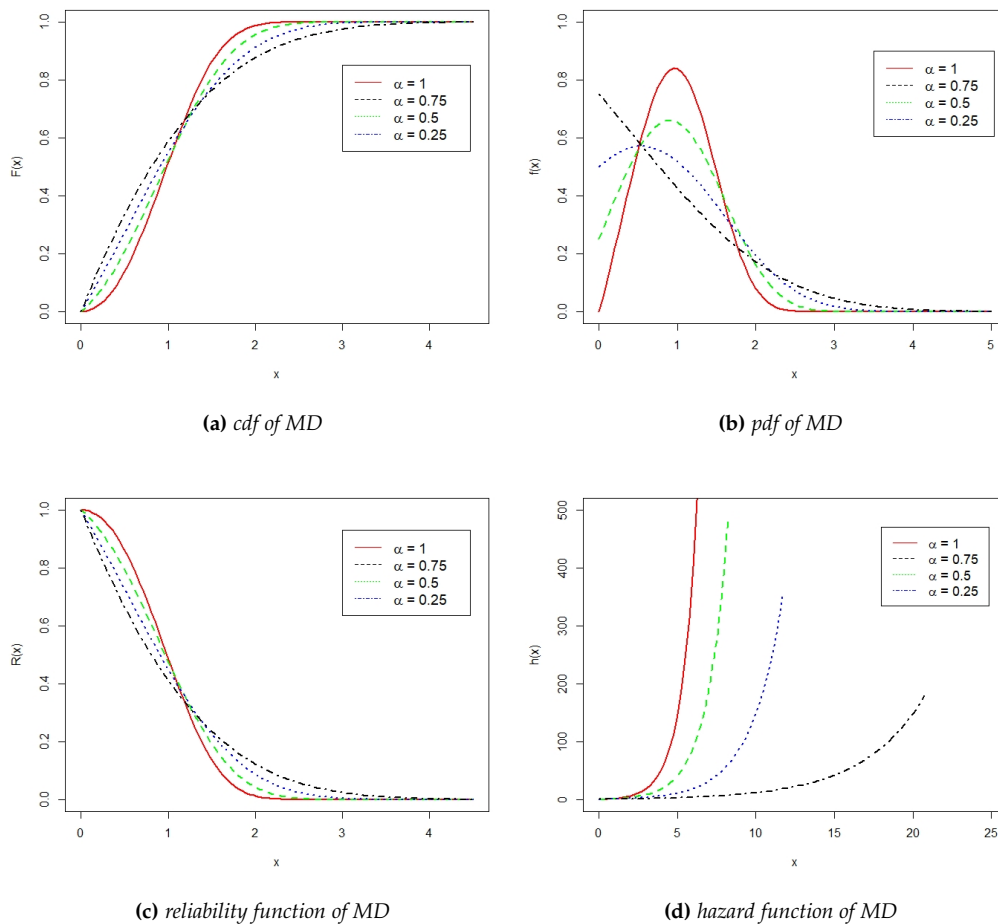


Figure 1: pdf, cdf, reliability and hazard functions of Muth Distribution.

A natural extension is also considered in Jodra et. al. [6] by adding a scale parameter named as Scaled Muth distribution. A transformed distribution for Muth distribution called power Muth (PM) distribution proposed by Jodra et. al. [7]. The exponentiated PM distribution and Inverse PM distribution will be proposed by Irshad et. al. [8] and Chesneau & Agiwal [9]. Some other literature on Muth distribution are discussed in Almarashi & Elgarhy [10], Al-Babtain et.al.

[11], Bicer et. at. [12]. In Figure 1, the hazard rate shows the failure rate is increasing. It has explained that the failure rate occurs in UBT shape when we take the inverse transformation of usual distributions given Sharma et. al. [4]. In the case of Invese PM distribution it is found that the behavior of hazard rate is in UBT shape. In this article, we have proposed a transformed distribution which is termed as the IM distribution. All the work of this article is arranged in different sections as: In section 2, statistical properties of proposed distribution are discussed. In section 3, we obtained the estimates of the parameter α using MLE and MPSE. In section 4, we have computed the expression for asymptotic confidence interval in case of MLE and MPSE. In section 5, the scale transformation of IM distribution has taken to estimate the parameters. In section 6, the simulation study has done to compute the estimates of parameters for both IM and scaled inverse Muth (SIM) distributions respectively. In section 7, the real data analysis is done to show the applicability of SIM distribution. Finally, the conclusion of this article is written in section 8.

2. INVERSE MUTH DISTRIBUTION

Let Y be a random variable follows the Muth distribution with pdf in equation (1) and cdf in equation (2), on taking inverse transformation as $X = \frac{1}{Y}$, the pdf of IM distribution is obtained as

$$f(x; \alpha) = \begin{cases} \frac{1}{x^2} (e^{\alpha/x} - \alpha) \cdot \exp\left\{\frac{\alpha}{x} - \frac{1}{\alpha}(e^{\alpha/x} - 1)\right\} & x > 0, \alpha \in (0, 1] \\ 0 & otherwise \end{cases} \quad (5)$$

The cdf is given by,

$$F(x; \alpha) = \exp\left\{\frac{\alpha}{x} - \frac{1}{\alpha}(e^{\alpha/x} - 1)\right\} \quad x > 0, \alpha \in (0, 1] \quad (6)$$

Some statistical properties of IM distribution are discussed as below:

2.1. Reliability and Hazard Function of IM Distribution

Importance of any lifetime distribution is based on its reliability and hazard rate. By using equation (5) and (6) the reliability and hazard function of the IM distribution are obtained as

$$R(t) = 1 - \exp\left\{\frac{\alpha}{t} - \frac{1}{\alpha}(e^{\alpha/t} - 1)\right\} \quad t > 0, \alpha \in (0, 1] \quad (7)$$

$$h(t) = \frac{f(t)}{R(t)} = \frac{(e^{\alpha/t} - \alpha) \cdot \exp\left\{\frac{\alpha}{t} - \frac{1}{\alpha}(e^{\alpha/t} - 1)\right\}}{t^2 \cdot \left(1 - \exp\left\{\frac{\alpha}{t} - \frac{1}{\alpha}(e^{\alpha/t} - 1)\right\}\right)} \quad t > 0, \alpha \in (0, 1] \quad (8)$$

The above equation (7) and (8) show the reliability and hazard function respectively and the graphical representation of these are given in Figure 2. We observed the behavior of hazard rate as UBT shape in Figure 2. As increases the value of parameter α , the peak of hazard rate also increases.

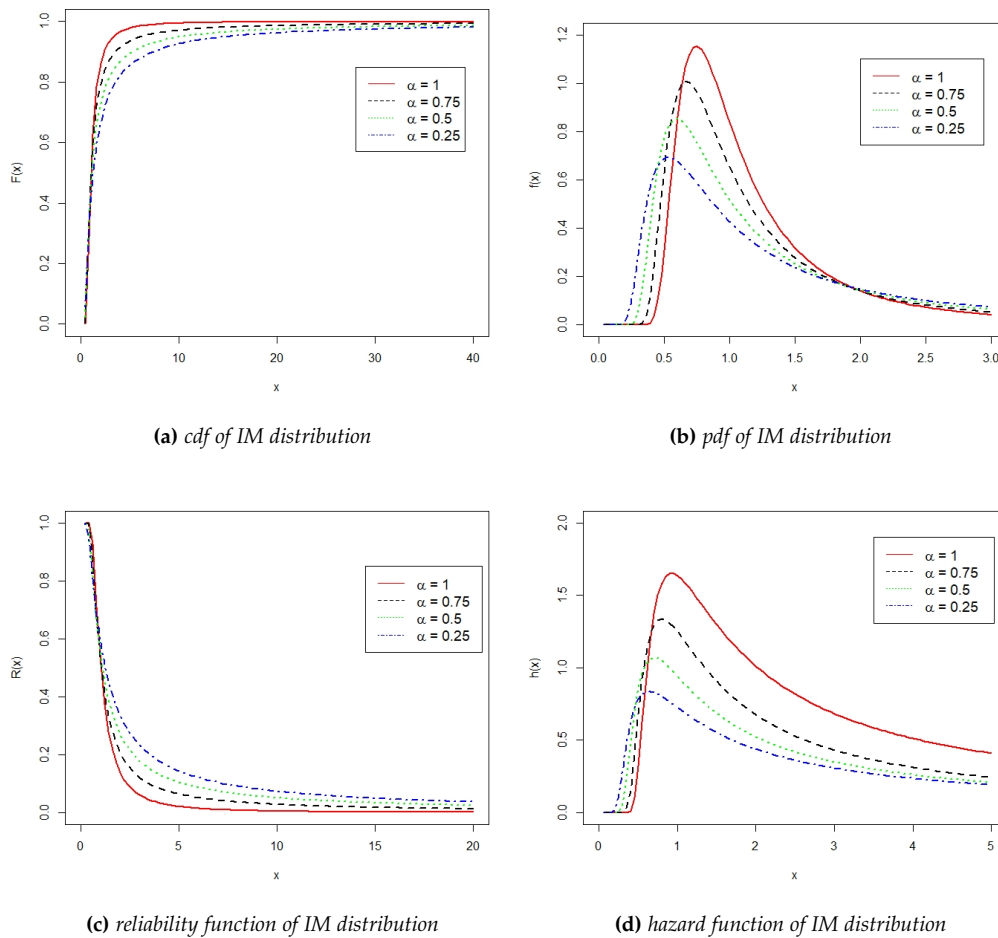


Figure 2: pdf, cdf, reliability and hazard functions of IM Distribution.

2.2. Quantile Function

Quantile function for the cdf $F_X(x)$ is defined as,

$$Q_X(u) = \inf\{x \in R : F_X(x) \geq u\} \quad 0 < u < 1 \quad (9)$$

It shows u^{th} quantile of an integer valued random variable, is also an integer. It indicates that if $F_X(x)$ be a continuous and strictly increasing, then quantile function of X is defined as

$$Q_X(u) = F_X^{-1}(u) \quad 0 < u < 1 \quad (10)$$

To find the quantile function for the IM distribution, it has to solve $F(x, \alpha) = u ; x > 0$ with respect to x for any $\alpha \in (0, 1]$ and $u \in (0, 1)$ i.e.

$$u = \exp\left(\frac{\alpha}{x} + \frac{1}{\alpha} - \frac{1}{\alpha} e^{\frac{\alpha}{x}}\right)$$

$$\log(u) - \frac{\alpha}{x} - \frac{1}{\alpha} = -\frac{1}{\alpha} e^{\frac{\alpha}{x}} \quad (11)$$

Multiplying by $e^{(\log(u) - \frac{\alpha}{x} - \frac{1}{\alpha})}$ on both side in equation (11), we get

$$\left(\log(u) - \frac{\alpha}{x} - \frac{1}{\alpha}\right) \cdot e^{(\log(u) - \frac{\alpha}{x} - \frac{1}{\alpha})} = -\frac{e^{-\frac{1}{\alpha} \cdot u}}{\alpha} \quad (12)$$

To solve equation (12), here we use a generalized integro-exponential function, Lambert-W function. It has applicability in computer algebra system and in mathematics given by Corless et al. [13]. The Lambert W function is defined as the solution of,

$$W(z) \cdot \exp(W(z)) = z \quad (13)$$

Where, z is complex function. If z is a real number such that If z is a real number such that $z \geq -\frac{1}{e}$ then $W(z)$ becomes a real function having two possible real branches. If the real branch taking value in $(-\infty, -1]$ is called negative branch and denoted by $W_{-1}(z)$ where $-\frac{1}{e} \leq z \leq 0$. The real root branch taking values in $[-1, \infty)$ is called the principle branch and denoted by $W_0(z)$ where $z \geq -\frac{1}{e}$, we shall use the negative branch which is satisfies the following properties, $W_{-1}(-\frac{1}{e}) = -1$, $W_{-1}(z)$ is decreasing as z increases to 0 and $W_{-1}(z)$ tends to $-\infty$ as z tends to 0 see Jodra [14].

By using equations (12) and (13), we obtained that $(\log(u) - \frac{\alpha}{x} - \frac{1}{\alpha})$ is the Lambert-W function of the real argument $(-\frac{e^{-\frac{1}{\alpha} \cdot u}}{\alpha})$, then, the explicit expression for Q_x in terms of Lambert-W function.

$$x = \frac{\alpha^2}{\alpha \cdot \log(u) - \alpha \cdot W\left(-\frac{e^{-\frac{1}{\alpha} \cdot u}}{\alpha}\right) - 1} \quad (14)$$

It gives the Quantile function of IM distribution.

Now for any $\alpha \in (0, 1]$, $x > 0$ and $u \in (0, 1)$ it ensure that,

$$\left(\log(u) - \frac{\alpha}{x} - \frac{1}{\alpha}\right) < -1$$

And it also be checked that,

$$\left(-\frac{e^{-\frac{1}{\alpha} \cdot u}}{\alpha}\right) \in \left(-\frac{1}{e}, 1\right)$$

By using the negative branch of Lambert W function the Quantile function of IM distribution in terms of negative branch of Lambert W function as,

$$x_u = \frac{\alpha^2}{\alpha \cdot \log(u) - \alpha \cdot W_{-1}\left(-\frac{e^{-\frac{1}{\alpha} \cdot u}}{\alpha}\right) - 1} \quad (15)$$

Where, x_u gives the u^{th} quantile of IM distribution.

2.3. Moments of the IM distribution

Let X be a random variable follows IM distribution with pdf in equation (5) then the k^{th} raw moment is defined as:

$$\begin{aligned} \mu'_k &= \int_0^\infty x^k \cdot f(x; \alpha) dx \\ \mu'_k &= \int_0^\infty x^k \cdot \frac{1}{x^2} \left(e^{\alpha/x} - \alpha\right) e^{\left\{\frac{\alpha}{x} - \frac{1}{\alpha} \cdot (e^{\alpha/x} - 1)\right\}} dx \\ I &= \mu'_k = \int_0^\infty x^{k-2} \cdot \left(e^{\alpha/x} - \alpha\right) e^{\left\{\frac{\alpha}{x} - \frac{1}{\alpha} \cdot (e^{\alpha/x} - 1)\right\}} dx \\ I &= \int_0^a x^{k-2} \cdot \left(e^{\alpha/x} - \alpha\right) e^{\left\{\frac{\alpha}{x} - \frac{1}{\alpha} \cdot (e^{\alpha/x} - 1)\right\}} dx \\ &+ \int_a^\infty x^{k-2} \cdot \left(e^{\alpha/x} - \alpha\right) e^{\left\{\frac{\alpha}{x} - \frac{1}{\alpha} \cdot (e^{\alpha/x} - 1)\right\}} dx \end{aligned}$$

$$I = I_1 + I_2$$

Where,

$$I_1 = \int_0^a x^{(k-2)} \cdot (e^{\frac{\alpha}{x}} - \alpha) \cdot e^{\{\frac{\alpha}{x} - \frac{1}{\alpha} \cdot (e^{\frac{\alpha}{x}} - 1)\}} dx$$

$$I_2 = \int_a^\infty x^{(k-2)} \cdot (e^{\frac{\alpha}{x}} - \alpha) \cdot e^{\{\frac{\alpha}{x} - \frac{1}{\alpha} \cdot (e^{\frac{\alpha}{x}} - 1)\}} dx$$

Now proceeding with integration I_2

$$I_2 = \int_a^\infty x^{(k-2)} \cdot (e^{\frac{\alpha}{x}} - \alpha) \cdot e^{\{\frac{\alpha}{x} - \frac{1}{\alpha} \cdot (e^{\frac{\alpha}{x}} - 1)\}} dx$$

To check the convergence or divergence of integral I_2 , we use the limit comparison test which state that if

1. $f(x)$ and $g(x) > 0$ on $[a, \infty)$
2. $f(x)$ and $g(x)$ both are continuous on $[0, \infty)$ and
3. $\lim_{x \rightarrow \infty} \frac{f(x)}{g(x)} = L > 0$ where, L is some finite positive number.

then $\int_a^\infty f(x) dx$ and $\int_a^\infty g(x) dx$ either both converge or both diverge.

For I_2 , Let,

$$f_1(x) = \int_a^\infty x^{(k-2)} \cdot (e^{\frac{\alpha}{x}} - \alpha) \cdot e^{\{\frac{\alpha}{x} - \frac{1}{\alpha} \cdot (e^{\frac{\alpha}{x}} - 1)\}} \text{ and,}$$

$$g_1(x) = x^{(k-2)}$$

$f_1(x)$ and $g_1(x) > 0$ as well as continuous for $[a, \infty)$ for $k = 1, 2, 3, \dots$
 now,

$$\begin{aligned} \lim_{x \rightarrow \infty} \frac{f_1(x)}{g_1(x)} &= \lim_{x \rightarrow \infty} (e^{\frac{\alpha}{x}} - \alpha) \cdot e^{\{\frac{\alpha}{x} - \frac{1}{\alpha} \cdot (e^{\frac{\alpha}{x}} - 1)\}} \\ &= (1 - \alpha) \cdot e^0 \\ &= (1 - \alpha) > 0 \quad \alpha \in (0, 1] \end{aligned}$$

$$\int_a^\infty g_1(x) dx = \int_a^\infty x^{(k-2)} dx = \int_a^\infty \frac{1}{x^{-(k-2)}} dx$$

$\therefore \int_a^\infty \frac{1}{x^n} dx$ is convergent if $n > 1$ and divergent for $n \leq 1$.

So, $\int_a^\infty \frac{1}{x^{-(k-2)}} dx$ is convergent if $(2-k) > 1$ or $k < 1$. But we have $k > 0$ ($k = 1, 2, 3, \dots$).

Then it shows that $\int_a^\infty g_1(x) dx$ is divergent for all $k \geq 1$ and by using limit comparison test for convergence of an improper integral, $\int_a^\infty f_1(x) dx$ is also divergent i.e. integral

$$I_2 = \int_a^\infty x^{(k-2)} \cdot (e^{\frac{\alpha}{x}} - \alpha) \cdot e^{\{\frac{\alpha}{x} - \frac{1}{\alpha} \cdot (e^{\frac{\alpha}{x}} - 1)\}} dx \text{ is divergent for all the value of } k \geq 1.$$

By using the property of convergence of integral, if we have an integral $I = I_1 + I_2$ then I is convergent iff I_1 and I_2 both are convergent. If any one of the I_1 and I_2 is divergent then the integral I is also divergent. Thus we found that integral I also become a divergent. Hence the moment for the IM distribution does not exist.

2.4. Measures of Skewness and Kurtosis

In the above section, we found that the moment of the IM distribution does not exist, so we cannot obtain Pearson's measure of skewness and kurtosis based on moments. Therefore by using

the quantile function, it may be possible to obtain Galton's measures of skewness and Moor's measures of kurtosis mentioned in Gilchrist [15]. These measures are defined as:

$$G(\alpha) = \frac{x_{3/4}(\alpha) + x_{1/4}(\alpha) - 2x_{1/2}(\alpha)}{x_{3/4}(\alpha) - x_{1/4}(\alpha)} \quad (16)$$

$$K(\alpha) = \frac{x_{7/8}(\alpha) - x_{5/8}(\alpha) + x_{3/8}(\alpha) - x_{1/8}(\alpha)}{x_{3/4}(\alpha) - x_{1/4}(\alpha)} \quad (17)$$

Where, $x_{i/4}$; $i = 1, 2, 3$ denote the i^{th} quartile and $x_{i/8}$; $i = 1, 2, \dots, 7$ denote the i^{th} octile for this distribution. Galton's measure of skewness $G(\cdot)$ lies between $(-1, 1)$. If $G(\cdot) > 0$ it is called positive or right skewed and if $G(\cdot) < 0$ it is called negative skewed. For a perfect symmetrical distribution, $G(\cdot) = 0$. Galton's measures of skewness $G(\alpha)$ and Moor's measures of kurtosis $K(\alpha)$ for IM distribution are calculated at different value of α in Table 1. From the Table 1, we observed that all values of skewness are greater than zero for different values of parameter, thus IM distribution is a positive or right skewed distribution.

Table 1: Skewness and kurtosis of IM distribution

α	Skewness	Kurtosis
0.1	0.4759	2.1413
0.2	0.4741	2.1385
0.3	0.4695	2.1301
0.4	0.4607	2.1108
0.5	0.4465	2.0733
0.6	0.4264	2.0109
0.7	0.4008	1.9207
0.8	0.3710	1.8080
0.9	0.3388	1.6861
1.0	0.3060	1.5698

3. PARAMETER ESTIMATION

3.1. Maximum likelihood estimation

Let x_1, x_2, \dots, x_n be a random sample of size of n from IM distribution with unknown parameter α having pdf equation (5). Likelihood function for the sample x_1, x_2, \dots, x_n as follows,

$$L(x; \alpha) = \prod_{i=1}^n \frac{1}{x_i^2} \left(e^{\alpha/x_i} - \alpha \right) \cdot \exp \left(\frac{\alpha}{x_i} - \frac{1}{\alpha} (e^{\alpha/x_i} - 1) \right) \quad (18)$$

$$\log(L(x; \alpha)) = -2 \sum_{i=1}^n \log(x_i) + \sum_{i=1}^n \log \left(e^{\alpha/x_i} - \alpha \right) + \sum_{i=1}^n \left(\frac{\alpha}{x_i} - \frac{1}{\alpha} (e^{\alpha/x_i} - 1) \right) \quad (19)$$

MLE is the value of unknown parameter α which maximize the equation (18). To get estimated value of α , we take partial derivative of equation (19) w.r.t. α and equating to zero i.e.

$$\frac{\partial}{\partial \alpha} \log(L(x; \alpha)) = 0$$

$$\sum_{i=1}^n \frac{(e^{\alpha/x_i} - 1)}{x_i (e^{\alpha/x_i} - \alpha)} + \sum_{i=1}^n \frac{1}{x_i} + \frac{1}{\alpha^2} \sum_{i=1}^n e^{\alpha/x_i} - \frac{1}{\alpha} \sum_{i=1}^n \frac{e^{\alpha/x_i}}{x_i} - \frac{n}{\alpha^2} = 0 \quad (20)$$

Now we have to solve equation (20) to get $\hat{\alpha}_{ml}$ and check that this solution to maximizes equation (18) following condition has to be satisfies:

$$\left[\frac{\partial^2}{\partial \alpha^2} \log(L(x; \alpha)) \right]_{\alpha=\hat{\alpha}_{ml}} < 0 \quad (21)$$

Where, $\hat{\alpha}_{ml}$ is the estimated value of α which obtained from equation (20). We observed that it is not in closed form, so we cannot solve it analytically. Newton-Raphson iteration method used which gives the numerical solution of equation (20) for α .

3.2. Maximum product spacing

Maximum product spacing estimation (MPSE) method is an alternative to MLE which is proposed by Cheng & Amin [16] and Ranney [17]. MLE does not give better performance or fails in the case of three or more parameters exist, remarked in Cheng & Traylor [18], and MLE does not perform satisfactorily for heavy tailed distribution which is discussed in Pitman [19]. Let us consider x_1, x_2, \dots, x_n be a random sample of size 'n' drawn from the IM distribution having cdf in equation (6).

Let $x_{i:n}$ be i^{th} order statistic and the spacing function D_i 's is defined as,

$$D_i = \left[F(x_{i:n}; \alpha) - F(x_{(i-1):n}; \alpha) \right] \quad (22)$$

For x_0 and x_{n+1} , $F(x_0; \alpha) = 0$ and $F(x_{n+1}; \alpha) = 1$ respectively.
 at $i=1$,

$$D_1 = \exp\left(\frac{\alpha}{x_1} - \frac{1}{\alpha}(e^{\alpha/x_1} - 1)\right) \quad (23)$$

at $i=n+1$,

$$D_{n+1} = 1 - F(x_{n:n}; \alpha)$$

$$D_{n+1} = 1 - \exp\left(\frac{\alpha}{x_n} - \frac{1}{\alpha}(e^{\alpha/x_n} - 1)\right) \quad (24)$$

For $i = 2, 3, \dots, n$ the expression is

$$D_i = \left[F(x_{i:n}; \alpha) - F(x_{(i-1):n}; \alpha) \right]$$

$$D_i = \exp\left(\frac{\alpha}{x_i} - \frac{1}{\alpha}(e^{\alpha/x_i} - 1)\right) - \exp\left(\frac{\alpha}{x_{i-1}} - \frac{1}{\alpha}(e^{\alpha/x_{i-1}} - 1)\right) \quad (25)$$

Then the product of spacing function is defined as

$$S = \prod_{i=1}^{n+1} D_i \quad (26)$$

MPSE is the value of α which maximize the product spacing function given in equation (26).

Taking the log of both side of equation (26)

$$\log(S) = \sum_{i=1}^{n+1} \log(D_i)$$

$$\log(S) = \log(D_1) + \log(D_{n+1}) + \sum_{i=2}^n \log(D_i)$$

$$\log(S) = \log\left[\exp\left(\frac{\alpha}{x_1} - \frac{1}{\alpha}(e^{\alpha/x_1} - 1)\right)\right] + \log\left[1 - \exp\left(\frac{\alpha}{x_n} - \frac{1}{\alpha}(e^{\alpha/x_n} - 1)\right)\right]$$

$$+ \sum_{i=2}^n \log\left[\exp\left(\frac{\alpha}{x_i} - \frac{1}{\alpha}(e^{\alpha/x_i} - 1)\right) - \exp\left(\frac{\alpha}{x_{i-1}} - \frac{1}{\alpha}(e^{\alpha/x_{i-1}} - 1)\right)\right] \quad (27)$$

To find the estimated value of α which maximize the equation (26) we use the method of optimization. For this we have to differentiate the equation (27) w.r.t. α and equate to zero,

$$\frac{\partial}{\partial \alpha} (\log(S)) = 0 \quad (28)$$

On solving the above equation it found an estimated value of $\alpha = \hat{\alpha}_{mp}$, and to satisfy the condition of maximization by the value $\alpha = \hat{\alpha}_{mp}$, i.e.

$$\left[\frac{\partial^2}{\partial \alpha^2} \log(S) \right]_{\alpha=\hat{\alpha}_{mp}} < 0 \quad (29)$$

The expression given in equation (27) and (28) together is not easy to solve and it is not in closed form. For the solution of this and to find the estimated value of α which maximize the product of spacing function given in equation (26) by satisfying the condition in equation (29) and we have used some numerical method to find the numerical solution of equation (28).

4. ASYMPTOTIC CONFIDENCE INTERVAL

We have obtained both MLE and MPSE of the parameter which are not in explicit form. So the exact distribution of the estimator is quite difficult to obtain. The authors Cheng & Amin [16], Ghosh & Jammalamadaka [20], Anatolyev [21] and Singh et. al. [22] have used MPSE method in their papers and explained the MPSE method is asymptotically equivalent to MLE method. By using the concept of large sample theory we may write the asymptotic distribution for the estimators as,

$$(\hat{\theta} - \theta) \equiv N(0, I^{-1}(\hat{\theta})); \quad (30)$$

where,

$\hat{\theta}$ is the estimate of parameter

θ is the true value of parameter

$I^{-1}(\hat{\theta})$ is the inverse of Fisher information matrix

For m parameters $\theta_1, \theta_2, \theta_3, \dots, \theta_m$ involved in a distribution the $m \times m$ Fisher information matrix is defined as

$$I(\hat{\theta}) = \begin{bmatrix} I_{1,1} & I_{1,2} & \cdots & I_{1,m} \\ I_{2,1} & I_{2,2} & \cdots & I_{2,m} \\ \vdots & \vdots & \vdots & \vdots \\ I_{m,1} & I_{m,2} & \cdots & I_{m,m} \end{bmatrix}$$

Where, $I_{i,j} = -E \left(\frac{\partial^2(L)}{\partial \theta_i \partial \theta_j} \right); \quad i, j = 1, 2, 3, \dots, m$

And the estimated variance for $\hat{\theta}$ is given by:

$$Var(\hat{\theta}) = I_{i,j}^{-1} = -E \left(\frac{\partial^2(L)}{\partial \theta^2} \right)_{\theta=\hat{\theta}}^{-1}; \quad \text{here } i = j \quad (31)$$

This is the diagonal element of the inverse of Fisher information matrix. Therefore, the two sided $100(1 - \alpha^*)$ % confidence interval for the θ is

$$\hat{\theta} \pm Z_{\alpha^*/2} \sqrt{Var(\hat{\theta})}; \quad (32)$$

Where, α^* is the level of significance and $Z_{\alpha^*/2}$ is upper $\alpha^*/2$ % point of standard normal distribution.

For the IM distribution, asymptotic confidence interval defined for the MLE is defined as:

$$\hat{\alpha}_{ml} \pm Z_{\alpha^*/2} \sqrt{Var(\hat{\alpha}_{ml})} \quad (33)$$

In the case of MPSE defined as :

$$\hat{\alpha}_{mp} \pm Z_{\alpha^*/2} \sqrt{Var(\hat{\alpha}_{mp})} \quad (34)$$

5. SCALE TRANSFORMATION OF IM DISTRIBUTION

We take a natural transformation (extension) of random variable by including a scale parameter say $\beta > 0$. The scale transformation is taken as $Z = \beta X$. Then the cdf of Z is given as,

$$F_Z(z) = \exp \left\{ \frac{\alpha \cdot \beta}{z} - \frac{1}{\alpha} \left(e^{\frac{\alpha \cdot \beta}{z}} - 1 \right) \right\}; \quad \alpha \in (0, 1] \text{ and } \beta > 0 \quad (35)$$

the pdf is given by

$$f_Z(z; \alpha, \beta) = \frac{1}{\beta \cdot z^2} \left(e^{\frac{\alpha \cdot \beta}{z}} - \alpha \right) \exp \left\{ \frac{\alpha \cdot \beta}{z} - \frac{1}{\alpha} \left(e^{\frac{\alpha \cdot \beta}{z}} - 1 \right) \right\}; \quad \alpha \in (0, 1] \text{ and } \beta > 0 \quad (36)$$

Since, the distribution of Z is obtained by the scaling transformation of X which follows the IM distribution with parameter α . So the new distribution of Z is called scaled inverse Muth (SIM) distribution. Here, it is noticeable that Z comes from X follows IM distribution, on taking scale transformation by adding a scale parameter β , thus SIM distribution has some properties as similar to IM distribution, like as moments of this distribution also does not exist etc. The quantile function for SIM is defined as:

$$Q_Z(u; \alpha, \beta) = \beta \cdot Q(u; \alpha); \quad 0 < u < 1$$

where $Q(u; \alpha)$ is the quantile function for IM distribution. So it becomes as

$$z_u = \frac{\beta \cdot \alpha^2}{\alpha \cdot \log(u) - \alpha \cdot W_{-1} \left(\frac{-e^{-\frac{1}{\alpha}} \cdot u}{\alpha} \right) - 1} \quad (37)$$

6. SIMULATION STUDY

We have given numerical illustration of the results based on simulation study. We calculated the estimates of parameters, bias and confidence limit for parameter, based on generated random sample from IM distribution. The method of estimation MLE and MPS are used to compare the MSE of parameters. Less MSE gives more efficient method of estimation. We generated 10000 random samples for different sizes to find the estimates for each sample and calculated their MSE and bias using formula :

$$MSE = \frac{1}{N} \sum_{i=1}^N (\hat{\alpha}_i - \alpha)^2 \text{ and } bias = \frac{1}{N} \sum_{i=1}^N (\hat{\alpha}_i - \alpha), \quad \text{where } N = 10000$$

R-codes are used to all the numerical computation. To compute the numerical values first we generated a uniform random sample $U = u_1, u_2, u_3, \dots, u_n$ of size n then generated random sample from both distribution by using their quantile function where 'u' is the uniform random sample. For each value of u_i we get x_i . In equation (15) and (37) $W_{-1}()$ is the lambert-W function which is calculated by "lambertWm1()" command from package "lamW" in 'R', Adler [23].

6.1. Simulation study for IM distribution

To generate the random sample from IM distribution, we have used the quantile function equation (15). We used different sample size $n = (15, 25, 50, 75, 100, 125)$ for each true value of parameter $\alpha = (0.3, 0.5, 0.7)$. In Table 2, we have given average value of MLE and MPSE of parameter α along with their respective MSEs, average value of bias, average length of confidence interval (CI) and average of the upper limit (UL) and lower limit (LL) of confidence interval for $\alpha = 0.3, 0.5$, and 0.7 . The output of simulation study is based on Table 2, explained as: for both method of estimation, MSE decreases as the sample size increases. For the small value of shape parameter α , MPSE has

less MSE than MLE only for small sample, and for the large sample, MLE has less MSE than MPSE. From Table 2, it is observed that for large value of α within its range $\alpha \in (0, 1]$, MLE has less MSE than MPSE to all sample size. In the case of MLE, bias is positive for each value of parameter and mostly negative in MPSE method. As usual, the average length of the CI decreases as the sample size increases for both the method MLE and MPSE. In Table 2, somewhere we found that LL of CI and UL of CI is going to outside of range of $\alpha \in (0, 1]$, but IM distribution is defined for only $\alpha \in (0, 1]$. For this we take 0.0000* for $LL < 0$ and 1.0000* for $UL > 1$.

6.2. Simulation study for SIM distribution

To generate the random sample from SIM distribution we have used the quantile function equation (37). We have used different sample size $n = (15, 25, 50, 75, 100, 125)$ for different value of shape parameter α and scale parameter β . All the numerical value of average value of MLE and MPSE of parameter α and β along with their respective MSEs, average value of bias, average length of CI and average of the upper limit (UL) and lower limit (LL) of CI estimates presented in Table [3, 4, 5, 6, 7]. From these Tables, we can observe that MSE of the estimates of shape parameter α and scale parameter β , decreases as the sample size increases in case of MLE as well as in MPSE. At the fixed value of β and small value α , MPSE gives less MSE than MLE. It indicates that MPSE gives better estimates than MLE. For large value of $\alpha \in (0, 1]$ at the same β , MLE gives less MSE than MPSE for all different sample sizes. Length of the CI decreases as the sample size increases in both the cases MLE and MPSE. MLE has mostly positive bias whereas MPSE has mostly negative bias. 0.0000* and 1.0000* defined same as above in section 6.1.

Table 2: MLE and MPS estimate for $\alpha = 0.3, 0.5$ and 0.7

	n	MLE						MPS					
		Est.	bias	MSE	CI			Est.	bias	MSE	CI		
					LL	UL	length				LL	UL	length
$\alpha = 0.3$	15	0.3954	0.0954	0.0497	0.0000*	0.8375	0.8375	0.2827	-0.0173	0.0323	0.0000*	0.7870	0.7870
	25	0.3544	0.0544	0.0307	0.0069	0.7019	0.6950	0.2661	-0.0339	0.0251	0.0000*	0.6493	0.6493
	50	0.3227	0.0227	0.0155	0.0776	0.5679	0.4903	0.2557	-0.0443	0.0152	0.0000*	0.5192	0.5192
	75	0.3149	0.0149	0.0105	0.1161	0.5136	0.3976	0.2624	-0.0376	0.0105	0.0531	0.4716	0.4185
	100	0.3108	0.0108	0.0078	0.1405	0.4811	0.3406	0.2662	-0.0338	0.0087	0.0885	0.4438	0.3554
	125	0.3097	0.0097	0.0060	0.1584	0.4610	0.3026	0.2755	-0.0245	0.0065	0.1194	0.4317	0.3123
$\alpha = 0.5$	15	0.5441	0.0441	0.0371	0.9732	0.1149	0.8583	0.3996	-0.1004	0.0454	0.0000*	0.9135	0.9135
	25	0.5329	0.0329	0.0261	0.8612	0.2046	0.6566	0.4250	-0.0750	0.0321	0.0541	0.7960	0.7419
	50	0.5157	0.0157	0.0133	0.7429	0.2884	0.4545	0.4464	-0.0536	0.0168	0.2025	0.6904	0.4879
	75	0.5098	0.0098	0.0090	0.6943	0.3252	0.3691	0.4545	-0.0455	0.0110	0.2615	0.6476	0.3861
	100	0.5099	0.0099	0.0068	0.6683	0.3515	0.3168	0.4654	-0.0346	0.0082	0.3015	0.6293	0.3278
	125	0.5094	0.0094	0.0054	0.6509	0.3679	0.2830	0.4678	-0.0322	0.0061	0.3219	0.6137	0.2918
$\alpha = 0.7$	15	0.7007	0.0007	0.0253	0.3139	1.0000*	0.6861	0.5485	-0.1515	0.0527	0.0980	0.9990	0.9010
	25	0.7083	0.0083	0.0189	0.4124	1.0000*	0.5876	0.6048	-0.0952	0.0307	0.2790	0.9307	0.6518
	50	0.7097	0.0097	0.0110	0.5028	0.9165	0.4137	0.6435	-0.0565	0.0143	0.4256	0.8614	0.4357
	75	0.7079	0.0079	0.0076	0.5389	0.8769	0.3380	0.6558	-0.0442	0.0098	0.4802	0.8313	0.3511
	100	0.7079	0.0079	0.0056	0.5614	0.8543	0.2928	0.6678	-0.0322	0.0065	0.5173	0.8183	0.3011
	125	0.7041	0.0041	0.0042	0.5731	0.8350	0.2618	0.6732	-0.0268	0.0051	0.5392	0.8073	0.2681

Est.: Estimate; MSE: Mean Square Error; CI: Confidence interval; UL: Upper limit; LL: Lower limit.

Table 3: MLE and MPS estimate for $\alpha = 0.3$ and $\beta = 2$

	n	MLE						MPS					
		Est.	bias	MSE	CI			Est.	bias	MSE	CI		
					UL	LL	length				UL	LL	length
$\alpha = 0.3$	15	0.4302	0.1302	0.0606	0.8548	0.0056	0.8492	0.3325	0.0325	0.0386	0.8613	0.0000*	0.8613
	25	0.3856	0.0856	0.0369	0.7171	0.0540	0.6630	0.3128	0.0128	0.0268	0.7014	0.0000*	0.7014
	50	0.3422	0.0422	0.0181	0.5782	0.1063	0.4719	0.2886	-0.0114	0.0156	0.5496	0.0276	0.5220
	75	0.3254	0.0254	0.0113	0.5184	0.1324	0.3861	0.2887	-0.0113	0.0105	0.4960	0.0815	0.4146
	100	0.3219	0.0219	0.0085	0.4888	0.1549	0.3339	0.2774	-0.0226	0.0075	0.4552	0.0997	0.3555
	125	0.3224	0.0224	0.0077	0.4716	0.1733	0.2983	0.2937	-0.0063	0.0070	0.4500	0.1373	0.3127
$\beta = 2$	15	2.0570	0.0570	0.1831	2.7382	1.3758	1.3624	1.9418	-0.0582	0.1756	2.6697	1.2139	1.4558
	25	2.0256	0.0256	0.1004	2.5621	1.4890	1.0730	1.9670	-0.0330	0.0881	2.5401	1.3940	1.1460
	50	2.0114	0.0114	0.0499	2.3998	1.6229	0.7769	1.9697	-0.0303	0.0437	2.3773	1.5621	0.8152
	75	2.0082	0.0082	0.0328	2.3284	1.6879	0.6405	1.9694	-0.0306	0.0304	2.2993	1.6395	0.6598
	100	2.0112	0.0112	0.0243	2.2892	1.7332	0.5560	1.9750	-0.0250	0.0247	2.2636	1.6864	0.5771
	125	1.9968	-0.0032	0.0185	2.2433	1.7503	0.4929	1.9732	-0.0268	0.0193	2.2262	1.7203	0.5058

Table 4: MLE and MPS estimate for $\alpha = 0.5$ and $\beta = 2$

	n	MLE						MPS					
		Est.	bias	MSE	CI			Est.	bias	MSE	CI		
					UL	LL	length				UL	LL	length
$\alpha = 0.5$	15	0.5675	0.0675	0.0432	0.9683	0.1668	0.8015	0.4415	-0.0585	0.0417	0.9266	0.0000*	0.9266
	25	0.5524	0.0524	0.0317	0.8630	0.2417	0.6213	0.4630	-0.0370	0.0288	0.8150	0.1110	0.7040
	50	0.5315	0.0315	0.0172	0.7520	0.3110	0.4411	0.4776	-0.0224	0.0162	0.7138	0.2413	0.4724
	75	0.5163	0.0163	0.0108	0.6971	0.3354	0.3617	0.4740	-0.0260	0.0109	0.6641	0.2839	0.3802
	100	0.5171	0.0171	0.0087	0.6736	0.3606	0.3130	0.4833	-0.0167	0.0084	0.6459	0.3207	0.3252
	125	0.5123	0.0123	0.0070	0.6525	0.3721	0.2804	0.4833	-0.0167	0.0065	0.6280	0.3387	0.2893
$\beta = 2$	15	2.0673	0.0673	0.1349	2.6636	1.4710	1.1926	1.9923	-0.0077	0.1134	2.6630	1.3216	1.3414
	25	2.0262	0.0262	0.0766	2.4799	1.5725	0.9074	1.9826	-0.0174	0.0797	2.4791	1.4860	0.9931
	50	2.0042	0.0042	0.0347	2.3231	1.6854	0.6377	1.9838	-0.0162	0.0332	2.3209	1.6466	0.6743
	75	2.0093	0.0093	0.0236	2.2724	1.7463	0.5261	1.9884	-0.0116	0.0231	2.2624	1.7144	0.5480
	100	2.0038	0.0038	0.0172	2.2303	1.7774	0.4529	1.9930	-0.0070	0.0180	2.2275	1.7584	0.4691
	125	2.0014	0.0014	0.0143	2.2043	1.7985	0.4058	1.9917	-0.0083	0.0170	2.2007	1.7826	0.4180

Table 5: MLE and MPS estimate for $\alpha = 0.7$ and $\beta = 2$

	n	MLE						MPS					
		Est.	bias	MSE	CI			Est.	bias	MSE	CI		
					UL	LL	length				UL	LL	length
$\alpha=0.7$	15	0.7055	0.0055	0.0289	1.0000*	0.3277	0.6723	0.5808	-0.1192	0.0437	1.0000*	0.1437	0.8563
	25	0.7167	0.0167	0.0218	1.0000	0.4270	0.5730	0.6253	-0.0747	0.0269	0.9437	0.3068	0.6369
	50	0.7187	0.0187	0.0142	0.9237	0.5138	0.4099	0.6600	-0.0400	0.0149	0.8762	0.4438	0.4324
	75	0.7118	0.0118	0.0097	0.8795	0.5440	0.3355	0.6717	-0.0283	0.0100	0.8457	0.4977	0.3480
	100	0.7111	0.0111	0.0077	0.8566	0.5656	0.2910	0.6786	-0.0214	0.0080	0.8283	0.5289	0.2994
	125	0.7089	0.0089	0.0059	0.8393	0.5784	0.2609	0.6795	-0.0205	0.0061	0.8131	0.5458	0.2673
$\beta=2$	15	2.0806	0.0806	0.1020	2.6046	1.5566	1.0480	2.0263	0.0263	0.0918	2.6177	1.4349	1.1828
	25	2.0385	0.0385	0.0566	2.4285	1.6486	0.7799	2.0085	0.0085	0.0578	2.4347	1.5824	0.8523
	50	2.0078	0.0078	0.0257	2.2763	1.7392	0.5370	1.9905	-0.0095	0.0235	2.2740	1.7071	0.5669
	75	2.0117	0.0117	0.0185	2.2317	1.7916	0.4401	2.0021	0.0021	0.0181	2.2307	1.7736	0.4571
	100	2.0037	0.0037	0.0132	2.1932	1.8141	0.3790	1.9980	-0.0020	0.0135	2.1935	1.8024	0.3911
	125	2.0063	0.0063	0.0106	2.1761	1.8366	0.3395	2.0005	0.0005	0.0119	2.1750	1.8260	0.3490

Table 6: MLE and MPS estimate for $\alpha = 0.3$ and $\beta = 5$

	n	MLE						MPS					
		Est.	bias	MSE	CI			Est.	bias	MSE	CI		
					UL	LL	length				UL	LL	length
$\alpha=0.3$	15	0.4282	0.1282	0.0589	0.8552	0.0012	0.8540	0.3231	0.0231	0.0375	0.8626	0.0000*	0.8626
	25	0.3846	0.0846	0.0383	0.7175	0.0517	0.6658	0.2996	-0.0004	0.0282	0.6955	0.0000*	0.6955
	50	0.3452	0.0452	0.0188	0.5815	0.1090	0.4725	0.2840	-0.0160	0.0169	0.5469	0.0211	0.5258
	75	0.3359	0.0359	0.0119	0.5284	0.1434	0.3850	0.2880	-0.0120	0.0117	0.4960	0.0801	0.4159
	100	0.3265	0.0265	0.0085	0.4933	0.1597	0.3336	0.2967	-0.0033	0.0089	0.4732	0.1202	0.3530
	125	0.3161	0.0161	0.0061	0.4657	0.1666	0.2991	0.2896	-0.0104	0.0070	0.4464	0.1328	0.3136
$\beta=5$	15	5.0498	0.0498	0.9296	6.7910	3.3085	3.4825	4.7917	-0.2083	0.8598	6.6624	2.9209	3.7415
	25	5.0434	0.0434	0.6235	6.4279	3.6589	2.7690	4.8389	-0.1611	0.5573	6.3059	3.3719	2.9340
	50	5.0169	0.0169	0.3575	6.0060	4.0279	1.9781	4.8789	-0.1211	0.3539	5.9168	3.8409	2.0759
	75	5.0488	0.0488	0.2548	5.8586	4.2390	1.6196	4.9499	-0.0501	0.2534	5.7944	4.1053	1.6891
	100	5.0276	0.0276	0.2150	5.7291	4.3261	1.4030	4.9380	-0.0620	0.2150	5.6565	4.2196	1.4369
	125	5.0530	0.0530	0.1917	5.6877	4.4183	1.2694	4.9720	-0.0280	0.1821	5.6200	4.3240	1.2960

Table 7: MLE and MPS estimate for $\alpha = 0.3$ and $\beta = 10$

	n	MLE						MPS					
		Est.	bias	MSE	CI			Est.	bias	MSE	CI		
					UL	LL	length				UL	LL	length
$\alpha=0.3$	15	0.4349	0.1349	0.0623	0.8606	0.0092	0.8514	0.3290	0.0290	0.0377	0.8659	0.0000*	0.8659
	25	0.3855	0.0855	0.0389	0.7182	0.0528	0.6654	0.3053	0.0053	0.0284	0.6994	0.0000*	0.6994
	50	0.3503	0.0503	0.0197	0.5860	0.1146	0.4714	0.2899	-0.0101	0.0173	0.5521	0.0277	0.5244
	75	0.3424	0.0424	0.0121	0.5344	0.1504	0.3840	0.2998	-0.0002	0.0120	0.5065	0.0931	0.4134
	100	0.3273	0.0273	0.0086	0.4941	0.1605	0.3336	0.3002	0.0002	0.0093	0.4765	0.1240	0.3525
	125	0.3237	0.0237	0.0070	0.4728	0.1745	0.2983	0.2916	-0.0084	0.0062	0.4482	0.1350	0.3132
$\beta=10$	15	9.9635	-0.0365	3.4750	13.3824	6.5447	6.8377	9.4550	-0.5450	3.4249	13.1285	5.7816	7.3469
	25	10.0247	0.0247	2.6036	12.7796	7.2697	5.5099	9.5618	-0.4382	2.4351	12.4525	6.6711	5.7814
	50	9.9386	-0.0614	1.5441	11.8934	7.9838	3.9096	9.6508	-0.3492	1.5991	11.6994	7.6022	4.0972
	75	10.0207	0.0207	1.1687	11.6192	8.4223	3.1969	9.7578	-0.2422	1.2321	11.4079	8.1076	3.3003
	100	10.0328	0.0328	1.0610	11.4341	8.6315	2.8026	9.7869	-0.2131	1.0286	11.2072	8.3667	2.8405
	125	10.0279	0.0279	0.8687	11.2806	8.7752	2.5054	9.8581	-0.1419	0.8287	11.1387	8.5774	2.5613

7. REAL DATA ANALYSIS

The real data have been used to show the applicability of the SIM distribution. The results show this model is more appropriate than some other fitted model for this data. The data represent the active repair time (in hrs.) for airborne communication transceiver given in Jorgensen [24]. The data is given as below:

0.50	0.60	0.60	0.70	0.70	0.70	0.80	0.80
1.00	1.00	1.00	1.00	1.10	1.30	1.50	1.50
1.50	1.50	2.00	2.00	2.20	2.50	2.70	3.00
3.00	3.30	4.00	4.00	4.50	4.70	5.00	5.40
5.40	7.00	7.50	8.80	9.00	10.20	22.00	24.50

For the fitting of above real data to the proposed model we used Kolmogorov–Smirnov test (K–S test). In order to compare the models we used negative log-likelihood function define as $-\log L(\hat{\alpha}, \hat{\beta})$ values, Akaike information criteria (AIC) values defined by $AIC = -2\log(L) + 2q$ and Bayesian information criterion (BIC) values defined $BIC = -2\log(L) + q \cdot \log(n)$ by BIC where, $\hat{\alpha}_{ml}$, $\hat{\beta}_{ml}$ are the estimates of parameter α and β by using MLE method, q is the number of parameters and n is the sample size. The best fitted distribution is that distribution which gives the lower values of $-\log(L)$, AIC and BIC.

From the Table 8 it is obtained that SIM distribution give best fit among some other popular distributions. And the MLE of parameters of SIM and some other distributions given in Table 9. Figure 3 shows that empirical cdf and fitted cdf plot for SIM and some other distributions.

Table 8: Comparison criterion values for different distribution.

Model	AIC	BIC	$-\log(L)$	k-s statistic	p-value
SIMD ($x; \alpha, \beta$)	182.6664	182.3504	89.3332	0.0869	0.9231
EPLD ($x; \alpha, \beta, \theta$)	186.5721	191.6387	90.2861	0.0909	0.8627
PLD ($x; \beta, \theta$)	195.8854	199.2631	95.9427	0.1346	0.4637
GLD ($x; \alpha, \theta$)	199.8218	203.1995	97.9107	0.1660	0.2201

SIMD:Scaled inverse Muth distribution; **EPLD:** Exponentiated power Lindley distribution; **PLD:** Power Lindley distribution; **GLD:** Generalized Lindley distribution.

Table 9: MLE for the parameters of different distributions.

Model	θ	β	α
SIMD ($x; \alpha, \beta$)	-	1.5464	0.2630
EPLD ($x; \alpha, \beta, \theta$)	3.5472	0.2901	30.8299
PLD ($x; \beta, \theta$)	0.5867	0.7988	-
GLD ($x; \alpha, \theta$)	0.3588	-	0.7460

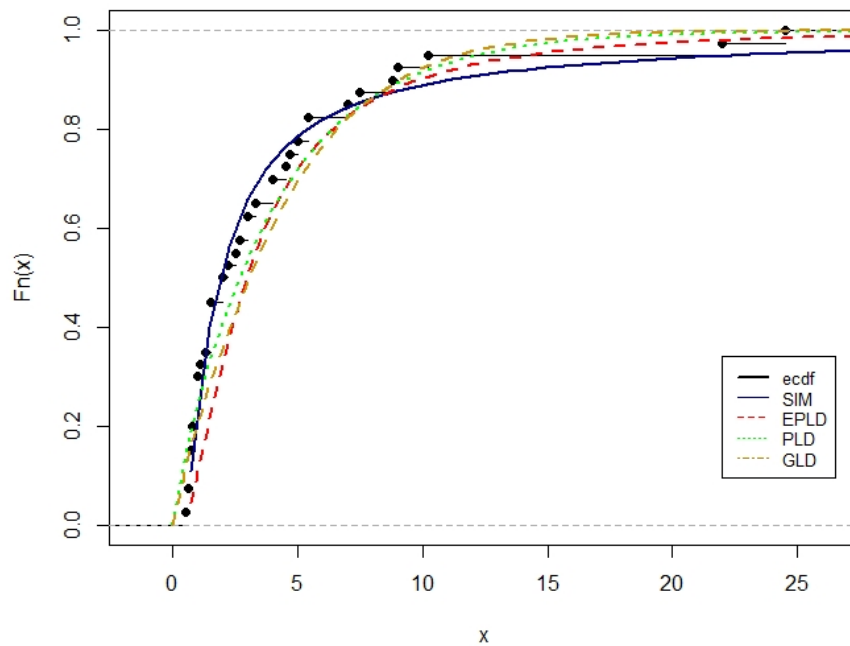


Figure 3: Empirical cdf and fitted cdf plot.

ACKNOWLEDGEMENT

Authors are deeply indebted to the Editor-in-Chief (Rykov Vladimir) and anonymous referees for their valuable suggestions to improve the quality of the original manuscript. Agni Saroj acknowledges research fellowship (373/NFSCJUNE2019) from UGC, New Delhi.

REFERENCES

- [1] Martz, H. F., & Waller, R. (1982). Bayesian Reliability Analysis. JOHN WILEY & SONS, INC., 605 THIRD AVE., NEW YORK, NY 10158, 1982, 704.
- [2] Bennett, S. (1983). Log-logistic regression models for survival data. *Journal of the Royal Statistical Society: Series C (Applied Statistics)*, 32(2), 165-171.
- [3] Langlands, A. O., Pocock, S. J., Kerr, G. R., & Gore, S. M. (1979). Long-term survival of patients with breast cancer: a study of the curability of the disease. *Br med J*, 2(6200), 1247-1251.
- [4] Sharma, V. K., Singh, S. K., & Singh, U. (2014). A new upside-down bathtub shaped hazard rate model for survival data analysis. *Applied Mathematics and Computation*, 239, 242-253.
- [5] Muth, E. J. (1977). Reliability models with positive memory derived from the mean residual life function. *Theory and applications of reliability*, 2, 401-436.
- [6] Jodra, P., Jimenez-Gamero, M. D., & Alba-Fernandez, M. V. (2015). On the Muth distribution. *Mathematical Modelling and Analysis*, 20(3), 291-310.
- [7] Jodra, P., Gomez, H. W., Jimenez-Gamero, M. D., & Alba-Fernandez, M. V. (2017). The power Muth distribution. *Mathematical Modelling and Analysis*, 22(2), 186-201.
- [8] Irshad, M. R., Maya, R., & Krishna, A. (2021). Exponentiated Power Muth Distribution and Associated Inference. *Journal of the Indian Society for Probability and Statistics*, 22(2), 265-302.
- [9] Chesneau, C., & Agiwal, V. (2021). Statistical theory and practice of the inverse power Muth distribution. *Journal of Computational Mathematics and Data Science*, 1, 100004.
- [10] Almarashi, A. M., & Elgarhy, M. (2018). A new muth generated family of distributions with applications. *J. Nonlinear Sci. Appl*, 11, 1171-1184.
- [11] Al-Babtain, A. A., Elbatal, I., Chesneau, C., & Jamal, F. (2020). The transmuted Muth generated class of distributions with applications. *Symmetry*, 12(10), 1677.
- [12] Bicer, C., Bakouch, H. S., & Bicer, H. D. (2021). Inference on Parameters of a Geometric Process with Scaled Muth Distribution. *Fluctuation and Noise Letters*, 20(01), 2150006.
- [13] Corless, R. M., Gonnet, G. H., Hare, D. E., Jeffrey, D. J., & Knuth, D. E. (1996). On the LambertW function. *Advances in Computational mathematics*, 5(1), 329-359.
- [14] Jodra, P. (2010). Computer generation of random variables with Lindley or Poisson-Lindley distribution via the Lambert W function. *Mathematics and Computers in Simulation*, 81(4), 851-859.
- [15] Gilchrist, W. (2000). Statistical modelling with quantile functions. Chapman and Hall/CRC.
- [16] Cheng, R. C. H., & Amin, N. A. K. (1983). Estimating parameters in continuous univariate distributions with a shifted origin. *Journal of the Royal Statistical Society: Series B (Methodological)*, 45(3), 394-403.
- [17] Ranney, B. (1984). The maximum spacing method. An estimation method related to the maximum likelihood method. *Scandinavian Journal of Statistics*, 93-112.
- [18] Cheng, R. C. H., & Traylor, L. (1995). Non-regular maximum likelihood problems. *Journal of the Royal Statistical Society: Series B (Methodological)*, 57(1), 3-24.
- [19] Pitman, E. J. (1979). Some basic theory for statistical inference (vol. 7). Chapman and Hall, London.
- [20] Ghosh, K., & Jammalamadaka, S. R. (2001). A general estimation method using spacings. *Journal of Statistical Planning and Inference*, 93(1-2), 71-82.
- [21] Anatolyev, S., & Kosenok, G. (2005). An alternative to maximum likelihood based on spacings. *Econometric Theory*, 21(2), 472-476.
- [22] Singh, U., Singh, S. K., & Singh, R. K. (2014). A comparative study of traditional estimation methods and maximum product spacings method in generalized inverted exponential distribution. *Journal of Statistics Applications & Probability*, 3(2), 153.
- [23] Adler, A. (2017). lamW: Lambert-W function, R package version 1.3.0.
- [24] Jorgensen, B. (1982). Statistical properties of the generalized inverse Gaussian distribution (Vol. 9). Springer.

Hybrid Deep Resnet With Inception Model For Optical Character Recognition In Gujarati Language

^{*1}Mr. Sanket B. Suthar, ²Dr. Amit R. Thakkar

^{*1}Department of Information Technology,
Chandubhai S. Patel Institute of Technology (CSPIT),
Faculty of technology & Engineering (FTE),
Charotar University of science and Technology (CHARUSAT), Changa, Anand, India.
*Email: bsutharsanket@gmail.com

²Department of Information Technology,
Chandubhai S. Patel Institute of Technology (CSPIT),
Faculty of technology & Engineering (FTE),
Charotar University of science and Technology (CHARUSAT), Changa, Anand, India.
Email:amitrthakkar6@gmail.com

Abstract

In the Optical Character Recognition (OCR) system, achieving high recognition performance is important. OCR and visual perception are affected by the inclined characters in each language. Deep learning methods play an important role in the OCR field, which can outperform humans with higher recognition performance. So, in this research, a hybrid deep learning technique is applied to recognize the Gujarati language characters. Initially, Gujarati characters collected from different sources are pre-processed using different techniques. Adaptive Weiner Filter (AWF) is used for noise removal, Binarization, and contrast enhancement is done by Contrast Limited Adaptive Histogram Equalization (CLAHE) method. Finally, a hybrid deep ResNet with Inception model (GoogleNet) is suggested to perform character recognition in the Gujarati language. This hybrid architecture also performs feature extraction tasks, considered a major task in OCR. Python tool is utilized to illustrate the proposed methodology and solve the mathematical model. Scanned documents containing Gujarati characters are engaged to evaluate the robustness of the proposed methodology. Using various performance parameters, the influence of the proposed methodology is examined and its results compared with various deep learning algorithms.

Index terms: Gujarati language, Optical character recognition (OCR), pre-processing, adaptive filtering, Hybrid deep learning algorithms.

I. Introduction

Demand for handheld gadgets is increasing quickly with time in the digitization world. Handheld gadgets also require an efficient and easy tool to input the data. Input using a standard keyboard obliges time and determination, mostly for Indian scripts. Because, they have a huge complex character set that makes the input system difficult to use a normal keyboard [1]. With a simple keyboard, tiny handheld gadgets have a lot of benefits using online words identification system. In India, the Gujarati language belongs to the Devnagari family of languages, and it is instigated in the western state of India

that is Gujarat. Fifty million people of the state speak this language. It is a widely spoken language and has inherited rich cultural and literature properties, but few types of research only concentrate on identifying Gujarati characters from handwritten documents [2, 3]. There are several numbers of handwritten and printed documents available in Gujarati script, and it is essential to preserve those pamphlets in digital format from an efficient distribution and legal and historical perspective [4].

Scanning is considered one of the best methods to transform pamphlets into a digital layout. Still, searching, retrieving and editing the information in a scanned document is considered another difficult task [5]. It is an important task to retrieve the data from the scanned pamphlet. Recognition based and recognition free methods are two important techniques used to retrieve any information from the document [6]. OCR system [7] is a recognition-based method that transforms document images into readable text format. For various Indian regional scripts like Tamil, Malayalam, Telugu, Kannada, Oriya, Bangla, Devanagari and Gurumuki, a small amount of research related to character recognition has been carried out [8]. Researchers are looking forward to inventing new methods for accurately identifying the characters due to the demand for low-cost OCR systems [9, 10]. This paper concentrates on the identification of optical characters in the Gujarati language.

There are only very few works in the literature on the recognition of Gujarati language scripts [11]. In previous years, machine learning methods and conventional pattern recognition approaches have been used in the OCR framework. But, it requires an efficient method to satisfy the need and requirements of users to enhance the marketability of the OCR system using efficiency and economy [12, 13]. Several methods and techniques are used to find the best OCR system to achieve a better recognition rate. Since the last few years, machine learning and deep learning methods have emerged as promising solutions for these OCR problems. Due to the satisfactory results in this area, researchers are making several efforts to extend deep learning architectures [14, 15].

A major objective of this study is to make a structure that automatically identifies the optical characters from a set of scanned documents. Major contributions of this research are defined as follows:

- To perform the different pre-processing methods to make character recognition tasks very simple.
- To design a hybrid deep learning technique that can efficiently recognize a Gujarati character with maximum recognition accuracy.
- To reduce the computational complexity of this entire system by performing a recognition process using a hybrid deep learning algorithm.

The remaining section of this research is ordered as follows: Section 1 introduces the Gujarati language and the advantage of using the OCR framework. Section 2 depicts recent work related to our research methodology and problems in previous research. The proposed methodology is elaborated in section 3. Section 4 illustrates simulation outcomes and considerations of the proposed methodology, and Section 5 provides the conclusion and future enhancement of our research work.

II. Literature review

Generally, the electronic document analysis framework widely uses OCR for character identification. This method has been very useful for extracting text from a scanned document or image and is used in image processing, Natural language processing and pattern recognition. Rakesh Kumar Sethi and Kalyan Kumar Mohanty [16] developed a deep learning technique for optical Odia character classification. There was little progress in handwriting character recognition (HCR) for a small vocabulary for neatly hand-typed characters and new line isolated words. Moreover, a small amount of research work had been done on Odia's character recognition process. In this article, different transfer learning methods like VGG16 and ResNet 50 were utilized to perform the character recognition process, and the performance was compared with existing CNN based techniques.

Ambadas Shinde and Yogesh Dandawate [17] developed a convolutional neural network architecture for handwritten based Marathi text identification. Different authors performed character recognition by different techniques. In computer vision, deep learning algorithms were considered an important technique that correctly predicts the scanned document's characters. In general, handwritten Devanagari characters were considered difficult to identify, which was overcome with the help of deep learning methods. In this article, manually written Marathi words have been precisely identified using an OCR system based on a Convolutional Neural Network (CNN). Also, manually written Devanagari text written in the Marathi language was obtained by developing a character segmentation free technique that replicates the perceived words in printed form.

The Gujarati language normally contains many confusing characters that lead to misclassification. Vishal A. Naik and Apurva A. Desai [18] for online handwritten Gujarati character recognition. So, the classification accuracy of confusing characters was increased with the multi-layer classification method. Initially, training was performed by the polynomial kernel using Support Vector Machine (SVM) in the first classification layer. In the second layer, SVM with linear kernel was utilized to classify confusing letters when the first layer returns a letter with some letters on training data. Finally, both layers perform classification using features obtained from a hybrid feature set that contains dominant point and zoning features based on regularized chain code features.

Optimized Self-Organizing Map (SOM) network was developed by Om Prakash Jena et al. [19] to recognize printed Odia characters and digits. For Odia language, the SOM network was created to build up an OCR framework that effectively performs the character identification task. Some characteristics like shape, different content styles, subordinate conditions of characters and their context make challenges in the Odia character recognition framework. The proposed SOM network was advanced with certain structural features like height, cross-section, width, and end points to obtain 97.55% recognition accuracy.

Dibyasundar Das et al. [20] developed a multi-objective Jaya Convolutional Network (MJCN) for handwritten OCR. This technique tries to learn significant features directly from the images. This MJCN technique contained a convolution layer, an activation layer, a multiplication layer and had a multi-objective Jaya Optimizer (MJO). Over a local neighbourhood connection, the convolution layer explores significant patterns in an image, and the multiplication layer develops the convolutional response to a more compact feature space. MJO algorithm was utilized to optimize the initial weight value in the network. Minimizing intra-class variance and maximising inter-class distance were the main objectives of the MJO algorithm. Standard classifiers were used to recognize the characters from different datasets.

III. Proposed methodology

In the script of Gujarathi, nearly 34 consonants and 12 vowels are available, and such consonants are termed as Vyanjan and Vowels are called Swar. In this proposed work, the own datasets are collected from the vowels and consonants of the Gujarathi language. In which, OCR is necessary for understanding such data to both machinery and humans. Besides, OCR is considered superior, and this is because; process controlling during data production is not required in it. This also suppresses the issue of the identification of optically processed characters. Both the printed and the handwritten characters are verified by OCR. However, the input data quality mainly decides its overall performance. To classify a similar set of characters from the wide data varieties, a classifier is necessary. The ResNet and Inception model is considered a superior method for classifying similar sets. The Gujarati characters are classified in this research work by hybridising such approaches. Figure 1 represents the phases tangled in the proposed technique.

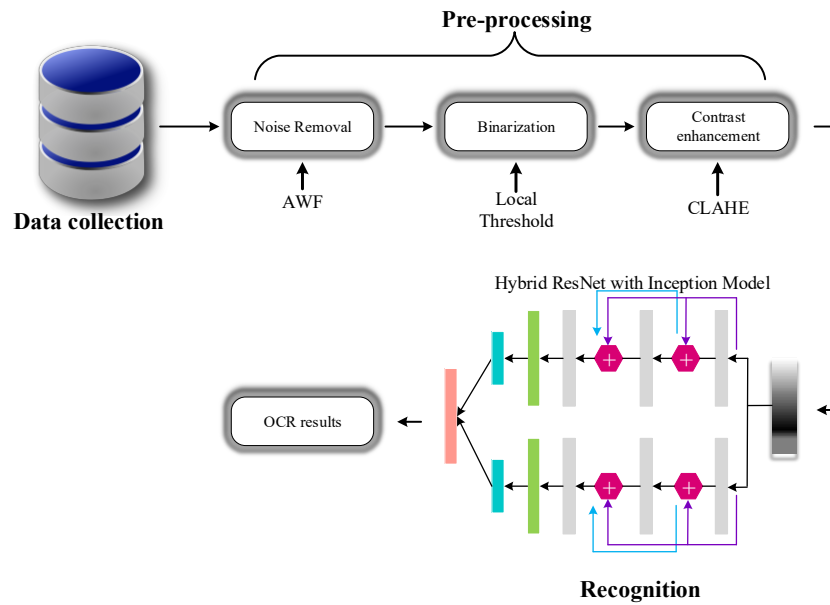


Figure 1: Workflow of the proposed methodology

This research focuses on offline OCR using a collection of Printed (laser and Machine printed) Gujarati characters from different sources like magazines, newspapers and books, etc. Initially, the dataset is pre-processed using different methods like noise removal technique using Adaptive Wiener Filter (AWF), Binarization, and Contrast Limited Adaptive Histogram Equalization (CLAHE) technique for contrast improvement. After that, the classification approach is done with the help of hybrid deep ResNet with Inception model (GoogleNet) architecture, which significantly achieves better recognition accuracy on poor quality text images. This hybrid algorithm can perform better classification results than any other conventional technique.

I. Pre-processing

After data acquisition, it should be properly pre-processed with different techniques. In some cases, the collected data is of poor quality due to the blurred image. So, pre-processing phase is essential to remove noise and variability in the input image. Different kinds of pre-processing methods like noise removal, Binarization, skew detection and correction, and image contrast enhancement are done with the help of different techniques. The character recognition task becomes simpler with a pre-processed image that organizes the image in a correct format [21].

A. Noise removal

Wiener filtering is assumed as one of the best methods to eliminate noise from digital images. Based on a local variance of the image, AWF [22] modifies the output of the filter. The main goal of this method is to minimize the mean square error between the original image and the reconstructed image. Compared to previous filtering techniques, this filtering is very useful to preserve the edges and high-frequency area of the images. In this filtering, some adjustments are created to make the image better. Various window alternatives are applied to deal with different situations and automatically pick the best one. At smooth areas, center sample in the moving window must be ignored to suppress intuitively annoying singularities, but properly utilized in uneven areas. Before performing the AWF method, the images from the datasets are initially transformed into grey scale images.

The AWF is given in equation (1), for a particular pixel location (a_1, a_2)

$$AWF[I(a_1, a_2)] = \mu + \frac{\sigma^2 - \sigma_n^2}{\sigma^2} (I(a_1, a_2) - \mu) \quad (1)$$

where, input image is denoted as I , mean μ and variance (σ^2) are calculated from the set \mathfrak{N} of $(N * M)$ local neighborhood of every single pixel. Hence,

$$\mu = \frac{1}{MN} \sum_{a_1, a_2 \in \mathfrak{N}} I(a_1, a_2) \quad (2)$$

$$\sigma^2 = \frac{1}{MN} \sum_{a_1, a_2 \in \mathfrak{N}} I^2(a_1, a_2) - \mu^2 \quad (3)$$

In addition, the variance of noise is denoted as σ_n .

B. Binarization

In the character recognition task, binarization is considered an important phase. Several amounts of binarization methods are available in previous research in which most of them are utilized for a particular image type. The major objective of this technique is to preserve significant data and reduce the amount of information present in the image. Overall threshold and local threshold are two different classes presented in the gray scale images. In overall threshold, single threshold is utilized in a whole image to create background class and text, while threshold values are determined locally (pixel-by-pixel or area-by-area) in local threshold. Given below expression is used to compute threshold Th of every single pixel locally.

$$Th = (1-k)m + k.m + k \frac{\sigma}{R(m-M)} \quad (4)$$

Here, minimum image grey level is mentioned by M , a standard deviation of all pixels in window is denoted as σ , an average of whole pixels in the window is mentioned by (m, R) mentions the maximum deviation of grayscale on all windows and k is set to 0.5 [23].

C. Contrast enhancement

An enhancement function is offered to all the neighborhood pixels, and a transformation function is acquired from that corresponding pixels. CLAHE [24] method is exploited to maximize the image's contrast. The stages of CLAHE method is explained below:

Stage 1: Input image

Stage 2: Clip limit, distribution parameter type, dynamic range (number of bins in histogram transform function), and number of regions from column and row direction are considered as input data.

Stage 3: Original image is separated into a number of regions.

Stage 4: In tile (i.e. contextual region), apply the process.

Stage 5: Clipped histogram and Gray level mapping are created. Whole pixels of contextual regions are equally distributed in every single gray level. The average number of pixels in a gray level image is represented by the given below expression.

$$M_a = \frac{M_x * M_y}{M_g} \quad (5)$$

Here, M_a mentions the average number of pixels, M_g represents the contextual area in the total gray level, total pixels in direction X and Y of the contextual region is mentioned by M_x , and M_y respectively, finally, M_{CL} and M_{clip} denotes the clip limit and the total number of clips respectively. Given below expression is used to compute the actual clip limit.

$$M_{CL} = M_{clip} * M_a \quad (6)$$

Stage 6:For creating an enhanced image, introduce the gray level mapping. This process exploits four different pixel clusters and applies a mapping function to overlap every single drawing slate over the partially sliced images. This entire process is replicated to accomplish the desired result, which gives improved pixels on image.

II. Recognition

In this research, the Gujarati character identification method is done with the help of a hybrid algorithm, which integrates two different deep learning algorithms like CNN. Different convolution and subsampling layers are tracked by more than one fully connected layer. Normally, a fully connected layer is considered a usual multilayer neural network, and it clasps output which is defined as class score. The input image is convolved by the convolutional layers, which utilize several filters (learnable weights) to convolve the image and the pooling layer down samples the image. Average pooling and max pooling are two different kinds of functions in the pooling layer. CNN converts input images over different stacked layers from original pixels to obtain the final class score. Also, CNN structures are used as building blocks for different semantic segmentation models. In our work, two different deep learning algorithms named ResNet [25] and Inception (GoogLeNet)[26]model are hybridized to perform character recognition in the Gujarati language. Description of ResNet and Inception model are explained in the next section.

A. ResNet

In 2016, Microsoft researchers developed ResNet model, which achieved 96.4% classification accuracy and won the ImageNet Large Scale Visual Recognition Competition (ILSVRC). This network contains 152 deep layers and contains a unique structure that presents residual blocks as shown in figure 2.

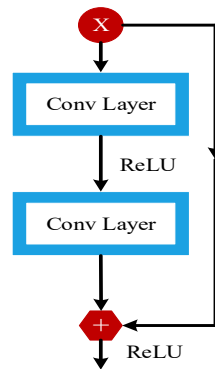


Figure 2: Basic structure of a deep residual network

It also utilize identity skip connections to discourse the problem of training a deep structure. The residual block's function is to copy the input of layers and forwards them into a subsequent layer. The vanishing gradient problem is exceeded with the help of identity skip connection in which an upcoming layer learns something different from the familiar input.

B. Inception model

In 2014, Google researchers developed the GoogleNet architecture, also known as the Inception model. This design won ILSVRC as a top-five with 93.3% classification accuracy. It contains 22 layers and introduces a building block named as Inception model. It does not follow the usual consecutive procedure. However, it exploits the network layer, pooling layer, and large and small convolution layers that are calculated in parallel. For dimensionality reduction, a 1x1 convolution operation is

performed by the convolution layers. By saving memory and computational cost, dimensionality reduction and parallelism process significantly minimize the number of parameters and operations. The building blocks of the core Inception model is displayed in the given below figure 3.

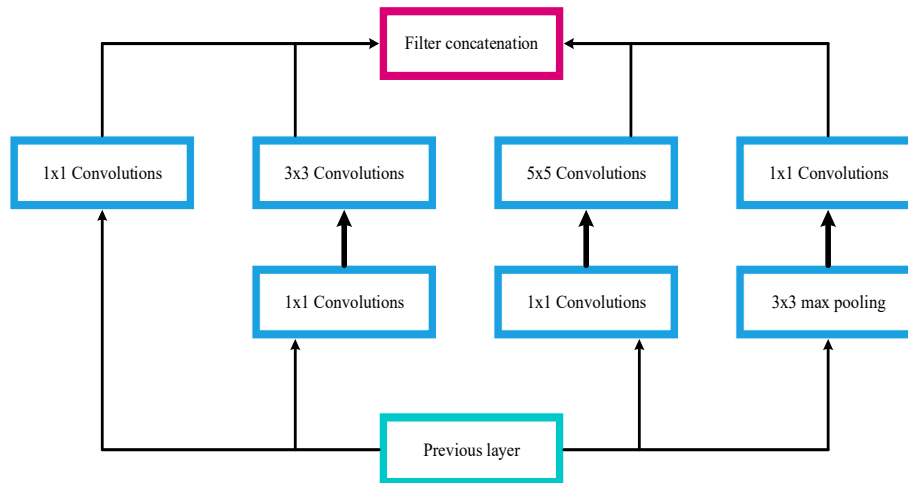


Figure 3: Core blocks in Inception module

C. Hybrid ResNet with Inception model for character recognition

This research combines the benefits of both ResNet and Inception models to improve the classification accuracy of Gujarati characters recognition with this proposed hybrid model. The inception model and residual network demonstrate their capability to increase thousands of layers by offering better performance as well as enhanced efficiency. Many residual blocks with identity mapping are presented in the residual network, and several convolution layers are presented in the deep convolution network named as Inception model. This Gujarati character recognition aims to recognize the character type by allocating and tagging separate pixels with several frequency bands into separate modules. A deep hybrid network structure is developed in this research to absorb deep features of Gujarati characters also offer better recognition accuracy performance without many pre-processing steps. The hybrid structure contains three convolutional layers and one average pooling layer. Outputs of every single layer form the input to every single, consecutive layer. Also, only one fully connected cascaded residual block is presented in the network, which is shown in figure 4.

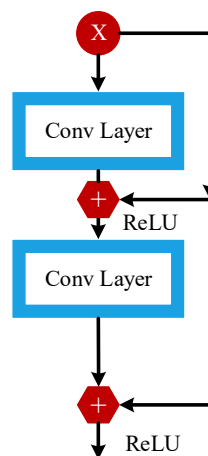


Figure 4: Residual block with fully connected cascaded layers (changed type)

Every convolutional layer accepts inputs from all preceding convolutional layers in the residual model. For our work, three convolutional layers are enough. Generally, the convolution operation is applied to the input data by convolutional layers, and the pooling operation is applied by the average pooling layer in a hybrid model. Also, these operations are performed before feeding data to the classifier. The Adam optimisation algorithm optimises the network model for its faster convergence speed. Also, this technique is a computationally effective one and less complex to sound. For our collected data, the batch size is set to 17, and the initial learning rate is 0.001. Figure 5 demonstrates the general scheme for combined Inception-ResNet modules.

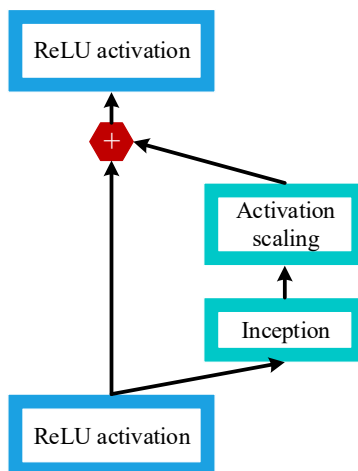


Figure 5: The general schema for scaling combined Inception-ResNet modules.

Convolutional layers

After performing convolution operations to the input image, it transforms the image by rectified linear unit (ReLU) function. Three convolutional layers are utilized in which everyone has nine filters making nine feature maps. Given below, expression (7) expresses each kernel's operation.

$$X^i = \varphi(W^i * X^{i-1} + \beta^i) \quad (7)$$

Here, $*$ is a convolution operator that convolves the filter W^i with the input data X^{i-1} adds the bias term β^i and then applies the rectifier function φ and yields the feature map X^i . The size of the convolutional filter is sixteen units, in which every single layer uses nine filters in the proposed hybrid model. Input is padded by each filter where the output has the same dimensions as the input tensor. The length of the convolution stride is 1. The glorot uniform weight initialization method is utilized in the convolution layers to initialize the weight, and the bias terms are initialized with 0. An element-wise operation is applied by ReLU activation function φ on the input data x , which is defined in the given below expression.

$$\varphi(x) = \max(x, 0) \quad (8)$$

In this work, 1D convolutional kernels are used where each and every pixel is represented as one vector with only one label. The final structure of hybrid ResNetInception architecture is presented in figure 6, and it contains only two residual blocks.

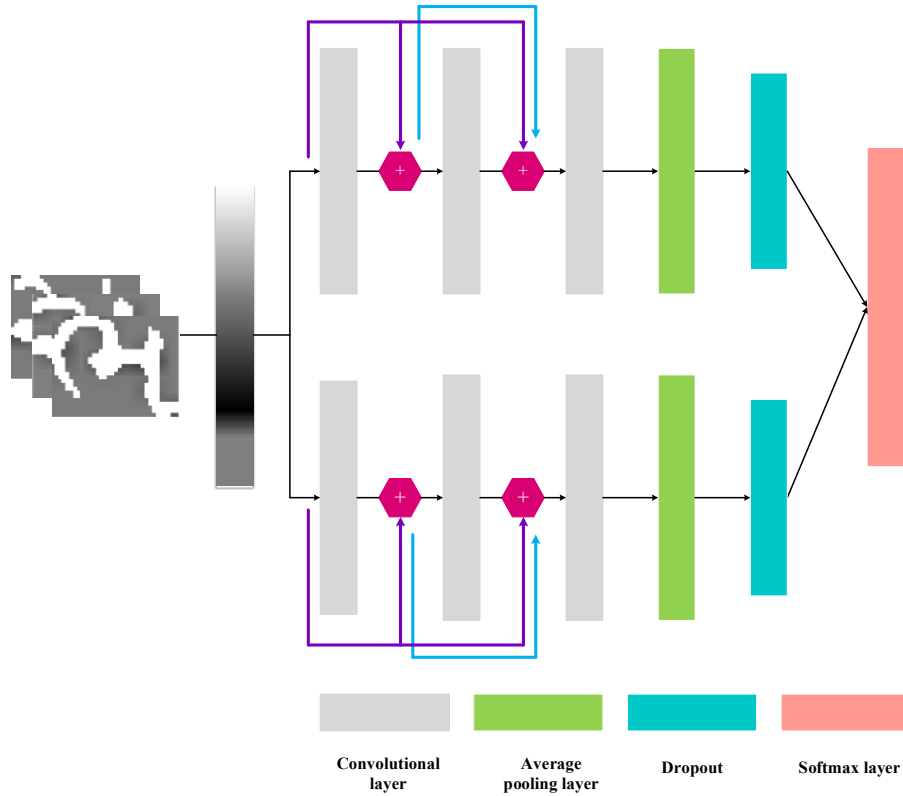


Figure 6: Hybrid deep ResNet-Inception architecture

Two residual models are ultimately connected in this network in which the given below expression express the function of the upper residual model.

$$\begin{aligned}
 X^1 &= \varphi(W^1 * X^0 + \beta^1) \\
 X^2 &= \varphi(W^2 * (X^0 + X^1)\beta^2) \\
 X^3 &= \varphi(W^3 * (X^0 + X^1 + X^2)\beta^3) \\
 X^4 &= AvgP(X^3)
 \end{aligned} \tag{9}$$

Equation 10 defines the function of the lower residual model.

$$\begin{aligned}
 X'^1 &= \varphi(W'^1 * X^0 + \beta^1) \\
 X'^2 &= \varphi(W'^2 * (X'^0 + X'^1)\beta^2) \\
 X'^3 &= \varphi(W'^3 * (X'^0 + X'^1 + X'^2)\beta^3) \\
 X'^4 &= AvgP(X'^3)
 \end{aligned} \tag{10}$$

The parallelism feature of the Inception component is stimulated by the Inception module so that lower and upper residual models work in parallel. Convolution of the operation is done by the first three lines in the equation and third convolutional layer X^3 and X'^3 feeds the output to the average pooling layer, then apply dropout technique.

Pooling layers

Average pooling is performed by only one pooling layer with a stride and filter size of 2. The below expression express this average pooling function. Equation 11 defines the average pooling function.

$$X^i = AvgP(X^{i-1}) \tag{11}$$

Here, $AvgP$ mentions the average pooling function and the input data from the previous convolutional layer is mentioned as X^{i-1} . In neural networks, dropout is performed to minimize interdependent learning between neurons. A dropout technique with a probability of 0.25 is directly

applied in the final stage after performing maximum pooling. Because, there is no fully connected layer apart from the Softmax classifier.

Softmax classifier

In a multi-class problem, Softmax assigns decimal probabilities to each class. Those decimal probabilities must add up to 1.0. The softmax activation function in the output layer obtains the probabilities of each input element belonging to a label and represents a categorical distribution over class labels. In this research, totally 34 classes are assigned to recognize 34 characters in the Gujarati language.

IV. Simulation results and analysis

This section deals with implementing OCR in the Gujarati language using a hybrid deep learning algorithm in the Matlab tool. Performance of the proposed methodology is estimated in terms of different parameters like detection accuracy, precision, recall, F-1 measure and character error rate (CER). Different kinds of existing pre-trained deep learning algorithms like AlexNet, ResNet, and GoogleNet architectures are implemented to equate the performance of the suggested technique.

I. Dataset explanation

To implement this work, the dataset containing Gujarati characters is collected by ourselves from different sources. The prepared dataset contains 10,200 characters containing 34 Gujarati consonants of 300 characters for each. The structure of dataset is displayed in table 2. Printed (laser and Machine printed) Gujarati characters from different sources like magazines, newspapers and books etc., are utilized to collect the dataset. The samples for Gujarati numerals were poised from 300 persons of dissimilar age groups, professional backgrounds and genders. Sample images from the dataset are displayed in figure 7.

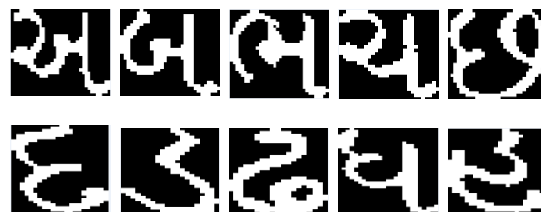


Figure 7: Sample images from the dataset

II. Experiment on dataset

The collected data is divided into 80% for training and 20% for testing in this research. Approaches closely related to our proposed methodology are implemented to equate the performance of our hybrid model. Conventional techniques like AlexNet, ResNet, and GoogleNet are implemented in this work.

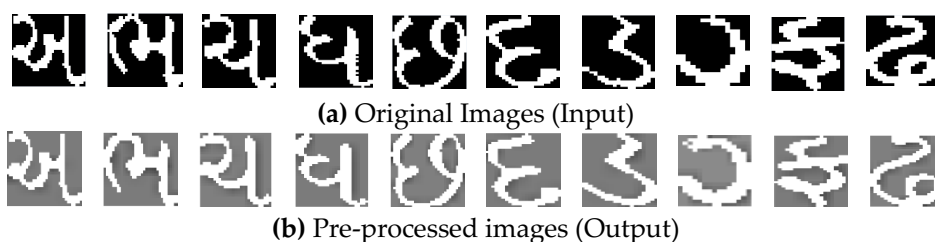


Figure 8: Output images after performing pre-processing steps

Figure 8 displays the original images as well as pre-processed images. This image only contains 10 sample characters from the collected dataset and the pre-processed images of that sample characters.

Table 1: Configuration parameters for proposed hybrid deep neural network

Layer	Image size	Kernel size	No of filters	Stride	Activation
Input	28*38	-	-	-	-
Convolution	24*24	5*5	9	1	Relu-Inception
Convolution	12*12	3*3	9	1	Relu-Inception
Convolution	10*10	2*2	9	1	Relu-Inception
Max pooling	5*5	3*3	2	2	Relu-Inception
Drop out (0.25)	5*5	-	-	-	-
Output	-	-	-	-	Softmax

Table 1 mentions the configuration parameter for the proposed hybrid model. This hybrid deep learning algorithm uses three convolutional layers with stride size 1. Also, all the convolutional layer functions with the ReLu-Inception activation function. Drop out technique is applied with a 0.25 probability value. Finally, the output is obtained by joining the Softmax layer as the output layer. In this architecture, the initial learning rate is set as 0.001, and the batch size is 17.

III. Performance analysis

Some standard measures such as Precision, Recall, F1 measure, and accuracy are used to evaluate the performance of the hybrid model, in which they are based on a confusion matrix. The output is either a correctly recognized character or an incorrectly recognized character in the character recognition problem. True Positive (TP), True Negative (TN), False Positive (FP) and False Positive (FP) are four different categories used to estimate the performance of the proposed methodology. TP defines that the actual characters are correctly recognized as actual characters, FP explains that some other characters are incorrectly recognized as actual characters, TN describes that some other characters are correctly recognized as other characters, and FN indicates that the actual characters are incorrectly recognized as some other characters. The performance metrics like precision, recall, accuracy, and F1 measure are evaluated by these four categories. Precision (P) measure is the fraction of all recognized characters to the total number of typescripts in the dataset. The recall is a fraction between correctly recognised characters and the number of characters that should have been recognized. F1 score or balanced F-score is the harmonic mean of precision and recall. Finally, accuracy is a quantity of correctness of the character recognition. In OCR related frameworks, CER is defined as the percentage of inaccurate typescripts in the system output.

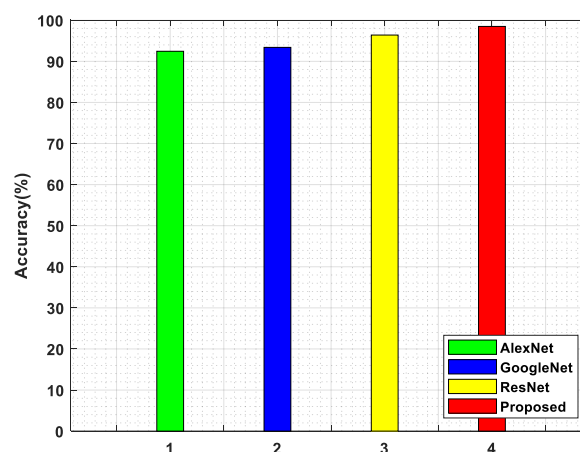


Figure 9: Performance comparison of accuracy

Figure 9 displays the performance comparison of accuracy. Additionally, the performance of the suggested classifier is compared with existing pre-trained models like AlexNet, GoogleNet and ResNet. Our proposed hybrid model exceeds all previous methods in terms of higher accuracy compared to existing methods. For instance, the proposed hybrid methodology obtains 98.5% accuracy, and the existing methods like GoogleNet obtain 93.4%, ResNet obtains 96.4%, and AlexNet obtains 92.45%. The higher accuracy is that the proposed hybrid model only uses three convolution layers for further processing, while the others use a different number of convolution layers. In general, the quality of the results is decreased with more convolutional layers.

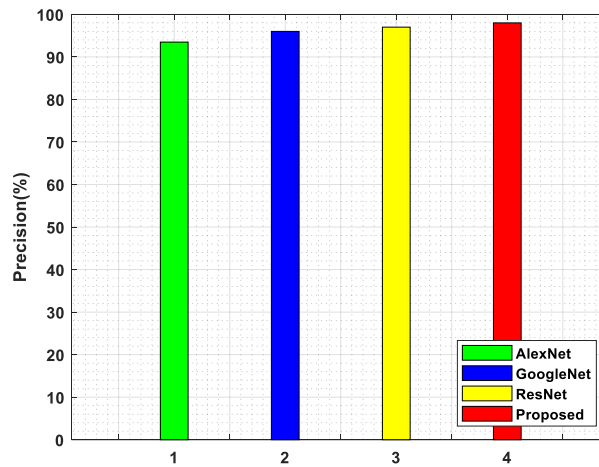


Figure 10: Performance comparison of precision

The comparative analysis of precision metrics is displayed in figure 10. The performance of the proposed hybrid structure is compared with existing methodologies like AlexNet, GoogleNet and ResNet architecture. The figure analysis shows that the proposed methodology obtains 98% accuracy in which GoogleNet obtains 96%, ResNet attains 97%, and AlexNet achieves 93.48%. The proposed methodology exceeds all conventional methods using higher precision value.

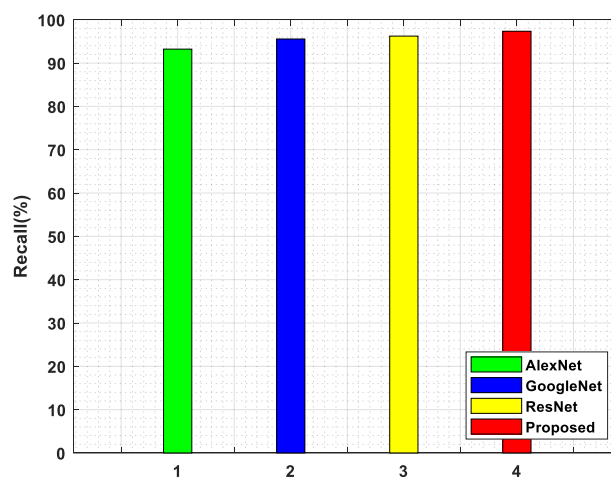


Figure 11: Performance comparison of Recall

Figure 11 demonstrates the performance analysis of recall metric. From the figure analysis, it is shown that the proposed hybrid model obtains 97.35% recall in which existing methods like GoogleNet

obtains 95.56% recall value, ResNet attains 96.23% recall. Finally, AlexNet achieves 93.22% recall value. Compared to existing methodologies, our proposed method obtains high recall in our collected dataset.

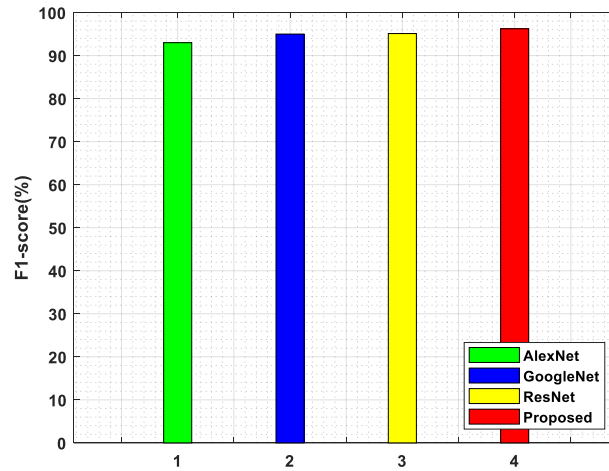


Figure 12: Performance comparison of F1-score

Figure 12 displays the performance comparison of the F1-score. The proposed hybrid model attains a 96.23% score while existing methodologies like AlexNet, GoogleNet and ResNet obtain 93%, 95% and 95.12% F1-score. From the figure analysis, it is clearly shown that the proposed methodology beats all conventional methodologies using a high score value.

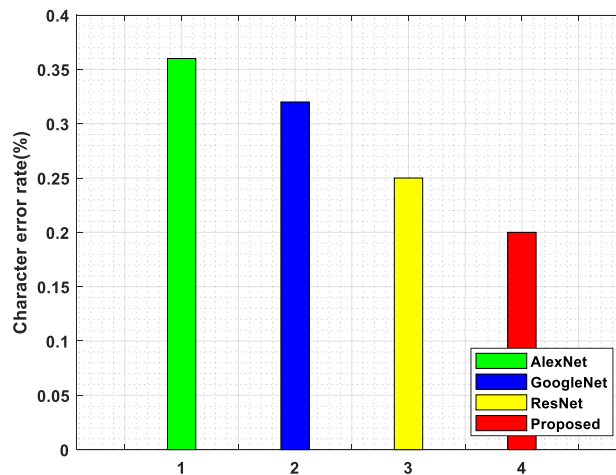


Figure 13: Performance comparison of Character error rate

Figure 13 shows the Character error rate evaluation of the proposed hybrid model with conventional techniques like GoogleNet, ResNet as well as AlexNet classifiers. When comparing the performance of classifiers, the character error rate is minimum for the proposed hybrid model with 0.20%. Existing methodologies like AlexNet, GoogleNet, ResNet obtain 0.36%, 0.32% and 0.25% error which is comparatively higher than the proposed method. The reason for less error is that both feature selection and character recognition process are done by hybrid model, which shows less character recognition rate in the proposed methodology. Moreover, the hybrid model has advantages like robustness, speed learning, and generalization to the same input. These are considered the significance of the hybrid model, which minimizes the error rate in character recognition compared to the existing pre-trained models.

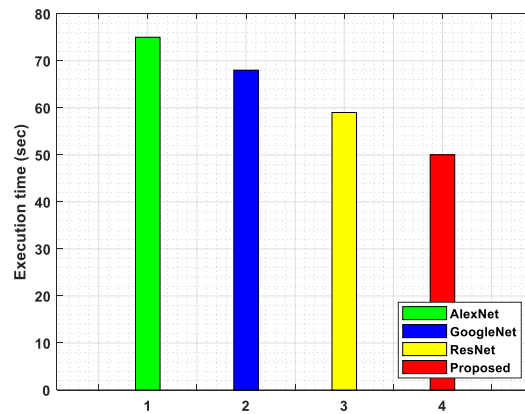


Figure 14: Execution time analysis

Figure 14 shows the execution time analysis of the proposed hybrid model and existing pre-trained models like AlexNet, GoogleNet and ResNet. Compared to the existing pre-trained models, the proposed hybrid model takes 50 seconds to complete the recognition process. This is due to the hybrid model's fast learning process that helps speedily identify the characters.

V. Conclusion

In today's world, most people are e-readers. But, very few e-books are available in the Gujarati language, and most pamphlets are in the form of hardcopy. It needs a digitization method to change those hardcopies into editable text format. OCR is a technique for converting scanned documents into digitized text. So also, for the Gujarati language, the OCR system is required. Plenty of researchers is making efforts to create an efficient OCR system for Indian languages like Marathi, Gujarati and many more. So, in this article, a hybrid ResNet-Inception model is proposed to detect the characters from the collection of scanned documents. Simulation is carried out using the Python tool, and the performance of hybrid methodology is calculated by means of different parameters. Also, it is compared with diverse deep-learning procedures to show the effectiveness of the proposed methodology. The simulation result indicates that the proposed deep hybrid architecture achieves 98.5% accuracy for character recognition, 3.73% higher than ALEXNet, 3.94% greater than GoogleNet and 1.51% superior to ResNet.

References

- [1] Islam, N., Islam, Z., Noor, N. (2017 Oct 3). A survey on optical character recognition system. *arXiv preprint arXiv:1710.05703*.
- [2] Joshi, D.S., Risodkar, Y.R. (2018 Feb 8). Deep learning based Gujarati handwritten character recognition. In 2018 *International Conference On Advances in Communication and Computing Technology (ICACCT) IEEE* 563-566.
- [3] Pareek, J., Singhanian, D., Kumari, R.R., Purohit, S. (2020 Jan 1). Gujarati Handwritten Character Recognition from Text Images. *Procedia Computer Science*. 171: 514-23.
- [4] Naik, V.A., Desai, A.A. (2017 Jul 3). Online handwritten Gujarati character recognition using SVM, MLP, and K-NN. In 2017 *8th International Conference on Computing, Communication and Networking Technologies (ICCCNT) IEEE* 1-6.
- [5] Sharma, A.K., Thakkar, P., Adhyaru, D.M., Zaveri, T.H. (2019 Apr). Handwritten Gujarati Character Recognition Using Structural Decomposition Technique. *Pattern Recognition and Image Analysis*. 29(2): 325-38.

- [6] Sharma, A.K., Adhyaru, D.M., Zaveri, T.H. (2018). A novel cross correlation-based approach for handwritten Gujarati character recognition. *In Proceedings of First International Conference on Smart System, Innovations and Computing. Springer, Singapore.* 505-513.
- [7] Chaudhuri, A., Mandaviya, K., Badelia, P., Ghosh, S.K. (2017). Optical character recognition systems. *In Optical Character Recognition Systems for Different Languages with Soft Computing.* Springer, Cham. 9-41.
- [8] Avadesh, M., Goyal, N. (2018 Apr 24). Optical character recognition for sanskrit using convolution neural networks. *In 2018 13th IAPR International Workshop on Document Analysis Systems (DAS).* IEEE. 447-452.
- [9] Sharma, R., Mudgal, T. (2019). Primitive feature-based optical character recognition of the Devanagari script. *In Progress in Advanced Computing and Intelligent Engineering.* Springer, Singapore. 249-259.
- [10] Bebartta, H.N., Mohanty, S. (2017 Jul). Algorithm for segmenting script-dependant portion in a bilingual Optical Character Recognition system. *Pattern Recognition and Image Analysis.* 27(3): 560-8.
- [11] Audichya, M.K., Saini, J.R. (2017). A study to recognize printed Gujarati characters using tesseract OCR. *Int. J. Res. Appl. Sci. Eng. Technol.* 5: 1505-10.
- [12] Jain, A.A., Arolkar, H.A. A Survey of Gujarati Handwritten Character [1] Recognition Techniques. *International Journal for Research in Applied Science & Engineering Technology (IJRASET),* ISSN. 2321-9653.
- [13] Vakharwala, P., Chhabda, R., Painter, V., Pawar, U., Dastoor, S. (2020 May 15). Performance Analysis of Various Trained CNN Models on Gujarati Script. *In International Conference on Information and Communication Technology for Intelligent Systems.* Springer, Singapore. 483-492.
- [14] Althobaiti, H., Lu, C. (2017 Mar 22). A survey on Arabic Optical Character Recognition and an isolated handwritten Arabic Character Recognition algorithm using encoded freeman chain code. *In 2017 51st Annual Conference on Information Sciences and Systems (CISS).* IEEE 1-6.
- [15] Ahmad, I., Wang, X., Li, R., Rasheed, S. (2017 Feb 2). Offline Urdu Nastaleeq optical character recognition based on stacked denoising autoencoder. *China Communications* 14(1): 146-57.
- [16] Sethi, R.K., Mohanty, K.K. (2020 July 07). Optical Odia Character Classification using CNN and Transfer Learning: A Deep Learning Approach.
- [17] Shinde, A., Dandawate, Y. Convolutional Neural Network Based Handwritten Marathi Text Recognition.
- [18] Naik, V.A., Desai, A.A. (2019). Multi-layer classification approach for online handwritten Gujarati character recognition. *In Computational Intelligence: Theories, Applications and Future Directions- Volume II.* Springer, Singapore 595-606.
- [19] Jena, O.P., Pradhan, S.K., Biswal, P.K., Nayak, S. (2020 Mar 13). Recognition of Printed Odia Characters and Digits using Optimized Self-Organizing Map Network. *In 2020 International Conference on Computer Science, Engineering and Applications (ICCSEA) IEEE.* 1-6.
- [20] Das, D., Nayak, D.R., Dash, R., Majhi, B. (2020 Nov). MJCN: Multi-objective Jaya Convolutional Network for handwritten optical character recognition. *Multimedia Tools and Applications* 79(43): 33023-42.
- [21] Bui, Q.A., Mollard, D., Tabbone, S. (2017 Nov 9). Selecting automatically pre-processing methods to improve OCR performances. *In 2017 14th IAPR International Conference on Document Analysis and Recognition (ICDAR).* IEEE 1: 169-174.
- [22] Suresh, S., Lal, S., Chen, C., Celik, T. (2018 Apr 10). Multispectral satellite image denoising via adaptive cuckoo search-based wiener filter. *IEEE transactions on geoscience and remote sensing.* 56(8): 4334-45.

- [23] Kaundilya, C., Chawla, D., Chopra, Y. (2019 Mar 13). Automated text extraction from images using OCR system. In 2019 6th *International Conference on Computing for Sustainable Global Development (INDIACom)*. IEEE 145-150.
- [24] Garg, D., Garg, N.K., Kumar, M. (2018 Oct). Underwater image enhancement using blending of CLAHE and percentile methodologies. *Multimedia Tools and Applications*. 77(20): 26545-61.
- [25] He, K., Zhang, X., Ren, S., Sun, J. (2016). Deep residual learning for image recognition. In: *Proceedings of the IEEE conference on computer vision and pattern recognition*. 770-778.
- [26] Szegedy, C., Liu, W., Jia, Y., Sermanet, P., Reed, S., Anguelov, D., Erhan, D., Vanhoucke, V., Rabinovich, A. (2015). Going deeper with convolutions. In: *Proceedings of the IEEE conference on computer vision and pattern recognition*. 1-9.

RELIABILITY ANALYSIS AND PROFIT OPTIMIZATION OF BRIQUETTE MACHINE BY CONSIDERING NEGLECTED FAULTS

Divesh Garg¹, Reena Garg¹

¹J.C. Bose University of Science and Technology, YMCA, Faridabad, India

diveshgarg29@gmail.com,

reenagargymca@gmail.com

Abstract

Sustainable energy plays a significant role in socio-economic advancement by raising the standard of living of all human beings. Briquetting is the process of compaction of biomass residues into solid fuels in order to increase the effectiveness of thermal capacity, combustion rate, calorific value to name a few. In this paper, we consider not only the occurrence of minor/ major faults but also the other neglected faults such as abnormal sound, overheating of the motor unit, vibration, etc. Such neglected faults may not affect the working of the system at a time but their ignorance may convert into major faults in the future. An ordinary repairman can easily rectify all machine faults except some major faults for which an expert repairman is required. Moreover, we analyse the availability of the system and optimize system profit by using the Artificial Bee Colony optimization algorithm. Furthermore, a graphical study of these parameters is presented.

Keywords: Briquette machine, Profit, Base state, Transition probability, Regenerative Point Graphical Technique (RPGT).

I. Introduction

Ongoing international efforts to reduce CO₂ emission from the consumption of energy lead us towards renewable energy sources. Production of biomass helps us in achieving a neutral CO₂ emission which balances the rate of growth of biomass. Sharma et al. [20] discussed varying contents of carbon, oxygen, and hydrogen provide us various effects on the conversion process of energy. Cellulose, hemicellulose, and lignin are the three main polymers of biomass.

The process of heating biomass up to approximately 200-300 degrees Celsius is sometimes known as Torre-faction (roasting, slow pyrolysis). Nowadays, Torre-faction becomes a widely discussed technology because of its potential to enable the use of extra biomass resources and make it one of the main energy sources of the present time. One of the main purposes of the Torrefaction process is to produce biomass that resembles coal mostly in terms of its properties as a solid fuel. Due to such reasons torrefied biomass is often called bio-coal. Many authors published their works on describing several parameters which are necessary for its use as solid fuel and introduced bio coal into the energy market [21].

Briquetting or densification is the process of pressurizing loose biomass into a compacted fuel known as briquettes. It helps us to produce an energy content with a smaller amount of dampness.

Briquettes are consistent in shape which results in smooth utilization and storage equipment lessening the handling, storage space, and transport expenses. Sawdust, cotton stalk, edible nutshell, coconut shell, paper and coconut mixture cocoa shell, and a lot more are the samples of biomass investigations so far [18]. Raju et al. [15] analysed that such biomass briquettes can be utilized not only for housing purposes like cooking, warming, and barbecuing but for agriculture and food industries also. Nowadays, as the necessity for an alternative energy source is high, we should focus on developing new biomass briquettes using biomass wastes [17,19].

Okwu and Omonigho [14] used saw dust and water hyacinth plant along with cassava starch as binder for the production of solid briquettes by developing a movable and light weighted briquette machine. Obtained parameters were better performing as compared to the traditional energy sources in terms of profit, high calorific value, less moisture content etc. Fikri and Sartika [4] constituted a bio-charcoal briquette obtained from organic wastes, they used simple random sampling method in order to obtain different compositions of organic wastes for comparative analysis.

Lubwama et al. [13] developed a bio-composite briquette from coffee and rice husks with proportionate groundnut shells and studied its several attributes. This briquette performs better over other single constituent briquettes. Kumar et al. [10] compared biomass briquette and charcoal briquette in order to find that which briquette has higher calorific value and also the effect of the addition of binder. Senchi & Kofa [22] investigated the intrinsic properties of corncob as well as un-carbonized rice husk base briquettes to check their fuel efficiencies. They concluded that briquette produces from corncob is far better than the rice husk briquette in terms of low moisture content, moderate ash content, and high viability. Garg and Garg [24] analysed the reliability parameters of a briquette machine with deviation in demand. Aliyu et al. [1] developed a composite briquette using corn cobs and orange peels which are easily available in some parts of Niger state, Nigeria to overcome the issue of lack of electricity supply. Obtained results give a strong hope of the development of such briquettes in those areas where there is less electricity supply or no electricity supply at all. Rane and Narvel [16] redesign the organisation based on Blockchain-IoT integrated architecture to improve the agility in their routine operations. In order to monitor its operations, they installed a sensor based industrial pump and suggested predictive measures for the management of such assets. They concluded that the new technology increases the decentralisation capacity and allowed autonomous coordination among devices. Asni and Andiappan [25] discussed Fuzzy Multi-Objective Optimal Design of a Biomass Combined Power and Heat System Considering System Reliability, Cost, and Flexibility.

Singh et al. [23] developed a mathematical model and evaluated reliability measures of power generation system by using the Boolean function technique in which lengthy calculations are involved. Garg et al. [5] utilized RPGT technique to analysed the performance parameter of a single unit briquetting system. Also, Barak et al. [3] used RPGT successfully to find reliability measures of a milk plant. So, we calculate various measures such as busy period, machine availability, mean time to system failure (MTSF), expected number of ordinary/expert repairman visits, and profit for the developed system quickly by using RPGT [12]. Moreover, we optimize profit by utilizing Artificial Bee Colony (ABC) [7,8]. Step by step working algorithm is also presented for ABC.

Generally, we consider two kinds of faults in the operation of a briquette-making machine: Minor and Major [6]. Minor faults are responsible for the degradation of the whole operating unit but major faults lead towards the complete failure of the unit. Apart from those two faults, some other faults sometimes may convert into major faults if ignored. Vibrations of the machine, overheating, unusual sounds are some examples of such faults [11]. We usually neglect such faults but their ignorance may lead to complete failure of the operating unit. Various faults necessitate the use of different repair facilities, since an ordinary repairman is unable to adequately address all

major faults [2]. None of the researchers considered above discussed faults simultaneously. To fill this gap, we present a system consisting of minor, major as well as neglected faults for the development of a briquette machine.

This paper is structured as follows: A detailed introduction of the related topic is presented in Section I. Assumptions and notations are discussed thoroughly in Sections II and III, respectively. In Sections IV and V, we developed a state transition diagram and a research methodology flowchart, respectively. Calculation of all transition probabilities as well as mean Sojourn times for each state of the transition diagram are estimated in Section VI. Different measures are calculated and optimized by using various algorithms in order to find maximum profit in Section VII. In Section VIII, detailed analyses along with graphical representations of obtained results are discussed. Section IX concludes our work with future scope.

II. Assumptions

- Inspection/Failures/Repairs are analytically independent.
- All Faults are self-announcing.
- The Faults are exponentially distributed and repair rate are arbitrary.
- Once the system has failed, no more failures can occur.

III. Notations

$\lambda/\gamma/\lambda_2$: Machine complete/neglected failure rate

O/On: Operative/Operative under neglected fault

F_i : Machine failed & under inspection

F_{rM} : Minor Fault & under repair

F_{iM} : Major Fault & under inspection

FrO/FrE : Machine under repair by ordinary/expert repairmen

a/b : Minor/Major Fault Probabilities

p/q : Major fault repair Probability

$i(t)/I(t)$: fault inspection time p.d.f/c.d.f

$h(t)/H(t)$: major fault inspection time p.d.f/c.d.f

$g_1(t)/G_1(t)$: Minor fault repair-time by ordinary repairmen p.d.f/c.d.f

$g_2(t)/G_2(t)$: Major fault repair-time by Ordinary repairmen p.d.f/c.d.f

$g_3(t)/G_3(t)$: Major fault repair-time by Expert repairmen p.d.f/c.d.f

IV. State Transition diagrams

The state S_0, S_1 are the available-states, S_2, S_3, S_4, S_5 , and S_6 are failed states as shown in Figure 1. We assume that S_0 is the base state.

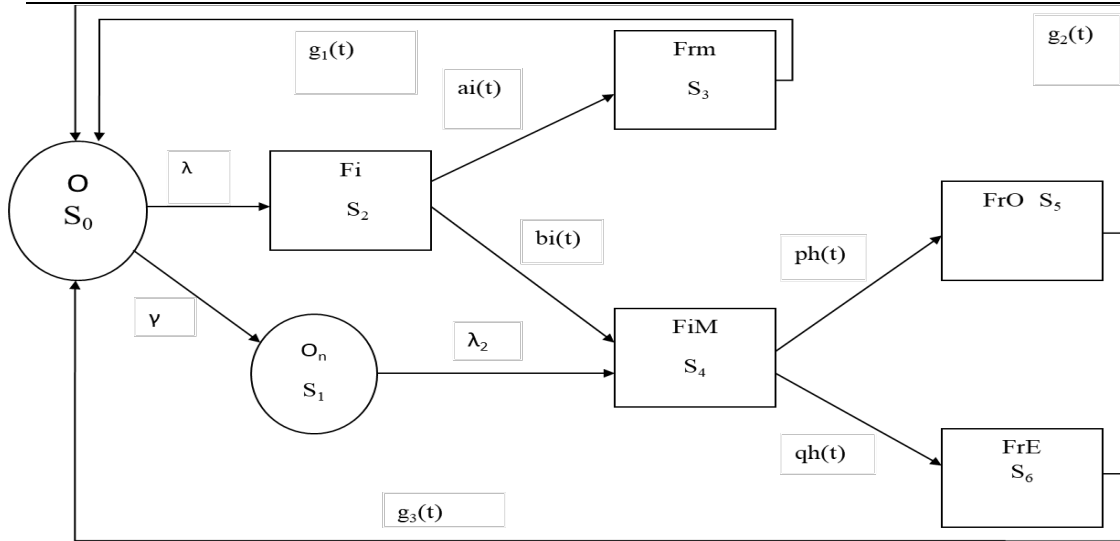


Figure 1: State transition diagram

V. Research Methodology Flowchart

The flowchart of the proposed methodology is shown in fig. 2

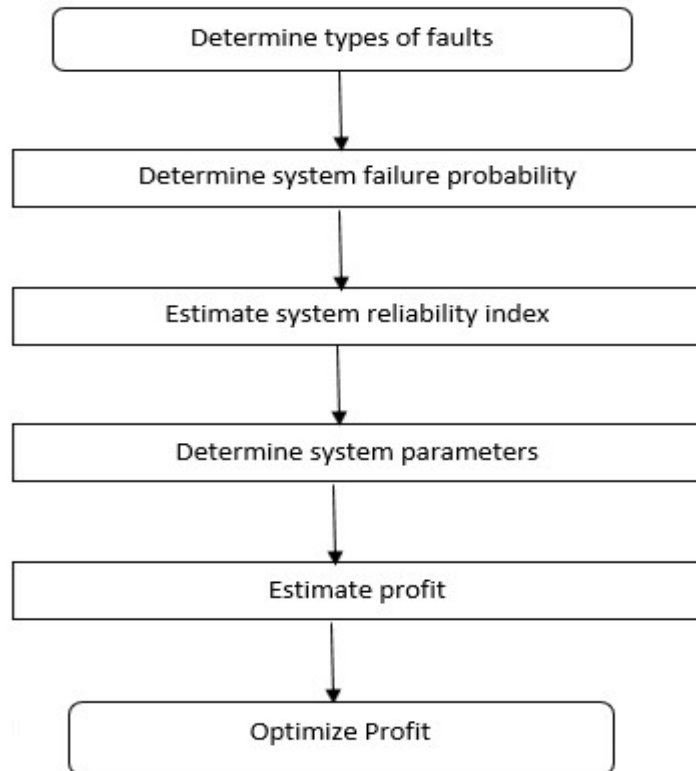


Figure 2: Research Methodology Flowchart

VI. Research Methodology Flowchart

In this section, all transition probabilities and mean sojourn times are shown in Table 1 and Table 2, respectively.

$q_{i,j}(t)$: probability distribution function from regenerative state i to j .

$p_{i,j}(t)$: State transition probability from regenerative state i to j .

$$p_{i,j}(t) = q_{i,j}^*(0)$$

where * stand for Laplace transform

Table 1: Transition Probabilities

$q_{ij}(t)$	$p_{ij} = q_{ij}^*(0)$
$q_{0,1} = \gamma e^{-(\lambda+\gamma)t}$	$p_{0,1} = \gamma/(\lambda + \gamma)$
$q_{0,2} = \lambda e^{-(\lambda+\gamma)t}$	$p_{0,2} = \lambda/(\lambda + \gamma)$
$q_{1,4} = \lambda_2 e^{-(\lambda_2)t}$	$p_{1,4} = 1$
$q_{2,3} = ai(t)$	$p_{2,3} = ai^*(0)$
$q_{2,4} = bi(t)$	$p_{2,4} = bi^*(0)$
$q_{3,0} = g_1(t)$	$p_{3,0} = g_1^*(0)$
$q_{4,5} = ph(t)$	$p_{4,5} = ph^*(0)$
$q_{4,6} = qh(t)$	$p_{4,6} = qh^*(0)$
$q_{5,0} = g_2(t)$	$p_{5,0} = g_2^*(0)$
$q_{6,0} = g_3(t)$	$p_{6,0} = g_3^*(0)$

$$p_{01} + p_{02} = 1, p_{23} + p_{24} = 1, p_{45} + p_{46} = 1,$$

Mean sojourn time can be calculated as follows:

$$\mu_i = \int_0^{\infty} R_i(t) dt = R_i^*(0)$$

Where, $R_i(t)$ is the reliability of system at time t.

Table 2: Mean Sojourn Times

$R_i(t)$	$\mu_i = R_i^*(0)$
$R_0 = e^{-(\lambda+\gamma)t}$	$\mu_0 = 1/(\lambda + \gamma)$
$R_1 = e^{-(\lambda_2)t}$	$\mu_1 = 1/\lambda_2$
$R_2 = I(t)$	$\mu_2 = -i^*(0)$
$R_3 = G_1(t)$	$\mu_3 = -g_1^*(0)$
$R_4 = H(t)$	$\mu_4 = -h^*(0)$
$R_5 = G_2(t)$	$\mu_5 = -g_2^*(0)$
$R_6 = G_3(t)$	$\mu_6 = -g_3^*(0)$
$q_{6,0} = g_3(t)$	$p_{6,0} = g_3^*(0)$

Now, transition probability factors are given as:

$$V_{0,1} = \frac{\gamma}{\lambda+\gamma}, \quad V_{0,2} = \frac{\lambda}{\lambda+\gamma}, \quad V_{0,3} = \frac{\lambda}{\lambda+\gamma} a,$$

$$V_{0,4} = \frac{1}{\lambda+\gamma}b , \quad V_{0,5} = \frac{1}{\lambda+\gamma} [p\gamma + bp\lambda], \quad V_{0,6} = \frac{1}{\lambda+\gamma} [q\gamma + bq\lambda]$$

VII. Measures of System Effectiveness

Briquetting Machine Parameters are evaluated by utilizing RPGT and “0” as a base state.

I. Mean time to system-failure

MTSF is the average time predicted until a system fails for the first time. By fig. 1, S₀ and S₁ are the only operative states that can be transited before reaching the Failed State. MTSF per unit time is represented in Table 3.

$$MTSF = V_{0,0}\mu_0 + V_{0,1}\mu_1 = \frac{1}{\lambda+\gamma} + \frac{\gamma}{\lambda+\gamma} \left(\frac{1}{\lambda_2}\right) = \frac{1}{\lambda+\gamma} \left[1 + \frac{1}{\lambda_2}\right]$$

Table 3: Effect of λ_1, γ & λ_2 on MTSF

λ	$\gamma=0.001, \lambda_2=0.025$	$\gamma=0.003, \lambda_2=0.025$	$\gamma=0.003, \lambda_2=0.025$	$\gamma=0.001, \lambda_2=0.005$
0.005	233.3333	275	300	200
0.01	127.2727	169.2308	200	109.0909
0.015	87.5	122.2222	150	75
0.02	66.66667	95.65217	120	57.14286
0.025	53.84615	78.57143	100	46.15385
0.03	45.16129	66.66667	85.71429	38.70968
0.035	38.88889	57.89474	75	33.33333
0.04	34.14634	51.16279	66.66667	29.26829
0.045	30.43478	45.83333	60	26.08696
0.05	27.45098	41.50943	54.54545	23.52941

II. Machine Availability

Let A be the probability that the unit in is working state at time t. Here, S₀ and S₁ are only operative states and all states are regenerative states. Using regenerative point graphical technique, the proportion of steady-state machine availability is given by

$$A = \frac{V_{0,0}\mu_0 + V_{0,1}\mu_1}{\sum_{i=0}^6 V_{0,i}\mu_i}$$

$$A = \frac{N}{D}$$

$$N = \frac{1}{\lambda+\gamma} \left[1 + \frac{\gamma}{\lambda_2}\right]$$

$$D = V_{0,0}\mu_0 + V_{0,1}\mu_1 + V_{0,2}\mu_2 + V_{0,3}\mu_3 + V_{0,4}\mu_4 + V_{0,5}\mu_5 + V_{0,6}\mu_6$$

$$= \frac{1}{\lambda+\gamma} + \frac{\gamma}{\lambda+\gamma} \left(\frac{1}{\lambda_2}\right) + \frac{\lambda}{\lambda+\gamma} \left(\frac{1}{\alpha}\right) + \frac{\lambda}{\lambda+\gamma} \left(\frac{1}{\alpha_1}\right) + \frac{[\gamma+b\lambda]}{\lambda+\gamma} \left(\frac{1}{\beta}\right) + \frac{[p\gamma+bp\lambda]}{\lambda+\gamma} \left(\frac{1}{\alpha_2}\right) + \frac{[q\gamma+bq\lambda]}{\lambda+\gamma} \left(\frac{1}{\alpha_3}\right)$$

$$= \frac{1}{\lambda+\gamma} \left[1 + \left(\frac{\gamma}{\lambda_2}\right) + \left(\frac{\lambda}{\alpha}\right) + \left(\frac{\lambda}{\alpha_1}\right) + \frac{[\gamma+b\lambda]}{\beta} + \frac{[p\gamma+bp\lambda]}{\alpha_2} + \frac{[q\gamma+bq\lambda]}{\alpha_3}\right]$$

Machine availability values of the given system are shown in Table 4:

Table 4: Machine availability

λ	$\alpha=0.8, \beta=0.8$	$\alpha=0.8, \beta=0.0.9$	$\alpha=0.9, \beta=0.8$	$\alpha=0.9, \beta=0.9$
0.005	0.289917598	0.289969009	0.289665715	0.2897171
0.01	0.293154824	0.29325821	0.29273926	0.29284256
0.015	0.296354714	0.296510608	0.295778765	0.295934484
0.02	0.29951791	0.299726819	0.298784793	0.298993409
0.025	0.30264504	0.302907442	0.301757893	0.30201986
0.03	0.305736716	0.306053066	0.304698604	0.305014351
0.035	0.308793539	0.309164264	0.307607452	0.307977387
0.04	0.311816095	0.312241599	0.310484952	0.310909461
0.045	0.314804956	0.315285621	0.313331609	0.313811054
0.05	0.317760683	0.318296867	0.316147915	0.318296867

III. Busy Period

Let B be the likelihood that the repairmen are occupied with fixing the unit caused to failure at time t. From the state Transition Diagram, the repairmen busy at states j=2, 3, 4, 5 & 6. For base state '0', the busy period is given in Table 5.

$$B = \frac{N_2}{D}$$

$$N_2 = V_{0,2}\mu_2 + V_{0,3}\mu_3 + V_{0,4}\mu_4 + V_{0,5}\mu_5 + V_{0,6}\mu_6$$

$$= \frac{\lambda}{\lambda+\gamma} \left(\frac{1}{\alpha}\right) + \frac{\lambda}{\lambda+\gamma} \left(\frac{a}{\alpha_1}\right) + \frac{1[\gamma+b\lambda]}{\lambda+\gamma} \left(\frac{1}{\beta}\right) + \frac{1[p\gamma+bp\lambda]}{\lambda+\gamma} \left(\frac{1}{\alpha_2}\right) + \frac{1[q\gamma+bq\lambda]}{\lambda+\gamma} \left(\frac{1}{\alpha_3}\right)$$

$$= \frac{1}{\lambda+\gamma} \left[\left(\frac{\gamma}{\lambda_2}\right) + \left(\frac{\lambda a}{\alpha_1}\right) + \frac{[\gamma+b\lambda]}{\beta} + \frac{[p\gamma+bp\lambda]}{\alpha_2} + \frac{[q\gamma+bq\lambda]}{\alpha_3} \right]$$

Table 5: Busy period

λ	$\alpha=0.8, \beta=0.8$	$\alpha=0.8, \beta=0.0.9$	$\alpha=0.9, \beta=0.8$	$\alpha=0.9, \beta=0.9$
0.005	0.99287427	0.993050337	0.993226466	0.993402658
0.01	0.987115457	0.987463579	0.987695796	0.988044328
0.015	0.981423063	0.98193933	0.98222638	0.982743492
0.02	0.975795946	0.976476547	0.976817204	0.977499231
0.025	0.970232988	0.97107421	0.971467279	0.972310643
0.03	0.964733099	0.96573132	0.966175637	0.967176847
0.035	0.959295212	0.960446902	0.96094133	0.962096979
0.04	0.953918284	0.955220001	0.955763432	0.957070193
0.045	0.948601297	0.950049684	0.950641036	0.952095663
0.05	0.943343253	0.944935036	0.945573254	0.947172577

IV. Expected visits by repairmen

let V be the number of repairmen visits for repair in time (0, t]. From the state Transition Diagram, the repairmen visit anew for repair at j=2. For base state '0', the expected visits by repairmen are given in Table 6.

$$V = \frac{V_{0,2}}{\sum_{i=0}^6 V_{0,i} \mu_i}$$

$$= \frac{\lambda}{\lambda+\gamma} + \frac{1}{\lambda+\gamma} \left[1 + \left(\frac{\gamma}{\lambda_2} \right) + \left(\frac{\lambda}{\alpha} \right) + \left(\frac{\lambda\alpha}{\alpha_1} \right) + \frac{[\gamma+b\lambda]}{\beta} + \frac{[p\gamma+bp\lambda]}{\alpha_2} + \frac{[qr+bq\lambda]}{\alpha_3} \right]$$

Table 6: Repairmen visits

λ	$\alpha=0.8, \beta=0.8$	$\alpha=0.8, \beta=0.0.9$	$\alpha=0.9, \beta=0.8$	$\alpha=0.9, \beta=0.9$
0.005	0.007091959	0.007093217	0.007094475	0.007095733
0.01	0.011986402	0.011990629	0.011993449	0.011997681
0.015	0.016824395	0.016833246	0.016838167	0.016847031
0.02	0.02160691	0.021621981	0.021629524	0.021644626
0.025	0.026334895	0.026357729	0.026368398	0.026391289
0.03	0.031009278	0.031041364	0.031055645	0.031087827
0.035	0.035630965	0.035673742	0.035692107	0.035735031
0.04	0.040200842	0.0402557	0.040278602	0.040333672
0.045	0.044719775	0.044788057	0.044815935	0.04488451
0.05	0.049188612	0.049271613	0.049304891	0.049271613

V. Profit

we consider particular case and function for analysing the system profit \

$g1(t) = \alpha 1e-\alpha 1t$, $g2(t) = \alpha 2e-a2t$, $g3(t) = \alpha 3e-\alpha 3t$, $i(t) = \alpha e-\alpha t$, $h(t) = \beta e-\beta t$

and $P = P1 A0 - P2 B0- pP3 V0- qP4 V0- P5$

Where

P1 = Revenue per unit time while the system is in up-state

P2 = Loss due to busy period of repairmen

P3 = Price of ordinary repairmen involved in the repair

P4 = Price of Expert repairmen involved in the repair

P5 = Downstate reduction & other costs

The System profit is shown in table 7:

Table 7: Profit

λ	$\alpha=0.8, \beta=0.8$	$\alpha=0.8, \beta=0.0.9$	$\alpha=0.9, \beta=0.8$	$\alpha=0.9, \beta=0.9$
0.005	29499.44914	29510.0002	29520.64369	29531.20225
0.01	29152.74694	29173.60808	29187.67066	29208.55639
0.015	28810.04339	28840.97977	28858.38534	28889.37249
0.02	28471.26972	28512.05245	28532.7268	28573.59516
0.025	28136.3587	28186.7647	28210.63546	28261.17012
0.03	27805.24465	27865.05644	27892.05302	27952.0443
0.035	27477.86337	27546.86892	27576.92246	27646.16569
0.04	27154.15209	27232.14464	27265.18797	27343.48341
0.045	26834.04943	26920.82739	26956.79495	27043.94761
0.05	26517.4954	26612.86212	26651.68996	26747.1146

VI. ABC Algorithm

Step-1: Formulate the fitness function and randomly initialize the honey bee.

Step-2: Find an applicant food source position for each utilized honey bee and estimate the nectar amount fitness function of food sources.

Step-3: Calculate the pi (probability Values) for the solution.

Step-4: for each onlooker, the bee chooses a food source depending on a pi and generates an applicant solution.

Step-5: select the better food source position.

Step-6: Memorize the best solution found so far.

Step-7: Locate the surrendered food sources and produce new situations for depleted food sources

Step-8: Repeat steps 2 onwards till the end criterion is met.

All constraints limits are reflected in Table 8.

Table 8: Repair, inspection and failure rate parameter constraints limits

Parameters	λ	γ	λ_2	α	β	α_1	α_2	α_3
Min	0.001	0.002	0.005	0	0	0.1	0.2	0.2
Max	0.05	0.1	0.05	0.9	0.9	0.9	0.9	0.9

Table 9 shows ABC's optimal profit function values for various repair and failure rates.

Table 8: Constraints limits

ABC Results (Profit)	λ	γ	λ_2	α	β	α_1	α_2	α_3
29637.091	0.002	0.003	0.019	0.87	0.0878	0.0892	0.9	0.889
29668.051	0.002	0.002	0.047	0.731	0.878	0.463	0.895	0.894
29589.136	0.006	0.003	0.05	0.891	0.895	0.871	0.89	0.883
29504.176	0.002	0.004	0.006	0.9	0.9	0.871	0.851	0.806
29640.821	0.015	0.002	0.047	0.891	0.894	0.879	0.895	0.845
29745.041	0.001	0.002	0.01	0.9	0.883	0.578	0.9	0.9
29702.85	0.002	0.002	0.005	0.753	0.752	0.844	0.9	0.9
29719.59	0.003	0.002	0.044	0.88	0.849	0.9	0.9	0.9
29747.066	0.001	0.002	0.005	0.829	0.898	0.597	0.9	0.739
29762.308	0.001	0.002	0.005	0.852	0.9	0.872	0.9	0.9

VIII. Results and Discussion

In this section, different graphs for MTSF, availability, and profit are drawn by considering the particular cases. Fig. 3 represents the reciprocal of MTSF with respect to the failure rate. In Fig. 4, a graph of availability versus failure rate is shown. It is easy to check that availability decreases with the increase in failure rate and increases with the higher value of inspection rate. Fig. 5 reflects the graphs between profit and failure rates. Profit goes down with an increase in failure

rate but depicts the same behaviour as the inspection rate. The validation of the proposed work is ensured by the expected trends on the following graphs.

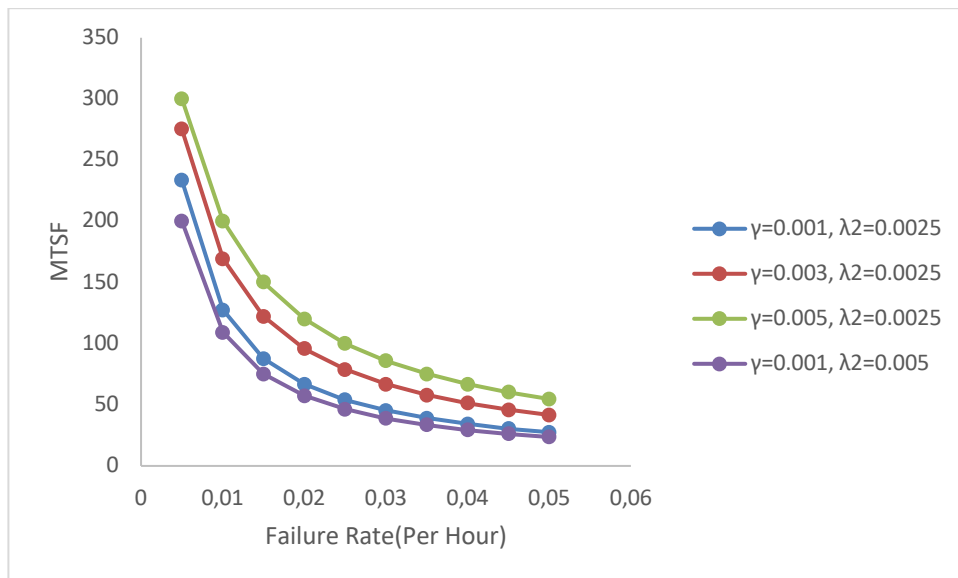


Figure 3- Effect of different parameters on MTSF

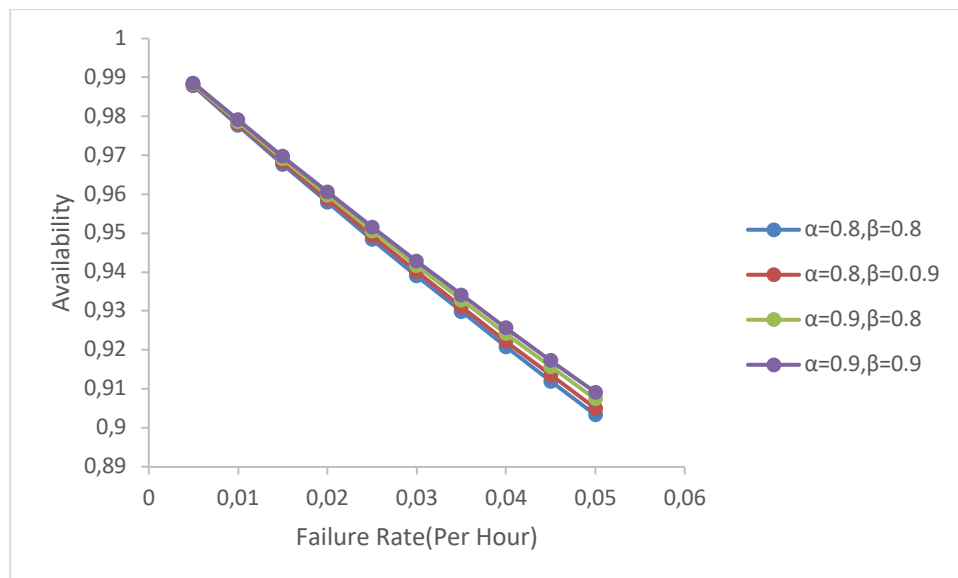


Figure 4- Availability Vs Failure Rate

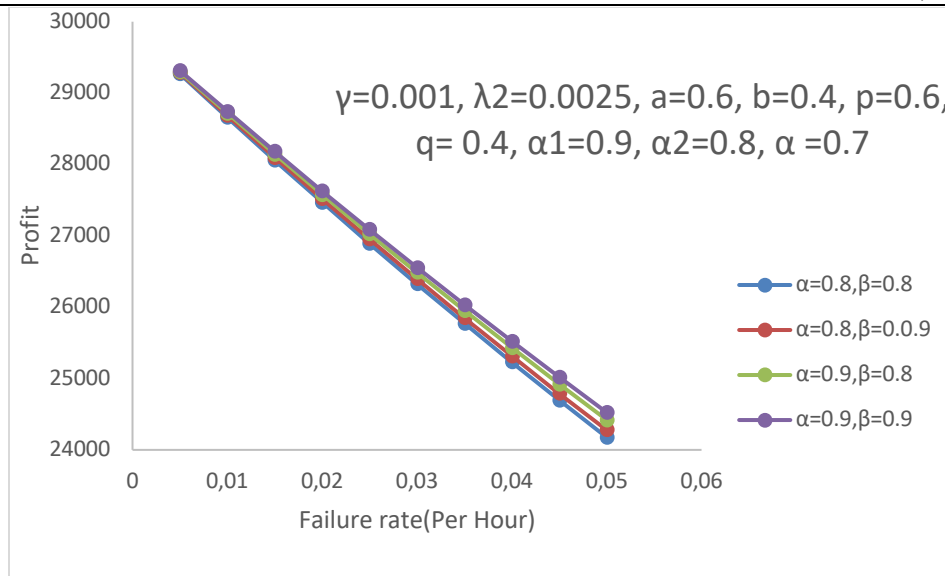


Figure 5- Profit Vs Failure Rate

Biomass is one of the easily available energy sources which can be used for bioenergy to generate electricity, heat, and various other forms of energy. Biomass briquettes produced by a piston press are less expensive than coal. It also has a higher burning capacity and lowers ash concentration than coal and wood. Industries using such briquettes are more profitable as compare to traditional energy sources. Briquettes are environment friendly due to its less carbon emission nature.

IX. Conclusion and future scope

Neglected faults along with different faults in the bio-coal briquette machine have been analysed and formulated. All three parameters MTSF, availability, and profit drop as the failure rate increases and rise as the inspection rate increases. Artificial Bee colony optimization algorithm is effectively applied to organize simultaneously repair, inspection, and failure rate parameters for an ideal degree of system profit. The optimum value for Profit by ABC algorithm for repair and failure rate parameters ($\lambda, \gamma, \lambda_2, \alpha, \beta, \alpha_1, \alpha_2, \alpha_3$) is 29762.308. That means the briquetting machine is quite profitable. Therefore, Biomass briquettes are of practical significance in any apparatus intended for the combustion of coal or wood. Some adjustments to the operating parameters are required to achieve maximum profit. Also, a preventive maintenance policy or periodic rest which will help practitioners to avoid such conversion of neglected faults into major faults.

The Briquetting system tends to fail when neglected faults are ignored. The concept of preventive maintenance was not taken care of in this manuscript. In future, we wish to work on the profit optimization of two-unit briquetting system considering neglected Faults with Preventive Maintenance.

References

- [1] Aliyu, M., Mohammed, I. S., Usman, M., Dauda, S. M. and Igbetua, I. J. (2020). Production of composite briquettes (orange peels and corn cobs) and determination of its fuel properties. *Agric Eng Int: CIGR Journal*, 22(2):133-144.
- [2] Attahiru, W. L., Alfa, S. and Zhao, Y. Q. (1998). Stochastic analysis of a repairable system with three units and two repair facilities. *Microelectronics Reliability*, 38(4):585-595.

- [3] Barak, M. S., Garg, R. and Kumar, A. (2021). Reliability measures analysis of a milk plant using RPGT. *Life Cycle Reliab Saf Eng*, 10:295-302.
- [4] Fakri, E. and Sartika, C. (2018). Study on the Use and Composition of Bio-Charcoal Briquettes Made of Organic Waste. *Journal of Ecological Engineering*, 19(2):81-88.
- [5] Garg, D. and Garg, R. (2022). Performance analysis of the briquette machine considering aneglected faults with preventive maintenance. *Int J Syst Assur Eng Manag*, <https://doi.org/10.1007/s13198-022-01621-5>.
- [6] Garg, D., Garg, R. and Garg, V. (2020). Inspecting Briquette Machine with Different Faults. *Recent Advances in Computer Science and Communications*, 13(1).
- [7] Karaboga, D. and Akay, B. (2009). A comparative study of Artificial Bee Colony algorithm. *Applied Mathematics and Computation*, 214(1):108-132.
- [8] Karaboga, D., Gorkemli, B., Ozturk, C. and Karaboga, N. (2014). A comprehensive survey: artificial bee colony (ABC) algorithm and applications, *Artif. Intell. Rev.*, 42 (1) 21-57.
- [9] Kongprasert, N., Wangphanich, P. and Jutilarptavorn, A. (2019). Charcoal briquettes from Madan wood waste as an alternative energy in Thailand. *Procedia manufacturing* 30:128-135.
- [10] Kumar, J. A., Kumar, K.V., Petchimuthu, M., Iyahraja, S. and Kumar, D. V. (2020). Comparative analysis of briquettes obtained from biomass and charcoal. *Materials Today: Proceedings*, 45(2): 857-861.
- [11] Kumar, R. and Bhatia, P. (2011). Reliability and cost analysis of one-unit centrifuge system with single repairman and inspection. *Pure Applied Math. Sci.*, 74:113-121.
- [12] Kumar, A., Garg, D. and Goel, P. (2019). Mathematical modeling and behavioral analysis of a washing unit in paper mill. *Int J Syst Assur Eng Manag*, 10:1639–1645.
- [13] Lubwama, M., Yiga, V. A., Muhairwe, F., and Kihedu, J. (2019). Physical and combustion properties of agricultural residue bio-char bio-composite briquettes as sustainable domestic energy sources. *Renewable Energy*, 148:1002-1016.
- [14] Okwu, M. O. and Omonigho, O. B. (2018). Development of a Light Weight Briquetting Machine for Small and Medium Scale Enterprise. *FUPRE Journal of Scientific and Industrial Research*, 2(1):71-87.
- [15] Raju, C. A. I., Jyothi, K. R., Satya, M. and Praveena, U. (2014). Studies on development of fuel briquettes for household and industrial purpose. *International Journal of Research in Engineering and Technology*, 3(2):54-63.
- [16] Rane, S. B., Narvel, Y. A. M. (2021). Re-designing the business organization using disruptive innovations based on blockchain-IoT integrated architecture for improving agility in future Industry 4.0. *Benchmarking: An International Journal*, 28(5):1883-1908.
- [17] Romallosa, A. R. D. and Kraft, E. (2017). Feasibility of Biomass Briquette Production from Municipal Waste Streams by Integrating the Informal Sector in the Philippines. *Resources*, 6(12):01-19.
- [18] Roy, R., Kundu, K., Kar, S., Dahake, V. R. and Ranjan, P. (2015). Production and evaluation of briquettes made from dry leaves, wheat straw, saw dust using paper pulp and cow dung as binder. *Research front*, 3:51-58.
- [19] Sanap, R., Nalawade, M., Shende, J. and Patil, P. (2016). Automatic screw press briquette making machine. *International Journal of Novel Research in Electrical and Mechanical Engineering*, 3(1):19-23.
- [20] Sharma, M. K., Priyank, G. and Sharma, N. (2015). Biomass Briquette Production: A Propagation of Non-Convention Technology and Future of Pollution Free Thermal Energy Sources. *American Journal of Engineering Research*, 4(2):44-50.
- [21] Shuklal, S. and Vyas, S. (2015). Study of Biomass Briquettes, Factors Affecting Its Performance and Technologies Based on Briquettes. *IOSR Journal of Environmental Science, Toxicology and Food Technology*, 9:37-44.

-
- [22] Senchi, G. F. and Kofa, I. D. (2020). Preparation of Biomass Briquettes from Corncob and Uncarbonized Rice Residues. *ICONIC RESEARCH AND ENGINEERING JOURNALS* 4(1):33-39
- [23] Singh, J. and Jaswal, R. A. (2013). Evaluation of reliability parameter of thermal power plant by BFT. *International Journal of Advanced Engineering Technology*, 4(3): 79-81.
- [24] Garg, D. and Garg, R. (2021). Reliability modelling and performance analysis of bio-coal manufacturing system with deviation in demand. *Life Cycle Reliab Saf Eng*, 10:403-409.
- [25] Asni, T. and Andiappan, V. (2021). Optimal Design of Biomass Combined Heat and Power System using Fuzzy Multi-Objective Optimisation: Considering System Flexibility, Reliability, and Cost. *Process Integr Optim Sustain*, 5:207–229.

A new method for generating distributions with an application to Weibull distribution

M. A. LONE

•

Department of Statistics, University of Kashmir, Srinagar, India
murtazastat@gmail.com

I. H. DAR

•

Department of Statistics, University of Kashmir, Srinagar, India
ishfaqh@gmail.com

T. R. JAN*

•

Department of Statistics, University of Kashmir, Srinagar, India
drtrjan@gmail.com

Abstract

In the literature of probability theory, it has been noticed that the classical probability distributions do not furnish an ample fit and fail to model the real-life data with a non-monotonic hazard rate behaviour. To overcome this limitation, researchers are working in the refinement of these distributions. In this paper, a new method has been presented to add an extra parameter to a family of distributions for more flexibility and potentiality. We have specialized this method to two-parametric Weibull distribution. A comprehensive mathematical treatment of the new distribution is provided. We provide closed-form expressions for the density, cumulative distribution, reliability function, hazard rate function, the r -th moment, moment generating function, and also the order statistics. Moreover, we discussed mean residual life time, stress strength reliability and maximum likelihood estimation. The adequacy of the proposed distribution is supported by using two real lifetime data sets as well as simulated data.

Keywords: Weibull distribution, hazard rate function, survival function, mean residual life, Maximum likelihood estimation.

1. INTRODUCTION

Weibull distribution is a well known life time distribution in reliability engineering and failure analysis. The Weibull distribution is used in modelling the engineering, biological, weather forecasting and hydrological data sets. It does not impart an admissible fit for some applications, especially, when the hazard rates are bathtub, upside down bathtub, or bimodal shapes. To overcome these limitations, several researchers have developed various modifications and extensions of the Weibull distribution to model various types of data. Many extensions and generalizations of the Weibull distribution have accomplished the above purpose. Among these, Xie and Lai [1] introduced the additive Weibull distribution, Mudholkar et al. [2] proposed exponentiated Weibull (EW) distribution by adding an extra parameter to the Weibull distribution

which provides bathtub shaped hazard rate function. Xie et al. [3] proposed the the extended Weibull distribution. Carrasco et al. [4] presented generalized modified Weibull (GMW) distribution. Modified Weibull by Lai et al. [5]; extended flexible Weibull by Bebbington et al. [6]. The exponential-Weibull distribution by Cordeiro et al. [7]. Lee et al. [8] and Alzaatreh et al. [9] proposed methods of generalized continuous and discrete distributions.

Mahdavi and Kundu [10] proposed a method called the Alpha Power Transformation (APT) and it is useful to assimilates skewness to a family of distributions. Let $F(x)$ be the cumulative distribution function (cdf) of a continuous random variable X , then they define the APT of $F(x)$ for $x \in \mathbb{R}$ as follows

$$F_{APT}(x) = \begin{cases} \frac{\alpha^{F(x)} - 1}{\alpha - 1} ; \alpha \in \mathbb{R}^+, & \alpha \neq 1 \\ F(x) & ; \alpha = 1 \end{cases}$$

and the corresponding probability density function (pdf) as

$$f_{APT}(x) = \begin{cases} \frac{\log \alpha}{\alpha - 1} f(x) \alpha^{F(x)} ; \alpha \in \mathbb{R}^+, & \alpha \neq 1 \\ f(x) & ; \alpha = 1 \end{cases}$$

They applied the proposed method to a one-parameter exponential distribution and generated a two-parameter Alpha Power Exponential distribution.

Recently, Ijaz et al. [11] proposed a new family of distributions named as New Alpha Power Trasformed family (NAPT) of distributions. They employed exponential distribution in NAPT family and derived a new distribution called New Alpha Power Trasformed exponential (NAPTE) distribution. Let $F(x)$ be the cdf of a continuous random variable X , then they define the NAPT of $F(x)$ for $x \in \mathbb{R}$ as follows

$$F_{NAPT}(x) = \alpha^{-\log\left(\frac{1}{F(x)}\right)} ; \quad \alpha > 0$$

and the corresponding pdf as

$$f_{NAPT}(x) = \frac{\log(\alpha) \alpha^{-\log\left(\frac{1}{F(x)}\right)} f(x)}{F(x)} ; \quad \alpha > 0$$

The following are the primary motivations for disposing Ratio Transformation (RT) method in practise:

- A straightforward and efficient method for adding an extra parameter to an existing distributions.
- To enhance the characteristics and flexibility of existing distributions.
- It is quite easy to use, hence it can be used quite effectively for data analysis purposes.
- To present the extended version of the baseline distribution that includes closed forms of cdf, reliability function as well as hazard rate function.
- To provide better fits than the other modified models having the same or higher number of parameters.

The remainder of the paper is organized as follows: In section 2 a new family of probability distributions called RT has been highlighted and some general properties of this family have been discussed. In section 3, RTW distribution has been considered, some special cases are presented and its structural properties including moments, moment generatin function, mean residual life and mean waiting time, order statistic and stress-strength reliability have been discussed. In section 4, Maximum likelihood estimators of unknown parameter as well as simulation study have been carried out. In secton 5, Two real life data sets have been analyzed to illustrate the potency of the proposed model. Finally, the paper is concluded in section 6.

2. GENERAL PROPERTIES OF RT METHOD

Let $F(x)$ be the cdf of a continuous random variable X , then the Ratio transformation of $F(x)$ for $x \in \mathbb{R}$, is defined as follows

$$F_{RT}(x) = \frac{F(x)}{1 + \alpha - \alpha^{F(x)}}; \quad \alpha > 0 \quad (1)$$

Clearly, $F_{RT}(x)$ is a proper cdf. If $F(x)$ is an absolute continuous distribution function with the pdf $f(x)$, then $F_{RT}(x)$ is also an absolute continuous distribution function with the pdf

$$f_{RT}(x) = f(x) \frac{(1 + \alpha - \alpha^{F(x)} (1 - F(x) \log \alpha))}{(1 + \alpha - \alpha^{F(x)})^2}; \quad \alpha > 0 \quad (2)$$

A useful expansion for the cdf and pdf in (1) and (2) are respectively given by

$$F_{RT}(x) = \sum_{j=0}^{\infty} \sum_{k=0}^{\infty} a_{jk} (F(x))^{k+1} \quad (3)$$

where,

$$a_{jk} = \frac{(j \log \alpha)^k}{k! (1 + \alpha)^{j+1}}$$

and

$$f_{RT}(x) = f(x) \left[1 - \frac{\alpha^{F(x)}}{1 + \alpha} (1 - F(x) \log \alpha) \right] \sum_{j=0}^{\infty} \sum_{k=0}^{\infty} b_{jk} F^k(x) \quad (4)$$

where,

$$b_{jk} = \frac{(j+1)(j \log \alpha)^k}{(1 + \alpha)^{j+1} k!}$$

The reliability function $R_{RT}(x)$ is given by

$$R_{RT}(x) = \frac{1 + \alpha - \alpha^{F(x)} - F(x)}{1 + \alpha - \alpha^{F(x)}}; \quad \alpha > 0 \quad (5)$$

The hazard rate function $h_{RT}(x)$ is given by

$$h_{RT}(x) = f(x) \frac{(1 + \alpha - \alpha^{F(x)} (1 - F(x) \log \alpha))}{(1 + \alpha - \alpha^{F(x)}) (1 + \alpha - \alpha^{F(x)} - F(x))}; \quad \alpha > 0 \quad (6)$$

If $R(x)$ and $h(x)$ are the reliability and hazard rate functions of f respectively, then the hazard rate $h_{RT}(x)$ can be written as

$$h_{RT}(x) = h(x) R(x) \frac{(1 + \alpha - \alpha^{F(x)} (1 - F(x) \log \alpha))}{(1 + \alpha - \alpha^{F(x)}) (1 + \alpha - \alpha^{F(x)} - F(x))}; \quad \alpha > 0 \quad (7)$$

From (7), it is clear that

$$\lim_{x \rightarrow -\infty} h_{RT}(x) = \frac{1}{\alpha} \lim_{x \rightarrow -\infty} h(x)$$

and,

$$\lim_{x \rightarrow \infty} h_{RT}(x) = \lim_{x \rightarrow \infty} h(x)$$

3. RTW DISTRIBUTION AND ITS PROPERTIES

Let $\Theta = (\alpha, \lambda, \beta)^T$. From (2), The continuous random variable X follows RTW distribution if its cdf, with scale parameter $\lambda > 0$ and shape parameters $\alpha > 0, \beta > 0$, for $x \in \mathbb{R}^+$ is given by

$$F_{RTW}(x, \Theta) = \frac{1 - e^{-\lambda x^\beta}}{1 + \alpha - \alpha^{1 - e^{-\lambda x^\beta}}}; \quad \alpha > 0 \quad (8)$$

and the corresponding pdf is

$$f_{RTW}(x, \Theta) = \frac{\lambda \beta x^{\beta-1} e^{-\lambda x^\beta} \left(1 + \alpha - \alpha^{1 - e^{-\lambda x^\beta}} \left(1 - (1 - e^{-\lambda x^\beta}) \log \alpha\right)\right)}{\left(1 + \alpha - \alpha^{1 - e^{-\lambda x^\beta}}\right)^2}; \quad \alpha > 0 \quad (9)$$

Using (3) and (4), the cdf and pdf in (8) and (9) can be respectively written as

$$F_{RTW}(x, \Theta) = \sum_{j=0}^{\infty} \sum_{k=0}^{\infty} \sum_{l=0}^{k+1} a_{jkl} e^{-l \lambda x^\beta}$$

where,

$$a_{jkl} = \frac{(j \log \alpha)^k \binom{k+1}{l} (-1)^l}{k! (1 + \alpha)^{j+1}}$$

and

$$f_{RTW}(x, \Theta) = x^{\beta-1} \left[1 - \frac{\alpha^{(1 - e^{-\lambda x^\beta})}}{1 + \alpha} (1 - \log \alpha (1 - e^{-\lambda x^\beta})) \right] \sum_{j=0}^{\infty} \sum_{k=0}^{\infty} \sum_{l=0}^k b_{jkl} e^{-\lambda(l+1)x^\beta}$$

where,

$$b_{jkl} = \frac{\lambda \beta (j+1) (j \log \alpha)^k \binom{k}{l} (-1)^l}{(1 + \alpha)^{j+1} k!}$$

The reliability function $R_{RTW}(x, \Theta)$ and the hazard rate function $h_{RTW}(x, \Theta)$ for $x \in \mathbb{R}^+$ are, respectively, given by

$$R_{RTW}(x, \Theta) = \frac{\alpha \left(1 - \alpha^{-e^{-\lambda x^\beta}}\right) + e^{-\lambda x^\beta}}{1 + \alpha - \alpha^{1 - e^{-\lambda x^\beta}}}; \quad \alpha > 0 \quad (10)$$

$$h_{RTW}(x, \Theta) = \frac{\lambda \beta x^{\beta-1} e^{-\lambda x^\beta} \left(1 + \alpha - \alpha^{1 - e^{-\lambda x^\beta}} \left(1 - (1 - e^{-\lambda x^\beta}) \log \alpha\right)\right)}{\left(1 + \alpha - \alpha^{1 - e^{-\lambda x^\beta}}\right) \left(\alpha \left(1 - \alpha^{-e^{-\lambda x^\beta}}\right) + e^{-\lambda x^\beta}\right)}; \quad \alpha > 0$$

The behaviour of the hazard rate function at extremes for different values of shape parameter β .

$$h(0) = \begin{cases} \infty & \text{for } 0 < \beta < 1, \\ \frac{\lambda}{\alpha} & \text{for } \beta = 1, \\ 0 & \text{for } \beta > 1, \end{cases} \quad h(\infty) = \begin{cases} 0 & \text{for } 0 < \beta < 1, \\ \lambda & \text{for } \beta = 1, \\ \infty & \text{for } \beta > 1. \end{cases}$$

Remark: When $\alpha = 1$, the RTW distribution becomes the Weibull distribution. In that situation the shapes for hazard rate function are conspicuous in the literature. The seven important special cases of RTW distribution are presented in table 1

Figure 1 depicts some plots of the RTW density for selected parameter values. Plots of the hazard rate function of the RTW distribution for selected parameter values are displayed in Figure 2.

Table 1: Sub-cases of the RTW Distribution

α	λ	β	Reduced model
-	1	-	RT one-parameter Weibull distribution
1	-	-	Two-parameter Weibull distribution
1	1	-	One-parameter Weibull distribution
-	-	2	RT-Rayleigh distribution
1	-	2	Rayleigh distribution
-	-	1	RT-exponential distribution
1	-	1	Exponential distribution

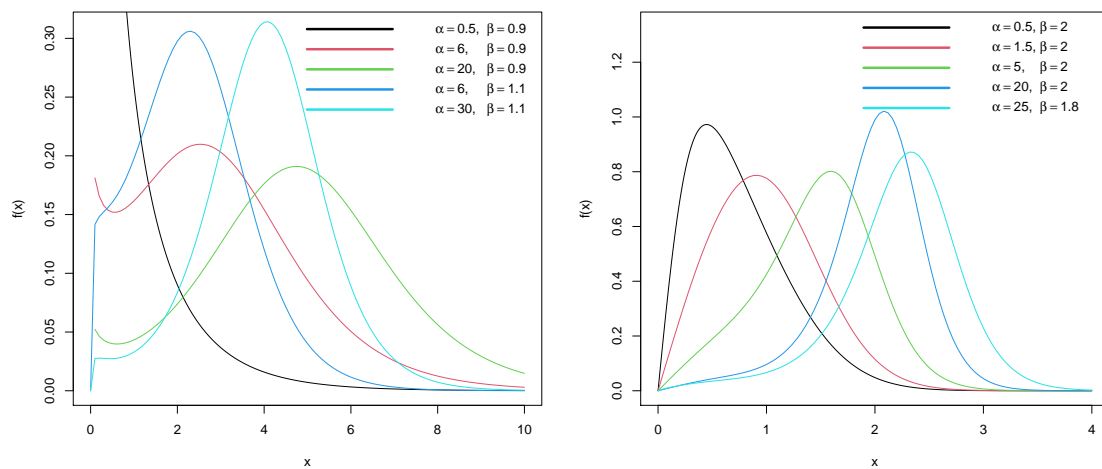


Figure 1: Plots of the RTW density for $\lambda = 1$ and various values of α and β .

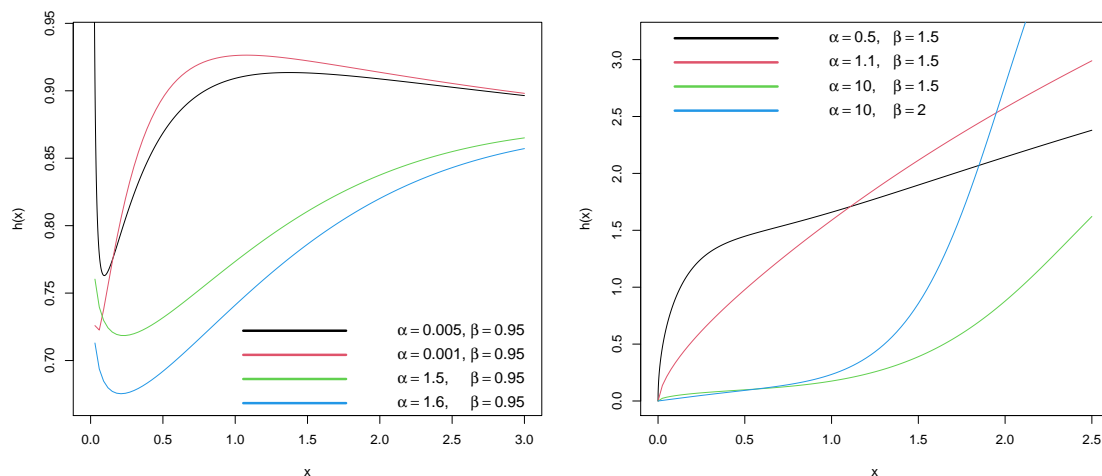


Figure 2: Plots of the RTW hazard rate function for $\lambda = 1$ and various values of α and β .

3.1. Moment and moment generating function

In this subsection, the r th moment and the moment generating function of the RTW distribution are obtained by using the following series representations.

$$\alpha^{-x} = \sum_{k=0}^{\infty} \frac{(-\log \alpha)^k x^k}{k!} \quad (11)$$

$$(1-x)^{-2} = \sum_{k=0}^{\infty} (k+1)x^k; \quad |x| < 1, \quad (12)$$

$$(1-x)^{-1} = \sum_{k=0}^{\infty} x^k; \quad |x| < 1, \quad (13)$$

The r th moment of X can be obtained as

$$\begin{aligned} E(X^r) &= \int_0^{\infty} x^r f(x) dx \\ &= \frac{1}{(1+\alpha)^2} \int_0^{\infty} x^r \lambda \beta x^{\beta-1} e^{-\lambda x^{\beta}} \left(1 + \alpha - \alpha^{1-e^{-\lambda x^{\beta}}} \left(1 - (1 - e^{-\lambda x^{\beta}}) \log \alpha \right) \right) \\ &\quad \times \left(1 - \frac{\alpha^{1-e^{-\lambda x^{\beta}}}}{1+\alpha} \right)^{-2} dx \end{aligned} \quad (14)$$

By substituting $1 - e^{-\lambda x^{\beta}} = y$ in (14), we get

$$E(X^r) = \sum_{j=0}^{\infty} \frac{1}{(1+\alpha)^{j+1}} \left(\int_0^1 \left(\frac{-1}{\lambda} \log(1-y) \right)^{\frac{r}{\beta}} \left(\alpha^{jy} + \frac{\alpha^{(j+1)y}(j+1)\log \alpha}{1+\alpha} y \right) dy \right) \quad (15)$$

Again, substituting $\frac{-1}{\lambda} \log(1-y) = x$ in (15), we get the final expression as

$$E(X^r) = \sum_{j=0}^{\infty} \sum_{k=0}^{\infty} \frac{\lambda \alpha^j (-\log \alpha)^k}{(1+\alpha)^{j+1} k!} \Gamma\left(\frac{r}{\beta} + 1\right) \{A + B\}$$

where,

$$A = \frac{j^k}{(\lambda(k+1))^{\frac{r}{\beta}+1}}$$

and

$$B = \frac{\alpha \log \alpha (j+1)^{k+1}}{1+\alpha} \left(\frac{1}{(\lambda(k+1))^{\frac{r}{\beta}+1}} - \frac{1}{(\lambda(k+2))^{\frac{r}{\beta}+1}} \right)$$

and the moment generating function can be obtained as

$$M_X(t) = \int_0^{\infty} e^{tx} f(x) dx$$

by using the same procedure as above, we get the final expression for moment generating function as

$$\sum_{i=0}^{\infty} \sum_{j=0}^{\infty} \sum_{k=0}^{\infty} \frac{\lambda t^i \alpha^j (-\log \alpha)^k}{(1+\alpha)^{j+1} k! i!} \Gamma\left(\frac{i}{\beta} + 1\right) \{C + D\}$$

where,

$$C = \frac{j^k}{(\lambda(k+1))^{\frac{1}{\beta}+1}}$$

and

$$D = \frac{\alpha \log \alpha (j+1)^{k+1}}{1+\alpha} \left(\frac{1}{(\lambda(k+1))^{\frac{1}{\beta}+1}} - \frac{1}{(\lambda(k+2))^{\frac{1}{\beta}+1}} \right)$$

3.2. Mean residual life and mean waiting time

Suppose that X is a continuous random variable with reliability function $R(x)$, the mean residual life is the expected additional lifetime given that a component has survived until time t . The mean residual life function, say $\mu(t)$, is given by

$$\mu(t) = \frac{1}{R(t)} \left(E(t) - \int_0^t x f(x) dx \right) - t \tag{16}$$

where

$$E(t) = \sum_{j=0}^{\infty} \sum_{k=0}^{\infty} \frac{\lambda \alpha^j (-\log \alpha)^k}{(1+\alpha)^{j+1} k!} \Gamma\left(\frac{1}{\beta} + 1\right) \left\{ \frac{j^k}{(\lambda(k+1))^{\frac{1}{\beta}+1}} + \frac{\alpha \log \alpha (j+1)^{k+1}}{1+\alpha} \right. \\ \left. \times \left(\frac{1}{(\lambda(k+1))^{\frac{1}{\beta}+1}} - \frac{1}{(\lambda(k+2))^{\frac{1}{\beta}+1}} \right) \right\} \tag{17}$$

and

$$\int_0^t x f(x) dx = \sum_{j=0}^{\infty} \sum_{k=0}^{\infty} \frac{\alpha j^k (-\log \alpha)^k}{(1+\alpha)^{j+1} k!} \left\{ \frac{1}{\lambda^{\frac{1}{\beta}} (k+1)^{\frac{1}{\beta}+1}} \gamma\left(\lambda(k+1)t^{\beta}, \frac{1}{\beta} + 1\right) \right. \\ \left. + \frac{(j+1) \log \alpha}{1+\alpha} \left[\frac{\gamma\left(\lambda(k+1)t^{\beta}, \frac{1}{\beta} + 1\right)}{\lambda^{\frac{1}{\beta}} (k+1)^{\frac{1}{\beta}+1}} - \frac{\gamma\left(\lambda(k+1)t^{\beta}, \frac{1}{\beta} + 1\right)}{\lambda^{\frac{1}{\beta}} (k+2)^{\frac{1}{\beta}+1}} \right] \right\} \tag{18}$$

Substituting (10), (17) and (18) in (16), $\mu(t)$ can be written as

$$\mu(t) = \frac{1+\alpha - \alpha^{1-e^{-\lambda t^{\beta}}}}{\alpha(1 - \alpha^{-e^{-\lambda t^{\beta}}}) + e^{-\lambda t^{\beta}}} \sum_{j=0}^{\infty} \sum_{k=0}^{\infty} \frac{\alpha^j (-\log \alpha)^k}{(1+\alpha)^{j+1} k!} \\ \times \left(A' + B' \frac{-j^k}{\Gamma\left(\frac{1}{\beta} + 1\right)} (C' + D') \right) - t$$

where,

$$A' = \frac{j^k}{(\lambda(k+1))^{\frac{1}{\beta}+1}}, \\ B' = \frac{\alpha \log \alpha (j+1)^{k+1}}{1+\alpha} \left(\frac{1}{(\lambda(k+1))^{\frac{1}{\beta}+1}} - \frac{1}{(\lambda(k+2))^{\frac{1}{\beta}+1}} \right), \\ C' = \frac{\gamma\left(\lambda(k+1)t^{\beta}, \frac{1}{\beta} + 1\right)}{\lambda^{\frac{1}{\beta}} (k+1)^{\frac{1}{\beta}+1}}$$

and

$$D' = \frac{(j+1)\log\alpha}{1+\alpha} \left[\frac{\gamma\left(\lambda(k+1)t^\beta, \frac{1}{\beta} + 1\right)}{\lambda^{\frac{1}{\beta}}(k+1)^{\frac{1}{\beta}+1}} - \frac{\gamma\left(\lambda(k+1)t^\beta, \frac{1}{\beta} + 1\right)}{\lambda^{\frac{1}{\beta}}(k+2)^{\frac{1}{\beta}+1}} \right]$$

where $\gamma(a, b) = \int_0^a x^{b-1}e^{-x}dx$ is the lower incomplete gamma function.

The mean waiting time represents the waiting time elapsed since the failure of an object on condition that this failure had occurred in the interval $[0, t]$. The mean waiting time of X , say $\bar{\mu}(t)$, is defined by

$$\bar{\mu}(t) = t - \frac{1}{F(t)} \int_0^t xf(x)dx. \tag{19}$$

Substituting (8) and (18) in (19), we get

$$\begin{aligned} \bar{\mu}(t) = t - \frac{1+\alpha - \alpha^{1-e^{-\lambda t^\beta}}}{1 - e^{-\lambda t^\beta}} & \sum_{j=0}^{\infty} \sum_{k=0}^{\infty} \frac{\alpha^j j^k (-\log\alpha)^k}{(1+\alpha)^{j+1} k!} \left\{ \frac{1}{\lambda^{\frac{1}{\beta}}(k+1)^{\frac{1}{\beta}+1}} \right. \\ & \times \gamma\left(\lambda(k+1)t^\beta, \frac{1}{\beta} + 1\right) + \frac{(j+1)\log\alpha}{1+\alpha} \left[\frac{\gamma\left(\lambda(k+1)t^\beta, \frac{1}{\beta} + 1\right)}{\lambda^{\frac{1}{\beta}}(k+1)^{\frac{1}{\beta}+1}} \right. \\ & \left. \left. - \frac{\gamma\left(\lambda(k+1)t^\beta, \frac{1}{\beta} + 1\right)}{\lambda^{\frac{1}{\beta}}(k+2)^{\frac{1}{\beta}+1}} \right] \right\} \end{aligned}$$

3.3. Order Statistics

Let X_1, X_2, \dots, X_n be a random sample of size n , and let $X_{r:n}$ denote the r th order statistic, then, the pdf of $X_{r:n}$, say $f_{r:n}(x)$ is given by

$$f_{r:n}(x) = \frac{n!}{(r-1)!(n-r)!} F(x)^{r-1} f(x) (1-F(x))^{n-r}. \tag{20}$$

Substituting (8) and (9) in (20), we get

$$\begin{aligned} f_{r:n}(x) = \frac{\lambda\beta x^{\beta-1} e^{-\lambda x^\beta} \left(1 + \alpha - \alpha^{1-e^{-\lambda x^\beta}} \left(1 - (1 - e^{-\lambda x^\beta}) \log\alpha \right) \right)}{B(r, n-r+1) \left(1 + \alpha - \alpha^{1-e^{-\lambda x^\beta}} \right)^{n+1}} \\ \times \left(1 - e^{-\lambda x^\beta} \right)^{r-1} \left(\alpha \left(1 - \alpha^{-e^{-\lambda x^\beta}} \right) + e^{-\lambda x^\beta} \right)^{n-r} \end{aligned}$$

where $B(a, b)$ is the beta function.

3.4. Stress Strength Reliability

Suppose X_1 and X_2 be independent strength and stress random variables respectively, where $X_1 \sim RTW(\alpha_1, \lambda_1, \beta)$ and $X_2 \sim RTW(\alpha_2, \lambda_2, \beta)$, then the stress strength reliability $\mathbb{P}(X_1 > X_2)$, say SSR , is defined as

$$SSR = \int_{-\infty}^{\infty} f_1(x)F_2(x)dx$$

Table 2: Average values of MLEs and the corresponding MSEs(n=50).

Parameter λ	α	β	MLE			MSE		
			$\hat{\lambda}$	$\hat{\alpha}$	$\hat{\beta}$	$\hat{\lambda}$	$\hat{\alpha}$	$\hat{\beta}$
1	0.5	1	1.18927	0.75566	0.74107	0.27647	0.71977	0.04782
		1.5	1.22622	0.87384	1.51407	0.40466	0.58467	0.07297
		2	1.18561	0.77796	1.98113	0.24700	0.61990	0.11475
	1	1	1.08698	1.18120	1.04943	0.23511	1.10633	0.03877
		1.5	1.12510	1.27644	1.55446	0.24403	1.12121	0.09897
		2	1.13204	1.28600	2.04414	0.29381	1.45360	0.17665
	1.5	1	1.04126	1.72249	1.05876	0.27080	2.20896	0.05698
		1.5	1.08026	1.78405	1.54105	0.28238	2.09977	0.10365
		2	1.07287	1.81606	2.12707	0.27423	1.89261	0.24845
2	1	0.98987	2.07177	1.07668	0.24656	2.17639	0.07918	
	1.5	0.98794	2.19104	1.60992	0.22690	2.61831	0.17018	
	2	0.98397	2.19145	2.15508	0.22988	2.63456	0.31296	
2	0.5	1	2.28613	0.68043	1.02709	0.30981	0.33733	0.03757
		1.5	2.16929	0.57581	1.57420	0.19697	0.27864	0.07851
		2	2.23597	0.60438	2.09259	0.30316	0.31276	0.11952
	1	1	2.17700	1.19918	1.04533	0.51708	1.12488	0.03843
		1.5	2.21341	1.27536	1.55452	0.49046	1.11322	0.09883
		2	2.15140	1.33614	2.09166	0.55797	1.57897	0.15442
	1.5	1	2.05912	1.74110	1.05653	0.55367	2.22683	0.05775
		1.5	2.00179	1.58862	1.61057	0.45244	1.48239	0.15847
		2	1.95160	1.56072	2.18486	0.52078	2.38803	0.27118
	2	1	1.99288	2.15485	1.09058	0.58386	2.18773	0.10266
		1.5	2.01983	2.26075	1.58730	0.53255	2.56440	0.15576
		2	1.99596	2.23927	2.14504	0.58591	3.79841	0.27387

The stress strength reliability SSR, is obtained by using (8) , (9), (11), (12) and (13) and is given by

$$\begin{aligned}
 SSR = & \lambda_1 \sum_{j=0}^{\infty} \sum_{k=0}^{\infty} \sum_{l=0}^{\infty} \sum_{m=0}^{\infty} \frac{\alpha_1^j \alpha_2^k k^m (-\log \alpha_1)^l (-\log \alpha_2)^m}{(1 + \alpha_1)^{j+1} (1 + \alpha_2)^{k+1} l! m!} \left\{ \left(j^l + \frac{\alpha_1 \log \alpha_1 (j+1)^{l+1}}{1 + \alpha_1} \right) \right. \\
 & \times \frac{\lambda_2}{[(l+1)\lambda_1 + m\lambda_2][(l+1)\lambda_1 + (m+1)\lambda_2]} \\
 & \left. - \frac{\lambda_2 \alpha_1 \log \alpha_1 (j+1)^{l+1}}{(1 + \alpha_1)[(l+2)\lambda_1 + (m+1)\lambda_2][(l+2)\lambda_1 + m\lambda_2]} \right\}
 \end{aligned}$$

Table 3: Average values of MLEs and the corresponding MSEs(n=100).

Parameter	MLE			MSE				
	λ	α	β	$\hat{\lambda}$	$\hat{\alpha}$	$\hat{\beta}$		
1	0.5	1	1.12427	0.85980	1.01394	0.16520	0.36686	0.02039
		1.5	1.10945	0.64163	1.49813	0.08311	0.15675	0.04790
		2	1.03860	0.51790	2.00760	0.04648	0.11094	0.08922
	1	1	1.09751	1.20162	1.00568	0.13615	0.44997	0.02630
		1.5	1.09006	1.14954	1.52710	0.14385	0.47309	0.05824
		2	1.07148	1.14295	2.07225	0.17511	0.69167	0.12353
	1.5	1	1.04769	1.66319	1.01968	0.17384	1.08369	0.02691
		1.5	1.05555	1.68631	1.54287	0.19368	1.20057	0.07301
		2	1.05153	1.64619	2.06356	0.17319	1.02013	0.14828
2	1	0.96890	2.04959	1.05881	0.19612	1.91723	0.04225	
	1.5	1.02776	2.05201	1.52135	0.15814	1.90158	0.04479	
	2	1.02772	2.04339	2.02851	0.15842	1.92072	0.07969	
2	0.5	1	2.20157	0.64279	1.00275	0.20282	0.21313	0.01958
		1.5	2.15936	0.60787	1.50924	0.18855	0.18872	0.03718
		2	2.20967	0.64716	2.00121	0.25218	0.27663	0.07502
	1	1	2.14197	1.15711	1.03218	0.35039	0.70753	0.03321
		1.5	2.12690	1.14278	1.55439	0.36045	0.69360	0.06954
		2	2.22353	1.21377	1.98709	0.51312	1.10397	0.09771
	1.5	1	2.09963	1.74911	1.03669	0.50675	1.89731	0.03895
		1.5	2.05345	1.67112	1.55151	0.33247	0.93642	0.06657
		2	2.06760	1.68920	2.06563	0.37754	1.67294	0.15132
	2	1	1.92617	2.06013	1.05836	0.42906	1.98756	0.04258
		1.5	2.01885	2.20664	1.55748	0.40409	1.79326	0.08481
		2	1.99881	2.13749	2.07929	0.41542	2.86112	0.14579

4. STATISTICAL INFERENCE

4.1. Maximum Likelihood Estimators

Let x_1, x_2, \dots, x_n be a random sample from RTW distribution, then the logarithm of the likelihood function is

$$\begin{aligned}
 l = & n \log \alpha + n \log \beta + (\beta - 1) \sum_{i=1}^n \log x_i - \lambda \beta \sum_{i=1}^n x_i - 2 \sum_{i=1}^n \log \left(1 + \alpha - \alpha^{1 - e^{-\lambda x_i^\beta}} \right) \\
 & + \sum_{i=1}^n \log \left[1 + \alpha - \alpha^{1 - e^{-\lambda x_i^\beta}} \left(1 - \log \alpha \left(1 - e^{-\lambda x_i^\beta} \right) \right) \right] \quad (21)
 \end{aligned}$$

The MLEs of α , λ and β are obtained by partially differentiating (21) with respect to the corresponding parameters and equating to zero, we have

$$\frac{\partial l}{\partial \alpha} = \sum_{i=1}^n \frac{1 + (1 - e^{-\lambda x_i^\beta})^2 \alpha^{-e^{-\lambda x_i^\beta}} \log \alpha}{1 + \alpha - \alpha^{1 - e^{-\lambda x_i^\beta}} (1 - (1 - e^{-\lambda x_i^\beta}) \log \alpha)} - 2 \sum_{i=1}^n \frac{1 - (1 - e^{-\lambda x_i^\beta}) \alpha^{-e^{-\lambda x_i^\beta}}}{1 + \alpha - \alpha^{1 - e^{-\lambda x_i^\beta}}} \quad (22)$$

$$\frac{\partial l}{\partial \beta} = \frac{n}{\beta} + (1 - \lambda) \sum_{i=1}^n x_i + \alpha \lambda \beta \log \alpha \sum_{i=1}^n x_i^{\beta-1} e^{-\lambda x_i^\beta} \alpha^{-e^{-\lambda x_i^\beta}} \times \left[\frac{\alpha}{1 + \alpha - \alpha^{1 - e^{-\lambda x_i^\beta}}} - \frac{(1 - e^{-\lambda x_i^\beta}) \log \alpha}{1 + \alpha - \alpha^{1 - e^{-\lambda x_i^\beta}} (1 - (1 - e^{-\lambda x_i^\beta}) \log \alpha)} \right] \quad (23)$$

$$\frac{\partial l}{\partial \lambda} = \frac{n}{\lambda} + \beta \sum_{i=1}^n x_i - \alpha \log \alpha \sum_{i=1}^n x_i^\beta e^{-\lambda x_i^\beta} \alpha^{-e^{-\lambda x_i^\beta}} \left[\frac{2}{1 + \alpha - \alpha^{1 - e^{-\lambda x_i^\beta}}} - \frac{(1 - e^{-\lambda x_i^\beta}) \log \alpha}{1 + \alpha - \alpha^{1 - e^{-\lambda x_i^\beta}} (1 - (1 - e^{-\lambda x_i^\beta}) \log \alpha)} \right] \quad (24)$$

The above three equations (22),(23) and (24) are not in closed form. thus, it is difficult to calculate the values of the parameters α , β and λ . However, R software can be used to get the MLE.

4.2. Simulation study

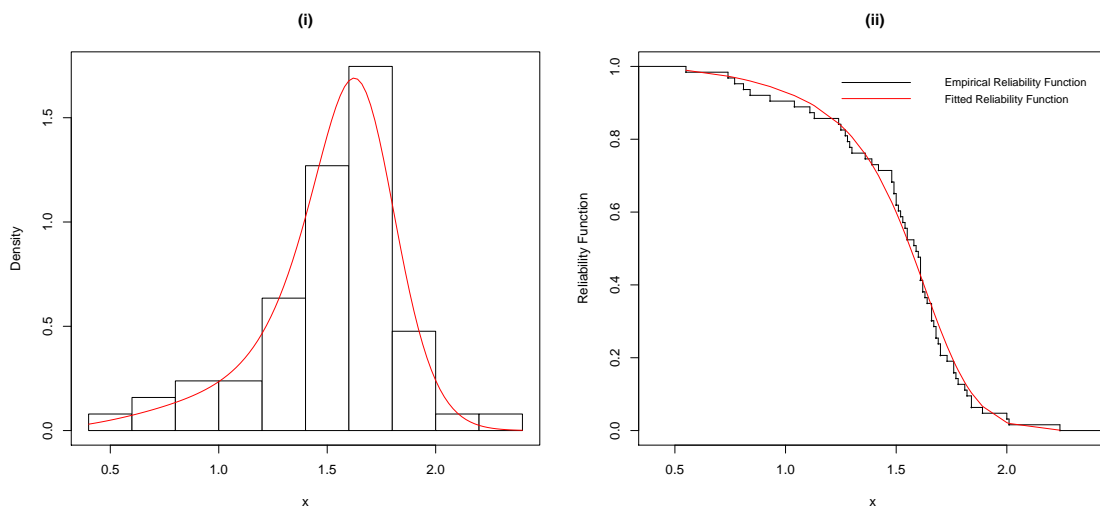


Figure 3: (i) The relative histogram and the fitted RTW distribution. (ii) The fitted RTW reliability function and empirical reliability function for first data set.

The simulation study has been performed using R Software to show the behaviour of the MLEs in terms of the sample size n . Two sets of sample ($n=50$, $n=100$) each replicated 100 times with different values of parameters $\lambda = (1, 2)$, $\alpha = (0.5, 1, 1.5, 2)$ and $\beta = (1, 1.5, 2)$ were

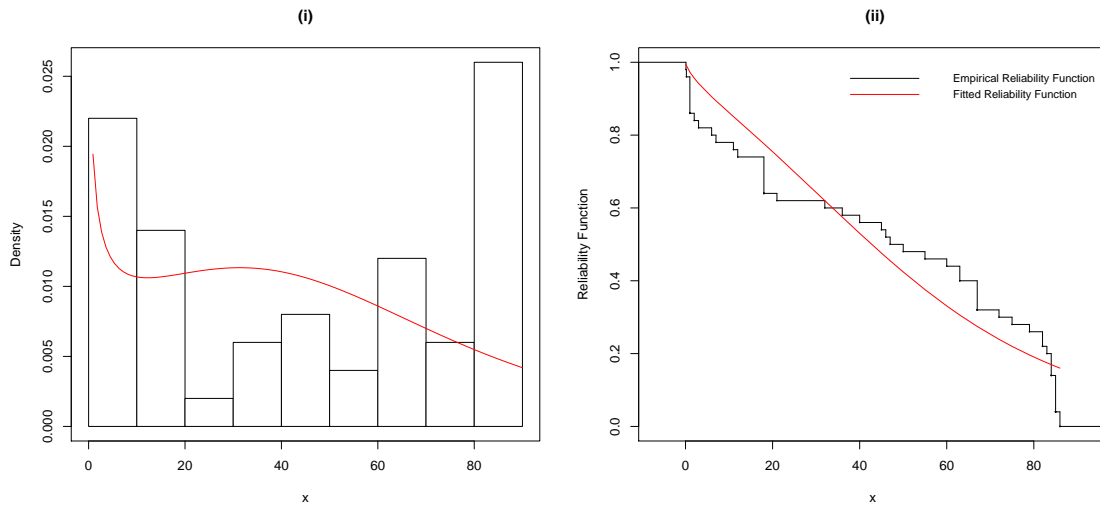


Figure 4: (i) The relative histogram and the fitted RTW distribution. (ii) The fitted RTW reliability function and empirical reliability function for second data set.

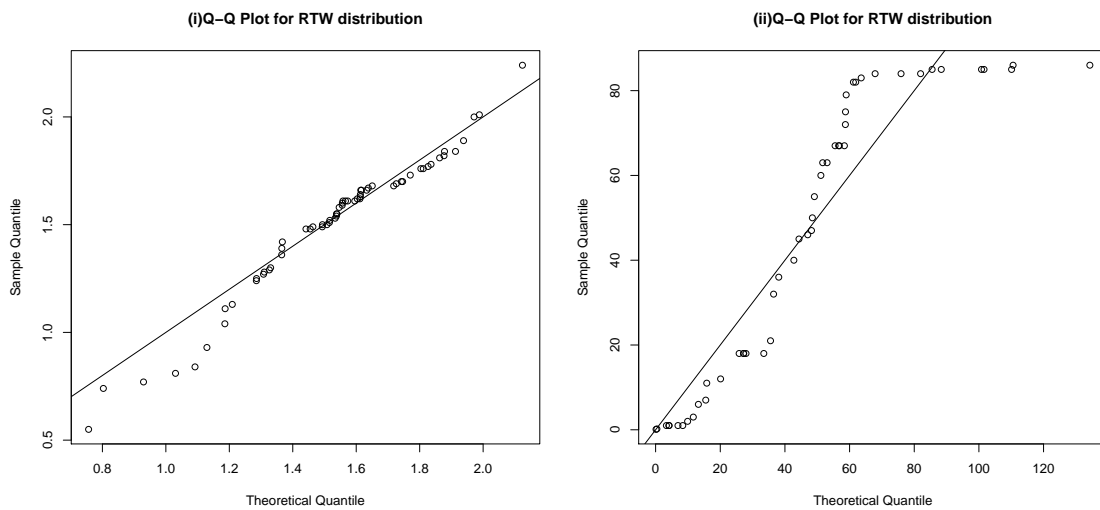


Figure 5: Q-Q plot for the RTW distribution for data set first and data set second, respectively.

generated from RTW. In each setting, the average values of MLEs and the corresponding empirical mean squared errors (MSEs) were obtained. The simulation results are presented in table 2 and table 3. From tables 2 and 3, it can be seen that the estimates are stable and quite close to the true parameter values. As the sample size increases the MSE decreases in all the cases.

5. APPLICATIONS

In this section, we analyse two data sets to describe the significance and flexibility of the RTW distribution. The data set first reported by Nassar et al. [12], originally published by Smith and Naylor [13], corresponding to strengths of 1.5 cm glass fibers, measured at the National Physical Laboratory, England. The data are as follows: 0.55, 0.93, 1.25, 1.36, 1.49, 1.52, 1.58, 1.61, 1.64, 1.68, 1.73, 1.81, 2, 0.74, 1.04, 1.27, 1.39, 1.49, 1.53, 1.59, 1.61, 1.66, 1.68, 1.76, 1.82, 2.01, 0.77, 1.11, 1.28,

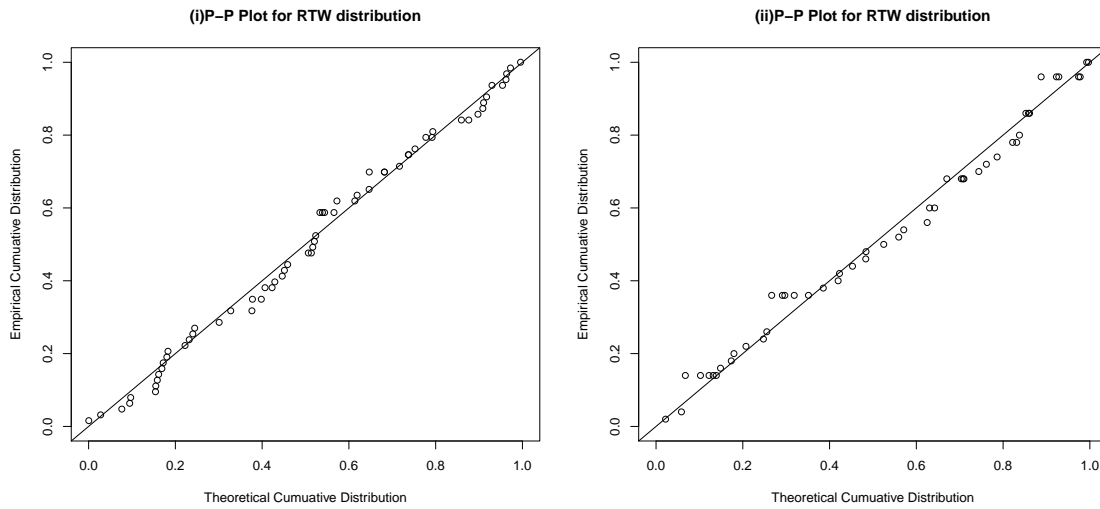


Figure 6: P-P plot for the RTW distribution for data set first and data set second, respectively.

Table 4: MLEs (standard errors in parentheses), K-S Statistic, and p-values for the first data set.

Model	$\hat{\alpha}$	Estimates		Statistics	
		$\hat{\beta}$	$\hat{\lambda}$	K-S	p-value
RTW	9.49959 (6.00647)	3.261905 (0.69075)	0.72053 (0.40517)	0.08745	0.72090
APW	10.86178 (12.72527)	4.48322 (0.76269)	0.19483 (0.10826)	0.12249	0.30090
APIW	193.05946 (267.40709)	3.87688 (0.30960)	0.63654 (0.1823435)	0.21627	0.00551
MW	0.03088 (0.04349)	6.37442 (0.96544)	0.04087 (0.02476)	0.13341	0.21210
TW	0.92496 (0.21931)	5.97478 (0.74495)	1.80960 (0.07553)	0.15191	0.10920
LW	0.53504 (0.48673)	4.94433 (0.65927)	0.77920 (0.18296)	0.13673	0.18950
ZBLL	0.25140 (0.06121)	18.41002 (3.05420)	1.82436 (0.04629)	0.13053	0.23330
APE	145351 (23726.57)	-	2.15458 (0.09901)	0.22099	0.00425
W	-	5.77962 (0.57515)	0.05978 (0.02047)	0.15232	0.10750

1.42, 1.5, 1.54, 1.6, 1.62, 1.66, 1.69, 1.76, 1.84, 2.24, 0.81, 1.13, 1.29, 1.48, 1.5, 1.55, 1.61, 1.62, 1.66, 1.7, 1.77, 1.84, 0.84, 1.24, 1.3, 1.48, 1.51, 1.55, 1.61, 1.63, 1.67, 1.7, 1.78, 1.89.

The second data set was reported by Elbatal et al. [14], originally published by Aarset [15], which represents the failure times of 50 devices. The data are as follows: 0.1, 0.2, 1, 1, 1, 1, 2, 3,

Table 5: $-2l(\hat{\theta})$, AIC, AICC, BIC for the first data set.

Model	$-2l(\hat{\theta})$	AIC	AICC	BIC
RTW	22.16977	28.16977	28.57655	34.59917
APW	26.94826	32.94826	33.35504	39.37766
APIW	75.77237	81.77237	82.17915	88.20177
MW	29.78938	35.78938	36.19616	42.21878
TW	30.28635	36.28635	36.69313	42.71576
LW	28.42141	34.42141	34.82819	40.85081
ZBLL	24.23729	30.23729	30.64407	36.66669
APE	67.56511	71.56511	71.76511	75.85138
W	30.41369	34.41369	34.61369	38.69995

Table 6: MLEs (standard errors in parentheses), K-S Statistic, and p-values for the second data set.

Model	Estimates			Statistics	
	$\hat{\alpha}$	$\hat{\beta}$	$\hat{\lambda}$	K-S	p-value
RTW	6.28982 (2.80293)	0.71267 (0.12226)	0.17523 (0.10967)	0.16014	0.15390
APW	4.51340 (4.01925)	0.83571 (0.13558)	0.05854 (0.03910)	0.17492	0.09379
APIW	62.22037 (86.31937)	0.59918 (0.05672)	1.14499 (0.39802)	0.27478	0.00105
MW	0.01863 (0.00375)	0.37305 (0.18838)	0.04043 (0.03113)	0.19432	0.04583
TW	0.00010 (0.42067)	0.94905 (0.12873)	44.91508 (12.90900)	0.1928	0.04860
LW	0.91774 (0.69388)	0.88097 (0.12668)	0.04050 (0.04259)	0.18488	0.06555
ZBLL	20.23812 (4.33771)	2.25295 (0.46228)	0.00273 (0.00091)	0.23307	0.00874
APE	2.64622 (1.90895)	-	0.02687 (0.00474)	0.17657	0.08851
W	-	0.94770 (0.11778)	0.02719 (0.01375)	0.19313	0.04800

6, 7, 11, 12, 18, 18, 18, 18, 18, 21, 32, 36, 40, 45, 46, 47, 50, 55, 60, 63, 63, 67, 67, 67, 67, 72, 75, 79, 82, 82, 83, 84, 84, 84, 85, 85, 85, 85, 86, 86.

We compare the fit of the proposed RTW distribution with its sub-model Weibull (W) distribution and with several other competitive models, namely Alpha Power Weibull (APW) (see [12]), Alpha Power Inverse Weibull (APIW) (see [16]), Modified Weibull (MW) (see [17]), Transmuted Weibull (TW) (see [18]), Lindley Weibull (LW) (see [19]), Zografos–Balakrishnan log-logistic

Table 7: $-2l(\hat{\theta})$, AIC, AICC, BIC for the second data set.

Model	$-2l(\hat{\theta})$	AIC	AICC	BIC
RTW	470.2143	476.2143	476.7360	481.9504
APW	479.2431	485.2431	485.7648	490.9791
APIW	519.9063	525.9063	526.4280	531.6423
MW	478.9685	484.9685	485.4902	490.7045
TW	482.0043	488.0043	488.5261	493.7404
LW	479.5173	485.5173	486.0390	491.2534
ZBLL	517.3178	523.3178	523.8396	529.0539
APE	480.5838	484.5838	484.8391	488.4078
W	482.0038	486.0038	486.2591	489.8278

(ZBLL) (see [20]), and Alpha Power Exponential (APE) (see [10]), their corresponding density functions for $x > 0$ are as follows

$$\text{APW } f(x) = \frac{\log \alpha}{\alpha - 1} \lambda \beta \alpha^{1-e^{-\lambda x^\beta}} x^{\beta-1} e^{-\lambda x^\beta}$$

$$\text{APIW } f(x) = \frac{\log \alpha}{\alpha - 1} \lambda \beta x^{-(\beta+\alpha)} e^{-\lambda x^{-\beta}} \alpha^{e^{-\lambda x^{-\beta}}}$$

$$\text{MW } f(x) = (\alpha + \lambda \beta x^{\beta-1}) e^{-\alpha x - \lambda x^\beta}$$

$$\text{TW } f(x) = \frac{\beta}{\lambda} \left(\frac{x}{\lambda}\right)^{\beta-1} e^{-\left(\frac{x}{\lambda}\right)^\beta} \left(1 - \alpha + 2\alpha e^{-\left(\frac{x}{\lambda}\right)^\beta}\right)$$

$$\text{LW } f(x) = \frac{\beta \alpha^2}{\alpha + 1} \lambda \beta x^{\beta-1} + \lambda^2 \beta x^{2\beta-1} e^{-\alpha(\lambda x)^\beta}$$

$$\text{ZBLL } f(x) = \frac{\beta}{\lambda^\beta \Gamma(\alpha)} x^{\beta-1} \left(1 + \left(\frac{x}{\lambda}\right)^\beta\right)^{-2} \left(\log \left(1 + \left(\frac{x}{\lambda}\right)^\beta\right)\right)^{\alpha-1}$$

$$\text{APE } f(x) = \frac{\log \alpha}{\alpha - 1} \lambda e^{-\lambda x} \alpha^{1-e^{-\lambda x}}$$

where $\alpha, \beta, \lambda > 0$ and $\Gamma(\alpha) = \int_0^\infty x^{\alpha-1} e^{-x} dx$ is the gamma function.

From Table 4, Table 5, Table 6 and Table 7, it is evident that RTW distribution has lowest $-2l(\hat{\theta})$, AIC, AICC, BIC, K-S values and highest p-value among all the other competitive models. Hence the proposed model yields the better fit than the other models for both data sets.

The relative histogram and the fitted RTW distribution of the data set first and second are shown in Figures 3(i) and 4(i), respectively. The plots of the fitted RTW reliability function and empirical reliability function of the data set first and second are shown in Figures 3(ii) and 4(ii), respectively. The Q-Q plots for data set first and second are shown in Figure 5(i) and 5(ii) respectively. Also, The P-P plots for data set first and second are shown in Figure 6(i) and 6(ii) respectively that allows us to differentiate between the empirical distribution of the data with the RTW distribution. These graphical goodness of fit measures clearly support the results in

Tables 4, Table 5, Table 6 and Table 7.

6. CONCLUSION

A new family of distributions has been introduced called RT method. RT method has been specialized on the two-parameter Weibull distribution and a new three-parameter RTW distribution has been introduced. We have discussed various properties of RTW distribution. It has been realized that the three-parameter RTW distribution has more flexibility in terms of the hazard rate function and the density function. The effectiveness of the proposed model is compared with other existing models by using goodness of fit measures. The model has been fitted to two different real life data sets, the figures show that the proposed model provides better fit for both data sets in comparison to all other competitive models.

REFERENCES

- [1] Ming Xie and Chin Diew Lai. Reliability analysis using an additive weibull model with bathtub-shaped failure rate function. *Reliability Engineering & System Safety*, 52(1):87–93, 1996.
- [2] Govind S Mudholkar, Deo Kumar Srivastava, and Marshall Freimer. The exponentiated weibull family: A reanalysis of the bus-motor-failure data. *Technometrics*, 37(4):436–445, 1995.
- [3] Min Xie, Y Tang, and Thong Ngee Goh. A modified weibull extension with bathtub-shaped failure rate function. *Reliability Engineering & System Safety*, 76(3):279–285, 2002.
- [4] Jalmar MF Carrasco, Edwin MM Ortega, and Gauss M Cordeiro. A generalized modified weibull distribution for lifetime modeling. *Computational Statistics & Data Analysis*, 53(2):450–462, 2008.
- [5] CD Lai, Min Xie, and DNP Murthy. A modified weibull distribution. *IEEE Transactions on reliability*, 52(1):33–37, 2003.
- [6] Mark Bebbington, Chin-Diew Lai, and Ričardas Zitikis. A flexible weibull extension. *Reliability Engineering & System Safety*, 92(6):719–726, 2007.
- [7] Gauss M Cordeiro, Edwin MM Ortega, and Artur J Lemonte. The exponential–weibull lifetime distribution. *Journal of Statistical Computation and simulation*, 84(12):2592–2606, 2014.
- [8] Carl Lee, Felix Famoye, and Ayman Y Alzaatreh. Methods for generating families of univariate continuous distributions in the recent decades. *Wiley Interdisciplinary Reviews: Computational Statistics*, 5(3):219–238, 2013.
- [9] Ayman Alzaatreh, Carl Lee, and Felix Famoye. T-normal family of distributions: A new approach to generalize the normal distribution. *Journal of Statistical Distributions and Applications*, 1(1):1–18, 2014.
- [10] Abbas Mahdavi and Debasis Kundu. A new method for generating distributions with an application to exponential distribution. *Communications in Statistics-Theory and Methods*, 46(13):6543–6557, 2017.
- [11] Muhammad Ijaz, Wali Khan Mashwani, Atilla Göktaş, and Yuksel Akay Unvan. A novel alpha power transformed exponential distribution with real-life applications. *Journal of Applied Statistics*, pages 1–16, 2021.
- [12] M Nassar, A Alzaatreh, M Mead, and O Abo-Kasem. Alpha power weibull distribution: Properties and applications. *Communications in Statistics-Theory and Methods*, 46(20):10236–10252, 2017.
- [13] Richard L Smith and JC918854 Naylor. A comparison of maximum likelihood and bayesian estimators for the three-parameter weibull distribution. *Journal of the Royal Statistical Society: Series C (Applied Statistics)*, 36(3):358–369, 1987.
- [14] I Elbatal, M Elgarhy, and BM Golam Kibria. Alpha power transformed weibull-g family of distributions: Theory and applications. *Journal of Statistical Theory and Applications*, 2021.
- [15] Magne Vollan Aarset. How to identify a bathtub hazard rate. *IEEE Transactions on Reliability*, 36(1):106–108, 1987.

- [16] Abdulkareem M Basheer. Alpha power inverse weibull distribution with reliability application. *Journal of Taibah University for Science*, 13(1):423–432, 2019.
- [17] Ammar M Sarhan and Mazen Zaindin. Modified weibull distribution. *APPS. Applied Sciences*, 11:123–136, 2009.
- [18] Gokarna R Aryal and Chris P Tsokos. Transmuted weibull distribution: A generalization of the weibull probability distribution. *European Journal of pure and applied mathematics*, 4(2):89–102, 2011.
- [19] Gauss M Cordeiro, Ahmed Z Afify, Haitham M Yousof, Selen Cakmakyapan, and Gamze Ozel. The lindley weibull distribution: properties and applications. *Anais da Academia Brasileira de Ciências*, 90(3):2579–2598, 2018.
- [20] Konstantinos Zografos and Narayanaswamy Balakrishnan. On families of beta-and generalized gamma-generated distributions and associated inference. *Statistical methodology*, 6(4):344–362, 2009.

SKIP-LOT SAMPLING PLAN OF TYPE SKSP-T WITH GROUP ACCEPTANCE SAMPLING PLAN AS REFERENCE PLAN UNDER BURR-TYPE XII DISTRIBUTION

S. Suganya

•

Assistant Professor, Department of Statistics,
PSG College of Arts & Science,
Coimbatore, Tamil Nadu, India
suganstat@gmail.com

K. Pradeepa Veerakumari

•

Assistant Professor, Department of Statistics,
Bharathiar University,
Coimbatore, Tamil Nadu, India
pradeepaveerakumari@buc.ac.in

Abstract

This paper clearly assigns skip-lot sampling plan of type SkSP-T with Group Acceptance sampling plan is designing and Burr type XII distribution is applied to determine the lifetime of the product. The new proposed plan parameters are determined by using the two-point method on the Operating Characteristics curve together with consistent producer and consumer risks are specified. Tables are simulated for various parametric values of SkSP-T, Group acceptance sampling plan and Burr type XII distribution. Skip-lot sampling plan of type SkSP-T is also compared with Group acceptance single sampling plan and skip-lot sampling plan of type SkSP-2 with group acceptance sampling plan using Burr type XII distribution. Further, the efficiency of the proposed plan is discussed. Numerical illustration and examples are given to justify the efficiency of the proposed plan.

Keywords: Burr type XII distribution, Group Acceptance Sampling Plan, Skip-lot sampling plan of type SkSP-T.

I. Introduction

Statistical Quality Control (SQC) use statistical mechanisms to supervise the quality of products and maintenance. Acceptance sampling plans are followed by Statistical Quality Control tools and it is used to provide the "good quality of finished products". Acceptance sampling plan is a decision-making tool. It is a technique that deals with accepting or not the lot to be found on sampling inspection that delivers the quality of products manufactured by industries. Today's scientific world the area of acceptance sampling and statistical quality control has been enhanced by various quality control engineers, manufacturing industries, statisticians, biologists, researchers and etc. The most important areas of Acceptance Sampling plan is classified into four broad categories.

Dodge [8] introduced skip-lot sampling plans. It is an expansion of CSP. In general, the skip-lot sampling plan is the function of continuous sampling plans. The initial skip-lot sampling plan

is a single determination or test for verifying the lots acceptance or rejection. It is called the skip-lot sampling plan of type SkSP-1. Skip-lot sampling plan is bulk materials or products produced in successive lots. The SkSP-1 sampling plan was proposed without considering the concept of reference sampling plan. The structure of lot-by-lot sampling inspection plans and the condition is made for inspecting only a fraction of submitted lots. It is called the skip lot sampling plans. Dodge and Perry [9] introduced Skip-lot Sampling Plan of type SkSP-2. It is an extension of skip-lot sampling plan of type SkSP-1 and based on the origin of continuous sampling plan of CSP-1. Soundararajan and Vijayaraghavan [18] introduced the new system of skip-lot sampling plan; it is designated as SkSP-3. Skip-lot sampling plan of type SkSP-V is introduced by Balamurali and Chi-Hyuck Jun [6]. It is based on the concept of continuous sampling plan of type CSP-V. Skip-lot sampling plans are efficient in acceptance sampling system and it is used to reduce inspections. In skip-lot sampling system, the quality of submitted lots is extremely good and it is acceptable. Skip-lot sampling plans are best when the defective-free production in the production process.

Tightened multilevel plans that include three levels designed by Fordice [10]. Kandasamy and Govindaraju [11] used Markov Chain techniques to find the characteristics function of CSP-T plan. Balamurali [4] proposed Modified Tightened Three level Continuous sampling plan. Balamurali and Chi-Hyuck Jun [5] proposed a modified CSP-T sampling procedure.

Pradeepa Veerakumari and Suganya [15] introduced tightened three levels Skip-lot sampling plan, which is designated as SkSP-T. Skip-lot sampling plan of type SKSP-T is based on the concept of continuous sampling plan of types CSP-T and CSP-M modified tightened three level continuous sampling plans and skip-lot sampling plan of type SkSP-2. Sampling levels are fixed by using CSP-M procedure; sampling fractions are taken from the CSP-T procedure and other concepts are taken by modified CSP-T and SkSP-2 procedures. In SkSP-T sampling plan, the sampling frequency (f) is minimized by every skipping inspection level. The Operating Characteristic functions and operating procedures are derived for SkSP-T plan. SkSP-T plan vary among normal and skipping inspection with three levels. Skip-lot sampling plan starts with normal inspection using various reference sampling plans. In skipping inspection entire lots in the structure of construction and the skipping inspections are continued. The number of consecutive conforming lots or batches reaches some pre-specified clearance number i continue to normal inspection. If i consecutive lots are cleared with normal inspection, using skipping inspection with fraction f appear; if another i consecutive conforming lots are passed under fractional inspection, the fraction (f) is bisected to $f/2$, and then to $f/4$ provided no non-conforming is found. Then the non-conforming is found in skipping inspection the system goes to normal inspection.

II. Design of SkSP-T plan with Group acceptance sampling plan as Reference plan

This section skip-lot sampling plan of type SkSP-T plan using group acceptance sampling plan as a reference plan. Then the skip-lot sampling plan parameters are i - clearance number and f -sampling frequency or fraction of submitted lots inspected in the skipping inspection. The attribute Group acceptance sampling plan for the necessary parameters the number of groups (g), acceptance number (c) and pre-defined (r). The following quantities of the plan parameters are stated as t -time of the experiment, t_q/t_{q_0} , α , β producer and consumer risks respectively. Therefore the operating procedure for the new proposed plan as follows

Step1: Initiate SkSP-T procedure with normal inspection using the group acceptance sampling plan as a reference plan. Select a random sample of size n from the lot and distribute r items in g groups and pre-defined experiment time t_0 .

Step2: When i successive lots are accepted on normal inspection, discontinue normal inspection and switch to skipping inspection.

Step3: On skipping inspection, inspect only a fraction f of the lots selected at random, level 1.

Step4: After i consecutive lots in succession is accepted at level 1, then switches to skipping inspection with a fraction of $f/2$, level 2.

Step5: After i consecutive lots in succession is accepted at level 2, the system then switches to skipping inspection with a fraction of $f/4$, level 3.

Step6: If a lot is rejected on any of the skipping level, the system then reverts back to normal inspection.

Assume that the lifetime of the submitted products follows any accelerating lifetime distribution using the Cumulative Distribution Function (CDF) of F . Then, the probability of the failure of an item before experiment time to is given by,

$$p = F(t_0) \tag{1}$$

The Operating Characteristics Function of SkSP-T plan is given by

$$P_a(p) = \frac{P^i(f_2 f_3 (1-P^i) + f_1 f_3 P^i (1-P^i) + f_1 f_2 P^{2i})}{f_1 f_2 f_3 (1-P^i) + P^i(f_2 f_3 (1-P^i) + f_1 f_3 P^i (1-P^i) + f_1 f_2 P^{2i})} \tag{2}$$

The new proposed sampling plan of skip-lot sampling plan of type SkSP-T plan parameters are determined by using the two point's method on the Operating Characteristics (OC) curve together with consistent producer and consumer risks are specified. The two-point approach is used in the new proposed plan to find the proposed plan parameters such that producer and consumer risks are satisfied simultaneously. Let p_1 - Producer's risk ($1-\alpha$) at AQL (Acceptable Quality Level) and p_2 - Consumer's risk (β) at LQL (Limiting Quality Level).

$$p_1 = \sum_{i=0}^c \binom{rg}{i} p_1^i (1 - p_1)^{rg-i} \tag{3}$$

$$p_2 = \sum_{i=0}^c \binom{rg}{i} p_2^i (1 - p_2)^{rg-i} \tag{4}$$

To specified by the producer's and consumer's risk used by Acceptable Quality Level and Limiting Quality level as follows

$$P_a(p_1) = \frac{P^i(f_2 f_3 (1-P^i) + f_1 f_3 P^i (1-P^i) + f_1 f_2 P^{2i})}{f_1 f_2 f_3 (1-P^i) + P^i(f_2 f_3 (1-P^i) + f_1 f_3 P^i (1-P^i) + f_1 f_2 P^{2i})} \geq 1 - \alpha \tag{5}$$

$$P_a(p_2) = \frac{P^i(f_2 f_3 (1-P^i) + f_1 f_3 P^i (1-P^i) + f_1 f_2 P^{2i})}{f_1 f_2 f_3 (1-P^i) + P^i(f_2 f_3 (1-P^i) + f_1 f_3 P^i (1-P^i) + f_1 f_2 P^{2i})} \leq \beta \tag{6}$$

The Average Sample Number (ASN) of SkSP-T plan with Group acceptance sampling plan as reference plan is given by

$$P_a(p_2) = \frac{n(f_1 f_2 f_3)}{f_1 f_2 f_3 (1-P^i) + P^i(f_2 f_3 (1-P^i) + f_1 f_3 P^i (1-P^i) + f_1 f_2 P^{2i})} \tag{7}$$

Equations 3 and 4 are substituting in equation 5 and 6 respectively. Using the new proposed plan parameters is simulating the specified values of Acceptable Quality Level and Limiting Quality level (AQL and LQL). Equations 5 and 6 are satisfied at the same time. Aslam *et.al* [1] used to find the minimum ASN values at Limiting Quality Level instead of Acceptable Quality Levels we will use the same simulation process.

The following constraints used to simulate the optimal plan parameter values,

Minimize

$$ASN(p_2)$$

Subject to

$$P_a(p_1) = \frac{P^i(f_2 f_3 (1 - P^i) + f_1 f_3 P^i (1 - P^i) + f_1 f_2 P^{2i})}{f_1 f_2 f_3 (1 - P^i) + P^i(f_2 f_3 (1 - P^i) + f_1 f_3 P^i (1 - P^i) + f_1 f_2 P^{2i})} \geq 1 - \alpha$$

$$P_a(p_2) = \frac{P^i(f_2 f_3 (1 - P^i) + f_1 f_3 P^i (1 - P^i) + f_1 f_2 P^{2i})}{f_1 f_2 f_3 (1 - P^i) + P^i(f_2 f_3 (1 - P^i) + f_1 f_3 P^i (1 - P^i) + f_1 f_2 P^{2i})} \leq \beta$$

The above constraints used to calculate the proposed plan parameter values. The values are tabulate in table 1 and 2. From table 1 number of tester $r = 5$ and table 2 number of tester $r = 10$.

III. Burr-type XII Distribution

In present situations, products are manufactured and guaranteed with high reliability. In order to know the lifetime information of a particular product, a destructive experiment is made on it. Since the process is long and time-consuming, the lifetime is truncated for a pre-specified time. This experiment is terminated in two cases, when the number of failure item exceeds the expected number of failures or when the pre-specified time is attained. Let t_q be true percentiles life and t_{q_0} be specified percentiles life. Assume that the lifetime of the submitted product follows the Burr-

type XII distribution with known and unknown shape parameters.

Burr [7] proposed the new distribution, which is called Burr Distribution. It is mainly based on log-logistic distribution. Zimmer and Burr [19] have used Burr distribution to find out the values of degrees of skewness and kurtosis. Rodriguez [17] developed Burr type XII distribution to generate distribution function of skewness and kurtosis also derives the area of the plane. Lio *et al.* [12] developed acceptance sampling plan for percentiles of Birnbaum- Saunders model and proposed that the acceptance sampling plans based on mean may not satisfy the requirement of engineers on the specific percentile of strength or breaking stress. Lio *et. al.*, [13] developed percentiles of Burr type XII distribution of single sampling plan when the life test is truncated at a pre-specified time. Aslam *et.al* [1] developed the skip-lot sampling plan of type SkSP-2 with GASP as reference plan using Burr distribution. Aslam derived the percentiles of median life. Aslam is compared mean life percentile (with [12]) and median life percentiles. It concludes that median life percentile is better than mean life percentile.

Aslam *et.al.*, [2] implemented the Two-Stage improved group plans for Burr type XII Distributions. Aslam.*et.al* [3] developed the RGS (Repetitive Group Sampling) plan using Burr-type XII distribution. Ismail *et. al.*, [14] develop two and three parameters are estimating in Burr type XII distribution using expected maximization (EM) algorithm. Rao *et al.*, [17] using Burr type XII distribution to estimate the multi-component stress strength reliability and estimate its parameters.

The Cumulative distribution function is given by

$$F(t) = 1 - [1 + (t/\eta)^b]^{-k} \quad t \geq 0, \eta \geq 0, b \geq 0, k > 0 \quad (8)$$

Here, b and k are the shape parameters and η is the scale parameter. When k=1, the Burr-type XII distribution converts to log-logistic distribution. The 100qth percentile of Burr-type XII distribution is given as

$$t_q = \eta \left[\left(\frac{1}{1-q} \right)^{\frac{1}{k}} - 1 \right]^{1/b} \quad (9)$$

The median life of the Burr-type XII distribution is given by

$$m = \eta \left[\frac{1-(0.5)^{1/k}}{(0.5)^{1/k}} \right]^{1/b} \quad (10)$$

When the shape parameters k and b are fixed, the median is proportional to the scale parameter η . The p based on the 100qth percentile of the Burr-type XII distribution is

$$p = 1 - \left[1 + \left[\frac{\gamma \delta_q}{t_q/t_{q0}} \right]^b \right]^{-k} \quad (11)$$

Where

$$\gamma = \left[\left(\frac{1}{1-q} \right)^{1/k} - 1 \right]^{1/b} \quad (12)$$

Where p is based on the median life, it is given by

$$p = 1 - \left[\frac{1}{1+(\delta_q \gamma / (t_q/t_{q0}))^b} \right]^k \quad (13)$$

Where

$$\gamma = \left[\frac{1-(0.5)^{1/k}}{(0.5)^{1/k}} \right]^{1/b} \quad (14)$$

IV. Determination of Sample Size

Step 1: Find the value of p_2 from equation 3 for shape parameter k=2 and q=0.5 by changing another shape parameter b=0.5 to 1.

Step 2: Set the evaluated Probability of Acceptance value P_a (p_2), and $t_q/t = 2, 4, 6, 8, 10, 12$.

Step 3: Find the ASN value at LQL level and other parameter values fixed.

V. Numerical Illustration

From table 1 and 2, Acceptable Quality Level (p_1) and Limiting Quality level (p_2) values are fixed by deriving the ASN at AQL (p_1) level and ASN at LQL (p_2) level. From table 2 number of tester's r increases, the group g decreases. From table 1 and 2, r , g , i , f_1 , f_2 , and f_3 values are fixed by changing the AQL and LQL values. It concludes that some small changes are made in Skip lot sampling plan of type SkSP-T with Group Acceptance Sampling Plan ASN at AQL values are very small compared to ASN at LQL.

From tables 3, 4, 5 and 6 shape parameters k and b values are fixed to find the percentiles ratios. The number of tester's r increases 5 to 10 then the group g decreases. The shape parameter b increase 0.5 to 1 also the number of group g is increasing. Consider the tables, table 3, 4, 5 and 6 simulating the values from Average Sample Number at Limiting Quality Level (ASN at p_2) and Probability of Acceptance at Acceptable Quality Level ($P_a(p)$ at p_1) using 50th percentile ratio. Table 5 and 6 noticed that shape parameter b increases 0.5 to 1 maximum of all the LQL values are same and the probability of Acceptance values are almost equaled. For $b=2$ and $k=1$ for $q_{0.5}$ or 50th percentile the Burr type XII distribution is converted into the log-logistic distribution.

The life distribution is burr type XII distribution is assumed and the experimenter is interested and focused on showing that the true unknown 50th ($q_{0.5}$) percentile life $t_{0.5}$ is at least 4000hrs. Consider the shape parameter $k=2$ and $b=0.5$ and the producer and consumer risks are fixed by $\alpha = 0.05$ and $\beta = 0.05$. The experimenter is stopped at desire percentile lifetime $t=4000$ hrs. Hence the parameter of Skip lot sampling plan of type SkSP-T with Group Acceptance Sampling Plan as reference plan using Burr type XII distribution indexed through ASN at AQL and LQL levels used various parameters. From table 5, then the parameter value $c=1$, $f_1=0.25$, $f_2=0.125$ and $f_3=0.0625$. At the time the quality engineer can apply SkSP-T with Group Acceptance Sampling Plan using Burr type XII distribution as follows: high probability acceptance ($P_a(p_1)$) is 0.9876 and the minimum ASN at LQL level is 4.38 and the product lifetime is 4000hrs. Hence the lot is accepted or rejected for no failure and one failure found in 4000hrs. It concludes that only one failure occurred in 167 days and the probability of acceptance $0.9876 \approx 0.99$ or 99%. In this example is compared to Aslam *et. al* [1] skip-lot sampling plan of type SkSP-2 with GASP with Burr Type XII distribution and Aslam *et.al* [3] Repetitive acceptance single sampling plan with Burr type XII distribution it concludes that Skip-lot sampling plan of type SkSP-T is more efficient. Skip-lot sampling plan of type SkSP-T with Burr type XII distribution has more probability of acceptance and minimum ASN at AQL and LQL levels compared with SkSP-2 with Burr type XII distribution.

From table 7, Skip-lot sampling plan of type SkSP-T with Group Acceptance Sampling Plan is compared with an existing Group acceptance sampling plan. And also calculate the corresponding Probability of Acceptance value. Let us consider the various group of Acceptable Quality and Limiting Quality levels are used and by fixed the number of tester r value (5 and 10), then calculate the group size for an existing plan and proposed plan. It concludes that the new proposed plan provides the very less number of group size and the already existing plan has more number of group size. For this table AQL=0.01 and LQL=0.02 and the number of tester $r = 10$, then the number of testers for existing plan to test the product under inspection is 130 and the proposed plan to test the product under inspection is 8. And this table is also compared with Aslam *et. al* [1] skip-lot sampling plan of type SkSP-2 with GASP with Burr Type XII distribution. It concludes that the new proposed plan has more efficient than GASP and SkSP-2 with Burr distribution.

Table 1: Skip-lot sampling plan of type SkSP-T with Group Acceptance Sampling Plan as a reference plan based on truncated life tests for $r = 5$

AQL (p ₁)	LQL (p ₂)	Optimal parameters							
		g	i	c	f ₁	f ₂	f ₃	ASN at (p ₁)	ASN at (p ₂)
0.001	0.002	552	2	4	0.1	0.05	0.025	135	1898
	0.003	150	2	1	0.15	0.075	0.0375	62	841
	0.004	98	2	1	0.2	0.1	0.05	36	458
	0.005	37	2	1	0.25	0.125	0.0625	12	36
	0.006	11	2	0	0.3	0.15	0.075	5	16
0.003	0.005	220	2	4	0.1	0.05	0.025	83	744
	0.0065	64	2	1	0.15	0.075	0.0375	38	274
	0.007	16	2	0	0.2	0.1	0.05	11	34
	0.0075	14	2	0	0.25	0.125	0.0625	10	32.8
	0.008	8	2	0	0.3	0.15	0.075	5	11.6
0.005	0.007	43	2	1	0.1	0.05	0.025	23	49.8
	0.008	11	2	0	0.15	0.075	0.0375	7	12.6
	0.009	7	2	0	0.2	0.1	0.05	4	7.66
	0.01	6	2	0	0.25	0.125	0.0625	4	6.54
	0.011	4	2	0	0.3	0.15	0.075	3	5.43
0.01	0.02	10	2	0	0.1	0.05	0.025	9	34.7
	0.03	5	2	0	0.15	0.075	0.0375	2	12.2
	0.04	4	2	0	0.2	0.1	0.05	2	10
	0.05	3	2	0	0.25	0.125	0.0625	1	9
	0.06	2	2	0	0.3	0.15	0.075	1	7.8

Table 2: Skip-lot sampling plan of type SkSP-T with Group Acceptance Sampling Plan as a reference plan based on truncated life tests for $r = 10$

AQL (p ₁)	LQL (p ₂)	Optimal parameters							
		g	i	c	f ₁	f ₂	f ₃	ASN at (p ₁)	ASN at (p ₂)
0.001	0.002	275	2	4	0.1	0.05	0.025	134	1866
	0.003	75	2	1	0.15	0.075	0.0375	62.7	835
	0.004	48	2	1	0.2	0.1	0.05	35.7	432
	0.005	18	2	1	0.25	0.125	0.0625	11.9	31.9
	0.006	6	2	0	0.3	0.15	0.075	5.14	15
0.003	0.005	110	2	4	0.1	0.05	0.025	83.4	740
	0.0065	31	2	1	0.15	0.075	0.0375	35.4	236
	0.007	8	2	0	0.2	0.1	0.05	10.4	30
	0.0075	7	2	0	0.25	0.125	0.0625	9.89	28.5
	0.008	4	2	0	0.3	0.15	0.075	4.86	10.4
0.005	0.007	21	2	1	0.1	0.05	0.025	21.2	45.9
	0.008	6	2	0	0.15	0.075	0.0375	6.51	11.6
	0.009	4	2	0	0.2	0.1	0.05	4.12	7.2
	0.01	3	2	0	0.25	0.125	0.0625	3.31	5.74
	0.011	3	2	0	0.3	0.15	0.075	2.97	5.15
0.01	0.02	5	2	0	0.1	0.05	0.025	8.95	35.1
	0.03	2	2	0	0.15	0.075	0.0375	3	11.8
	0.04	2	2	0	0.2	0.1	0.05	2	10.2
	0.05	1	2	0	0.25	0.125	0.0625	2	7.61
	0.06	1	2	0	0.3	0.15	0.075	1	7.09

Table 3: Parameters for Skip-lot sampling plan of type SkSP-T with Group Acceptance Sampling Plan as a reference plan for the total failure under the Burr type XII distribution

		r = 5, δq = 0.5								r = 5, δq = 1							
β	t_q/t_{q0}	g	c	i	f_1	f_2	f_3	ASN at p_2	Pa(p)	g	c	i	f_1	f_2	f_3	ASN at p_2	Pa(p)
0.25	2	8	9	2	0.10	0.050	0.0250	91.17	0.9500	6	9	2	0.10	0.050	0.0250	99.19	0.9558
	4	7	6	2	0.15	0.075	0.0375	70.14	0.9504	5	6	2	0.15	0.075	0.0375	62.29	0.9498
	6	5	3	2	0.20	0.10	0.05	69.45	0.9498	4	3	2	0.20	0.10	0.05	83.86	0.9501
	8	4	2	2	0.25	0.125	0.0625	58.87	0.9503	3	2	2	0.25	0.125	0.0625	74.46	0.9504
	10	4	2	2	0.30	0.15	0.075	58.79	0.9502	3	2	2	0.30	0.15	0.075	55.86	0.9499
	12	3	1	2	0.35	0.175	0.0875	47.18	0.9499	2	1	2	0.35	0.175	0.0875	53.73	0.9494
0.20	2	7	7	2	0.10	0.050	0.0250	111.3	0.9998	5	7	2	0.30	0.15	0.075	111.3	0.9996
	4	5	3	2	0.15	0.075	0.0375	89.44	0.9836	3	2	2	0.20	0.10	0.05	89.44	0.9841
	6	3	1	2	0.15	0.075	0.0375	58.41	0.9616	2	1	2	0.10	0.050	0.0250	58.41	0.9618
	8	3	0	2	0.20	0.10	0.05	60.64	0.950	1	0	2	0.30	0.15	0.075	60.64	0.9589
	10	3	0	2	0.15	0.075	0.0375	58.37	0.9755	3	1	2	0.15	0.075	0.0375	58.37	0.9759
	12	3	0	2	0.30	0.15	0.075	47.33	0.9862	1	0	2	0.30	0.15	0.075	47.44	0.9861
0.10	2	6	6	2	0.10	0.050	0.0250	128.4	0.9880	4	5	2	0.15	0.075	0.0375	128.4	0.9881
	4	4	2	2	0.20	0.10	0.05	90.89	0.9832	2	1	2	0.30	0.15	0.075	90.89	0.9826
	6	3	1	2	0.10	0.05	0.0250	58.16	0.9613	1	0	2	0.20	0.10	0.05	58.16	0.9606
	8	2	0	2	0.20	0.10	0.05	60.64	0.9596	1	0	2	0.35	0.175	0.0875	60.64	0.9550
	10	2	0	2	0.40	0.20	0.10	58.37	0.9749	1	0	2	0.45	0.225	0.1125	58.37	0.9810
	12	2	0	2	0.45	0.225	0.1125	47.33	0.9859	1	0	2	0.30	0.15	0.075	47.33	0.9918
0.05	2	5	4	2	0.15	0.075	0.0375	120.4	0.9877	3	4	2	0.10	0.050	0.0250	120.4	0.9968
	4	3	2	2	0.20	0.10	0.05	90.89	0.9830	2	1	2	0.15	0.075	0.0375	90.89	0.9927
	6	2	0	2	0.25	0.125	0.0625	58.41	0.9608	2	1	2	0.10	0.050	0.0250	58.41	0.9977
	8	2	0	2	0.35	0.175	0.0875	60.64	0.9592	1	0	2	0.20	0.10	0.05	60.64	0.9669
	10	2	0	2	0.40	0.20	0.10	58.37	0.9747	2	0	2	0.15	0.075	0.0375	58.37	0.9847
	12	2	0	2	0.45	0.225	0.1125	47.33	0.9856	2	0	2	0.25	0.125	0.0625	47.33	0.9865

Table 4: Parameters for Skip-lot sampling plan of type SkSP-T with Group Acceptance Sampling Plan as a reference plan for the total failure under the Burr type XII distribution

		r = 10, δq = 0.5								r = 10, δq = 1							
β	t_q/t_{q0}	g	c	i	f_1	f_2	f_3	ASN at p_2	Pa(p)	g	c	i	f_1	f_2	f_3	ASN at p_2	Pa(p)
0.25	2	4	9	2	0.10	0.050	0.0250	91.17	0.9504	3	9	2	0.15	0.075	0.0375	99.19	0.9551
	4	4	6	2	0.15	0.075	0.0375	70.14	0.9504	3	6	2	0.10	0.050	0.0250	70.14	0.9474

	6	3	3	2	0.20	0.10	0.05	69.45	0.9498	2	3	2	0.20	0.10	0.05	69.45	0.9583
	8	2	2	2	0.25	0.125	0.0625	58.87	0.9502	2	2	2	0.25	0.125	0.0625	69.45	0.9533
	10	2	2	2	0.30	0.15	0.075	58.79	0.9501	2	2	2	0.20	0.10	0.05	58.79	0.9513
	12	2	1	2	0.35	0.175	0.0875	47.18	0.9497	2	1	2	0.35	0.175	0.0875	47.18	0.9552
0.20	2	3	7	2	0.10	0.050	0.0250	111.3	0.9998	2	7	2	0.30	0.15	0.075	111.3	0.9996
	4	2	3	2	0.15	0.075	0.0375	89.44	0.9836	1	2	2	0.20	0.10	0.05	89.44	0.9841
	6	2	1	2	0.15	0.075	0.0375	58.41	0.9616	1	1	2	0.15	0.075	0.0375	58.41	0.9618
	8	1	0	2	0.10	0.050	0.0250	60.64	0.9627	1	1	2	0.50	0.25	0.125	60.64	0.9619
	10	1	0	2	0.20	0.10	0.05	58.37	0.9754	1	1	2	0.10	0.050	0.0250	58.37	0.9759
	12	1	0	2	0.30	0.15	0.075	47.33	0.9862	1	1	2	0.35	0.175	0.0875	47.44	0.9989
0.10	2	3	6	2	0.10	0.050	0.0250	128.4	0.9886	2	5	2	0.15	0.075	0.0375	128.4	0.9881
	4	2	2	2	0.20	0.10	0.05	90.89	0.9832	1	1	2	0.30	0.15	0.075	90.89	0.9825
	6	2	1	2	0.10	0.05	0.0250	58.16	0.9613	1	1	2	0.25	0.125	0.0625	58.16	0.9923
	8	1	0	2	0.10	0.050	0.0250	60.64	0.9631	1	1	2	0.10	0.050	0.0250	60.64	0.9974
	10	1	0	2	0.15	0.075	0.0375	58.37	0.9860	1	1	2	0.50	0.25	0.125	58.37	0.9983
	12	1	0	2	0.20	0.10	0.05	47.33	0.9919	1	0	2	0.10	0.050	0.0250	47.38	0.9977
0.05	2	2	4	2	0.15	0.075	0.0375	120.4	0.9877	2	4	2	0.10	0.050	0.0250	120.4	0.9967
	4	1	1	2	0.25	0.125	0.0625	90.89	0.9830	1	1	2	0.15	0.075	0.0375	90.89	0.9926
	6	1	1	2	0.20	0.10	0.05	58.41	0.9652	1	1	2	0.25	0.125	0.0625	58.41	0.9963
	8	1	0	2	0.10	0.050	0.0250	60.64	0.9828	1	1	2	0.45	0.225	0.1125	60.64	0.9669
	10	1	0	2	0.15	0.075	0.0375	58.37	0.9747	1	0	2	0.10	0.050	0.0250	58.37	0.9846
	12	1	0	2	0.20	0.10	0.05	47.33	0.9856	1	0	2	0.30	0.15	0.075	47.33	0.9864

Table 5: Parameters for Skip-lot sampling plan of type SkSP-T with Group Acceptance Sampling Plan as a reference plan for the total failure under the Burr type XII distribution

		r = 5, δq = 0.5								r = 5, δq = 1							
β	t_q/t_{q0}	g	c	I	f_1	f_2	f_3	ASN at p^2	Pa(p)	g	c	i	f_1	f_2	f_3	ASN at p^2	Pa(p)
0.25	2	8	6	2	0.10	0.050	0.0250	13.2662	0.9952	5	7	2	0.10	0.050	0.0250	13.2662	0.9942
	4	6	3	2	0.15	0.075	0.0375	4.38	0.9882	6	6	2	0.15	0.075	0.0375	4.38	0.9876
	6	5	1	2	0.20	0.10	0.05	4.38	0.9873	3	2	2	0.20	0.10	0.05	4.38	0.9866
	8	4	1	2	0.25	0.125	0.0625	4.38	0.9857	4	2	2	0.25	0.125	0.0625	4.38	0.9855
	10	4	1	2	0.30	0.15	0.075	4.38	0.9904	4	2	2	0.30	0.15	0.075	4.38	0.9894
	12	4	1	2	0.40	0.20	0.10	4.38	0.9897	3	1	2	0.35	0.175	0.0875	4.37	0.9893
0.20	2	7	5	2	0.10	0.050	0.0250	13.2662	0.9953	5	7	2	0.30	0.15	0.075	13.2662	0.9960
	4	4	2	2	0.15	0.075	0.0375	4.38	0.9882	3	2	2	0.25	0.125	0.0625	4.38	0.9881
	6	4	2	2	0.50	0.25	0.125	4.38	0.9872	3	1	2	0.15	0.075	0.0375	4.38	0.9870

	8	2	0	2	0.20	0.10	0.05	4.38	0.9856	1	0	2	0.30	0.15	0.075	4.38	0.9854
	10	2	0	2	0.35	0.175	0.0875	4.38	0.9898	3	1	2	0.35	0.175	0.0875	4.38	0.9896
	12	2	0	2	0.30	0.15	0.075	4.38	0.9895	1	0	2	0.40	0.20	0.10	4.38	0.9896
0.10	2	6	4	2	0.10	0.050	0.0250	13.2662	0.9949	4	5	2	0.15	0.075	0.0375	13.2662	0.9949
	4	4	2	2	0.20	0.10	0.05	4.37	0.9708	2	1	2	0.15	0.075	0.0375	4.37	0.9880
	6	4	1	2	0.10	0.05	0.0250	4.38	0.9866	1	0	2	0.20	0.10	0.05	4.38	0.9871
	8	2	0	2	0.25	0.125	0.0625	4.38	0.9856	1	0	2	0.30	0.15	0.075	4.38	0.9856
	10	2	0	2	0.40	0.20	0.10	4.38	0.9903	1	0	2	0.40	0.20	0.10	4.38	0.9895
	12	2	0	2	0.45	0.225	0.1125	4.8	0.9816	1	0	2	0.45	0.225	0.1125	4.8	0.9888
0.05	2	5	4	2	0.15	0.075	0.0375	13.2662	0.9945	3	4	2	0.10	0.050	0.0250	13.2662	0.9969
	4	3	1	2	0.25	0.125	0.0625	4.38	0.9876	2	1	2	0.10	0.050	0.0250	4.38	0.9848
	6	2	0	2	0.20	0.10	0.05	4.38	0.9869	2	1	2	0.20	0.10	0.05	4.38	0.9864
	8	2	0	2	0.15	0.075	0.0375	4.38	0.9856	1	0	2	0.20	0.10	0.05	4.38	0.9848
	10	2	0	2	0.35	0.175	0.0875	4.38	0.9898	2	0	2	0.25	0.125	0.0625	4.38	0.9899
	12	2	0	2	0.40	0.20	0.10	4.38	0.9896	2	0	2	0.35	0.175	0.0875	4.38	0.9896

Table 6: Parameters for Skip-lot sampling plan of type SkSP-T with Group Acceptance Sampling Plan as a reference plan for the total failure under the Burr type XII distribution

		r = 10, $\delta q = 0.5$								r = 10, $\delta q = 1$							
β	t_q/t_{q0}	g	c	i	f_1	f_2	f_3	ASN at p^2	Pa(p)	g	c	i	f_1	f_2	f_3	ASN at p^2	Pa(p)
0.25	2	5	9	2	0.10	0.050	0.0250	13.2662	0.9948	3	9	2	0.10	0.050	0.0250	13.2662	0.9948
	4	5	6	2	0.15	0.075	0.0375	4.38	0.9874	3	6	2	0.15	0.075	0.0375	4.38	0.9878
	6	4	3	2	0.20	0.10	0.05	4.37	0.9867	2	3	2	0.20	0.10	0.05	4.38	0.9871
	8	3	2	2	0.25	0.125	0.0625	4.38	0.9855	2	2	2	0.25	0.125	0.0625	4.38	0.9855
	10	3	2	2	0.30	0.15	0.075	4.38	0.9899	2	2	2	0.30	0.15	0.075	4.38	0.9898
	12	2	1	2	0.35	0.175	0.0875	4.38	0.9895	2	1	2	0.35	0.175	0.0875	4.37	0.9893
0.20	2	4	7	2	0.10	0.050	0.0250	13.2662	0.9979	2	7	2	0.30	0.15	0.075	13.2662	0.9999
	4	3	3	2	0.15	0.075	0.0375	4.38	0.9878	1	2	2	0.25	0.125	0.0625	4.38	0.9867
	6	2	1	2	0.15	0.075	0.0375	4.38	0.9868	1	1	2	0.15	0.075	0.0375	4.38	0.9868
	8	1	0	2	0.10	0.050	0.0250	4.38	0.9849	1	1	2	0.30	0.15	0.075	4.38	0.9899
	10	1	0	2	0.35	0.175	0.0875	4.38	0.9898	1	1	2	0.35	0.175	0.0875	4.38	0.9895
	12	1	0	2	0.50	0.25	0.125	4.38	0.9892	2	1	2	0.40	0.20	0.10	4.38	0.9982
0.10	2	4	6	2	0.10	0.050	0.0250	13.2662	0.9947	2	5	2	0.15	0.075	0.0375	13.2662	0.9895
	4	2	2	2	0.20	0.10	0.05	4.37	0.9878	1	1	2	0.15	0.075	0.0375	4.37	0.9903
	6	2	1	2	0.30	0.15	0.075	4.38	0.9866	1	1	2	0.20	0.10	0.05	4.38	0.9919
	8	1	0	2	0.25	0.125	0.0625	4.38	0.9856	1	1	2	0.30	0.15	0.075	4.38	0.9938
	10	1	0	2	0.35	0.175	0.0875	4.38	0.9894	1	1	2	0.40	0.20	0.10	3.97	0.9983

	12	1	0	2	0.45	0.225	0.1125	4.8	0.9896	1	0	2	0.45	0.225	0.1125	4.8	0.9934
0.05	2	3	4	2	0.15	0.075	0.0375	13.2662	0.9944	2	4	2	0.10	0.050	0.0250	13.2662	0.9968
	4	1	1	2	0.30	0.15	0.075	4.38	0.9875	1	1	2	0.10	0.050	0.0250	4.38	0.9847
	6	1	1	2	0.40	0.20	0.10	4.38	0.9876	1	1	2	0.20	0.10	0.05	4.38	0.9955
	8	1	0	2	0.25	0.125	0.0625	4.38	0.9856	1	1	2	0.20	0.10	0.05	4.38	0.9914
	10	1	0	2	0.35	0.175	0.0875	4.38	0.9897	1	0	2	0.25	0.125	0.0625	4.38	0.9899
	12	1	0	2	0.40	0.20	0.10	4.38	0.9895	1	0	2	0.35	0.175	0.0875	4.38	0.9896

Table 7: Comparison of GASP with SkSP-T with GASP as reference plan using Burr type XII distribution

		r = 5			r = 10		
p_1	p_2	Group Acceptance Sampling plan	Proposed Plan (SkSP-T with Burr type XII)	Probability of Acceptance at $P_a(p_1)$	Group Acceptance Sampling plan	Proposed Plan (SkSP-T with Burr type XII)	Probability of Acceptance at $P_a(p_1)$
0.001	0.002	200	13	0.9959	130	8	0.9973
	0.005	162	7	0.9978	45	5	0.9964
	0.01	53	5	0.9973	25	3	0.9981
	0.15	38	4	0.9973	14	2	0.9976
	0.02	25	4	0.9966	10	2	0.9979
	0.03	17	3	0.9974	8	2	0.9989
0.005	0.02	142	9	0.9955	113	7	0.9977
	0.03	62	6	0.9973	38	5	0.9956
	0.04	31	4	0.9977	21	3	0.9966
	0.05	18	3	0.9972	12	2	0.9973
	0.06	13	2	0.9961	8	2	0.9978
	0.07	7	2	0.9974	5	2	0.9982

VI. CONCLUSION

The new proposed skip-lot sampling plan of type SkSP-T with Group Acceptance Sampling Plan will be useful when the lifetime of the product follows the Burr type XII distribution with known and unknown shape parameters. The proposed SkSP-T with GASP has been compared with SkSP-2 with GASP and Group Acceptance Sampling Plan. The comparison results have specified that the SkSP-T with Group Acceptance Sampling Plan is more efficient than the SkSP-2 and existing Group Acceptance Sampling Plan. From the illustration, it is noticed that the SkSP-T has more probability of acceptance compared with other existing plans. Producer and consumer risks are reduced while compared with SkSP-2 and RGASP under Burr type XII distribution. The article also provides a detailed procedure for designing and selecting the plan parameters. An attempt has been made in this paper in developing Skip lot sampling plans ensuring reduce the frequency of sampling inspection and total inspection cost and also reducing the defectives products. The necessary tables and examples are contributed and applied for the formulation of the new proposed sampling plan.

References

- [1] Aslam M, Balamurali, S, Chi-Hyuck Jun and Mujahid Rasool (2011). Optimal Designing of Skip-lot sampling plan of type SkSP-2 with group acceptance sampling plan as reference

- plan under Burr type XII distribution, *Journal of Statistical Computation and Simulation*, 83:37-51.
- [2] Aslam M, Y. L. Lio, Muhammad Azam and Chi-Hyuck Jun (2012) Two-Stage Improved Group plans for Burr type XII Distributions, *American Journal of Mathematics and Statistics*, 2:pp. 33-39.
- [3] Aslam M, Y. L. Lio and Chi-Hyuck Jun (2013). Repetitive acceptance sampling plans for Burr type XII percentiles, *International Journal of Advanced Manufacturing Technology*, 68: 495-507.
- [4] Balamurali, S., (2002) Modified Tightened Three level Continuous sampling plan, *Economic Quality Control*, 17: 221-234.
- [5] Balamurali, S., and Chi-Hyuck Jun, (2004). Modified CSP-T sampling procedures for Continuous production process, *Quality Technology and Quantitative Management*, 1(2):175-188.
- [6] Balamurali S and Chi-Hyuck Jun, (2010): "A new system of skip-lot sampling plans having a provision for reducing a normal inspection", *Applied Stochastic Models Business Industries*, 27:348-353.
- [7] Burr L. W. (1942). Cumulative frequency functions, *The Annals of Mathematical Statistics*, 13:215-232.
- [8] Dodge H.F. (1955). Skip-Lot sampling plan, *Industrial Quality Control*, 11:3-5.
- [9] Dodge H.F. and Perry, R.L. (1970). A System of Skip-lot Plans for Lot-by-lot inspection, *American Society for Quality Control Technical Conference Transactions*, Chicago, Illinois, 1971, 469-477.
- [10] Fordice J.J. (1972). A Tightened Multi-Level Continuous Sampling Plan CSPT, Report No.QEM 21230-10, *Ammunition Procurement and Supply Agency*, Joliet, Illinois.
- [11] Kandasamy, C. and Govindaraju, K., (1993) Selection of CSP-T plans", *Communication in Statistics - Simulation and Computation*, 22: 265-283.
- [12] Lio Y L, Tsai T. R and Wu S. J (2010). Acceptance sampling plans from truncated life tests based on the Birnbaum- Saunders distribution for percentiles, *Communications in Statistics: Simulation and Computation*, 39:119-136.
- [13] Lio, Y. L., Tsai T.-R. and Wu, S.-J. (2010). Acceptance sampling plans from truncated life tests based on the Burr type XII percentiles, *Journal of the Chinese Institute of Industrial Engineers*, 27:pp. 270-280.
- [14] Nor Hidayah Ismail and Zarina mohd Khalid (2014) Estimation of 2- and 3-parameter Burr Type XII distributions using EM algorithm, *Malaysian Journal of Fundamental and Applied Sciences*, 10:74-81
- [15] Pradeepa Veerakumari .K and Suganya. S (2016). A New System of SkSP-T with Single Sampling Plan as Reference Plan, *Research Journal of Mathematics and Statistics*, 4:1-6.
- [16] Rao, G. S., Aslam, M. and Kundu, D. (2015). Burr-XII Distribution Parametric Estimation and Estimation of Reliability of Multi-component Stress-Strength, *Communications in Statistics -Theory and Methods*, 44: 4953-4961.
- [17] Rodriguez, R. N. (1977). A Guide to the Burr Type XII Distributions, *Biometrika*, 64: 129-134.
- [18] Soundararajan, V and Vijayaraghavan, R (1989): A new system of skip-lot inspection plans of type SkSP-3, *Quality for Process and Development*, Wiley Eastern.
- [19] Zimmer, W. J. and Burr I. W. (1963). Variable Sampling Plans Based on Non-Normal Populations, *Industrial Quality Control*, 3:18-26.

Some Properties and Different Estimation Methods for Inverse $A(\alpha)$ Distribution with an Application to Tongue Cancer Data

SHREYA BHUNIA* AND PROLOY BANERJEE

•

Department of Mathematics and Statistics, Aliah University, Kolkata, India
shreyabhunia.stat@gmail.com and proloy.stat@gmail.com

*Corresponding author E-mail: shreyabhunia.stat@gmail.com

Abstract

The inverted distribution is the distribution of the reciprocal of a random variable that follows a specified distribution. Here, a new one parameter inverse $A(\alpha)$ distribution has been introduced, which is the reciprocal of the $A(\alpha)$ distribution. An account of mathematical and statistical properties of the new distribution such as survival characteristics, quantile functions, mode, order statistics, ageing intensity function and stochastic ordering have been derived and discussed. Furthermore, from the frequentist view point we discussed several estimation approaches including maximum likelihood method, method of maximum product of spacings, ordinary and weighted least square methods, Cramér-Von-Mises estimation and Anderson-Darling estimation methods. These methods are compared for both small and large samples by performing an extensive numerical simulation. The flexibility of the new lifetime distribution is demonstrated by modeling a tongue cancer data. The result indicates the superiority for proposed model compared to some popular competing ones.

Keywords: Inverse distribution, Estimation methods, Hazard rate function, Lifetime distribution

1. INTRODUCTION

In several applied fields of research such as engineering, medical sciences, economics, biological sciences etc., analyzing and modeling complex datasets are the most essential parts. Albeit in literature there exists many well known standard distributions, sometimes it may not always reflect the real world scenario. So, the researchers aspire to extend structures of the probability models. Recently, [1] introduced a new one parameter $A(\alpha)$ distribution and the applicability of the distribution is investigated by analyzing three datasets. A continuous random variable Y is said to follow an $A(\alpha)$ distribution if its probability density function (pdf) is of the form;

$$f_Y(y) = \frac{1}{y^2} \exp \left[\frac{1}{\alpha} \left(1 - \exp \left(\frac{\alpha}{y} \right) \right) + \frac{\alpha}{y} \right]; y > 0 \quad (1)$$

and is denoted by $Y \sim A(\alpha)$. The corresponding cumulative distribution function (cdf) of Y is given by,

$$F_Y(y) = \exp \left[\frac{1}{\alpha} \left(1 - \exp \left(\frac{\alpha}{y} \right) \right) \right]; y > 0 \quad (2)$$

with scale parameter $\alpha > 0$.

In statistical literature there are various methods for proposing new distributions by using baseline distributions. For example, [2] introduced a general method for obtaining more flexible distributions by adding a new parameter to an existing family of distributions, Quadratic rank

transmutation map (QRTM) [3], DUS transformation [4], α -power transformation method [5] etc. In this context, finding inversion of univariate probability distributions and their applicability under the inverse transformation method is one of the preferred areas of research in recent times. Sometimes it has been found that inverted version of the distributions are much more effective to explore additional aspects of the phenomena that non-inverted distribution cannot. For instances, inverse exponential distribution is studied by [6], inverse Weibull distribution is studied by [7], [8] studied inverse Lindley distribution, inverse Xgamma distribution is studied by [9], inverse power Lindley distribution by [10], inverted Gamma distribution by [11], inverse Kumaraswamy distribution is studied by [12].

In this present study, we have also introduced the inverted version of the $A(\alpha)$ distribution using the same technique and named it as the inverse $A(\alpha)$ distribution. The new distribution is flexible to model positive real datasets which possesses increasing hazard rate function. Another beauty of this distribution includes heavy-tail, unimodal, parsimonious in parameter and easy to use. The objectives of this article are: (i) to obtain some mathematical properties for inverse $A(\alpha)$ distribution and (ii) to estimate the unknown parameter of the model from frequentist perspectives. The maximum likelihood estimation (MLE), method of maximum product of spacings (MPS), ordinary least square estimation (OLS) and weighted least square estimation (WLS), Cramér-Von-Mises estimation (CVM) and the method of Anderson-Darling (AD) are considered as frequentist methods for parameter estimation. Also we compare these estimation procedures on the basis of root mean square error (RMSE) values for different sample sizes and different parameter values using Monte-Carlo simulation technique. Furthermore, to the best of our knowledge, no attempt has been made to compare all of these estimators for the inverse $A(\alpha)$ distribution along with mathematical and statistical properties. Additionally, to illustrate the flexibility of this distribution a tongue cancer patient data has been analyzed.

The remainder of this article is organized as follows. In Section 2, the new distribution has been introduced. Different statistical properties and associated measures of Inv- $A(\alpha)$ distribution have been discussed in Section 3. Different classical estimation procedures for the parameter of inverse $A(\alpha)$ distribution have been considered in Section 4. In Section 5, a simulation study is conducted to compare the various obtained estimators. Empirical application based on a real dataset is discussed in Section 6. Finally, concluding remarks are given in Section 7.

2. THE INVERTED $A(\alpha)$ DISTRIBUTION

A new probability distribution, termed as inverted or inverse- $A(\alpha)$ distribution has been introduced in this section. By origin, this distribution is the reciprocal of the $A(\alpha)$ distribution and for simplicity throughout this study we use the notation Inv- $A(\alpha)$ for this new lifetime model. Here we consider the random variable Y having the density function (1), then the cdf of the inverted random variable $X = \frac{1}{Y}$ is defined as

$$F_X(x) = \mathcal{P}[X \leq x] = 1 - F_Y\left(\frac{1}{X}\right) = 1 - \exp\left[\frac{1}{\alpha}(1 - \exp(\alpha x))\right]; x > 0. \quad (3)$$

Now, by differentiating $F_X(x)$ given in (3) the pdf of the Inv- $A(\alpha)$ distribution is obtained and expressed as follows;

$$f_X(x) = \exp\left[\frac{1}{\alpha}(1 - \exp(\alpha x)) + \alpha x\right]; x > 0 \quad (4)$$

and $\alpha > 0$ is the scale parameter. The Inv- $A(\alpha)$ distribution is an one parameter family of continuous probability distributions on the positive real line.

The plots of pdf and cdf function of Inv- $A(\alpha)$ distribution for different choices of scale parameter α are shown in Figures 1a and 1b respectively. The plots reveal that the Inv- $A(\alpha)$ density can be decreasing, unimodal and right skewed.

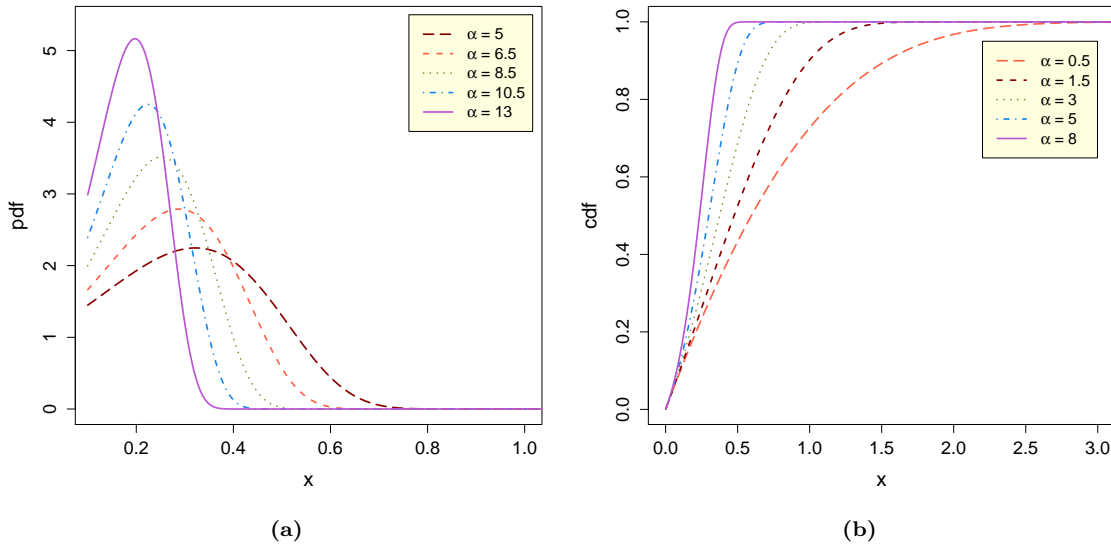


Figure 1: The pdf and cdf plots of $Inv-A(\alpha)$ distribution for different parameter choices.

3. SOME STATISTICAL PROPERTIES

3.1. Reliability characteristics

The survival function (sf) and hazard rate function (hrf) are the basic characteristics of any lifetime distributions. Both the measures are commonly employed to describe and model the fundamental properties of a variety of survival datasets. The survival function $\mathbb{S}(t)$, which is defined as the probability that an individual or an item is survived at least t ($t \geq 0$) unit of time and denoted as $\mathbb{S}(t) = P(X \geq t) = 1 - F(t)$.

Thus, the sf of the $Inv-A(\alpha)$ distribution is defined as,

$$\mathbb{S}(t) = e^{\frac{1}{\alpha}(1-e^{\alpha t})} \tag{5}$$

The hazard rate function, also known as the failure rate function, is another key feature to consider when measuring a real-life phenomenon with a lifetime distribution. It can be interpreted as the conditional probability of failure, given it has survived upto at least the time t ($t \geq 0$) and is defined as $h(t) = \frac{f(t)}{1-F(t)} = \frac{f(t)}{\mathbb{S}(t)}$; where $f(t)$ is the pdf and $\mathbb{S}(t)$ is the sf of the corresponding distribution. Therefore, the hrf for the $Inv-A(\alpha)$ distribution is given by,

$$h(t) = \frac{e^{\frac{1}{\alpha}(1-e^{\alpha t})+\alpha t}}{e^{\frac{1}{\alpha}(1-e^{\alpha t})}} = e^{\alpha t} \tag{6}$$

The ratio between the lifetime probability density and its distribution function is characterised as the reversed (or proportional) hazard rate function (rhrf) of a random life phenomena. For the $Inv-A(\alpha)$ distribution the rhrf is given as follows,

$$H(t) = \frac{f(t)}{F(t)} = \frac{e^{\frac{1}{\alpha}(1-e^{\alpha t})+\alpha t}}{1 - e^{\frac{1}{\alpha}(1-e^{\alpha t})}} \tag{7}$$

Another similar measure is cumulative hazard function and is defined as follows [13]:

$$\Lambda(t) = -\log \mathbb{S}(t) = -\log \left[e^{\frac{1}{\alpha}(1-e^{\alpha t})} \right] = \frac{1}{\alpha} (e^{\alpha t} - 1) \tag{8}$$

So, clearly from expression (6) we can see that the hazard rate function is increasing for $\alpha > 0$. The shape of the hazard rate is displayed in figure 2b for different choices of α , whereas figure 2a represents the shape of the survival function.

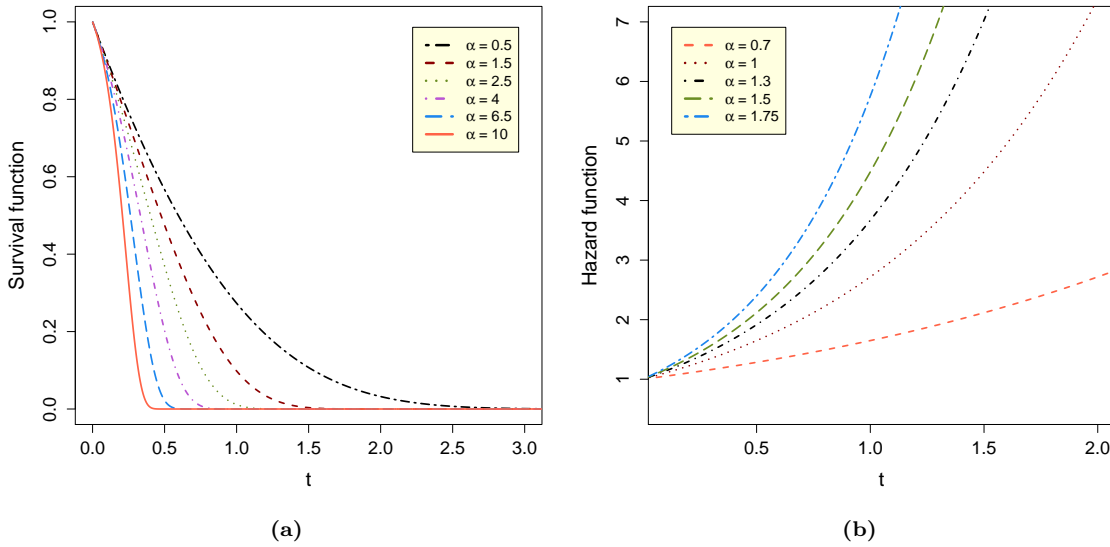


Figure 2: The survival and hazard plots of $Inv-A(\alpha)$ distribution for different parameter choices.

The shape of the hazard rate function can also be derived mathematically by using the following lemma.

Lemma 1. Suppose $f(t)$, for $t > 0$ is the density function of a positive real valued continuous random variable. $f'(t)$ is the derivative of $f(t)$ and

$$\eta(t) = -\frac{f'(t)}{f(t)}.$$

Then if $\eta'(t) > 0$ for all $t > 0$ then the hazard rate function is an increasing function of t .

Proof. [14].

Here,

$$\eta(x) = e^{\alpha x} - \alpha.$$

After differentiating with respect to x , we have

$$\eta'(x) = \alpha e^{\alpha x}; \quad \alpha > 0.$$

It is clearly seen that $\eta'(x) > 0$ for $x > 0$. Therefore, the distribution has increasing hazard rate function.

3.2. Quantile functions, median and mode

The q^{th} quantile function x_q of $Inv-A(\alpha)$ distribution will be obtained by solving the following equation

$$F(x_q) = q \quad \text{where, } 0 < q < 1.$$

Therefore, $1 - e^{\frac{1}{\alpha}(1 - e^{\alpha x_q})} = q$

$$x_q = \frac{1}{\alpha} \log [1 - \alpha \log(1 - q)]. \tag{9}$$

Thus, the median (or 2^{nd} quartile) of the proposed distribution is obtained by substituting $q = \frac{1}{2}$ in (9).

i.e.,
$$X_{\frac{1}{2}} = Q_2 = \frac{1}{\alpha} \log \left[1 - \alpha \log \left(\frac{1}{2} \right) \right] = \frac{1}{\alpha} \log [1 + \alpha \log 2]. \tag{10}$$

Similarly, the 1st and 3rd quartiles are obtained by replacing $q = \frac{1}{4}$ and $q = \frac{3}{4}$ respectively. Thus expressions for the 1st and 3rd quartiles are as follows.

$$Q_1 = \frac{1}{\alpha} \log \left[1 - \alpha \log \left(\frac{3}{4} \right) \right] \quad \text{and} \quad Q_3 = \frac{1}{\alpha} \log [1 + \alpha \log 4].$$

Now, the mode of the inverse $A(\alpha)$ distribution denoted by x_m will be derived by solving the equation $f'(x; \alpha) = 0$, for which $f''(x) < 0$. The solution x_m will be the mode of the distribution for which $f(x)$ attains the maximum value. Therefore, the mode of the proposed distribution is obtained by solving the differentiation expressed as

$$\frac{\partial}{\partial x} e^{\left[\frac{1}{\alpha}(1-e^{\alpha x}) + \alpha x \right]} = 0 \tag{11}$$

After simplification, we get

$$x_m = \frac{\log \alpha}{\alpha} \tag{12}$$

It is noted that, though the mode of $A(\alpha)$ distribution exists but it cannot be expressed in a closed form. However, in our study of Inv- $A(\alpha)$ distribution, we see that the mode exists with an explicit form.

3.3. Order statistics

In nonparametric statistics and inference, order statistics are one of the useful techniques. In life testing and reliability analysis order statistics have a wide range of applications. Let us assume that $X_{(1)}, X_{(2)}, \dots, X_{(n)}$ be the order statistics of a random sample X_1, X_2, \dots, X_n drawn from a continuous population with cdf $F_X(x)$ and pdf $f_X(x)$. Therefore under these assumptions pdf and cdf of the order statistics $X_{(r)}$, $r = 1, 2, \dots, n$ is expressed as

$$f_r(x) = \frac{n!}{(r-1)!(n-r)!} f(x) F^{(r-1)}(x) [1 - F(x)]^{(n-r)}; \quad r = 1, 2, \dots, n \tag{13}$$

and

$$F_r(x) = \sum_{i=r}^n \binom{n}{i} F_X^i(x) [1 - F_X(x)]^{(n-i)}. \tag{14}$$

Now, by using the pdf (4) and cdf (3) in equation (13), we can easily derive the pdf of r^{th} order statistic for the Inv- $A(\alpha)$ distribution as in the following expression

$$\begin{aligned} f_{X_{(r)}}(x) &= \frac{n!}{(r-1)!(n-r)!} \left\{ 1 - e^{\frac{1}{\alpha}(1-e^{\alpha x})} \right\}^{(r-1)} \left\{ e^{\frac{1}{\alpha}(1-e^{\alpha x})} \right\}^{(n-r+1)} e^{\alpha x} \\ &= \frac{n!}{(r-1)!(n-r)!} \sum_{k=0}^{r-1} \binom{r-1}{k} (-1)^k e^{\alpha x} \left[e^{\frac{1}{\alpha}(1-e^{\alpha x})} \right]^{(n-r+k+1)}. \end{aligned} \tag{15}$$

While using equation (3) in (14) the cdf of r^{th} order statistic becomes,

$$F_{X_{(r)}}(x) = \sum_{i=r}^n \sum_{k=0}^i \binom{n}{i} \binom{i}{k} (-1)^k e^{\frac{n}{\alpha}(1-e^{\alpha x})}. \tag{16}$$

In particular, the densities of the smallest and largest order statistics of the Inv- $A(\alpha)$ distribution are obtained by substituting $r = 1$ and n simultaneously in the expression (15). Hence the pdf of the smallest order statistic $X_{(1)}$ is expressed as,

$$f_{X_{(1)}}(x) = n e^{\left\{ \frac{n}{\alpha}(1-e^{\alpha x}) + \alpha x \right\}}$$

and the pdf of the largest order statistic $X_{(n)}$ is as follows,

$$f_{X_{(n)}}(x) = n \sum_{k=0}^{n-1} \binom{n-1}{k} (-1)^k e^{\left\{ \frac{(1-e^{\alpha x})(k+1)}{\alpha} + \alpha x \right\}}.$$

3.4. Ageing intensity function

Ageing intensity (AI) function has been developed by [15] and according to him, a unimodal failure rate can be represented as either approximately decreasing or approximately increasing or approximately constant. [16] investigated various features of AI functions, whereas [17] discussed AI function in the field of reliability theory. The AI function for a positive random variable X , denoted by $L_X(t)$, for any $t > 0$. The ratio of the instantaneous failure rate to a baseline failure rate is used to calculate the AI function. It is defined as

$$L_X(t) = \frac{h(t)}{H(t)},$$

$$= \frac{-tf(t)}{S(t)\ln S(t)}, t > 0.$$

Where $f(\cdot)$ and $S(\cdot)$ are the probability density function and survival function of the random variable X respectively. $H(t)$ is failure rate average and it can be written as $H(t) = (\int_0^t h(u)du)/t$. Now, if $X \sim \text{Inv-}A(\alpha)$ then the expression for the AI function is obtained as

$$L_X(t) = -\frac{\alpha t e^{\alpha t}}{1 - e^{\alpha t}}. \tag{17}$$

AI function is uniquely determined by the failure rate function, however the converse is not true. The stronger the ageing tendency of the related random variable, the higher the value of the AI function. If the failure rate is a constant then the $AI = 1$, If the failure rate is increasing then the $AI > 1$, if the failure rate is decreasing then the $AI < 1$.

3.5. Stochastic ordering

The notion of stochastic ordering was first suggested by [18] and used to demonstrate the comparative behaviour of two positive continuous random variables. Suppose X and Y are the two random variables with respective cdfs F_X and F_Y , then X is said to be smaller than Y in the following cases

- Stochastic order ($X \leq_{st} Y$) if $F_X(x) \geq F_Y(x)$ for all x ;
- Hazard rate order ($X \leq_{hr} Y$) if $h_X(x) \geq h_Y(x)$ for all x ;
- Mean residual life order ($X \leq_{mrl} Y$) if $m_X(x) \leq m_Y(x)$ for all x ;
- Likelihood ratio order ($X \leq_{lr} Y$) if $\frac{f_X(x)}{f_Y(x)}$ decreases in x .

The aforementioned relationship are well known for establishing stochastic ordering of distributions.

$$X \leq_{lr} Y \implies X \leq_{hr} Y \implies X \leq_{mrl} Y$$

$$\Downarrow$$

$$X \leq_{st} Y$$

When the required conditions are met, the $\text{Inv-}A(\alpha)$ distribution is ordered with regard to the strongest likelihood ratio ordering, as shown by the following theorem.

Theorem 1. let, $X \sim \text{Inv-}A(\alpha_1)$ and $Y \sim \text{Inv-}A(\alpha_2)$. If $\alpha_1 < \alpha_2$, then $X \leq_{lr} Y$ and hence it implies other orderings.

Proof. According to the definition, the Likelihood ratio is defined as

$$\xi(x) = \frac{f_X(x)}{f_Y(x)} = \frac{\exp\left[\frac{1}{\alpha_1}(1 - \exp(\alpha_1 x)) + \alpha_1 x\right]}{\exp\left[\frac{1}{\alpha_2}(1 - \exp(\alpha_2 x)) + \alpha_2 x\right]}$$

$$\implies \log \xi(x) = \frac{1}{\alpha_1} - \frac{e^{\alpha_1 x}}{\alpha_1} - \frac{1}{\alpha_2} + \frac{e^{\alpha_2 x}}{\alpha_2} + (\alpha_1 - \alpha_2)x$$

Now differentiating with respect to x , we get

$$\begin{aligned} \frac{\xi'(x)}{\xi(x)} &= (\alpha_1 - \alpha_2) + e^{\alpha_2 x} - e^{\alpha_1 x} \\ \Rightarrow \xi'(x) &= \xi(x) \{(\alpha_1 - \alpha_2) + e^{\alpha_2 x} - e^{\alpha_1 x}\} \\ &\Rightarrow \xi'(x) < 0 \quad \text{if } \alpha_1 < \alpha_2. \end{aligned}$$

Therefore, $\xi(x)$ is decreasing function in x if $\alpha_1 < \alpha_2$ and hence $X \leq_{lr} Y$. The remaining orderings can also be established in similar manner.

4. METHODS OF ESTIMATION

In this section, we describe some parameter estimation techniques for Inv- $A(\alpha)$ distribution under frequentist view point. In particular, the methods which we have discussed here, those are: maximum likelihood estimation (MLE), maximum product of spacings (MPS), ordinary least square (OLS) and weighted least square estimation (WLS), Cramér-Von-Mises estimation (CVM) and Anderson-Darling (AD) estimation.

4.1. Method of Maximum Likelihood

Here, we discuss the maximum likelihood estimation (MLE) method for estimating the unknown scale parameter α . Several desirable properties like consistency, asymptotic efficiency and invariance make this estimation technique most popular among others [19]. Let X_1, X_2, \dots, X_n be an observed random sample from Inv- $A(\alpha)$ distribution with pdf (4) and the MLE for the unknown parameter is derived as follows. The likelihood function is defined as

$$L(x) = \prod_{i=1}^n f(x_i; \alpha) = \prod_{i=1}^n \exp \left[\frac{1}{\alpha} (1 - \exp(\alpha x_i)) + \alpha x_i \right].$$

So, the log-likelihood function becomes

$$\log L = \frac{n}{\alpha} - \frac{1}{\alpha} \sum_{i=1}^n e^{\alpha x_i} + \alpha \sum_{i=1}^n x_i. \tag{18}$$

After differentiating $\log L$ in (18) with respect to α and equating to zero, we get the system of non-linear equation as,

$$\begin{aligned} \frac{\delta \log L}{\delta \alpha} &= \frac{1}{\alpha^2} \sum_{i=1}^n e^{\alpha x_i} - \frac{1}{\alpha} \sum_{i=1}^n x_i e^{\alpha x_i} - \frac{n}{\alpha^2} + \sum_{i=1}^n x_i = 0. \\ \Rightarrow \sum_{i=1}^n e^{\alpha x_i} - \alpha \sum_{i=1}^n x_i e^{\alpha x_i} + \alpha^2 \sum_{i=1}^n x_i &= n. \end{aligned} \tag{19}$$

The solution of the above non-linear equation (19) gives the MLE for the parameter α . As the equation cannot be solved analytically, therefore some iteration techniques like Newton-Raphson method may be adopted to obtain the MLE.

4.2. Method of maximum product of spacings

For the estimation of unknown parameters of continuous univariate distributions, the maximum product of spacings (MPS) approach provides a strong alternative to MLE. [20] initially discussed the use of MPS estimation method whereas [22] demonstrated that this technique as efficient as the MLE and consistent across a wider range of situations. [21] developed the MPS approach as an approximation to the Kullback–Leibler information measure independently. Recently, [23], [24], [25], [26] etc. applied this approach in parameter estimation problem.

According to the procedure, the uniform spacings of a random sample drawn from the Inv- $A(\alpha)$ distribution are defined as

$$\mathbb{D}_i(\alpha) = F(x_{i:n}; \alpha) - F(x_{i-1:n}; \alpha), \quad i = 1, 2, \dots, n + 1.$$

Where, $F(x_{0:n}; \alpha) = 0$ and $F(x_{n+1:n}; \alpha) = 1$. Clearly, $\sum_{i=1}^{n+1} \mathbb{D}_i(\alpha) = 1$.

The maximum product of spacings estimate $\hat{\alpha}_{MPS}$ is obtained by maximizing the geometric mean of the spacings,

$$\mathbb{G}(\alpha) = \left[\prod_{i=1}^{n+1} \mathbb{D}_i(\alpha) \right]^{1/(n+1)}$$

with respect to α , or equivalently, by maximizing the logarithm of the geometric mean of sample spacings:

$$\eta(\alpha) = \frac{1}{n+1} \sum_{i=1}^{n+1} \log \mathbb{D}_i(\alpha). \quad (20)$$

The estimate $\hat{\alpha}_{MPS}$ of the parameter α can be obtained by solving the following non-linear equation.

$$\begin{aligned} & \frac{e^{\frac{1}{\alpha}(1-e^{\alpha x_1})} \left\{ \frac{1}{\alpha} x_1 e^{\alpha x_1} - \frac{1}{\alpha^2} (e^{\alpha x_1} - 1) \right\}}{1 - e^{\frac{1}{\alpha}(1-e^{\alpha x_1})}} + \\ & \sum_{i=2}^n \left[\frac{e^{\frac{1}{\alpha}(1-e^{\alpha x_{i-1}})} \left\{ \frac{1}{\alpha^2} (e^{\alpha x_{i-1}} - 1) - \frac{1}{\alpha} x_{i-1} e^{\alpha x_{i-1}} \right\} - e^{\frac{1}{\alpha}(1-e^{\alpha x_i})} \left\{ \frac{1}{\alpha^2} (e^{\alpha x_i} - 1) - \frac{1}{\alpha} x_i e^{\alpha x_i} \right\}}{e^{\frac{1}{\alpha}(1-e^{\alpha x_{i-1}})} - e^{\frac{1}{\alpha}(1-e^{\alpha x_i})}} \right] \\ & + \frac{1}{\alpha^2} (e^{\alpha x_n} - 1) - \frac{1}{\alpha} x_n e^{\alpha x_n} = 0 \quad (21) \end{aligned}$$

Since the above non-linear equation is not having a closed form solution, it cannot be solved analytically. Therefore, we derived it numerically in next section by using some iteration technique.

4.3. Ordinary and weighted least square estimation

The ordinary least square and the weighted least square are the two conventional estimation procedures were developed by [27] in context of the parameters estimation of the Beta distribution. Let, $x_{(1)}, x_{(2)}, \dots, x_{(n)}$ be the ordered sample of size n from a distribution function $F(x_{i:n}; \alpha)$. Then the ordinary least square estimator $\hat{\alpha}_{OLS}$ can be obtained by minimizing

$$OLS = \sum_{i=1}^n \left[F(x_{i:n}; \alpha) - \frac{i}{n+1} \right]^2,$$

with respect to α . Now, the OLS estimator for the parameter of Inv- $A(\alpha)$ distribution can be obtained by solving the following non-linear equation

$$\sum_{i=1}^n \left(1 - e^{\frac{1}{\alpha}(1-e^{\alpha x_i})} - \frac{i}{n+1} \right) e^{\frac{1}{\alpha}(1-e^{\alpha x_i})} \left\{ \frac{1}{\alpha^2} (e^{\alpha x_i} - 1) - \frac{1}{\alpha} x_i e^{\alpha x_i} \right\} = 0 \quad (22)$$

Similarly, the weighted least square estimate (WLS) of the unknown parameter can be obtained by minimizing the following expression

$$WLS = \sum_{i=1}^n \omega_i \left[F(x_{i:n}; \alpha) - \frac{i}{n+1} \right]^2,$$

with respect to α and $\omega_i = \frac{(n+1)^2(n+2)}{i(n-i+1)}$ be the weight function at the i^{th} point.

Using equation (3) in the above expression and differentiating with respect to α we obtained $\hat{\alpha}_{WLS}$ by solving the following non-linear equation

$$\sum_{i=1}^n \frac{(n+1)^2(n+2)}{i(n-i+1)} \left(1 - e^{\frac{1}{\alpha}(1-e^{\alpha x_i})} - \frac{i}{n+1} \right) e^{\frac{1}{\alpha}(1-e^{\alpha x_i})} \left\{ \frac{1}{\alpha^2} (e^{\alpha x_i} - 1) - \frac{1}{\alpha} x_i e^{\alpha x_i} \right\} = 0. \quad (23)$$

4.4. Minimum distance estimators

In this subsection, we briefly present two estimation approaches for the unknown parameter α of the proposed lifetime distribution based on the minimization, with respect to α , of the goodness-of-fit statistics. This class of statistics is defined based on the discrepancies between the estimate of the cdf and the empirical distribution function [28], [29].

4.4.1 Cramér-Von-Mises estimation

The Cramér-Von-Mises (CVM) estimator is a sort of minimal distance estimator, computed based on the discrepancies between the estimate of the cumulative distribution function and the empirical distribution function. This estimator is also known as maximum goodness of fit estimator. For more details about this method we refer [28, 29, 30] etc. [31] justified the use of Cramér-Von-Mises type minimal distance estimators by demonstrating that their bias is lower than that of other minimum distance estimators.

Let $x_1 < x_2 < \dots < x_n$ be the ordered samples from the pdf (4). Then the Cramér-Von-Mises estimator $\hat{\alpha}_{CVM}$ can be obtained by minimizing ζ with respect to α , where

$$\begin{aligned} \zeta &= \frac{1}{12n} + \sum_{i=1}^n \left(F(x_i) - \frac{2i-1}{2n} \right)^2 \\ &= \frac{1}{12n} + \sum_{i=1}^n \left(1 - e^{\frac{1}{\alpha}(1-e^{\alpha x_i})} - \frac{2i-1}{2n} \right)^2 \end{aligned}$$

Thus, CVM estimator can be obtained by solving the following non-linear equation

$$\sum_{i=1}^n \left(1 - e^{\frac{1}{\alpha}(1-e^{\alpha x_i})} - \frac{2i-1}{2n} \right) e^{\frac{1}{\alpha}(1-e^{\alpha x_i})} \left\{ \frac{1}{\alpha^2} (e^{\alpha x_i} - 1) - \frac{1}{\alpha} x_i e^{\alpha x_i} \right\} = 0. \quad (24)$$

4.4.2 Anderson-Darling estimation

The Anderson-Darling (AD) estimator is another type of minimal distance estimator that is based on the Anderson-Darling statistic, is an alternative to traditional statistical tests for detecting sample distributions departure from normality [32]. The AD estimate, $\hat{\alpha}_{AD}$ of the parameter is obtained by minimizing the following expression with respect to α ,

$$\mathbb{A} = -n - \frac{1}{n} \sum_{i=1}^n (2i-1) [\log F(x_{i:n}) + \log(1 - F(x_{n+1-i:n}))].$$

After minimizing the above expression with respect to α , we have the following nonlinear equation which will be solved numerically to obtain the AD estimator.

$$\sum_{i=1}^n (2i-1) \left[2e^{\frac{1}{\alpha}(1-e^{\alpha x_i})} - 1 \right] \left\{ \frac{1}{\alpha} x_i e^{\alpha x_i} - \frac{1}{\alpha^2} (e^{\alpha x_i} - 1) \right\} = 0. \quad (25)$$

5. SIMULATION STUDY FOR DIFFERENT ESTIMATION METHODS

In this section, a Monte Carlo simulation study has been performed to investigate the behaviour of the proposed estimators. The performance is evaluated based on the root mean square error (RMSE) values of the following six estimates namely, maximum likelihood estimate (MLE), maximum product spacing (MPS), ordinary least square (OLS), weighted least square (WLS), Cramér-Von-Mises (CVM) and Anderson-Darling (AD) estimate. We generate $K=1000$ random samples X_1, X_2, \dots, X_n of sizes $n = 10, 25, 50, 75, 100$ from $Inv-A(\alpha)$ distribution by using inverse transformation method. The initial choices of parameter are taken as $\alpha = 0.1, 0.5, 1.0, 3.0, 5.0$. We calculate the ML, MPS, OLS, WLS, CVM, AD estimates for all choices of the scale parameter. Numerical outcomes are constructed in Table 1 where the average estimates and corresponding RMSE values are displayed.

Table 1: Average estimate values and the associated RMSEs for Inv- $A(\alpha)$ distribution

Parameter choice	Sample sizes (n)	$\hat{\alpha}_{MLE}$	$\hat{\alpha}_{MPS}$	$\hat{\alpha}_{OLS}$	$\hat{\alpha}_{WLS}$	$\hat{\alpha}_{CVM}$	$\hat{\alpha}_{AD}$
$\alpha = 0.1$	10	0.334841	0.071176	0.322474	0.353796	0.426889	0.169213
		0.007426	0.000912	0.007035	0.008026	0.010337	0.002189
	25	0.189182	0.061142	0.180246	0.174847	0.224161	0.123333
		0.002820	0.001229	0.002538	0.002367	0.003926	0.000738
	50	0.145191	0.068292	0.124540	0.124579	0.146387	0.108763
		0.001429	0.001002	0.000776	0.000777	0.001467	0.000277
	75	0.128844	0.071494	0.116508	0.116079	0.130995	0.105799
		0.000912	0.000901	0.000522	0.000508	0.000980	0.000183
	100	0.123515	0.076731	0.112897	0.114688	0.123671	0.106887
		0.000744	0.000736	0.000408	0.000464	0.000749	0.000218
$\alpha = 0.5$	10	0.752290	0.436867	0.716765	0.739353	0.844578	0.572157
		0.007978	0.001996	0.006855	0.007569	0.010897	0.002282
	25	0.595096	0.438685	0.578822	0.575220	0.627734	0.526648
		0.003007	0.001939	0.002493	0.002379	0.004040	0.000843
	50	0.548418	0.454349	0.523074	0.524836	0.547285	0.509773
		0.001531	0.001444	0.000730	0.000785	0.001495	0.000309
	75	0.530561	0.460606	0.515562	0.516496	0.531643	0.506529
		0.000966	0.001246	0.000492	0.000522	0.001000	0.000206
	100	0.525595	0.468765	0.512467	0.515438	0.524463	0.508000
		0.000809	0.000988	0.000394	0.000488	0.000774	0.000253
$\alpha = 1.0$	10	1.275037	0.904548	1.226252	1.223553	1.425039	1.077413
		0.008697	0.003018	0.007155	0.007069	0.013441	0.002448
	25	1.103888	0.918020	1.079842	1.076663	1.133836	1.030476
		0.003285	0.002592	0.002525	0.002424	0.004232	0.000964
	50	1.053224	0.941482	1.022732	1.026182	1.049406	1.010681
		0.001683	0.001850	0.000719	0.000828	0.001562	0.000338
	75	1.033451	0.950529	1.015402	1.017632	1.033153	1.007198
		0.001058	0.001564	0.000487	0.000558	0.001048	0.000228
	100	1.028529	0.961345	1.012633	1.016743	1.025899	1.00906
		0.000902	0.001222	0.000399	0.000529	0.000819	0.000286
$\alpha = 3.0$	10	3.356249	2.809940	3.258877	3.224152	3.430144	3.098857
		0.011266	0.006010	0.008186	0.007088	0.013602	0.003126
	25	3.136043	2.857535	3.090781	3.091121	3.160051	3.042742
		0.004302	0.004505	0.002871	0.002882	0.005062	0.001352
	50	3.070314	2.903247	3.024113	3.032452	3.058492	3.013378
		0.002224	0.003060	0.000763	0.001026	0.001850	0.000423
	75	3.044011	2.920498	3.016559	3.022434	3.039508	3.009221
		0.001392	0.002514	0.000524	0.000709	0.001249	0.000292
	100	3.038722	2.939091	3.014403	3.021810	3.031602	3.012286
		0.001224	0.001926	0.000455	0.000690	0.000999	0.000389
$\alpha = 5.0$	10	5.426122	4.735217	5.287511	5.219631	5.491406	5.11804
		0.013475	0.008373	0.009092	0.006945	0.01554	0.003733
	25	5.16381	4.809465	5.102561	5.104967	5.184119	5.052456
		0.005180	0.006025	0.003243	0.003319	0.005822	0.001659
	50	5.084771	4.872474	5.026128	5.038306	5.06668	5.015507
		0.002681	0.004033	0.000826	0.001211	0.002109	0.00049
	75	5.053036	4.896338	5.018092	5.026767	5.045195	5.010834
		0.001677	0.003278	0.000572	0.000846	0.001429	0.000343
	100	5.047319	4.92115	5.016312	5.026294	5.036646	5.014891
		0.001496	0.002493	0.000516	0.000831	0.001159	0.000471

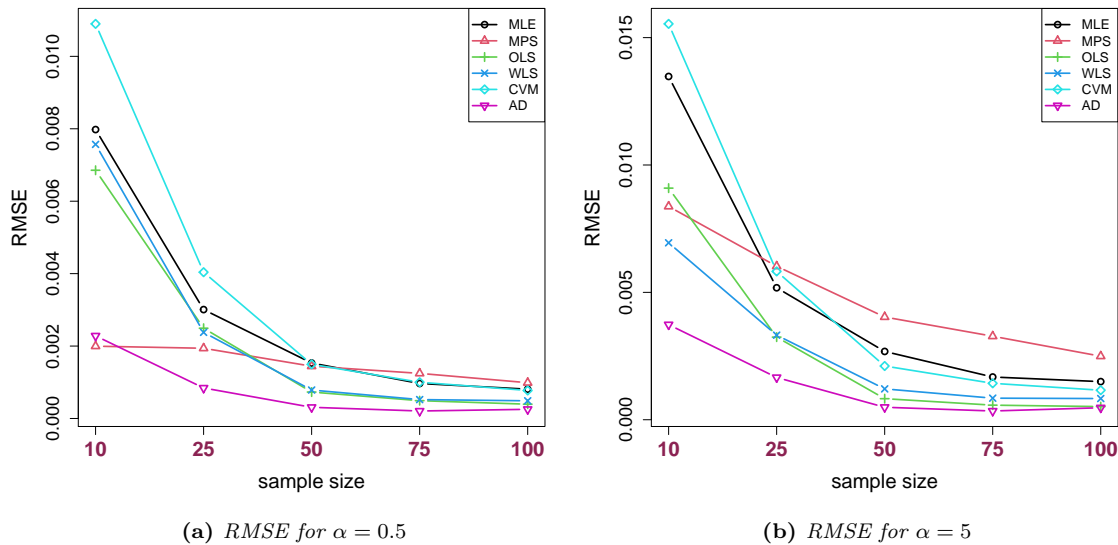


Figure 3: RMSE of $\hat{\alpha}$ under the six different estimation methods with the variation of sample size n

According to Table 1, as the sample size increases, the RMSE of ML, MPS, OLS, WLS, CVM and AD estimates of the scale parameter decrease. Hence, all the estimators hold the property of consistency. Also, it has been observed that the RMSE of the ML, MPS, WLS, CVM and AD estimates increase with the increment of the scale parameter. For small size of sample $n=10$, the performance of MPS estimate is effective when $\alpha < 1$. Overall, the AD estimate is most effective among all the estimates as it produces the least RMSE value for most of the cases we have considered in our study. The results are also verified from the Figure 3.

6. REAL DATA APPLICATION OF THE INV- $A(\alpha)$ DISTRIBUTION

A real dataset has been considered with the goal of evaluating the potentiality of the Inv- $A(\alpha)$ distribution by comparing it with some other well known distributions already available in literature. Inverse exponential (IE) [6], inverse Xgamma (IXg) [9], inverse Lindley (IL) [8], inverse Gamma (IG) [11], inverse Kumaraswamy (IK) [12], inverse Weibull (IW) [7], inverted Nadarajah–Haghighi (INH) [33], Exponentiated inverse Rayleigh (EIR) [34], Inverse power Lindley (IPL) [10] are the few distributions belong to the inverse family have been selected as the competitive models. The parameters of the considered models have been estimated through the MLE approach.

The data consists of death times (in weeks) of 52 patients having tongue cancer with an aneuploid DNA profile discussed by [35] and given by [36]. Recently, [37] used this dataset in their study. Patients with sexually transmitted illnesses who had a paraffin-embedded sample of malignant tissue obtained were chosen and the time frames to reinfection were estimated. Using a flow cytometer, the tissue samples were evaluated to see if the tumour had an aneuploid (abnormal) or diploid (normal) DNA profile, as described by [35].

In ordered to make comparison among the considered models some criterion includes $2 \times$ negative log-likelihood ($-2 \ln L$), Akaike Information Criterion (AIC), Corrected AIC (CAIC), Bayesian information criterion (BIC) and Hannan-Quinn information criterion (HQIC) are utilized. A model with minimum values of these statistics are considered to be the best model. Further, we also use goodness of fit tests such as Kolmogorov-Smirnov (K-S), Cramér-Von-Mises (CVM) and Anderson-Darling (AD) tests along with their corresponding P Values. The MLE with respective standard error (in parentheses) of the parameters and values of $-2 \ln L$, AIC, BIC, CAIC and HQIC and the numerical values of K-S, CVM and AD statistics along with their corresponding P values are displayed in Table 2 and 3 respectively. It has been observed that the Inv- $A(\alpha)$ distribution

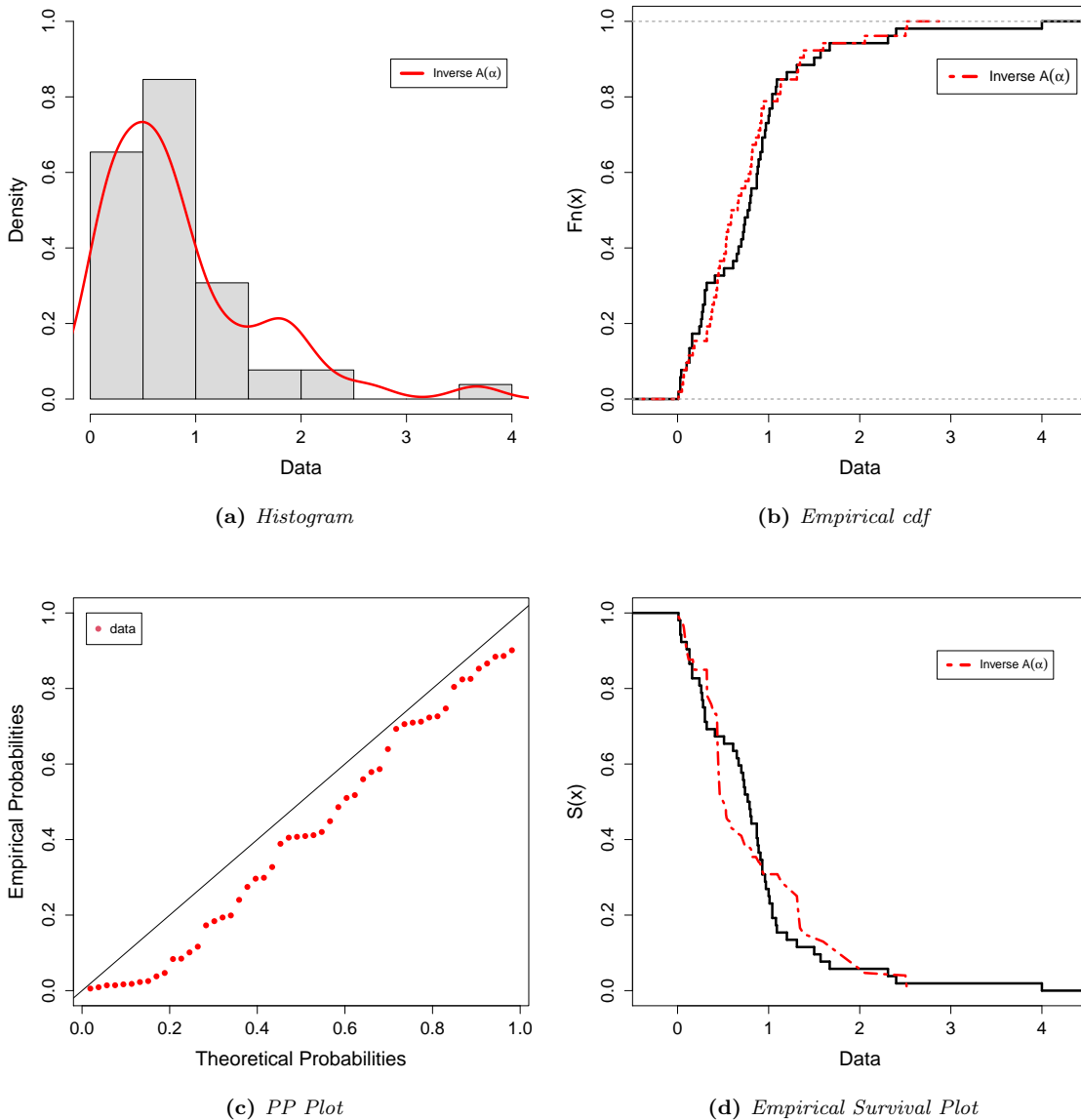


Figure 4: Empirical pdf, cdf, pp and sf plots for the tongue cancer data

have the lowest values for all goodness-of-fit statistics and the largest P value among all other competitive models. As a result, our proposed model outperformed the other models for the tongue cancer data.

Figure 4 shows a plot of estimated histogram, empirical cdf, PP-plot and a plot of the survival functions modified by the suggested theoretical models onto the empirical survival function (Kaplan-Meier estimate), which may be used to verify the goodness of fit for the proposed model. A graphical technique based on total time on test (TTT) plot is also used here to identify the shapes of the data. According to [38], the hrf is constant if the TTT plot is visually portrayed as a straight diagonal, the hrf is increasing (or decreasing) if the TTT plot is concave (or convex). The hrf is U-shaped (bathtub) if the TTT plot is firstly convex and then concave, if not, the hrf is unimodal. The TTT plot in Figure 5 indicates that the empirical hrf of the tongue cancer dataset is ‘monotonically increasing’. Hence the proposed lifetime model $Inv-A(\alpha)$ might be a good fit for the cancer data theoretically.

Table 2: Analytical results of the $Inv-A(\alpha)$ distribution and the other competing models for the tongue cancer data

Model	Estimates (SE)	$-2 \log L$	AIC	CAIC	BIC	HQIC
$Inv-A(\alpha)$	0.2333 (0.1187)	80.9634	82.9634	83.0434	84.9146	83.7114
IE (θ)	0.1766 (0.0245)	146.0563	148.0563	148.1363	150.0075	148.8044
IXg (θ)	0.3741 (0.0351)	216.1880	218.1880	220.1393	218.2680	218.9361
IL (θ)	0.3112 (0.0310)	191.1509	193.1509	193.2309	195.1021	193.8989
IG (α, β)	0.5805 (0.0953) 0.1025 (2.3912)	133.2271	137.2271	137.4720	141.1295	138.7232
IK (α, β)	2.5056 (0.3860) 1.6592 (0.3184)	88.4087	92.4087	92.6536	96.3112	93.9048
IW (α, β)	0.4113 (0.0790) 0.6745 (0.0619)	121.5629	125.5629	125.8078	129.4654	127.0590
INH (α, β)	1.2836 (0.4463) 0.4228 (0.0580)	107.3259	111.3259	111.5708	115.2284	112.8220
EIR (α, σ)	0.1706 (0.0256) 0.0283 (0.0049)	161.3631	165.3631	165.6080	169.2656	166.8592
IPL (α, β)	0.5790 (0.0497) 0.7788 (0.1020)	122.8562	126.8562	127.1011	130.7587	128.3524

Table 3: Goodness of fit measures of the $Inv-A(\alpha)$ distribution and the other competing models for the tongue cancer data

Model	K-S	P value	CVM	P value	AD	P value
$Inv-A(\alpha)$	0.13896	0.26783	0.22006	0.23203	1.13202	0.29461
IE (θ)	0.40253	9.606×10^{-8}	2.52648	4.603×10^{-7}	12.57664	1.153×10^{-5}
IXg (θ)	0.51125	3.130×10^{-12}	4.93455	0.00000	28.18699	1.153×10^{-5}
IL (θ)	0.48784	3.563×10^{-11}	4.04569	0.00000	23.22221	1.153×10^{-5}
IG (α, β)	0.27891	6.130×10^{-4}	1.21856	6.903×10^{-4}	6.15950	8.319×10^{-4}
IK (α, β)	0.20757	2.265×10^{-2}	0.41892	6.405×10^{-2}	2.08487	8.278×10^{-2}
IW (α, β)	0.21708	1.488×10^{-2}	0.81699	6.410×10^{-3}	4.48490	5.123×10^{-3}
INH (α, β)	0.19485	3.857×10^{-2}	0.63488	1.800×10^{-2}	3.51034	1.531×10^{-2}
EIR (α, σ)	0.34511	8.350×10^{-6}	2.08864	5.598×10^{-6}	9.97822	1.867×10^{-5}
IPL (α, β)	0.21509	1.627×10^{-2}	0.81766	6.386×10^{-3}	4.5175	4.941×10^{-3}

7. CONCLUSION

In medical science and reliability engineering, development of a distribution with an increasing hazard rate function constitutes a considerable practical interest. In this article, we have presented an $Inv-A(\alpha)$ distribution with some properties such as quantile function, median, reliability function, hazard rate function, order statistics, ageing intensity function etc. The flexibility of this distribution primarily depends on the reliability behaviour as the distribution has an increasing hazard rate function. This feature of such distribution enhances the applicability to the real world. For instance, it describes the real scenarios which are more likely to fail with age, either of a human being or a machine whose parts wear out.

The model parameter is estimated through the ML estimation, maximum product of spacings estimation, ordinary and weighted least square estimation, CVM and AD estimation respectively.

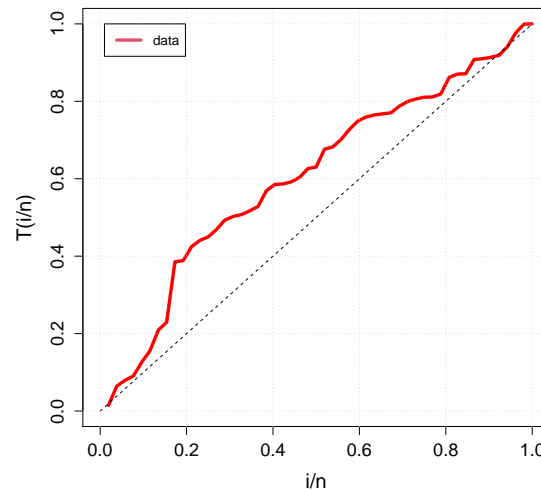


Figure 5: TTT plot for the Tongue cancer data

The Monte Carlo simulation study has been performed to investigate the performance of the obtained estimators and it is noticed that all the estimators are asymptotically unbiased and consistent. Among all the traditional estimation methods, Anderson-Darling method outperforms the others. Furthermore, we consider tongue cancer data to exhibit the applicability of the Inv- $A(\alpha)$ distribution in the field of bio-medical science. To examine the superiority of the proposed model, we compared it with some competitive models and found that our model has the best fittings amongst them based on the goodness of fit measures. Therefore, we hope that our new proposed model from the family of inverse probability distribution might be taken as a viable choice to analyze several medical science data.

REFERENCES

- [1] Alshenawy, R. (2020). A new one parameter distribution: properties and estimation with applications to complete and type II censored data. *Journal of Taibah University for Science, Taylor & Francis*, 14(1):11–18.
- [2] Marshall, A. W. and Olkin, I. (1997). A new method for adding a parameter to a family of distributions with application to the exponential and Weibull families. *Biometrika, Oxford University Press*, 84(3):641–652.
- [3] William, T. S. and Ian, R. C. B. (2009). The alchemy of probability distributions: beyond Gram-Charlier expansions, and a skew-kurtotic-normal distribution from a rank transmutation map. *arXiv preprint arXiv:0901.0434*.
- [4] Kumar, D., Singh, U. and Singh, S. K. (2015). A method of proposing new distribution and its application to Bladder cancer patients data. *J. Stat. Appl. Pro. Lett*, 2(3):235–245.
- [5] Mahdavi, A. and Kundu, D. (2017). A new method for generating distributions with an application to exponential distribution. *Communications in Statistics-Theory and Methods, Taylor & Francis*, 46(13):6543–6557.
- [6] Keller, A. Z., Kamath, A. R. R and Perera, U. D. (1982). Reliability analysis of CNC machine tools. *Reliability engineering, Elsevier*, 3(6):449–473.
- [7] Calabria, R. and Pulcini, G. On the maximum likelihood and least-squares estimation in the inverse Weibull distribution. *Statistica Applicata*, 2(1):53–66.
- [8] Sharma, V. K., Singh, S. K. and Singh, U. and Agiwal, V. (2015). The inverse Lindley distribution: a stress-strength reliability model with application to head and neck cancer data. *Journal of Industrial and Production Engineering, Taylor & Francis*, 32(3): 162–173.

- [9] Yadav, A. S., Maiti, S. S. and Saha, M. (2021). The inverse xgamma distribution: statistical properties and different methods of estimation. *Annals of Data Science, Springer*, 8(2): 275–293.
- [10] Barco, K. V. P., Mazucheli, J. and Janeiro, V. (2017). The inverse power Lindley distribution. *Communications in Statistics-Simulation and Computation, Taylor & Francis*, 46(8): 6308–6323.
- [11] Abid, S. H. and Al-Hassany, S. A. (2016). On the inverted gamma distribution. *International Journal of Systems Science and Applied Mathematics*, 1(3): 16–22.
- [12] Abd AL-Fattah, A. M., El-Helbawy, A. A. and Al-Dayian, G. R. (2017). Inverted Kumaraswamy Distribution: Properties and Estimation. *Pakistan Journal of Statistics*, 33(1).
- [13] Sakthivel, K. M. and Dhivakar, K. (2021). Transmuted Sine-Dagum Distribution and its Properties. *Reliability: Theory & Applications*, 16,4 (65):150–166.
- [14] Ronald, E. G. (1980). Bathtub and Related Failure Rate Characterizations. *Journal of the American Statistical Association*, 75(371):667–672.
- [15] Jiang, R., Ji, P., and Xiao, X. (2003). Aging property of unimodal failure rate models. *Reliability Engineering & System Safety, Elsevier*, 79(1): 113–116.
- [16] Nanda, A. K., and Bhattacharjee, S., and Alam, S. S. (2007). Properties of aging intensity function. *Statistics & probability letters, Elsevier*, 77(4): 365–373.
- [17] Bhattacharjee, S., Nanda, A. K. and Misra, S. Kr. (2013). Reliability analysis using ageing intensity function. *Statistics & Probability Letters, Elsevier*, 83(5): 1364–1371.
- [18] Shanthikumar, J. G. (1994). Stochastic orders and their applications. *Academic Press*.
- [19] Casella, G., and Berger, R. L. (2021). Statistical inference. *Cengage Learning*.
- [20] R. C. H. Cheng. and N. A. K., Amin. (1983). Maximum product of spacings estimation with applications to the lognormal distribution. *Journal of the Royal Statistical Society: Series B*, 45(3): 394–403.
- [21] Bo, Ranneby. (1984). The Maximum Spacing Method. An Estimation Method Related to the Maximum Likelihood Method. *Scandinavian Journal of Statistics*, 11(2):93–112.
- [22] F. P. A. Coolen. and M. J. Newby. (1991). The Maximum Spacing Method. An Estimation Method Related to the Maximum Likelihood Method. *Kwantitatieve Methoden*, 37:19–32.
- [23] Kaushik. G., and S. Rao., J. (2001). A general estimation method using spacings. *Journal of Statistical Planning and Inference*, 93:71–82.
- [24] T. S. T. Wong and W. K. Li. (2006). A Note on the Estimation of Extreme Value Distributions Using Maximum Product of Spacings. *IMS Lecture Notes-Monograph Series*, 52:272–283.
- [25] Singh., U., Singh., S. K. and Rajwant., K. S. (2014). The Maximum Spacing Method. An Estimation Method Related to the Maximum Likelihood Method. *Journal of Statistics Applications and Probability*, 3(2):179–188.
- [26] Mazucheli, J., Ghitany, ME. and Louzada, F. (2017). Comparisons of ten estimation methods for the parameters of Marshall–Olkin extended exponential distribution. *Communications in Statistics-Simulation and Computation, Taylor & Francis*, 46(7):5627–5645.
- [27] James J. S., Venkatraman, S. and James, R. W. (1988). Least-squares estimation of distribution functions in johnson’s translation system. *Journal of Statistical Computation and Simulation*, 29(4):271–297.
- [28] D’Agostino, R. B. (1986). Goodness-of-fit-techniques. *CRC press*, 68.
- [29] Luceño, Alberto. (2006). Fitting the generalized Pareto distribution to data using maximum goodness-of-fit estimators. *Computational Statistics & Data Analysis, Elsevier*, 51(2): 904–917.
- [30] Louzada, F., Ramos, P., L. and Perdoná, G., SC. (2016). Different estimation procedures for the parameters of the extended exponential geometric distribution for medical data. *Computational and mathematical methods in medicine, Hindawi*, 2016.
- [31] Macdonald, P. D. M. (1971). Comments and queries comment on “an estimation procedure for mixtures of distributions” by choi and bulgren. *Journal of the Royal Statistical Society: Series B (Methodological)*, 33(2): 326–329.

- [32] Anderson, T. W. and Darling, D. A. (1952). Asymptotic theory of certain "goodness of fit" criteria based on stochastic processes. *The annals of mathematical statistics, JSTOR*, 193–212.
- [33] Tahir, M. H., Cordeiro, G. M., Ali, S., Dey, S. and Manzoor, A. (2018). The inverted Nadarajah–Haghighi distribution: estimation methods and applications. *Journal of Statistical Computation and Simulation, Taylor & Francis*, 88(14): 2775–2798.
- [34] Rao, G. S. and Mbwambo, S. (2019). Exponentiated inverse Rayleigh distribution and an application to coating weights of iron sheets data. *Journal of probability and statistics, Hindawi*, 2019.
- [35] Sickle-Santanello, B. J., Farrar, W. B., Decenzo, J., F., Keyhani-Rofagha, S., Klein, J., Pearl, D., Laufman, H. and O'Toole, R. V. (1988). Technical and statistical improvements for flow cytometric DNA analysis of paraffin-embedded tissue. *Cytometry: The Journal of the International Society for Analytical Cytology*, 9(6):594–599.
- [36] Klein, J. P. and Moeschberger, M. L. (2003). Survival analysis: techniques for censored and truncated data. *Springer*, 1230.
- [37] Bantan, R., Hassan, A. S., Elsehetry, M. and Kibria, B. M. (2020). Half-logistic xgamma distribution: Properties and estimation under censored samples. *Discrete Dynamics in Nature and Society, Hindawi*, 2020.
- [38] Aarset, M. V. (1987). How to identify a bathtub hazard rate. *IEEE Transactions on Reliability, IEEE*, 36(1):106–108.

SAFETY AT WORK: A COMPLEX OR AN EXCEEDINGLY SIMPLE MATTER?

Rodrigo F. S. Gomes^{*1}, Leandro Gauss², Fabio Sartori Piran³, Daniel Pacheco
Lacerda⁴

•

^{1, 2, 3, 4}PPGEPS/GMAP. Graduate Program in Production & System Engineering. Universidade
do Vale do Rio dos Sinos, São Leopoldo/RS – Brazil.

E-mail: ¹rodrigofrank@edu.unisinos.br, ²lgauss@unisinos.br, ³fpiran@unisinos.br,
⁴dlacerda@unisinos.br

* Corresponding author

Abstract

This paper uses the concept of inherent simplicity stemming from the Theory of Constraints to explain whether safety at work is a complex or an exceedingly simple matter. In this context, the study seeks to explore the causalities that govern safety at work, identifying its constructs and presenting logic propositions based on the theory-building blocks: classification, correlation, and causal consistency. To support the research, a dataset composed of 46 work-related accident investigation reports from an elevator industry in Latin America was carefully analyzed using association rules. Moreover, direct observations grounded on inductive reasoning were used to speculate plausible causes concerning the effect of work-related accidents. The research strategy followed common strategies of theory building to reach common sense: theory-to-practice and practice-to-theory. As a result, a conceptual proposition is postulated based on the reasoning that safety at work is governed by very few constructs, and that its complexity is explained through the two elements from inherent simplicity: degrees of freedom (interdependencies between constructs) and harmony (conflicts resolution within the work environment). From the practitioners' perspective, the study also offers directions towards safety improvements at the organizational level by considering the impact of the interdependencies between constructs in safety at work.

Keywords: Inherent simplicity. Safety at work. Theory of constraints. Theory building. Causation

I. Introduction

The field of safety science is advancing very slowly, despite an increasing volume of research activity and publication [1]. On one side, a massive body of knowledge is available in literature in a form of cases, frameworks, mathematical models, and systematic literature reviews. On the other side, practitioners are struggling to improve safety practices within organizations without considering theories and published shreds of evidence. While this disharmony between theory and practice in safety science is verified, society remains to deal with social and economic impacts arising from ineffective safety management.

According to ILO [2], more than 2.8 million deaths per year result from occupational accidents or work-related diseases. When considering non-fatal work-related injuries, this number increases to approximately 376.8 million a year. Moreover, the burden resulting from such ineffective safety management accounts for economic losses estimated at 3.94% of the global Gross Domestic Product [3–5].

This pragmatic reality shall draw the attention of researchers and practitioners due to its impact on society. This is because a healthy and safe work environment not only is desirable from the workers' perspective but also contributes considerably to labor productivity and promotes economic growth [6]. Furthermore, safety at work promotes worker motivation, increases productivity by reducing costs related to work-related health problems, and relieves pressure on public and private health systems.

Based on such a challenging scenario, a step back seems to be necessary. Rather than propose solutions to address just a piece of this issue, it is necessary to make sure that safety at work is well understood in academia and within organizations.

In this context, this paper aims at identifying the constructs and presenting propositions to explain the causalities that govern safety at work. In addition, this study explores how the definition of complexity should be understood in the field of safety science, and what is the prevailing definition. This is fundamental to draw attention to the main factors that affect safety, and how their interdependencies might increase or decrease the complexity of the system.

In that reasoning, the theoretical discussion of this study is structured on building blocks proposed by Whetten [9], and consistent with the three stages of science proposed by Goldratt [10]: classification, correlation, and causation consistency. As a major theoretical outcome of this research, the causalities that govern safety at work and its complexity are explained through the two elements of inherent simplicity: degrees of freedom (interdependencies between constructs) and harmony (determined by the belief that every internal conflict can be removed by eliminating improper assumptions).

From a managerial's perspective, this study is useful for practitioners to put efforts on critical constructs that impact the overall safety management system to make it simpler and harmonious, instead of acting to reach local optima.

Finally, this study also has a side contribution in extending the applications of Theory of Constraints (TOC) to the field of safety. Since literature is particularly lacking in investigative studies on the theoretical and practical implications of TOC principles [11], this research contributes to closing this gap since no previous study is found connecting inherent simplicity and safety science.

This article is organized as follows: Section II outlines a comprehensive review of the concept of inherent simplicity. The work method is described in Section III. In Section IV the results are presented and a narrative of theoretical discussion is conducted. Finally, the main conclusions and limitations of the study are summarized in Section V.

II. Inherent simplicity

The concept of inherent simplicity is a principle from the Theory of Constraints [10] in which is postulated that any part of reality is governed by very few elements and that any conflict can be eliminated [12]. In its earliest stage, TOC focused on production system optimization before being recognized as an operations management theory to foster the process of ongoing improvement. Further on, TOC became a global management philosophy applied to various areas such as production, supply chain, project, and other fields [11]. In the theoretical field, TOC also satisfies the virtues of a good theory, such as uniqueness, parsimony, and generalizability [13].

Goldratt [10] outlined that TOC is grounded in its practicability, and unlike in common sense, "theory in science must be practical, otherwise, it is not theory but just an empty scholastic speculation" (p.32). This is consistent with the assumption that the purpose of good theory shouldn't be other than describe and explain how things actually work, and in so doing to help us improve our actions in this world [14]. The concept of inherent simplicity can also be understood as a practical way of viewing reality. However, reality usually looks complex to us, and Goldratt took for granted the foundation of modern science from Newton: "*Natura valde simplex est et sibi consona*" (nature is exceedingly simple and harmonious with itself). It does mean that if we deep dive enough into observing phenomena, we'll find that there are very few elements at the base that govern the whole system. Reality is, therefore, built in wonderful simplicity [12]. The interpretation of Goldratt from Newton's quote is also consistent with the principle of bounded rationality (Simon, 1957, pp. 198-199): "the capacity of the human mind for formulating and solving complex problems is very small compared with the size of the problems whose solution is required for objectively rational behavior in the real world". In other terms, the key to simplification of the choice process is rather the goal of "maximizing", the goal of "satisfying", i.e. finding a course of action is good enough". This association of concepts was postulate by Eden and Ronen [8] and in-deep described by Naor et al. [13] for further readings. The prevailing definition of complexity is that the more entities the system has, the more complex the system is. Thus, by following this approach to compare the complexity of the systems 'A' and 'B' represented in Figure 1, the system 'B' is more complex than 'A' because the quantity of entities that comprise the system 'B' is higher than 'A'. However, since we are more interested in understanding, predicting, and controlling the system instead of just describing it, this study follows Goldratt's approach to define complexity by the following: the more degrees of freedom the system has, the more complex it is [12].

The concept of degrees of freedom might be clear for physicists or engineers but it is not under overall comprehension. In short, Goldratt explains that it means the minimum number of points (or entities) you have to touch in order to impact the whole system. For example, in the case of system 'B', by impacting the bottom circle, the whole system is impacted, i.e. it has only one degree of freedom. On the other hand, system 'A' has five degrees of freedom, which is harder to control and predict due to its magnitude. This becomes clear by observing the absence of arrows in the system, which means that there are no interdependencies between the entities. Figure 1 illustrates the reasoning of complexity based on inherent simplicity.

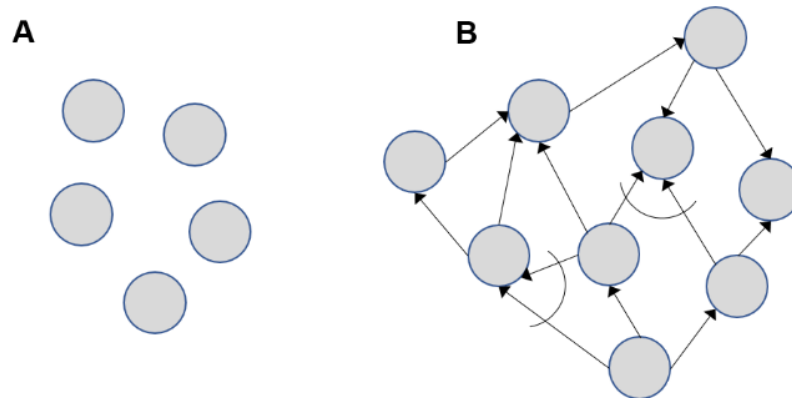


Figure 1 – *The reasoning of complexity* [12]

Safety at work also might look complex to researchers and practitioners. One possible reason for that is the lack of comprehension about what plausible constructs govern this phenomenon, and how these constructs are interconnected to define the degrees of freedom that govern the system. Seeking the same logic applied to safety science, if the constructs that govern safety at work are identified, and the propositions between them are clear, it is possible to decipher the level of complexity of this matter.

III. Research Design

This study is based on 18 months of direct observations and primary data analysis concerning investigation reports of work-related accidents occurred in an elevator industry. The industry’s activities are spread out over 12 countries across Latin America, covering one industrial facility in Brazil and more than 75 service operating units across the region. During this period, the first researcher had close contact with a reality-based source of data, in which scope it is included both manufacturing and service areas in the twelve countries where the organization has an operational presence.

The work method used both common strategies of theory building: theory-to-practice and practice-to-theory [7, 14] as shown in Figure 2.

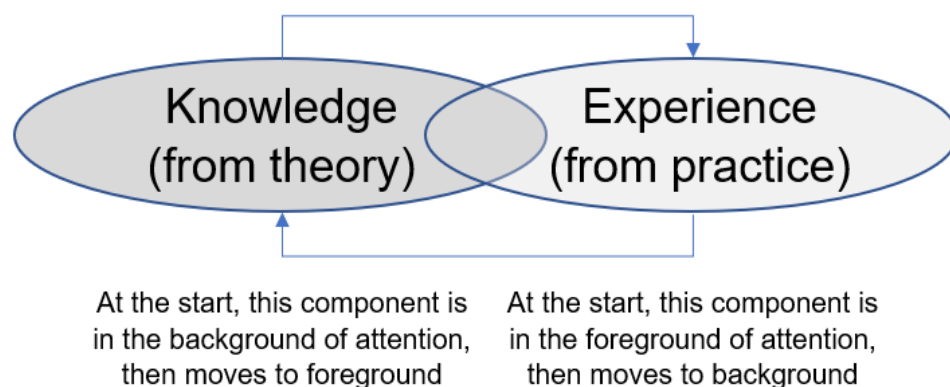


Figure 2 – *General method of theory building in applied disciplines. Source: Adapted from Lynham (2002)* [14]

Initially, the researchers observed an effect: the occurrence of work-related accidents as an issue with significant social and economic impacts worldwide. Then, following the stages proposed by Goldratt [10], the focus moved to speculate plausible causes to explain this phenomenon. To do that, a research question was therefore defined, and awareness about the research problem was sought based on specialized literature.

The next step accounted for the use of a theory-to-practice approach to assume that very few constructs govern safety at work. In that reasoning, the principle of inherent simplicity derived from TOC was reviewed and the theory was framed in the field of safety. As a second stream, the research moved on to the practice-to-theory approach through reality-based data collection to analyze and come up with theoretical and practical contributions to safety science, exploring how and why the constructs that govern safety at work are interconnected and seeking to uncover underlying issues to explain its complexity. A detailed step-by-step of the work method is depicted in Figure 3.

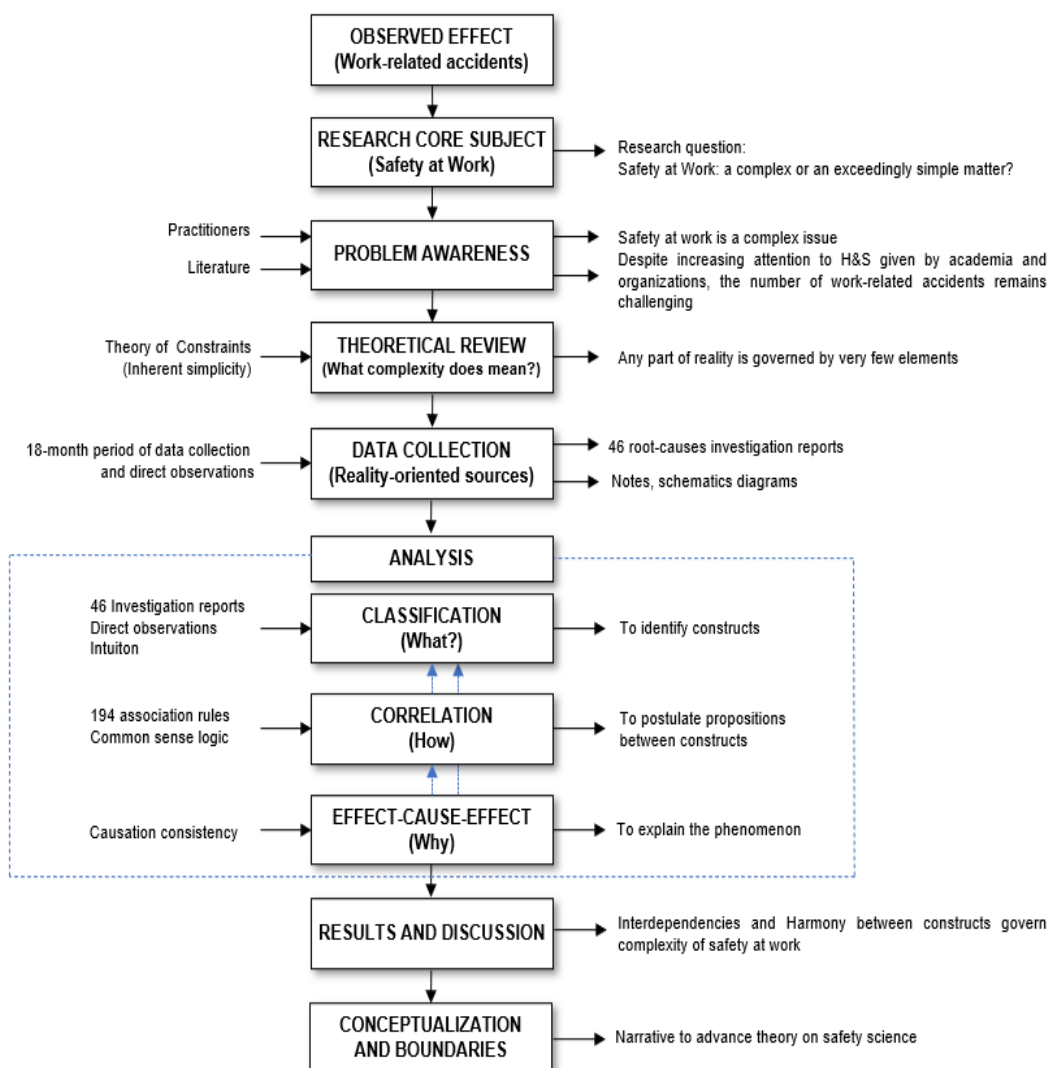


Figure 3 – Core research subject

The first researcher examined in depth the existing body of documents in the occupational health and safety management system (OHSMS), the structural functioning of the case unit, and how health and safety (H&S) fits into the organization's strategic planning. Also, several job site visits were conducted to observe how the work is done, the resources available, level of technical knowledge, procedures, routine instructions, task planning, and personal protective equipment (PPE) usage.

Data retrieved from the OHSMS was studied through a business intelligence (B.I.) dashboard covering the period between oct-19 to mar-21. Forty-six root-causes investigation reports listed in Table 1 were collected and analyzed with the support of three specialists. The specialists are H&S managers in charge of the three main operations within the organization: the factory located in Brazil, field operations in Brazil, and field operations in other Latin American countries. In addition, an organizational psychologist supported the discussion when behavioral aspects were reported as contributive causes to the accidents.

Table 1 – Root-causes investigation reports

Country	Working hours	Root-causes investigation reports derived from lost-time accidents	
		Factory	Services
Argentina	403,000	-	1
Brazil	14,000,000	1	28
Chile	1,387,000	-	4
Colombia	1,256,000	-	2
Costa Rica	91,000	-	1
Mexico	978,000	-	3
Panama	2,918,000	-	2
Paraguay	372,000	-	1
Peru	1,049,000	-	1
Uruguay	163,000	-	2

Each root-cause investigation report followed a structured template based on 9 categories and 41 data fields (see appendix A 1). The outcome of this analysis was to identify and classify the most frequent factors that impacted work-related accidents.

Moreover, a data mining through the algorithm *Apriori* was powered to identify association rules between factors, i.e., what antecedent factors (named *lhs*) impact the other consequent ones (named *rhs*), and how strong is this correlation. It consists of a data mining algorithm that systematically controls the exponential growth of candidate itemsets [16]. The parameters support (supp=0.5), and confidence (conf=0.8) were set up as thresholds based on adopted criteria from previous studies [17, 18].

The parameter support determines how often a rule applies to a given dataset. Besides, it aims to identify the most relevant rules [20] in the dataset. Confidence, in turn, determines how frequently consequent factors [*rhs*] appear in relationships that contain antecedents [*lhs*]. It is used to measure the strength of an association rule, expressed as the times a specific itemset is found together with a specific item out of the total times this specific itemset is found in the entire dataset [18]. In other words, the greater confidence of rule $\{X\} \Rightarrow \{Y\}$, the greater the probability of $\{Y\}$ being present in events that contain $\{X\}$ [21].

An additional measure used in that research is the ‘lift’. The lift of an association rule is responsible for measuring the difference between the number of times {X} and {Y} co-occur and the expected frequency of such co-occurrence if they were statistically independent [22]. In that reasoning, high levels of lift mean that the consequent factor is scarcer within the population and more frequent within the specific itemset.

For this step, a script loaded in software RStudio was used for data processing (see appendix A2). Additional explanations about the use of association rules can be found in the work of Zhang and Zhang [16] and other mentioned literature. Furthermore, examples of how to explore cause-effect relationships using association rules in the H&S field can be found in the studies of Cheng et al. [23], Mirabadi and Sharifian [24], and Verma et al. [25].

Through this technique, 194 associated rules were retrieved to support the correlation stage. The structure of rules is presented in Table 2 and can be interpreted as follows: based on a dataset with N events, the rule [n1], for example, associates the antecedent factor A to the consequent factor C. The support of this rule can vary between 0 – 1. A minimum support threshold is used to select the most frequent (and hopefully important) factors’ combinations. Confidence, similarly, is understood as an estimate of the conditional probability of factors co-occur in a rule (0 – 1). Finally, the lift value of 1 indicates that the factors are co-occurring in the database as expected under independence. Values greater than 1 indicate that the items are associated, and lower than 1 indicate an absence of association [22].

Table 2 – Structure of association rules

Rule	lhs	rhs	support	confidence	lift	count
[n1]	{antecedent A}	=> {consequent C}	0 - 1	0 - 1	0 - ∞	1 - N
[n2]	{antecedent A, antecedent B}	=> {consequent D}	0 - 1	0 - 1	0 - ∞	1 - N

Besides the investigation reports, other general documents were carefully analyzed, e.g the strategic planning 2020-2025, OHSMS manual, and H&S policies. From these documents, it was possible to situate expected management commitment as well as H&S in the strategic context of the organization, in order to check against reality through direct observations.

Direct observations were conducted in the course of the same period of the primary data collection. It followed as possible, a semi-structured approach as follows: (1) to verify the work being performed, such as the use of tools and personal protective equipment, printed instructions, work environment, etc; (2) to conduct an informal conversation to understand the task routine, capabilities required to the task, and capacity to foreseeing risks; (3) to verify the leadership commitment from the worker’s perspectives, and possible behavioral impacts from externalities, such as COVID-19, personal issues. Yet, the informal approach was given to avoid the feeling of pressure when formal questions for interviews could bring up.

Moreover, additional factors were observed at the job sites beyond the technical field. The education level and behavioral aspects, such as lack of concentration and lack of awareness were considered as well. Also, the observations were not limited to job sites. Management meetings and reactions from the occurrence of accidents were also observed. Preliminary speculations from the direct observations were registered in notes and schematic diagrams to reach common-sense logic. Furthermore, confirmation questions were frequently used at the end of any informal approach: “if I understood well this effect was caused by this fact. Am I right?”.

The relevance of the direct observations is based on the fact that it is rarely found whether in literature or in reality-based practices, pieces of evidence related to explain the safe work, i.e. a deep analysis of what went good, and the factors that led to a work environment in which safety culture is intrinsic. As an outcome of the use of both association rules and direct observations, a framework is proposed to explain the causalities that govern safety at work since it allows the researcher to observe, in practice, the effect-cause-effect stage.

Based on the framework elaborated, the first researcher was encouraged to use verbalized intuition with other researchers and practitioners [10] to practice simplicity, parsimony, and to reach common sense.

In that reasoning, principles of causal consistency derived from the Theory of Constraints Thinking Processes were also used to explain each proposition presented in the framework: causality existence, causality clarity, the sufficiency of cause, and additional cause [26]. As a result, a conceptualization of complexity in safety at work is postulated.

In the next session, results are discussed throughout a combined approach of the three main stages that every science has gone through [9, 10]. The classification stage was associated with the 'what', correlation with the 'how', and effect-cause-effect with the 'why'. Finally, the researchers sought to define limitations in time and context for the propositions. These contextual factors are critical to set the boundaries of generalizability in which the propositions are postulated.

IV. Results and Discussion

I. Classification (building block 'what')

This stage sought to explore what constructs logically impact safety at work. In this context, the criteria of comprehensiveness and parsimony supported the researchers to determine whether a factor should be considered as a variable to explore the causalities of safety at work. In short, it was sought for relevance and value-added of each variable to explain phenomena [9]. One primary instance of identifying these constructs was based on an inductive approach and intuition. Initially, it was considered plausible factors that influence phenomena (safety at work). For instance, technical expertise is a plausible factor to impact positively safety. However, even in case of considering this example a common sense, it does not explain what is its level of importance, how this factor is connected to others, and what is its effect on the whole system.

In addition, the analysis and classification of primary data and the findings obtained through direct observations supported the researchers in that stage. Numerous factors came up with this process, including training, task planning, years of experience, education level, availability of proper tools, personal protective equipment usage, adequate instruction. However, at this point in time, no correlation was checked, and each factor was considered an independent one. In that reasoning, consistent with the concept of inherent simplicity, the system primarily seemed to be very complex (see Figure 4)



Figure 4 – Factors that impact safety at work

The next step was to practice simplicity and parsimony, considering that theory should have a minimum of complexity and few assumptions. Each variable was considered as a potential factor to impact safety at work. Next, every variable was associated with a construct as a theoretical element wherein the variable is encompassed. A minimum number of constructs was sought in order to reach simplicity and decrease complexity.

In that reasoning, after the data analysis, an interactive process of verbalizing the factors grouped in constructs with other researchers, H&S experts, and workers was conducted to reach common sense. In this context, variables were grouped into constructs to reach a higher level of abstraction, keeping the properties of comprehensiveness. For instance, variables such as technical training, safety training, hazard analysis were grouped into the construct ‘knowledge’. This is because ‘knowledge’ encompasses several factors associated with the necessity of knowing, for example, ‘what to do’, ‘how to do’, ‘what are the risks involved’, ‘how to mitigate the risks’.

As an outcome of this stage, a set of constructs were defined as satisfactory based on the logic of ‘good enough’ [8] to explore phenomena of interest (see Figure 5). This is because these four theoretical elements (knowledge, planning, behavior, and performance measure) sufficiently encompass in a form of constructs all variables identified in the classification stage.

In the next sub-session, the propositions between how these constructs are connected are outlined.

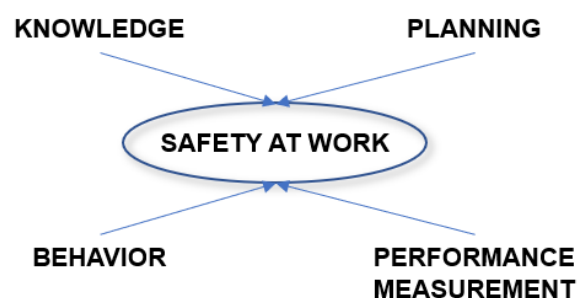


Figure 5 – Constructs associated with safety at work

II. Correlation (building block ‘how’)

Once the minimum necessary constructs to explore phenomena of interest are identified, the next stage aimed to define how they are connected (co-related). Although this stage is based on careful observations and often involves a quantitative approach, the question ‘why’ is not asked at all. Rather the question ‘how’ is the center of interest [10]. Based on that reasoning, the propositions were structured with the use of 194 association rules, as shown in Table 3.

Table 3 – Association rules

Rule	Lhs	rhs	support	confidence	lift	count
[34]	{Inappropriate JHA}	=> {Lost time Accident}	0.6415	1	1.1522	34
[70]	{Trained to the task}	=> {Diminishing Risks}	0.6038	0.8889	1.1778	32
[76]	{Trained to the task}	=> {Lost time Accident}	0.6792	1	1.1522	36
[79]	{Diminishing Risks}	=> {Daily routine}	0.6415	0.8500	1.1551	34
[100]	{Diminishing Risks}	=> {Lost time Accident}	0.7547	1	1.1522	40
[145]	{Trained to the task, Working in regular time}	=> {Unappropriate JHA}	0.5283	0.8000	1.2471	28
[155]	{On-time, Trained to task}	=> {Diminishing Risks}	0.5283	0.9333	1.2367	28

Also, the researchers sought to take benefit from the direct observation of works being performed safely. This is because the set of investigation reports analyzed is about ‘how things went wrong’ (unsafe work). However, seeking for broadening the research perspective, the researchers also focused to verify ‘how things go safe’ (work safely), to confirm some association rules and intuition. According to Whetten [9], although the researcher may be unable to test all the links (propositions between constructs), restrictions in methods do not invalidate the inherent causal nature of theory. In this reasoning, and consistent with the understanding that most of what passes for theory in organizational studies consists of approximations [27], the connections and the propositions between constructs are introduced in the framework depicted in Figure 6.

The framework is comprised of fours constructs, and it should be read as the following narrative: knowledge is the starting point. It is represented by work elements such as ‘what to do’, how to do’, ‘what are the risks’ and ‘how to eliminate/neutralize/mitigate the risks’. Knowledge is a construct presented in every type of work. This is consistent with the investigation reports analyzed and coherent with the direct observations conducted throughout the research. In both situations of work safely or work unsafely, knowledge (or the lack of knowledge) is present as a plausible construct that partially governs and explains phenomena of interest. In the case of safety at work, it also represents a baseline since common sense is that knowledge is critical for working safely.

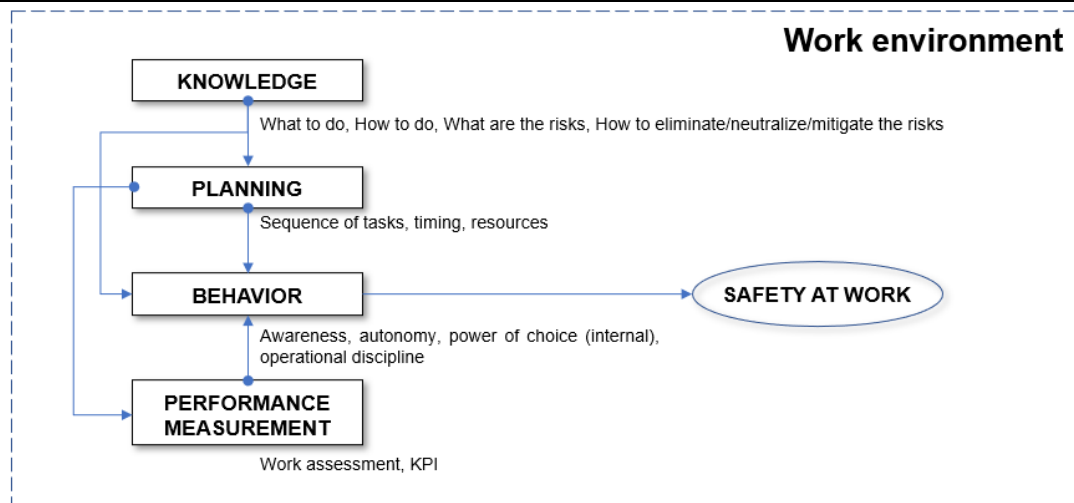


Figure 6 – Propositions that govern safety at work

However, knowledge is necessary but far away as sufficient to explain phenomena safety at work. This is consistent with the association rules, e.g. rules [70, 76, 155]. According to those rules, even workers trained to perform their tasks can get involved in lost-time accidents. This association is highly represented in rule [76], in which 36 out of 46 investigation reports analyzed, the worker was trained to the task in question (confidence = 1; lift = 1.1522). Moreover, our observations confirmed that trained workers might diminish risks due to possible reasons, such as their work experience or due to the fact they never had a work-related accident before. Thus, other plausible constructs are necessary to explain what governs safety at work.

Knowledge is connected to construct planning. This reasoning is explained by conceptualizing planning as the way the work is expected to be done, in which sequence of tasks, timing, and with what resources. Following this logic, it sounds clear that ‘to plan’ depends on ‘to know’. By defining a good sequence of tasks, a standard operational procedure, or an estimation for a set of tasks to be completed, it is fundamental to know what is this activity about, how the activities are performed, and what resources are available. Planning also represents the way of performing a task. Well-defined tasks are the ones where the resources, timing, and logical sequence of each activity are established to raise productivity without taking out safety is a core aspect.

The question to be responded at this point in time is whether knowledge and planning are sufficient to defining the minimum constructs that govern safety at work. If so, an expert performing a well-planned task would be ever working safely. Our intuition indicates not, and also the association rules, e.g. rules [34, 59, 145] in which confidence and lift present a high level. Firstly (rule [34]), the lack of operational discipline in doing job hazard analysis (JHA) is associated with trained works. It means that even experts do not follow the planning. Second (rule [59]), resources such as personal protective equipment do not guarantee safety at work. Investigation reports indicated that very often accidents occur with employees equipped with PPEs. This suggests such a level of personal confidence that nothing wrong can happen, and risks are ignored. Finally (rule [145]), diminishing risk is highly associated with lost time accidents, and therefore, the behavioral aspect is another plausible construct to be considered.

In this context, behavior is a comprehensive construct. It is present in the literature in numerous studies about accident prevention, such as in the studies of Han et al. [28] and Li et al. [29]. Also, motivation and work behavior are present in a robust body of knowledge in social sciences [30]. Consistent with the existing literature, results of the association rules put light on the effects of

behavior in the work environment, verified in the consequent factor 'diminishing risks', and based on its high association with lost-time accidents (rule [100]). This comprehensiveness is expressed in the proposed framework through the fact that behavior is the most interconnected construct in the system. All other constructs are connected to it, and it is the only one directly connected to the work.

In that reasoning, both knowledge and planning are connected to construct behavior by one of the two directional flows presented in the framework. Both constructs impact the way a person behaves at work. This was verified through direct observations carefully conducted besides the association rules. For instance, consider a worker performing maintenance services. If he/she lacks the required knowledge about what to do and how to perform a repair, or if the worker does not know the risks associated with the task, a potential risk for an incident to occur is increased as the worker tries to perform the task. Also, if the timing defined for the service is inadequate, or if necessary resources are not available, the worker's behavior is impacted negatively, leading towards the opposite direction of safety at work.

Behavior is, therefore, a key construct in the proposed framework. In the context of this research, it is represented by four elements: awareness, autonomy, power of choice, and operational discipline. Each of these elements plays an important role in safety at work. Awareness is the state of being conscious of something. More specifically, it is the ability to directly know and perceive, or to be aware of events. Autonomy, in turn, is a condition of self-government, and that needs to be outlined by managers. It is an important element to neutralize risks arising from externalities. Next is the power of choice, which means the attitude of using awareness and autonomy to every decision at work. Finally, operational discipline means doing the right thing, the right way, every time. It encompasses the other constructs towards promoting safety at work. From another direction, behavior is also impacted by another construct, represented by the way workers are measured. The performance measurement did not come up with the analysis of investigation reports. Rather, it emerged through the inductive approach and it is consistent with the theory of constraints. Goldratt [10] pointed out that the way an organization defines its work assessment and KPIs impact how workers behave at all levels. For instance, even in the case of an expert performing a well-planned task, if the KPIs are not consistent with the timing required for the task and with the resources available, the behavior is impacted. This is deeply explained by social cognitive theory (SCT), which explains behavior in organizations in terms of the reciprocal causation among the person, the environment, and the behavior itself [30]. Because of these combined influences, under SCT organizational participants would at the same time be products and producers of their motivation, their respective environments, and their behaviors. In that reasoning, SCT and TOC justify the connection between performance measurement and work behavior.

Finally, performance measurement is also connected with planning. This is because performance assessment is intrinsically related to a comparison between what is realized versus what was planned. Moreover, KPIs and targets are typically defined based on strategic planning and organization capabilities (resources). For instance, the expected sales growth rate of a Retail store is defined in management reviews. The organization may expect more sales if more sellers are working for them, or, in the case of use of technologies to increase sales, e.g. web platforms. Both examples are resources, and resources are associated with planning.

The four constructs are interconnected in the boundaries of the work environment, as previously depicted in Figure 6. It represents a system to explain what are the constructs that govern safety at work, and how they are connected.

The work environment is characterized by both external (e.g. market regulations) and internal (organizational culture) existing factors in any work environment that might impact positively or negatively any construct. It plays a critical role for safety at work since it acts directly in promoting (dis)harmony between the connections, and therefore, affects the level of complexity as further explained in sub-session IV.

Internal consistency and parsimony were sought to sustain every proposition's argument. Each construct in the system has a certain number of in-out connections. In this context, behavior represents the central construct because it is connected with all constructs and it is directly connected with phenomena safety at work. It follows the reasoning of considering 'to behave' an expression of 'acting', such as 'working'. Therefore, work behavior is positively or negatively impacted by knowledge, planning, and performance measurement, and all framed into the work environment.

The next session seeks for exploring the causation consistency.

III. Effect-cause-effect (building block 'why')

The previous sections were extremely helpful. 'What' and 'How' provide a framework for interpreting patterns in empirical observations [9]. However, only 'why' explains phenomena. Existing literature in the field of safety science often lacks explaining causation, being limited to verified correlations. The inherent limitation of any correlation, e.g. findings from association rules, is the lack of understanding of the cause-and-effect relationships between the propositions [10]. After identifying the constructs and exploring the reasoning of how they are connected, the next stage accounted for asking the question why?. In other words, the researchers are focused on what might be causing the existence of each proposition to explain safety at work as the effect of interest.

This stage is aimed no longer just to observe what already exists to explain phenomena, but also to use logical derivations based on existing causes to uncover underlying issues and predict the outcome of entirely new situations. Moreover, this stage accounts for fulfilling the minimum requirements of the conceptualization phase of theory building [7].

At this theory-development stage, logic replaces data as the basis for evaluation [9]. This is consistent with the use of common sense proposed by Goldratt [10] to go through the effect-cause-effect stage. Goldratt outlines that it represents the third stage of science, and the most important one because only at this stage there is a widely accepted recognition that the subject is actually a theory-building.

Therefore, the starting point of this stage is to become aware of an effect. The 'effect' of interest in this research is 'safety at work', and in the context of this study, safety at work means the action of working safely. "One effect is enough", said Dr. Goldratt, and the effect comes together with a challenging question: Is 'safety at work' a complex or exceedingly simple matter?

Once the effect and a challenging question are defined, more information is not much needed. Rather, to think and to speculate of plausible causes grounded in common sense are the next step [7, 10, 12]. To do that, principles of causation consistency derived from the theory of constraints thinking processes are applied for each proposition: causality existence, causality clarity, the sufficiency of cause, and additional cause [26]. In that reasoning, the causal consistencies are presented in 5 through a narrative for each connection, and thus, the framework is translated into confirmable propositions or knowledge claims to an explicit connection between the conceptualization phase and practice [31].

Table 4 – *Causation consistency*

Connection	Causal consistency
Knowledge → Planning	Knowledge is presented in every type of work. In the context of safety at work, it is a baseline. Knowledge impacts planning because ‘to plan’ any activity requires knowledge about the nature of the work to be performed. Causal existence is evidenced by examples to sustain that this connection is always the case. For instance, to plan the construction of a house, a common sense is that a body of knowledge is necessary, e.g. what raw materials are required, the method of how to do it, the sequence of tasks, the risks involved in the work, and what other resources are needed. This reasoning is applied to construction but also any other type of work. Planning might be also be impacted by the work environment, in which the proposed framework is represented by the boundary via dashed line (see Figure 6). This is because both external (e.g. macroeconomy, market regulations) and internal factors (organizational culture) existing in any work environment might positively or negatively any construct.
Knowledge and Planning → Behavior	Knowledge and planning are necessary but not sufficient to explain safety at work. Even experts performing well-planned tasks might work unsafely. A common sense to explain why knowledge and planning are not enough is to consider the behavior at work. If a worker behaves diminishing risks or if presents a lack of awareness, the knowledge and planning will not be sufficient at all. Therefore, by common sense, behavior is another necessary construct to explain the phenomena of interest. However, it is still needed to explain the causal existence of this proposition. It is assumed the way a worker behaves performing a task is impacted by his/her knowledge and how well the task was planned. This logic is explained also by examining accidents associated with knowledge in two ways: (1) the worker with the proper knowledge to perform a task and the one with a lack of knowledge to do so. In the first case, the proper knowledge can lead the worker to behave and work safely, but also an excess of confidence can lead to failures in following safety procedures. In the second case, the lack of necessary knowledge can lead the worker to unconsciously put himself/herself at risk. The same reasoning is applied to planning. If the sequence of tasks is carefully designed, proper resources are available, and timing is adequate for the task (a general harmony), the worker with autonomy and power of choice is predicted to work safely. This explanation put light on the causal existence and clarity of this proposition. However, sufficiency is not reached yet. There is speculation that people within the organizations are

Connection	Causal consistency
	responsive to the way they are measured. By considering it as a plausible, relevant, and necessary construct to explain the complexity of safety at work, performance measurement (as a construct) was added to the framework.
Planning → Performance Measurement	Performance measurement is connected by planning. This connection is intrinsically observed in management reviews and strategic planning. The definition of key performance indicators (KPIs) considers the organization's planning because it takes into account capabilities, resources, timing, and the work environment influences. For instance, typical planning for the construction of vertical buildings in Brazil varies between 36 and 48 months. This general planning cascades several other sub-plannings to define all that is needed to accomplish each phase of the project. KPIs for each phase and each task are also defined. Therefore, clarity and the existence of causation between planning and performance are verified. Another way to reach common sense that performance measurement is impacted by planning is by exploring the main KPIs of an industry. Productivity, for instance, is a performance measure that considers the ratio outputs/inputs. To increase productivity, practitioners evaluate how the activity is planned to be performed, including resources usage, quality of processes, and lead times. Following that reasoning, a KPI defined without taking into account planning sounds like no sense.
Performance Measurement → Behavior	Within organizations "people behave under influence of how they are measured". This quote retrieved from principles of the theory of constraints [10] is consistent with the existing literature about social cognitive theory (SCT) which explains behavior in organizations in terms of the reciprocal causation among the person, the environment, and the behavior itself [30]. It is important to highlight that behavior is the most interconnected construct in the proposed framework. Based on both theories it is assumed that the way a worker behaves at work is impacted by how the performance is measured, and also by his knowledge and how well is the planning of the task to be performed. Clarity of this proposition can be reached by examining productivity. For instance, consider a production line used to produce 22 elevators per day (just quantity). This level of productivity is consistent with the resources available (machinery, personnel, and tooling), and all workers are focused only on pushing forward the production line to reach the target. However, based on some organizational changes and observing that the production was also full of wastes, managers decide to consider efficiency instead of production volume as the performance measurement. Then, workers start to carefully look after the inputs to avoid any waste to maximize efficiency. This example comes up with pieces of evidence of why performance measurement impacts behavior. In this logic, The behavior characterized by a higher level of attention to avoid wastes was influenced by the changes in the performance measure.
Behavior → Safety at work	Finally, behavior is directed connected to safety at work, because in the context of this research it means the phenomena of working safely (co-existence). In more practical words, the action of working safely. Behavior is, therefore, a key construct in the proposed framework due to its high interconnection with other constructs. Moreover, besides being impacted

Connection	Causal consistency
	by knowledge, planning, and performance measurement, it represents the utmost connection to the phenomena, expressed through a few elements such as worker’s awareness, autonomy, power of choice, and operational discipline. The existence of causation between behavior and safety at work is well-known in literature and also between practitioners. This is consistent with the concepts of behavior-based safety (BBS), as well as voluntary safety programs within organizations to raise safety awareness as a tentative to prevent accidents. Each of the mentioned elements of behavior at work plays a critical role in safety at work. In the instance of safety at work, they encompass the action of doing the right thing, the right way, every time.

IV. The complexity of safety at work

A major outcome from the stages of classification, correlation, and causation consistency, is to underlying the issues that govern safety at work, and therefore, its complexity. Through the comprehension about what minimum constructs are sufficient to explain safety at work, how they are connected and why, this research’s seed is postulated:

Proposition: The complexity of safety work is a function of the degrees of freedom and harmony between constructs that govern the work environment within an organization.

Every organization has an unique system as depicted in Figure 6, represented by the individual and collective knowledge, the work planning, and the performance measurement system. The way these constructs are connected impacts the behavior of workers, and therefore defines the complexity of safety at work.

Although each connection between constructs has generalizability, which means that it can be verified in every organization, it does not mean it is harmonious. The concept of inherent simplicity is grounded in two main beliefs: simplicity and harmony: Simplicity is expressed by the fact that there are very few elements that govern the whole system. Harmony, in turn, is expressed by considering that any conflict can be eliminated [12].

The framework and propositions depicted in Figure 6 follow the same reasoning that Figure 1(B). It demonstrates that a system to represent safety at work might be exceedingly simple. This is possible since the system is comprised of four interconnected constructs that represent only one degree of freedom. However, this is necessary but not sufficient. The harmony between constructs is also a key factor.

Organizations usually face serious problems to properly address well-defined internal processes, and local optima is preferable instead of thinking as a whole. Moreover, problems arise from conflicts and disharmonies. As a result, organizations increase the number of system’s degrees of freedom, fail in eliminating conflicts, and tend to address safety as a very complex matter. This explains the challenges often faced by larger organizations. For instance, the disconnection between the planning department and the operations (who perform the work) or changes in the performance measurement system without taking into account the resources needed, causes disharmony and adds degrees of freedom to the system. Following the inherent simplicity concept, more points have to be touched by management in that case.

Therefore, we postulate that the complexity of safety at work is based on inherent simplicity, governed by very few constructs (knowledge, planning, performance measurement, and behavior), and simply explained as a function of the system's degrees of freedom and harmony between of constructs that govern the work environment within an organization.

IV. The complexity of safety at work

A major outcome from the stages of classification, correlation, and causation consistency, is to underlying the issues that govern safety at work, and therefore, its complexity. Through the comprehension about what minimum constructs are sufficient to explain safety at work, how they are connected and why, this research's seed is postulated:

Proposition: The complexity of safety work is a function of the degrees of freedom and harmony between constructs that govern the work environment within an organization.

Every organization has an unique system as depicted in Figure 6, represented by the individual and collective knowledge, the work planning, and the performance measurement system. The way these constructs are connected impacts the behavior of workers, and therefore defines the complexity of safety at work.

Although each connection between constructs has generalizability, which means that it can be verified in every organization, it does not mean it is harmonious. The concept of inherent simplicity is grounded in two main beliefs: simplicity and harmony: Simplicity is expressed by the fact that there are very few elements that govern the whole system. Harmony, in turn, is expressed by considering that any conflict can be eliminated [12].

The framework and propositions depicted in Figure 6 follow the same reasoning that Figure 1(B). It demonstrates that a system to represent safety at work might be exceedingly simple. This is possible since the system is comprised of four interconnected constructs that represent only one degree of freedom. However, this is necessary but not sufficient. The harmony between constructs is also a key factor.

Organizations usually face serious problems to properly address well-defined internal processes, and local optima is preferable instead of thinking as a whole. Moreover, problems arise from conflicts and disharmonies. As a result, organizations increase the number of system's degrees of freedom, fail in eliminating conflicts, and tend to address safety as a very complex matter.

This explains the challenges often faced by larger organizations. For instance, the disconnection between the planning department and the operations (who perform the work) or changes in the performance measurement system without taking into account the resources needed, causes disharmony and adds degrees of freedom to the system. Following the inherent simplicity concept, more points have to be touched by management in that case.

Therefore, we postulate that the complexity of safety at work is based on inherent simplicity, governed by very few constructs (knowledge, planning, performance measurement, and behavior), and simply explained as a function of the system's degrees of freedom and harmony between of constructs that govern the work environment within an organization.

V. Conclusion

This study was framed into the conceptualization phase of theory building to identify and to present propositions between constructs to explain the causalities that govern safety at work. By following a general method of theory building in applied sciences, and consistent with the principle of inherent simplicity from TOC, our findings indicate the existence of four constructs that govern safety at work: knowledge, planning, behavior, and performance measurement. Moreover, each construct and its interconnections comprised a set of propositions expressed through a conceptual framework that explains the underlying issues in safety at work and put behavior as a key element. Furthermore, as a result of our analysis based on the stages in which every science has gone through (classification, correlation, and causal consistency), the phenomenon of safety at work was represented as a system in which the level of complexity depends on the interdependencies between constructs and harmony.

A major theoretical outcome from this research is a conceptualization narrative that defines the complexity of safety at work as a consequence of degrees of freedom (interdependencies between constructs) and harmony (absence of conflicts between constructs). We postulate that as much interdependent and harmonious is the system the less complex is safety at work. In that reasoning, both circumstances affect safety at work and determine whether safety at work is a complex or exceedingly simple matter.

Although foster future research is highly encouraged to cover other phases of this theoretical model, this study presents generalizability regarding temporal and contextual factors discussed. Finally, from the practitioner's perspective, our findings contribute to the improvement of safety practices at the organizational level by redefining their structures, connections and focusing on behavior-based safety under a broader perspective.

References

- [1] Rae A, Provan D, Aboelssaad H, et al. A manifesto for Reality-based Safety Science. *Safety Science* 2020; 126: 104654.
- [2] ILOSTAT. Statistics on safety and health at work, <https://ilostat.ilo.org/topics/safety-and-health-at-work/> (2021, accessed 3 April 2021).
- [3] Brocal F, González C, Sebastián MA, et al. Standardized risk assessment techniques: A review in the framework of occupational safety. In: van Gulijk C. Haugen S. BAVJEKT (ed) *Safety and Reliability - Safe Societies in a Changing World - Proceedings of the 28th International European Safety and Reliability Conference, ESREL 2018*. CRC Press/Balkema, pp. 2889–2896.
- [4] ILO. International Labour Organization Web Page, <https://www.ilo.org/global/topics/safety-and-health-at-work/lang--en/index.htm> (2020, accessed 15 July 2020).
- [5] Wang Y, Chen H, Liu B, et al. A systematic review on the research progress and evolving trends of occupational health and safety management: A bibliometric analysis of mapping knowledge domains. *Front Public Heal*; 8. Epub ahead of print 2020. DOI: 10.3389/fpubh.2020.00081.
- [6] Heuvel S van den, Zwaan L van der, Dam L van, et al. *Estimating the costs of work-related accidents and ill-health: An analysis of European data sources - European Risk Observatory*. Luxembourg: European Agency for Safety and Health at Work, 2017. Epub ahead of print 2017. DOI: 10.2802/566789.
- [7] Swanson RA, Chermack TJ. *Theory Building in Applied Disciplines*. San Francisco, CA, 2013. Epub ahead of print 2013. DOI: 10.1108/jchrm-06-2013-0023.
- [8] Eden Y, Ronen B. *Approximately right not precisely wrong: Cost accounting pricing and decision making*. Great Barrington, MA: The North River Press, 2007.

- [9] Whetten DA. What constitutes a Theoretical Development? *Acad Manag Rev* 1989; 14: 490–495.
- [10] Goldratt EM. *What is the thing called Theory of Constraints and it should be implemented?* New York, NY, United States: The North River Press, 1990.
- [11] Ikeziri LM, Souza FB de, Gupta MC, et al. Theory of constraints: review and bibliometric analysis. *Int J Prod Res* 2018; 57: 1–35.
- [12] Goldratt EM. *The Choice*. Great Barrington, MA: The North River Press, 2008.
- [13] Naor M, Bernardes ES, Coman A. Theory of constraints: Is it a theory and a good one? *Int J Prod Res* 2013; 51: 542–554.
- [14] Lynham SA. General Method of Theory Building in Applied Disciplines. *Adv Dev Hum Resour* 2002; 4: 221–241.
- [15] Simon HA. *Models of man*. Hoboken, NJ: Wiley, 1957.
- [16] Zhang S, Zhang C. *Association Rule Mining - Models and Algorithms. Lecture Notes in Artificial Intelligence*. Berlin: Springer, <https://www.springer.com/gp/book/9783540435334> (2002, accessed 11 October 2020).
- [17] Isa N, Kamaruzzaman NA, Ramlan MA, et al. Market Basket Analysis of Customer Buying Patterns at Corm Café. *Int J Eng Technol* 2018; 7: 119–123.
- [18] Kouzlis-loukas M. *Analysing Customer Baskets*. Erasmus School of Economics, 2014.
- [19] Gauss L, Lacerda DP, Cauchick Miguel PA. Module-based product family design: systematic literature review and meta-synthesis. *Journal of Intelligent Manufacturing*. Epub ahead of print 2020. DOI: 10.1007/s10845-020-01572-3.
- [20] Alves FLD. *Data mining como suporte a tomada de decisão na priorização de estoques*. 2020.
- [21] Tan PN, Steinbach M, Karpatne A, et al. *Introduction to Data Mining*. 2nd ed. New York: Pearson, <https://www-users.cs.umn.edu/~kumar001/dmbook/index.php> (2018).
- [22] Hahsler M, Hornik K. New probabilistic interest measures for association rules. *Intell Data Anal* 2008; 11: 437–455.
- [23] Cheng C-W, Lin C-C, Leu S-S. Use of association rules to explore cause-effect relationships in occupational accidents in the Taiwan construction industry. *Saf Sci* 2010; 48: 436–444.
- [24] Mirabadi A, Sharifian S. Application of association rules in Iranian Railways (RAI) accident data analysis. *Saf Sci* 2010; 48: 1427–1435.
- [25] Verma A, Khan SD, Maiti J, et al. Identifying patterns of safety related incidents in a steel plant using association rule mining of incident investigation reports. *Saf Sci* 2014; 70: 89–98.
- [26] Ermel APC, Lacerda DP, Morandi MIWM, et al. Literature Reviews: Modern Methods for Investigating Scientific and Technological Knowledge. In: *Literature Reviews: Modern Methods for Investigating Scientific and Technological Knowledge*. Springer International Publishing, 2021. Epub ahead of print 2021. DOI: 10.1007/978-3-030-75722-9.
- [27] Weick KE. What Theory is Not, Theorizing Is. *Adm Sci Q* 1995; 40: 385.
- [28] Han S, Lee S, Peña-Mora F. Framework for a resilience system in safety management: A simulation and visualization approach. In: W. T (ed) *Proceedings of the International Conference on Computing in Civil and Building Engineering*. University of Illinois at Urbana-Champaign, United States: Nottingham, <https://www.scopus.com/inward/record.uri?eid=2-s2.0-85069842960&partnerID=40&md5=f86ce5dd2d85bd49b1ceae1cef2ea53c> (2010).
- [29] Li H, Lu M, Hsu S-C, et al. Proactive behavior-based safety management for construction safety improvement. *Saf Sci* 2015; 75: 107–117.
- [30] Porter LW, Bigley GA, Steers RM. *Motivation and Work Behavior*. 7th ed. Mc-Graw Hill/Irwin, 2002.
- [31] Cohen BP. *Developing sociological knowledge: Theory and method*. 2nd ed. Chicago, IL: Nelson-Hall, 1989.

Appendix

A 1 – Structure of the investigation report

Category	Data field (required information)
Time-horizon (n=3)	Fiscal year Month Sequence
Location (n=5)	Business Unit Operation Unit Country Branch Geographic region
Individual (n=6)	Age Scholar level Technical background Job function Years of experience Years working for the company
Accident data (n=9)	Type of accident, e.g. Elevator. Equipment Lost days Level of severity Body's part affected Nature of illness/injury Weekday Shift Location where the accident occurred
Process planning (n=7)	Task condition, e.g. routine, non-routine Job site (OTD status), e.g. on-time, delayed Worked hours in the circumstances of the event PPE: Was appropriate PPE being used? (Y/N) Tools: Were there appropriate tools available? (Y/N) JHA: Was it performed (Y/N) JHA: Was it performed according to the task? (Y/N)
Previous accidents/sanctions/audits (n=3)	Previous accident reported? (Y/N) Previous sanctions in the last 12 months? (Y/N) Audited in the last 12 months? (Y/N)
Training (n=3)	Hours of training(last 12 months) 10 rules training up to date? (Y/N) Has been trained for the task being performed (Y/N)
Behavior	Behavioral assessment in the last 12 months? (Y/N) Behavioral change observed recently? Psychological test performed during onboarding?
Violated rules	Technical rule violated?, e.g. PPE usage, fall protection etc Behavioral trap associated with the accidente?, e.g. Diminishing risks, lack of concentration etc.

A 2 – Script R for association rules

R Studio v. 4.0.5

```
# Require packages
if(!require(readxl)) install.packages("readxl")
if(!require(arules)) install.packages("arules")
if(!require(arulesViz)) install.packages("arulesViz")
if(!require(tidyr)) install.packages("tidyr")

# Load packages
library(readxl)
library(arules)
library(arulesViz)
library(tidyr)

# Load dataset
data <- read_excel("Lost-time accidents Report.xlsx", sheet='DATA')
View(data)

# Adjust dataset
data_aj <- dados [, c(-2,-3,-4,-5,-6,-7,-8,-9)]
View(data_aj)

# Convert dataset into file .csv
write.csv(dados_aj, "AR.csv", quote=FALSE, row.names=FALSE)

# Convert dataset into transaction format
tr <- read.transactions('AR.csv', format = 'basket', sep=',')
tr
summary(tr)

# Create association rules
rules = apriori(tr, parameter=list(suppor = 0.5, conf = 0.8, minlen = 1, maxlen = 3))
rules
inspect(head(rules))

# Remove redundant rules
rules = rules[!is.redundant(rules)]
rules
inspect(rules)
result = inspect(rules)

# Print association rules
write.csv2(result, "Association rules.csv")
```

Gumbel Marshall-Olkin Lomax: A new distribution for reliability modelling

ELEBE E. NWEZZA

Department of Mathematics and Statistics,
Alex Ekwueme federal University Ndufu-Alike, Nigeria
Correspondence email address:elebe.nwezza@funai.edu.ng •
Uchenna U. Uwadi

Department of Mathematics and Statistics,
Alex Ekwueme federal University Ndufu-Alike, Nigeria
uchenna.uwadi@funai.edu.ng •
C.K. Acha

Department of Statistics, Micheal Okpara University of Agriculture, Umudike,
Nigeria.
specialgozie@yahoo.com •
Christian Osagie

Environmental and Natural Sciences,
Brandenburg University of Technology, Cottbus-Senftenberg,
Senftenberg, Germany
osagichr@b-tu.de

Abstract

A new distribution for modeling the two approaches (physical and actuarial) of reliability problems is introduced. The statistical properties including the moments, mode, quantile function are derived. Some reliability measures including the mean residual life and hazard rate are derived. An alternative measure for total time of test (TTT) for evaluation of the interfailure times is derived. The unknown parameters of the new distribution are estimated using the maximum likelihood approach. Furthermore, the asymptotic consistency of the estimated parameters is evaluated through a simulation study. Two real-life datasets were used to illustrate the applicability of the new distribution and comparison with already existing distributions.

Keywords: Lomax distribution, Reliability, Moment, Total time of test, Maximum likelihood

1. INTRODUCTION

There have been growing needs to provide solutions associated with reliability problems found in life testing, structural reliability, machine maintenance using probability distribution [1]. Many classical distributions including Weibull, Log-normal, Birnbaum-Saunders, Inverse normal, gamma, exponential, geometric, Poisson have been applied in reliability studies where interest is on nonrepairable system [2]. However, [1] noted that it may be difficult to differentiate among these distributions while fitting failure datasets but stated that the failure rate function provides distinguishing features for these distributions. [3] furthermore, pointed out that distributions with bathtub shape failure rate function describing the decreasing, normal or constant, and increasing failure rate of component would have wide applicability in reliability studies. Most of the classical

distributions do not exhibit bathtub-shape hazard rate function [4]. However, a distribution to analyze business failure which is referred to as Lomax distribution was introduced by [5]. The application of Lomax distribution has been found in many other areas including income, size cities, reliability modeling [6], see [7] for more details. The Lomax distribution has been extended by introducing one or more additional parameter such as Marshall-Olkin Lomax due to [8], gamma Lomax by [9], exponential Lomax by [10], logistic-Lomax by [11] and McDonald Lomax distribution by [7]. The major aim of this paper is to introduce a new and more flexible extended Lomax distribution that will provide better fit and for modeling reliability datasets amongst other datasets from different areas of study. The reversed-J-shape, constant, and J-shape among many other shapes are the characterizations of the failure rate function shape of the new distribution. These shapes of failure rate function are suitable for modeling increasing failure rate (IFR), no-ware out and decreasing failure rate (DFR) datasets. Some statistical properties of this distribution are discussed and comparison with other existing distribution having Lomax distribution as baseline was made. The rest of the paper is organized as follows. The new distribution is derived in section two. In Section 3, the statistical properties of the distribution are derived and presented while the reliability measures are derived in Section 4. The Entropy and parameter estimation of the distribution are respectively considered in Sections 5 and 6. The asymptotic consistence of the maximum likelihood estimates is considered in Section 7 while the applications to real-life data sets are done in Section 8. The concluding remark is presented in Section 9.

2. THE NEW DISTRIBUTION

A class of distribution having distribution function as defined by equation(1) was introduced by[12].

$$G(x) = e^{-Bp^{\frac{1}{\sigma}} \left[\frac{F(x;\xi)}{1-F(x;\xi)} \right]^{-\frac{1}{\sigma}}}; \tag{1}$$

where $B = e^{\frac{\mu}{\sigma}}$. Define $F(x;\xi) = 1 - \left(1 + \frac{x}{\lambda}\right)^{-\alpha}$ in eq(1), where $\xi = (\alpha, \lambda)$ is the parameter vector, the cumulative density function (cdf) of the new distribution referred to as Gumbel Marshall-Olkin-Lomax (GMO-Lomax) is given by

$$G(x) = e^{-Bp^{\frac{1}{\sigma}} \left[\left(1 + \frac{x}{\lambda}\right)^{\alpha} - 1 \right]^{-\frac{1}{\sigma}}}. \tag{2}$$

The density function corresponding to equation (2) is obtained as

$$g(x) = \frac{Bp^{\frac{1}{\sigma}} \alpha \left(1 + \frac{x}{\lambda}\right)^{\alpha-1} e^{-Bp^{\frac{1}{\sigma}} \left[\left(1 + \frac{x}{\lambda}\right)^{\alpha} - 1 \right]^{-\frac{1}{\sigma}}}}{\lambda \sigma \left[\left(1 + \frac{x}{\lambda}\right)^{\alpha} - 1 \right]^{\frac{1}{\sigma}+1}}. \tag{3}$$

Furthermore, equation(3) can also be obtained using **Theorem 1**.

Theorem 1. Let X and Y be two random variables, if Y follows Gumbel distribution, then, $X = \lambda \left[\left(1 + pe^Y\right)^{\frac{1}{\alpha}} - 1 \right]$ follows GMO-Lomax distribution.

Proof. Given that the random variable Y follows Gumbel distribution, its pdf is given as

$$h(y) = \frac{B}{\sigma} e^{-\frac{y}{\sigma}} e^{-Be^{-\frac{y}{\sigma}}}. \tag{4}$$

For $X = \lambda \left[\left(1 + pe^Y\right)^{\frac{1}{\alpha}} - 1 \right]$, the partial derivative w.r.t. x is obtained as

$$\frac{\partial y}{\partial x} = \frac{\alpha}{\lambda \left(1 + \frac{x}{\lambda}\right) \left[1 - \left(1 - \frac{x}{\lambda}\right)^{-\alpha}\right]}.$$

The density function of X is defined as $g(x) = h(y) \left| \frac{\partial y}{\partial x} \right|$. Substituting the value of Y in $h(y)$ and $\left| \frac{\partial y}{\partial x} \right|$ and simplifying yields

$$g(x) = \frac{B p^{\frac{1}{\sigma}} \alpha \left(1 + \frac{x}{\lambda}\right)^{\alpha-1} e^{-B p^{\frac{1}{\sigma}} \left[\left(1 + \frac{x}{\lambda}\right)^{\alpha} - 1\right]^{\frac{1}{\sigma}}}}{\lambda \sigma \left[\left(1 + \frac{x}{\lambda}\right)^{\alpha} - 1\right]^{\frac{1}{\sigma} + 1}}.$$

■

Some possible shapes of GMO-Lomax pdf, including monotone decreasing, monotone increasing, right-skewed, among other shapes are shown in Figure 1.

3. STATISTICAL PROPERTIES

Some of the GMO-Lomax statistical properties such as Quantile function, moments, moment generating function, mode are derived and presented in this section.

3.1. Quantile function

The quantile function is very important in probability distribution, θ^{th} , percentile and random number generation for a distribution can be obtained using the quantile function. Using the probability integral transform [13], the quantile function of GMO-Lomax is obtained as

$$Q_X(u) = \lambda \left(\left\{ 1 + B^\sigma p \left[\log \left(u^{-1} \right) \right]^{-\sigma} \right\}^{\frac{1}{\alpha}} - 1 \right). \tag{5}$$

Using **Theorem 2**, the quantile function of GMO-Lomax can also be obtained.

Theorem 2. Given that a random variable, Y , follows Gumbel distribution, then the quantile function of GMO-Lomax is defined by $Q_X(u) = F^{-1} \left\{ 1 + p^{-1} e^{-G^{-1}(u)} \right\}^{-1}$; where $G^{-1}(\cdot)$ denotes the quantile function of Gumbel distribution and $F^{-1}(\cdot)$ denotes the quantile function of Lomax distribution.

Proof. Equation(1) can also be re-written as

$$G(y) = \int_{-\infty}^y \frac{B}{\sigma} e^{-\frac{t}{\sigma}} e^{B e^{-\frac{t}{\sigma}}} dt, \tag{6}$$

where $y = \log \left[\frac{F(x)}{p[1-F(x)]} \right]$.

By probability integral transform, the quantile function of a random variable, X , having a well-defined cdf, $F(x)$, is given by $x = F^{-1}(u)$, where $u = F(x)$. Then, the quantile function of Gumbel distribution is given by

$$y = G^{-1}(u) = \log \left\{ \left[B^{-1} \log \left(u^{-1} \right) \right]^{-\sigma} \right\}. \tag{7}$$

Furthermore, the quantile function of Lomax distribution is given by

$$x = F^{-1}(u) = \lambda \left[\left(1 - u \right)^{-\frac{1}{\alpha}} - 1 \right]. \tag{8}$$

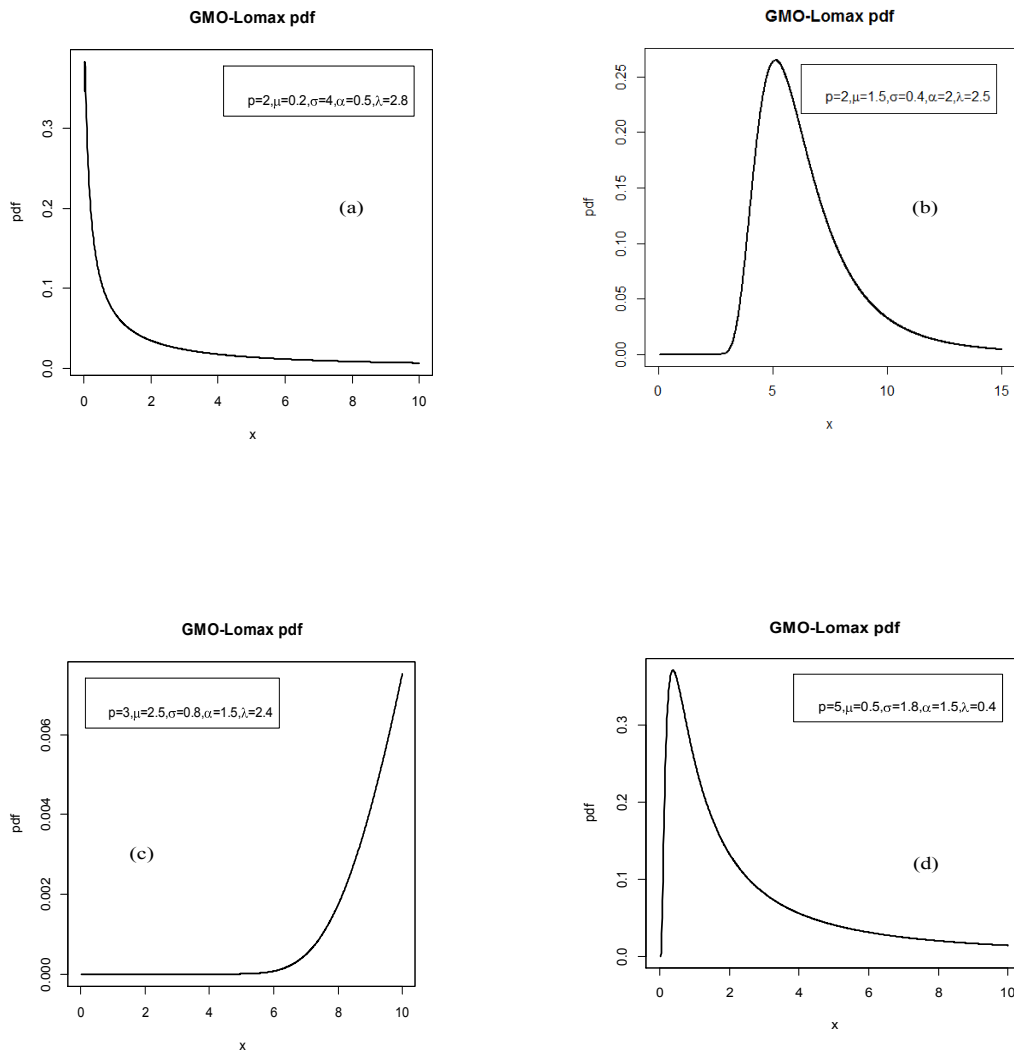


Figure 1: Some possible shapes of GMO-Lomax pdf: a) monotone decreasing b) unimodal c) monotone increasing d) right-skewed.

From equation(6)

$$\begin{aligned}
 x &= F^{-1} \left[1 + p^{-1} e^{-y} \right]^{-1} \\
 &= F^{-1} \left[1 + p^{-1} e^{-G^{-1}(u)} \right]^{-1} \\
 &= F^{-1} \left(\left\{ 1 + pB^\sigma \left[\log(u^{-1}) \right]^{-\sigma} \right\}^{-1} \right). \tag{9}
 \end{aligned}$$

Substituting the value of $u = \left\{ 1 + pB^\sigma \left[\log(u^{-1}) \right]^{-\sigma} \right\}^{-1}$ in equation(9) and simplifying yields

$$Q_X(u) = \lambda \left(\left\{ 1 + B^\sigma p \left[\log(u^{-1}) \right]^{-\sigma} \right\}^{\frac{1}{\alpha}} - 1 \right).$$

■

3.2. Moments

Corollary 1. The n^{th} non-central moment of GMO-Lomax random variable, X denoted by $E(X^n)$ is obtained as $E(X^n) = \lambda^n \sum_{j=0}^{\infty} \psi_j \Gamma(1 - j\sigma)$

Proof.

$$\begin{aligned} E(X^n) &= \int_0^{\infty} \left\{ \lambda \left[(1 + pe^y)^{\frac{1}{\alpha}} - 1 \right] \right\}^n \frac{B}{\sigma} e^{-\frac{y}{\sigma}} e^{-Be^{-\frac{y}{\sigma}}} dy \\ &= \frac{B\lambda^n}{\sigma} \int_0^{\infty} (1 + pe^y)^{\frac{n}{\alpha}} \left[1 - (1 + pe^y)^{-\frac{1}{\alpha}} \right]^n e^{-\frac{y}{\sigma}} e^{-Be^{-\frac{y}{\sigma}}} dy \\ &= \frac{B\lambda^n}{\sigma} \sum_{i,j=0}^{\infty} (-1)^i \binom{n}{i} \binom{\frac{n-i}{\alpha}}{j} p^j \int_0^{\infty} e^{iy} e^{-\frac{y}{\sigma}} e^{-Be^{-\frac{y}{\sigma}}} dy \\ &= \frac{B\lambda^n}{\sigma} \sum_{i,j=0}^{\infty} (-1)^i \binom{n}{i} \binom{\frac{n-i}{\alpha}}{j} p^j \int_0^{\infty} e^{-\frac{y}{\sigma}(1-j\sigma)} e^{-Be^{-\frac{y}{\sigma}}} dy \end{aligned} \tag{10}$$

Letting $x = Be^{-\frac{y}{\sigma}}$ implies that $dy = -\frac{\sigma}{x} dx$ and equation(10) becomes

$$\begin{aligned} E(X^n) &= B\lambda^n \sum_{i,j=0}^{\infty} (-1)^i \binom{n}{i} \binom{\frac{n-i}{\alpha}}{j} p^j B^{j\sigma-1} \int_0^{\infty} x^{-j\sigma} e^{-x} dx \\ &= \lambda^n \sum_{j=0}^{\infty} \psi_j \Gamma(1 - j\sigma), \end{aligned}$$

where

$$\psi_j = \sum_{i=j}^{\infty} (-1)^i \binom{n}{i} \binom{\frac{n-i}{\alpha}}{j} p^j B^{j\sigma}.$$

■

3.3. Moment generating function

The moment generating function (mgf) of a random variable with well-defined density function, $f(x)$, is defined by $M_X(t) = E(e^{tX})$. For a random variable with pdf defined as in equation(3) then, the mgf is given by

$$\begin{aligned} M_X(t) &= \int_0^{\infty} e^{tx} \frac{Bp^{\frac{1}{\sigma}} \alpha \left(1 + \frac{x}{\lambda}\right)^{\alpha-1} e^{-Bp^{\frac{1}{\sigma}} \left[\left(1 + \frac{x}{\lambda}\right)^{\alpha} - 1\right]^{-\frac{1}{\sigma}}}}{\lambda \sigma \left[\left(1 + \frac{x}{\lambda}\right)^{\alpha} - 1\right]^{\frac{1}{\sigma}+1}} dx \\ &= \frac{Bp^{\frac{1}{\sigma}} \alpha}{\lambda \sigma} \sum_{i,j=0}^{\infty} \frac{(-1)^{i+j}}{i!} \binom{\frac{i}{\sigma} + \frac{1}{\sigma} + j}{j} \left(Bp^{\frac{1}{\sigma}}\right)^i \int_0^{\infty} e^{tx} \left(1 + \frac{x}{\lambda}\right)^{-\alpha \left(\frac{i}{\sigma} + \frac{1}{\sigma} + j\right) - 1} dx \\ M_X(t) &= \sum_{j=0}^{\infty} \varphi_j \Gamma\left(-\frac{\alpha(j\sigma + i + 1)}{\sigma}, t\lambda\right), \end{aligned}$$

where

$$\varphi_j = \frac{Bp^{\frac{1}{\sigma}} \alpha}{\sigma} \sum_{j=i}^{\infty} \sum_{i,j=0}^{\infty} \frac{(-1)^{i+j}}{i!} \binom{\frac{i}{\sigma} + \frac{1}{\sigma} + j}{j} \left(Bp^{\frac{1}{\sigma}}\right)^i (-1\lambda)^{\frac{\alpha(j\sigma+i+1)}{\sigma}}.$$

3.4. Mode

The mode of a distribution plays an important role in life distribution. It defines the most likely failure time of an object when failure is of consideration. The mode of GMO-Lomax is obtained as the value of x that satisfies $\frac{\partial \log(g(x))}{\partial x} = 0$ given in equation (11)

$$\frac{\alpha - 1}{\lambda \left(1 + \frac{x}{\lambda}\right)} + \frac{B\alpha p^{\frac{1}{\sigma}}}{\sigma\lambda} \left(1 + \frac{x}{\lambda}\right)^{\alpha-1} \left[\left(1 + \frac{x}{\lambda}\right)^{\alpha} - 1\right]^{-\left(\frac{1}{\sigma}+1\right)} - \frac{\left(\frac{1}{\sigma} + 1\right) \alpha \left(1 + \frac{x}{\lambda}\right)^{\alpha-1}}{\lambda \left[\left(1 + \frac{x}{\lambda}\right)^{\alpha} - 1\right]} = 0 \quad (11)$$

4. RELIABILITY MEASURES

4.1. Hazard rate function

Generally, the hazard rate function is defined as the conditional probability of failure, given that a component has survived up to time x . [4] note that the hazard rate function is an important quantity which characterizes life phenomena. Denoting the hazard rate function as $R(x)$, the hazard rate function is defined as $\frac{g(x)}{S(x)}$, where $S(x)$ represents the survival function. Suppose a random variable X follows GMO-Lomax distribution, the hazard rate function associated to GMO-Lomax is given by

$$R(x) = \frac{Bp^{\frac{1}{\sigma}} \left(1 + \frac{x}{\lambda}\right)^{\alpha-1}}{\lambda\sigma \left[\left(1 + \frac{x}{\lambda}\right)^{\alpha} - 1\right]^{\frac{1}{\sigma}+1} \left[e^{Bp^{\frac{1}{\sigma}} \left[\left(1 + \frac{x}{\lambda}\right)^{\alpha} - 1\right]^{-\frac{1}{\sigma}}} - 1 \right]}.$$

Figure 2 shows some possible shapes of the GMO-Lomax hazard rate function which include decreasing hazard rate function which captures the high failure rate at the initial phase (infant mortality), the constant hazard rate function representing the period of stability of the component, and the increasing hazard rate function capturing the increase in failure rate as the component begins to wear-out.

4.2. Mean residual life function

Given that a random variable, X , denotes the lifetime of a component. The mean residual life function denoted by $m(t)$ defines the expected value of the remaining lifetime of a component after a fixed point t . Suppose the random variable, X , follows GMO-Lomax distribution, then

$$\begin{aligned} m(t) &= E(X - t | X > t) \\ &= \frac{1}{1 - G(t)} \int_t^{\infty} 1 - G(u) du, \end{aligned} \quad (12)$$

where $G(\cdot)$ is as defined in equation(2), substituting in equation(12) and simplifying yields

$$m(t) = \sum_{k=0}^{\infty} \psi_k \left(1 + \frac{t}{\lambda}\right)^{-\alpha\left(\frac{j}{\sigma}+k\right)} \left\{ \sum_{j=0}^{\infty} \psi_j \frac{[\lambda\sigma + t\alpha(1+i+j\sigma)] \left(1 + \frac{t}{\lambda}\right)^{-\alpha\left(\frac{1}{\sigma}+\frac{1}{\sigma}+j\right)}}{(1+i+j\sigma) [\alpha(1+i+j\sigma) - \sigma]} - t \right\},$$

where

$$\psi_k = \sum_{i,k=j}^{\infty} \frac{(-1)^j}{j!} \left(iBp^{\frac{1}{\sigma}}\right)^j \binom{\frac{j}{\sigma} + k - 1}{k}$$

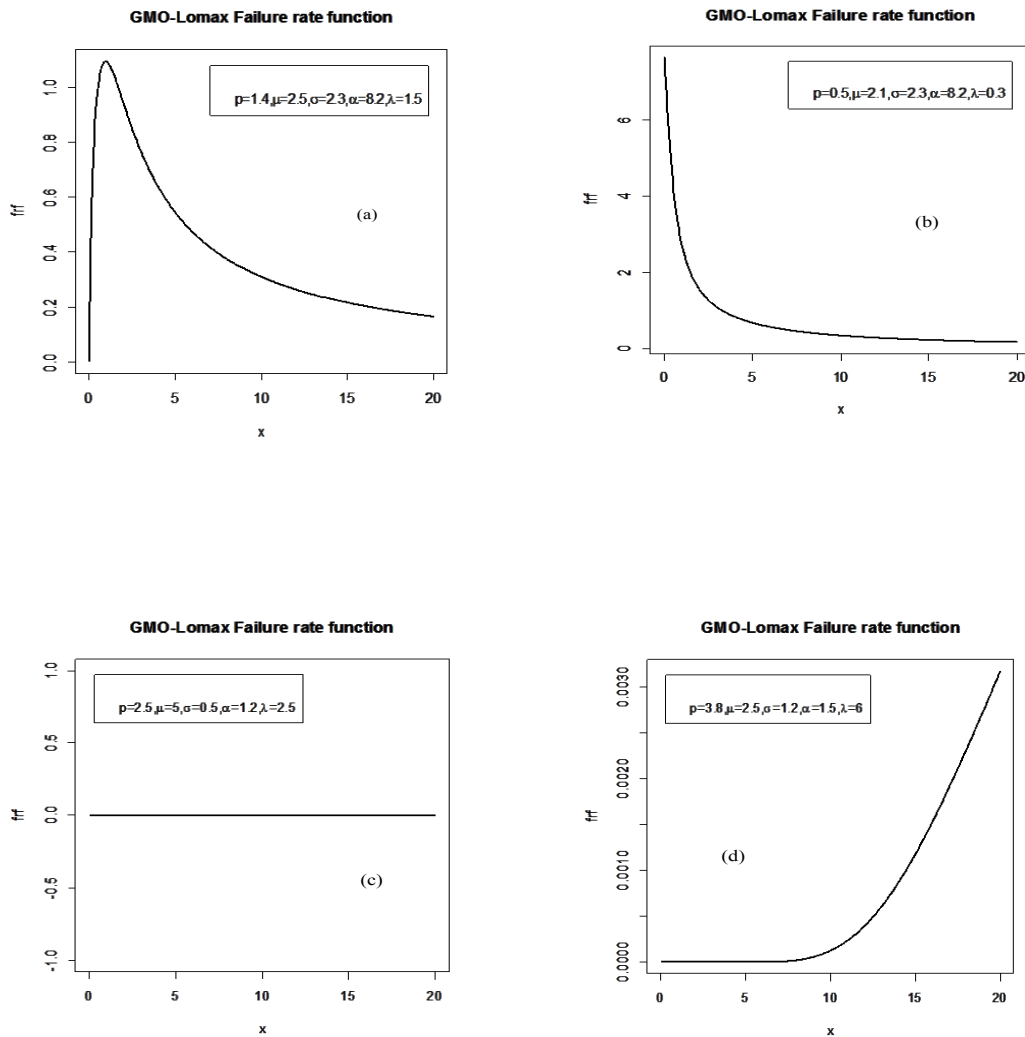


Figure 2: Some possible shapes of GMO-Lomax failure rate function: a) right-skewed b) monotone decreasing c) constant d) monotone increasing.

and

$$\psi_j = Bp^{\frac{1}{\sigma}} \sum_{i=0}^{\infty} \frac{(-1)^i}{i!} \left(Bp^{\frac{1}{\sigma}} \right)^i \binom{\frac{j}{\sigma} + k - 1}{k}$$

5. RELIABILITY

Suppose the random variables, X and Y , represent, respectively, the strength and stress of a component. The measure of performance of the component (that is the component reliability) having strength, X when subjected to random stress, Y , denoted by R is defined as $R = P(Y < X)$. Let X and Y , respectively, follow GMO-Lomax with some different parameters, then, R , is defined by

$$\begin{aligned} R &= \int_0^\infty g(x; B_1, p_1, \sigma, \alpha, \lambda) P(Y < X) dx \\ &= \int_0^\infty g(x; B_1, p_1, \sigma, \alpha, \lambda) G(x; B_2, p_2, \sigma, \alpha, \lambda) dx \\ &= \int_0^\infty \frac{B_1 p_1^{\frac{1}{\sigma}} \alpha}{\lambda \sigma \left[\left(1 + \frac{x}{\lambda}\right)^\alpha - 1 \right]^{\frac{1}{\sigma} + 1}} e^{-\left(B_1 p_1^{\frac{1}{\sigma}} + B_2 p_2^{\frac{1}{\sigma}}\right) \left[\left(1 + \frac{x}{\lambda}\right)^\alpha - 1 \right]^{-\frac{1}{\sigma}}} dx \\ &= \sum_{j=0}^\infty C_j B_1 p_1^{\frac{1}{\sigma}}, \end{aligned}$$

where $B_1 = e^{\frac{\mu_1}{\sigma}}$, $B_2 = e^{\frac{\mu_2}{\sigma}}$ and $C_j = \sum_{i=0}^\infty \frac{(-1)^i}{i!} \binom{\frac{i}{\sigma} + \frac{1}{\sigma} + j}{j} \frac{\left(B_1 p_1^{\frac{1}{\sigma}} + B_2 p_2^{\frac{1}{\sigma}}\right)^i}{(1+i+j\sigma)}$.

5.1. Lorenz curve

The Lorenz curve was established by [14] to graphical represent the distribution of wealth in a population. However, [15] established relationship between the Lorenz curve and the total time on test (TTT). The TTT graphically detects the possible change in the pattern of failures [16]. Hence, if a random variable, X , follows GMO-Lomax such that it denotes the failure times of a component or an individual, then the Lorenz curve is defined as

$$L(\varphi) = \frac{1}{\mu} \int_0^z x f(x) dx \tag{13}$$

Substituting equation (3) in equation (14), we have

$$\begin{aligned} L(\varphi) &= \frac{B p^{\frac{1}{\sigma}} \alpha}{\mu \lambda \sigma} \int_0^z \frac{x \left(1 + \frac{x}{\lambda}\right)^{\alpha-1} e^{-B p^{\frac{1}{\sigma}} \left[\left(1 + \frac{x}{\lambda}\right)^\alpha - 1 \right]^{-\frac{1}{\sigma}}}}{\left[\left(1 + \frac{x}{\lambda}\right)^\alpha - 1 \right]^{\frac{1}{\sigma} + 1}} dx \\ &= \frac{B p^{\frac{1}{\sigma}} \alpha}{\mu \lambda \sigma} \sum_{i=0}^\infty \frac{(-1)^i}{i!} \left(B p^{\frac{1}{\sigma}}\right)^i \int_0^z x \left(1 + \frac{x}{\lambda}\right)^{\alpha-1} \left[\left(1 + \frac{x}{\lambda}\right)^\alpha - 1 \right]^{-\left(\frac{1}{\sigma} + \frac{1}{\sigma} + 1\right)} dx \\ &= \frac{B p^{\frac{1}{\sigma}} \alpha}{\mu \lambda \sigma} \sum_{i,j=0}^\infty \frac{(-1)^{i+j}}{i!} \left(B p^{\frac{1}{\sigma}}\right)^i \binom{\frac{i}{\sigma} + \frac{1}{\sigma} + 1}{j} \int_0^z x \left(1 + \frac{x}{\lambda}\right)^{-\alpha \left(\frac{i}{\sigma} + \frac{1}{\sigma} + j\right) - 1} dx \\ &= \frac{1}{\mu} \sum_{j=0}^\infty (-1)^j \Psi_j, \end{aligned}$$

where μ is the first non-central moment and

$$\Psi_j = \sum_{i=j}^{\infty} \frac{(-1)^i \binom{\frac{i}{\sigma} + \frac{1}{\sigma} + 1}{j} (Bp^{\frac{1}{\sigma}})^{i+1} (1 + \frac{z}{\lambda})^{-\alpha(\frac{i}{\sigma} + \frac{1}{\sigma} + j)}}{i!(1+i+j\sigma)[\alpha(1+i+j\sigma) - \sigma]} \times \left[\lambda\sigma \left\{ \left(1 + \frac{z}{\lambda}\right)^{\alpha(\frac{i}{\sigma} + \frac{1}{\sigma} + j)} - 1 \right\} - z\alpha(1+i+j\sigma) \right]$$

6. ORDER STATISTICS

Suppose $X_1 < X_2 < \dots < X_n$ are ordered random sample of size n from GMO-Lomax population. The density function of the h^{th} order statistics ($h = 1, 2, \dots, n$), say, $g_{h:n}(x)$, is obtained as

$$g_{h:n}(x) = \frac{g(x)}{B(h, n-h+1)} \sum_{j=0}^{n-h} (-1)^j \binom{n-h}{j} G(x)^{h+j-1} \tag{14}$$

Substituting equations (2) and (3) in equation(14) and simplifying yields

$$g_{h:n}(x) = \frac{g(x)}{B(h, n-h+1)} \sum_{j=0}^{n-h} (-1)^j \binom{n-h}{j} \sum_{m=0}^{\infty} \varphi_m,$$

where $\varphi_m = \frac{Bp^{\frac{1}{\sigma}} \alpha}{\lambda\sigma} \sum_{k=m}^{\infty} \frac{(-1)^k}{k!} [Bp^{\frac{1}{\sigma}}(h+j)]^k (1 + \frac{x}{\lambda})^{-\alpha(\frac{k}{\sigma} + \frac{1}{\sigma} + m) - 1}$.

7. ENTROPY

Suppose a random variable, X , follows GMO-Lomax, the uncertainty associated with a value of X is measured using entropy. The Rényi entropy introduced by [17] generalizes the Shannon entropy and it is defined by

$$I_R(\gamma) = \frac{1}{1-\gamma} \log \left[\int_{\mathbb{V}} g^\gamma(x) dx \right], \tag{15}$$

where $g(x)$ is the pdf of GMO-Lomax, then

$$\begin{aligned} I_R(\gamma) &= \frac{1}{1-\gamma} \log \left[\left(\frac{Bp^{\frac{1}{\sigma}} \alpha}{\lambda\sigma} \right)^\gamma \int_0^\infty \frac{(1 + \frac{x}{\lambda})^{\gamma(\alpha-1)} e^{-\gamma Bp \left[(1 + \frac{x}{\lambda})^\alpha - 1 \right]^{-\frac{1}{\sigma}}}}{\left[(1 + \frac{x}{\lambda})^\alpha \right]^{\gamma(\frac{1}{\sigma} + 1)}} dx \right] \\ &= \frac{1}{1-\gamma} \log \left(Bp^{\frac{1}{\sigma}} \alpha \right) + \log(\lambda\sigma) + \frac{1}{1-\gamma} \log \left(\sum_{j=0}^{\infty} \varphi_j \right), \end{aligned}$$

where $\varphi_j = \sum_{i=j}^{\infty} \frac{(-1)^i}{i!} \left(\gamma Bp^{\frac{1}{\sigma}} \right)^i \binom{\frac{i}{\sigma} + \frac{\gamma}{\sigma} + \gamma + j - 1}{j}$.

8. PARAMETER ESTIMATION

Let X_1, X_2, \dots, X_n be a radom sample of size n from GMO-Lomax population. The unknown parameters of GMO-Lomax are estimated using the maximum likelihood method. The log-likelihood function is obtained as

$$\begin{aligned} \ell(\Theta) &= \frac{n\mu}{\sigma} + \frac{n}{\sigma} \log(p) + n \log(\alpha) + (\alpha - 1) \sum_{i=1}^n \log\left(1 + \frac{x_i}{\lambda}\right) - e^{\frac{\mu}{\sigma}} p^{\frac{1}{\sigma}} \sum_{i=1}^n \left[\left(1 + \frac{x_i}{\lambda}\right)^\alpha - 1\right]^{-\frac{1}{\sigma}} \\ &= -n \log(\lambda) - n \log(\sigma) - \left(\frac{1}{\sigma} + 1\right) \sum_{i=1}^n \left[\left(1 + \frac{x_i}{\lambda}\right)^\alpha - 1\right]. \end{aligned} \tag{16}$$

The corresponding score functions of equation(16) are given below

$$\begin{aligned} \frac{\partial \ell(\Theta)}{\partial \sigma} &= \frac{n\mu}{\sigma^2} - \frac{n}{\sigma^2} \log(p) + \frac{e^{\frac{\mu}{\sigma}} p^{\frac{1}{\sigma}}}{\sigma^2} \sum_{i=1}^n \left[\left(1 + \frac{x_i}{\lambda}\right)^\alpha - 1\right]^{-\frac{1}{\sigma}} [\mu + \log(p)] - \frac{n}{\sigma} \\ &\quad - \frac{1}{\sigma^2} e^{\frac{\mu}{\sigma}} p^{\frac{1}{\sigma}} \sum_{i=1}^n \log\left[\left(1 + \frac{x_i}{\lambda}\right)^\alpha - 1\right] \left[\left(1 + \frac{x_i}{\lambda}\right)^\alpha - 1\right]^{-\frac{1}{\sigma}} + \frac{1}{\sigma^2} \sum_{i=1}^n \left[\left(1 + \frac{x_i}{\lambda}\right)^\alpha - 1\right]. \end{aligned}$$

$$\frac{\partial \ell(\Theta)}{\partial \mu} = \frac{1}{\sigma} \left[n - e^{\frac{\mu}{\sigma}} p^{\frac{1}{\sigma}} \sum_{i=1}^n \left[\left(1 + \frac{x_i}{\lambda}\right)^\alpha - 1\right]^{-\frac{1}{\sigma}} \right].$$

$$\frac{\partial \ell(\Theta)}{\partial p} = \frac{n}{\sigma p} \left[n - e^{\frac{\mu}{\sigma}} p^{\frac{1}{\sigma}} \sum_{i=1}^n \left[\left(1 + \frac{x_i}{\lambda}\right)^\alpha - 1\right]^{-\frac{1}{\sigma}} \right].$$

$$\begin{aligned} \frac{\partial \ell(\Theta)}{\partial \lambda} &= \frac{(1 - \alpha)}{\lambda^2} \sum_{i=1}^n \frac{x_i}{\left(1 + \frac{x_i}{\lambda}\right)} + \frac{\alpha}{\sigma \lambda^2} e^{\frac{\mu}{\sigma}} p^{\frac{1}{\sigma}} \sum_{i=1}^n x_i \left(1 + \frac{x_i}{\lambda}\right)^{\alpha-1} \left[\left(1 + \frac{x_i}{\lambda}\right)^\alpha - 1\right]^{-\left(\frac{1}{\sigma}+1\right)} \\ &\quad - \left(\frac{1}{\sigma} + 1\right) \frac{\alpha}{\lambda^2} \sum_{i=1}^n x_i \left(1 + \frac{x_i}{\lambda}\right)^{\alpha-1}. \end{aligned}$$

$$\begin{aligned} \frac{\partial \ell(\Theta)}{\partial \alpha} &= \frac{n}{\alpha} + \sum_{i=1}^n \log\left(1 + \frac{x_i}{\lambda}\right) - \left(\frac{1}{\sigma} + 1\right) \sum_{i=1}^n \log\left(1 + \frac{x_i}{\lambda}\right) \left(1 + \frac{x_i}{\lambda}\right)^\alpha \\ &\quad + \frac{e^{\frac{\mu}{\sigma}} p^{\frac{1}{\sigma}}}{\sigma} \log(\alpha) \sum_{i=1}^n \left[\left(1 + \frac{x_i}{\lambda}\right)^\alpha - 1\right]^{-\left(\frac{1}{\sigma}+1\right)} \log\left(1 + \frac{x_i}{\lambda}\right) \left(1 + \frac{x_i}{\lambda}\right)^\alpha. \end{aligned}$$

The maximum likelihood estimators for the nknown parameters of GMO-Lomax are obtained by equating the score functions to zero respectively and solving simultaneously for the parameters. However, the score functions are non-linear to x and there are no closed form solutions for the estimators. The estimates for the parameters can be obtained using iterative numeric optimization methods.

9. SIMULATION

The maximum likelihood estimates of GMO-Lomax parameters were examined for asymptotic consistence using simulation study. Random samples of sizes 50, 75, 125 and 200 were generated using equation(5) with initial parameter values $\Omega = (p = 2.3, \mu = 2, \sigma = 1.8, \alpha = 0.5, \lambda = 1.2)$. For each sample size and $N = 1000$, the parameter estimates $\hat{\Omega}_i = (\hat{p}_i, \hat{\mu}_i, \hat{\sigma}_i, \hat{\alpha}_i, \hat{\lambda}_i)$ were evaluated for $i = 1, 2, \dots, N$. The Mean value $\bar{\Omega}$, Bias, Mean Square Error (MSE) were all computed. The values in Table 1 indicate that as the sample size increases, the MSE decreases and the Mean value converges to the initial parameter values as required under first asymptotic theorem.

Table 1: Summary of the simulation study.

Initial parameter value	Sample size (n)	Mean value	Bias	MSE
$p=2.3$ $\mu = 2$ $\sigma = 1.8$ $\alpha = 0.5$ $\lambda = 1.2$	50	2.2598	-0.0402	0.0022
		1.9324	-0.0676	0.0085
		1.8466	0.0466	0.0033
		0.5232	0.0232	0.0007
		3.5942	2.3943	5.7900
	75	2.3081	0.0081	0.0006
		1.9758	-0.0242	0.0038
		1.8537	0.0537	0.0037
		0.5239	0.0239	0.0007
		3.3466	2.1466	4.6753
	125	2.3016	0.0016	0.0003
		1.9344	-0.0655	0.0065
		1.7939	-0.0061	0.0006
		0.5028	0.0028	0.0001
		2.9596	1.7596	3.1669
	200	2.2918	-0.0082	0.0003
		1.8786	-0.1214	0.0161
		1.7641	-0.0359	0.0018
		0.4903	-0.0097	0.0001
		2.7963	1.5962	2.6032

10. APPLICATIONS

In this section, we illustrate the applicability of the GMO-Lomax using two real-life datasets. Comparison with other existing distributions including McDonald Lomax (McLomax) Beta-Lomax, Lomax of Lomax, Marshall-Olkin Lomax(MOL), Logistic Lomax(logisticL), and exponentiated Lomax(Exp Lomax)) are done using goodness-of-fit statistics including Cramer-von Misses (W), Anderson Darling (A), Kolmogorov Smirnov (K-S) test, Akaike Information Criterion (AIC), and Bayesian Information Criterion (BIC). Generally, the smaller the values of these statistics, the better the distribution fits the data set. The total test on time (TTT) to illustrate the empirical failure rate behavior of the two data sets was done.

First data set used which was reported by [18] is on the Kevlar 49/epoxy strands failure when the pressure is at 90% stress level while the second data set reported by [19] is on the lifetimes of 50 industrial device put on life test at time zero. The estimated cramer-von Misses (W^*), and Anderson Darling (A^*) together with the computed K-S, AIC, BIC, and negative log-likelihood of the two datasets are shown in Tables 3 and 5. The parameter estimates of the competing distributions with the standard errors in parentheses for the first and second data set are respectively shown in Table 2 and 4. Tables 3 and 5 show that the goodness-of-fit statistics values associated with GMO-Lomax are the least among the competing distribution, implying that GMO-Lomax distribution provided adequate fit for the two data sets respectively. The plots of the estimated pdfs with the histograms of the datasets and cdfs with the empirical cdf of the two data sets are shown in Figures 3 and 4. Figure 3 showed a close fit of the dataset’s histogram, however, the goodness-of-fit statistics values in Table 3 indicate the numerical difference of how well the various competing distributions actually fit the dataset. Figure 4 clearly show that the GMO-Lomax provided a better fit on the histogram of the second dataset among other competing distributions. Furthermore, the empirical TTT of the failure rates for the two datasets are shown in Figure 5. The Figure 5 shows that the datasets constitute constant and monotone-increasing failure rate.

Table 2: Results of parameter estimates for the first dataset(standard errors).

Distribution					
GMO-Lomax($p, \mu, \sigma, \alpha, \lambda$)	5.0148 (371.7516)	0.5808 (74.1372)	3.5797 (0.6937)	33.6301 (27.8848)	6.5039 (6.5015)
McLomax(a, b, α, λ, c)	0.8243 (0.1279)	6.0317 (17.3009)	1.6613 (4.5598)	4.1831 (7.2706)	3.1728 (2.8795)
Beta-Lomax(a, b, α, λ)	0.8897 (0.1177)	4.2914 (108.5245)	7.6109 (189.4789)	36.09837 (94.9773)	
Lomax(α, λ)	15.4125 (20.9761)	14.7618 (21.3217)			
MOL(p, α, λ)	1.3640 (0.8281)	8.9718 (10.9643)	6.9621 (11.1955)		
LogisticsL(β, α, λ)	1.2869 (0.1089)	38.9985 (31.6599)	24.4089 (20.3205)		
Exp-Lomax(θ, α, λ)	0.8846 (0.1201)	31.0501 (71.2834)	33.3998 (80.0430)		

Table 3: Results of the goodness-of-fit-statistics for the first dataset.

Distribution	W^*	A^*	K-S	AIC	BIC	$-\ell$
GMO-Lomax	0.0985	0.5926	0.0653	208.9945	209.6261	99.4973
McLomax	0.1440	0.8452	0.0967	213.9501	227.0257	101.9751
Beta-Lomax	0.1934	1.0843	0.0925	213.6633	224.1238	102.8817
Lomax	0.2107	1.1665	0.0864	210.4693	215.6995	103.2346
MOL	1.515	8.2009	0.6336	212.2111	220.0565	103.1056
LogisticsL	0.5828	3.1709	0.1065	233.0110	240.8564	113.5055
Exp-Lomax	0.1914	1.0749	0.0926	211.6259	219.4713	102.8129

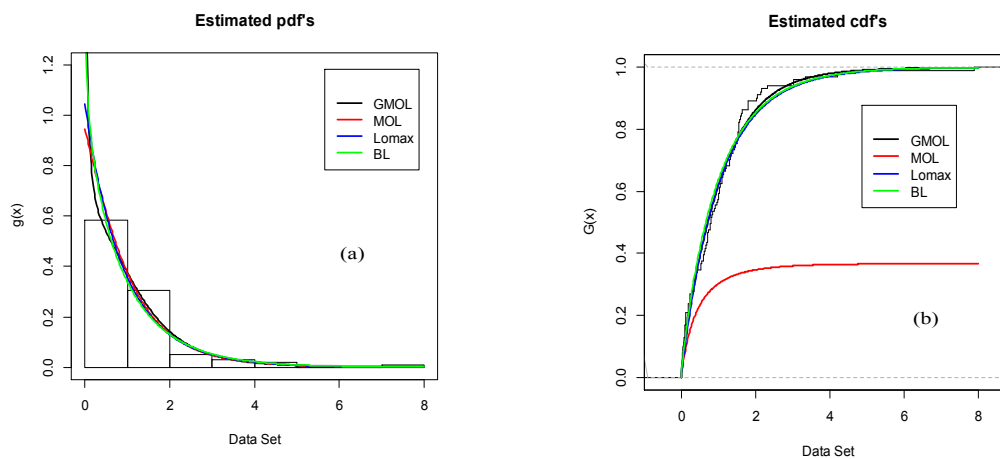


Figure 3: Estimated plots for the first dataset: a) competing pdfs b) empirical cdf with competing cdf.

Table 4: Results of parameter estimates for the second dataset (standard errors).

Distribution					
GMO-Lomax($p, \mu, \sigma, \alpha, \lambda$)	7.3403 (83.8036)	1.8975 (11.5748)	5.5264 (1.5003)	60.0204 (38.3307)	341,1701 (211.1367)
McLomax(a, b, α, λ, c)	0.8345 (0.1398)	63.7855 (54.4193)	1.1889 (0.6347)	105.2354 (51.0148)	8.1853 (4.0484)
Beta-Lomax(a, b, α, λ)	0.5273 (0.1464)	0.0915 (0.0277)	37.2292 (11.0337)	162.6509 (26.1937)	
Lomax(α, λ)	5.1659 (2.5299)	205.1413 (110.9948)			
MOL(p, α, λ)	3.9229 (2.3716)	4.3019 (1.8419)	83.7042 (52.2756)		
LogisticsL(β, α, λ)	8.7631 (1.1127)	0.1069 (0.0038)	0.0022 (0.0005)		
Exp-Lomax(θ, α, λ)	0.8464 (0.1547)	3.9194 (1.6727)	176.1126 (88.7161)		

Table 5: Results of the goodness-of-fit-statistics for the second dataset.

Distribution	W^*	A^*	K-S	AIC	BIC	$-\ell$
GMO-Lomax	0.3725	2.3066	0.1641	479.9236	489.4837	234.9618
McLomax	0.3898	2.4432	0.2277	481.2248	490.7849	235.6124
Beta-Lomax	0.4871	2.9544	0.2124	492.1212	499.7693	242.0606
Lomax	0.8010	4.5753	0.8014	490.7842	494.6083	243.3921
MOL	1.5131	7.7835	0.8757	491.1396	496.8757	242.5698
LogisticsL	0.8579	4.7819	0.2566	521.2151	526.9511	257.6075
Exp-Lomax	0.5455	3.2668	0.1999	492.8816	498.0960	243.1799

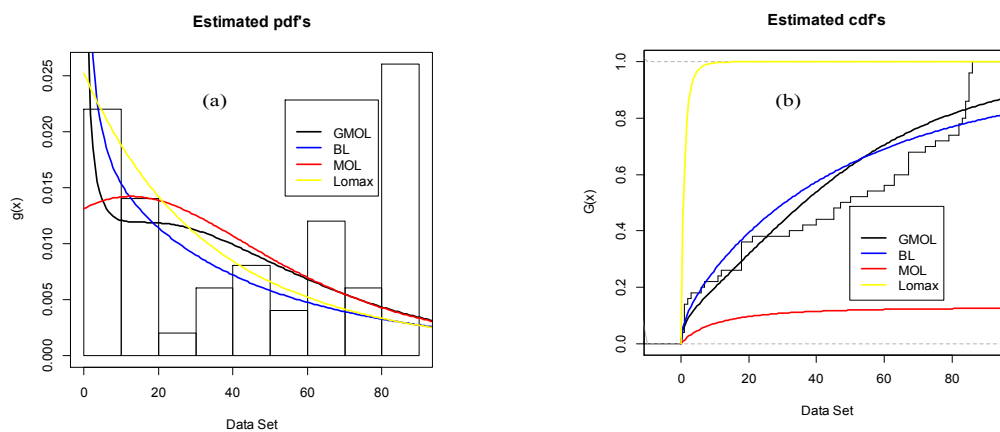


Figure 4: Estimated plots for the second dataset: a) competing pdfs b) empirical cdf with competing cdf.

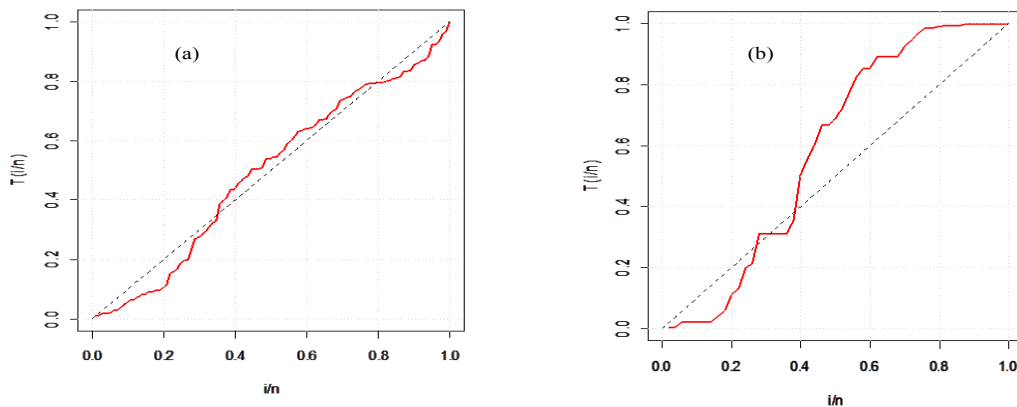


Figure 5: Plots of Total time on test: a) First dataset b) second dataset.

11. CONCLUSION

We have introduced a new five parameter distribution for modeling reliability problems. The statistical properties and some reliability measures of the new distribution are derived. The unknown parameters of the distribution are estimated using the maximum likelihood approach. Furthermore, the maximum likelihood estimates of the new distribution were examined for asymptotic consistence and were found to conform to the first order asymptotic theorem. Two real-life data sets were used to illustrate the applicability of the new distribution and comparison with other existing distributions indicates that the new distribution provided better fit for the two data sets. The constant and monotone-increasing failure shapes shown in the TTT plots are indications of the suitability of GMO-Lomax distribution which has constant and monotone-increasing failure rate shapes amongst other possible shapes in modelling the two datasets.

REFERENCES

- [1] Barlow, R. E. and Proschan, F. Mathematical theory of reliability, John Wiley and Sons Inc., New York, U.S.A., 1996.
- [2] Rauusand, M. and Hoyland, A. System reliability theory, models, statistical methods and applications, Second Edition, John Wiley and Sons Inc., New Jersey, U.S.A., 2004.
- [3] Meniconi, M. and Barry, D. M. (1996). The Power function distribution: A useful and simple distribution to assess electrical component reliability. *Microelectron. Reliab.*, 36(9):1207-1212.
- [4] Nadarajah, S. (2009). Bathtub-Shape failure rate functions. *Journal of Qual. Quant.*, 43:855-863.
- [5] Lomax, K. S. (1954). Marshall-Olkin extended Lomax distribution and its application to Censored Data. *Journal of the American Statistical Association*, 49(268):847-852.
- [6] Ahsanullah, M. (1991). Record values of the Lomax distribution. *Statistica Neerlandica*, 45:21-29.
- [7] Refaie, M.K. A. (2019). A New extension of the Lomax distribution with statistical properties and applications to failure and service times data sets. *Journal of Mathematics and Statistics*, 15:1-11.
- [8] Ghitany, M. E. Al-Awadhi, F. A. and Alkhalafan, L. A. (2007). Marshall-Olkin extended Lomax distribution and its application to Censored Data. *Communications in Statistics-Theory and Methods*, 36(10):1855-1866.

- [9] Cordeiro, G. M. Edwin, M. M. Ortega, E. M. M. and Popović, B. V. (2013) The gamma-Lomax distribution. *Journal of Statistical Computation and Simulation*, <http://doi.org/10.1080/00949655.2013.822869>.
- [10] El-Bassiouny, A. H. Abdo, N. F. and Shahem, H. S. (2015). Exponential Lomax distribution. *International journal of computer applications* , 121(13): 24-29.
- [11] Zubair, M. Cordeiro G. M. Tahir M. H. Mahmood, M. and Mansoor, M.(2017). A study of logistic Lomax distribution and its applications. *Journal of probability and statistical sciences*, 15:29-46.
- [12] Nwezza, E. E. Ogbuehi, C. V. Uwadi, U. U. and Omekara, C O. (2020). A new Gumbel generated family of distribution, properties, bivariate distribution and applications. *American Journal of Applied Mathematics and Statistics*,8:9-20.
- [13] Casella, G. and Berger, R. L. *Statistical Inference*, Second Edition, Duxbury, USA, 2002.
- [14] Lorenz, M. O. (1905). Methods of measuring the concentration of wealth. *American Statistical Association*,9(70):209-219.
- [15] Chandra, M. and Singpurwalla, N. The Gini index, the Lorenz curve, and the total time on test transform. Research report, The George Washington University, Institute for management Science and engineering, Washington, D.C. 20052, 1978.
- [16] Kvaløy, J. T. and Lindqvist, B. H.(1998). TTT-based tests for trend in repairable systems data. *Reliability engineering and system safety*, 60:13-28.
- [17] Rényi, A. (1961). On measures of entropy and information. *Hungarian academy of Sciences Budapest Hungary*, 547-561.
- [18] Al-Aqtash, R. Lee, C. and Famoye, F. (2014) Gumbel-Weibull distribution: properties and applications. *Journal of Modern Applied Statistical Methods*, 13(2):201-225.
- [19] Cordeiro, G. M. Alizadeh, M. Ozel, G. Hosseini, B. Ortega, E.M. M. and Altun, E. (2016). The generalized odd log-logistic family of distributions: properties, regression models and applications. *Journal of Statistical Computation and Simulation*, <http://doi.org/10.1080/00949655.2016.1238088>,

A Novel Transformation: Based on Inverse Trigonometric Lindley Distribution

D. KUMAR*, P. K. CHAURASIA**, P. KUMAR* AND A. CHAURASIA***



* Department of Statistics, Banaras Hindu University, Varanasi-221005, India

**Narayan Institute of Agricultural Sciences, Gopal Narayan Singh University, Jamuhar-821305, India

***School of Interdisciplinary Studies, DY Patil International University, Pune-411044, India

chaurasiaprashantvns@gmail.com

Abstract

As we see that the present era is directly depending upon various kinds of machines. In other words, we can say that we are fully surrounded by machines. Machines are assembled with many components and each component has its own importance. For proper functioning of a machine, these components should be up to date. Therefore, for smooth functioning, we have to make replacement of the component before its failure. In this present paper, we propose a new transformation which is purely based on inverse trigonometry with lindley distribution for the first time and so, named "Inverse Trigonometric Lindley Distribution". It find its various properties like survival function, hazard rate function, moments, conditional moments, order statistics, entropy measurement etc. Maximum likelihood estimator have also considered for estimation of parameter. To know the paternal behavior of the model, different real datasets have been considered. To understand the behavior of estimators at the long run, simulation study is being performed in detail.

Keywords: Lindley distribution, Renyi entropy, Moments, Maximum likelihood estimator, Simulation Study

1. INTRODUCTION

Survival and reliability analysis play an important role in the field of statistics. These are devising several noteworthy real life applications in many areas of applied and medical sciences, such as engineering, public health, actuarial science, biomedical studies, demography, industrial reliability, etc. In this era, each activity is dealt by the machines which are gathered by the help of different components. It is required to keep each and every component up to date, so that machines can run or function efficiently. In addition, before failure of that component, there is the need of replacement. But, the key matter is to estimate the appropriate time of replacement and decide the best policy to adopt with regard to replacement. Therefore, the main objective is to study about the behavior of the life of components individually as well as through suitable lifetime models. In relevant literatures, there is a list of different lifetime distributions along with their theoretical discussion to identify correct guess at which we replace the components so that system could work without failure. There are vital role of Survival and Hazard rate function in lifetime data analysis. Using these functions, we can identify the nature of a chosen model.

If we look back in literature, many authors used several transformations. For example, Power transformation was used by Gupta et al. (1998), Quadratic Rank Transmutation Map (QRTM) developed by Shaw and Buckley (2005), trigonometry based transformations like SS-transformation proposed by Kumar et al. (2015) and Chesneau et al. (2018), Mahmood, Z., and Chesneau, C. (2019), logarthim based transformation proposed by Maurya et al.(2016), DUS-transformation proposed by Kumar et al. (2015) and its generalization have done by Maurya et al. (2017),

generalization through QRTM have done by Yadav et al. (2019) etc. Their numerous statistical results have been obtained and deliberated its various shapes of hazard rate patterns in means of increasing, decreasing, upper side down etc. If we see literature, we get there are only few transformation that are based on inverse trigonometry.

In this paper, we propose a novel transformation based on "Inverse Trigonometric Lindley Distribution", which is related to inverse trigonometric function and lindley distribution. We also discuss its various characteristic and properties as well as identify its various hazard rate patterns. For simplicity, applicability and suitability in real life scenario different datasets have been considered. Simulation study is also being carried out to know the behavior of the estimators at the long-run.

2. A NEW TRANSFORMATION USING TRIGONOMETRIC FUNCTION

We introduce a new transformation using trigonometric function and It is denoted by $G(x)$:

$$G(x) = K * \tan^{-1} F(x) \quad (1)$$

where, K is $\frac{1}{\tan^{-1}(1)}$.

Theorem 1. The function $G(x)$ possesses the properties of a cdf.

Proof. Let $f(x)$ be a pdf associated to the cdf $F(x)$ is continuous with $F(x) \in [0,1]$,

$$\lim_{x \rightarrow +\infty} F(x) = 1 \quad \lim_{x \rightarrow -\infty} F(x) = 0$$

and $f(x) = F'(x)$ almost everywhere with $f(x) \geq 0$. Let us now investigate sufficient conditions for $G(x)$ to be a cdf.

- $G(-\infty) = 0$ and $G(+\infty) = 1$.

$$\begin{aligned} G(x) &= K * \tan^{-1} F(x) \\ G(-\infty) &= K * \tan^{-1} F(-\infty) \\ G(-\infty) &= 0 \end{aligned}$$

and

$$\begin{aligned} G(+\infty) &= K * \tan^{-1} F(x) \\ G(+\infty) &= K * \tan^{-1} F(+\infty) \\ G(+\infty) &= 1 \end{aligned}$$

- G is non decreasing function.

Let us prove that $G(x_2) - G(x_1) \geq 0$.

$$\begin{aligned} G(x_1) &= K * \tan^{-1} F(x_1) \\ G(x_2) &= K * \tan^{-1} F(x_2) \\ G(x_2) - G(x_1) &= K * [\tan^{-1} F(x_2) - \tan^{-1} F(x_1)] \\ G(x_2) - G(x_1) &= K * [\tan^{-1} F(x_2) - \tan^{-1} F(x_1)] > 0 \end{aligned}$$

where, $F(x_2) > F(x_1)$.

The above expression $G(x_2) - G(x_1)$ is positive if $x_2 > x_1$.

- G is Right Continuous.

$\tan^{-1} F(x)$ are right continuous function of x , then $G(x)$ is right continuous function of x .

Thus, we can say that our transformation is a cdf.

The pdf and hazard rate of our transformation is given by

$$g(x) = K * \frac{f(x)}{1 + (F(x))^2} \tag{2}$$

$$h(x) = K * \frac{f(x)}{\{1 - (F(x))^2\} \{1 - K * \tan^{-1} F(x)\}} \tag{3}$$

3. A NEW TRANSFORMATION WITH SOME RELATED NEW DISTRIBUTIONS

- Consider the Uniform Distribution $[0, \theta]$, we have $F(x) = \frac{x}{\theta}$; $0 \leq x \leq \theta$ then,

$$G(x) = K * \tan^{-1} \left(\frac{x}{\theta} \right)$$

$$g(x) = K * \frac{1}{\theta \left\{ 1 + \left(\frac{x}{\theta} \right)^2 \right\}}$$

$$h(x) = K * \frac{1}{\theta \left\{ 1 + \left(\frac{x}{\theta} \right)^2 \right\} \left\{ 1 - K * \tan^{-1} \left(\frac{x}{\theta} \right) \right\}}$$

- Consider the logistic distribution with parameters $\mu \in R$ and $s > 0$, we have $F(x) = \frac{1}{1 + e^{-\frac{x-\mu}{s}}}$, $x \in R$ then,

$$G(x) = K * \tan^{-1} \left(\frac{1}{1 + e^{-\frac{x-\mu}{s}}} \right)$$

$$g(x) = K * \frac{e^{-\frac{x-\mu}{s}}}{\left\{ s \left(1 + e^{-\frac{x-\mu}{s}} \right)^2 \right\} \left\{ 1 + \left(\frac{1}{1 + e^{-\frac{x-\mu}{s}}} \right)^2 \right\}}$$

$$h(x) = K * \frac{e^{-\frac{x-\mu}{s}}}{\left\{ s \left(1 + e^{-\frac{x-\mu}{s}} \right)^2 \right\} \left\{ 1 + \left(\frac{1}{1 + e^{-\frac{x-\mu}{s}}} \right)^2 \right\} \left\{ 1 - K * \tan^{-1} \left(\frac{1}{1 + e^{-\frac{x-\mu}{s}}} \right) \right\}}$$

- Consider the Cauchy distribution with parameters $x_0 \in R$ and $a > 0$, we have $F(x) = \frac{1}{\pi} \arctan \left(\frac{x-x_0}{a} \right) + \frac{1}{2}$, $x \in R$

$$G(x) = K * \tan^{-1} \left(\frac{1}{\pi} \arctan \left(\frac{x-x_0}{a} \right) + \frac{1}{2} \right)$$

$$g(x) = K * \frac{a}{\pi \{a^2 + (x-x_0)^2\} \left\{ 1 + \left(\frac{1}{\pi} \arctan \left(\frac{x-x_0}{a} \right) + \frac{1}{2} \right)^2 \right\}}$$

$$h(x) = K * \frac{a}{\pi \{a^2 + (x-x_0)^2\} \left\{ 1 + \left(\frac{1}{\pi} \arctan \left(\frac{x-x_0}{a} \right) + \frac{1}{2} \right)^2 \right\} \left\{ 1 - K * \tan^{-1} \left(\frac{1}{\pi} \arctan \left(\frac{x-x_0}{a} \right) + \frac{1}{2} \right) \right\}}$$

- Consider the Normal distribution with parameters $\mu \in R$ and $\sigma > 0$, we have

$$F(x) = \int_{-\infty}^x -\frac{1}{\sqrt{2\pi\sigma^2}} e^{-\frac{(t-\mu)^2}{2\sigma^2}} dt = \Phi(x), \quad x \in R,$$

$$G(x) = K * \tan^{-1} (\Phi(x))$$

$$g(x) = \frac{e^{-\frac{(x-\mu)^2}{2\sigma^2}}}{\sqrt{2\pi\sigma^2} \{1 + (\Phi(x))^2\}}$$

$$h(x) = \frac{e^{-\frac{(x-\mu)^2}{2\sigma^2}}}{\sqrt{2\pi\sigma^2} \{1 + (\Phi(x))^2\} \{1 - K * \tan^{-1} (\Phi(x))\}}$$

- Consider the Exponential Distribution with parameter $\theta > 0$, we have $F(x) = 1 - e^{-\theta x}$; $\theta > 0, x > 0$ then,

$$G(x) = K * \tan^{-1} (1 - e^{-\theta x})$$

$$g(x) = K * \frac{\theta e^{-\theta x}}{1 + (1 - e^{-\theta x})^2}$$

$$h(x) = K * \frac{\theta e^{-\theta x}}{\{1 + (1 - e^{-\theta x})^2\} \{1 - K * \tan^{-1} (1 - e^{-\theta x})\}}$$

- Consider the Lindley Distribution with parameter $\theta > 0$, we have $F(x) = 1 - \left\{ \left(1 + \frac{\theta x}{\theta + 1}\right) e^{-\theta x} \right\}$; $\theta > 0, x > 0$ then,

$$G(x) = K * \tan^{-1} \left\{ 1 - \left(\left(1 + \frac{\theta x}{\theta + 1}\right) e^{-\theta x} \right) \right\} \quad (4)$$

$$g(x) = k * \left(\frac{\theta^2}{\theta + 1} \right) \frac{(1 + x)e^{-\theta x}}{1 + \left\{ 1 - \left(\left(1 + \frac{\theta x}{\theta + 1}\right) e^{-\theta x} \right) \right\}^2} \quad (5)$$

$$h(x) = \left(\frac{\theta^2}{\theta + 1} \right) \frac{(1 + x)e^{-\theta x}}{1 + \left\{ 1 - \left(\left(1 + \frac{\theta x}{\theta + 1}\right) e^{-\theta x} \right) \right\}^2 \left\{ 1 - K * \tan^{-1} \left\{ 1 - \left(\left(1 + \frac{\theta x}{\theta + 1}\right) e^{-\theta x} \right) \right\} \right\}} \quad (6)$$

In order to illustrate the potential of applicability of $IT_{lin}(\theta)$, The shapes of the cdf and pdf are shown in Figures 1 and 2 respectively for different value of θ .

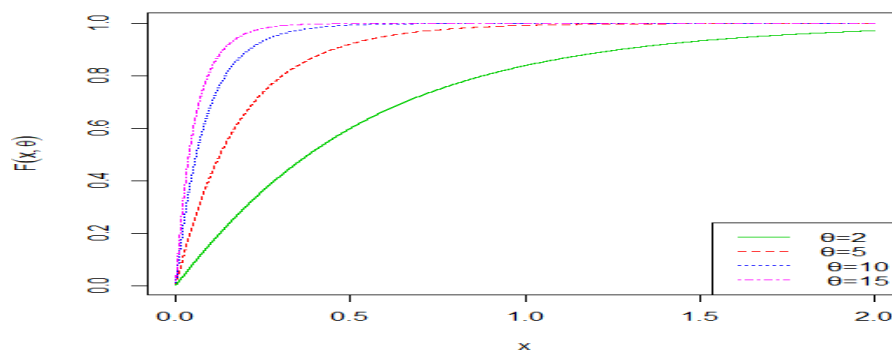


Figure 1: Plots of Cumulative distribution function for different values of θ

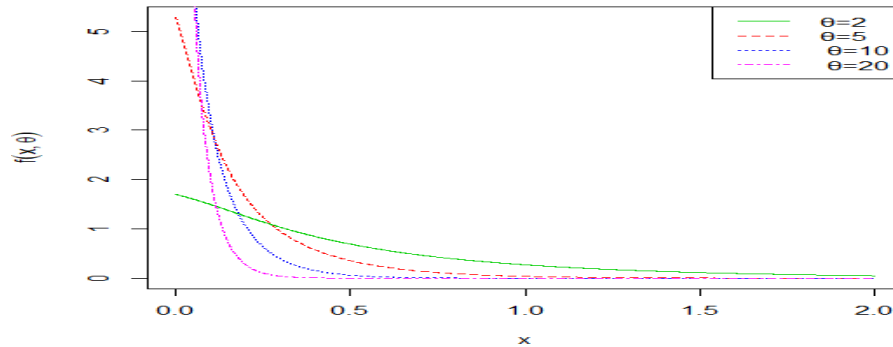


Figure 2: Plots of Probability density function for different values of θ

4. SURVIVAL ANALYSIS

In this section we present the survival function, the hazard function and the cumulative hazard rate function for the $IT_{lin}(\theta)$ -distribution.

Survival Function

It is define as the probability that an individual survives larger than, t: $S(t) = P(\text{an individual survives larger than } t)$

$= P(T > t)$, where T denote the survival time.

The cdf $F(t)$ of T, is given as $S(t) = 1 - P(\text{an individulas fails before } t) = 1 - F(t)$.

Hence, the Survival Function of $IT_{lin}(\theta)$ -distribution is obtained as follows:-

$$S(t) = 1 - \left[K * \tan^{-1} \left\{ 1 - \left(\left(1 + \frac{\theta t}{\theta + 1} \right) e^{-\theta t} \right) \right\} \right] \quad (7)$$

The behavior of the survival rate function, for different values of θ is shown are Fig. 3.

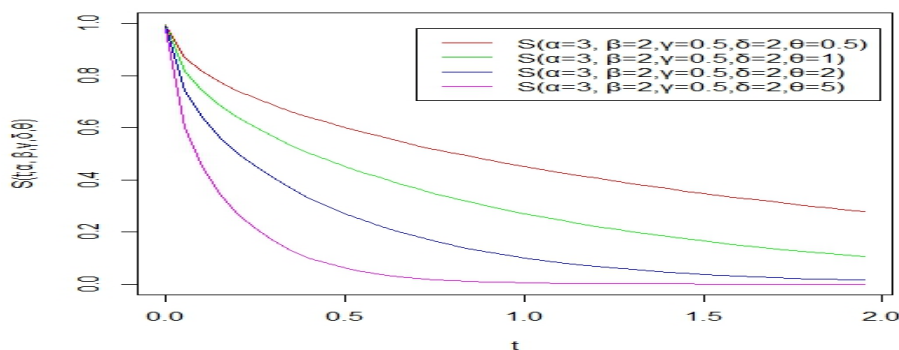


Figure 3: Plots of Survival Rate Function for different values of θ

Hazard Rate Function

It is defined as the probability of failure during a very small time interval, assuming that the individual has survived to the begining of the interval, or as the limit of the probability that an

individual fails in a very short interval, $t + \Delta t$, given that the individual has survived to time t :

$$h(t) = \lim_{\Delta x \rightarrow 0} \frac{\Pr(\text{an individual fails an interval } (t + \Delta t) \text{ given the individual has survived to } t)}{\Delta t}$$

It is defined as the terms of CDF $F(t)$ and PDF $f(t)$ is given as,

$$h(t) = \frac{f(t)}{1 - F(t)}$$

The hazard rate function, $h(t)$ of the $IT_{lin}(\theta)$ -distribution are given by

$$h(t) = \left(\frac{\theta^2}{\theta + 1} \right) \frac{(1 + t)e^{-\theta t}}{1 + \left\{ 1 - \left(\left(1 + \frac{\theta t}{\theta + 1} \right) e^{-\theta t} \right) \right\}^2 \left\{ 1 - K * \tan^{-1} \left\{ 1 - \left(\left(1 + \frac{\theta t}{\theta + 1} \right) e^{-\theta t} \right) \right\} \right\}} \quad (8)$$

Figure 4 illustrates these shapes for selected parameter values.

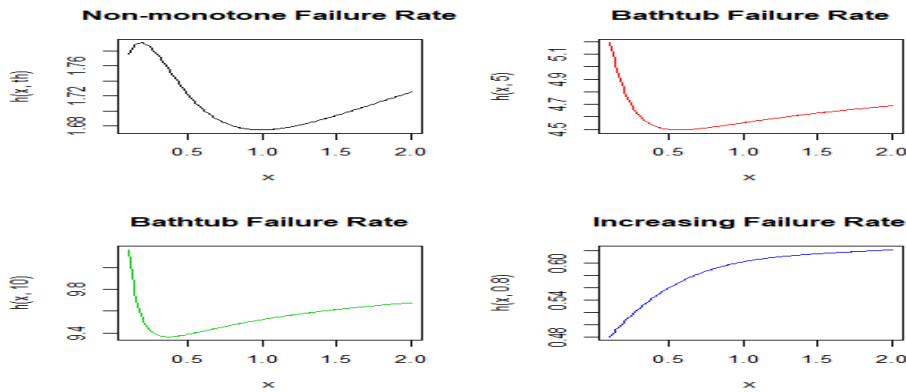


Figure 4: Plots of Hazard Rate Function for different values of θ

5. MOMENTS PROPERTIES

The expression of the moment, are defined as

$$\begin{aligned} E(X^r) &= \int_0^{\infty} x^r g(x) dx \\ &= k * \left(\frac{\theta^2}{\theta + 1} \right) \int_0^{\infty} x^r \frac{(1 + x)e^{-\theta x}}{1 + \left\{ 1 - \left(\left(1 + \frac{\theta x}{\theta + 1} \right) e^{-\theta x} \right) \right\}^2} dx \\ &= k * \left(\frac{\theta^2}{\theta + 1} \right) \int_0^{\infty} x^r (1 + x) e^{-\theta x} \left[1 + \left\{ 1 - \left(\left(1 + \frac{\theta x}{\theta + 1} \right) e^{-\theta x} \right) \right\}^2 \right]^{-1} dx \end{aligned}$$

Using expansion $\left[1 + \{F(x)\}^2 \right]^{-1} = \sum_{k=0}^{\infty} (-1)^k \{F(x)\}^{2k}$ in equation (21) we get,

$$= \sum_{k=0}^{\infty} (-1)^k K * \left(\frac{\theta^2}{\theta + 1} \right) \int_0^{\infty} x^r (1 + x) e^{-\theta x} \left\{ 1 - \left(\left(1 + \frac{\theta x}{\theta + 1} \right) e^{-\theta x} \right) \right\}^{2k} dx$$

Using expansion of $\{1 - F(x)\}^{2k} = \sum_{l=0}^{2k} \binom{2k}{l} (-1)^l \{F(x)\}^l$ in equation (22) we get,

$$= \sum_{k=0}^{\infty} \sum_{l=0}^{2k} (-1)^{k+l} \binom{2k}{l} K * \left(\frac{\theta^2}{\theta + 1} \right) \frac{1}{(\theta + 1)^l} \int_0^{\infty} x^r (1 + x) e^{-\theta x(1+l)} \{1 + \theta + \theta x\}^l dx$$

$$= \sum_{k=0}^{\infty} \sum_{l=0}^{2k} \sum_{m=0}^l (-1)^{k+l} \binom{2k}{l} \binom{l}{m} K * \left(\frac{\theta^2}{\theta+1} \right) \frac{\theta^m}{(\theta+1)^l} \int_0^{\infty} x^r e^{-\theta x(1+l)} \{1+x\}^{m+1} dx$$

Using expansion of $(1+x)^{m+1} = \sum_{n=0}^{m+1} \binom{m+1}{n} x^n$ and gamma function we get expression of r^{th} moments as,

$$E(X^r) = K * \frac{\theta^2}{\theta+1} \sum_{k=0}^{\infty} \sum_{l=0}^{2k} \sum_{m=0}^l \sum_{n=0}^{m+1} (-1)^{k+l} \binom{2k}{l} \binom{l}{m} \binom{m+1}{n} \frac{\theta^m}{(1+\theta)^l} \frac{(n+r)!}{(\theta+\theta l)^{n+r+1}} \quad (9)$$

where, K is $\frac{1}{\tan^{-1}(1)}$.

In particular, the first four moments of X are as follows:

$$E(X) = K * \frac{\theta^2}{\theta+1} \sum_{k=0}^{\infty} \sum_{l=0}^{2k} \sum_{m=0}^l \sum_{n=0}^{m+1} (-1)^{k+l} \binom{2k}{l} \binom{l}{m} \binom{m+1}{n} \frac{\theta^m}{(1+\theta)^l} \frac{(n+1)!}{(\theta+\theta l)^{n+2}} \quad (10)$$

$$E(X^2) = K * \frac{\theta^2}{\theta+1} \sum_{k=0}^{\infty} \sum_{l=0}^{2k} \sum_{m=0}^l \sum_{n=0}^{m+1} (-1)^{k+l} \binom{2k}{l} \binom{l}{m} \binom{m+1}{n} \frac{\theta^m}{(1+\theta)^l} \frac{(n+2)!}{(\theta+\theta l)^{n+3}}$$

$$E(X^3) = K * \frac{\theta^2}{\theta+1} \sum_{k=0}^{\infty} \sum_{l=0}^{2k} \sum_{m=0}^l \sum_{n=0}^{m+1} (-1)^{k+l} \binom{2k}{l} \binom{l}{m} \binom{m+1}{n} \frac{\theta^m}{(1+\theta)^l} \frac{(n+3)!}{(\theta+\theta l)^{n+4}}$$

$$E(X^4) = K * \frac{\theta^2}{\theta+1} \sum_{k=0}^{\infty} \sum_{l=0}^{2k} \sum_{m=0}^l \sum_{n=0}^{m+1} (-1)^{k+l} \binom{2k}{l} \binom{l}{m} \binom{m+1}{n} \frac{\theta^m}{(1+\theta)^l} \frac{(n+4)!}{(\theta+\theta l)^{n+5}}$$

The variance, skewness and kurtosis of T can be obtained using the following relationships:
 $Var(X) = E(X^2) - (E(X))^2$, $Skewness(X) = \frac{E(X-E(X))^3}{(Var(X))^{3/2}}$ and $Kurtosis(X) = \frac{E(X-E(X))^4}{(Var(X))^2}$.

6. ORDER STATISTICS

Let $f(x)$ and $F(x)$ be the pdf and cdf respectively, then for $r=1,2,\dots,n$ be the pdf $f_r(x)$ of r^{th} order statistics $X_{r:n}$ is

$$\begin{aligned} f_r(x) &= \frac{n!}{(r-1)!(n-r)!} F^{r-1}(x) [1-F(x)]^{n-r} f(x) \\ &= \frac{n!}{(r-1)!(n-r)!} \sum_{i=0}^{n-r} (-1)^i \binom{n-r}{i} F^{r+i+1}(x) f(x) \end{aligned} \quad (11)$$

Now using pdf and cdf in equation we have,

$$\begin{aligned} f_r(x) &= \frac{n!}{(r-1)!(n-r)!} K * \frac{\theta^2}{\theta+1} \sum_{i=0}^{n-r} (-1)^i \binom{n-r}{i} \frac{(1+x)e^{-\theta x}}{\left[1 + \left\{1 - \left(1 + \frac{\theta x}{\theta+1}\right)e^{-\theta x}\right\}^2\right]} \\ &\quad \left[K * \tan^{-1} \left\{1 - \left(1 + \frac{\theta x}{\theta+1}\right)e^{-\theta x}\right\} \right]^{r+i+1} \end{aligned} \quad (12)$$

And corresponding to r^{th} order statistics of cdf $F_r(x)$ is ,

$$\begin{aligned} F_r(x) &= \sum_{i=r}^n \binom{n}{i} F^i(x) [1-F(x)]^{n-i} \\ &= \sum_{i=r}^n \sum_{j=0}^{n-i} \binom{n}{i} \binom{n-i}{j} (-1)^j F^{i+j}(x) \end{aligned} \quad (13)$$

Using equation we get,

$$\sum_{i=r}^n \sum_{j=0}^{n-i} \binom{n}{i} \binom{n-i}{j} (-1)^j \left[K * \tan^{-1} \left\{ 1 - \left(\left(1 + \frac{\theta x}{\theta + 1} \right) e^{-\theta x} \right) \right\} \right]^{i+j} \quad (14)$$

7. RENYI ENTROPY

An entropy of a random variable X is a measure of variation of the uncertainty. Renyi entropy is defined by

$$R_\gamma = \frac{1}{1-\gamma} \ln \left(\int f^\gamma(x) dx \right) \quad (15)$$

Where $\gamma > 0$ and $\gamma \neq 1$. Substitute (5) in above expression, we have

$$R_\gamma = \frac{1}{1-\gamma} \log \left(k * \left(\frac{\theta^2}{\theta + 1} \right) \frac{(1+x)e^{-\theta x}}{1 + \left\{ 1 - \left(\left(1 + \frac{\theta x}{\theta + 1} \right) e^{-\theta x} \right) \right\}^2} \right)^\gamma dx \quad (16)$$

Solve the equation(16) anatically and we get final result are:

$$R_\gamma = \frac{1}{1-\gamma} + \ln \sum_{k=0}^{\infty} \sum_{l=0}^{2k} \sum_{p=0}^l \sum_{m=0}^{\infty} (-1)^{k+l} \binom{2k}{l} \binom{\gamma}{m} \binom{l}{p} \frac{(\gamma + k - 1)^{[k]}}{k!} \frac{\Gamma m + p + 1}{[\theta(\gamma + l)]^{m+p+1}} \quad (17)$$

8. ESTIMATION

In this section, we briefly discuss the maximum likelihood estimators (MLE's) of the $IT_{lin}(\theta)$ distribution.

Let $\underline{x} = (x_1, \dots, x_n)$ be a random sample of size n from $IT_{lin}(\theta)$, then the log likelihood function $l(\theta|\underline{x})$ can be written as

$$l(\theta|\underline{x}) = -n * \ln(\tan^{-1}(1)) + n * \ln \left(\frac{\theta^2}{1+\theta} \right) - \theta \sum x + \sum (\ln(1+x)) + \sum \left[\ln \left\{ 1 + \left(1 - \left(1 + \frac{\theta x}{1+\theta} \right) e^{-\theta x} \right) \right\}^2 \right] \quad (18)$$

Therefore, to obtain MLE's of estimated θ , we can maximise the equation directly w.r.t θ or we can solve the following Non- Linear equation by using Newton-Raphson method. Since this equation is not closed form and can not be solved analytically. So, we have to use some numerical technique such as Newton-Raphson method for the solution.

9. SIMULATION ALGORITHM AND STUDY

9.1. Inverse cdf method

One of the most simplest and common method to generating random variates is based on the inverse cdf. For arbitrary cdf, define $F^{-1}(u) = \min \{x; F(x) \geq u\}$, see Sharma et al.(2016). In case of $IT_{lin}(\theta)$ distribution, inverse cdf cannot be obtained easily, so we proposed the use of Newton's method for the solution of the Cdf of $IT_{lin}(\theta)$ distribution. The algorithm used for this purpose is as follows:

- Step 1. Set n, θ and initial value x^0 .
- Step 2. Generate U Uniform(0,1).
- Step 3. Update x^0 by the using Newton's formula.
 $x^* = x^0 - H(x^0, \theta)$

where $H(x^0, \theta) = \frac{F(x^0, \theta) - U}{f(x^0, \theta)}$; $f(\cdot)$ and $F(\cdot)$ are given equation respectively.

Step 4. If $|x^0 - x^*| \leq \epsilon$, then store $x = x^*$ as a sample from $IT_{lin}(\theta)$.

Step 5. If $|x^0 - x^*| > \epsilon$, then, set $x^0 = x^*$ and goto step 3.

Step 6. Repeat steps 2-5, n times for x_1, x_2, \dots, x_n , respectively.

9.2. Simulation Study

In this section, we present the results of the long run guarantee of the proposed lifetime distribution. To verify the behaviour of the proposed lifetime model in terms of mean square error (MSE), bias confidence interval and width of the confidence interval of the maximum likelihood estimator (MLE) of θ . Here we generate 15000 different random sample of size n (n= 10,15,20,25,30,40,90,160,250 and 400) for the consider true value of parameter θ ($\theta= 0.5, 1$ and 2).

Table 1: ML estimates, MSE, Bias, Confidence Interval and width of CI for the true value of parameter is 0.5.

n	mle	mse	Bais	LCL	UCL	width
10	0.5600	0.0239	0.0600	(0.4756, 0.6444)		0.1688
15	0.5058	0.0116	0.0058	(0.4553, 0.5563)		0.1009
20	0.5052	0.0071	0.0052	(0.4674, 0.5430)		0.0755
25	0.5088	0.0056	0.0088	(0.4783, 0.5392)		0.0608
30	0.5093	0.0049	0.0093	(0.4839, 0.5247)		0.0507
40	0.5088	0.0037	0.0088	(0.4897, 0.5077)		0.0380
90	0.5011	0.0032	0.0011	(0.4928, 0.5094)		0.0166
160	0.5020	0.0009	0.0020	(0.4973, 0.5067)		0.0094
250	0.5017	0.0006	0.0017	(0.4987, 0.5047)		0.0060
400	0.5013	0.0004	0.0013	(0.4993, 0.5031)		0.0037

Table 2: ML estimates, MSE, Bias, Confidence Interval and width of CI for the true value of parameter is 1.

n	mle	mse	bais	LCL	UCL	width
10	1.0758	0.0897	0.0758	(0.9059, 1.2456)		0.3397
15	1.0516	0.0530	0.0516	(0.9414, 1.1617)		0.2203
20	1.0377	0.0367	0.0377	(0.9563, 1.1190)		0.1627
25	1.0312	0.0287	0.0312	(0.9666, 1.0958)		0.1292
30	1.0302	0.0237	0.0302	(0.9765, 1.0840)		0.1075
40	1.0233	0.0172	0.0233	(0.9833, 1.0633)		0.0800
90	1.0106	0.0069	0.0106	(0.9931, 1.0282)		0.0350
160	1.0063	0.0038	0.0063	(0.9965, 1.0161)		0.0196
250	1.0041	0.0025	0.0041	(0.9978, 1.0103)		0.0125
400	1.0022	0.0015	0.0022	(0.9983, 1.0061)		0.0078

Table 3: ML estimates, MSE, Bias, Confidence Interval and width of CI for the true value of parameter is 2.

n	mle	mse	Bais	Confidence Inteval	width
10	2.1632	0.3061	0.1632	(1.7950, 2.5312)	0.7362
15	2.1555	0.1921	0.1555	(1.9110, 2.3999)	0.4889
20	2.1491	0.1472	0.1491	(1.9663, 2.3318)	0.3655
25	2.1295	0.1102	0.1295	(1.9847, 2.2743)	0.2895
30	2.1025	0.0810	0.1025	(1.9835, 2.2214)	0.2378
40	2.1215	0.0715	0.1215	(2.0314, 2.2116)	0.1802
90	2.0862	0.0274	0.0862	(2.0469, 2.1256)	0.0786
160	2.1008	0.0235	0.1008	(2.0785, 2.1231)	0.0446
250	2.0976	0.0180	0.0976	(2.0833, 2.1118)	0.0285
400	2.0959	0.0144	0.0959	(2.0870, 2.1048)	0.0178

The results are consider in all Tables (Table 1,2 and 3), which show the average of the 15000 MLE's together with their MSE, Bias, 95% of confidence interval and width of the confidence interval of true value of the parameter of the proposed lifetime distribution. For all considered true value of the parameter θ ;the MSE and bias are decreases as sample size increased. These results suggest that the MLE have performed consistently 95% confidence interval and width of the paramter θ also decreases as sample size increases.

10. REAL DATA MODELING

In the present section, we have considered two data sets, which are initially proposed by Efron, B (1998). The data represents the patients of two groups suffering from head and neck cancer disease. The data set of first group represents the survival times of 51 head and neck cancer patients treated with radiotherapy whereas the other group of data set represents the survival times of 45 head and neck cancer patients treated with combined radiotherapy and chemotherapy. The data sets are as follows:

Data(A): 6.53, 7, 10.42, 14.48, 16.10, 22.70, 34, 41.55, 42, 45.28, 49.40, 53.62, 63, 64, 83, 84, 91, 108, 112, 129, 133,133, 139, 140, 140, 146, 149, 154, 157, 160, 160, 165, 146, 149, 154, 157, 160, 160, 165, 173, 176, 218, 225, 241, 248, 273,277, 297, 405, 417, 420, 440, 523, 583, 594, 1101, 1146, 1417.

Data(B): 12.20, 23.56, 23.74, 25.87, 31.98, 37, 41.35, 47.38, 55.46, 58.36, 63.47, 68.46, 78.26, 74.47, 81,43, 84, 92, 94, 110, 112, 119, 127, 130, 133, 140, 146, 155, 159, 173, 179, 194, 195, 209, 249, 281, 319, 339, 432, 469, 519, 633, 725, 817, 1776.

To check the validity of the considered model for the above data sets A and B using Kologorov-Smirnov Statistics (K-S), Akaike information criterion (AIC), and Bayes information criterion (BIC) and log-likelihood criterion. We compare the applicability of this model for the above data sets over Inverse Rayleigh distribution (IRD), Generalized inverted exponential distribution (GIED), Inverse exponential distribution (IED) and Lindley distribution (LD) have discussed and it is found that the considered model is quite flexible than the other four, see Table.

Table 4: The values of different statistical measures for the Data Set (A)

Distributions	AIC	BIC	-LL	K-S test value
GIED	773.18	777.30	384.59	0.2453
IRD	840.13	842.06	419.06	0.6039
ITLD	721.25	723.31	359.62	0.2433
IED	773.37	775.43	385.68	0.2875
LD	765.74	767.80	381.87	0.2453

Table 5: The values of different statistical measures for the Data Set (B)

Distributions	AIC	BIC	-LL	K-S test value
GIED	572.43	576.04	284.21	0.1901
IRD	962.71	964.49	480.35	0.3783
ITLD	559.45	561.25	278.72	0.1223
IED	571.06	572.86	284.53	0.1823
LD	593.23	595.04	295.61	0.2942

10.1. TTT Plot

The total-time-on-test (TTT) plot is a graphical procedure to get some idea about the shape of the hazard function. We have used the empirical version of the scaled TTT plot, [Aarset (1987)]. We have plotted the empirical version of the scaled TTT transform of the both data set (data set A and B) in figure 5 and 6. Since the empirical version of the scaled TTT transform is concave and convex both, it indicates the hazard function is increasing and decreasing both.

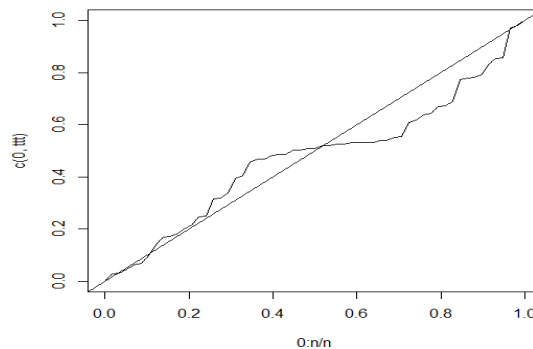


Figure 5: The empirical scaled TTT transform of the data set A

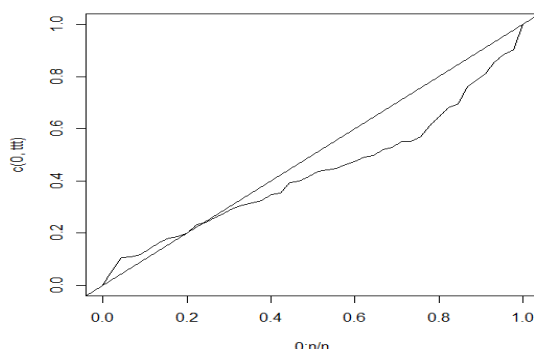


Figure 6: The empirical scaled TTT transform of the data set B

11. CONCLUSIONS

In this work, we have proposed a new transformation using trigonometric function along with Lindley distribution. So, the name of distribution is "Inverse Trigonometric Lindley Distribution" as it uses lindley distribution as the baseline distribution. Some of its important various statistical/mathematical properties including shape, survival function, hazard rate, moments and associated measures, order statistics are discussed and renyi entropy of the proposed distribution have been derived. The method of maximum likelihood estimation has also been discussed for estimating the parameter. For depth understanding, we have deliberated real life scenarios as two real data sets of survival of head and neck cancer patients are considered to illustrate the applicability of the discussed model. It is found that our invented model provides better fit to the given data set, which has been well verified by graphical illustrations.

REFERENCES

- [1] Lindley, D. (1958): Fiducial distributions and Bayes theorem. *J.R.Stat.Soc.Ser.B* 20:102107.
- [2] Kumar, D., Singh, S.K. and Singh, U. (2017): Life Time Distributions: Derived from some Minimum Guarantee Distribution. *Sohag J. Math.* 4, No. 1, 7-11 (2017).
- [3] Singh, S. K., Singh, U., Yadav, A. S., and Vishwkarma, P. K. (2015). On the estimation of stress strength reliability parameter of inverted exponential distribution. *International Journal of Scientific World*, 3(1), 98-112.
- [4] Sharma, V. K., Singh, S. K., Singh, U., and Merovci, F. (2016). The generalized inverse Lindley distribution: A new inverse statistical model for the study of upside-down bathtub data. *Communications in Statistics-Theory and Methods*, 45(19), 5709-5729.
- [5] Shanker, R. (2015). Shanker distribution and its applications. *International journal of statistics and Applications*, 5(6), 338-348.
- [6] Sharma, V. K., Singh, S. K., Singh, U., and Agiwal, V. (2015). The inverse Lindley distribution: a stress-strength reliability model with application to head and neck cancer data. *Journal of Industrial and Production Engineering*, 32(3), 162-173.
- [7] Maurya, S. K., Kaushik, A., Singh, S. K., and Singh, U. A new class of exponential transformed Lindley distribution and its Application to Yarn Data.
- [8] Nadarajah, S., and Haghighi, F. (2011). An extension of the exponential distribution. *Statistics*, 45(6), 543-558.
- [9] Efron, B. (1988). Logistic regression, survival analysis, and the Kaplan-Meier curve. *Journal of the American statistical Association*, 83(402), 414-425.
- [10] Kumar, D., Singh, U., Singh, S. K., and Chaurasia, P. K. (2018). A new lifetime distribution: Some of its statistical properties and application. *J. Stat. Appl. Prob.* 7, 413-422.

- [11] Kumar, D., Singh, U., and Singh, S. K. (2015). A new distribution using Sine function-its application to bladder cancer patients data. *Journal of Statistics Applications and Probability*, 4(3), 417.
- [12] Kumar, D., Singh, U., and Singh, S. K. (2015). A method of proposing new distribution and its application to Bladder cancer patients data. *J. Stat. Appl. Pro. Lett*, 2(3), 235-245.
- [13] Kumar, D., Singh, S. K., Singh, U., Kumar, P. and Chaurasia, P. K. (2018): Statistical Properties and Application of a Lifetime Model Using Sine Function. *International Journal of Creative Research Thoughts*, vol. 6(2); pp: 993-1002. ISSN: 2320-2882.
- [14] Chesneau, C., Bakouch, H. S., and Hussain, T. (2019). A new class of probability distributions via cosine and sine functions with applications. *Communications in Statistics-Simulation and Computation*, 48(8), 2287-2300.
- [15] Oluyede, B. O., and Yang, T. (2015). A new class of generalized Lindley distributions with applications. *Journal of Statistical Computation and Simulation*, 85(10), 2072-2100.
- [16] Shaw, W. T., and Buckley, I. R. (2007). The alchemy of probability distributions: Beyond gamma-Charlier and Cornish-Fisher expansions, and skew-normal or kurtotic-normal distributions. Submitted, Feb, 7, 64.
- [17] Gupta, R. C., Gupta, P. L., and Gupta, R. D. (1998). Modeling failure time data by Lehman alternatives. *Communications in Statistics-Theory and methods*, 27(4), 887-904.
- [18] Asgharzadeh, A., Bakouch, H. S., and Esmaeili, L. (2013). Pareto Poisson-Lindley distribution with applications. *Journal of Applied Statistics*, 40(8), 1717-1734.
- [19] Nadarajah, S., Bakouch, H. S., and Tahmasbi, R. (2011). A generalized Lindley distribution. *Sankhya B*, 73(2), 331-359.
- [20] Merovci, F., and Elbatal, I. (2013). Transmuted Lindley-geometric distribution and its applications. arXiv preprint arXiv:1309.3774.
- [21] Al-Babtain, A., Eid, A. M., Ahmed, A. H. N., and Merovci, F. (2015). THE FIVE PARAMETER LINDLEY DISTRIBUTION. *Pakistan Journal of Statistics*, 31(4).
- [22] Ghitany, M. E., Al-Mutairi, D. K., and Nadarajah, S. (2008). Zero-truncated Poisson-Lindley distribution and its application. *Mathematics and Computers in Simulation*, 79(3), 279-287.
- [23] Ghitany, M. E., Atieh, B., and Nadarajah, S. (2008). Lindley distribution and its application. *Mathematics and computers in simulation*, 78(4), 493-506.
- [24] Mahmood, Z., and Chesneau, C. (2019). A New Sine-G Family of Distributions: Properties and Applications.
- [25] Maurya, S. K., Kaushik, A., Singh, S. K., and Singh, U. (2017). A new class of distribution having decreasing, increasing, and bathtub-shaped failure rate. *Communications in Statistics-Theory and Methods*, 46(20), 10359-10372.
- [26] Aarset, M. V. (1987). How to identify a bathtub hazard rate. *IEEE Transactions on Reliability*, 36(1), 106-108.
- [27] Casella, G., and Berger, R. L. (1990). *Statistical Inference*. Belmont: Wadsworth. Casella *Statistical Inference* 1990.
- [28] Johnson, N. L. (1970). L. and Kotz, S.(1970). *Continuous Univariate Distributions-1*.
- [29] Johnson, N. L. Kotz (1970). *Distributions in statistics, continuous univariate distributions-2*.
- [30] Lawless, J. F. (2011). *Statistical models and methods for lifetime data (Vol. 362)*. John Wiley and Sons.

Study on Acceptance Sampling Plan For Truncate Life Tests Based on Percentiles Using Gompertz Frechet Distribution

S.JAYALAKSHMI, S.VIJILAMERY



(1).Assistant Professor, Department of Statistics, Bharathiar University

(2).Research Scholar, Department of Statistics, Bharathiar University

E.mail: statjayalakshmi16@gmail.com ,vijilamerysrsj@gmail.com

Abstract

In this paper, Acceptance Sampling approaches useful for minimizing the cost and time of the submitted lots. In this busy world expect the Quality assurance and reliability of the product is very high. So, use the truncated life tests in acceptance sampling plan. Time truncated life tests in sampling plan are used to certain reach a decision on the product. Therefore, Gompertz Frechet Distribution is considered as model for a life time random variable when the lifetime test is truncated at pre-determined time. The operating characteristic functions of the sampling plans and Producer's risk is also discussed. The results are illustrated by an example.

Keywords: Gompertz Frechet Distribution, Single Sampling Plan, truncated life time test, Consumer's risk;

1. INTRODUCTION

Acceptance sampling plan constitutes one of the oldest techniques in Statistical Quality Control. It has an important role on common quality control techniques used in the manufacturing industry. It is desired to be a protective and efficient to make sure the quality control of such items. The sampling plan is determined to accept or reject a lot of items based on the life span time of the items is called reliability acceptance sampling plan. In a truncated life test using Single Sampling Plan, time is a main factor in check and fit the quality of the items. When the lifetime test suggests that the average life of items is lesser than the pre determined one, the lot of products is rejected, otherwise it is accepted. Accepting lots are ready for the production, while rejecting lots may be returned to the trader. For the main objective of minimizing the test time and cost, a truncated lifetime test may be run to determine the minimum sample size to make certain average lifetime of products when the lifetime test is stopped at a pre-determined time.

In the scheme of the truncated lifetime test is the number of defects 'd' and comparing the acceptance number 'c'. If the defects are lesser than acceptance number $d < c$, accept the lot and otherwise reject the lot. If defects are lesser than acceptance number c , is get before time t_0 put an end to the test and improve, the better quality of the product in the production management. In truncated life test use to find the minimum sample size to make certain an average life of items with specified confidence level P^* .

The Reliability Acceptance Sampling Plan for percentiles using various distributions are: Epstein (1954) designed acceptance sampling plan depends on life test presuming that the life time of a product follows the exponential distribution. Cameron. J.M (1952) has developed and designing tables for constructing and computing the Operating Characteristics of Single Sampling Plans. Gupta and Groll (1961) originated an acceptance sampling when the lifetime test truncated at a pre-fixed time and assumes to using the design of lifetime as gamma distribution.

Kantam and Rosaiah (1998) progress an acceptance sampling plan based on model for truncated pre determined lifetime random variable using the half logistic distribution. Kantam et al. (2001) evolved the sampling plan for lifetime follows log-logistic distribution with known shape parameter explaining an illustration with examples. Rosaiah et.al(2005) determines that the life time of the items follows the inverse Rayleigh distribution and origin the acceptance sampling for life tests. Al-Nassar, A.D. and Al-Omari, A.I. (2013) has developed an acceptance sampling plan depends up on truncated lifetime tests for exponentiated Frechet distribution. Rao et al. (2014) constructed the Exponentiated half log logistic distribution and its percentile estimator for designing acceptance sampling plans applying the similar method depend on its percentiles.

Kaviyarasu. V and Fawaz. P (2017) has designed an acceptance sampling plan of single sampling plan uses to truncated life tests based on percentiles using Weibull-Poisson distribution. Jayalakshmi.S, Neena Krishna P.K (2021) has developed a Special Type Double Sampling Plan for Life Tests Based on Percentiles Using Exponentiated Frechet distribution.

This paper mainly focusing the designing of an acceptance sampling plans truncated life test based on percentiles using Gompertz Frechet distribution. Oguntunde et. al (2019) has developed by Gompertz Frechet distribution properties and applications. The real time application of Gompertz Frechet distributions are reliability studies, hydrology, finance and so on.

2. GOMPERTZ FRECHET DISTRIBUTION

The life time distribution of the product follows as Gompertz Frechet distribution with the scale parameter is α and shape parameters are β, γ, θ . The Cumulative Distribution Function (CDF) and Probability Density Function (PDF) of the Gompertz Frechet distribution is given by

$$F(x, \alpha, \beta, \gamma, \theta) = 1 - \exp\left[\left(\frac{\theta}{\gamma}\right)\left(1 - \left(1 - \exp\left[\left(\frac{\alpha}{x}\right)^\beta\right]^{-\gamma}\right)\right)\right] \quad (1)$$

and

$$f(x, \alpha, \beta, \gamma, \theta) = \theta\beta\alpha^\beta x^{-\beta-1} \left[\exp\left[-\frac{\alpha}{x}\right]^\beta \left(\exp\left[-\frac{\alpha}{x}\right]^\beta\right)^{-\gamma-1} * \exp\left[\frac{\theta}{\gamma}\left(1 - \left(1 - \exp\left[\left(\frac{\alpha}{x}\right)^\beta\right]^{-\gamma}\right)\right)\right]\right] \quad (2)$$

where $\alpha > 0, \beta > 0, \gamma > 0, \theta > 0$

2.1. Percentile Estimator

The q^{th} percentile function of the any distribution is given below,

$$Pr(T \leq t_q) = q \quad (3)$$

$$t_q = \alpha \left[-\log\left[1 - \frac{\gamma}{\theta} \left[\log(1 - q)\right]^{-\frac{1}{\gamma}}\right]^{-\frac{1}{\beta}}\right] \quad (4)$$

$$\alpha = \frac{t_q}{\phi_q} \quad (5)$$

where

$$\phi_q = \left[-\log\left[1 - \frac{\gamma}{\theta} \left[\log(1 - q)\right]^{-\frac{1}{\gamma}}\right]^{-\frac{1}{\beta}}\right] \quad (6)$$

$$\delta_q = \frac{t}{t_q} \quad (7)$$

Replacing the value of scale parameter α by 5 in 1 then we obtained the Cumulative Distribution Function of Gompertz Frechet distribution is

$$F(t, \alpha, \beta, \gamma, \theta) = 1 - \exp\left[\frac{\theta}{\gamma}\left(1 - \left(1 - \exp\left[\frac{-1}{\phi_q \delta_q}\right]^\beta\right)^{-\gamma}\right)\right] \quad (8)$$

Taking a first derivative of partial differentiation with respect to δ , we get

$$\frac{\partial(t, \delta)}{\partial \delta} = \frac{1 - \exp\left(\frac{\theta}{\gamma}\right)}{\phi_q(\delta_q^2)} \left[\gamma\left(1 - \exp\left[\frac{-1}{\phi_q \delta_q}\right]^\beta\right)^{-\gamma-1} \beta \exp\left(1 - \exp\left[\frac{-1}{\phi_q \delta_q}\right]^{2\beta-1}\right)\right] \quad (9)$$

3. DESIGNING OF SINGLE SAMPLING PLAN THROUGH GOMPERTZ FRECHET DISTRIBUTION

Single Sampling Plan is the key for all attribute acceptance sampling. The elementary form of single sampling plan is relates with dichotomous situations in which the inspection results can be classified into two classes of outcomes such as accept and reject of the lot. A sampling inspection scheme in which a decision to accept or reject an inspection lot is based on the inspection of a single sample. A single sampling plan consists of a single sample size with associated acceptance number(c). If taking random sample size n from the Lot size N then conducting the inspection with the number of defectives (d) found and compared to an Acceptance number (c). If the number of defectives found is less than or equal to acceptance number (c), the lot is accepted. Otherwise, the lot is rejected. For a single sampling plan, one sample of items is selected at random from a lot and the disposition of the lot is determined from the resulting information. The random sample size values of Single Sampling Plan follows Binomial Distribution denoted by $B(n, c, p)$. It has developed procedure of single sampling plan whose parameter p is assigned to follow Gompertz Frechet distribution with parameters $\delta_0 = \frac{t_q}{t_q^0}$ Where, t and t_q^0 are the specified time test duration and specified $100q^{th}$ percentile of the Gompertz Frechet distribution respectively. According to Cameron (1952), the smallest size n can be given by satisfying,

$$\sum_{i=0}^c \binom{n}{i} (p)^i (1-p)^{(n-i)} \quad (10)$$

Where, $(1-p^*)$ is the consumer risk and p^* is the probability of accepting the good lot.

4. OPERATING PROCEDURE FOR ACCEPTANCE SINGLE SAMPLING PLAN THROUGH GOMPERTZ FRECHET DISTRIBUTION PERCENTILES FOR LIFE TESTING

The operating procedure of the suggested plan is follows as:

- Taking a sample of size n within a test for time t_0
- Find the number of defectives d and comparing the acceptance number c .
 - i If $d > c$, reject the lot.
 - ii If $d \leq c$, accept the lot.
- If $d > c$, is get before time t_0 , put an end to the test and improve the better quality of the product in the production management.

4.1. Minimum sample size for 10^{th} percentile using Gompertz Frechet Distribution

For a predetermined P^* , our sampling plan is described by $(n, c, t/t_q)$. Here we observe that acceptably exhaust sized lots and also that the binomial distribution can be applied. The study is to determine for given values of P^* ($0 < P^* < 1$), t_q^0 and c, the smallest non-negative integer n required to assured that $t_q < t_q^0$ must satisfy

Step 1: Find the value of ϕ for fixing the values of parameters are θ, β, γ and $q=0.10$.

Step 2: Set the calculate value of $\phi = 0.7785$, $c=0$ to 10, and $t/t_q = 0.9, 0.95, 1.0, 1.1, 1.25, 1.5, 1.6, 1.65$

Find the minimum value of n satisfying

$$L(p) = \sum_{i=0}^c \binom{n}{i} (p)^i (1-p)^{(n-i)} \leq (1-p^*) \quad (11)$$

where p^* is the probability of accepting the good lot.

Table 1: Gives the minimum sample size 'n' for the specified 10th percentile value $t_{0.10}^0$ of Gompertz Frechet Distribution to exceed the actual 10th percentile value $t_{0.10}$, with probability p^* and acceptance number c using binomial approximation

P^*	c	$t/t_{0.10}$								
		0.9	0.95	1	1.1	1.2	1.25	1.5	1.6	1.65
0.75	0	8	6	4	2	1	1	1	1	1
	1	20	9	5	4	4	3	3	2	2
	2	26	24	18	8	7	6	5	4	3
	3	32	28	13	7	6	6	5	4	4
	4	40	37	28	13	8	7	7	6	6
	5	66	58	43	29	27	14	12	9	8
	6	71	63	58	46	33	27	18	13	10
	7	86	69	60	57	43	32	27	22	17
	8	92	89	78	65	54	42	31	28	19
	9	116	104	93	82	67	55	44	36	20
10	125	105	95	86	74	66	59	43	32	
0.90	0	10	7	5	4	3	2	1	1	1
	1	26	10	7	6	5	3	2	2	2
	2	33	25	19	9	8	7	6	5	3
	3	44	30	23	10	7	7	5	4	4
	4	56	41	29	14	9	9	8	8	7
	5	67	59	47	30	28	23	20	17	13
	6	72	65	59	46	36	32	28	26	21
	7	87	81	72	59	54	43	38	34	26
	8	94	89	79	66	57	51	48	42	36
	9	126	123	102	96	80	72	59	52	41
10	128	120	116	92	78	67	56	42	39	
0.95	0	11	8	7	5	4	3	1	1	1
	1	28	12	8	7	5	4	3	2	2
	2	38	25	20	12	9	7	6	4	3
	3	49	34	25	15	8	7	6	5	4
	4	57	45	31	15	10	10	9	8	7
	5	69	63	48	32	28	25	23	20	18
	6	76	66	60	49	47	35	30	27	24
	7	90	82	73	62	55	48	41	39	35
	8	105	94	89	72	68	59	52	47	42
	9	128	124	103	99	82	79	61	57	43
10	139	125	117	98	83	79	62	59	53	
0.99	0	20	15	8	6	4	3	1	1	1
	1	30	20	10	8	7	6	5	3	2
	2	40	25	20	13	9	8	7	6	5
	3	58	36	29	16	12	12	12	12	10
	4	75	54	42	35	20	20	20	19	14
	5	96	63	51	33	32	31	29	29	27
	6	102	92	81	60	57	48	46	39	38
	7	118	106	99	82	71	64	59	44	42
	8	167	158	104	99	87	73	61	59	45
	9	183	160	113	103	94	81	78	62	59
10	199	181	179	154	121	108	96	79	61	

4.2. Operating Characteristic Function

The operating characteristic function of the sampling plan gives the probability of accepting the lot $L(p)$ with,

$$L(p) = \sum_{i=0}^c \binom{n}{i} (p)^i (1-p)^{(n-i)} \tag{12}$$

The producer's risk α is the probability of rejecting a lot when $t_q > t_q^0$. And for the given producer's risk α , p as a function of d_q should be simulated satisfying the condition given by Cameron (1952) as

$$\sum_{i=0}^c \binom{n}{i} (p)^i (1-p)^{(n-i)} > (1-\alpha) \tag{13}$$

Where, $p=F(t, \delta_0)$ and $F(.)$ can be obtained as a function of d_q for the sampling plan developed, $d_{0.1}$ values are obtained at the producers risk $\alpha=0.05$.

Table 2: Operating characteristic values of the sampling plan $(n, c, t/t_{0.10}^0)$ for given p^* under Gompertz Frechet distribution

P^*	n	$t/t_{0.10}$	$(t_{0.10})/(t_{0.10}^0)$							
			1.95	2	2.5	2.75	3	3.25	3.5	4
0.75	18	1.0	0.0019	0.0059	0.7651	0.9160	0.9756	0.9944	0.9990	0.9999
	8	1.1	0.0124	0.0548	0.7748	0.9276	0.9836	0.9971	0.9995	0.9999
	7	1.2	0.0875	0.0911	0.8284	0.9428	0.9853	0.9972	0.9996	0.9999
	6	1.25	0.1412	0.1920	0.8381	0.9627	0.9993	0.9993	0.9999	1.0000
	5	1.5	0.3024	0.3382	0.9919	0.9994	0.9999	0.9999	1.0000	1.0000
	4	1.6	0.3073	0.3442	0.9964	0.9998	0.9999	1.0000	1.0000	1.0000
	3	1.65	0.4340	0.4143	0.9997	0.9999	1.0000	1.0000	1.0000	1.0000
0.90	19	1.0	0.0020	0.0066	0.7748	0.9160	0.9756	0.9971	0.9995	0.9999
	9	1.1	0.0157	0.0694	0.7902	0.9428	0.9853	0.9986	0.9990	0.9999
	8	1.2	0.1074	0.1942	0.8284	0.9506	0.9917	0.9944	0.9998	0.9999
	7	1.25	0.1725	0.2116	0.8747	0.9631	0.9919	0.9990	0.9999	1.0000
	6	1.5	0.2267	0.2812	0.9899	0.9992	0.9999	0.9999	1.0000	1.0000
	3	1.6	0.4022	0.4304	0.9957	0.9997	0.9999	1.0000	1.0000	1.0000
	3	1.65	0.4340	0.4327	0.9996	0.9999	1.0000	1.0000	1.0000	1.0000
0.95	20	1.0	0.0023	0.0074	0.7651	0.9160	0.9756	0.9944	0.9990	0.9999
	12	1.1	0.0268	0.0721	0.7748	0.9276	0.9836	0.9971	0.9995	0.9999
	9	1.2	0.1272	0.1977	0.7902	0.9428	0.9853	0.9972	0.9999	0.9999
	7	1.25	0.1725	0.2116	0.8284	0.9506	0.9919	0.9990	0.9999	1.0000
	6	1.5	0.2267	0.2815	0.9899	0.9992	0.9999	0.9999	1.0000	1.0000
	4	1.6	0.4024	0.4344	0.9950	0.9997	0.9999	1.0000	1.0000	1.0000
	3	1.65	0.4422	0.4443	0.9995	0.9999	1.0000	1.0000	1.0000	1.0000
0.99	20	1.0	0.0027	0.0074	0.7750	0.9650	0.9840	0.9945	0.9992	0.9999
	13	1.1	0.0310	0.0855	0.8546	0.9681	0.9850	0.9988	0.9997	0.9999
	9	1.2	0.1272	0.1978	0.8685	0.9986	0.9895	0.9989	0.9999	0.9999
	8	1.25	0.2007	0.2404	0.9879	0.9993	0.9899	0.9990	0.9999	1.0000
	7	1.5	0.2561	0.2811	0.9950	0.9995	0.9999	0.9996	1.0000	1.0000
	6	1.6	0.4875	0.4361	0.9996	0.9998	0.9999	1.0000	1.0000	1.0000
	5	1.65	0.5110	0.5985	0.9998	0.9999	1.0000	1.0000	1.0000	1.0000

5. ILLUSTRATION WITH REAL LIFE APPLICATIONS

Assuming that the conduct an inspection of the lifetime of battery saver of Smart Watch. The study was based on inspection lifetime product which follows a Gompertz Frechet distribution. The Gompertz Frechet distribution has a three shape parameters it uses to fixing a value of length, breath and thickness of the battery saver of smart watch as $\theta=6, \beta=3, \gamma=0.06$ respectively. Figure 1 represents the example for Battery Saver of Smart Watch.



Figure 1: Battery Saver of Smart Watch

An Experimenter wants to conduct the runtime of experiment is 3000hrs but the laboratory has the testers to true percentile life time $t_{0.10}=1800$ hrs, $c=2, \alpha = 0.05, \beta=0.05$, then, $\phi=0.7785$ is computed from the equation get under the percentile estimator and the minimum ratio, $t/t_{0.10}^0=1.0$ and minimum sample size is $n=20$ get the information from the Table 1. The probability of acceptance is characterized by $(n, c, t/t_{0.10}^0) = (20, 2, 1.0)$ with $p^* = 0.95$ under Gompertz Frechet distribution the values from Table 2 are given below.

t_q/t_q^0	1.95	2	2.5	2.75	3	3.25	3.5	4
L(p)	0.0023	0.074	0.7651	0.9160	0.9756	0.9944	0.9990	0.9999

Figure 2 represents the Two point Operating Characteristic curve for Single Sampling Plan using 10th percentile for Gompertz Frechet Distribution. The Acceptable Reliability Level (ARL) and Limiting Reliability Level (LRL) are determined through producer’s confidence level (1- α) and consumer’s level β . An product is considered as $t_{0.10} \geq t_{0.10}^0$ and otherwise it is considered to be a bad of the product. The Reliability acceptance Sampling plan is considered as good one of the product if both risks are minimized. It reveals that if the true 10th percentile is almost equal to the essential 10th percentile ($t_{0.10}/t_{0.10}^0 = 1.0$) the producer’s risk nearly 0.9757 (1-0.023). The producer’s risk is an almost nearly equal to Zero whenever the actual 10th percentile is greater than or equal to 3 times the specified 10th percentile.

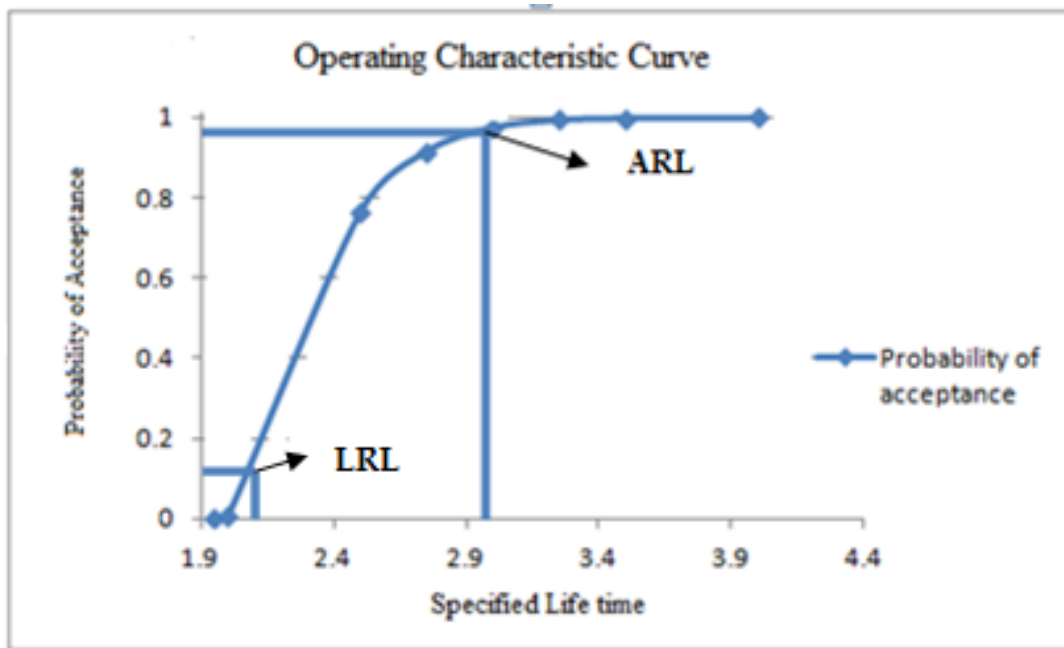


Figure 2: Operating Characteristic curve for Single Sampling Plan using 10th percentile for Gompertz Frechet Distribution

5.0.1 Real Data Application

We consider the real data application was recorded from Bi and Gui (2017). The dataset describes strength of carbon fibers tested under tension at Gauge lengths of 20mm. The observations are as given below:

	1.312,	1.314,	1.479,	1.552,	1.700,	1.803,	1.861,	1.865,	1.944,	1.958,
1.966,	1.997,	2.006,	2.021,	2.027,	2.055,	2.063,	2.098,	2.140,	2.179,	2.224,
2.240,	2.253,	2.270,	2.272,	2.274,	2.301,	2.301,	2.359,	2.382,	2.382,	2.426,
2.434,	2.435,	2.478,	2.490,	2.511,	2.514,	2.535,	2.554,	2.566,	2.570,	2.586,
2.629,	2.633,	2.642,	2.648,	2.684,	2.697,	2.726,	2.770,	2.773,	2.800,	2.809,
2.818,	2.821,	2.848,	2.880,	2.954,	3.067,	3.084,	3.090,	3.096,	3.128,	3.233,
3.433,	3.585	3.585.								

First, we should check the given sample comes from Gompertz Frechet Distribution by the goodness of fit test and model selection criteria. So, we have to use the Q-Q Plot, Shapiro-wilk test, kolmogrov smirnov test and Histogram. Figure 3 graphically represents the Histogram satisfies the Normality of the given data. We get the result of KS test statistic is 0.039 and the Shapiro-Wilk test is 0.991. Figure 4 represents the graphically satisfies the Q-Q plot of the given

data. Hence, the Gompertz Frechet Distribution could also provide reasonable goodness of fits for data set.

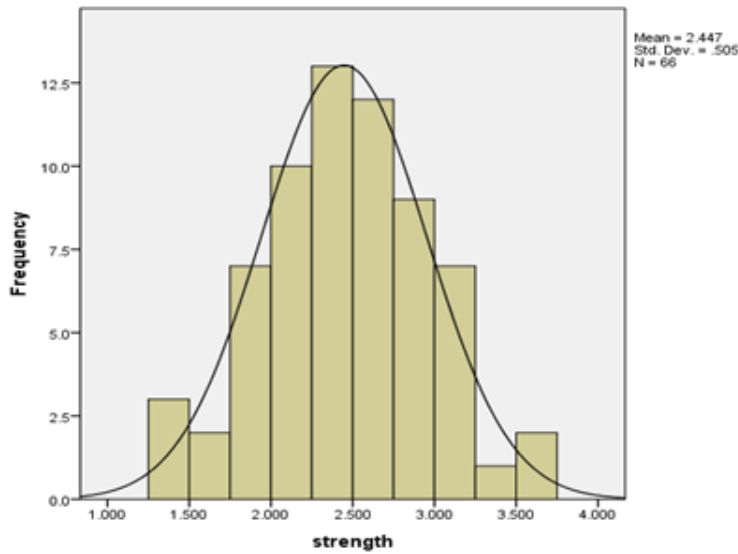


Figure 3: Histogram

Experimenter wants to make runtime of the experiment for 300 hrs. Further, the laboratory has the testers to actual percentile life time $t_{0.10}=150$ hrs, $c=2$, $\alpha = 0.05$, $\beta=0.05$, then, $\phi=0.7785$ is calculated from the equation get under percentile estimator and the minimum ratio, $t/t_{0.10}=1.6$ from Table 1 the minimum sample size from the obtained information is $n=57$. The probability of acceptance for the triplet values $(n, c, t/t_{0.10}) = (57, 9, 1.6)$.

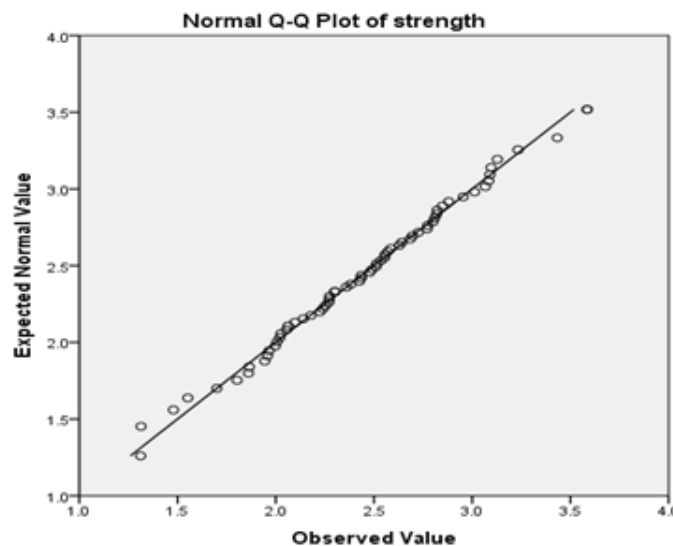


Figure 4: Q-Q Plot

Since there were no items with a failure time less than or equal to 300 hrs in the given sample of $n = 57$ observations, the experimenter would accept the lot, assuming the 10th percentile lifetime $t_{0.10}$ of at least 150 hrs with a confidence level of $p^* = 0.95$.

6. CONSTRUCTION OF THE TABLE

The procedure uses to construction of Table 3 for the minimum ratio of true mean life for specified mean life for the acceptability of a lot with a producer’s risk of 0.05.

Step 1: Find the value of ϕ for fixing the values of parameters are θ, β, γ and $q=0.10$.

Step 2: Set the evaluated $\phi, c=0$ to 10, and $t/t_q = 0.9, 0.95, 1.0, 1.1, 1.25, 1.5, 1.6, 1.65, 1.7$.

Step 3: Find the smallest value of n satisfying where P^* is the probability of accepting the good lot.

Step 4: For the n value obtained find the ratio $d_{0.1}$ such that 13 where, $p = F\left(\frac{t_q}{t_q^0}\right) * \frac{1}{(d_q)}$ and $d_q = \frac{t_q^0}{t_q}$.

Table 3: Minimum ratio of true mean life to specified mean life for the acceptability of a lot with producer’s risk of 0.05 using Gompertz Frechet Distribution

P^*	c	t/t_q^0								
		0.9	0.95	1	1.1	1.2	1.25	1.5	1.6	1.65
0.75	0	1.224	1.263	1.299	1.406	1.500	1.510	1.696	1.809	1.866
	1	0.783	0.846	0.896	0.900	0.901	1.086	1.175	1.282	2.083
	2	0.665	0.725	0.764	0.780	0.799	0.802	0.812	0.836	0.879
	3	0.364	0.457	0.552	0.593	0.682	0.718	0.725	0.756	0.779
	4	0.354	0.366	0.398	0.416	0.420	0.448	0.465	0.476	0.498
	5	0.254	0.266	0.277	0.298	0.314	0.352	0.365	0.398	0.406
	6	0.157	0.177	0.184	0.198	0.201	0.226	0.2365	0.308	0.311
	7	0.117	0.123	0.137	0.153	0.187	0.199	0.207	0.216	0.238
	8	0.139	0.139	0.149	0.153	0.169	0.198	0.206	0.209	0.211
	9	0.104	0.115	0.127	0.138	0.157	0.184	0.199	0.208	0.214
	10	0.043	0.061	0.075	0.107	0.115	0.120	0.130	0.139	0.142
0.90	0	1.297	1.342	1.386	1.504	1.612	1.633	1.860	1.984	2.046
	1	0.896	0.936	1.089	1.188	1.276	1.362	1.467	1.578	1.68
	2	0.734	0.756	0.768	0.772	0.796	0.803	0.813	0.822	0.846
	3	0.573	0.598	0.608	0.611	0.627	0.697	0.747	0.768	0.783
	4	0.477	0.498	0.502	0.699	0.739	0.753	0.763	0.788	0.792
	5	0.365	0.379	0.399	0.409	0.416	0.427	0.438	0.448	0.468
	6	0.267	0.279	0.288	0.291	0.301	0.316	0.328	0.338	0.340
	7	0.217	0.226	0.238	0.247	0.257	0.268	0.277	0.289	0.299
	8	0.190	0.199	0.201	0.227	0.238	0.249	0.257	0.266	0.278
	9	0.117	0.124	0.145	0.153	0.167	0.178	0.203	0.218	0.224
	10	0.098	0.106	0.118	0.126	0.138	0.146	0.158	0.188	0.199
0.95	0	1.334	1.394	1.443	1.568	1.684	1.713	1.964	2.095	2.161
	1	0.899	0.946	1.189	1.288	1.376	1.462	1.567	1.688	1.709
	2	0.739	0.766	0.779	0.880	0.896	0.903	0.913	0.922	0.946
	3	0.583	0.608	0.618	0.621	0.637	0.707	0.757	0.788	0.793
	4	0.487	0.508	0.512	0.709	0.749	0.793	0.773	0.798	0.802
	5	0.375	0.389	0.409	0.419	0.416	0.437	0.448	0.458	0.468
	6	0.277	0.289	0.298	0.301	0.311	0.326	0.338	0.358	0.360
	7	0.227	0.236	0.248	0.257	0.267	0.278	0.287	0.299	0.309
	8	0.191	0.209	0.211	0.237	0.248	0.259	0.267	0.276	0.298
	9	0.127	0.134	0.155	0.163	0.177	0.188	0.213	0.228	0.234
	10	0.099	0.116	0.128	0.136	0.148	0.156	0.168	0.198	0.199
0.99	0	1.435	1.494	1.551	1.690	1.820	1.860	2.156	2.300	2.372
	1	0.909	0.946	1.189	1.288	1.376	1.462	1.567	1.688	1.709
	2	0.759	0.766	0.779	0.880	0.896	0.903	0.913	0.922	0.946
	3	0.593	0.608	0.618	0.621	0.637	0.707	0.757	0.788	0.793
	4	0.507	0.508	0.512	0.709	0.749	0.793	0.773	0.798	0.802
	5	0.395	0.389	0.409	0.419	0.416	0.437	0.448	0.458	0.468
	6	0.297	0.289	0.298	0.301	0.311	0.326	0.338	0.358	0.360
	7	0.237	0.236	0.248	0.257	0.267	0.278	0.287	0.299	0.309
	8	0.201	0.209	0.211	0.237	0.248	0.259	0.267	0.276	0.298
	9	0.137	0.144	0.165	0.173	0.187	0.188	0.223	0.238	0.244
	10	0.109	0.126	0.138	0.146	0.158	0.166	0.1788	0.208	0.219

7. CONCLUSION

In this article, reliability acceptance single sampling plan is developed based on the Gompertz Frechet distribution in directed to construct a decision of the lot. The single sampling plan gets the minimum sample size and Operating Characteristic values of the producer’s risk. Tables and values are provided and applied to develop an acceptance sampling plans for real life application. In real life data application can be revealed that there were no items with a failure time less than or equal to 300 hrs in the given sample of $n = 57$ observations, the experimenter

would accept the lot.

REFERENCES

- [1] Al-Nassar, A.D. and Al-Omari, A.I. (2013) Acceptance sampling plan based on truncated life tests for exponentiated Frechet distribution. *Journal of Statistics and Management Systems*,16(1):13-24.
- [2] Cameron.J.M. (1952) Tables for constructing and computing the Operating Characteristics of Single Sampling Plans *Industrial Quality Control* ,Vol. 11, pp. 37-39.
- [3] Epstein, B. (1954) Truncated life tests in the exponential case *Annals of Mathematical Statistics* ,Vol. 25, pp. 555-564.
- [4] Gupta, S.S. and Groll, P. A. (1961) Gamma distribution in acceptance sampling based on life tests. *Journal of the American Statistical Association*,Vol. 56, pp. 942-970.
- [5] Jayalakshmi.S, Neena Krishna P.K (2020) Designing of Special Type Double Sampling Plan for Life Tests Based on Percentiles Using Exponentiated Frechet Distribution *RTA*,No 1 (61) Volume 16, March 2021.
- [6] Kantam, R.R.L. and Rosaiah, K. and Rao, G.S. (1998). Half logistic distribution in acceptance sampling based on life tests. *IAPQR Transaction* ,Vol. 23, pp. 117-125.
- [7] Kantam, R.R.L. and Rosaiah, K. and Rao, G.S. (2001) Acceptance sampling based on life tests: Log-Logistic model *Journal of Applied Statistics* ,Vol. 28: 121-128.
- [8] V Kaviyarasu, P Fawaz (2017) Design of acceptance sampling plan for life tests based on percentiles using Weibull-Poisson distribution. *Int J Stat Appl Math* Vol.2(5):51-57.
- [9] Pelumi E. Oguntunde, Mundher A. Khaleel, Mohammed T. Ahmed and Hilary I. Okagbue (2019), The Gompertz Frechet distribution: Properties and applications. *Cogent Mathematics Statistics*,6: 1568662. <https://doi.org/10.1080/25742558.2019.1568662>.
- [10] Rosaiah,K. and Kantam, R.R.L (2005) Acceptance sampling based on the inverse Rayleigh distribution. *Economic Quality Control*Vol.20, pp. 277-286.
- [11] Rao, G. S, and Naidu, Ch. R. (2014), Acceptance Sampling Plans for Percentiles based on the Exponentiated half log logistic distribution *Applications and Applied Mathematics: An International Journal*,9(1): 39-53.

EXPLICIT TIME DEPENDENT SOLUTION OF A TWO- STATE RETRIAL QUEUEING MODEL WITH HETEROGENOUS SERVERS

¹Neelam Singla, ²Sonia Kalra (Corresponding Author)

•

¹Associate Professor
Department of Statistics
Punjabi University
Patiala, Punjab (147002)
neelgagan2k3@yahoo.co.in

²Assistant Professor
University School of Business
Chandigarh University,
Gharuan, Mohali (Punjab) 140413
soniakalra276@gmail.com

Abstract

In this paper, two dimensional state retrial queueing system with two non - identical parallel servers is considered. Incoming calls (primary calls) arrive at the server according to a Poisson process. Repeating calls also follows the same fashion. Service times of two servers follow exponential distribution with different rates. An incoming call that finds the servers busy, joins an orbit and retries after some random amount of time. Time dependent probabilities of exact number of arrivals and exact number of departures at when the servers are free or when one server is busy or when both servers are busy are derived for the system. Finally busy period distribution obtained to illustrate the system dynamics.

Keywords: Retrial, Queueing, Arrivals, Departures, Heterogeneous Servers

I. Introduction

Recently retrial queues are paid much attention because they have applications in performance analysis of various systems such as call centers, computer networks and telecommunication systems. Retrial queues are characterized by the fact that arriving customers when could not able to receive service may enter a virtual queue (orbit) and retry for service again after some random amount of time. The analyse of retrial queueing models are much more difficult than without retrials and explicit results are obtained only in a few special cases.

Retrial queueing models are often used for the performance and reliability modeling of computer systems and communication networks. The reason is that the return of customers plays a special role in many of these systems or in other practical applications. Some applications of retrial

queues can be found in Li and Yang [1], Janssens [2], Tran-Gia and Mandjes [3], Onur et al. [4] and the detailed overviews of retrial queues are given in Falin and Templeton [5], Artalejo [6], Falin and Artalejo [7], Artalejo [8], Falin [9].

Queues with non-identical parallel servers (heterogeneous servers) can be widely used for modeling real systems with heterogeneous environment. Heterogeneous servers are allocated in banks, hospitals, telecommunication and business centers. Customers arrive according to a Poisson process at a rate λ . The servers have a tendency to serve the same type of job but with different service rates μ_1 & μ_2 .

The classical transient results for the M/M/1 queueing model provide slight perception about the behavior of a queueing system through a fixed time t , but Pegden and Rosenshine [10] have given the probability of exact number of arrivals in the system and exact number of departures from the system by a given time for the classical queueing model M/M/1/ ∞ . This measures supplies better insight into the behavior of a queueing system than the probability of the exact number of units in the system at a given time.

In this paper, we obtained the time dependent probabilities of the exact number of arrivals in the system and exact number of departures from the system for a retrial queueing system with two servers having unequal service rates. Many authors have studied systems with two non-identical parallel servers. Satty [11] studied a continuous time first come first served queueing system with two parallel servers each with different service rate. He obtained the steady state probabilities for the number of units in the system/ queue. Gumbel [12] studied the steady state probabilities for the number of units in the system by considering a more general queueing problem having a finite number of servers, each with different service rate. Morse [13] also considered two servers with different service rates and obtained the steady state solutions.

The paper is organized as follows: In Section 2, the full description of the model is discussed. In Section 3, we defined the two-dimensional state model and derived its difference-differential equations. The time dependent solution for the model is also obtained in this section. Then the main performance measures of the system and a special case are derived in Section 4. In Section 5, several numerical examples are discussed. The busy period distribution for the system is obtained in Section 6 and finally the paper ends with a conclusion.

II. Model Description

I. Assumption and Notation

The queueing system investigated in this paper is described by the following assumptions:

- 1) The arrival of primary calls follow a Poisson distribution with parameter λ .
- 2) The repeated calls to each server follow a Poisson distribution with parameter θ .
- 3) Service times are exponentially distributed with parameters μ_1 and μ_2 for the first and second channel respectively.
- 4) When the channels are empty, an arriving unit/ repeating unit joins the first channel with probability a_1 and the second channel with probability a_2 .
- 5) The stochastic process involved viz. arrival of units, departures of unit and retrials are statistically independent.

Laplace transformation $\bar{f}(s)$ of $f(t)$ given by

$$\bar{f}(s) = \int_0^\infty e^{-st} f(t) dt, \quad \text{Re}(s) > 0$$

The Laplace inverse of

$$\frac{Q(p)}{P(p)} \text{ is } \sum_{k=1}^n \sum_{l=1}^{m_k} \frac{t^{m_k-l} e^{a_k t}}{(m_k-l)!(l-1)!} \times \frac{d^{l-1} Q(p)}{dp^{l-1} P(p)} (p - a_k)^{m_k} \forall p = a_k, a_i \neq a_k \text{ for } i \neq k$$

where,

$$P(p) = (p - a_1)^{m_1} (p - a_2)^{m_2} \dots \dots \dots (p - a_n)^{m_n}$$

Q(p) is a polynomial of degree $< m_1 + m_2 + m_3 + \dots \dots \dots m_n - 1$.

The Laplace inverse of $\bar{N}_{n_1, n_2, n_3}^{a, b, c}(s) = \frac{1}{(s+a)^{n_1} (s+b)^{n_2} (s+c)^{n_3}}$ is

$$N_{n_1, n_2, n_3}^{a, b, c}(t) = \sum_{l=1}^{n_3} \sum_{m=1}^l \frac{e^{-at} t^{n_3-l} (-1)^{m+1} \binom{l-1}{m-1} (\prod_{g_1=0}^{l-m-1} (n_1 + g_1)) (\prod_{g_2=0}^{m-2} (n_2 + g_2))}{(n_3-l)! (m-1)! (b-a)^{n_2+m-1} (c-a)^{n_1+l-m}}$$

$$+ \sum_{l=1}^{n_2} \sum_{m=1}^l \frac{e^{-bt} t^{n_2-l} (-1)^{m+1} \binom{l-1}{m-1} (\prod_{g_1=0}^{l-m-1} (n_1 + g_1)) (\prod_{g_2=0}^{m-2} (n_3 + g_2))}{(n_2-l)! (m-1)! (a-b)^{n_3+m-1} (c-b)^{n_1+l-m}}$$

$$+ \sum_{l=1}^{n_1} \sum_{m=1}^l \frac{e^{-ct} t^{n_1-l} (-1)^{m+1} \binom{l-1}{m-1} (\prod_{g_1=0}^{l-m-1} (n_2 + g_1)) (\prod_{g_2=0}^{m-2} (n_3 + g_2))}{(n_1-l)! (m-1)! (a-c)^{n_3+m-1} (b-c)^{n_2+l-m}}$$

If $L^{-1}\{f(s)\} = F(t)$ and $L^{-1}\{g(s)\} = G(t)$, then

$L^{-1}\{f(s)g(s)\} = \int_0^t F(u)G(t-u)du = F * G$, $F * G$ is called the convolution of F and G.

III. The Two-Dimensional State Model

I. Definitions

$P_{i,j,0}(t)$ = Probability that there are exactly i arrivals in the system and j departures from the system by time t when both servers are free.

$P_{i,j,1,k}(t)$ = Probability that there are exactly i arrivals in the system, j departures from the system by time t when one server is free and that unit is in the kth channel. $k = 1, 2$.

$P_{i,j,2}(t)$ = Probability that there are exactly i arrivals in the system and j departures from the system by time t when both servers are busy.

$P_{ij}(t)$ = Probability that there are exactly i arrivals in the system and j departures from the system by time t.

$$P_{ij}(t) = P_{i,j,0}(t) + P_{i,j,1,1}(t) + P_{i,j,1,2}(t) + P_{i,j,2}(t) \quad \forall i, j \quad i \geq j$$

$$P_{i,j,1}(t) = P_{i,j,1,1}(t) + P_{i,j,1,2}(t)$$

also

$$P_{i,j,0}(t) = 0, i < j; P_{i,j,1,k}(t) = 0 \ \& \ P_{i,j,2}(t) = 0, i \leq j. \quad k=1,2$$

Initially

$$P_{0,0,0}(0) = 1; P_{i,j,0}(0) = 0, P_{i,j,1,k}(0) = 0 \ \& \ P_{i,j,2}(0) = 0, i, j \neq 0. \quad k=1,2.$$

II. The difference – differential equations governing the system are

$$\frac{d}{dt} P_{i,j,0}(t) = -(\lambda + (i-j)\theta) P_{i,j,0}(t) + \mu_1 P_{i-1,j,1,1}(t) + \mu_2 P_{i-1,j,1,2}(t) \quad i \geq j \geq 0 \quad (1)$$

$$\frac{d}{dt} P_{1,0,1,1}(t) = -(\lambda + \mu_1) P_{1,0,1,1}(t) + \lambda a_1 P_{0,0,0}(t) \quad (2)$$

$$\frac{d}{dt} P_{1,0,1,2}(t) = -(\lambda + \mu_2) P_{1,0,1,2}(t) + \lambda a_2 P_{0,0,0}(t) \quad (3)$$

$$\frac{d}{dt} P_{i,j,1,1}(t) = -(\lambda + \mu_1 + (i-j-1)\theta) P_{i,j,1,1}(t) + \lambda a_1 P_{i-1,j,0}(t) + (i-j)\theta a_1 P_{i,j,0}(t) + \mu_2 P_{i,j-1,2}(t) \quad i > j > 0 \quad (4)$$

$$\frac{d}{dt} P_{i,j,1,2}(t) = -(\lambda + \mu_2 + (i-j-1)\theta) P_{i,j,1,2}(t) + \lambda a_2 P_{i-1,j,0}(t) + (i-j)\theta a_2 P_{i,j,0}(t) + \mu_1 P_{i,j-1,2}(t) \quad i > j > 0 \quad (5)$$

$$\frac{d}{dt} P_{i,0,2}(t) = -(\lambda + \mu_1 + \mu_2) P_{i,0,2}(t) + \lambda \delta_{i,2} \{P_{i-1,0,1,1}(t) + P_{i-1,0,1,2}(t)\} + \lambda (1 - \delta_{i-2,j}) P_{i-1,0,2}(t) \quad i \geq 2 \quad (6)$$

$$\frac{d}{dt} P_{i,j,2}(t) = -(\lambda + \mu_1 + \mu_2) P_{i,j,2}(t) + (i-j-1)\theta \{P_{i,j,1,1}(t) + P_{i,j,1,2}(t)\} + \lambda \{P_{i-1,j,1,1}(t) + P_{i-1,j,1,2}(t)\} + \lambda (1 - \delta_{i-2,j}) P_{i-1,j,2}(t) \quad i > 2, i > j > 0 \quad (7)$$

where $\delta_{i-2,j} = \begin{cases} 1, & \text{when } i - 2 = j \\ 0, & \text{otherwise} \end{cases}$

$$\delta_{i,2} = \begin{cases} 1, & \text{when } i = 2 \\ 0, & \text{otherwise} \end{cases}$$

Using Laplace transformation $\bar{f}(s)$ of $f(t)$ given by

$$\bar{f}(s) = \int_0^\infty e^{-st} f(t) dt, \quad \text{Re}(s) > 0$$

in the equations (1) - (7) along with the initial conditions. We have

$$(s + \lambda + (i-j)\theta)\bar{P}_{i,j,0}(s) = \mu_1 \bar{P}_{i-j,1,1}(s) + \mu_2 \bar{P}_{i-j,1,2}(s) + P_{i,j,0}(0) \quad i \geq j \geq 0 \quad (8)$$

$$(s + \lambda + \mu_1)\bar{P}_{1,0,1,1}(s) = \lambda a_1 \bar{P}_{0,0,0}(s) \quad (9)$$

$$(s + \lambda + \mu_2)\bar{P}_{1,0,1,2}(s) = \lambda a_2 \bar{P}_{0,0,0}(s) \quad (10)$$

$$(s + \lambda + \mu_1 + (i-j-1)\theta)\bar{P}_{i,j,1,1}(s) = \lambda a_1 \bar{P}_{i-1,j,0}(s) + (i-j)\theta a_1 \bar{P}_{i,j,0}(s) + \mu_2 \bar{P}_{i,j-1,2}(s) \quad i > j > 0 \quad (11)$$

$$(s + \lambda + \mu_2 + (i-j-1)\theta)\bar{P}_{i,j,1,2}(s) = \lambda a_2 \bar{P}_{i-1,j,0}(s) + (i-j)\theta a_2 \bar{P}_{i,j,0}(s) + \mu_1 \bar{P}_{i,j-1,2}(s) \quad i > j > 0 \quad (12)$$

$$(s + \lambda + \mu_1 + \mu_2)\bar{P}_{i,0,2}(s) = \lambda \delta_{i,2} \{\bar{P}_{i-1,0,1,1}(s) + \bar{P}_{i-1,0,1,2}(s)\} + \lambda (1 - \delta_{i-2,j})\bar{P}_{i-1,j,2}(s) \quad i \geq 2 \quad (13)$$

$$(s + \lambda + \mu_1 + \mu_2)\bar{P}_{i,j,2}(s) = (i-j-1)\theta \{\bar{P}_{i,j,1,1}(s) + \bar{P}_{i,j,1,2}(s)\} + \lambda \{\bar{P}_{i-1,j,1,1}(s) + \bar{P}_{i-1,j,1,2}(s)\} + \lambda (1 - \delta_{i-2,j})\bar{P}_{i-1,j,2}(s) \quad i > 2, i > j > 0 \quad (14)$$

$$\text{where } \delta_{i-2,j} = \begin{cases} 1, & \text{when } i - 2 = j \\ 0, & \text{otherwise} \end{cases}$$

$$\delta_{i,2} = \begin{cases} 1, & \text{when } i = 2 \\ 0, & \text{otherwise} \end{cases}$$

III. Solution of the Problem

Solving equations (8) to (14) recursively, we have

$$\bar{P}_{0,0,0}(s) = \frac{1}{s + \lambda} \quad (15)$$

$$\bar{P}_{1,1,0}(s) = \left(\frac{\lambda a_1}{(s + \lambda + \mu_1)(s + \lambda)^2} + \frac{\lambda a_2}{(s + \lambda + \mu_2)(s + \lambda)^2} \right) \quad (16)$$

$$\bar{P}_{i,2,0}(s) = \frac{\mu_1 \mu_2}{(s + \lambda + (i-2)\theta)} \left[\frac{1}{(s + \lambda + \mu_1 + (i-2)\theta)} + \frac{1}{(s + \lambda + \mu_2 + (i-2)\theta)} \right] \bar{P}_{i,0,2}(s) \quad i \geq 3 \quad (17)$$

$$\bar{P}_{1,0,1,1}(s) = \frac{1}{s + \lambda} \frac{\lambda a_1}{(s + \lambda + \mu_1)} \quad (18)$$

$$\bar{P}_{1,0,1,2}(s) = \frac{1}{s + \lambda} \frac{\lambda a_2}{(s + \lambda + \mu_2)} \quad (19)$$

$$\bar{P}_{2,1,1,1}(s) = \frac{\lambda a_1}{(s + \lambda + \mu_1)} \bar{P}_{1,1,0}(s) + \left[\frac{\mu_2}{(s + \lambda + \mu_1)} \left(\frac{\lambda}{(s + \lambda + \mu_1 + \mu_2)} \right) \{\bar{P}_{1,0,1,1}(s) + \bar{P}_{1,0,1,2}(s)\} \right] \quad (20)$$

$$\bar{P}_{2,1,1,2}(s) = \frac{\lambda a_2}{(s + \lambda + \mu_2)} \bar{P}_{1,1,0}(s) + \left[\frac{\mu_1}{(s + \lambda + \mu_2)} \left(\frac{\lambda}{(s + \lambda + \mu_1 + \mu_2)} \right) \{\bar{P}_{1,0,1,1}(s) + \bar{P}_{1,0,1,2}(s)\} \right] \quad (21)$$

$$\bar{P}_{i,1,1,1}(s) = \left(\frac{\mu_2}{(s + \lambda + \mu_1 + (i-2)\theta)} \frac{\lambda^{i-1}}{(s + \lambda + \mu_1 + \mu_2)^{i-1}} \{\bar{P}_{1,0,1,1}(s) + \bar{P}_{1,0,1,2}(s)\} \right) \quad i > 2 \quad (22)$$

$$\bar{P}_{i,1,1,2}(s) = \left(\frac{\mu_1}{(s + \lambda + \mu_2 + (i-2)\theta)} \frac{\lambda^{i-1}}{(s + \lambda + \mu_1 + \mu_2)^{i-1}} \{\bar{P}_{1,0,1,1}(s) + \bar{P}_{1,0,1,2}(s)\} \right) \quad i > 2 \quad (23)$$

$$\bar{P}_{i,0,2}(s) = \frac{\lambda^{i-1}}{(s + \lambda + \mu_1 + \mu_2)^{i-1}} \{\bar{P}_{1,0,1,1}(s) + \bar{P}_{1,0,1,2}(s)\} \quad i > 1 \quad (24)$$

$$\bar{P}_{i,j,2}(s) = \left(\sum_{k=1}^{i-j} \left(\frac{\lambda}{s + \lambda + \mu_1 + \mu_2} \right)^{i-j-k} \eta'_k(s) \{\bar{P}_{j+k,j,1,1}(s) + \bar{P}_{j+k,j,1,2}(s)\} \right) \quad i \geq j+2, j \geq 1 \quad (25)$$

$$\text{where } \eta'_k(s) = \begin{cases} 1 & \text{for } k = 1 \\ \left(1 + \frac{(k-1)\theta}{s + \lambda + \mu_1 + \mu_2} \right) & \text{for } k = 2 \text{ to } i - j - 1 \\ \frac{(k-1)\theta}{s + \lambda + \mu_1 + \mu_2} & \text{for } k = i - j \end{cases}$$

$$\bar{P}_{i,i-1,1,1}(s) = \frac{\lambda a_1}{(s + \lambda + \mu_1)} \bar{P}_{i-1,i-1,0}(s) + \frac{\theta a_1}{(s + \lambda + \mu_1)} \bar{P}_{i,i-1,0}(s) + \frac{\mu_2}{(s + \lambda + \mu_1)} \bar{P}_{i,i-2,2}(s) \quad i > 2 \quad (26)$$

$$\bar{P}_{i,i-1,1,2}(s) = \frac{\lambda a_2}{(s+\lambda+\mu_2)} \bar{P}_{i-1,i-1,0}(s) + \frac{\theta a_2}{(s+\lambda+\mu_2)} \bar{P}_{i,i-1,0}(s) + \frac{\mu_1}{(s+\lambda+\mu_2)} \bar{P}_{i,i-2,2}(s) \quad i > 2 \tag{27}$$

$$\bar{P}_{i,j,1,1}(s) = \frac{\lambda a_1}{(s+\lambda+\mu_1+(i-j-1)\theta)} \bar{P}_{i-1,j,0}(s) + \frac{(i-j)\theta a_1}{(s+\lambda+\mu_1+(i-j-1)\theta)} \bar{P}_{i,j,0}(s) + \frac{\mu_2}{(s+\lambda+\mu_1+(i-j-1)\theta)} \left(\sum_{k=0}^{i-j} \left(\frac{\lambda}{s+\lambda+\mu_1+\mu_2} \right)^{i-j-k} \eta'_k(s) \{ \bar{P}_{j+k,j-1,1,1}(s) + \bar{P}_{j+k,j-1,1,2}(s) \} \right) \quad i \geq j+2, j \geq 2 \tag{28}$$

$$\text{where } \eta'_k(s) = \begin{cases} 1 & \text{for } k = 0 \\ \left(1 + \frac{k\theta}{s + \lambda + \mu_1 + \mu_2} \right) & \text{for } k = 1 \text{ to } i - j - 1 \\ \frac{k\theta}{s + \lambda + \mu_1 + \mu_2} & \text{for } k = i - j \end{cases}$$

$$\bar{P}_{i,j,1,2}(s) = \frac{\lambda a_2}{(s+\lambda+\mu_2+(i-j-1)\theta)} \bar{P}_{i-1,j,0}(s) + \frac{(i-j)\theta a_2}{(s+\lambda+\mu_2+(i-j-1)\theta)} \bar{P}_{i,j,0}(s) + \frac{\mu_1}{(s+\lambda+\mu_2+(i-j-1)\theta)} \left(\sum_{k=0}^{i-j} \left(\frac{\lambda}{s+\lambda+\mu_1+\mu_2} \right)^{i-j-k} \eta'_k(s) \{ \bar{P}_{j+k,j-1,1,1}(s) + \bar{P}_{j+k,j-1,1,2}(s) \} \right) \quad i \geq j+2, j \geq 2 \tag{29}$$

$$\text{where } \eta'_k(s) = \begin{cases} 1 & \text{for } k = 0 \\ \left(1 + \frac{k\theta}{s + \lambda + \mu_1 + \mu_2} \right) & \text{for } k = 1 \text{ to } i - j - 1 \\ \frac{k\theta}{s + \lambda + \mu_1 + \mu_2} & \text{for } k = i - j \end{cases}$$

$$\bar{P}_{i,i,0}(s) = \left(\frac{\lambda}{(s+\lambda)} \right) \left[\frac{\mu a_1}{(s+\lambda+\mu_1)} + \frac{\mu a_2}{(s+\lambda+\mu_2)} \right] \bar{P}_{i-1,i-1,0}(s) + \left(\frac{\theta}{(s+\lambda)} \right) \left[\frac{\mu a_1}{(s+\lambda+\mu_1)} + \frac{\mu a_2}{(s+\lambda+\mu_2)} \right] \bar{P}_{i,i-1,0}(s) + \left(\frac{\mu_1+\mu_2}{(s+\lambda)} \right) \left[\frac{1}{(s+\lambda+\mu_1)} + \frac{1}{(s+\lambda+\mu_2)} \right] \bar{P}_{i,i-2,2}(s) \quad i > 1 \tag{30}$$

$$\begin{aligned} & \bar{P}_{i,j,0}(s) \\ &= \frac{\mu_1}{(s+\lambda+(i-j)\theta)} \left\{ \frac{\lambda a_1}{(s+\lambda+\mu_1+(i-j)\theta)} \bar{P}_{i-1,j-1,0}(s) + \frac{(i-j+1)\theta a_1}{(s+\lambda+\mu_1+(i-j)\theta)} \bar{P}_{i,j-1,0}(s) \right. \\ &+ \left. \frac{\mu_2}{(s+\lambda+\mu_1+(i-j)\theta)} \left(\sum_{k=0}^{i-j+1} \left(\frac{\lambda}{s+\lambda+\mu_1+\mu_2} \right)^{\{(i-j)+1\}-k} \eta'_k(s) \{ \bar{P}_{(j-1)+k,j-2,1,1}(s) + \bar{P}_{(j-1)+k,j-2,1,2}(s) \} \right) \right\} \\ &+ \frac{\mu_2}{(s+\lambda+(i-j)\theta)} \left\{ \frac{\lambda a_2}{(s+\lambda+\mu_2+(i-j)\theta)} \bar{P}_{i-1,j-1,0}(s) + \frac{(i-j+1)\theta a_2}{(s+\lambda+\mu_2+(i-j)\theta)} \bar{P}_{i,j-1,0}(s) \right. \\ &+ \left. \frac{\mu_1}{(s+\lambda+\mu_2+(i-j)\theta)} \left(\sum_{k=0}^{i-j+1} \left(\frac{\lambda}{s+\lambda+\mu_1+\mu_2} \right)^{\{(i-j)+1\}-k} \eta'_k(s) \{ \bar{P}_{(j-1)+k,j-2,1,1}(s) + \bar{P}_{(j-1)+k,j-2,1,2}(s) \} \right) \right\} \quad i > j \geq 3 \tag{31} \end{aligned}$$

$$\text{where } \eta'_k(s) = \begin{cases} 1 & \text{for } k = 0 \\ \left(1 + \frac{k\theta}{s + \lambda + \mu_1 + \mu_2} \right) & \text{for } k = 1 \text{ to } i - j \\ \frac{k\theta}{s + \lambda + \mu_1 + \mu_2} & \text{for } k = i - j + 1 \end{cases}$$

Taking the Inverse Laplace transform of equations (15) to (31), we have

$$P_{0,0,0}(t) = e^{-\lambda t} \tag{32}$$

$$P_{1,1,0}(t) = \lambda \mu_1 a_1 (te^{-\lambda t}) e^{-(\lambda+\mu_1)t} + \lambda \mu_2 a_2 (te^{-\lambda t}) e^{-(\lambda+\mu_2)t} \tag{33}$$

$$P_{i,2,0}(t) = \mu_1 \mu_2 e^{-(\lambda+(i-2)\theta)t} \left(\frac{1}{(\mu_1+(i-2)\theta)} - \frac{e^{-(\mu_1+(i-2)\theta)t}}{(\mu_1+(i-2)\theta)} \right) * P_{i,0,2}(t) + \mu_1 \mu_2 e^{-(\lambda+(i-2)\theta)t} \left(\frac{1}{(\mu_2+(i-2)\theta)} - \frac{e^{-(\mu_2+(i-2)\theta)t}}{(\mu_2+(i-2)\theta)} \right) * P_{i,0,2}(t)$$

$$\frac{e^{-(\mu_2+(i-2)\theta)t}}{(\mu_2+(i-2)\theta)} * P_{i,0,2}(t) \quad i \geq 3 \quad (34)$$

$$P_{1,0,1,1}(t) = \lambda a_1 e^{-\lambda t} \times \left(\frac{1}{\mu_1} - \frac{e^{-\mu_1 t}}{\mu_1} \right) \quad (35)$$

$$P_{1,0,1,2}(t) = \lambda a_2 e^{-\lambda t} \times \left(\frac{1}{\mu_2} - \frac{e^{-\mu_2 t}}{\mu_2} \right) \quad (36)$$

$$P_{2,1,1,1}(t) = \lambda a_1 e^{-(\lambda+\mu_1)t} * P_{1,1,0}(t) + \left(\lambda \mu_2 e^{-(\lambda+\mu_1)t} \left(\frac{1}{\mu_1+\mu_2} - \frac{e^{-(\mu_1+\mu_2)t}}{\mu_1+\mu_2} \right) * \{P_{1,0,1,1}(t) + P_{1,0,1,2}(t)\} \right) \quad (37)$$

$$P_{2,1,1,2}(t) = \lambda a_2 e^{-(\lambda+\mu_2)t} * P_{1,1,0}(t) + \left(\lambda \mu_1 e^{-(\lambda+\mu_2)t} \left(\frac{1}{\mu_1+\mu_2} - \frac{e^{-(\mu_1+\mu_2)t}}{\mu_1+\mu_2} \right) * \{P_{1,0,1,1}(t) + P_{1,0,1,2}(t)\} \right) \quad (38)$$

$$P_{i,1,1,1}(t) = \left[\left(\mu_2 \lambda^{i-1} e^{-(\lambda+\mu_1+(i-2)\theta)t} \left\{ \frac{1}{(\mu_1+\mu_2)^{i-1}} - e^{-(\mu_1+\mu_2)t} \sum_{r=0}^{i-2} \frac{(t)^r}{r!} \frac{1}{(\mu_1+\mu_2)^{i-r}} \right\} \right) * \{P_{1,0,1,1}(t) + P_{1,0,1,2}(t)\} \right] \quad i > 2 \quad (39)$$

$$P_{i,1,1,2}(t) = \left[\left(\mu_1 \lambda^{i-1} e^{-(\lambda+\mu_2+(i-2)\theta)t} \left\{ \frac{1}{(\mu_1+\mu_2)^{i-1}} - e^{-(\mu_1+\mu_2)t} \sum_{r=0}^{i-2} \frac{(t)^r}{r!} \frac{1}{(\mu_1+\mu_2)^{i-r}} \right\} \right) * \{P_{1,0,1,1}(t) + P_{1,0,1,2}(t)\} \right] \quad i > 2 \quad (40)$$

$$P_{i,0,2}(t) = \left(\lambda^{i-1} \frac{t^{i-2}}{(i-2)!} e^{-(\lambda+\mu_1+\mu_2)t} \right) * P_{1,0,1,1}(t) + \left(\lambda^{i-1} \frac{t^{i-2}}{(i-2)!} e^{-(\lambda+\mu_1+\mu_2)t} \right) * P_{1,0,1,2}(t) \quad i > 1 \quad (41)$$

$$P_{i,j,2}(t) = \left(\left(\lambda^{i-j-1} \frac{t^{i-j-2}}{(i-j-2)!} e^{-(\lambda+\mu_1+\mu_2)t} \right) * \{P_{j+1,j,1,1}(t) + P_{j+1,j,1,2}(t)\} \right) + \left(\sum_{k=2}^{i-j-1} \left(\lambda^{i-j-k} \frac{t^{i-j-k-1}}{(i-j-k-1)!} e^{-(\lambda+\mu_1+\mu_2)t} \right) * \{P_{j+k,j,1,1}(t) + P_{j+k,j,1,2}(t)\} \right) + \left(\sum_{k=2}^{i-j-1} \left(\lambda^{i-j-k} (k-1) \theta \frac{t^{i-j-k}}{(i-j-k)!} e^{-(\lambda+\mu_1+\mu_2)t} \right) * \{P_{j+k,j,1,1}(t) + P_{j+k,j,1,2}(t)\} \right) + \left((i-j-1) \theta e^{-(\lambda+\mu_1+\mu_2)t} \right) * \{P_{i,j,1,1}(t) + P_{i,j,1,2}(t)\} \quad i \geq j+2, j \geq 1 \quad (42)$$

$$P_{i,i-1,1,1}(t) = \lambda a_1 e^{-(\lambda+\mu_1)t} * P_{i-1,i-1,0}(t) + \theta a_1 e^{-(\lambda+\mu_1)t} * P_{i,i-1,0}(t) + \mu_2 e^{-(\lambda+\mu_1)t} * P_{i,i-2,2}(t) \quad i > 2 \quad (43)$$

$$P_{i,i-1,1,2}(t) = \lambda a_2 e^{-(\lambda+\mu_2)t} * P_{i-1,i-1,0}(t) + \theta a_2 e^{-(\lambda+\mu_2)t} * P_{i,i-1,0}(t) + \mu_1 e^{-(\lambda+\mu_2)t} * P_{i,i-2,2}(t) \quad i > 2 \quad (44)$$

$$P_{i,j,1,1}(t) = \lambda a_1 e^{-(\lambda+\mu_1+(i-j-1)\theta)t} * P_{i-1,j,0}(t) + (i-j) \theta a_1 e^{-(\lambda+\mu_1+(i-j-1)\theta)t} * P_{i,j,0}(t) + \left[\mu_2 \lambda^{i-j} e^{-(\lambda+\mu_1+(i-j-1)\theta)t} \left\{ \frac{1}{(\mu_1+\mu_2)^{i-j}} - e^{-(\mu_1+\mu_2)t} \sum_{r=0}^{i-j-1} \frac{(t)^r}{r!} \frac{1}{(\mu_1+\mu_2)^{i-j-r}} \right\} * \{P_{j,j-1,1,1}(t) + P_{j,j-1,1,2}(t)\} \right] + \left[\mu_2 e^{-(\lambda+\mu_1+(i-j-1)\theta)t} \sum_{k=1}^{i-j-1} \lambda^{i-j-k} \left\{ \frac{1}{(\mu_1+\mu_2)^{i-j-k}} - e^{-(\mu_1+\mu_2)t} \sum_{r=0}^{i-j-k-1} \frac{(t)^r}{r!} \frac{1}{(\mu_1+\mu_2)^{i-j-k-r}} \right\} * \{P_{j+k,j-1,1,1}(t) + P_{j+k,j-1,1,2}(t)\} \right] + \left[\mu_2 e^{-(\lambda+\mu_1+(i-j-1)\theta)t} \sum_{k=1}^{i-j-1} \lambda^{i-j-k} (k\theta) \left\{ \frac{1}{(\mu_1+\mu_2)^{i-j-k+1}} - e^{-(\mu_1+\mu_2)t} \sum_{r=0}^{i-j-k} \frac{(t)^r}{r!} \frac{1}{(\mu_1+\mu_2)^{i-j-k+1-r}} \right\} * \{P_{j+k,j-1,1,1}(t) + P_{j+k,j-1,1,2}(t)\} \right]$$

$$+ \left[\mu_2(i-j)\theta e^{-(\lambda+\mu_1+(i-j-1)\theta)t} \times \left(\frac{1}{(\mu_1+\mu_2)} - \frac{e^{-(\mu_1+\mu_2)t}}{(\mu_1+\mu_2)} \right) * \{P_{i,j-1,1,1}(t) + P_{i,j-1,1,2}(t)\} \right]$$

$i \geq j+2, j \geq 2$ (45)

$$P_{i,j,1,2}(t) = \lambda a_2 e^{-(\lambda+\mu_2+(i-j-1)\theta)t} * P_{i-1,j,0}(t) + (i-j)\theta a_2 e^{-(\lambda+\mu_2+(i-j-1)\theta)t} * P_{i,j,0}(t)$$

$$+ \left[\mu_1 \lambda^{i-j} e^{-(\lambda+\mu_2+(i-j-1)\theta)t} \left\{ \frac{1}{(\mu_1+\mu_2)^{i-j}} - e^{-(\mu_1+\mu_2)t} \sum_{r=0}^{i-j-1} \frac{(t)^r}{r! (\mu_1+\mu_2)^{i-j-r}} \right\} * \{P_{j,j-1,1,1}(t) + P_{j,j-1,1,2}(t)\} \right] +$$

$$\left[\mu_1 e^{-(\lambda+\mu_2+(i-j-1)\theta)t} \sum_{k=1}^{i-j-1} \lambda^{i-j-k} \left\{ \frac{1}{(\mu_1+\mu_2)^{i-j-k}} - e^{-(\mu_1+\mu_2)t} \sum_{r=0}^{i-j-k-1} \frac{(t)^r}{r! (\mu_1+\mu_2)^{i-j-k-r}} \right\} * \{P_{j+k,j-1,1,1}(t) + P_{j+k,j-1,1,2}(t)\} \right] +$$

$$\left[\mu_1 e^{-(\lambda+\mu_2+(i-j-1)\theta)t} \sum_{k=1}^{i-j-1} \lambda^{i-j-k} (k\theta) \left\{ \frac{1}{(\mu_1+\mu_2)^{i-j-k+1}} - e^{-(\mu_1+\mu_2)t} \sum_{r=0}^{i-j-k} \frac{(t)^r}{r! (\mu_1+\mu_2)^{i-j-k+1-r}} \right\} * \{P_{j+k,j-1,1,1}(t) + P_{j+k,j-1,1,2}(t)\} \right]$$

$$+ \left[\mu_1(i-j)\theta e^{-(\lambda+\mu_2+(i-j-1)\theta)t} \times \left(\frac{1}{(\mu_1+\mu_2)} - \frac{e^{-(\mu_1+\mu_2)t}}{(\mu_1+\mu_2)} \right) * \{P_{i,j-1,1,1}(t) + P_{i,j-1,1,2}(t)\} \right]$$

$i \geq j+2, j \geq 2$ (46)

$$P_{i,i,0}(t) = \left(\lambda \mu_1 a_1 e^{-\lambda t} \left(\frac{1}{\mu_1} - \frac{e^{-\mu_1 t}}{\mu_1} \right) + \lambda \mu_2 a_2 e^{-\lambda t} \left(\frac{1}{\mu_2} - \frac{e^{-\mu_2 t}}{\mu_2} \right) \right) * P_{i-1,i-1,0}(t) +$$

$$\left(\mu_1 \theta a_1 e^{-\lambda t} \left(\frac{1}{\mu_1} - \frac{e^{-\mu_1 t}}{\mu_1} \right) + \mu_2 \theta a_2 e^{-\lambda t} \left(\frac{1}{\mu_2} - \frac{e^{-\mu_2 t}}{\mu_2} \right) \right) * P_{i-1,i,0}(t) +$$

$$\left(\mu_1 \mu_2 e^{-\lambda t} \left(\frac{1}{\mu_1} - \frac{e^{-\mu_1 t}}{\mu_1} \right) + \mu_1 \mu_2 e^{-\lambda t} \left(\frac{1}{\mu_2} - \frac{e^{-\mu_2 t}}{\mu_2} \right) \right) * P_{i,i-2,2}(t)$$

$i > 1$ (47)

$$P_{i,j,0}(t) = \mu_1 \lambda a_1 e^{-(\lambda+(i-j)\theta)t} \left(\frac{1}{\mu_1+(i-j)\theta} - \frac{e^{-(\mu_1+(i-j)\theta)t}}{\mu_1+(i-j)\theta} \right) * P_{i-1,j-1,0}(t) +$$

$$\mu_1(i-j+1)\theta a_1 e^{-(\lambda+(i-j)\theta)t} \left(\frac{1}{\mu_1+(i-j)\theta} - \frac{e^{-(\mu_1+(i-j)\theta)t}}{\mu_1+(i-j)\theta} \right) * P_{i,j-1,0}(t) +$$

$$\left[\mu_1 \mu_2 \lambda^{i-j+1} \left[\sum_{l=1}^{i-j+1} \sum_{m=1}^l \frac{e^{-(\lambda+(i-j)\theta)t} t^{(i-j+1)-l} (-1)^{m+1} \binom{l-1}{m-1} (\prod_{g_1=0}^{l-m-1} (1+g_1)) (\prod_{g_2=0}^{m-2} (1+g_2))}{((i-j+1)-l)!(m-1)! (\mu_1)^m (\mu_1+\mu_2-(i-j)\theta)^{1+l-m}} - \frac{e^{-(\lambda+\mu_1+(i-j)\theta)t}}{(\mu_1)^{(i-j+1)}(\mu_1-(i-j)\theta)} + \frac{e^{-(\lambda+\mu_1+\mu_2)t}}{(\mu_1+\mu_2-(i-j)\theta)^{(i-j+1)}(\mu_1-(i-j)\theta)} \right] * \{P_{j-1,j-2,1,1}(t) + P_{j-1,j-2,1,2}(t)\} \right] +$$

$$\left[\mu_1 \mu_2 \sum_{k=1}^{i-j} \lambda^{(i-j+1)-k} \left[\sum_{l=1}^{(i-j+1)-k} \sum_{m=1}^l \frac{e^{-(\lambda+(i-j)\theta)t} t^{((i-j+1)-k)-l} (-1)^{m+1} \binom{l-1}{m-1} (\prod_{g_1=0}^{l-m-1} (1+g_1)) (\prod_{g_2=0}^{m-2} (1+g_2))}{(((i-j+1)-k)-l)!(m-1)! (\mu_1)^m (\mu_1+\mu_2-(i-j)\theta)^{1+l-m}} - \frac{e^{-(\lambda+\mu_1+(i-j)\theta)t}}{(\mu_1)^{((i-j+1)-k)}(\mu_1-(i-j)\theta)} + \frac{e^{-(\lambda+\mu_1+\mu_2)t}}{(\mu_1+\mu_2-(i-j)\theta)^{((i-j+1)-k)}(\mu_1-(i-j)\theta)} \right] * \{P_{(j-1)+k,j-2,1,1}(t) + P_{(j-1)+k,j-2,1,2}(t)\} \right] +$$

$$\left[\mu_1 \mu_2 \sum_{k=1}^{i-j} (k\theta) \lambda^{(i-j+1)-k} \left[\sum_{l=1}^{((i-j+1)-k)+1} \sum_{m=1}^l \frac{e^{-(\lambda+(i-j)\theta)t} t^{(((i-j+1)-k)+1)-l} (-1)^{m+1} \binom{l-1}{m-1} (\prod_{g_1=0}^{l-m-1} (1+g_1)) (\prod_{g_2=0}^{m-2} (1+g_2))}{(((i-j+1)-k)+1)-l)!(m-1)! (\mu_1)^m (\mu_1+\mu_2-(i-j)\theta)^{1+l-m}} - \frac{e^{-(\lambda+\mu_1+(i-j)\theta)t}}{(\mu_1)^{(((i-j+1)-k)+1)}(\mu_1-(i-j)\theta)} + \frac{e^{-(\lambda+\mu_1+\mu_2)t}}{(\mu_1+\mu_2-(i-j)\theta)^{(((i-j+1)-k)+1)}(\mu_1-(i-j)\theta)} \right] * \{P_{(j-1)+k,j-2,1,1}(t) + P_{(j-1)+k,j-2,1,2}(t)\} \right]$$

$$\begin{aligned}
 & + \left[\mu_1 \mu_2 (i-j+1) \theta \left[\frac{e^{-(\lambda+(i-j)\theta)t}}{(\mu_1)(\mu_1+\mu_2-(i-j)\theta)} - \frac{e^{-(\lambda+\mu_1+(i-j)\theta)t}}{(\mu_1)(\mu_1-(i-j)\theta)} + \frac{e^{-(\lambda+\mu_1+\mu_2)t}}{(\mu_1+\mu_2-(i-j)\theta)(\mu_1-(i-j)\theta)} \right] * \{P_{i,j-2,1,1}(t) + \right. \\
 & \quad \left. P_{i,j-2,1,2}(t)\} \right] + \\
 & \quad \mu_2 \lambda a_2 e^{-(\lambda+(i-j)\theta)t} \left(\frac{1}{\mu_2+(i-j)\theta} - \frac{e^{-(\mu_2+(i-j)\theta)t}}{\mu_2+(i-j)\theta} \right) * P_{i-1,j-1,0}(t) + \\
 & \quad \mu_2 (i-j+1) \theta a_2 e^{-(\lambda+(i-j)\theta)t} \left(\frac{1}{\mu_2+(i-j)\theta} - \frac{e^{-(\mu_2+(i-j)\theta)t}}{\mu_2+(i-j)\theta} \right) * P_{i,j-1,0}(t) + \\
 & \quad \left[\mu_1 \mu_2 \lambda^{i-j+1} \left[\sum_{l=1}^{i-j+1} \sum_{m=1}^l \frac{e^{-(\lambda+(i-j)\theta)t} t^{(i-j+1)-l} (-1)^{m+1} \binom{l-1}{m-1} (\prod_{g_1=0}^{l-m-1} (1+g_1)) (\prod_{g_2=0}^{m-2} (1+g_2))}{((i-j+1)-l)!(m-1)! (\mu_2)^m (\mu_1+\mu_2-(i-j)\theta)^{1+l-m}} - \right. \right. \\
 & \quad \left. \frac{e^{-(\lambda+\mu_2+(i-j)\theta)t}}{(\mu_2)^{(i-j+1)}(\mu_2-(i-j)\theta)} + \frac{e^{-(\lambda+\mu_1+\mu_2)t}}{(\mu_1+\mu_2-(i-j)\theta)^{(i-j+1)}(\mu_2-(i-j)\theta)} \right] * \{P_{j-1,j-2,1,1}(t) + P_{j-1,j-2,1,2}(t)\} + \\
 & \quad \left[\mu_1 \mu_2 \sum_{k=1}^{i-j} \lambda^{(i-j+1)-k} \left[\sum_{l=1}^{(i-j+1)-k} \sum_{m=1}^l \frac{e^{-(\lambda+(i-j)\theta)t} t^{((i-j+1)-k)-l} (-1)^{m+1} \binom{l-1}{m-1} (\prod_{g_1=0}^{l-m-1} (1+g_1)) (\prod_{g_2=0}^{m-2} (1+g_2))}{(((i-j+1)-k)-l)!(m-1)! (\mu_2)^m (\mu_1+\mu_2-(i-j)\theta)^{1+l-m}} - \right. \right. \\
 & \quad \left. \frac{e^{-(\lambda+\mu_2+(i-j)\theta)t}}{(\mu_2)^{((i-j+1)-k)}(\mu_2-(i-j)\theta)} + \frac{e^{-(\lambda+\mu_1+\mu_2)t}}{(\mu_1+\mu_2-(i-j)\theta)^{((i-j+1)-k)}(\mu_2-(i-j)\theta)} \right] * \{P_{(j-1)+k,j-2,1,1}(t) + \\
 & \quad \left. P_{(j-1)+k,j-2,1,2}(t)\} + \mu_1 \mu_2 \sum_{k=1}^{i-j} (k\theta) \lambda^{(i-j+1)-k} \right. \\
 & \quad \left. \left[\left(\frac{\sum_{l=1}^{((i-j+1)-k)+1} \sum_{m=1}^l \frac{e^{-(\lambda+(i-j)\theta)t} t^{(((i-j+1)-k)+1)-l} (-1)^{m+1} \binom{l-1}{m-1} (\prod_{g_1=0}^{l-m-1} (1+g_1)) (\prod_{g_2=0}^{m-2} (1+g_2))}{(((i-j+1)-k)+1)-l)!(m-1)! (\mu_2)^m (\mu_1+\mu_2-(i-j)\theta)^{1+l-m}}}{e^{-(\lambda+\mu_1+\mu_2)t}} + \frac{e^{-(\lambda+\mu_1+\mu_2)t}}{(\mu_2)^{(((i-j+1)-k)+1)}(\mu_2-(i-j)\theta)} + \frac{e^{-(\lambda+\mu_1+\mu_2)t}}{(\mu_1+\mu_2-(i-j)\theta)^{((i-j+1)-k)+1}(\mu_2-(i-j)\theta)} \right) \right. \\
 & \quad \left. * \{P_{(j-1)+k,j-2,1,1}(t) + P_{(j-1)+k,j-2,1,2}(t)\} \right] \\
 & + \left[\mu_1 \mu_2 (i-j+1) \theta \left[\frac{e^{-(\lambda+(i-j)\theta)t}}{(\mu_2)(\mu_1+\mu_2-(i-j)\theta)} - \frac{e^{-(\lambda+\mu_2+(i-j)\theta)t}}{(\mu_2)(\mu_2-(i-j)\theta)} + \frac{e^{-(\lambda+\mu_1+\mu_2)t}}{(\mu_1+\mu_2-(i-j)\theta)(\mu_2-(i-j)\theta)} \right] * \{P_{i,j-2,1,1}(t) + \right. \\
 & \quad \left. P_{i,j-2,1,2}(t)\} \right] \quad i > j \geq 3 \tag{48}
 \end{aligned}$$

IV. Measures of Effectiveness

I. The Laplace transform of the probability $P_i(t)$ that exactly i units arrive by time t is :

$$\bar{P}_i(s) = \sum_{j=0}^i \bar{P}_{i,j}(s) = \frac{\lambda^i}{(s+\lambda)^{i+1}} ; i > 0 \tag{49}$$

And its Inverse Laplace transform is

$$P_i(t) = \frac{e^{-\lambda t} (\lambda t)^i}{i!} \tag{50}$$

The basic assumption on primary arrivals is that it forms a Poisson process and above analysis of abstract solution also verifies the same.

II. The probability that exactly j customers have been served by time t. $P_j(t)$ in terms of $P_{i,j}(t)$ is given by:

$$P_j(t) = \sum_{i=j}^{\infty} P_{i,j}(t)$$

III. From the abstract solution of our model, we verified that the sum of all possible probabilities is one i.e. taking summation over i and j on equations (15)-(31) and adding, we get

$$\sum_{i=0}^{\infty} \sum_{j=0}^i \{ \bar{P}_{i,j,0}(s) + \bar{P}_{i,j,1,1}(s) + \bar{P}_{i,j,1,2}(s) + \bar{P}_{i,j,2}(s) \} = \frac{1}{s}$$

Taking inverse Laplace transformation, we get

$$\sum_{i=0}^{\infty} \sum_{j=0}^i \{ P_{i,j,0}(t) + P_{i,j,1,1}(t) + P_{i,j,1,2}(t) + P_{i,j,2}(t) \} = 1,$$

which is a verification of our results.

IV. Converting two-state model into single state model:

Define $Q_{n,m}(t)$ as the probability that there are n customers in the system at time t and the servers are free or busy according as $m=0,1,2$.

The probability of exactly n customers in the system at time t in terms of $P_{i,j,0}(t)$ and $P_{i,j,m}(t)$:

When the server is free, it is defined by probability $Q_{n,0}(t)$

$$Q_{n,0}(t) = \sum_{j=0}^{\infty} P_{j+n,j,0}(t)$$

In this case, the number of customers in the orbit is calculated with the help of following formula:

$n = (\text{number of arrivals} - \text{number of departures})$

When only one server ($m=1$) is busy, it is defined by probability $Q_{n,m,k}(t)$

$$Q_{n,m,k}(t) = \sum_{j=0}^{\infty} P_{j+n+m,j,m,k}(t) \quad (\mathbf{k = 1, 2})$$

In this case, the number of customers in the orbit is calculated with the help of following formula:

$n = (\text{number of arrivals} - \text{number of departures} - m)$

When both servers ($m=2$) are busy, it is defined by probability $Q_{n,m}(t)$

$$Q_{n,m}(t) = \sum_{j=0}^{\infty} P_{j+n+m,j,m}(t)$$

In this case, the number of customers in the orbit is calculated with the help of following formula:

$n = (\text{number of arrivals} - \text{number of departures} - m)$

Using above definitions and letting $\mu_1 = \mu_2 = 1$ from the equations (1) to (7) the set of equations in statistical equilibrium are:

$$(\lambda + n\theta) Q_{n,0} = Q_{n,1} \quad n \geq 0 \quad (51)$$

$$(\lambda + n\theta + 1) Q_{n,1} = \lambda a_1 Q_{n,0} + (n+1)\theta a_1 Q_{n+1,0} + Q_{n,2} \quad n \geq 0 \quad (52)$$

$$(\lambda + n\theta + 1) Q_{n,1,2} = \lambda a_2 Q_{n,0} + (n+1)\theta a_2 Q_{n+1,0} + Q_{n,2} \quad n \geq 0 \quad (53)$$

$$(\lambda + 2) Q_{n,2} = \lambda Q_{n,1} + (n+1)\theta Q_{n+1,1} + \lambda Q_{n-1,2}(1 - \delta_{n,0}) \quad n \geq 0 \quad (54)$$

where $\delta_{n,0} = \begin{cases} 1, & \text{when } n = 0 \\ 0, & \text{when } n \geq 1 \end{cases}$

Using $Q_{n,1,1} + Q_{n,1,2} = Q_{n,1}$ and letting $a_1 = a_2 = \frac{1}{2}$ in equations (51) to (54) then the set of equations are:

$$(\lambda + n\theta) Q_{n,0} = Q_{n,1} \quad n \geq 0 \quad (55)$$

$$(\lambda + n\theta + 1) Q_{n,1} = \lambda Q_{n,0} + (n+1)\theta Q_{n+1,0} + 2Q_{n,2} \quad n \geq 0 \quad (56)$$

$$(\lambda + 2) Q_{n,2} = \lambda Q_{n,1} + (n+1)\theta Q_{n+1,1} + \lambda Q_{n-1,2}(1 - \delta_{n,0}) \quad n \geq 0 \quad (57)$$

where $\delta_{n,0} = \begin{cases} 1, & \text{when } n = 0 \\ 0, & \text{when } n \geq 1 \end{cases}$

which coincide with the results (2.1) - (2.3) of Falin and Templeton [5].

V. Special Case:

When there are two servers then various probabilities can be obtained from equations (32) to (48) by letting $\mu_1 = \mu_2 = \mu$, $a_1 = a_2 = \frac{1}{2}$ and using the relation $P_{i,j,1,1}(t) + P_{i,j,1,2}(t) = P_{i,j,1}(t)$, we get

$$P_{1,0,1}(t) = \lambda e^{-\lambda t} \times \left(\frac{1}{\mu} - \frac{e^{-\mu t}}{\mu} \right) \quad (58)$$

$$P_{1,1,0}(t) = \lambda \mu (t e^{-\lambda t}) e^{-(\lambda + \mu)t} \quad (59)$$

$$P_{i,0,2}(t) = \left(\lambda^{i-1} \frac{t^{i-2}}{(i-2)!} e^{-(\lambda+2\mu)t} \right) * P_{1,0,1}(t) \quad i > 1 \quad (60)$$

$$P_{i,i,0}(t) = \lambda \mu e^{-\lambda t} \left(\frac{1}{\mu} - \frac{e^{-\mu t}}{\mu} \right) * P_{i-1,i-1,0}(t) + \mu \theta e^{-\lambda t} \left(\frac{1}{\mu} - \frac{e^{-\mu t}}{\mu} \right) * P_{i,i-1,0}(t) \\
 + 2\mu^2 e^{-\lambda t} \left(\frac{1}{\mu} - \frac{e^{-\mu t}}{\mu} \right) * P_{i,i-2,2}(t) \quad i > 1 \quad (61)$$

$$P_{2,1,1}(t) = \lambda e^{-(\lambda+\mu)t} * P_{1,1,0}(t) + 2\lambda \mu e^{-(\lambda+\mu)t} \left(\frac{1}{2\mu} - \frac{e^{-2\mu t}}{2\mu} \right) * P_{1,0,1}(t) \quad (62)$$

$$P_{i,1,1}(t) = \left[2\mu \lambda^{i-1} e^{-(\lambda+\mu+(i-2)\theta)t} \left\{ \frac{1}{(2\mu)^{i-1}} - e^{-2\mu t} \sum_{r=0}^{i-2} \frac{(t)^r}{r!} \frac{1}{(2\mu)^{i-r}} \right\} \right] * P_{1,0,1}(t) \quad i > 2 \quad (63)$$

$$P_{i,i-1,1}(t) = \lambda e^{-(\lambda+\mu)t} * P_{i-1,i-1,0}(t) + \theta e^{-(\lambda+\mu)t} * P_{i,i-1,0}(t) + 2\mu e^{-(\lambda+\mu)t} * P_{i,i-2,2}(t) \quad i > 2 \quad (64)$$

$$P_{i,2,0}(t) = 2\mu^2 e^{-(\lambda+(i-2)\theta)t} \left(\frac{1}{(\mu+(i-2)\theta)} - \frac{e^{-(\mu+(i-2)\theta)t}}{(\mu+(i-2)\theta)} \right) * P_{i,0,2}(t) \quad i \geq 3 \quad (65)$$

$$P_{i,j,2}(t) = \left(\lambda^{i-j-1} \frac{t^{i-j-2}}{(i-j-2)!} e^{-(\lambda+2\mu)t} \right) * P_{j+1,j,1}(t) + \sum_{k=2}^{i-j-1} \left(\lambda^{i-j-k} \frac{t^{i-j-k-1}}{(i-j-k-1)!} e^{-(\lambda+2\mu)t} \right) * P_{j+k,j,1}(t) \\
 + \sum_{k=2}^{i-j-1} \left(\lambda^{i-j-k} (k-1) \theta \frac{t^{i-j-k}}{(i-j-k)!} e^{-(\lambda+2\mu)t} \right) * P_{j+k,j,1}(t) + ((i-j-1)\theta e^{-(\lambda+2\mu)t}) * P_{i,j,1}(t) \quad i \geq j+2, j \geq 1 \quad (66)$$

$$P_{i,j,1}(t) = \lambda e^{-(\lambda+\mu+(i-j-1)\theta)t} * P_{i-1,j,0}(t) + (i-j)\theta e^{-(\lambda+\mu+(i-j-1)\theta)t} * P_{i,j,0}(t) \\
 + 2\mu \lambda^{i-j} e^{-(\lambda+\mu+(i-j-1)\theta)t} \left\{ \frac{1}{(2\mu)^{i-j}} - e^{-2\mu t} \sum_{r=1}^{i-j-1} \frac{(t)^r}{r!} \frac{1}{(2\mu)^{i-j-r}} \right\} * P_{j,j-1,1}(t) \\
 + 2\mu e^{-(\lambda+\mu+(i-j-1)\theta)t} \sum_{k=1}^{i-j-1} \lambda^{i-j-k} \left\{ \frac{1}{(2\mu)^{i-j-k}} - e^{-2\mu t} \sum_{r=0}^{i-j-k-1} \frac{(t)^r}{r!} \frac{1}{(2\mu)^{i-j-k-r}} \right\} \\
 * P_{j+k,j-1,1}(t) + 2\mu e^{-(\lambda+\mu+(i-j-1)\theta)t} \sum_{k=1}^{i-j-1} \lambda^{i-j-k} (k\theta) \\
 \left\{ \frac{1}{(2\mu)^{i-j-k+1}} - e^{-2\mu t} \sum_{r=0}^{i-j-k} \frac{(t)^r}{r!} \frac{1}{(2\mu)^{i-j-k+1-r}} \right\} * P_{j+k,j-1,1}(t) + 2\mu(i-j)\theta e^{-(\lambda+\mu+(i-j-1)\theta)t} \\
 \times \left(\frac{1}{2\mu} - \frac{e^{-2\mu t}}{2\mu} \right) * P_{i,j-1,1}(t) \quad i \geq j+2, j \geq 2 \quad (67)$$

$$P_{i,j,0}(t) = \lambda \mu e^{-(\lambda+(i-j)\theta)t} \left(\frac{1}{\mu+(i-j)\theta} - \frac{e^{-(\mu+(i-j)\theta)t}}{\mu+(i-j)\theta} \right) * P_{i-1,j-1,0}(t) + \mu(i-j+1)\theta e^{-(\lambda+(i-j)\theta)t} \\
 \left(\frac{1}{\mu+(i-j)\theta} - \frac{e^{-(\mu+(i-j)\theta)t}}{\mu+(i-j)\theta} \right) * P_{i,j-1,0}(t) + 2\mu^2 \lambda^{i-j+1} \\
 \left[\frac{\sum_{l=1}^{i-j+1} \sum_{m=1}^l \frac{e^{-(\lambda+(i-j)\theta)t} t^{(i-j+1)-l} (-1)^{m+1} \binom{l-1}{m-1} \left(\prod_{g_1=0}^{m-1} (1+g_1) \right) \left(\prod_{g_2=0}^{m-2} (1+g_2) \right)}{((i-j+1)-l)!(m-1)! (\mu)^m (2\mu-(i-j)\theta)^{1+l-m}} - \frac{e^{-(\lambda+\mu+(i-j)\theta)t}}{(\mu)^{(i-j+1)} (\mu-(i-j)\theta)} \right] + \\
 \left[\frac{e^{-(\lambda+2\mu)t}}{(2\mu-(i-j)\theta)^{(i-j+1)} (\mu-(i-j)\theta)} \right] * P_{j-1,j-2,1}(t) + 2\mu^2 \sum_{k=1}^{i-j} \lambda^{(i-j+1)-k} \\
 \left[\frac{\sum_{l=1}^{(i-j+1)-k} \sum_{m=1}^l \frac{e^{-(\lambda+(i-j)\theta)t} t^{((i-j+1)-k)-l} (-1)^{m+1} \binom{l-1}{m-1} \left(\prod_{g_1=0}^{m-1} (1+g_1) \right) \left(\prod_{g_2=0}^{m-2} (1+g_2) \right)}{(((i-j+1)-k)-l)!(m-1)! (\mu)^m (2\mu-(i-j)\theta)^{1+l-m}} - \frac{e^{-(\lambda+\mu+(i-j)\theta)t}}{(\mu)^{(i-j+1)-k} (\mu-(i-j)\theta)} \right] + \\
 \left[\frac{e^{-(\lambda+2\mu)t}}{(2\mu-(i-j)\theta)^{(i-j+1)-k} (\mu-(i-j)\theta)} \right] * P_{(j-1)+k,j-2,1}(t) + 2\mu^2 \sum_{k=1}^{i-j} \lambda^{(i-j+1)-k} (k\theta) \\
 \left[\frac{\sum_{l=1}^{((i-j+1)-k)+1} \sum_{m=1}^l \frac{e^{-(\lambda+(i-j)\theta)t} t^{(((i-j+1)-k)+1)-l} (-1)^{m+1} \binom{l-1}{m-1} \left(\prod_{g_1=0}^{m-1} (1+g_1) \right) \left(\prod_{g_2=0}^{m-2} (1+g_2) \right)}{((((i-j+1)-k)+1)-l)!(m-1)! (\mu)^m (2\mu-(i-j)\theta)^{1+l-m}} - \frac{e^{-(\lambda+\mu+(i-j)\theta)t}}{(\mu)^{((i-j+1)-k)+1} (\mu-(i-j)\theta)} + \frac{e^{-(\lambda+2\mu)t}}{(2\mu-(i-j)\theta)^{((i-j+1)-k)+1} (\mu-(i-j)\theta)} \right] * P_{(j-1)+k,j-2,1}(t) + 2\mu^2 (i-j+1)\theta \\
 \left[\frac{e^{-(\lambda+(i-j)\theta)t}}{(\mu)(2\mu-(i-j)\theta)} - \frac{e^{-(\lambda+\mu+(i-j)\theta)t}}{(\mu)(\mu-(i-j)\theta)} + \frac{e^{-(\lambda+2\mu)t}}{(2\mu-(i-j)\theta)(\mu-(i-j)\theta)} \right] * P_{i,j-2,1}(t) \quad i > j \geq 3 \quad (68)$$

The above equations coincide with that of Singla & Kalra [14].

V. Numerical Solution

Using MATLAB programming the numerical results are generated for the case when $\rho (= \frac{\lambda}{\mu_1 + \mu_2}) = 0.3$, $\eta (= \frac{\theta}{\mu_1 + \mu_2}) = 0.6$, $r_1 (= \frac{\mu_1}{\mu_1 + \mu_2}) = 0.3$, $a_{1=} 0.4$, $a_{2=} 0.6$. From the numerical results, it is found that the sum of all the probabilities at any instant approaches to one. In table 1, we show some of the significant probabilities at different instants of time whose sum is found close to one.

Table 1: Some significant probabilities at different instants of time.

At time t=1						
P _{0,0}	P _{1,1,0}	P _{1,0,1,1}	P _{2,1,1,1}	P _{1,0,1,2}	P _{2,1,1,2}	P _{2,0,2}
0.7408	0.0495	0.0768	0.0069	0.0959	0.0046	0.0204

P _{3,0,2}	P _{3,1,2}	Sum
0.0018	0.0008	0.9975

At time t=5								
P _{0,0,0}	P _{1,1,0}	P _{2,2,0}	P _{3,3,0}	P _{1,0,1,1}	P _{2,1,1,1}	P _{3,2,1,1}	P _{1,0,1,2}	P _{2,1,1,2}
0.2231	0.2097	0.0947	0.0260	0.0693	0.0759	0.0330	0.0556	0.0463

P _{3,2,1,2}	P _{2,0,2}	P _{3,0,2}	P _{3,1,2}	P _{4,1,2}	P _{4,2,2}	P _{5,3,2}	Sum
0.0196	0.0341	0.0087	0.0315	0.0079	0.0107	0.0024	0.9147

At time t=10						
P _{0,0,0}	P _{1,1,0}	P _{2,2,0}	P _{3,3,0}	P _{5,2,0}	P _{5,5,0}	P _{1,0,1,1}
0.0498	0.1176	0.1378	0.1052	0.0579	0.0242	0.0189

P _{2,1,1,1}	P _{3,2,1,1}	P _{4,2,1,1}
0.0480	0.0572	0.0047

P _{4,3,1,1}	P _{1,0,1,2}	P _{2,1,1,2}	P _{3,2,1,2}	P _{4,3,1,2}	P _{5,4,1,2}	P _{6,5,1,2}	P _{2,0,2}	P _{3,0,2}	P _{3,1,2}
0.0433	0.0128	0.0288	0.0331	0.0249	0.0134	0.0055	0.0094	0.0028	0.0216

P _{4,1,2}	P _{4,2,2}	P _{5,3,2}	P _{6,3,2}	P _{6,4,2}	P _{7,4,2}	P _{7,5,2}	Sum
0.0069	0.0241	0.0174	0.0063	0.0089	0.0074	0.001	0.9062

At time t=20						
P _{1,1,0}	P _{2,2,0}	P _{3,3,0}	P _{4,4,0}	P _{5,5,0}	P _{6,6,0}	P _{7,6,0}
0.0132	0.0354	0.0627	0.0886	0.0876	0.0754	0.0071

P _{7,7,0}	P _{3,2,1,1}	P _{4,3,1,1}
0.2357	0.0148	0.0265

P _{5,4,1,1}	P _{6,5,1,1}	P _{7,6,1,1}	P _{3,2,1,2}	P _{4,3,1,2}	P _{5,4,1,2}	P _{6,5,1,2}	P _{1,0,2}	P _{5,3,2}
0.0353	0.0372	0.0741	0.0088	0.0155	0.0204	0.0213	0.0310	0.0119

P _{6,4,2}	P _{7,4,2}	P _{7,5,2}	Sum
0.0155	0.0080	0.0237	0.9497

At time t=40

P _{5,5,0}	P _{6,6,0}	P _{7,7,0}	P _{7,6,1,1}	P _{1,0,2}	P _{7,5,2}	Sum
0.0096	0.0180	0.9183	0.0242	0.0075	0.0027	0.9803

V. Busy Period Probabilities

In this section, we discuss some interesting numerical results about busy period distribution of the server and busy period distribution of the system.

The probability when the one or both servers are busy is given

$$P(\text{Servers one or both busy}) = \sum_{i>j \geq 0} (P_{i,j,1,1}(t) + P_{i,j,1,2}(t) + P_{i,j,2}(t))$$

The probability when the system is busy is given by

$$P(\text{System is busy}) = \sum_{i>j \geq 0} (P_{i,j,0}(t) + P_{i,j,1,1}(t) + P_{i,j,1,2}(t) + P_{i,j,2}(t))$$

The numerical results are generated using MATLAB programming for the desired probabilities. The probability when system is busy and the probability when one or both servers are busy for different values of $\rho (= \frac{\lambda}{\mu_1 + \mu_2})$ at $\eta (= \frac{\theta}{\mu_1 + \mu_2}) = 0.6$, $r_1 (= \frac{\mu_1}{\mu_1 + \mu_2}) = 0.3$, $a_1 = 0.4$, $a_2 = 0.6$ are listed in Table 2.

Table 2: Probability of system busy and one or both servers busy ($r_1 = 0.3$, $a_1 = 0.4$, $a_2 = 0.6$).

t	Probability (System busy) $\eta=0.6$			Probability (Servers busy) $\eta=0.6$		
	$\rho=0.3$	$\rho=0.6$	$\rho=0.9$	$\rho=0.3$	$\rho=0.6$	$\rho=0.9$
0	0	0	0	0	0	0
1	0.2082	0.3734	0.5045	0.2082	0.3732	0.5039
2	0.314	0.532	0.6826	0.3135	0.5294	0.6768
3	0.3754	0.6164	0.7685	0.3737	0.6088	0.754
4	0.4145	0.6684	0.8184	0.4111	0.6547	0.7949
5	0.441	0.7035	0.8504	0.4357	0.6838	0.8176
6	0.4598	0.7283	0.8699	0.4525	0.7028	0.8266
7	0.4733	0.7452	0.8759	0.4644	0.714	0.8207

In figure 1, probability (system busy) and probability (one or both servers busy) are studied by plotting these against time for the case ($\rho=0.6$, $\eta=0.6$, $r_1 = 0.3$, $a_1 = 0.4$, $a_2 = 0.6$). From this figure it is apparent that the probability when the system is busy always remains more than the probability when the (server / servers) are busy.

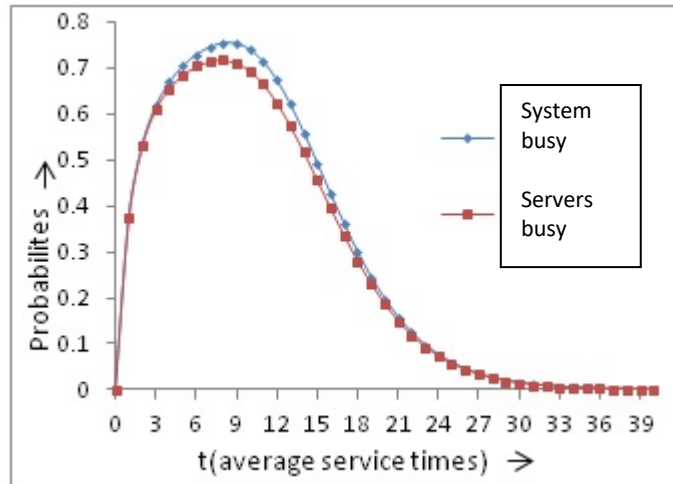


Figure 1 : Probability (system busy) and Probability (server/servers busy) against time for $\rho=0.6, \eta=0.6$

The probability (system busy) and the probability (one or both servers are busy) are plotted in figures 2 and 3 for different values of ρ for the case ($\eta=0.6, r_1 = 0.3, a_1 = 0.4, a_2 = 0.6$). From these figures it is clearly visible for higher values of value of ρ both the probabilities achieved greater highest values for some t , but this trend reverses for higher values of t .

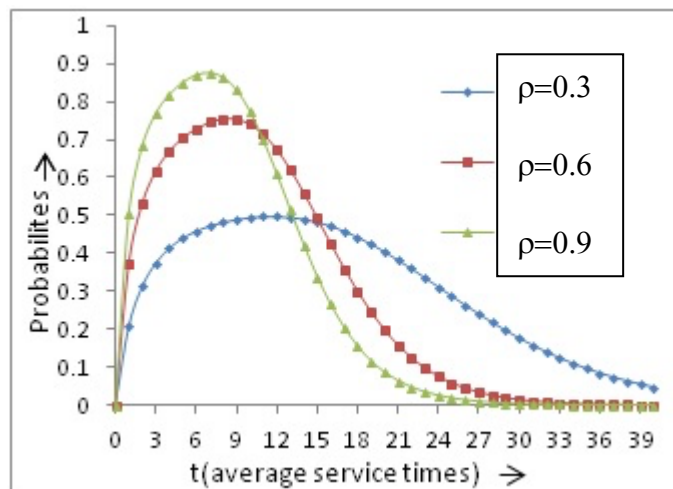


Figure 2: Effect of ρ on probability (system busy) against time

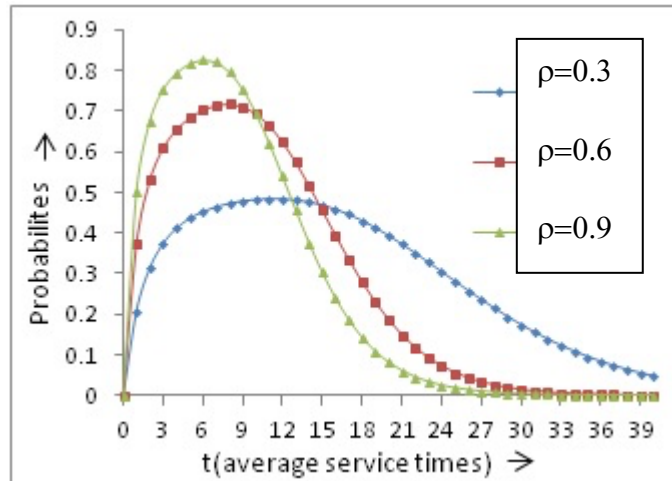


Figure 3: Effect of ρ on probability (servers busy) against time

VI. Conclusion

This paper considers a two state retrial queueing system having two non- identical parallel servers, which can be used in practical modeling of computer and communication systems. The transient state solution of the model is obtained and some measures of performance are derived. Due to the two-dimensional nature of the model under study, factors are clearly understood and well quantified. Further, the model can be converted into a model with the total number of customers in the system. Numerical results and busy period distribution demonstrate the influence of changing arrival rate on behavior of the system.

References

- [1] Li, H. and Yang, T. (1995). A single server retrial queue with server vacations and a finite number of input sources, *European Journal of Operational Research*, 85: 149-160.
- [2] Janssens, G.K. (1997). The quasi-random input queueing system with repeated attempts as a model for collision-avoidance star local area network, *IEEE Transaction on Communications*, 45: 360-364.
- [3] Tran-Gia, P. and Mandjes, M. (1997) Modeling of customer retrial phenomenon in cellular mobile networks, *IEEE Journal of Selected Areas in Communications*, 15: 1406-1414.
- [4] Onur, E., Delic, H., Ersoy, C. and Caglayan, M.U. (2002). Measurement-based replanning of cell capacities in GSM networks, *Computer Network*, 39: 749-767.
- [5] Falin, G.I. and Templeton, J.G.C. *Retrial queues*, Chapman and Hall, London, 1997.
- [6] Artalejo, J.R. (1998). Retrial queues with a finite number of sources, *J. Korean Math.Soc*, 35: 503-525.
- [7] Falin, G.I. and Artalejo, J.R. (1998). A finite source retrial queue, *European Journal of Operational Research*, 108: 409-424.
- [8] Artalejo, J.R. (1999). Accessible bibliography on retrial queues, *Mathematical and Computer Modelling*, 30:1-6.
- [9] Falin, G.I. (1993). A multiserver retrial queue with a finite number of sources of primary calls, *Mathematical and Computer Modelling*, 30: 33-49.
- [10] Pegden, C.D. and Rosenshine, M. (1982). Some new results for the M/M/1 queue, *Mgt Sci*, 28: 821-828.
- [11] Satty, T.L. *Elements of Queueing theory with applications*, Mc Graw Hill Book Co, 1961.

- [12] Gumbel, H. (1960). Waiting lines with heterogeneous servers, *Operations Research*, 8:504-511.
- [13] Morse, P.M. Queues, Inventories and Maintenance, John Wiley & Sons, Inc., New York, 1958.
- [14] Singla, N. and Kalra, S. (2018) Explicit Time Dependent Solution of a Two-State Retrial Queueing Model with Two Parallel Servers, *Int. J. Agricult. Stat. Sci*, 14: 419-429.
- [15] Kumari, N. (2011). An analysis of Some Continuous Time Queueing Systems with Feedback, *Ph.D Thesis*, Punjabi University, Patiala.

A Discrete Analogue of Teissier Distribution: Properties and Classical Estimation with Application to Count Data

BHUPENDRA SINGH¹, VARUN AGI WAL², AMIT SINGH NAYAL¹, ABHISHEK TYAGI^{1*}

•

¹Department of Statistics, Chaudhary Charan Singh University, Meerut-250004, India

²Indian Institute of Public Health, Hyderabad, Telangana, India.

bhupendra.rana@gmail.com

varunagiwal.stats@gmail.com

amitnayal009@gmail.com

*abhishektyagi033@gmail.com

Abstract

This article presents a novel discrete distribution with a single parameter, called the discrete Teissier distribution. It is noted that this model, with one parameter, offers a high degree of fitting flexibility as it is capable of modelling equi-, over-, and under-dispersed, positive and negative skewed, and increasing failure rate datasets. In this article, we have explored its numerous essential distributional features such as recurrence relation, moments, generating function, index of dispersion, coefficient of variation, entropy, survival and hazard rate functions, mean residual life and mean past life functions, stress-strength reliability, order statistics, and infinite divisibility. The classical point estimators have been developed using the method of maximum likelihood, method of moment, and least-squares estimation, whilst an interval estimation based on Fisher's information has also been presented. Finally, the applicability of the suggested discrete model has been demonstrated using two complete real datasets.

Keywords: COVID-19; Discrete Teissier distribution; Maximum Likelihood estimation; Method of moment estimation; Least square estimation

1. INTRODUCTION

In today's competitive world, the data generated from numerous sectors such as engineering, finance, and medical science, among others, is getting increasingly complicated. Therefore, we need distributions that are best suited for the analysis of this complex data. As a result, during the last three decades, developing a new probability distribution has become a major focus of statistical study. However, much of this research has focused on developing continuous probability distributions. But, there may be situations when discrete distributions are better appropriate for data modelling, or when the data generated is discrete. For example, in reliability engineering, the number of successful cycles before failure when a device is working in the cycle, the number of times a device is switched on/off; in survival analysis, the survival times for those suffering from diseases such as lung cancer or the period from remission to relapse may be recorded as the number of days/weeks, the number of deaths, or daily cases due to the COVID-19 pandemic observed over a specified duration, etc. Furthermore, the count phenomenon arises in many practical situations, such as the number of earthquakes that occur in a calendar year, the number of absences, the number of accidents, the number of species types in ecology, the number of insurance claims, and so on. Hence, it seems reasonable to model such scenarios using appropriate discrete distributions.

Due to the fact that conventional discrete distributions such as the Binomial, Poisson, Geometric, and Negative Binomial were insufficient to model a variety of discrete data. [21] suggested a novel approach in order to build a new discrete model through the survival function of a continuous model. [3] named this approach the survival discretization method. One of the most significant advantages of this technique is that the discrete distribution that has been developed preserves the same functional form of the survival function as its continuous counterpart. As a result of this feature, the various reliability properties of the distribution remain unaltered. According to this methodology, for a given continuous random variable (RV) X with survival function (SF) $S_X(x) = P(X \geq x)$, the discretized version can be derived as

$$\begin{aligned} P(Y = y) &= P(y \leq X \leq y + 1) \\ &= S_X(y) - S_X(y + 1); y = 0, 1, 2, 3, \dots \end{aligned} \quad (1)$$

Over the last two decades, this approach has gotten a lot of attention. Using this technique, [21] gave a discretized version of the normal distribution. Following this, [22] obtained discrete Rayleigh distribution. A comprehensive analysis of the evolution of the discrete distribution up to 2014 was provided by [3]. Then afterwards, a large number of significant discrete distributions have emerged in the literature. For example, [1], [11], [29], [28], [6], and the references cited therein. Most recently, [7] gave a discrete analogue of the odd Weibull-G family of distributions. They discussed the classical and Bayesian estimation and showed the applicability of the proposed family to count datasets.

In this paper, we have proposed the discrete analogue of the Teissier model [27] named discrete Teissier (DT) distribution using the survival discretization method. Recently, the Teissier distribution comes light when [26] introduced a two-parameter exponentiated Teissier distribution. The main objectives of proposing the DT model can be summarized as follows:

- An important objective of the proposed study is to provide a discrete model that has greater flexibility with less number of parameters so that the form of various distributional characteristics is easily manageable and easy to analyze the real datasets.
- The discrete data generated from many practical studies, such as mortality experiments, industrial experiments, etc., show constant or increasing failure rates, so we want to develop a discrete model with a monotonically increasing failure rate function.
- To produce a model that not only fit an equi-, over-, and under-dispersed real data, that is also capable of modelling a positively skewed, negatively skewed, platykurtic, and leptokurtic dataset.
- To provide consistently better fits than other well-known discrete models in the existing statistical literature.

The rest of the article is organized as follows: Section 2 introduces the one-parameter DT distribution. In Section 3 some important distributional and reliability characteristics are studied. In section 4, we estimate the parameter of DT distribution by different classical methods. In Section 5, numerical illustrations using empirical and real datasets have been presented. Finally, some concluding remarks are given in Section 6.

2. DISCRETE TEISSIER DISTRIBUTION

If X follows univariate continuous Teissier distribution with parameter α then its probability density function (PDF) and SF can be written as

$$f(x, \alpha) = \alpha(\exp(\alpha x) - 1) \exp(\alpha x - e^{\alpha x} + 1); \alpha > 0, x > 0, \quad (2)$$

$$S(x) = \exp(\alpha x - e^{\alpha x} + 1); \alpha > 0, x > 0. \quad (3)$$

Using the survival discretization approach (1), the DT distribution can be obtained as

$$\begin{aligned} p_y &= P[Y = y] = S_X(y) - S_X(y + 1) \\ &= \exp(1) \exp(\alpha y) (\exp(-e^{\alpha y}) - \exp(\alpha - e^{\alpha(y+1)})); y = 0, 1, 2, \dots, \alpha > 0. \end{aligned} \quad (4)$$

For ease of notation, after re-parametrization $\theta = \exp(\alpha)$, the probability mass function (PMF) in (4) can be written as

$$p_y = P[Y = y] = \exp(1)\theta^y(\exp(-\theta^y) - \theta \exp(-\theta^{(y+1)})); y = 0, 1, 2, \dots, \theta > 1. \quad (5)$$

The cumulative distribution function (CDF) corresponding to PMF (5) is

$$F(x) = 1 - \theta^{y+1} \exp(1 - \theta^{(y+1)}); y = 0, 1, 2, \dots, \theta > 1. \quad (6)$$

3. STATISTICAL PROPERTIES

3.1. The Shape of the Probability Mass Function

The PMF plots of the DT distribution for different parametric values are shown in Figure 1. The PMF of the suggested distribution may exhibit decreasing, bell-shaped, and unimodal (right-skewed) shapes, as seen in Figure 1. Furthermore, when θ is increased, the degree of asymmetry and peakedness of the PMF increases. The limiting behavior of DT distribution for various choices

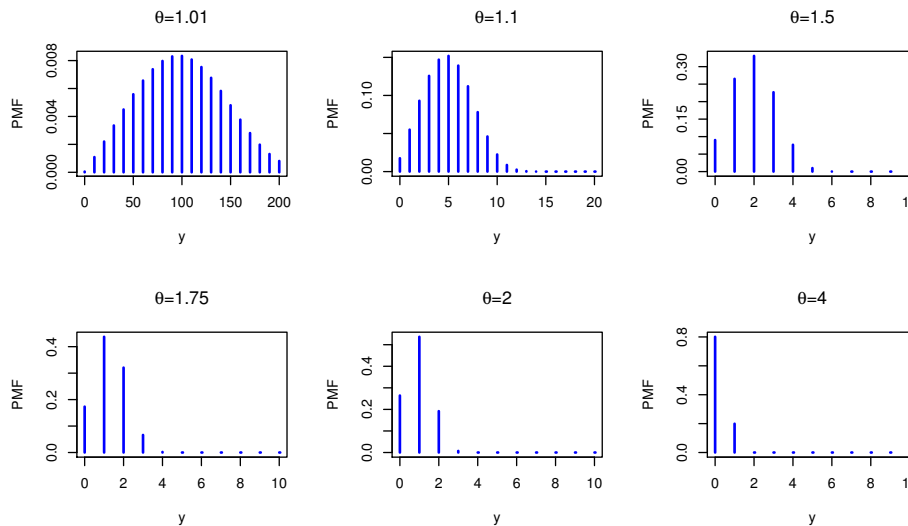


Figure 1: The shapes of PMF of DT distribution for various values of the parameter θ .

of parameters at the boundary points is:

(i). $\lim_{y \rightarrow \infty} p_y = 0$, (ii). $\lim_{\theta \rightarrow 1} p_y = 0$, (iii). $\lim_{\theta \rightarrow \infty} p_y = 1$, for $y = 0$ and $\lim_{\theta \rightarrow \infty} p_y = 0$, otherwise.

3.2. Recurrence Relation for Probabilities

The recursive relation shown below can be used to calculate probability mass for various values of y ,

$$P[Y = y + 1] = \frac{\theta(\exp(-\theta^{(y+1)}) - \theta \exp(-\theta^{(y+2)}))}{(\exp(-\theta^y) - \theta \exp(-\theta^{(y+1)}))} . P[Y = y]$$

It can be easily verifiable that $[P_Y(y)]^2 \geq P_Y(y + 1) . P_Y(y - 1)$ for all y . Hence, the DT distribution is log-concave. This concavity implies that the proposed distribution has a non-decreasing failure rate, strongly unimodal, remains log-concave if truncated and its all the moments exists. The convolution of the proposed model with any other discrete distribution is also unimodal and log-concave ([13],[10]).

3.3. Moments and related concepts

The moments of a probability distribution are important for measuring its different properties such as mean, variance, skewness, kurtosis, etc. The r^{th} raw moments ω'_r of the DT distribution can be obtained by using the relation

$$\begin{aligned} \omega'_r = E(Y^r) &= \sum_{y=0}^{\infty} y^r p_y \\ &= \exp(1) \sum_{y=1}^{\infty} \sum_{k=0}^{\infty} (-1)^k \frac{(y^r - (y-1)^r) \theta^{(k+1)y}}{|k|}. \end{aligned} \quad (7)$$

Using Equation (7), the first four raw moments of the DT distribution are

$$\omega'_1 = E(Y) = \exp(1) \sum_{y=1}^{\infty} \sum_{k=0}^{\infty} (-1)^k \frac{\theta^{(k+1)y}}{|k|}, \quad (8)$$

$$\omega'_2 = E(Y^2) = \exp(1) \sum_{y=1}^{\infty} \sum_{k=0}^{\infty} (-1)^k (2y - 1) \frac{\theta^{(k+1)y}}{|k|}, \quad (9)$$

$$\omega'_3 = E(Y^3) = \exp(1) \sum_{y=1}^{\infty} \sum_{k=0}^{\infty} (-1)^k (3y^2 - 3y + 1) \frac{\theta^{(k+1)y}}{|k|}, \quad (10)$$

$$\omega'_4 = E(Y^4) = \exp(1) \sum_{y=1}^{\infty} \sum_{k=0}^{\infty} (-1)^k (4y^3 - 6y^2 + 4y - 1) \frac{\theta^{(k+1)y}}{|k|}. \quad (11)$$

The variance of the DT distribution is

$$V(Y) = \exp(1) \sum_{y=1}^{\infty} \sum_{k=0}^{\infty} (-1)^k (2y - 1) \frac{\theta^{(k+1)y}}{|k|} - \left[\exp(1) \sum_{y=1}^{\infty} \sum_{k=0}^{\infty} (-1)^k \frac{\theta^{(k+1)y}}{|k|} \right]^2.$$

Using the raw moments in (8)-(11), we can easily find the skewness (Sk) and kurtosis (Kur) from the following relations

$$Sk = \frac{\omega'_3 - 3\omega'_2\omega'_1 + 2(\omega'_1)^3}{(Var(Y))^{3/2}} \quad \text{and} \quad Kur = \frac{\omega'_4 - 4\omega'_2\omega'_1 + 6\omega'_2(\omega'_1)^2 - 3(\omega'_1)^4}{(Var(Y))^2},$$

respectively.

The moment generating function (MGF) is an alternative representation of a probability distribution. It is an important tool to obtain various distributional characteristics. For the proposed model, it can be obtained as

$$\begin{aligned} M_Y(t) &= E[\exp(ty)] = \sum_{y=0}^{\infty} \exp(ty) p_y \\ &= 1 + \exp(1)\theta(\exp(t) - 1) \sum_{y=1}^{\infty} \exp(-\theta y) \cdot (\theta \exp(t))^{y-1}. \end{aligned}$$

The index of dispersion (IOD) is a technique for determining whether a data is equi-, under or over-dispersed. If the $IOD > 1 (< 1)$, it indicates the over-dispersion, (under-dispersion), while if $IOD = 1$, it is equi-dispersed. In the case of the proposed model, the IOD is

$$IOD = \frac{Var(Y)}{E(Y)} = \frac{\sum_{y=1}^{\infty} \sum_{k=0}^{\infty} (-1)^k (2y - 1) \frac{\theta^{(k+1)y}}{|k|} - \exp(1) \left[\sum_{y=1}^{\infty} \sum_{k=0}^{\infty} (-1)^k \frac{\theta^{(k+1)y}}{|k|} \right]^2}{\sum_{y=1}^{\infty} \sum_{k=0}^{\infty} (-1)^k \frac{\theta^{(k+1)y}}{|k|}}.$$

The coefficient of variation (CV) is a relative measure of dispersion and is generally used to compare two independent samples based on their variability. The higher value of CV indicates higher variability. For DT distribution, the CV can be obtained as

$$CV = \frac{(Var(Y))^{1/2}}{E(Y)} = \frac{\left(\sum_{y=1}^{\infty} \sum_{k=0}^{\infty} (-1)^k (2y-1) \frac{\theta^{(k+1)y}}{k} - \exp(1) \left[\sum_{y=1}^{\infty} \sum_{k=0}^{\infty} (-1)^k \frac{\theta^{(k+1)y}}{k} \right]^2 \right)^{1/2}}{\sum_{y=1}^{\infty} \sum_{k=0}^{\infty} (-1)^k \frac{\theta^{(k+1)y}}{k}}$$

It is not possible to get a closed-form of the above expressions, therefore, we use R software to demonstrate these characteristics numerically. Table 1 lists some numerical results of the mean, variance, skewness, kurtosis, IOD, and CV for the DT distribution under different setups of parametric values. From this table, it can be concluded that:

- The mean of the DT distribution decreases when the value of θ increases.
- From the observed values of skewness, we can conclude that the DT distribution can be used to model positively and negatively skewed data.
- The proposed model is appropriate for modelling leptokurtic and platykurtic datasets.
- The DT distribution can be used to analyze over-dispersed, under-dispersed, and equi-dispersed datasets.
- As the value of θ rises, the CV tends to increase.

Table 1: Descriptive measures at different values of the parameter θ .

θ	Descriptive Measures					
	Mean	Variance	Skewness	Kurtosis	IOD	CV
1.001	98.8320	8.2885	-20.5690	469.1044	0.0838	0.0291
1.005	94.5488	199.106	-3.6319	13.3240	2.1058	0.1492
1.010	81.4812	575.2569	-1.2399	0.4283	7.0599	0.2943
1.050	19.9959	81.0311	0.2090	-0.4210	4.0523	0.4501
1.100	9.9920	21.2957	0.2081	-0.4187	2.1312	0.4618
1.248	4.0301	4.0376	0.2035	-0.4075	1.0018	0.4985
1.750	1.2866	0.6969	0.1956	-0.4256	0.5416	0.6488
2.000	0.9422	0.4820	0.2086	-0.5048	0.5115	0.7368
2.500	0.5906	0.3074	0.2159	-0.9031	0.5205	0.9387

3.4. Entropy

Entropy is a crucial measure of complexity and uncertainty and is used in many fields including problems identification in statistics, statistical inference, physics, econometrics, and pattern recognition in computer science. One of the important entropy is Rényi entropy (RE) (see, [20]). For the DT distribution, the RE can be defined as ($\rho > 0, \rho \neq 1$)

$$I_R(\rho) = \frac{1}{1-\rho} \log \sum_{y=0}^{\infty} p_y^\rho = \frac{1}{1-\rho} \left(\rho + \log \sum_{y=0}^{\infty} \theta^{\rho y} (\exp(-\theta^y) - \theta \exp(-\theta^{(y+1)}))^\rho \right)$$

Another famous entropy called Shannon entropy (ShE) can be obtained as a particular case of RE as $\rho \rightarrow 1$, where $ShE = -E[\log P(y; \alpha)]$.

3.5. Survival and hazard rate functions

The SF and hazard rate function (HRF) of the DT distribution is respectively given by,

$$S(y; \theta) = P(Y \geq y) = \theta^y \exp(1 - \theta^y); y = 0, 1, 2, \dots$$

$$H(y; \theta) = P(Y = y | Y \geq y) = 1 - \theta \exp(\theta^y - \theta^{(y+1)}); y = 0, 1, 2, \dots$$

Figure 2 depicts various plots of HRF of the proposed model. From the HRF plot, it is easily visible that the HRF of the DT distribution is increasing. Also, $\lim_{y \rightarrow \infty} H(y; \theta) = \lim_{\theta \rightarrow \infty} H(y; \theta) = \lim_{\theta \rightarrow 1} H(y; \theta) = 1$. Moreover, the reversed hazard rate function (RHRF) and the second rate of failure (SRF) of the proposed model are

$$H^*(y; \theta) = P(Y = y | Y \leq y) = \frac{\exp(1)\theta^y (\exp(-\theta^y) - \theta \exp(-\theta^{(y+1)}))}{1 - \theta^{y+1} \exp(1 - \theta^{(y+1)})}; y = 0, 1, 2, \dots,$$

and

$$H^{**}(y; \theta) = \log \left[\frac{S(y)}{S(y+1)} \right] = \theta^y (\theta - 1) - \log \theta; y = 0, 1, 2, \dots$$

respectively.

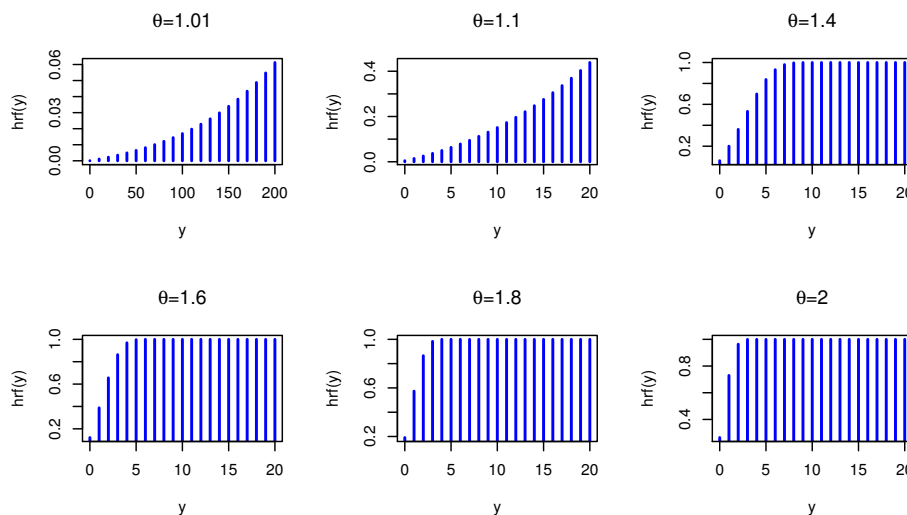


Figure 2: The shapes of HRF of DT distribution for various values of the parameter θ .

3.6. Mean residual lifetime and mean past lifetime function

The mean residual life (MRL) function is used extensively in a wide variety of areas, including reliability engineering, survival analysis, and biomedical research since it represents the ageing mechanism. It is well known that the MRL function characterizes the distribution function F uniquely since it contains all of the model's information. In discrete setup, the MRL, symbolized by $m(i)$, can be defined as

$$m(i) = E(Y - i | Y \geq i) = \frac{1}{S(i)} \sum_{j=i+1}^{\infty} S(j); i = 0, 1, 2, \dots$$

If Y has DT distribution with parameter θ , then the MRL function of Y is

$$m(i) = \frac{1}{\theta^i \exp(-\theta^{i+1})} \sum_{j=i+1}^{\infty} \theta^j \exp(-\theta^{j+1}).$$

The expected inactivity time function or mean past life (MPL) function, denoted by $m^*(i)$, measures the time elapsed since the failure of X given that the system has failed sometime before

'i'. It has many applications in a wide variety of areas, including reliability theory and survival analysis, actuarial research, and forensic science. In discrete setup, MPL function is defined as

$$m^*(i) = E(i - X | X < i) = \frac{1}{F(i-1)} \sum_{k=1}^i F(k-1); \quad i = 1, 2, \dots$$

By replacing the CDF (6) in the expression of $m^*(i)$, we can easily obtain the MPL for the proposed model.

3.7. Stress-strength analysis

The stress-strength ($S - S^*$) analysis is widely applicable in various areas including engineering, medical science, psychology etc. The probability of failure is based on the probability of S exceeding S^* . Suppose that the domain of S and S^* is positive, then the $S - S^*$ reliability (R) can be computed as

$$R = P[Y_S \leq Y_{S^*}] = \sum_{y=0}^{\infty} P_{Y_S}(y) S_{Y_{S^*}}.$$

If $Y_S \simeq \text{DT}(\theta_1)$ and $Y_{S^*} \simeq \text{DT}(\theta_2)$, then R can be expressed as

$$R = \theta_2 \exp(2) \sum_{y=0}^{\infty} (\theta_1 \theta_2)^y \exp(-\theta_2^{y+1}) \left(\exp(-\theta_1^y) - \theta_1 \exp(-\theta_1^{y+1}) \right). \quad (12)$$

Given the difficulty of obtaining an explicit expression for R in this instance, we show this feature quantitatively using the R software. Tables 2 illustrates the calculated values of R for various parameter combinations. From Table 2, we infer that for a fixed value of θ_2 , reliability increases as θ_1 increases, whereas for the particular value of θ_1 , $R \rightarrow 0$, as $\theta_2 \rightarrow \infty$.

Table 2: The numerical values of R for fixed values of θ_1 and θ_2 .

Parameter	θ_2					
	1.001	1.010	1.050	1.250	1.500	
θ_1	1.001	0.02093	0.00617	0.00024	0.00001	0.00000
	1.010	0.98078	0.49681	0.02554	0.00100	0.00026
	1.050	0.99974	0.97225	0.48476	0.02531	0.00636
	1.250	0.99999	0.99855	0.96300	0.43096	0.13811
	1.500	0.99999	0.99950	0.98739	0.73634	0.37738

3.8. Order statistics

The order statistics play a vital role in the construction of tolerance intervals for the distributions and drawing inferences on population parameters especially in survival analysis. Let Y_1, Y_2, \dots, Y_n be a random sample from the DT distribution. Also, let $Y_{(1)}, Y_{(2)}, \dots, Y_{(n)}$ represents the corresponding order statistics. Then the CDF of the r^{th} order statistic say $W = Y_{(r)}$ is given by

$$\begin{aligned} F_r(w) &= \sum_{i=r}^n \binom{n}{i} F^i(w) \cdot [1 - F(w)]^{n-i} \\ &= \sum_{i=r}^n \sum_{k=0}^{n-i} (-1)^k \binom{n}{i} \binom{n-i}{k} (1 - \theta^{(w+1)}) \exp(1 - \theta^{(w+1)})^{i+k}. \end{aligned} \quad (13)$$

The corresponding PMF of r^{th} order statistics is

$$\begin{aligned}
 f_r(w) &= F_r(w) - F_r(w - 1) \\
 &= \sum_{i=r}^n \sum_{k=0}^{n-i} (-1)^k \binom{n}{i} \binom{n-i}{k} \left\{ (1 - \theta^{w+1} \exp(1 - \theta^{(w+1)}))^{i+k} - (1 - \theta^w \exp(1 - \theta^w))^{i+k} \right\}.
 \end{aligned} \tag{14}$$

Particularly, by setting $r = 1$ and $r = n$ in Equation (14), we can obtain the PMF of minimum $\left(\{Y_{(1)}, \dots, Y_{(n)}\}\right)$ and the PMF of maximum $\left(\{Y_{(1)}, \dots, Y_{(n)}\}\right)$, respectively.

3.9. Infinite divisibility

In this section, the property of infinite divisibility of the DT distribution is examined. This property is critical in the theorems of probability theory, modelling problems, and waiting time distribution. A probability distribution with PMF p_x , $x = 0, 1, 2, \dots$ is infinite divisible if $p_x \leq e^{-1} \forall x = 1, 2, \dots$ [24]. For DT distribution with $\theta = 2$, we observe that $p_1 = 0.5366$ which is greater than $e^{-1} (= 0.3679)$. Hence in general, DT distribution is not infinitely divisible. Further, since the classes of self-decomposition and stable distributions, in their discrete concepts, are subclasses of infinitely divisible distributions, therefore a DT distribution can neither be self-decomposable nor stable in general.

4. CLASSICAL ESTIMATION

In this section, we address the problem of estimation through well-known estimation procedures like method of maximum likelihood, method of moment estimation, ordinary and weighted least squares estimation. In maximum likelihood estimation, we also derived the asymptotic distribution of the ML estimator and construct the asymptotic confidence interval (ACI) for the unknown parameter.

4.1. Method of maximum likelihood

Let Y_1, Y_2, \dots, Y_n be a random sample of size n with mean \bar{y} , then the likelihood-function (LF) for DT distribution can be written as

$$L(\underline{y}, \theta) = \exp(n)\theta^{n\bar{y}} \prod_{i=1}^n (\exp(-\theta^{y_i}) - \theta \exp(-\theta^{(y_i+1)})). \tag{15}$$

The log-likelihood (LL) function can be represented as

$$\log L(\underline{y}, \theta) = n + n\bar{y} \log \theta + \sum_{i=1}^n \log(\exp(-\theta^{y_i}) - \theta \exp(-\theta^{(y_i+1)})). \tag{16}$$

Taking the partial derivative of the LL function with respect to the parameter, we get the following normal-equation,

$$\frac{\partial \log L}{\partial \theta} = \frac{n\bar{y}}{\theta} + \sum_{i=1}^n \frac{E_1 E_2 - y_i \theta^{y_i-1}}{1 - \theta E_1} = 0, \tag{17}$$

where $E_1 = \exp(\theta^{y_i} - \theta^{y_i+1})$ and $E_2 = (y_i + 1) \theta^{y_i+1} - 1$.

The maximum likelihood (ML) estimator of θ can be found by simplifying Equation (17), but unfortunately, this equation does not yield an analytical solution. Therefore, we use an iterative approach such as Newton-Raphson (NR) to calculate the estimate computationally.

The ML estimator $\hat{\theta}$ of θ , is consistent and asymptotic Gaussian distribution with $\sqrt{n}(\hat{\theta} - \theta)$ follows $N(0, I^{-1}(\theta))$, where $I(\theta) = E\left(-\frac{\partial^2}{\partial \theta^2} \log f(y; \theta)\right)$. Therefore, the variance of the estimator $\hat{\theta}$ can be computed as $V(\hat{\theta}) \approx J^{-1}(\hat{\theta})$ where $J(\hat{\theta}) = -\left(\frac{\partial^2}{\partial \theta^2}\right)\Big|_{\theta=\hat{\theta}}$. The second-order partial derivative of the LL function is

$$\frac{\partial^2 \log L}{\partial \theta^2} = \sum_{i=1}^n \frac{(1-\theta E_1)(-y_i(y_i-1)\theta^{y_i-1} + E_1 E_2 E_3 + (y_i+1)^2 \theta^{y_i+1} E_1) + (-y_i \theta^{y_i} + \theta E_1 E_2)(E_3+1)E_1}{\theta(1-\theta E_1)^2} - \frac{n\bar{y}}{\theta^2},$$

where $E_3 = \theta^{y_i}(y_i - (y_i + 1)\theta)$. Hence, the $100 \times (1 - \gamma)\%$ ACI for the parameter θ is $\hat{\theta} \mp Z_{\gamma/2} \sqrt{V(\hat{\theta})}$, here $Z_{\gamma/2}$ is the upper $\gamma/2$ quantile of the standard Gaussian distribution.

4.2. Method of moment estimation

In this estimation process, firstly, we equate population moment(s) to the corresponding sample moment(s) and then solve this equation for the unknown parameter(s). In our case, the concerned equation is

$$\bar{y} = \sum_{i=1}^{\infty} \theta^i \exp(1 - \theta^i). \tag{18}$$

where \bar{y} represents the mean based on the RS y_1, y_2, \dots, y_n drawn from the DT distribution (5). We can obtain the method of moment (MOM) estimator $\hat{\theta}_{MOM}$, by solving Equation (18) for θ . Since Equation (18) does not provide the MOM estimator of θ in explicit form, so we can use numerical methods to compute $\hat{\theta}_{MOM}$.

4.3. Method of least squares estimation

Here, we present the regression-based estimation methods for estimating the model parameter. These approaches are known as the ordinary least square (OLS) and the weighted least square (WLS) estimators, and they were first suggested by [25]. The OLS and WLS estimators depend on the combination of the non-parametric and parametric distribution functions.

This method is widely used to estimate the parameters of a continuous model. Some authors utilize this technique to estimate the unknowns of a discrete model by considering the non-parametric CDF as a continuous type (see, [23]). Because discrete data is made up of ties observations, a non-parametric CDF that takes ties observations into account is more suited. In view of this, we use a different form of non-parametric CDF that relies on observation of relations. These methods can be described as follows:

Let Y_1, Y_2, \dots, Y_n be a random sample from $F(\cdot)$ in Equation (6), and $Y_{(1)} \leq Y_{(2)} \leq \dots \leq Y_{(n)}$ be the corresponding ordered values having r tie-runs with the length z_j for the j^{th} one, $j = 1, 2, \dots, r$, then the mean and variance of $F(Y_{(i)})$ are respectively as

$$E[F(Y_{(i)})] = 1 - \prod_{j=1}^i \frac{n_j - z_j}{n_j} \quad \text{and} \quad V[F(Y_{(i)})] = \left(1 - F(Y_{(i)})\right)^2 \sum_{j=1}^i \frac{z_j}{n_j(n_j - z_j)}.$$

The $V[F(X_{(i)})]$ is known as Greenwood's formula. The OLS and WLS estimators of the unknown parameter can be obtained by minimizing

$$W_1(\theta) = \sum_{i=1}^n \left(F(Y_{(i)}) - E[F(Y_{(i)})]\right)^2 \quad \text{and} \quad W_2(\theta) = \sum_{i=1}^n V[F(Y_{(i)})]^{-1} \left(F(Y_{(i)}) - E[F(Y_{(i)})]\right)^2,$$

respectively, with respect to the unknown parameter of the model.

Thus, in our case, the OLS estimator of the unknown parameter θ say $\hat{\theta}_{OLS}$ can be achieved by minimizing

$$W_1(\theta) = \sum_{i=1}^n \left(\theta^{y_i+1} \exp(1 - \theta^{y_i+1}) - \prod_{j=1}^i \frac{n_j - z_j}{n_j}\right)^2,$$

with respect to θ . Evenly, $\hat{\theta}_{OLS}$ can be determined by solving

$$\frac{\partial W_1(\theta)}{\partial \theta} = \sum_{i=1}^n \left[\theta^{y_i+1} \exp(1 - \theta^{y_i+1}) - \prod_{j=1}^i \frac{n_j - z_j}{n_j}\right] \xi(y_{i:n}; \theta) = 0,$$

where $\zeta(y_i; \theta) = (y_i + 1)\theta^{y_i}(1 - \theta^{y_i+1}) \exp(1 - \theta^{y_i+1})$.

The WLS estimator of θ , say $\hat{\theta}_{WLS}$, can be achieved by minimizing

$$W_2(\theta) = \sum_{i=1}^n V[F(Y_{(i)})]^{-1} \left(\theta^{y_i+1} \exp(1 - \theta^{y_i+1}) - \prod_{j=1}^i \frac{n_j - z_j}{n_j} \right)^2.$$

The estimator $\hat{\theta}_{WLS}$ can also be obtained by simplifying the following equation

$$\frac{\partial W_2(\theta)}{\partial \theta} = \sum_{i=1}^n V[F(Y_{(i)})]^{-1} \left[\theta^{y_i+1} \exp(1 - \theta^{y_i+1}) - \prod_{j=1}^i \frac{n_j - z_j}{n_j} \right] \zeta(y_{i:n}; \alpha) = 0.$$

5. NUMERICAL ILLUSTRATION

Here, we present the numerical illustrations of the proposed model based on the empirical and real datasets.

5.1. Using simulated data

In this sub-section, we observe the performance of different estimation techniques to estimate the unknown parameter of the proposed model. This assessment consists of the following steps:

1. Generate 2000 samples of sizes $n = 20, 25, \dots, 150$ from DT distribution with $\theta = 1.05, 1.5,$ and 3.0 . To generate the required RV Y from DT distribution we have used the general approach in which first we draw the pseudo-random value X from continuous Teissier distribution and then discretize this value to obtain Y . The following formula can be used to generate an RV X ,

$$Q(u) = \frac{1}{\alpha} \log \left[-W_{-1} \left(\frac{u-1}{\exp(1)} \right) \right]; 0 < u < 1,$$

where $\theta = \exp(\alpha)$ and W_{-1} denotes the Lambert function and its value can be easily obtained by the inbuilt R-function *lambertWm1* available in the package *lamW*.

2. Compute the ML, MOM, OLS, and WLS estimates for the 2000 samples, say $\hat{\theta}_\varphi^j; j = 1, 2, \dots, 2000; \varphi = \text{ML, MOM, OLS, and WLS}$. Also, we have computed the 95% ACI intervals for the above-generated samples.
3. Compute the mean-squared error (MSE) and average absolute bias (AB) for all point estimates, average width (AW) and coverage probability (CP), where

$$MSE = \frac{1}{2000} \sum_{j=1}^{2000} (\hat{\theta}_\varphi^j - \theta)^2, AB = \frac{1}{2000} \sum_{j=1}^{2000} |\hat{\theta}_\varphi^j - \theta|, AW = \frac{1}{2000} \sum_{j=1}^{2000} (UCL^j - LCL^j),$$
 and

$$CP = \frac{1}{2000} \sum_{j=1}^{2000} I(LCL^j < \theta < UCL^j),$$
 here, UCL^j and LCL^j denotes the upper and lower confidence limits for the j^{th} sample, respectively, and $I(\bullet)$ is the indicator function takes value 1, if $LCL^j < \theta < UCL^j$, and 0 otherwise.
4. The empirical results are shown in Figures 3-4.

From Figures 3-4, the following key conclusions can be made:

- The MSE decrease to zero as n tends to infinity. This shows the consistency of the estimators. Also, the AB decrease to zero as n becomes large.
- All the estimation procedures perform satisfactorily for different values of n and θ . However, the ML estimator works superior to other classical procedures with respect to MSE. The MOM estimator is the second choice of estimation since the MSE of these estimates is lesser than those obtained for OLS and WLS estimators.

- The AW of the ACI intervals decreases as we increase the sample size n .
- Here, the CP in the simulation of ACI intervals remains near about nominal value, this validates our simulation results.
- For the small value of the parameter θ , all estimation procedures work better as compare to the large value of θ . Also, as n becomes large, the considered estimation methods produce more or less similar results with respect to the MSE and AB.

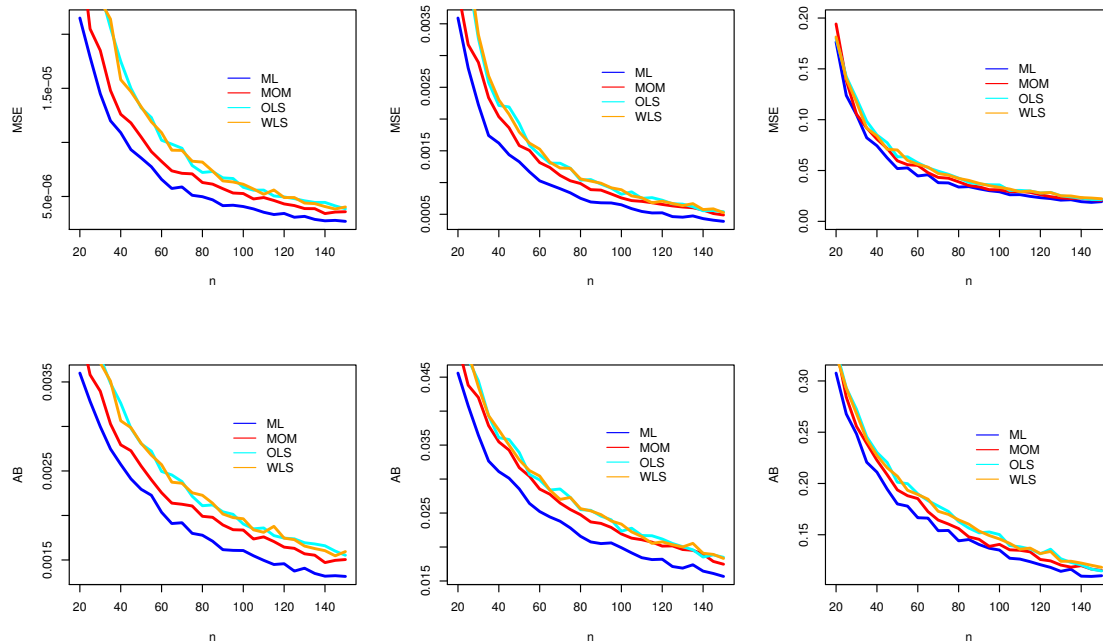


Figure 3: The MSEs and ABs of different estimators for (i) $\theta = 1.05$ (ii) $\theta = 1.50$ (iii) $\theta = 3.0$.

5.2. The real data application

In this part, we use two real datasets to demonstrate the relevance and superiority of the DT distribution. The two datasets are from two distinct areas, with the first representing daily COVID-19 cases in India and the second one consists survival times of a group of laboratory mice. The fitting capability of the proposed model has been compared to that of various well-known conventional and recently developed models. Table 3 has a list of the competitive models.

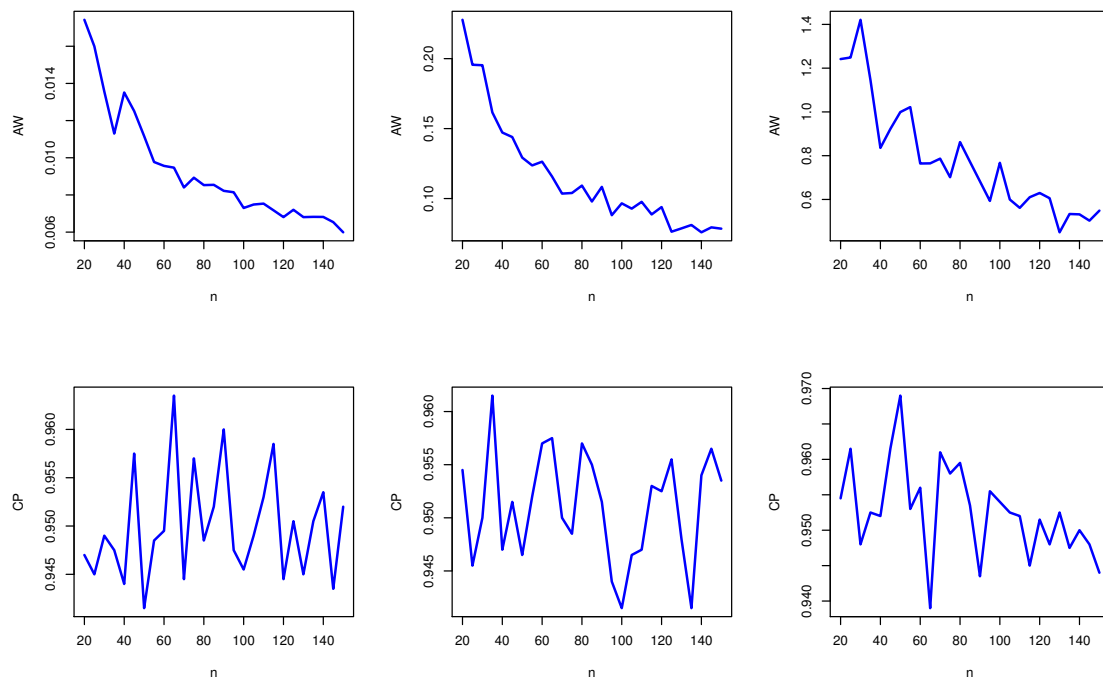


Figure 4: AW and CP for (i) $\theta = 1.05$ (ii) $\theta = 1.50$ (iii) $\theta = 3.0$.

Table 3: The competitive models.

Model	Parameter(s)	Abbreviation	References
Geometric	θ	Geo	-
Discrete Lindley	α	DsLi	[9]
Discrete Rayleigh	θ	DR	[22]
Discrete Poisson Lindley	α	DPL	[18]
Discrete Burr	(α, β)	DBr	[12]
Discrete Pareto	θ	DPa	[12]
Two Parameter Discrete Half Logistic	(α, β)	DHLo-II	[8]
Discrete Perks	(α, β)	DP	[28]
Discrete Weibull	(q, β)	DW	[19]
Discrete Logistic	(α, β)	DLOG	[4]
A Flexible discrete model with one parameter	α	DsFx-I	[5]
Poisson Bilal distribution	θ	PB	[2]

For comparison purposes, the estimation of the fitted models has been done through ML estimation. The model comparison is carried out based on $-LL$, Akaike information criterion (AIC), corrected Akaike information criterion (CAIC), Bayesian information criterion (BIC) and Kolmogorov-Smirnov (K-S) statistics using the open-source R software. However, there is another refined approach to find K-S statistics for detail see [17],[15], and [16]. Here, the lower value of these criteria except the p-value and the higher p-value indicates the best fit.

The first dataset (I): In the first application, we consider the daily new cases in India from 16 March 2021 to 08 April 2021. The data is available at <https://www.worldometers.info/coronavirus/country/india-sar/>. The original data values are 28869, 35838, 39643, 40950, 43815, 40611, 47264, 53419, 59069, 62291, 62631, 68206, 56119, 53158, 72182, 81441, 89019, 92998, 103793, 96557, 115269, 126315, 131893, 14482.

This dataset is modelled with DT and other competitive models. For ease of fitting, data have been divided by 10,000 and their floor values have been stored. Table 4 contains the estimated parameters and their corresponding standard errors (SEs) as well as the various fitting measures discussed earlier. From Table 4, we conclude that the DT model is the best-performed model among others since it has the lowest values of AIC, BIC, CAIC, HQIC, and K-S test statistics with the highest p-value. We have plotted the $-LL$ and CDF plots in Figure 5 (upper left and upper right panel). This figure not only confirms the unique existence of the ML estimate but also portrays that the fitted CDF closely follow the pattern of the empirical CDF for the considered data.

Table 4: The ML estimate (SE) and various goodness of fit measures under dataset I.

Model	ML estimate(SE)	-LL	AIC	BIC	CAIC	K-S	P-value
DT	1.1447 (0.0121)	61.6498	125.2997	126.4778	125.4815	0.12640	0.8374
DW	0.0035(0.0034), 2.5990 (0.4083)	61.1957	126.3914	128.7475	126.9628	0.12669	0.7907
DR	0.9844(0.0031)	61.8800	125.76	126.9381	125.9418	0.15186	0.6373
DP	0.0252(0.0208), 0.5020(0.0974)	62.2001	128.4003	130.7564	128.9717	0.13958	0.6869
DLOG	0.5860(0.05317), 7.4515(0.6792)	62.7109	129.4219	131.778	129.9934	0.13598	0.7166
PB	0.1136(0.0187)	67.2632	136.5266	137.7046	136.7084	0.30641	0.0169
DsLi	0.7920(0.0269)	67.8623	137.7246	138.9027	137.9064	0.31724	0.0120
DPL	0.2460(0.0396)	68.7832	139.5665	140.7445	139.7483	0.32841	0.0083
DHLo-II	0.8548(0.0316), 0.7729(0.0626)	69.1321	142.2644	144.6205	142.8358	0.35068	0.0038
DsFx-I	0.9020(0.0167)	71.0351	144.0703	145.2484	144.2521	0.81633	<0.0001
Geo	0.8716(0.0244)	71.6627	145.3255	146.5035	145.5073	0.29772	0.0284
DB	0.9261(0.0709), 6.6364(6.4802)	87.3628	178.7273	181.0834	179.2987	0.74374	<0.0001
DPa	0.6217(0.0603)	92.3961	186.7923	187.9703	186.9741	0.72802	<0.0001

Table 5 consists of ML, MOM, OLS, and WLS estimates with their SEs and 95% ACI intervals for θ . To compare different methods, the K-S statistics with associated p-values for all methods are also provided in Table 5. From Table 5, we can easily observe that all estimation methods perform quite satisfactorily as the p-values associated with K-S statistics is greater than 0.05.

Table 5: The different estimates, SE, and K-S with p-value under dataset I.

Method	Estimate	SE	K-S	P-value	ACI
ML estimate	1.1447	0.0121	0.1264	0.8374	[1.1209, 1.1683]
MOM	1.1372	0.0367	0.1544	0.6162	-
OLS	1.1561	0.0392	0.1633	0.5440	-
WLS	1.1561	0.0392	0.1633	0.5439	-

The second dataset (II): This dataset gives the survival times of a group of laboratory mice, which were exposed to a fixed dose of radiation at an age of 5 to 6 weeks [see, [14], pp. 445]. This group of mice lived in a conventional lab environment. The cause of death for each mouse was assigned after autopsy to be one of three things: thymic lymphoma (C1), reticulum cell sarcoma (C2), or other causes (C3). Here, we have used the dataset under C3 only. The mice are all died by the end of the experiment, so there is no censoring. The data values are:

40, 42, 51, 62, 163, 179, 206, 222, 228, 252, 259, 282, 324, 333, 341, 366, 385, 407, 420, 431, 441, 461, 462, 482, 517, 517, 524, 564, 567, 586, 619, 620, 621, 622, 647, 651, 686, 761, 763.

The above dataset is modelled with DT and DW, DR, PB, DsLi, DPL, Geo, DB, DPa models. The estimated parameters and other fitting measures are reported in Table 6. From the outcomes of Table 6, we conclude that the DT distribution is the best choice among other competitive models since it has the lowest values of $-LL$, AIC, BIC, CAIC, HQIC, and K-S statistics with the highest P-value. Figure 5 (lower left and lower right panel) also depicts that DT distribution has a unique ML estimate for the given data and it is well enough to model this data.

Table 6: The ML estimate (SE) and various goodness of fit measures under dataset II.

Model	ML estimate (SE)	-LL	AIC	BIC	CAIC	K-S	P-Value
DT	1.0024(0.0002)	262.0291	526.0581	527.7217	526.1663	0.0907	0.9049
DW	0.9999 (3.548e-07), 2.0772 (0.0318)	263.1519	530.3039	533.6310	530.6372	0.1008	0.8223
DR	0.9999 (5.874e-07)	263.1909	528.3818	530.0454	528.4899	0.1080	0.7525
PB	0.0020(0.0002)	267.1738	536.3476	538.0112	536.4557	0.1597	0.2723
DsLi	0.9951(0.0005)	266.9048	535.8097	537.4733	535.9178	0.1587	0.2797
DPL	0.0048(0.0005)	266.9121	535.8242	537.4878	535.9323	0.1588	0.2786
Geo	0.9975(0.0004)	273.9544	549.9088	551.5723	550.0169	0.2385	0.0236
DB	0.9282(0.0621), 2.3077(2.0575)	334.6387	673.2775	676.6046	673.6108	0.6803	<0.0001
DPa	0.8422(0.0231)	334.8421	671.6843	673.3478	671.7924	0.6801	<0.0001

Table 7 displays the ML, MOM, OLS, and WLS estimates with their SEs and 95% ACI intervals for θ . This table also contains the K-S statistics with associated p-values for all considered methods. From Table 7, we can easily observe that all estimation methods perform quite satisfactorily as the p-values associated with K-S statistics are greater than 0.05.

Table 7: The different estimates, SE and K-S with p-value under dataset II.

Method	Estimate	SE	K-S	P-Value	ACI
ML estimate	1.0024	0.0002	0.0907	0.9049	[1.0020, 1.0027]
MOM	1.0096	0.0022	0.2047	0.0759	-
OLS	1.0024	0.0004	0.0909	0.9034	-
WLS	1.0024	0.0004	0.0909	0.9034	-

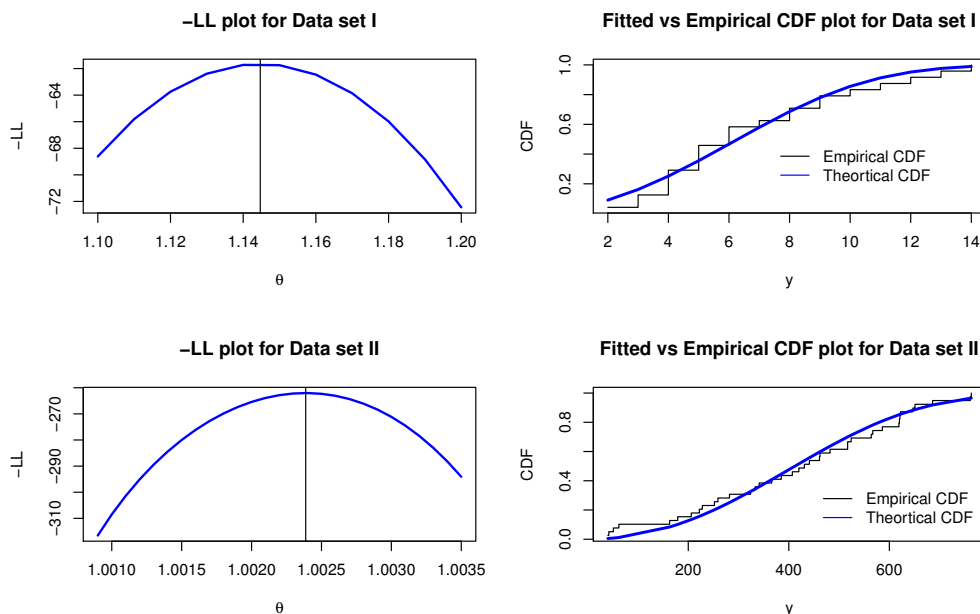


Figure 5: The $-LL$ and CDFs plots for dataset I and II.

6. CONCLUSION

In this article, a new one-parameter discrete Teissier distribution is obtained. It is observed that with one parameter, this model has great flexibility in terms of fitting as it is capable of modelling equi-, over and under-dispersed datasets. It is also capable of the modelling of

positively, negatively skewed and increasing failure datasets. In this article, various important distributional properties of DT distribution are discussed.

The unknown parameters of the proposed model are estimated under the various classical methods. An extensive simulation study is presented for the assessment of the various estimators under count data. Finally, the fitting capability of the proposed model for count data is illustrated using two real datasets. Hence, we can conclude that the suggested model may be used as an alternative model to some well-known existing models to analyze discrete data generated from various domains.

A future plan of action regarding the current study might be an examination of the censored data using the proposed model. We may investigate the load share model where the component failure time follows the DT distribution. The stress-strength parameter may also be examined using various censored data. In addition, a bivariate extension of the DT distribution can be developed.

ACKNOWLEDGEMENT

The authors would like to thank the editor and an anonymous referee for their careful reading of the manuscript and constructive suggestions, which significantly improved the earlier version of the manuscript. The last author is thankful to the Department of Science and Technology, India for providing financial aid for the research work under the Inspire Fellowship Program vide letter number DST/INSPIRE Fellowship/2017/IF170038.

CONFLICT OF INTEREST

The authors declare no conflicts of interest.

REFERENCES

- [1] Alamatsaz, M. H., Dey, S., Dey, T., & Harandi, S. S. (2016). Discrete generalized Rayleigh distribution. *Pakistan Journal of Statistics*, 32(1).
- [2] Altun, E. (2020). A new one-parameter discrete distribution with associated regression and integer-valued autoregressive models. *Mathematica Slovaca*, 70(4), 979-994.
- [3] Chakraborty, S. (2015). Generating discrete analogues of continuous probability distributions- A survey of methods and constructions. *Journal of Statistical Distributions and Applications*, 2(1), 6.
- [4] Chakraborty, S., & Chakravarty, D. (2016). A new discrete probability distribution with integer support on $(-\infty, \infty)$. *Communications in Statistics-Theory and Methods*, 45(2), 492-505.
- [5] Eliwa, M. S., & El-Morshedy, M. (2021). A one-parameter discrete distribution for over-dispersed data: statistical and reliability properties with applications. *Journal of Applied Statistics*, 1-21.
- [6] Eliwa, M. S., Alhussain, Z. A., & El-Morshedy, M. (2020). Discrete Gompertz-G family of distributions for over-and under-dispersed data with properties, estimation, and applications. *Mathematics*, 8(3), 358.
- [7] El-Morshedy, M., Eliwa, M. S., & Tyagi, A. (2021a). A discrete analogue of odd Weibull-G family of distributions: properties, classical and Bayesian estimation with applications to count data. *Journal of Applied Statistics*, 1-25.
- [8] El-Morshedy, M., Alizadeh, M., Al-Bossly, A., & Eliwa, M. S. (2021b). A Probability Mass Function for Various Shapes of the Failure Rates, Asymmetric and Dispersed Data with Applications to Coronavirus and Kidney Dymorphogenesis. *Symmetry*, 13(10), 1790.
- [9] Gómez-Déniz, E., & Calderín-Ojeda, E. (2011). The discrete Lindley distribution: properties and applications. *Journal of Statistical Computation and Simulation*, 81(11), 1405-1416.

- [10] Gupta, P. L., Gupta, R. C., and Tripathi, R. C. (1997). On the monotonic properties of discrete failure rates. *Journal of Statistical Planning and Inference*, 65(2), 255-268.
- [11] Jayakumar, K., & Babu, M. G. (2018). Discrete Weibull geometric distribution and its properties. *Communications in Statistics-Theory and Methods*, 47(7), 1767-1783.
- [12] Krishna, H., & Pundir, P. S. (2009). Discrete Burr and discrete Pareto distributions. *Statistical Methodology*, 6(2), 177-188.
- [13] Keilson, J., and Gerber, H. (1971). Some results for discrete unimodality. *Journal of the American Statistical Association*, 66(334), 386-389.
- [14] Lawless, J. F. (2003). *Statistical models and methods for lifetime data* (Vol. 362). John Wiley & Sons.
- [15] Lemeshko, B.Yu., Lemeshko, S.B. and Postovalov S.N. (2010) Statistic Distribution Models for Some Nonparametric Goodness-of-Fit Tests in Testing Composite Hypotheses. *Communications in Statistics - Theory and Methods*, 39: 460-471. DOI: 10.1080/03610920903140148
- [16] Lemeshko, B.Yu., Lemeshko, S.B. (2011) Models of Statistic Distributions of Nonparametric Goodness-of-Fit Tests in Composite Hypotheses Testing for Double Exponential Law Cases. *Communications in Statistics - Theory and Methods*, 40:2879-2892. DOI: 10.1080/03610926.2011.562770
- [17] Lemeshko B.Yu., Postovalov S.N. (2001) Application of the nonparametric goodness-of-fit Tests in testing composite hypotheses. *Optoelectronics, Instrumentation and Data Processing*. No.2. - P. 76-88.
- [18] Sankaran, M. (1970). "The discrete Poisson-Lindley distribution", *Biometrics.*, vol. 26, no. 1, pp. 145-149.
- [19] Nakagawa, T., & Osaki, S. (1975). The discrete Weibull distribution. *IEEE transactions on reliability*, 24(5), 300-301.
- [20] Renyi, A. (1961). On measures of entropy and information. *Mathematical Statistics and Probability*, 1, 547-561.
- [21] Roy, D. (2003). The discrete normal distribution. *Commun. Statist. Theor. Meth.* 32(10):1871-1883.
- [22] Roy, D. (2004). Discrete Rayleigh distribution. *IEEE Trans. Reliab.* 53:255-260.
- [23] Shafqat, M., Ali, S., Shah, I., & Dey, S. (2020). Univariate Discrete Nadarajah and Haghighi Distribution: Properties and Different Methods of Estimation. *Statistica*, 80(3), 301-330.
- [24] Steutel, F.W. & van Harn, K. (2004). *Infinite Divisibility of Probability Distributions on the Real Line*. New York: Marcel Dekker.
- [25] Swain, J. J., Venkatraman, S., & Wilson, J. R. (1988). Least-squares estimation of distribution functions in Johnson's translation system. *Journal of Statistical Computation and Simulation*, 29(4), 271-297.
- [26] Sharma, V. K., Singh, S. V., & Shekhawat, K. (2020). Exponentiated Teissier distribution with increasing, decreasing and bathtub hazard functions. *Journal of Applied Statistics*, 1-23.
- [27] Teissier, G. (1934). Recherches sur le vieillissement et sur les lois de la mortalité. *Annales de physiologie et de physicochimie biologique*, 10(2), 237-284.
- [28] Tyagi, A., Choudhary, N., & Singh, B. (2020). A new discrete distribution: Theory and applications to discrete failure lifetime and count data. *J. Appl. Probab. Statist*, 15, 117-143.
- [29] Tyagi, A., Choudhary, N., and Singh, B. (2019). Discrete additive Perks-Weibull distribution: Properties and applications. *Life Cycle Reliability and Safety Engineering*, 8(3), 183-199.

Costs of Age Replacement under Accelerated Life Testing with Censored Information

^{1,*}Intekhab Alam, ²Mohd Asif Intezar, ³Lalit Kumar Sharma, Mohammad Tariq Intezar⁴, Aqsa Irfan⁵

^{1,2,3}Department of Management, St. Andrews Institute of Technology & Management, Gurugram, Delhi (NCR), India

⁴Department of Law & Management
GD Goenka University, Gurugram, Haryana, India

⁵Department of Geology, Aligarh Muslim University, Aligarh, India

^{1,*}Email-intekhab.pasha54@gmail.com, ²Email-ap11_mgmt@saitm.org, ³Email-dean_mgmt@saitm.org, ⁴Email-m.tariq@gdgu.org, ⁵Email-aqsairfan.amu@gmail.com

*Corresponding author

Abstract

Accelerated life testing (ALTg) helps manufacturers to predict the various costs associated with the product under the warranty policy. The main aim of undertaking ALTg is the extended time of today's manufactured goods, the small-time among design and make public, and the difficulty of analysis of items that are continuously used in ordinary environments. Hence ALTg is used to offer quick information about the life distribution of products. We describe how to propose and analyze the accelerated life testing plans to develop the excellence and reliability of the item for consumption. We also focus on finding the expected cost rate and the expected total cost for age replacement in the pro-rate rebate warranty plan. The problem is studied using constant stress, under the hypothesis that the life spans of the units follow the Gompertz distribution (GD) for predicting the cost of age replacement in the warranty plan. The asymptotic variance and covariance matrix, confidence intervals for parameters, and respective errors are also obtained. A simulation study is carried out to show the statistical properties of distribution parameters.

Keywords: Accelerated Life Testing, Gompertz distribution, Warranty policy, Age-replacement, Type-I Censoring, Fisher Information matrix, Simulation Study.

I. Introduction

Nowadays, most producers are doing their finest to build up and get better the performance of their items to boost the requirement and increase faith between them and their purchaser. The producers face several disputes while developing manufactured goods, together with complicatedness in scheming the failure of the manufactured goods during the existing investigation era. To defeat many of the difficulties in normal reliability, testing ALTg techniques may be employed. It is significant to get better the performance of the manufactured goods, work towards the improvement of the item and conclude the issues that cause the undersized lifetime. Quantitative ALTg engages in identifying stress situations that will speed up the stoppage manner. Therefore, the failures may be observed in a shorter phase. The accelerated investigation situations may engage a superior stage of force, power, weight, speed, temperature, vibration, etc., and more than one stress may be operated depending on the item's nature. Information composed at such

accelerated circumstances is then extrapolated during a bodily suitable statistical representation to estimate the life span distribution at ordinary use circumstances.

In life testing analysis and reliability theories, the engineer may not constantly get absolute information on failure epochs for all investigational components. Information achieved from such researches is called censored information. The main reasons for censoring schemes are reducing the total time on investigation and the expenditure related to it. The censoring can make stability between total time used up for the experimentation, the number of components used in the test and the effectiveness of statistical assumption based on the experiment's outcomes. Type-I (time) censoring and Type- II (item) censoring are the frequent schemes. Here, we are only focusing on Type-I censoring scheme. Type I censoring occurs when an experiment finishes after a preset amount of time. There are several other censoring schemes, i.e., multiple censoring, progressive censoring, hybrid censoring and adaptive progressive hybrid censoring, etc.

According to Nelson [1], and Rao [2], the accelerated life test (ALT) is generally of three types. The first type is named the constant-stress ALT (CSALT). The next is the step-stress accelerated life test (SSALT). The third is progressive-stress ALT (PSALT). The stress is set aside at a constant level during the analysis in CSALT. In SSALT, the investigation circumstance varies at a known time or upon the happening of a specific number of failures. The stress practical to examination manufactured goods is constantly increasing with the point in PSALT. For an extensive review on these methods, (see Kim and Bai [3], AL-Hussaini and Abdel-Hamid [4, 5], Miller and Nelson [6]). These three techniques can decrease the testing time and accumulate a lot of human resources, material, and capital.

The key statement in ALT is that the mathematical model connecting the life span of the element and the stress is identified or can be assumed. In various situations, such life stress relationships are unknown and cannot be assumed, i.e. the information achieved from ALT cannot be extrapolated to use situation. So, in such situations, one more advanced method can be applied, which is partially accelerated life tests (PALTs). If the acceleration factor cannot be assumed as a known value, then PALT will be an excellent selection to carry out the life investigation. In PALTs, objects are experienced at both accelerated and use circumstances. PALTs: constant-stress PALT (CSPALT), step-stress PALT (SSPALT) and progressive-stress PALT (PSPALT) are the three frequently used types.

A rebate warranty policy is one of the mainly widespread types of warranty strategies. In a rebate plan, the seller refunds a customer some proportion of the sales worth if the manufactured goods are unsuccessful during the warranty era. Frequent examples of goods sold under rebate plans include batteries and tires. Objects sold under failure-free warranties might contain electronics and household machines. Rebate strategies also take two widespread forms: lump sum, and pro-rata rebates. If an article fails before the conclusion of the substance's warranty age, it is replaced or repaired as per common, however, only for the amount based on a price that depends on the age of the article at the point of failure. Basically, a pro-rate warranty decreases the value of your buy over time. This type of warranty is sometimes called a partial warranty since only a part of the original cost is covered. The producers shall only give incentives when they have the trust in the goods that their item has the capability to serve at least in the stated warranty period. Therefore, manufacturers need to test the reliability and performance of the goods before letting them serve in the marketplace. This can be done by using accelerated life testing on goods. Accelerated life testing also helps producers to predict the various costs connected with the item under the warranty policy.

Now, we present brief literature on ALT and warranty policies related to our study. El-Dessouky [7,8] described ALTg and age-replacement policy under warranty plan and also described maintenance service strategy under SSPALT using Type-II censored samples. Zhao and Xie [9] provided a structure to calculate the assurance outlay and risk under one-dimensional. At present, the two-dimensional and extended warranty has taken an important place in warranty policy analysis (Jack et al. [10], Gupta et al. [11], Huang et al. [12], Jung et al. [13], and Ye and Murthy [14]). However, it is very tough and tricky to design warranty plans and calculate warranty costs for new goods that have not been come into the market, because the failure rate of such types of products is not available. A literature review is presented by Murthy and Djameludin [15] on new item assurance by considering marketing, logistics, etc. A combined optimization method that concerned trustworthiness, service contract and price for new goods is presented by Huang et al. [16]. Xie and Ye. [17] proposed a comprehensive inexpensive guarantee cost forecast under the new item. In Yang [18], optimal 3-level accommodation ALT affairs were talked about to minimize the asymptotic about-face of best likelihood appraisal of the assurance cost. For an overview of accelerated believability experiments, one can refer to Meeker and Escobar [19]. Borgia et al. [20] presented a case study for the household's gadgets. Yang [21] proposed a technique for item population for predicting the warranty outlay and its confidence interval. Alam et al. [22] offered a study on age replacement policy under pro rebate warranty policy for Burr Type-X failure model using Type-II censoring scheme. Currently, Alam and Aquil [23] presented a study on SSPALT and provided its application in maintenance service policy for the generalized inverted exponential distribution. Alam et al. [24] handled constant-stress ALT under a progressive Type-II censoring scheme and also presented its application in the area of maintenance strategy. Almalki et al. [25] handled with constant stress ALTs model for Kumaraswamy failure model under the progressive censoring scheme.

In this work, we design ALT under Type-I censoring for GD and also provide the application of ALT in the field of warranty policy and this is the key factor of this study. In previous studies, a lot of study is available on ALT with different censoring schemes for different lifetimes model but few studies available that provide its application in the field of warranty policy The novelty of this study is that no earlier study is available for GD under pro-rata rebate warranty policy under Type-I censoring scheme.

The rest of the paper is organized as follows: Section 2 provides the introduction of GD and test procedure. The likelihood function, Fisher Information matrix, the inverse of Fisher Information matrix is developed in section 3. A simulation study is carried out in section 4. Estimation of shape parameter and reliability function is presented in section 5. The age-replacement policy for GD under pro-rate rebate warranty is presented in Section 6. Finally, a conclusion is made in section 7.

II. Model Description and Test Method

ALT is generally performed by one of the two approaches; (i) accelerated failure time, which means ALT is performed for the item by experiencing usual circumstances but more intensively than ordinary. This approach is excellent for items or components that are exercised on a continuous-time basis. (ii) Accelerated stress means ALT is performed with items or components at higher stress than usual. For designing ALT plans, the following points are needed

- (i) The stress application testing process.
- (ii) The stress levels selected and the type of stress to be applied in the investigation for each stress type.

- (iv) Relationship between life and stress which is expressed by the mathematical model.
- (v) At last, the proportion of experiment elements to be allocated to every level of stress.

Some authors dealt with constant stress, such as Abdel-Ghaly [26] tackled with an accelerated life test plan for the Pareto failure model and estimate reliability function and parameters of the model. Attia et al. [27,28] handled with Accelerated life test plan for Birnbaum-saunders and Generalized Logistic distributions using different censoring plans with constant stress. In the following section:

- (i) Stress G_j has k -levels.
- (ii) Assuming that G_u is normal use situation and fulfilling $G_u < G_1 < G_2 < G_3 < \dots < G_k$.
- (iii) There are m_j units put on the investigation at every stress stage.
- (iv) The test ends when r_j units attain among these s_j units.

This current study is dealt with Type-I censoring and constant stress with the assumption that the lifetime of the units follows the GD.

GD has wide popularity in relating human mortality, establishing actuarial tables, and other areas. Historically, it was firstly commenced by Gompertz [29]. GD has the following probability density function (*pdf*) and cumulative distribution function (*cdf*);

The *pdf* of the model is given as

$$f(x_{ij}, \tau_j, \gamma) = \tau_j \gamma e^{x_{ij}\gamma} e^{-\tau_j (e^{x_{ij}\gamma} - 1)}, \quad x_{ij} > 0, \tau_j > 0, \gamma > 0 \tag{1}$$

where γ and τ_j are scale and shape parameters, respectively.

The *cdf* of the model is given as

$$F(x_{ij}, \tau_j, \gamma) = 1 - e^{-\tau_j (e^{x_{ij}\gamma} - 1)}, \quad x_{ij} > 0, \tau_j > 0, \gamma > 0 \tag{2}$$

The Reliability function of the model is given as

$$S(x_{ij}, \tau_j, \gamma) = e^{-\tau_j (e^{x_{ij}\gamma} - 1)} \tag{3}$$

The Hazard function of the model is given as

$$h(x_{ij}, \tau_j, \gamma) = \tau_j \gamma e^{x_{ij}\gamma} \tag{4}$$

The pdf, cdf, Reliability, and hazard curves are shown in Figure1, Figure 2, Figure3, and Figure4, respectively.

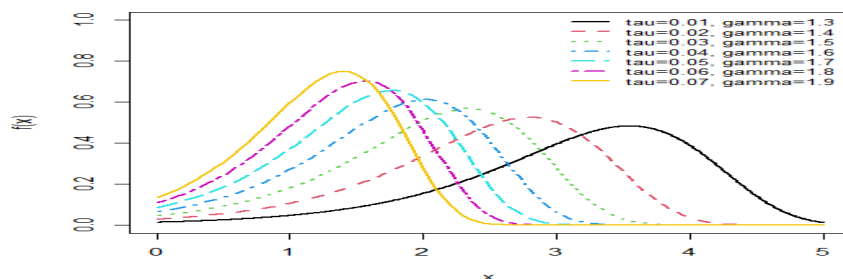


Figure 1: Probability density curve of GD

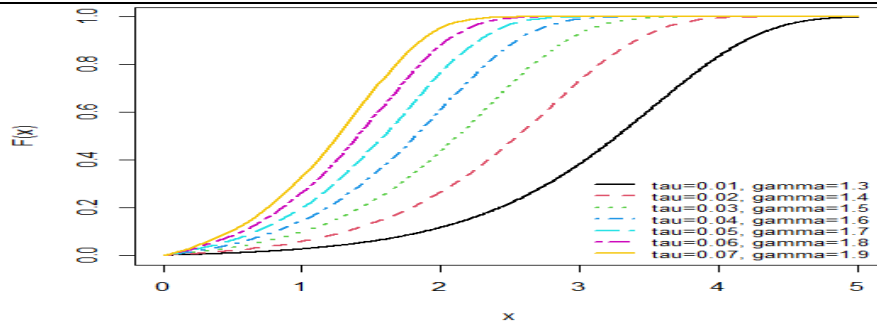


Figure2: Cumulative distribution curve of GD

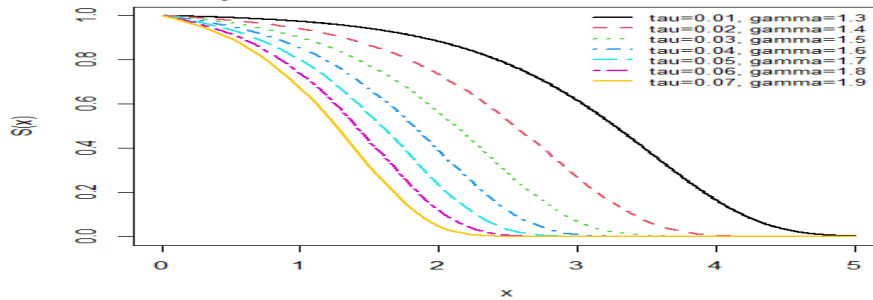


Figure3: Reliability curve of GD

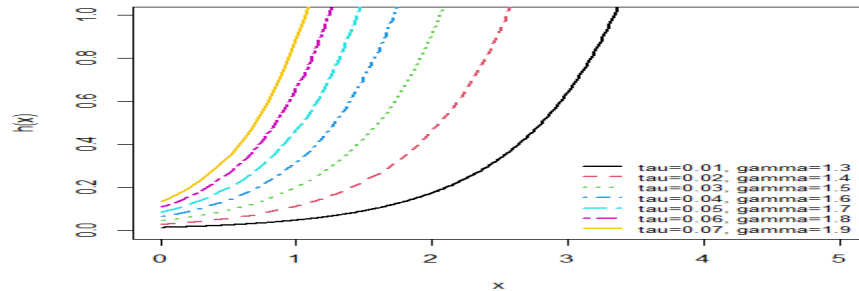


Figure4: Hazard curve of GD

GD possesses a unimodal *pdf* and has an increasing hazard curve for increasing values of τ and γ . Willekens [30] handled the associations of GD with other failure models. Wu et al. [31] proposed the weighted and unweighted least squares estimations for GD under censored and complete information. Chang and Tsai [32] intended the maximum likelihood estimates (MLEs), and accomplished the establishment for the exact confidence interval. Mohie El-Din [33] presented a study under generalized progressively hybrid censoring for GD.

This study is based on constant stress and Type-I censoring scheme. We have considered the Stress $G_j, j = 1, 2, \dots, k$ which affects the shape parameter of the used distribution, μ_j through the following equation (5) called the power rule model.

$$\tau_j = RG_j^{-f}; \quad R > 0, f > 0, \quad j = 1, 2, \dots, k \quad (5)$$

where R and f are the proportionality constant; and power of the applied stress respectively.

III. Estimation Process

In this section, the maximum likelihood (ML) estimation method is used. The reliability practitioner used this method because it is very robust and provides estimates of the parameters with excellent properties. At the stress level G_j , the authors constructed the likelihood function of an observation x (time to failure) and at each stress level G_j , s_j units were put on the test.

Therefore, $N = \sum_{j=1}^k s_j$ is the total number of components in the test. When a Type-I (time)

censoring scheme is adopted at each stress level, the experiment ends once the censoring time " x_0 " is reached. It is assumed that $r_j (\leq s_j)$ units are observed at the j th stress level before the test is terminated and $(s_j - r_j)$ units still carry on till the end of the analysis. In this situation, the likelihood function of the testing for GD model is taking the following form

$$L(x_{ij}, R, \gamma, f) = \prod_{j=1}^k \frac{s_j}{(s_j - r_j)!} \left[\prod_{i=1}^{r_j} f(x_{ij}, R, \gamma, f) \right] [1 - F(x_0)]^{s_j - r_j} \quad (6)$$

where x_0 is the time of cessation of the experiment and $\ln L(x_{ij}, R, \gamma, f) = \ln L$.

The log-likelihood function is obtained by taking the logarithm of the above equation (6) and given as

$$\begin{aligned} \ln L = & K + \sum_{j=1}^k r_j \ln(RG_j^{-f} \gamma) + \gamma \sum_{i=1}^{r_j} \sum_{j=1}^k x_{ij} - \sum_{i=1}^{r_j} \sum_{j=1}^k RG_j^{-f} (e^{\gamma x_{ij}} - 1) \\ & + \sum_{j=1}^k (s_j - r_j) RG_j^{-f} (e^{\gamma x_0} - 1) \end{aligned} \quad (7)$$

where K is the constant.

The ML estimates of γ, R and f can be estimated from the following three equations.

$$\frac{\partial \ln L}{\partial \gamma} = \sum_{j=1}^k r_j \gamma^{-1} + \sum_{i=1}^{r_j} \sum_{j=1}^k x_{ij} - \sum_{i=1}^{r_j} \sum_{j=1}^k R x_{ij} e^{\gamma x_{ij}} G_j^{-f} + \sum_{j=1}^k (s_j - r_j) RG_j^{-f} x_0 e^{\gamma x_0} = 0$$

$$\frac{\partial \ln L}{\partial f} = - \sum_{j=1}^k r_j \ln(G_j) + \sum_{i=1}^{r_j} \sum_{j=1}^k RG_j^{-f} \ln(G_j) (e^{\gamma x_{ij}} - 1) -$$

$$\sum_{j=1}^k (s_j - r_j) RG_j^{-f} \ln(G_j) (e^{\gamma x_0} - 1) = 0$$

$$\frac{\partial \ln L}{\partial R} = \sum_{j=1}^k r_j R^{-1} - \sum_{i=1}^{r_j} \sum_{j=1}^k G_j^{-f} (e^{\gamma x_{ij}} - 1) + \sum_{j=1}^k (s_j - r_j) G_j^{-f} (e^{\gamma x_0} - 1) = 0$$

It looks impossible to solve the above three non-linear equations manually. Therefore, an iterative technique (Newton-Raphson) can be used to get maximum likelihood estimates (MLEs) of parameters.

In mathematical statistics, the Fisher information or Information matrix is a technique of evaluating the amount of information that an observable random variable carries about an unknown parameter of a distribution. Simply, the Information matrix is the variance of the score or the expected value of the observed information.

The Information matrix for the Gompertz failure model under Type-I censoring is given as

$$F = \begin{bmatrix} \frac{-\partial^2 \ln L}{\partial \gamma^2} & \frac{-\partial^2 \ln L}{\partial \gamma \partial f} & \frac{-\partial^2 \ln L}{\partial \gamma \partial R} \\ \frac{-\partial^2 \ln L}{\partial f \partial \gamma} & \frac{-\partial^2 \ln L}{\partial f^2} & \frac{-\partial^2 \ln L}{\partial f \partial R} \\ \frac{-\partial^2 \ln L}{\partial R \partial \gamma} & \frac{-\partial^2 \ln L}{\partial R \partial f} & \frac{-\partial^2 \ln L}{\partial R^2} \end{bmatrix} \quad (8)$$

The elements of the matrix F are obtained by second partial derivatives of log-likelihood function with respect to parameters λ, q and U . Consequently, the elements are expressed by the following equations

$$\begin{aligned} \frac{\partial^2 \ln L}{\partial \gamma^2} &= -\sum_{j=1}^k r_j \gamma^{-2} - \sum_{i=1}^{r_j} \sum_{j=1}^k R x_{ij}^2 e^{\gamma x_{ij}} G_j^{-f} + \sum_{j=1}^k (s_j - r_j) R G_j^{-f} x_0^2 e^{\gamma x_0} \\ \frac{\partial^2 \ln L}{\partial f^2} &= -\sum_{i=1}^{r_j} \sum_{j=1}^k R G_j^{-f} \ln^2(G_j) \left(e^{\gamma x_{ij}} - 1 \right) + \sum_{j=1}^k (s_j - r_j) R G_j^{-f} \ln^2(G_j) \left(e^{\gamma x_0} - 1 \right) \\ \frac{\partial^2 \ln L}{\partial R^2} &= -\sum_{j=1}^k r_j R^{-2} \\ \frac{\partial^2 \ln L}{\partial f \partial \gamma} &= +\sum_{i=1}^{r_j} \sum_{j=1}^k R G_j^{-f} \ln(G_j) \left(x_{ij} e^{\gamma x_{ij}} \right) - \sum_{j=1}^k (s_j - r_j) R G_j^{-f} \ln(G_j) \left(x_0 e^{\gamma x_0} \right) \\ \frac{\partial^2 \ln L}{\partial f \partial R} &= \sum_{i=1}^{r_j} \sum_{j=1}^k G_j^{-f} \ln(G_j) \left(e^{\gamma x_{ij}} - 1 \right) - \sum_{j=1}^k (s_j - r_j) G_j^{-f} \ln(G_j) \left(e^{\gamma x_0} - 1 \right) \\ \frac{\partial^2 \ln L}{\partial \gamma \partial R} &= -\sum_{i=1}^{r_j} \sum_{j=1}^k x_{ij} e^{\gamma x_{ij}} G_j^{-f} + \sum_{j=1}^k (s_j - r_j) G_j^{-f} x_0 e^{\gamma x_0} \end{aligned}$$

Now, the variance-covariance matrix is the inverse of the Fisher Information matrix and given as

$$\Sigma = F^{-1} \quad (9)$$

$$\Sigma = \begin{bmatrix} \frac{-\partial^2 \ln L}{\partial \gamma^2} & \frac{-\partial^2 \ln L}{\partial \gamma \partial f} & \frac{-\partial^2 \ln L}{\partial \gamma \partial R} \\ \frac{-\partial^2 \ln L}{\partial f \partial \gamma} & \frac{-\partial^2 \ln L}{\partial f^2} & \frac{-\partial^2 \ln L}{\partial f \partial R} \\ \frac{-\partial^2 \ln L}{\partial R \partial \gamma} & \frac{-\partial^2 \ln L}{\partial R \partial f} & \frac{-\partial^2 \ln L}{\partial R^2} \end{bmatrix}^{-1} = \begin{bmatrix} AVar(\hat{\gamma}) & ACov(\hat{\gamma} \hat{f}) & ACov(\hat{\gamma} \hat{R}) \\ ACov(\hat{f} \hat{\gamma}) & AVar(\hat{f}) & ACov(\hat{f} \hat{R}) \\ ACov(\hat{R} \hat{\gamma}) & ACov(\hat{R} \hat{f}) & AVar(\hat{R}) \end{bmatrix} \quad (10)$$

$AVar$, $ACov$ are asymptotic variance and asymptotic covariance, respectively.

The $100(1 - \pi)\%$ approximated two-sided limits of confidence for parameters λ, U and q are given as

$$\hat{\gamma} \pm Z_{\pi/2} \sqrt{I_{11}^{-1}(\hat{\gamma}, \hat{f}, \hat{R})}, \hat{f} \pm Z_{\pi/2} \sqrt{I_{22}^{-1}(\hat{\gamma}, \hat{f}, \hat{R})} \text{ and } \hat{R} \pm Z_{\pi/2} \sqrt{I_{33}^{-1}(\hat{\gamma}, \hat{f}, \hat{R})}$$

$Z_{\pi/2}$ is the $100(1 - \pi/2)\%$ percentile of a standard normal variate.

IV. Simulation Results

In this section, we apply the Monte-Carlo simulation technique to examine the performances of the MLEs through their absolute relative bias (RAB) and mean square error (MSE). Using the invariance property of MLEs, we can estimate the MLEs of shape Parameter τ_j through the following expression;

$$\tau_j = RG_j^{-f}; \quad R > 0, f > 0, \quad j = 1, 2, \dots, k$$

The detailed steps are given below:

1. First, 1000 random samples of sizes 25, 50, 75, and 100 are generated from GD by inverse CDF method. Different initial values are selected for all sets of parameters.
2. The stress has three levels and the values of are $(G_1 = 1, G_2 = 1.5, G_3 = 2), s_j = \frac{n}{3}$ & $r_j = 60\% n_j, n$ is sample size.
3. The parameters of the model are estimated under Type-I censoring for all sample sizes.
4. The Newton-Raphson method is applied for solving all non-linear equations.
5. The estimates of the shape parameter μ_j are calculated from equation (5).
6. The RABs and MSEs are tabulated for all sets of (γ_0, R_0, f_0) .
7. We determine the MLEs of the scale parameter γ_u at the usual stress level $G_u = 0.5$ by the invariance property of MLEs,
8. The reliability function at the similar usual stress for various values γ, G, f and t_0 is calculated.

$$\hat{R}_u(t_0) = e^{-\tau_0 \left(e^{t_0 \gamma_0} - 1 \right)}$$

9. At mission time ($t_0 = 1.2, 1.5, 1.9$), the MLEs of reliability function are predicted in the same usual circumstances for every parameter set.

Table 1: The Estimates, Relative Bias and MSE of the parameters $(\gamma, G, f, \tau_1, \tau_2, \tau_3)$ under Type-I censoring

n	Parameters	$(\gamma_0 = 0.40, G_0 = 1.7, f_0 = 1)$			$(\gamma_0 = 1.2, G_0 = 1.7, f_0 = 1)$		
		Estimator	RABs	MSEs	Estimator	RABs	MSEs
25	γ	2.543	0.109	0.095	2.633	0.096	0.078
	G	2.765	0.116	0.097	1.873	0.109	0.074
	f	1.987	0.078	0.069	2.162	0.120	0.101
	τ_1	2.126	0.084	0.077	1.876	0.091	0.067
	τ_2	1.987	0.105	0.086	2.998	0.087	0.760
	τ_3	1.376	0.105	0.098	2.087	0.090	0.081

50	γ	2.830	0.086	0.076	1.876	0.098	0.076
	G	2.543	0.067	0.055	2.146	0.109	0.061
	f	2.791	0.077	0.061	1.998	0.123	0.097
	τ_1	1.162	0.054	0.040	1.989	0.094	0.051
	τ_2	2.788	0.054	0.031	1.360	0.080	0.042
	τ_3	2.197	0.049	0.055	1.786	0.076	0.057
	75	γ	2.139	0.044	0.042	2.345	0.069
G		2.349	0.054	0.044	2.492	0.050	0.051
f		2.046	0.065	0.054	2.052	0.072	0.086
τ_1		1.556	0.046	0.035	2.528	0.042	0.047
τ_2		2.290	0.048	0.040	1.404	0.039	0.037
τ_3		1.196	0.041	0.022	1.967	0.011	0.050
100		γ	2.252	0.018	0.029	2.763	0.064
	G	2.612	0.023	0.013	2.160	0.042	0.023
	f	1.313	0.113	0.010	1.885	0.045	0.031
	τ_1	1.950	0.027	0.014	1.443	0.062	0.069
	τ_2	2.322	0.031	0.023	2.111	0.018	0.016
	τ_3	1.089	0.032	0.023	1.025	0.033	0.025

Table 2:The Estimates, Relative Bias and MSE of the parameters $(\gamma, G, f, \tau_1, \tau_2, \tau_3)$ under Type-I censoring

n	Parameter s	$(\gamma_0 = 0.40, G_0 = 1.3, f_0 = 1)$			$(\gamma_0 = 1.2, G_0 = 1.3, f_0 = 1.9)$		
		Estimator	RABs	MSEs	Estimator	RABs	MSEs
25	γ	1.846	0.132	0.093	2.987	0.132	0.119
	G	1.425	0.123	0.110	1.171	0.115	0.099
	f	2.927	0.110	0.099	2.621	0.083	0.061
	τ_1	1.901	0.083	0.062	1.523	0.110	0.081
	τ_2	2.170	0.092	0.075	2.210	0.097	0.078
	τ_3	1.983	0.082	0.065	2.809	0.123	0.106
	50	γ	2.452	0.062	0.077	1.667	0.071
G		1.744	0.092	0.072	1.158	0.144	0.070
f		1.837	0.073	0.070	1.136	0.052	0.095
τ_1		1.164	0.081	0.058	1.283	0.074	0.061
τ_2		1.786	0.188	0.065	1.170	0.069	0.061
τ_3		1.564	0.068	0.065	2.986	0.088	0.079
75		γ	1.639	0.054	0.045	2.998	0.063
	G	1.919	0.089	0.063	2.791	0.081	0.056
	f	1.778	0.052	0.050	1.990	0.050	0.066
	τ_1	2.061	0.086	0.061	2.930	0.066	0.055
	τ_2	1.398	0.070	0.047	1.132	0.054	0.016
	τ_3	1.494	0.059	0.076	2.998	0.077	0.098

100	γ	1.052	0.030	0.037	1.997	0.049	0.056
	G	2.168	0.060	0.023	1.439	0.055	0.041
	f	2.016	0.043	0.061	1.967	0.042	0.055
	τ_1	1.192	0.050	0.019	1.209	0.055	0.066
	τ_2	1.921	0.059	0.033	1.432	0.032	0.014
	τ_3	2.595	0.042	0.016	2.955	0.030	0.084

V. Estimation of the survival functions and shape parameter at normal stress

In the following table, we estimate the survival function at the usual stress level $G_u = 0.5$ for various values of parameters γ, G, f and t_0 , also find the shape parameter for the same stress level.

Table3: Estimated reliability functions and shape parameter at normal stress

γ_0	G_0	f_0	τ_0	t_0	$R_u(t_0)$
0.40	1.7	1	3.332	1.2	0.543
				1.5	0.523
				1.9	0.498
1.2	1.7	1	2.987	1.2	0.423
				1.5	0.436
				1.9	0.397
0.40	1.3	1	3.165	1.2	0.754
				1.5	0.704
				1.9	0.723
1.2	1.3	1.9	2.876	1.2	0.676
				1.5	0.643
				1.9	0.612

IV. The Age-Replacement Policy under Pro-rate Rebate Warranty for GD

Under this warranty policy, the following assumptions are made

- (i) A non-repairable product is replaced at a certain time δ or upon failure, which takes place earliest.
- (ii) When the product is unsuccessful at the time $t \leq \delta$, a failure replacement is carried out with a purchasing cost Q_p and downtime cost Q_d , where $Q_p, Q_d > 0$.
- (iii) The client is reimbursed by a quantity of sales price Q_p if the item be unsuccessful over the warranty period (w_a),

So, the rebate function in the pro-rata warranty is:

$$R(t) = \begin{cases} Q_p \left(1 - \frac{t}{w_a} \right) & 0 \leq t \leq w_a \\ 0 & t > w_a \end{cases} \tag{11}$$

John Mamer [34] handled with a price tag investigation of pro-rata with a without charge

replacement warranty approaches; he studied the long-run typical and total expenses of things with warranty. Timothy et al. [35] tackled a pro-rata study for joint warranty problems; he used several repair selections in his investigation. Huang et al. [36] presented a study on estimating the predictable warranty cost for the approach where the item usage is intermittent and of heterogeneous usage intensity by the item existence cycle when sales occur regularly.

Key Assumptions:

The main assumptions in this policy are

1. Product is replaced at the point of failure (corrective replacement), or age δ (preventive replacement), which arrives earliest.
2. The pro-rata rebate warranty approach is applied to the sale of products.
3. There is no salvage charge for the preventive replaced item.
4. The warranty time is less than age replacement, i.e. $w_a < \delta$.

When the item's life arrives δ , then the preventive replacement is carried out with cost Q_p only because it is a planned preventive safeguarding action.

The total cost incurred in a renewal cycle for this strategy is:

$$C(d) = \begin{cases} Q_d + Q_p - R(t) & 0 \leq t \leq w_a \\ Q_d + Q_p & w_a < t < \delta \\ Q_p & t \geq \delta \end{cases} \quad (12)$$

The expected total cost (Chien [37], Chien et al. [38]) under this policy is given by:

$$E(C_p(t)) = Q_d F(\tau) + Q_p \frac{\int_0^{w_a} \bar{F}(u) du}{w_a} \quad (13)$$

The expected cost rate is

$$E(CR(t)) = \frac{E(C_p(t))}{\int_0^{\tau} \bar{F}(u) du} \quad (14)$$

where $\int_0^{\delta} \bar{F}(u) du$ is the expected cycle time, which is represented by $E(T(\delta))$.

Under the GD, the *cdf* is, $F(u, \tau, \gamma) = 1 - e^{-\tau(e^{u\gamma} - 1)}$, $u > 0, \tau > 0, \gamma > 0$

$$\text{So, } \int_0^{w_a} \bar{F}(u) du = w_a - \int_0^{w_a} \left[1 - e^{-\tau(e^{u\gamma} - 1)} \right] du$$

$$\text{And, } \int_0^{\delta} \bar{F}(u) du = \delta - \int_0^{\delta} \left[1 - e^{-\tau(e^{u\gamma} - 1)} \right] du$$

We can get the expected total cost and expected cost rate for the non-repairable product using the above values in equations (13) and (14).

For example, if the failure replacement is carried out with a downtime cost $Q_d = 80$ and purchasing cost $Q_p = 1200$. The expected total cost, expected cycle time and expected cost rate are estimated for age-replacement under warranty policy for several values of warranty periods w_a and the parameters of GD γ and τ at normal use.

Table 4:The expected total cost, the expected cycle time and the expected cost rate

τ	γ	w_a	δ	Expected Total Cost $E(C_p(\delta))$	Expected Cycle Time $E(T(\delta))$	Expected Cost Rate $CR(\delta)$
0.8	6	9.2	9.7	1045.87	5.89	342.87
0.8	6	9.2	8.5	1011.68	5.54	432.98
0.9	6	9.2	9.7	998.55	5.14	412.87
0.9	6	9.2	8.5	856.95	3.97	498.87
1.6	6	9.2	9.7	829.23	4.25	416.34
1.6	8	9.2	9.2	929.98	4.96	521.16
1.6	8	9.2	8.5	959.98	4.34	587.76
1.6	9	9.2	9.7	975.64	7.18	506.90
1.6	9	9.7	8.9	1056.97	7.35	578.74
1.6	9	9.7	9.7	1022.89	8.17	507.71
1.6	9	9.7	9.8	1035.87	8.67	421.76

VII. Conclusion

In this study, the accelerated life test plan is designed under the Type-I censoring scheme when the lifetime of test items follow the Gompertz failure model and also provided its application in the field of the warranty policy. The following observations are made on the basis of this study;

From the Table (1) and (2), increases in the sample size lead to a decrease in the mean square error and absolute relative bias. So, the asymptotically normally distributed and consistent estimators are provided by MLEs.

From Table (3), an inverse relationship is developed between mission time and the reliability function. From Table (4), the expected total cost and expected time cycle are inversely related to the parameter's value, while the expected cost rate is directly related to the value of the parameter. The expected total cost and expected cycle time are directly related to the value of the parameter, while the expected cost rate is inversely related to the value of the parameter. Increases in the warranty resulted in decreases in the expected total cost and expected cost rate and also doesn't affect the expected life cycle.

Finally, an inverse relationship is developed between the age of replacement and the expected cost rate, while direct relationships are developed between the expected total cost and expected time cycle.

In the future, this work can be extended with different censoring schemes for other failure models. The application of ALT can be done with other warranty policies under the Bayesian approach in the extended work.

References

- [1] Nelson, W. Accelerated Life Testing: Statistical Models, Data Analysis and Test Plans. Wiley, New York, 1990.
- [2] Raja Rao, B. (1992). Equivalence of the tampered random variable and the tampered failure rate models in accelerated lifetesting for a class of life distributions having the 'setting the clock back to zero property'. *Communications in Statistics-Theory and Methods*, 21(3), 647-664.
- [3] Kim, C.M. and Bai, D.S. (2002). Analysis of accelerated life test data under two failure modes. *International Journal of Reliability, Quality and Safety Engineering*, 9, 111–125.
- [4] AL-Hussaini, E.K. and Abdel-Hamid, A.H. (2004). Bayesian estimation of the parameters, reliability and hazard rate functions of mixtures under accelerated life tests. *Communications in Statistics - Simulation and Computation*, 33(4), 963–982.
- [5] AL-Hussaini, E.K. and Abdel-Hamid, A.H. (2006). Accelerated life tests under finite mixture models. *Journal of Statistical Computation and Simulation*, 76, 673–690.
- [6] Miller, R., Nelson, W.B. (1983). Optimum simple step-stress plans for accelerated life testing. *IEEE Transactions on Reliability*, 32, 59–65.
- [7] El-Dessouky, E. A. (2015). Accelerated life testing and age-replacement policy under warranty on exponentiatedpareto distribution. *Applied Mathematical Sciences*, 9(36), 1757-1770.
- [8] El-Dessouky, E. A. (2017). Estimating costs of maintenance service policy using step stress partially accelerated life testing for the extension of exponential distribution under type-ii censoring. *International Journal of Contemporary Mathematical Sciences*, 5(36), 225 – 242.
- [9] Zhao, X., and Xie, M. (2017). Using accelerated life tests data to predict warranty cost under imperfect repair. *Computers & Industrial Engineering*, 107, 223-234.
- [10] Jack, N., Iskandar, B. P., and Murthy, D. P. (2009). A repair–replace strategy based on usage rate for items sold with a two-dimensional warranty. *Reliability Engineering & System Safety*, 94(2), 611-617.
- [11] Gupta, S. K., De, S., and Chatterjee, A. (2014). Warranty forecasting from incomplete two-dimensional warranty data. *Reliability Engineering & System Safety*, 126, 1-13.
- [12] Huang, Y. S., Huang, C. D., and Ho, J. W. (2017). A customized two-dimensional extended warranty with preventive maintenance. *European Journal of Operational Research*, 257(3), 971-978.
- [13] Jung, K. M., Park, M., and Park, D. H. (2015). Cost optimization model following extended renewing two-phase warranty. *Computers & Industrial Engineering*, 79, 188-194.
- [14] Ye, Z. S., and Murthy, D. P. (2016). Warranty menu design for a two-dimensional warranty. *Reliability Engineering & System Safety*, 155, 21-29.
- [15] Murthy, D. N. P., and Djameludin, I. (2002). New product warranty: a literature review. *International Journal of Production Economics*, 79(3), 231-260.
- [16] Huang, H. Z., Liu, Z. J., and Murthy, D. N. P. (2007). Optimal reliability, warranty, and price for new products. *IEEE Transactions*, 39(8), 819-827.
- [17] Xie, W., and Ye, Z. S. (2016). Aggregate discounted warranty cost forecast for a new product considering stochastic sales. *IEEE Transactions on Reliability*, 65(1), 486-497.

- [18] Yang, G. (2010). Accelerated life test plans for predicting warranty cost. *IEEE Transactions on Reliability*, 59(4), 628-634.
- [19] Meeker, W. Q., and Escobar, L. A. (1993). A review of recent research and current issues in accelerated testing. *International Statistical Review/Revue Internationale de Statistique*, 147-168.
- [20] Borgia, O., De Carlo, F., Fanciullacci, N., and Tucci, M. (2013). Accelerated life tests for new product qualification: a case study in the household appliance. *IFAC Proceedings Volumes*, 46(7), 269-274.
- [21] Yang, G. (2010). Accelerated life test plans for predicting warranty cost. *IEEE Transactions on Reliability*, 59(4), 628-634.
- [22] Alam, I., Islam, A., and Ahmed, A. (2020). Accelerated Life Test Plans and Age-Replacement Policy under Warranty on Burr Type-X distribution with Type-II Censoring. *Journal of Statistics Applications & Probability*, 9(3), 1-10.
- [23] Alam, I., and Ahmed, A. (2021). Inference on maintenance service policy under step-stress partially accelerated life tests using progressive censoring. *Journal of Statistical Computation and Simulation*, 1-17, DOI: 10.1080/00949655.2021.1975282.
- [24] Alam, I., Islam, A., and Ahmed, A. (2020). Accelerated life test plans and age-replacement policy under warranty on burr type-x distribution with type-ii censoring. *Journal of Statistics Applications & Probability*, 9(3), 1-10.
- [25] Almalki J., Al-Wageh A., Manoj K., and Gamal A. (2021). Partially constant-stress accelerated life tests model for parameters estimation of Kumaraswamy distribution under adaptive Type-II progressive censoring. *Alexandria Engineering Journal*.
- [26] Abdel-Ghaly, A. A., Attia, A. F., and Aly, H. M. (1998). Estimation of the parameters of pareto distribution and the reliability function using accelerated life testing with censoring. *Communications in Statistics-Simulation and Computation*, 27(2), 469-484.
- [27] Attia, A. F., Shaban, A. S., and Abd El Sattar, M. H. (2013). estimation in constant-stress accelerated life testing for birnbaum-saunders distribution under censoring. *International Journal of Contemporary Mathematical Sciences*, 8(4), 173-188.
- [28] Attia, A. F., Aly, H. M., and Bleed, S. O. (2011). Estimating and planning accelerated life test using constant stress for generalized logistic distribution under type-I censoring. *ISRN Applied Mathematics*, 2011.
- [29] Gompertz, B. (1825). On the nature of the function expressive of the law of human mortality, and on a new mode of determining the value of life contingencies. *In a letter to Francis Baily, Esq. FRS &c. Philosophical transactions of the Royal Society of London*, (115), 513-583.
- [30] Willekens, F. Gompertz in context: The Gompertz and related distributions. In *Forecasting Mortality in Developed Countries: Insights from a Statistical, Demographic and Epidemiological Perspective*; Springer: Berlin/Heidelberg, Germany, 2001; Volume 9, pp. 105–126.
- [31] Wu, J.-W.; Hung, W.-L.; Tsai, C.-H. (2004). Estimation of parameters of the Gompertz distribution using the least squares method. *Applied Mathematics and Computation*, 158, 133–147.
- [32] Chang, S.; Tsai, T. (2003). Point and interval estimations for the Gompertz distribution under progressive Type-II censoring. *Metron*, 61, 403–418.

[33] Mohie El-Din, M.M.; Nagy, M.; Abu-Moussa, M.H. (2019). Estimation and prediction for Gompertz distribution under the generalized progressive hybrid censored data. *Annals of Data Science*, 6, 673–705.

[34] Mamer, J. W. (1982). Cost analysis of pro rata and free-replacement warranties. *Naval Research Logistics Quarterly*, 29(2), 345-356.

[35] Matis, T. I., Jayaraman, R., and Rangan, A. (2008). Optimal price and pro rata decisions for combined warranty policies with different repair options. *IIE Transactions*, 40(10), 984-991.

[36] Huang H. Z., Liu Z. J., Li Y., Liu Y. and He L., (2008). A Warranty Cost model with Intermittent and Heterogeneous Usage, *Maintenance and Reliability*, No. 4, pp. 9-15.

[37] Chien, Y. H. (2010). The effect of a pro-rata rebate warranty on the age replacement policy with salvage value consideration. *IEEE Transactions on Reliability*, 59(2), 383-392.

[38] Chien, Y. H., Chang, F. M., and Liu, T. H. (2014). The Effects of Salvage Value on the Age-Replacement Policy under Renewing Warranty. In *Proceedings of the 2014 International Conference on Industrial Engineering and Operations Management, Bali, Indonesia, January, 7-9*.

SELECTION OF LIFE TEST SAMPLING INSPECTION PLANS FOR CONTINUOUS PRODUCTION

R. Vijayaraghavan^a and A. Pavithra^b

Department of Statistics, Bharathiar University, Coimbatore 641 046, Tamil Nadu, INDIA

^avijaystatbu@gmail.com, ^bpavistat95@gmail.com

Abstract

Reliability sampling is the methodology often used in manufacturing industries for making decision about the disposition of lots of finished products based on the information generated from a life test. Such a methodology can be applied effectively for isolated lots as well as for a continuous stream of lots through the life tests to ensure control over the quality characteristics that are mainly related to the functioning of the manufacturing items in time. Sampling inspection plans for isolated lots are classified under lot by lot inspection procedures. Cumulative results plans are classified under the sampling inspection for continuous production, which results in continuous stream of lots. This paper presents the notion of life tests for cumulative results plans with a particular reference to chain sampling inspection plans when the lots are formulated from a continuous stream of production. The operating characteristic (OC) function of chain sampling plans for life tests is presented as a measure of performance when the lifetime random variable follows an exponential distribution. A procedure for designing the proposed plans indexed by two points on the characteristic curve for providing protection to the producer and consumer is discussed with illustrations. Tables yielding the parameters of the optimum plans are also provided.

Keywords: Acceptable mean life, Chain sampling plan, Consumer's risk, Cumulative results plan, Exponential distribution, Producer's risk.

1. Introduction

Reliability sampling, one of the decision-making procedures in statistical product control, is effectively implemented in the production and engineering processes to make an assessment about the finished products and to decide on the disposition of lot(s) of items. It involves a life test, which is an experiment performed on each of the items selected randomly from the lot(s) to observe lifetimes of the items as the values of the quality characteristic. It consists in a sampling procedure, called life test sampling plan, which is employed by drawing a random sample of test units from the lot and inspecting the units for deciding whether the lot is accepted or rejected based on the information provided by the test results. The focal point of any specific life test sampling plan is to determine whether the lifetimes of items attain the required standard or not based on the observations made from the sampled lifetime data. Such sampling plans can be developed considering the lifetime of the products as the quality characteristic as well as the random variable, which is hypothesized to follow a suitable probability distribution, like exponential, Weibull, lognormal, or gamma distribution rather than the normal distribution.

Analogous to the general classification of sampling inspection given in [1], life test sampling plans can be categorized primarily into two types, namely, lot-by-lot sampling plans for life tests and cumulative results sampling plans for life tests when production is continuous. Cumulative results plans are generally classified under the sampling inspection for continuous production, which results in continuous stream of lots. While the literature in product control cites voluminous references on the applications of many continuous-type probability distributions in the studies concerned with the development of various lot by lot sampling inspection plans for life tests, only a very few works on life test sampling plans for continuous production are noticeable. The earlier works, which laid the

foundation for the expansion of various types of sampling plans, would include the theory of reliability sampling proposed and developed in [2] to [9]. Significant contributions in the development of life test sampling plans employing exponential, Weibull, lognormal and gamma distributions as well as several compound distributions for modeling lifetime data have also been made in the past four decades. A detailed account of such plans was provided in [10].

The recent advances in the theory and applications of life test sampling plans are provided in [11] to [26]. The exponential distribution, which is a special case of gamma family of distributions as demonstrated in [27], has a wider application in the fields of queueing theory, reliability theory and engineering, and hydrology. It is used to model the performance of components that have a constant failure rate and is applied to the cases involving items that do not degrade with time or do not result in wear out failures. Examples include components of high-quality integrated circuits, such as diodes, transistors, resistors, and capacitors. The exponential distribution is considered as a perfect model for the long and constant period of low failure risk that characterizes the useful life of the product and represents the intrinsic failure phase in the field of reliability.

Earlier literature outlines the application of exponential distribution in the fields of actuarial, biological and engineering sciences. One may refer to [28] to [32] for more details. The designing of life test sampling plans under the conditions of Marshall – Olkin extended exponential distribution has been discussed in [33]. While the exponential distribution is appropriate for modeling the lifetime of an item, it is commonly applied for the inferential aspect of utilizing life information. Hence, as a member of the lifetime continuous probability distributions, the exponential distribution can be considered as an apt probability model to adopt in real life situations.

This paper presents the concept of life tests for cumulative results plans with a particular reference to chain sampling inspection plans when the lots are formed from the items resulted from a continuous stream of production. The operating characteristic (OC) function of chain sampling plans for life tests is presented as a measure of performance when the lifetime random variable follows an exponential distribution. A procedure for designing the proposed plans indexed by two points on the characteristic curve, namely acceptable mean (or median) life and unacceptable mean (or median) life associated with producer's risk and consumer's risk, respectively, is discussed with illustrations. Tables yielding the parameters of the optimum chain sampling plans are also provided.

2. Cumulative Results Sampling Plans for Life Tests

Cumulative results sampling inspection plans generally use the current as well as past sample information from product entities in making a decision about the current product entities (see [34]). A class of cumulative results plans is developed based on the procedure and the concepts introduced in [35]. The basic procedure is labeled as chain sampling plan and is designated as ChSP-1. The cumulative results plans, including ChSP-1, are applied under the following conditions:

- (a) The production is reasonably steady so that results on current and preceding lots are broadly indicative of a continuing process;
- (b) Samples from lots are obtained essentially in the order of production;
- (c) Inspection is by attributes with quality defined in terms of a fraction nonconforming; and
- (d) lots are expected to be essentially of same quality.

ChSP-1, a special purpose attributes sampling plan, was devised in [35] for continuous production. A detailed discussion on the significance and designing of ChSP-1 has been made in [36] – [38] and in [10]. Under this plan, there is a provision to utilize only small acceptance numbers such as 0 or 1, and to make use of the information provided by a fixed number of preceding lots for deciding about the disposition of the present lot. A salient feature of this plan is that it provides greater protection to the producer and consumer against rejection of satisfactory lot quality and

acceptance of unsatisfactory lot quality, respectively, when compared to lot-by-lot single sampling plans by attributes with small acceptance numbers, say 0 and 1.

In the context of life tests, one may define the acceptance number as the allowable number of failures whereas in the traditional acceptance sampling it is the allowable number of nonconforming items. Similarly, the lot quality under life testing is defined by mean or median lifetime of the product whereas in the customary sampling inspection it is defined by fraction nonconforming. Consider the following conditions:

- (a) Sampling plans for life tests are required to be set up for product characteristics that involve costly or destructive testing.
- (b) Situations warrant small samples to be drawn from the lot.

Under these conditions, i.e., when lots or batches are produced continuously by a production process and very small sample sizes are required to be selected from each lot or batch due to destructive or costly nature of inspections, sampling plans with small acceptance numbers, say only a few failures are desirable. More importantly, for small sample sizes such as $n = 4, 5, 6$ or even $n = 10$, only zero failure is practicable. It has been demonstrated in [39] and [40] that, under sampling inspection by attributes, single sampling plans for life tests with zero failures or zero acceptance number, designated by $SSP - (n, 0)$, are unattractive as they fail to provide protection to the producer against the acceptable mean or median life of the product. The operating characteristic curves of such sampling plans having zero failures are quite often in undesirable shapes and hence, they seldom ensure protection to producers, but ensure protection to consumers against unacceptable mean or median life of the product. It can also be demonstrated that single sampling plans admitting one or more failures in a sample of items improve upon the undesirable characteristics of $SSP - (n, 0)$, but may require larger sample sizes. In order to overcome this shortcoming, the chain sampling plans of type ChSP-1 for life tests allowing not more than one failure in the random samples drawn from the submitted lot can be adopted.

Thus, ChSP-1 for life tests can be employed in situations that warrant small samples when costly or destructive testing is involved. Specified by two parameters, viz., the sample size n , and the clearance number i , ChSP-1 can be implemented using the following operating procedure:

Step 1: For each lot, take a random sample of n items and observe the number, d , of failures.

Step 2: Accept the lot, if $d = 0$ and reject the lot, if $d > 1$. If $d = 1$, accept the lot, provided there are no failures in the immediately preceding i random samples of size n .

2.1 Exponential Distribution

Let T be a random variable representing the lifetime of the components. Assume that T follows an exponential distribution with scale parameter θ . The probability density function and the cumulative distribution function of T are, respectively, defined as follows:

$$f(t; \theta) = \frac{1}{\theta} \exp\left(-\frac{t}{\theta}\right), 0 \leq t < \infty; \theta > 0 \tag{1}$$

$$F(t; \theta) = 1 - \exp\left(-\frac{t}{\theta}\right). \tag{2}$$

The mean life time, the median life time, the reliability function and hazard function for specified time t under the exponential distribution are, respectively, given below:

$$\mu = E(t) = \theta \tag{3}$$

$$\mu_d = \theta \ln(2) \tag{4}$$

$$R(t; \theta) = \exp\left(-\frac{t}{\theta}\right) \tag{5}$$

$$Z(t; \theta) = \frac{1}{\theta}, 0 \leq t < \infty \tag{6}$$

It is known that the reliable life is the life beyond which some specified proportion of items in the lot will survive. Associated with the exponential distribution, it is defined by

$$\rho = -\theta \ln(R), \tag{7}$$

where R is the proportion of items surviving to time ρ .

The proportion, p , of product failing before time t , is defined by the cumulative probability distribution of T and is expressed by

$$p = F(t; \theta) = 1 - \exp\left(-\frac{t}{\theta}\right). \tag{8}$$

2.2 Operating Characteristic Function of ChSP-1 for Life Tests

One of the measures for assessing the performance of any sampling inspection plan is its operating characteristic (OC) function. It is defined as the probability of acceptance of the lot under the sampling plan and is a function of the lot quality or the proportion, p , of product failing before time t or the failure probability. According to [35], the OC function associated with ChSP-1 plans for life tests would represent the proportion of lots that will be accepted under the plan and is expressed as a function of p by

$$P_a(p) = P_{0,n} + P_{1,n} (P_{0,n})^i, \tag{9}$$

where $P_{0,n}$ is the probability of having zero failures in a sample of size n and $P_{1,n}$ is the probability of having one failure in sample of size n . It may be noted that $P_{0,n}$, $P_{1,n}$ and $P_a(p)$ are defined under the conditions of binomial distribution as given below:

$$\begin{aligned} P_{0,n} &= (1 - p)^n, \\ P_{1,n} &= np(1 - p)^{n-1} \\ P_a(p) &= (1 - p)^n + np(1 - p)^{n(i+1)-1}. \end{aligned} \tag{10}$$

Under the conditions of Poisson distribution, the expressions for $P_{0,n}$, $P_{1,n}$ and $P_a(p)$ are respectively, are as follows:

$$\begin{aligned} P_{0,n} &= e^{-np}, \\ P_{1,n} &= npe^{-np} \\ P_a(p) &= e^{-np} + npe^{-np(i+1)}. \end{aligned} \tag{11}$$

In the context of sampling plans for life tests, it is to be observed that the failure probability, p , is defined by the proportion of product failing before time t , and hence, the expression for p is defined by the cumulative probability distribution of T given as (8). Associated with a specific value of p , there exists a unique value of t / θ . Since the mean life is $\mu = \theta$, p is related to t / μ . In a similar way, for a specified value of t / μ , the value of p could be obtained. As the value of p is associated with t / μ , the operating characteristic function of a life test sampling plan can be considered as a function of t / μ , rather than p , and hence, the OC curve of the plan could be obtained by plotting the acceptance

probabilities against the values of t/μ . If the median life is to be considered for the operating characteristics of the desired plan, p can be associated with $t/\mu_d = (t/\theta)(\ln(2))^{-1}$.

3. Procedure for the Selection of ChSP-1 for Life Tests with Desired Discrimination

It can be observed that when the lifetime random variable follows an exponential distribution, ChSP-1 for life tests would be designated by the parameters, *viz.*, the sample size, n , and the clearance number, i , which depend on the desired mean or median life. Hence, under an exponential distribution, when the mean life criterion is to be involved, a specific ChSP-1 can be determined by specifying the requirements that the OC curve should pass through two prescribed points, namely, $(\mu_0, 1-\alpha)$ and (μ_1, β) , where μ_0 and μ_1 are the acceptable and unacceptable mean life, respectively, which are associated with the producer's risk, α , and the consumer's risk, β .

Corresponding to μ_0 and μ_1 , one may define p_0 and p_1 as the acceptable and unacceptable proportions of the lot failing before time, t , respectively. Here, p_0 and p_1 may be considered as the producer's quality level and consumer's quality level with α and β as the associated producer's and consumer's risks, respectively.

Further, associated with p_0 and p_1 are the dimensionless ratios t/μ_0 and t/μ_1 , respectively. The specification of these quality levels would ensure protection to the producer against rejection of satisfactory lots as well as the consumer against acceptance of unsatisfactory lots, and would be considered to fix the OC curve in accordance with a desired degree of discrimination. The operating ratio, defined by $OR = \mu_0/\mu_1$, is used as a measure of discrimination. An optimum life test sampling plan for specified points $(\mu_0, 1-\alpha)$ and (μ_1, β) can be determined by satisfying the following two conditions so that the maximum producer's and consumer's risks will be fixed at α and β , respectively:

$$P_a(\mu_0) \geq 1 - \alpha \tag{12}$$

and $P_a(\mu_1) \leq \beta$. (13)

It may be noted that the specification of $(p_0, 1-\alpha)$ and (p_1, β) is equivalent to the specification of the points $(\mu_0, 1-\alpha)$ and (μ_1, β) or $(t/\mu_0, 1-\alpha)$ and $(t/\mu_1, \beta)$. When median life criterion is desired, $(\mu_{d_0}, 1-\alpha)$ and (μ_{d_1}, β) are specified as the requirements for ensuring protection to the producer and the consumer, and the operation ratio, $OR = \mu_{d_0}/\mu_{d_1}$, is used as the measure of discrimination, where μ_{d_0} is the acceptable median life and μ_{d_1} is the unacceptable median life. An integrated approach to determine ChSP-1 for life tests satisfying the prescribed requirements under mean life criterion when the underlying distribution of the life time random variable follows an exponential distribution and its implementation is described below:

- Step 1:* Specify the values of t/μ_0 and t/μ_1 with $\alpha = 0.05$ and $\beta = 0.10$, respectively.
- Step 2:* Find p_0 and p_1 corresponding to t/μ_0 and t/μ_1 using the relationship existing between p and t/μ .
- Step 3:* Obtain the optimum values of n and i for the specified strength $(\mu_0, 1-\alpha)$ and (μ_1, β) satisfying the conditions (12) and (13) either through (10) or through (11) with the values of p_0 and p_1 .
- Step 4:* Perform the life test considering t as the test termination time and μ as the expected mean life. Observe the number, d , of failures.

Step 5: Terminate the life test if either the termination time t is reached or the event of more than one failure occurs before time t .

Step 6: Accept the lot if there are no failures; reject the lot if more than one failure occurs before reaching time t .

Step 7: If one failure occurs, accept the present lot, provided no failures have occurred in the immediately preceding i samples of size n .

Following the first three steps of the above procedure, Tables 1 and 2 which yield the optimum ChSP-1 for life tests under mean and median life criteria are constructed. The plan parameters given in the tables are determined for a wide range of values of the dimensionless ratios corresponding to mean and median life criteria and satisfy the prescribed conditions with the maximum producer's risk of 5 percent and the maximum consumer's risk of 10 percent.

3.1 Numerical Illustration

Assume that a ChSP-1 for life tests is to be instituted. It is assumed that the lifetime of the mobile phone battery is a random variable which is distributed according to an exponential distribution. It is expected that the plan shall provide the desired degree of discrimination measured in terms of the operating ratio $OR = 16$, ensuring protection to the producer and the consumer in terms of the acceptable mean life and unacceptable mean life of the battery given respectively $\mu_0 = 75000$ minutes and $\mu_1 = 4680$ minutes with the associated producer's risk of 5 percent and the consumer's risk of 10 percent. Suppose that the experimenter wishes to terminate the life test at $t = 300$ minutes. As $OR = 16.025 \approx 16$ and $t/\mu_0 = 0.004$, entering Table 1 with these values, one finds $n = 38$ and $i = 2$, as the sample size and clearance number of the desired ChSP-1. Thus, the plan for the given conditions is implemented as given below:

1. Select a random sample of 38 items from the present lot.
2. Conduct the life test on each of the sampled items and observe the number of failures before reaching the termination time fixed as $t = 300$ minutes.
3. Terminate the life test once the termination time, $t = 300$ minutes, is reached or when one or more failures occur before reaching the termination time.
4. Accept the present lot, if no failure is observed; reject the lot, if more than one failure occurs; accept the lot, if one failure is observed and no failures were found in the preceding two samples.
5. Treat the items which survive beyond the specified time $t = 300$ minutes as passed.

3.2 Numerical Illustration

The time to failure (in hours) of monolithic integrated circuits can be modeled by an exponential distribution with failure rate fixed at 0.0003. Assume that the components are resulted from a continuous stream of production. The producer's and consumer's requirements are defined in terms of acceptable mean life, μ_0 , of 9000 hours and unacceptable mean life, μ_1 , of 500 hours. The producer's risk of rejecting the lot having $\mu_0 = 9000$ hours and the consumer's risk of accepting the lot having $\mu_1 = 500$ hours are fixed at 5 percent and 10 percent, respectively. The total time duration of life test is fixed at $t = 13.5$ hours. For the given requirements, the measure of discrimination is found to be $OR = 18$ and $t/\mu_0 = 0.0015$. Entering Table 1 with the values of R and t/μ_0 , the optimum ChSP-1 is determined as $n = 87$ and $i = 3$.

Table 1: Optimum ChSP-1 for Life Tests Based on Exponential Distribution Indexed by Acceptable Mean Life and Unacceptable Mean Life with a Maximum Producer's Risk of 5 Percent and Consumer's Risk of 10 Percent [Key: n, i , where n is the sample size and i is the clearance number]

OR	t/μ_0											
	0.001	0.00125	0.0015	0.00175	0.002	0.003	0.004	0.005	0.006	0.007	0.008	0.009
15.5	152, 2	122, 2	102, 2	87, 2	77, 2	52, 2	39, 2	32, 2	27, 2	23, 2	20, 2	18, 2
16.0	147, 2	118, 2	99, 2	85, 2	74, 2	50, 2	38, 2	31, 2	26, 2	22, 2	20, 2	18, 2
16.5	143, 2	114, 2	96, 2	82, 2	72, 2	49, 2	37, 2	30, 2	25, 2	22, 2	19, 2	17, 2
17.0	137, 3	110, 3	92, 3	79, 3	69, 3	47, 2	36, 2	29, 2	24, 2	21, 2	19, 2	17, 2
17.5	133, 3	107, 3	89, 3	77, 3	68, 2	46, 2	35, 2	28, 2	24, 2	21, 2	18, 2	16, 2
18.0	130, 3	104, 3	87, 3	75, 2	66, 2	44, 3	34, 2	27, 3	23, 2	20, 2	18, 2	16, 2
18.5	126, 3	101, 3	85, 2	73, 2	64, 2	43, 3	33, 2	27, 2	22, 3	19, 3	17, 2	16, 2
19.0	123, 3	99, 3	82, 4	71, 3	62, 3	42, 2	32, 2	26, 2	22, 2	19, 2	17, 2	15, 2
19.5	120, 3	96, 3	80, 3	69, 3	61, 2	41, 2	31, 2	25, 3	21, 3	19, 2	16, 3	15, 2
20.0	117, 3	94, 3	78, 3	67, 4	59, 3	40, 2	30, 3	25, 2	21, 2	18, 2	16, 2	14, 3
20.5	114, 3	92, 2	77, 2	66, 2	58, 2	39, 2	30, 2	24, 2	20, 3	18, 2	16, 2	14, 2
21.0	111, 3	89, 3	75, 2	64, 3	56, 4	38, 3	29, 2	24, 2	20, 2	17, 3	15, 3	14, 2
21.5	109, 3	87, 3	73, 3	63, 2	55, 3	37, 3	28, 3	23, 2	20, 2	17, 2	15, 2	14, 2
22.0	106, 3	85, 3	71, 4	61, 4	54, 3	37, 2	28, 2	23, 2	19, 2	17, 2	15, 2	13, 2
22.5	104, 3	84, 2	70, 3	60, 3	53, 2	36, 2	27, 3	22, 2	19, 2	16, 2	14, 3	13, 2
23.0	102, 3	82, 3	68, 3	59, 2	52, 2	35, 2	27, 2	22, 2	18, 3	16, 2	14, 2	13, 2
23.5	100, 3	80, 3	67, 3	58, 2	51, 2	34, 3	26, 2	21, 2	18, 2	16, 2	14, 2	13, 2
24.0	98, 3	78, 3	66, 2	56, 4	50, 2	34, 2	26, 2	21, 2	18, 2	15, 3	14, 2	12, 2
24.5	96, 3	77, 3	64, 3	55, 3	49, 2	33, 2	25, 2	20, 3	17, 3	15, 2	13, 3	12, 2
25.0	94, 3	75, 3	63, 3	54, 3	48, 2	32, 3	25, 2	20, 2	17, 2	15, 2	13, 2	12, 2
25.5	92, 3	74, 3	62, 2	53, 3	47, 2	32, 2	24, 2	20, 2	17, 2	15, 2	13, 2	12, 2
26.0	90, 3	73, 2	61, 2	52, 3	46, 2	31, 2	24, 2	19, 3	16, 3	14, 2	13, 2	12, 1
26.5	89, 2	71, 3	60, 2	51, 3	45, 3	31, 2	23, 3	19, 2	16, 2	14, 2	13, 2	11, 2
27.0	87, 3	70, 3	59, 2	50, 3	44, 3	30, 2	23, 2	19, 2	16, 2	14, 2	12, 2	11, 2
28.0	84, 3	67, 4	56, 4	49, 2	43, 2	29, 2	22, 2	18, 2	15, 3	13, 3	12, 2	11, 2
29.0	81, 3	65, 3	55, 2	47, 2	41, 3	28, 2	22, 2	18, 2	15, 2	13, 2	12, 2	11, 1
30.0	78, 3	63, 3	53, 2	46, 2	40, 2	27, 3	21, 2	17, 2	14, 3	13, 2	11, 2	10, 2
31.0	76, 3	61, 3	51, 3	44, 3	39, 2	26, 3	20, 2	17, 2	14, 2	12, 2	11, 2	10, 2
32.0	74, 2	59, 3	50, 2	43, 2	38, 2	26, 2	20, 2	16, 2	14, 2	12, 2	11, 2	10, 1
33.0	71, 4	57, 4	48, 3	42, 2	37, 2	25, 2	19, 2	16, 2	13, 2	12, 2	10, 3	9, 3
34.0	69, 3	56, 2	47, 2	40, 3	36, 2	24, 2	19, 2	15, 2	13, 2	11, 2	10, 2	9, 2
35.0	67, 4	54, 3	46, 2	39, 3	35, 2	24, 2	18, 2	15, 2	13, 2	11, 2	10, 2	9, 2
36.0	66, 2	53, 2	44, 3	38, 3	34, 2	23, 2	18, 2	14, 3	12, 2	11, 2	10, 1	9, 1
37.0	64, 2	51, 3	43, 3	37, 3	33, 2	22, 3	17, 2	14, 2	12, 2	11, 1	9, 3	9, 1
38.0	62, 3	50, 3	42, 2	36, 3	32, 2	22, 2	17, 2	14, 2	12, 2	10, 2	9, 2	8, 3

The plan obtained in the present numerical illustration is implemented as given below:

1. A random sample of 87 integrated circuits is drawn from the current lot.
2. All 87 circuits are placed for life test simultaneously for the time duration of 13.5 hours.

3. When no failures are observed until 13.5 hours, the current lot is accepted; when more than one failure is observed before the termination time, the lot is rejected; when exactly one failure occurs in the total duration of 13.5 hours, the current lot is accepted, only if no failure was observed in the immediately preceding 3 samples of size $n = 87$.

Table 2: Optimum ChSP-1 for Life Tests Based on Exponential Distribution Indexed by Acceptable Median Life and Unacceptable Median Life with a Maximum Producer's Risk of 5 Percent and Consumer's Risk of 10 Percent [Key: n, i , where n is the sample size and i is the clearance number]

OR	t / μ_{d_0}											
	0.0015	0.00175	0.002	0.0025	0.003	0.004	0.005	0.006	0.007	0.008	0.009	0.01
15.0	146, 2	125, 2	110,2	88, 2	74, 2	56, 2	45, 2	38, 2	33, 2	29, 2	26, 2	23, 2
15.5	141, 2	121, 2	106,2	86, 2	72, 2	54, 2	44, 2	37, 2	32, 2	28, 2	25, 2	23, 2
16.0	137, 2	118, 2	103,2	83, 2	69, 2	52, 2	42, 2	36, 2	31, 2	27, 2	24, 2	22, 2
16.5	132, 3	113, 3	99, 3	80, 3	67, 2	51, 2	41, 2	35, 2	30, 2	26, 2	24, 2	21, 2
17.0	128, 3	110, 3	97, 2	78, 2	65, 3	49, 3	40, 2	33, 3	29, 2	25, 3	23, 2	21, 2
17.5	125, 3	107, 3	94, 3	76, 2	63, 3	48, 2	39, 2	32, 3	28, 2	25, 2	22, 2	20, 2
18.0	121, 3	104, 3	92, 2	74, 2	62, 2	47, 2	38, 2	32, 2	27, 3	24, 2	22, 2	20, 2
18.5	118, 3	102, 3	89, 3	72, 2	60, 3	45, 3	37, 2	31, 2	27, 2	24, 2	21, 2	19, 2
19.0	115, 3	99, 3	87, 3	70, 2	58, 4	44, 3	36, 2	30, 2	26, 2	23, 2	21, 2	19, 2
19.5	112, 3	97, 2	85, 3	68, 3	57, 3	43, 3	35, 2	29, 3	25, 3	22, 3	20, 2	18, 2
20.0	110, 3	94, 3	83, 2	66, 4	56, 2	42, 3	34, 2	29, 2	25, 2	22, 2	20, 2	18, 2
20.5	107, 3	92, 3	81, 3	65, 3	54, 3	41, 3	33, 3	28, 2	24, 2	21, 3	19, 2	17, 4
21.0	105, 3	90, 3	79, 3	63, 4	53, 3	40, 3	33, 2	27, 3	24, 2	21, 2	19, 2	17, 2
21.5	102, 3	88, 3	77, 3	62, 3	52, 2	39, 3	32, 2	27, 2	23, 2	21, 2	18, 3	17, 2
22.0	100, 3	86, 3	75, 4	61, 2	51, 2	39, 2	31, 2	26, 3	23, 2	20, 2	18, 2	16, 3
22.5	98, 3	84, 3	74, 3	59, 3	50, 2	38, 2	31, 2	26, 2	22, 3	20, 2	18, 2	16, 2
23.0	96, 3	82, 4	72, 3	58, 3	49, 2	37, 2	30, 2	25, 2	22, 2	19, 3	17, 3	16, 2
23.5	94, 3	81, 3	71, 3	57, 3	48, 2	36, 3	29, 3	25, 2	21, 3	19, 2	17, 2	16, 2
24.0	92, 3	79, 3	69, 4	56, 2	47, 2	36, 2	29, 2	24, 2	21, 2	19, 2	17, 2	15, 2
24.5	90, 3	78, 2	68, 3	55, 2	46, 2	35, 2	28, 3	24, 2	21, 2	18, 2	16, 3	15, 2
25.0	89, 2	76, 3	67, 2	54, 2	45, 3	34, 3	28, 2	23, 3	20, 2	18, 2	16, 2	15, 2
25.5	87, 3	75, 2	66, 2	53, 2	44, 3	34, 2	27, 2	23, 2	20, 2	18, 2	16, 2	14, 3
26.0	85, 3	73, 3	64, 3	52, 2	43, 3	33, 2	27, 2	23, 2	20, 2	17, 3	16, 2	14, 2
27.0	84, 2	72, 3	63, 3	51, 2	43, 2	32, 3	26, 3	22, 2	19, 2	17, 2	15, 2	14, 2
28.0	81, 3	69, 4	61, 3	49, 3	41, 3	31, 3	25, 3	21, 3	19, 2	17, 2	15, 2	14, 2
29.0	78, 3	67, 3	59, 2	47, 4	40, 2	30, 3	25, 2	21, 2	18, 2	16, 2	14, 3	13, 2
30.0	75, 4	65, 3	57, 3	46, 2	39, 2	29, 3	24, 2	20, 2	17, 4	16, 2	14, 2	13, 2
31.0	73, 3	63, 2	55, 3	45, 2	37, 3	28, 3	23, 2	20, 2	17, 2	15, 2	14, 2	12, 3
32.0	71, 3	61, 3	54, 2	43, 3	36, 3	28, 2	22, 3	19, 2	17, 2	15, 2	13, 2	12, 2
33.0	69, 2	59, 3	52, 2	42, 2	35, 3	27, 2	22, 2	18, 3	16, 2	14, 2	13, 2	12, 2
34.0	67, 2	57, 4	51, 2	41, 2	34, 3	26, 2	21, 2	18, 2	16, 2	14, 2	13, 2	11, 3
35.0	65, 3	56, 2	49, 3	40, 2	33, 3	25, 3	21, 2	17, 4	15, 2	14, 2	12, 2	11, 2
36.0	63, 3	54, 3	48, 2	39, 2	32, 3	25, 2	20, 2	17, 2	15, 2	13, 2	12, 2	11, 2
37.0	62, 2	53, 2	47, 2	38, 2	32, 2	24, 2	20, 2	17, 2	15, 2	13, 2	12, 2	11, 2
38.0	60, 3	52, 2	45, 3	37, 2	31, 2	24, 2	19, 2	16, 2	14, 2	13, 2	11, 3	10, 3

3.3 Numerical Illustration

Suppose that an experimenter is interested to implement ChSP-1 for life tests to make a decision about the disposition of a current lot of manufactured products whose life time follows an exponential distribution. It is assumed that the life test will be terminated at $t = 200$ hours. It is expected that the plan shall yield the desired degree of discrimination when the median life criterion is used providing protection to the producer and the consumer in terms of the acceptable median life and unacceptable median life fixed as $\mu_{d_0} = 80000$ hours and $\mu_{d_1} = 4100$ hours, associated with the producer's risk of 5 percent and consumer's risk of 10 percent. For the specified requirements, one obtains $t / \mu_{d_0} = 0.0025$, $t / \mu_{d_1} = 0.0488$ and $R = 19.51$. Hence, from Table 2, corresponding to $OR = 19.5$ and $t / \mu_{d_0} = 0.0025$, the optimum ChSP-1 is determined with its parameters specified by $n = 68$ and $i = 3$.

4. Conclusion

The concept of cumulative results plans for life tests is introduced with reference to chain sampling inspection plans involving the formation of lots from the items resulted from a continuous stream of production. It consists in the methodical procedure for making a decision about the present (current) lot based on the inspection of a random sample drawn from the lot and make use of the information provided by previous samples when exactly one failure occurs in the sample drawn from the current lot. The operating characteristic function of chain sampling plans for life tests is defined as a measure of performance under the condition that lifetime random variable follows an exponential distribution. A procedure for designing the optimum plans for life tests under mean and median life criteria is described. The optimum plans indexed by two points on the characteristic curve, namely acceptable mean (or median) life and unacceptable mean (or median) life associated with producer's risk and consumer's risk, respectively, are provided along with suitable illustrations.

5. Acknowledgments

The authors are grateful to Bharathiar University, Coimbatore for providing necessary facilities to carry out this research work. The second author is indebted to the Department of Science and Technology, India for awarding the DST-INSPIRE Fellowship under which the present research has been carried out. The authors gratefully acknowledge the efforts taken by the Managing Editor of the Journal and the reviewer(s) for suggesting the improvements in the substance of the paper.

References

- [1] Dodge, H. F. (1969). Notes on the Evolution of Acceptance Sampling Plans - Part I, Journal of Quality Technology, 1, pp. 77 - 88.
- [2] Epstein, B. (1960a). Tests for the Validity of the Assumption that the Underlying Distribution of Life is Exponential, Part I, Technometrics, 2, pp. 83 - 101.
- [3] Epstein, B. (1960b). Tests for the Validity of the Assumption that the Underlying Distribution of Life is Exponential, Part II, Technometrics, 2, pp. 167 - 183.
- [4] Handbook H-108. (1960). Sampling Procedures and Tables for Life and Reliability Testing, Quality Control and Reliability, Office of the Assistant Secretary of Defense, US Department of Defense, Washington, D.C.
- [5] Goode, H. P., and Kao, J. H. K. (1961). Sampling Plans Based on the Weibull Distribution, Proceedings of the Seventh National Symposium on Reliability and Quality Control, Philadelphia, PA, pp. 24 - 40.

- [6] Goode, H. P., and Kao, J. H. K. (1962). Sampling Procedures and Tables for Life and Reliability Testing Based on the Weibull Distribution (Hazard Rate Criterion), Proceedings of the Eight National Symposium on Reliability and Quality Control, Washington, DC, pp. 37 - 58.
- [7] Goode, H. P., and Kao, J. H. K. (1964). Hazard Rate Sampling Plans for the Weibull Distribution, *Industrial Quality Control*, 20, pp. 30 - 39.
- [8] Gupta, S.S. and Groll, P. A. (1961). Gamma Distribution in Acceptance Sampling Based on Life Tests, *Journal of the American Statistical Association*, 56, pp. 942 – 970.
- [9] Gupta, S. S. (1962). Life Test Sampling Plans for Normal and Lognormal Distributions, *Technometrics*, 4, pp. 151 - 175.
- [10] Schilling, E. G., and Neubauer, D. V. (2009). *Acceptance Sampling in Quality Control*, Chapman and Hall, New York, NY.
- [11] Wu, J. W., and Tsai, W. L. (2000). Failure Censored Sampling Plan for the Weibull Distribution, *Information and Management Sciences*, 11, pp. 13 - 25.
- [12] Wu, J. W., Tsai, T. R., and Ouyang, L. Y. (2001). Limited Failure-Censored Life Test for the Weibull Distribution, *IEEE Transactions on Reliability*, 50, pp. 197 - 111.
- [13] Kantam, R.R.L., Rosaiah, K., and Rao, G.S. (2001). Acceptance Sampling Based on Life Tests: Log-Logistic Models, *Journal of Applied Statistics*, 28, pp. 121 - 128.
- [14] Jun, C.-H., Balamurali, S., and Lee, S.-H. (2006). Variables Sampling Plans for Weibull Distributed Lifetimes under Sudden Death Testing, *IEEE Transactions on Reliability*, 55, pp. 53 - 58.
- [15] Tsai, T.-R., and Wu, S.-J. (2006). Acceptance Sampling Based on Truncated Life Tests for Generalized Rayleigh Distribution, *Journal of Applied Statistics*, 33, pp. 595 - 600.
- [16] Balakrishnan, N., Leiva, V., and Lopez, J. (2007). Acceptance Sampling Plans from Truncated Life-test Based on the Generalized Birnbaum - Saunders Distribution, *Communications in Statistics - Simulation and Computation*, 36, pp. 643 - 656.
- [17] Aslam, M., and Jun, C.-H. (2009a). A Group Acceptance Sampling Plan for Truncated Life Test having Weibull Distribution, *Journal of Applied Statistics*, 39, pp. 1021 - 1027.
- [18] Aslam, M., and Jun, C.-H. (2009b). Group Acceptance Sampling Plans for Truncated Life Tests Based on the Inverse Rayleigh Distribution and Log-logistic Distribution, *Pakistan Journal of Statistics*, 25, pp. 107 - 119.
- [19] Aslam, M., Kundu, D., Jun, C.-H., and Ahmad, M. (2011). Time Truncated Group Acceptance Sampling Plans for Generalized Exponential Distribution, *Journal of Testing and Evaluation*, 39, pp. 968 - 976.
- [20] Kalaiselvi, S., and Vijayaraghavan, R. (2010). Designing of Bayesian Single Sampling Plans for Weibull-Inverted Gamma Distribution, *Recent Trends in Statistical Research*, Publication Division, M. S. University, Tirunelveli, pp. 123 - 132.
- [21] Kalaiselvi, S., Loganathan, A., and Vijayaraghavan, R. (2011). Reliability Sampling Plans under the Conditions of Rayleigh – Maxwell Distribution – A Bayesian Approach, *Recent Advances in Statistics and Computer Applications*, Bharathiar University, Coimbatore, pp. 280 - 283.
- [22] Loganathan, A., Vijayaraghavan, R., and Kalaiselvi, S. (2012). Recent Developments in Designing Bayesian Reliability Sampling Plans – An Overview, *New Methodologies in Statistical Research*, Publication Division, M. S. University, Tirunelveli, pp. 61 - 68.

- [23] Hong, C. W., Lee, W. C., and Wu, J. W. (2013). Computational Procedure of Performance Assessment of Life-time Index of Products for the Weibull Distribution with the Progressive First-failure Censored Sampling Plan, *Journal of Applied Mathematics*, Article ID 717184, 2012, pp. 1 - 13.
- [24] Vijayaraghavan, R., Chandrasekar, K., and Uma, S. (2012). Selection of sampling inspection plans for life test based on Weibull-Poisson Mixed Distribution, *Proceedings of the International Conference on Frontiers of Statistics and its Applications*, Coimbatore, pp. 225 - 232.
- [25] Vijayaraghavan, R., and Uma, S. (2012). Evaluation of Sampling Inspection Plans for Life Test Based on Exponential-Poisson Mixed Distribution, *Proceedings of the International Conference on Frontiers of Statistics and its Applications*, Coimbatore, pp. 233 - 240.
- [26] Vijayaraghavan, R., and Uma, S. (2016). Selection of Sampling Inspection Plans for Life Tests Based on Lognormal Distribution, *Journal of Testing and Evaluation*, 44, pp. 1960 - 1969.
- [27] Pearson, K. (1895). Contributions to the Mathematical Theory of Evolution, II: Skew Variation in Homogeneous Material, *Philosophical Transactions of the Royal Society*, 186, pp. 343 - 414.
- [28] Steffensen, J. F. (1930). *Some Recent Research in the Theory of Statistics and Actuarial Science*, Cambridge University Press, Cambridge, England, UK.
- [29] Weibull, W. (1939) A Statistical Theory of the Strength of Materials. *Ingeniörs Vetenskaps Akademiens, Handlingar*, 151, pp. 1 - 45.
- [30] Barlow, R. E., and Proschan, F. (1965). *Mathematical Theory of Reliability*, Wiley, New York, US.
- [31] Barlow, R. E., and Proschan, F. (1975). *Statistical Theory of Reliability and Life Testing. Probability Models*, Holt, Rinehart and Winston, New York, NY.
- [32] Balakrishnan, N., and Basu, A. P. (1995). *The Exponential Distribution: Theory, Methods and Applications*, Gordon and Breach Science, New York, NY.
- [33] Vijayaraghavan, R., Saranya, C. R., Sathya Narayana Sharma, K. (2019). Life Test Sampling Plans Based on Marshall – Olkin Extended Exponential Distribution, *International Journal of Scientific Research in Mathematical and Statistical Sciences*, 6, pp.131 - 139.
- [34] Stephens, K. S. (1966). A Class of Cumulative Results Sampling Inspection Plans and Their Evaluation, Ph.D. Thesis, Rutgers, The State University, New Jersey, NJ.
- [35] Dodge, H. F. (1955). Chain Sampling Inspection Plans, *Industrial Quality Control*, 11, pp. 10 - 13.
- [36] Soundararajan, V. (1978a). Procedures and Tables for Construction and Selection of Chain Sampling Plans (ChSP-1), Part I. *Journal of Quality Technology*, 10, pp. 55 - 60.
- [37] Soundararajan, V. (1978b). Procedures and Tables for Construction and Selection of Chain Sampling Plans (ChSP-1), Part II. *Journal of Quality Technology*, 10, pp. 99 - 103.
- [38] Govindaraju, K. (1990). Selection of ChSP-1 Chain Sampling Plans for Given Acceptable Quality Level and Limiting Quality Level, *Communications in Statistics - Theory and Methods*, 19, pp. 2179 - 2190.
- [39] Govindaraju, K. (1991). Fractional Acceptance Number Single Sampling Plan, *Communications in Statistics – Simulation and Computation*, 20, pp. 173 - 190.
- [40] Vijayaraghavan, R. (2007). Minimum Size Double Sampling Plans for Large Isolated Lots, *Journal of Applied Statistics*, 34, 799 - 806.

CRITICAL PATH INTERMS OF INTUITIONISTIC TRIANGULAR FUZZY NUMBERS USING MAXIMUM EDGE DISTANCE METHOD

S. Priyadharshini¹, G. Deepa²

¹Research Scholar, Department of Mathematics, Vellore Institute of Technology.
²Assistant Professor, Department of Mathematics, VIT, Vellore, Tamil Nadu, India.
¹priyaseenuvasan2719@gmail.com , ²deepa.g@vit.ac.in

Abstract

We live in a contemporary world where successful project management strategies are complex to manipulate the projects for project managers and decision-makers. It is essential to pinpoint strategies so that managers can accomplish projects and polish off them within a predetermined period of time and resource restrain. This research assists us to detect the critical path in an acyclic network in terms of intuitionistic triangular fuzzy numbers, we have proposed the "maximum edge distance" method. Forward and backward algorithms are designed to find the optimal path for the proposed method. Numerical examples are also illustrated for the same. Verification is done using the path length ranking technique. Simulation results are included by the use of the C program and MATLAB. Finally, the comparison is made with the traditional forward and backward pass (existing method) technique to point out the conclusion.

Keywords: Critical path problem, Triangular fuzzy number, Intuitionistic Triangular Fuzzy Number, Acyclic network.

I. Introduction

A project is understood as a set of interconnected operations that must be executed out in a particular manner to generate a significant profit. A complex project implicates many interlinked activities depend upon labor force, machines, and materials; it was unfeasible for organizers to assemble and achieve an optimum schedule. However, due to the complexity of few projects come across in the late 1950's it was essential to introduce a new technique that will be more adequate and efficacious strategies. Two techniques were adopted by Operations Research namely, Project Evaluation and Review Technique and Critical Path Method. The former was developed by the US Naval Forces in 1957 while the latter was developed by James E. Kelley and Morgan R. walker [9]. CPM was first applied in 1966 for the construction of a major Skyscraper that is the former World Trade Center Twin Towers in New York City. CPM has more boons which were implemented by Mauchly Associates. CPM and PERT are predominantly time-oriented methods. The most noteworthy dissimilarity between CPM and PERT was in the utilization of the time estimates. The value of time assigns to be probabilistic in PERT although they were deterministic in CPM. It was widely known as a valuable tool for the look and programming for huge come. The concept of the critical path allows the decision-maker to control the project's cost and schedule, and it can improve the quality of the work. This method is commonly utilized in various industries to analyze and improve the efficiency of a project.

Adequate project management strategies are censorious to organizers and decision-makers to approach projects in the conflicting domain. Project Managers are required to observe which techniques can accomplish projects and execute them within a particular period [7]. Actually, owing to the uncertainty of data in addition to the discrepancy of quantities framework, it was often difficult to secure the designated activity time. Hence, Lofti Asker Zadeh proposed the

theory called fuzzy set theory which plays a significant aspect in this type of decision-making world [14]. There were several methods reported to solve the fuzzy critical path (FCP) problem in the open literature. The first method to find an optimal path called Fuzzy Program Evaluation and Review Technique (FPERT) was proposed by Chanas and Kamburowski [5]. FPERT assumes the time to find the critical path, whereas when the project managers have deterministic data to find a critical path they can use the Fuzzy Critical Path Method (FCPM). Stephen Dinakar and Rameshan [13] presented an approach to analyzing the critical path in a project network with octagonal fuzzy numbers. Balaganesan and Ganesan [3] proposed a new methodology to find the critical path where the imprecise parameters in the network diagram take the intuitionistic triangular fuzzy numbers instead of crisp numbers. N. Jose Parvin Praveena et.al proposed a new method called the new JOSE Algorithm to find FCP. This method was designed according to find the fuzzy critical path using 13 Parameters with a ranking method, namely the Euclidean ranking method. The dynamic encoding recursion of the critical path in terms of triskaidecagonal and Triskaidecagonal fuzzy numbers fuzzy critical Path was found [8]. Ravi Shankar Nowpada et.al presented a new analytical method for finding critical paths using a fuzzy project network. They have proposed a new defuzzification formula for trapezoidal fuzzy numbers and applied it to the float time for each activity in that project network and tabulated the values. With the use of table values, they found the critical path [11]. Thus, numerous papers are published on fuzzy critical path problems. Few among them are [1, 6 and 12].

The paper is organized as follows: In section 2, we review the basic definitions of fuzzy set theory. Section 3; focus on two different algorithms which are utilized to identify the intuitionistic fuzzy critical path. Numerical examples are illustrated to perform the proposed approach. The simulation result is included for one of the developed algorithms. Under results and discussions in section 4, the comparison is made with the existing method (Forward and backward pass computations). Section 5 concludes the paper.

II. Preliminaries

Definition 2.1 Fuzzy set [14]

Fuzzy sets are sets that are characterized by imprecise data with boundaries to express a degree of membership function in the closed unit interval $[0, 1]$.

Let P be a non-empty set. Then a fuzzy set X is a set having the form of ordered pairs $X = \{(p, \alpha_X(p)) : p \in P\}$ where the function $\alpha_X : P \rightarrow [0, 1]$ is called the membership function and $\alpha_X(p)$ is called the degree of membership of each element $p \in P$.

Definition 2.2 Intuitionistic Fuzzy set [2]

Let a set P be fixed. An intuitionistic fuzzy set X in P is an object having the form $X = \{(p, \alpha_X(p), \gamma_X(p)) : p \in P\}$ where the function $\alpha_X : P \rightarrow [0, 1]$ and $\beta_X : P \rightarrow [0, 1]$ defined the degree of membership and degree of non-membership respectively of the element $p \in P$ to the set X , which is a subset of P , and for every $p \in P$, $0 \leq \alpha_X(p) + \beta_X(p) \leq 1$.

The amount $\alpha_X(p) = 1 - \alpha_X(p) - \beta_X(p)$ is called the hesitation part, which may be either membership value or non-membership value or both.

Definition 2.3 Fuzzy Number [14]

Let \tilde{p} is said to be a fuzzy number if it satisfies the following condition,

- (i) $\alpha_X(p)$ is piecewise continuous
- (ii) $\alpha_X(p)$ is convex,
- (iii) $\alpha_X(p)$ is normal.

Definition 2.4 Triangular fuzzy number [14]

A triangular fuzzy number X can be defined by a triplet $(m, n, o; 1)$, where $m < n < o$; $m, n, o \in R$. The membership function $\alpha_x(p)$ is given as follows:

$$\alpha_x(p) = \begin{cases} \frac{x-m}{n-m}, & m \leq x < n \\ 1, & x = n \\ \frac{o-x}{o-n}, & n < x \leq o \\ 0, & \text{otherwise} \end{cases}$$

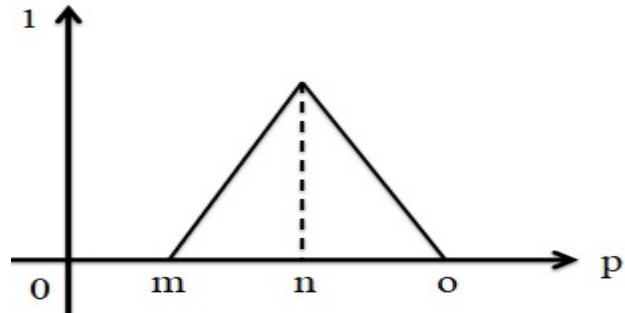


Fig.1. Triangular Fuzzy Number

Definition 2.5 Intuitionistic Triangular Fuzzy Number [2]

A intuitionistic triangular fuzzy number \tilde{X} can be defined by a triplet $(\tilde{m}, n, \tilde{o}; 1)$, where $\tilde{m} < m < n < o < \tilde{o}$; $\tilde{m}, n, \tilde{o} \in R$. The membership function is alike given in Definition 2.4. The non-membership function $\beta_x(p)$ is given as follows:

$$\beta_x(p) = \begin{cases} \frac{x-\tilde{m}}{n-\tilde{m}}, & \tilde{m} \leq x < n \\ 1, & x = n \\ \frac{\tilde{o}-x}{\tilde{o}-n}, & n < x \leq \tilde{o} \\ 0, & \text{otherwise} \end{cases}$$

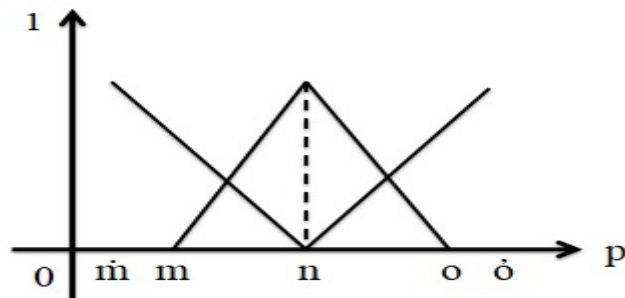


Fig.2. Intuitionistic Triangular Fuzzy Number

Definition 2.6 Addition operation on triangular fuzzy numbers [14]

Let $A = (m_1, n_1, o_1)$ and $B = (m_2, n_2, o_2)$ be two triangular fuzzy numbers, then $A \oplus B = (m_1 + m_2, n_1 + n_2, o_1 + o_2)$.

Definition 2.7 Subtraction operation on triangular fuzzy numbers [14]

Let $A = (m_1, n_1, o_1)$ and $B = (m_2, n_2, o_2)$ be two triangular fuzzy numbers, then $A - B = (m_1 - o_2, n_1 - n_2, o_1 - m_2)$.

Definition 2.8 Maximum operation for triangular fuzzy numbers [14]

Let $A = (m_1, n_1, o_1)$ and $B = (m_2, n_2, o_2)$ be two triangular fuzzy numbers then $L_{\max} = \max(A, B) = (\max(m_1, m_2), \max(n_1, n_2), \max(o_1, o_2))$.

Definition 2.9 Minimum operation for triangular fuzzy numbers [14]

Let $A = (m_1, n_1, o_1)$ and $B = (m_2, n_2, o_2)$ be two triangular fuzzy numbers then $L_{\min} = \min(A, B) = (\min(m_1, m_2), \min(n_1, n_2), \min(o_1, o_2))$.

Definition 2.10 Acyclic network [4]

A digraph is a graph each of whose edges are directed. Hence an acyclic digraph is a directed graph without cycle.

III. Methodology

I. General Algorithm for intuitionistic fuzzy critical path problem using intuitionistic triangular fuzzy numbers

Step 1:

Construct an acyclic network $G(V, E)$, where V is the set of vertices and E is the set of edges. Each arc lengths or edge weights corresponds to the cost, time etc., in practical problems.

Step 2:

Calculate all possible paths P_i , $i = 1$ to n from the source vertex 's' to the destination vertex 'd'.

Step 3:

The corresponding path lengths L_i , $i = 1$ to n using definition 2.6.

To calculate path length $P_i = \sum_{i=1}^n L_i$

Step 4:

After Calculating the path length for each possible path L_i , $i = 1$ to n , then find the path having the maximum value and rank it as first rank. The path which is ranked first is identified as the intuitionistic fuzzy critical path.

Numerical Example:

Step 1:

Construct an acyclic network $G(V, E)$ of Type V graph fuzziness using definition 2.12, where the edge weights are taken as an intuitionistic triangular fuzzy number. [3] [6]

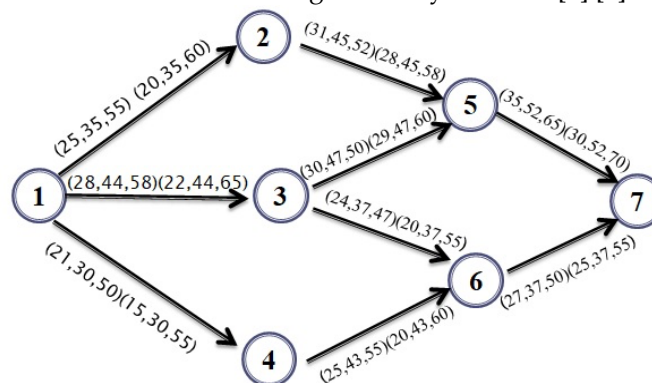


Fig. 3 Intuitionistic triangular fuzzy network

Step 2:

The possible paths are P_1 is 1-2-5-7, P_2 is 1-3-5-7, P_3 is 1-3-6-7 and P_4 is 1-4-6-7.

Step 3:

Consider Fig.3, calculate the path length, $P(L_i) = \sum_{i=1}^n L_i$. Calculated Values are tabulated below.

Table. 1 Results of the Network

Path (P _i)	Path length (L _i)	Ranking
P ₁ : 1-2-5-7	(91, 132, 172)(78, 132, 188)	2
P ₂ : 1-3-5-7	(93, 143, 173)(81, 143, 195)	1
P ₃ : 1-3-6-7	(79, 118, 155)(67, 118, 175)	3
P ₄ : 1-4-6-7	(73, 110, 155)(60, 110, 170)	4

From the table, the path P₁: 1-3-5-7, is identified as the intuitionistic fuzzy critical path because it has the highest value while calculating path length.

II Proposed Algorithm

Maximum Edge Distance Algorithm for intuitionistic fuzzy critical path (IFCP) problem using intuitionistic triangular fuzzy numbers

Notations used:

EL – Edge length

d[u, v] – Duration of the activity (u, v)

Adj [u] – Adjacent to node u

s – Source node

t – Destination node

(i) Forward procedure to calculate the IFCP

Step 1: Place all the vertices in Q = priority queue (1, 2, ..., n-1, n).

Step 2: Choose s = u = 1, choose the source node as permanent node. Set EL[u] = (0,0,0)(0,0,0).

Step 3: Extract the maximum edge distance.

For all $v \in \text{Adj}[u]$ that is for all edges emerging from u, calculate the following:

- (i) If u is incident to only one node v then, $EL[v] = EL[u] \oplus d[u, v]$ using definition 2.6
- (ii) If u is incident to more than one node v then, $EL [v] = \text{Max}_{v \in s} [(EL[u] \oplus d[u,v])]$ using definition 2.8

The new permanent node = v. Now, form the new priority queue by removing the source node s = u = 1 and the other nodes adjacent to u which are different from v.

Repeat step 3, until the permanent node = t. If so, terminate the execution of the algorithm.

Step 4: The intuitionistic fuzzy distance along the intuitionistic fuzzy critical path P namely intuitionistic fuzzy critical path length is denoted by D(P) and is defined as $D(P) = \sum_{(u,v) \in P} l_{uv}$, where l_{uv} is the path length. It is calculated using definition 2.6 and the corresponding path is the IFCP.

(ii) Backward procedure to calculate the IFCP

Step 1: Place all the vertices in Q = priority queue (n, n-1, ..., 2, 1).

Step 2: Choose t = u = n, that is choose the destination node as permanent node. Set EL[u] = (0,0,0)

Step 3: Extract the maximum edge distance.

For all $v \in \text{Adj}[u]$ that is for all edges incident on u , calculate the following:

- (i) If u is incident to only one node v then, $\text{EL}[u] = \text{EL}[v] \oplus d[u, v]$ using definition 2.6
- (ii) If u is incident to more than one node v then, $\text{EL}[u] = \text{Max}_{v \in s} [(\text{EL}[v] \oplus d[u, v])]$ using definition 2.8

The new permanent node = v . Now remove the destination node $u = t$ from the priority queue and the other nodes incident to u other than v .

Repeat step 3, until the permanent node = s . If so, terminate the execution of the algorithm.

Step 4: Calculate the edge distance by using step 4 as given in forward procedure to calculate the IFCP.

Numerical Example:

Consider fig. 3 to find the IFCP, Backward procedure of an algorithm 3.2 to calculate the IFCP will not work here, since the edges incident to the destination node as the same path length, because the network is constructed using directed graph. Hence, we apply forward procedure of an algorithm 3.2.

Step 1: $Q =$ priority queue (1, 2, 3, 4, 5, 6, 7)

Step 2: Let $S = u = 1$ (source node). $\text{EL}[1] = (0, 0, 0) (0, 0, 0)$.

Step 3: $2 \in \text{Adj}[1]$ $3 \in \text{Adj}[1]$ and $4 \in \text{Adj}[1]$

$$\begin{aligned} \text{EL}[2] &= \text{EL}[1] \oplus d[1,2] = (0, 0, 0) (0, 0, 0) + (25, 35, 55)(20, 35, 60) = (25, 35, 55)(20, 35, 60), \\ \text{EL}[3] &= \text{EL}[1] \oplus d[1,3] = (0, 0, 0) (0, 0, 0) + (28, 44, 58)(22, 44, 65) = (28, 44, 58)(22, 44, 65), \\ \text{EL}[4] &= \text{EL}[1] \oplus d[1,4] = (0, 0, 0) (0, 0, 0) + (21, 30, 50)(15, 30, 55) = (21, 30, 50)(15, 30, 55) \\ \text{EL}[v] &= \text{Max} \{ (\text{EL}[2], \text{EL}[3], \text{EL}[4]) \} \\ &= \text{Max} \{ (25, 35, 55)(20, 35, 60), (28, 44, 58)(22, 44, 65), (21, 30, 50)(15, 30, 55) \} \end{aligned}$$

$$\text{EL}[v] = (28, 44, 58)(22, 44, 65) = \text{EL}[3]$$

The new permanent node = 3

Remove source node 1, node 2 and node 4 from the priority queue.

New priority queue is $Q =$ Priority queue (5, 6, 7, 8)

$5 \in \text{Adj}[3]$, $6 \in \text{Adj}[3]$

$$\begin{aligned} \text{EL}[5] &= \text{EL}[3] \oplus d[3, 5] = (28, 44, 58)(22, 44, 65) + (30, 47, 50)(29, 47, 60) = (58, 91, 108) (51, 91, 125) \\ \text{EL}[6] &= \text{EL}[3] \oplus d[3, 6] = (28, 44, 58) (22, 44, 65) + (24, 37, 47)(20, 37, 55) = (52, 81, 105) (42, 81, 120) \\ \text{EL}[v] &= \text{Max} \{ \text{EL}[5], \text{EL}[6] \} = (58, 91, 108) (51, 91, 125) = \text{EL}[5] \end{aligned}$$

The new permanent node = 5

Remove source node 6 from the priority queue.

New priority queue is $Q =$ Priority queue (7)

$7 \in \text{Adj}[5]$

$$\text{EL}[7] = \text{EL}[5] \oplus d[5,7] = (58, 91, 108)(51, 91, 125) + (35, 52, 65)(30, 52, 70) = (93, 143, 173) (81, 143, 195)$$

The new permanent node = 7 = t = destination node.

Since, we reach the destination node we can stop the process.

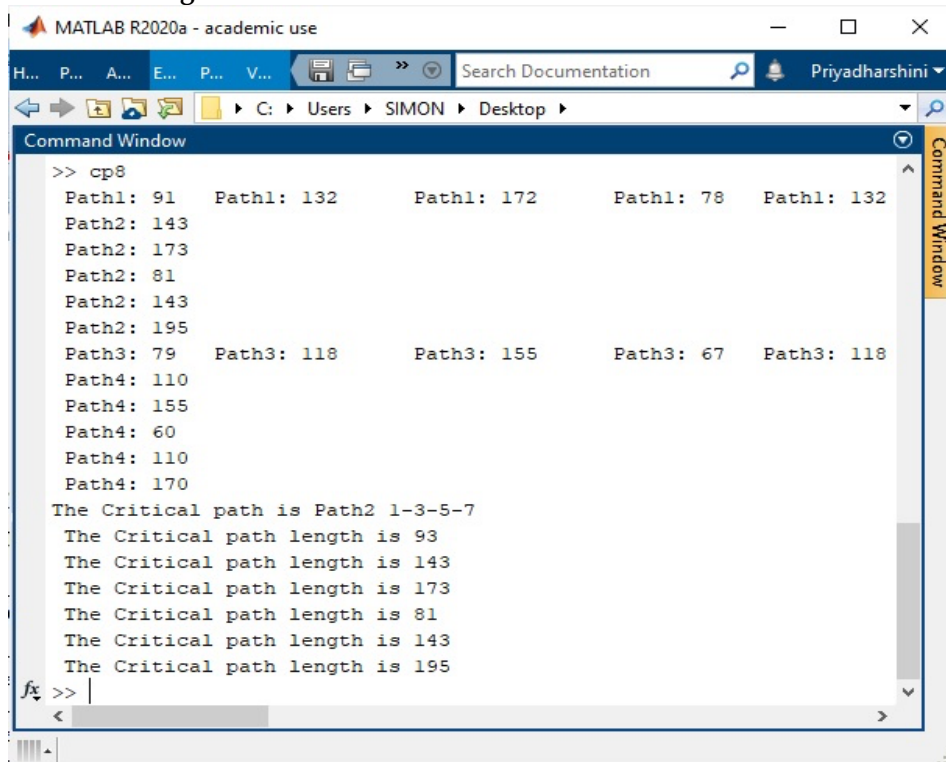
Step 4:

By using the formula stated in algorithm 3.2, $D(P) = \sum_{(u,v) \in P} l_{uv}$. The intuitionistic fuzzy critical path length is calculated that is (93, 143, 173) (81, 143, 195) and the corresponding intuitionistic fuzzy critical path is 1-3-5-7.

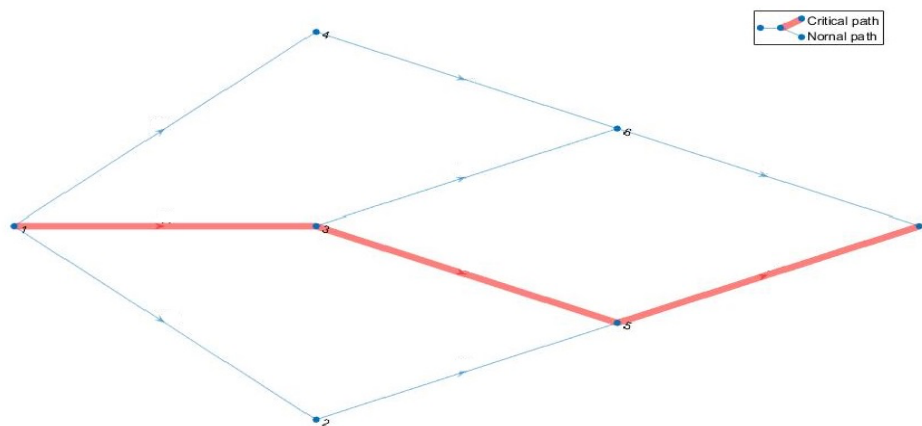
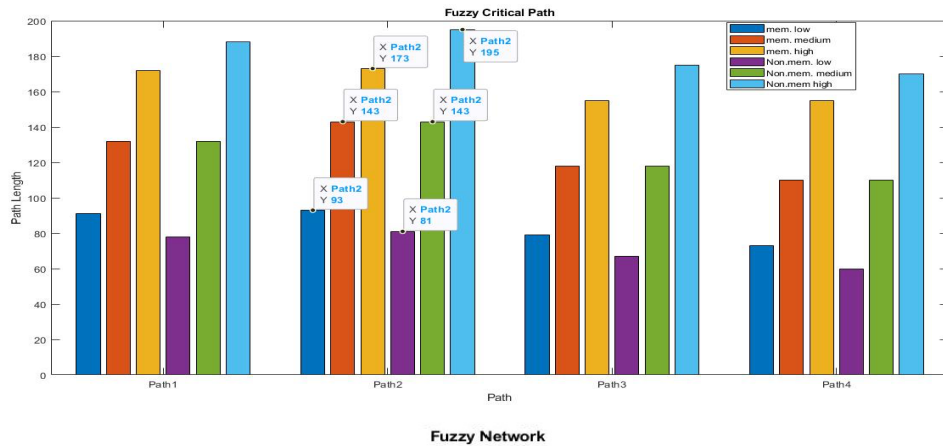
Simulation Result using C Program

```
NeuTroN DOS-C++ 0.77, Cpu speed: max 100% cycles, Frameskip 0, Program: TC
ENTER THE ACTIVITY(1,3):28 44 58 22 44 65
ENTER THE ACTIVITY(1,4):21 30 50 15 30 55
ENTER THE ACTIVITY(2,5):31 45 52 28 45 58
ENTER THE ACTIVITY(3,5):30 47 50 29 47 60
ENTER THE ACTIVITY(3,6):24 37 47 20 37 55
ENTER THE ACTIVITY(4,6):25 43 55 20 43 60
ENTER THE ACTIVITY(5,7):35 52 65 30 52 70
ENTER THE ACTIVITY(6,7):27 37 50 25 37 55
L1:    91    132    172    78    132    188
L2:    93    143    173    81    143    195
L3:    79    118    155    67    118    175
L4:    73    110    155    60    110    170
(L1)=398.000000,
(L2)=419.000000,
(L3)=360.000000,
(L4)=340.000000,
The Critical Path is 1-3-5-7
```

Simulation Result using MATLAB



```
MATLAB R2020a - academic use
C:\Users\SIMON\Desktop
Command Window
>> cp8
Path1: 91    Path1: 132    Path1: 172    Path1: 78    Path1: 132
Path2: 143
Path2: 173
Path2: 81
Path2: 143
Path2: 195
Path3: 79    Path3: 118    Path3: 155    Path3: 67    Path3: 118
Path4: 110
Path4: 155
Path4: 60
Path4: 110
Path4: 170
The Critical path is Path2 1-3-5-7
The Critical path length is 93
The Critical path length is 143
The Critical path length is 173
The Critical path length is 81
The Critical path length is 143
The Critical path length is 195
```



IV. Results and Discussions

Verification. For the sake of comparison, here verification is done using traditional forward and backward pass calculation.

Activity (i-j)	Duration	Earliest start Time(EST)	Earliest finish Time(EFT)	Latest finish Time(LFT)	Total Float
1-2	(25, 35, 55)(20, 35, 60)	(0,0,0) (0,0,0)	(25, 35, 55)(20, 35, 60)	(27,46,56)(23,46,67)	(2,11,1)(3,11,7)
1-3	(28,44,58)(22, 44, 65)	(0,0,0) (0,0,0)	(28,44,58)(22, 44, 65)	(28,44,58)(22,44,65)	<u>(0,0,0) (0,0,0)</u>
1-4	(21, 30, 50)(15, 30, 55)	(0,0,0) (0,0,0)	(21, 30, 50)(15, 30, 55)	(41,63,58)(36,63,80)	(20,33,8)(21,33,25)
2-5	(31, 45, 52)(28, 45, 58)	(25, 35, 55)(20, 35, 60)	(56,80,107)(48,80,118)	(58,91,108)(51,91,125)	(2,11,1)(3,11,7)
3-5	(30,47,50)(29,47,60)	(28,44,58)(22, 44, 65)	(58,91,108)(51,91,125)	(58,91,108)(51,91,125)	<u>(0,0,0) (0,0,0)</u>
3-6	(24,37,47)(20,37,55)	(28,44,58)(22, 44, 65)	(52,81,105)(42,81,120)	(66,106,123)(56,106,140)	(14,25,18)(14,25,20)
4-6	(25,43,55)(20,43,60)	(21, 30, 50)(15, 30, 55)	(46,73,105)(35,73,110)	(66,106,123)(56,106,140)	(20,33,18)(21,33,30)
5-7	(35,52,65)(30,52,70)	(58,91,108)(51,91,125)	(93,143,163)(81,143,195)	(93,143,163)(81,143,195)	<u>(0,0,0) (0,0,0)</u>
6-7	(27,37,50)(25,37,55)	(46,73,105)(35,73,115)	(73,110,155)(60,110,170)	(93,143,163)(81,143,195)	(20,30,58)(20,30,25)

Here path P₁:1-3-5-7 is identified as the intuitionistic fuzzy critical path.

The Comparison was done for the solution yield using the proposed method. Verification is done using the traditional forward and backward pass calculations. It is found that the result obtained in this paper, coincides with the result obtained through the existing methods. The iterations and time consumption used to find the critical path using maximum edge distance method was better than the existing method.

V. Conclusion

In this paper, we have developed a different algorithm namely the maximum edge distance method to find the optimal path in an intuitionistic fuzzy weighted directed graph with its edge weights as an intuitionistic triangular fuzzy number. The method proposed in this paper is an alternative way to identify the critical path in the fuzzy environment. This method has turned down the recurrence. The approximation of the project can be done effortlessly through this "Maximum edge distance" method. The reason to mention the word "effortless" is because that the completion time of the project given by this method will be optimized at its best as shown in the solution illustrated in the numerical example. Obviously and finally this method reduces the time consumption when compared to the regular methods used already (Forward and backward pass computations).

References

- [1] V. Anushya, and P. Balasowandari, "Fuzzy critical path with area measure", *International Journal of Pure and Applied Mathematics*, Vol.118, No.6, pp.167-173, 2018.
- [2] K. Atanassov, "Intuitionistic Fuzzy Sets", *Fuzzy Sets and Systems*, Vol. 20, No.1, pp.87-96. [http://dx.doi.org/10.1016/s0165-0114\(86\)80034-3](http://dx.doi.org/10.1016/s0165-0114(86)80034-3), 1986.
- [3] M. Balaganesan, and K. Ganesan, "An approach to find critical path in intuitionistic fuzzy environment", *International Journal of Pure and Applied Mathematics*, Vol.119, No.9, pp.395-403, 2018.
- [4] M. Blue, B. Bush, and J. Puckett, "Unified approach to fuzzy graph problems", *Fuzzy Sets and Systems*, Vol. 125, pp. 355-368, 2002.
- [5] S. Chanas, and J. Kamburowski, "The use of fuzzy Variables in PERT", *Fuzzy Sets and Systems*, Vol. 5, pp. 11-19, 1981.
- [6] S. Elizabeth, and L. Sujatha, "Project Scheduling method using triangular intuitionistic fuzzy numbers and triangular fuzzy numbers", *Applied Mathematical Sciences*, Vol.9, No.4, pp.185-198, 2015.
- [7] S. Elizabeth, L. Sujatha, and K. Bharathi, "On searching critical path in a project network under fuzzy environment", *National Conference on recent approaches of Mathematics to Science and Technology (NCRAM 2015)*, ISBN:978-81-929362-1-5, 2015.
- [8] N. Jose Parvin Praveena, C. Sagaya Nathan Stalin, and A. Rajkumar, "Critical Path Problem Through Intuitionistic Triskaidecagonal Fuzzy Number Using Two Different Algorithms", *Advances in Artificial Intelligence and Data Engineering*, volume 1133, pp 159-167, 2020.
- [9] Kelley, James; Walker, Morgan; "Critical-Path Planning and Scheduling", *1959 Proceedings of the Eastern Joint Computer Conference*, 1959.
- [10] Newell, Michael; Grashina, Marina; "The Project Management Question and Answer Book", *American Management Association*, pp. 98, 2003.
- [11] N. Ravi Shankar, V. Sireesha and P. Phani Bushan Rao, "An Analytical Method for Finding Critical Path in a Fuzzy Project Network", *Int. J. Contemp. Math. Sciences*, Vol. 5, 2010, No. 20, pp.953 – 962, 2010.
- [12] V. Sireesha, and N. Ravishankar, "A new approach to find total float time and critical path in a fuzzy project network", *International Journal of Engineering Science and Technology*, Vol.2, No. 4, pp.600-609, 2010.
- [13] D. Stephen Dinagar, and N. Rameshan, "A New Approach for Fuzzy Critical Path Method Using Octogonal Fuzzy Numbers", *International Journal of Pure and Applied Mathematics*, Vol. 119, No. 13, pp. 357-364, 2018.
- [14] L.A. Zadeh, "Fuzzy sets", *Information and Control*, Vol. 8, pp. 338-353, 1965.

Sentiment Analysis Performance and Reliability Evaluation Using an XLNet-based Deep Learning Approach

DHAVAL BHOI, DR. AMIT THAKKAR



CSPIT, Charotar University of Science and Technology, Changa-388421, Gujarat, India
dhavalbhoi.ce@charusat.ac.in

Abstract

Online reviews are now a global form of communication between consumers and E-commerce companies. When it comes to making day-to-day decisions, customers rely heavily on the availability of internet reviews, as well as their trustworthiness and performance. Due to the unique qualities of user reviews, customers are finding it increasingly difficult to define and examining the authenticity and reliability of sentiment evaluations. These sentiment classifications for user reviews can aid in understanding user feelings, review dependability, and customer perceptions of movie items. Deep Learning is a strong technique for learning several layers of data representations or features. When compared to traditional machine learning approaches, deep learning techniques yield better results. To assess, analyze, and weight the usefulness of each review comment, we employed the XLNet Deep Learning Model Approach on balanced movie review dataset. Experimental result demonstrates that the proposed deep learning model achieves higher performance evaluation than those of other classifiers.

Keywords: Sentiment Analysis, Machine Learning, Deep Learning, XLNet

1. INTRODUCTION

In recent years, the E-commerce industry has grown at a breakneck pace [1]. When a wide variety of items or products appear in customers' online shopping sites, however, determining their authenticity and trustworthiness becomes more complex, making it impossible to identify genuine goods from imitation or replica goods. Customers typically evaluate similar items based on quality information and pricing before making purchasing decisions.

According to studies, consumers who acquire information from online available posts or ratings are more interested in buying the product than those who just gather information from the manufacturer or producer. It implies that online remarks or sentiments left by previous consumers play a significant effect in the selection of online goods. According to a recent study, the number of online reviews are proportional to users' buy intent. Customers are more eager to buy if there are more online reviews [2]. Sentiment Analysis is a linguistic technique that involves extracting emotions from raw texts [3] [4]. It can be performed at Document Level, Sentence Level or Aspect Level shown in below Figure 1.

This is commonly used on social media posts and customer reviews to automatically determine whether some users are happy or unpleasant, as well as reasons. The original place of sentiment analysis or opinion mining is shown in Figure 2. The major purpose of this research is to demonstrate how deep learning may be used to perform sentiment analysis. It's a means of evaluating a document's, sentence's, or word's polarity. It is utilized in a wide range of industries, including marketing, medical diagnosis, education sector, film industries, and others, to aid businesses and customers. Based on the type of input, it can be broadly classified as Document Level sentiment Analysis, Sentence (or Line) Level Sentiment Analysis and Aspect (or Feature)

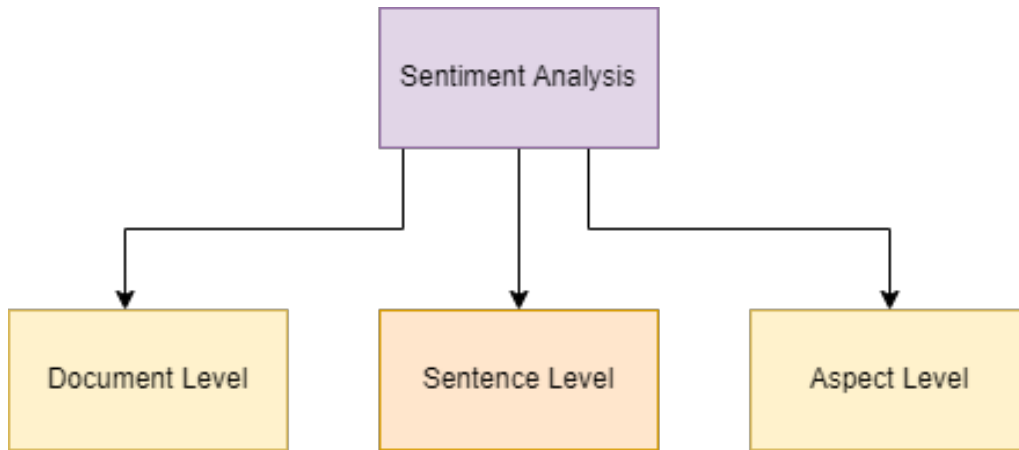


Figure 1: Levels of Sentiment Analysis

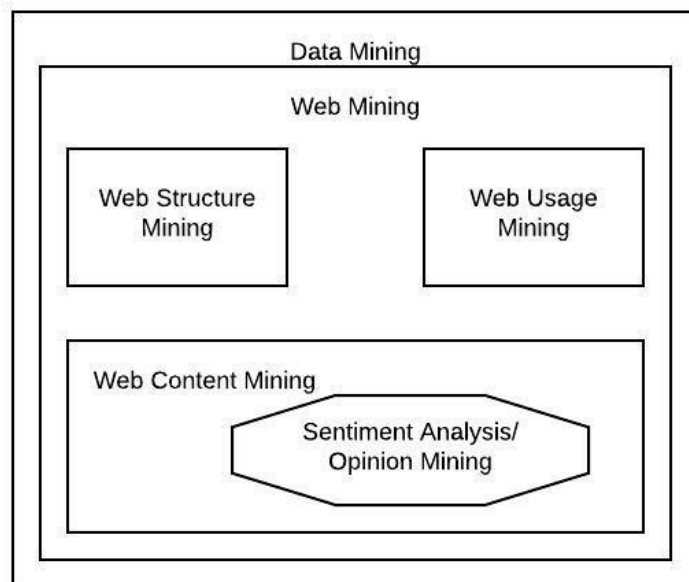


Figure 2: Place of Sentiment Analysis in Data Mining

level Sentiment Analysis [5]. The document's polarity is calculated by counting the number of times a positive or negative appears in a document. If there are more positive terms in a paper than negative words, it is determined that the document is positive. A sentence level check and a word level check can be performed in the same way as a document check [6]. The alternative method is termed Aspect Based, Entity Based, or Feature Based Sentiment Analysis, and it focuses on numerous characteristics of the situation [7]. Comment-based opinion mining or sentiment analysis is crucial for evaluating and examining the reliability of e-commerce items or products when human variables are involved. The e-commerce dependability evaluation results can be used in the iteration of product reliability design process, and offer product life cycle references management.

2. RELATED WORK

Different researchers had used earlier lexicon based approach, machine learning approach and deep learning based approach to perform classification of sentiment [8] [9].

The authors of [10] have used BOW [Bag of Words] feature extraction technique and applied Navie Bayes and Support Vector Machine classifier produce improved classification result.

In this study, a stacked residual LSTM [Long Short Term Memory] model was utilised to estimate sentiment intensity, which improved prediction accuracy [11].

In recent work, authors of [12] used an Amazon review dataset to test the baseline deep learning models for LSTM, GRU, Bi-LSTM, and Bi-GRU. These tactics ignore the importance of word order and the many distinct meanings that words can convey.

Recently, the authors used a supervised machine learning-based technique to analyse sentiment in product reviews. They improved the result by combining two separate word embedding techniques, word2vec and FastText Word Embedding, with a CNN Model. They improved their performance by using FastText as a word embedding technique and CNN as a deep learning model [13].

3. PROPOSED SYSTEM

To conduct this experiment, we employed a movie review dataset and associated binary sentiment polarity labels [14]. The primary rationale for selecting this dataset is that it is well-balanced. It comprises an equal number of positive and negative review data samples. We used an XLNet-based deep learning approach in the proposed method. The XLNetTokenizer is used to extract features from review text, and the XLNet deep learning model is used to train it. Figure 3 depicts the proposed approach's overall flow. The current reliability indices [15] mainly have time measurement and probability measurement for evaluation. Reliability is denoted as R. Function of Failure (F), Probability Density Function (f), and Failure Rate(λ) are the most commonly used probability measurements, whereas Mean Time To Failure (MTTF) and Mean Time Between Failures (MTBF) are the most common time measurements.

The possibility that a product or item will execute particular function for a certain amount of time duration under specified conditions without failure is known as reliability. To put it another way, if T is a product's time to failure, and the reliability function at time t is as shown in 1

$$R(t) = P(T > t) \quad (1)$$

The average time that it takes for an unfixable product or item to perform properly under given specific conditions until it fails is called MTTF. When the number of samples given is N and the life of sample I is t_i , the MTTF can be calculated as in 2

$$MTTF = \frac{1}{N} \sum_1^N t_i \quad (2)$$

If a product is repairable; the average continuous time between product or item failures during the operation or testing is called Mean Time Between Failure (MTBF), and it is calculated as shown in 3

$$MTBF = \int_0^{\infty} tf(t)dt \quad (3)$$

We have introduced the notion of Reliability for Sentiment (R_s), which is considered a weighted average of Sentimental Analysis Value (S) of products or items obtained from consumers' opinions, sentiments or evaluations about the product they've bought or used, weighted by the Importance or Usefulness (U) of a specific given review or comment. To quantify something, we use the following function shown in equation 4.

$$R_s = \frac{\sum S_i * U_i}{\sum U_i} \quad (4)$$

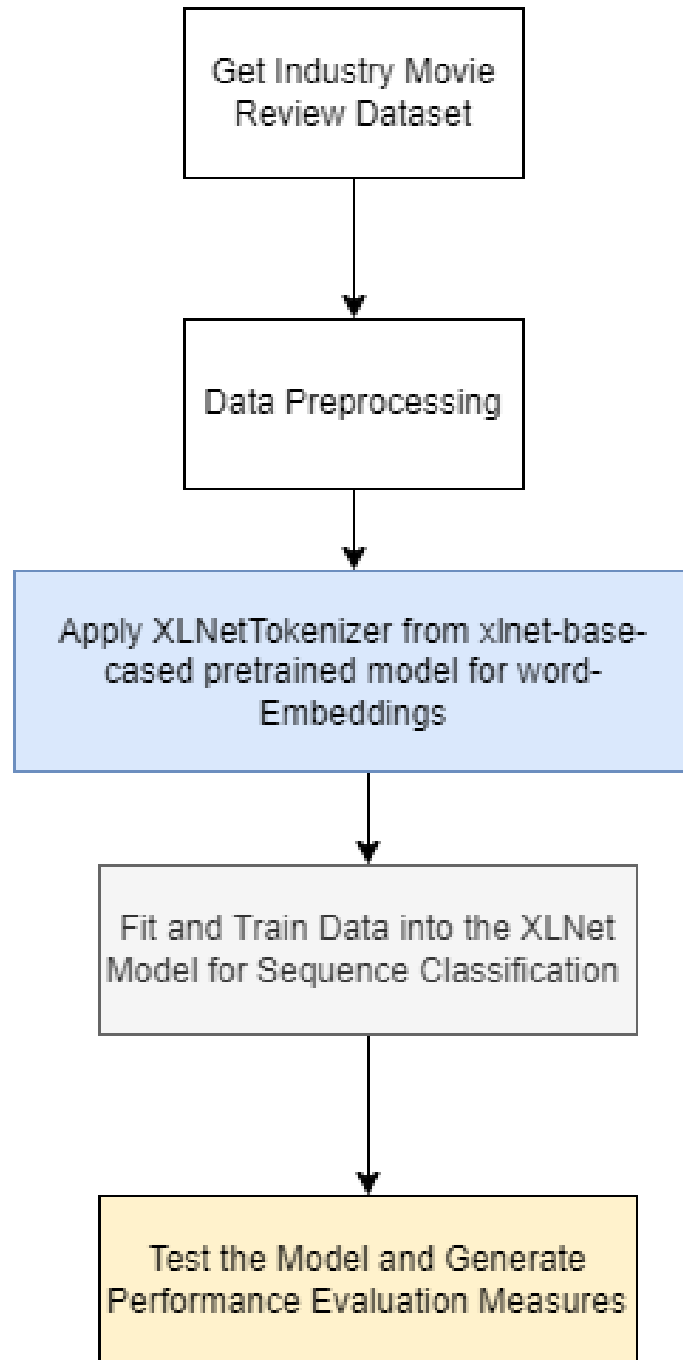


Figure 3: Proposed Approach

Sentiment analysis based on this metric of reliability can benefit not just consumers, but also businesses and organisations looking to enhance their operations and strategy.

We determined Accuracy, Precision, Recall, and F1-score [16] for performance evaluation, as given in the equations below 5, 6, 7 and 8. Precision and recall are balanced by the F-measure or F1-Score.

$$Accuracy = \frac{TP + TN}{TP + TN + FP + FN} \quad (5)$$

$$Precision = \frac{TP}{TP + FP} \quad (6)$$

$$Recall = \frac{TP}{TP + FN} \tag{7}$$

$$F1 = \frac{2 * TP}{2 * TP + FP + FN} \tag{8}$$

Where TP, TN, FP and FN are number of true positive, true negative, false positive and false negative samples in a review dataset.

4. RESULTS AND DISCUSSION

Based on the findings shown in table 1, we can conclude that our proposed deep learning model surpasses all existing machine learning methods, such as Logistic Regression, Naive Bayes classifier, and Support Vector Machine due to proper feature representation using XLNetTokenizer followed by XLNet Deep Learning Model. XLNet is the most recent and most advanced model to come from the burgeoning field of Natural Language Processing (NLP). XLNet is an autoregressive language model that uses a transformer architecture with recurrence to output the joint probability of a sequence of tokens hence it takes more time for training.

Table 1: Comparative Performance Result Analysis

Type of Model	Model Applied	Accuracy	Precision	Recall	F1-Score
Machine Learning Models	Naive Bayes	81.02	78.61	73.98	75.66
	Random Forest	84.76	83.39	77.84	80.52
	SVM	86.13	82.87	82.99	82.88
Deep Learning Model	XLNet	96.00	95.50	96.00	96.00

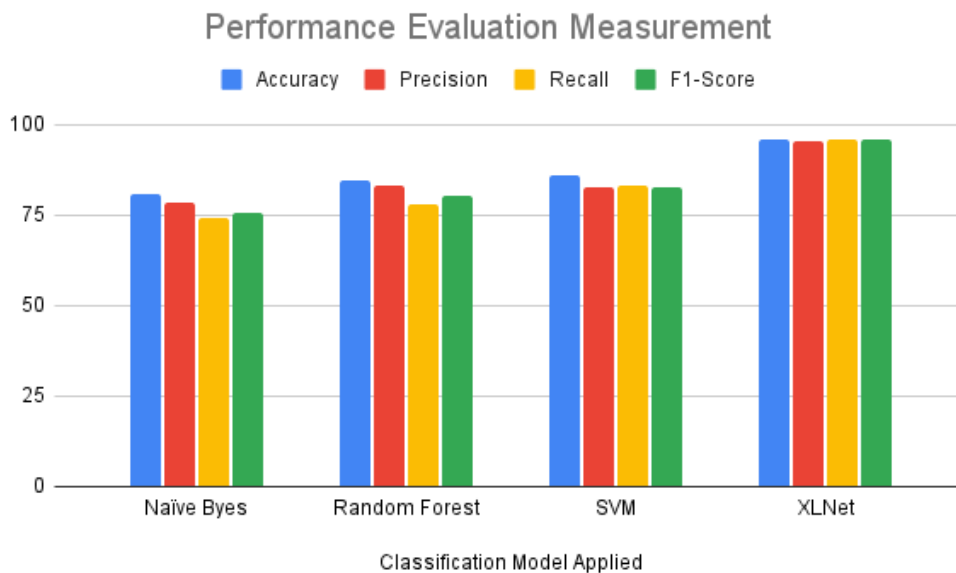


Figure 4: Performance Analysis Evaluation

In terms of F1-score, the suggested XLNet deep learning model performs 13.12 percent better than the top performing SVM machine learning model, as shown in Figure 4. We have enhanced accuracy, precision, and recall by 9.87 percent, 12.53 percent, and 13.02 percent, respectively.

5. CONCLUSION AND FUTURE WORK

All other machine learning models, including LR, NB, and SVM, are outperformed by our proposed deep learning methodology, XLNet. However, this method has the drawback of requiring more training time. We have applied our proposed approach on a dataset from the movie business; however, we can apply this model to other industry domains to determine how effective it is. As the proposed approach yields better results, it clearly tackles the reliability and performance issues based on sentiment analysis.

ACKNOWLEDGEMENT

The authors would like to thank the Principal and Dean of the Faculty of Technology and Engineering, as well as the Head of the U P U. Patel Department of Computer Engineering at CSPIT, Charotar University of Science and Technology, Changa, for their continuous suggestions, encouragement, guidance, and support in completing this research work. We want to express our gratitude to Management in particular for their moral guidance and encouragement.

DECLARATION OF CONFLICTING INTERESTS

The Author(s) declare(s) that there is no conflict of interest.

REFERENCES

- [1] Lakshmi P, StalinDavid D, Kalaria I, Jayadatta S, Sharma A, Saravanan D. Research on Collaborative Innovation of E-Commerce Business Model for Commercial Transactions. *Turkish Journal of Physiotherapy and Rehabilitation.*;32(3):787-94.
- [2] Zhang X, Xie G, Li D, Kang R. Reliability Evaluation Based on Sentiment Analysis of Online Comment. In2018 12th International Conference on Reliability, Maintainability, and Safety (ICRMS) 2018 Oct 17 (pp. 88-91). IEEE.
- [3] Devika, M.D. C, Sunitha Ganesh, Amal. (2016). Sentiment Analysis: A Comparative Study on Different Approaches. *Procedia Computer Science.* 87. 44-49. 10.1016/j.procs.2016.05.124.
- [4] Sriram B, Fuhry D, Demir E, Ferhatosmanoglu H, Demirbas M. Short text classification in twitter to improve information filtering. InProceedings of the 33rd international ACM SIGIR conference on Research and development in information retrieval 2010 Jul 19 (pp. 841-842).
- [5] Farooq U, Mansoor H, Nongaillard A, Ouzrout Y, Qadir MA. Negation Handling in Sentiment Analysis at Sentence Level. *J. Comput..* 2017 Sep 1;12(5):470-8.
- [6] Chen T, Xu R, He Y, Wang X. Improving sentiment analysis via sentence type classification using BiLSTM-CRF and CNN. *Expert Systems with Applications.* 2017 Apr 15;72:221-30.
- [7] Vanaja S, Belwal M. Aspect-level sentiment analysis on e-commerce data. In2018 International Conference on Inventive Research in Computing Applications (ICIRCA) 2018 Jul 11 (pp. 1275-1279). IEEE.
- [8] Taj S, Shaikh BB, Meghji AF. Sentiment analysis of news articles: A lexicon based approach. In2019 2nd International Conference on Computing, Mathematics and Engineering Technologies (iCoMET) 2019 Jan 30 (pp. 1-5). IEEE.
- [9] Long C, Ziyu G, Jinhong H, Jinye P. A survey on sentiment classification. *Journal of Computer Research and Development.* 2017 Jun 1;54(6):1150.
- [10] Zou H, Tang X, Xie B, Liu B. Sentiment classification using machine learning techniques with syntax features. In2015 International Conference on Computational Science and Computational Intelligence (CSCI) 2015 Dec 7 (pp. 175-179). IEEE.
- [11] Wang J, Peng B, Zhang X. Using a stacked residual LSTM model for sentiment intensity prediction. *Neurocomputing.* 2018 Dec 17;322:93-101.
- [12] Sachin S, Tripathi A, Mahajan N, Aggarwal S, Nagrath P. Sentiment analysis using gated recurrent neural networks. *SN Computer Science.* 2020 Mar;1(2):1-3.

- [13] Shah A. Sentiment Analysis Of Product Reviews Using Supervised Learning. *Reliability: Theory Applications*. 2021(SI 1 (60)).
- [14] Andrew L. Maas, Raymond E. Daly, Peter T. Pham, Dan Huang, Andrew Y. Ng, and Christopher Potts. (2011). Learning Word Vectors for Sentiment Analysis. *The 49th Annual Meeting of the Association for Computational Linguistics (ACL 2011)*
- [15] E. A. Elsayed, *Reliability Engineering*, 2nd ed., New Jersey: Wiley Sons, Inc., pp.3“5, 15“69, 2012.
- [16] Phan HT, Tran VC, Nguyen NT, Hwang D. Improving the performance of sentiment analysis of tweets containing fuzzy sentiment using the feature ensemble model. *IEEE Access*. 2020 Jan 3;8:14630-41.

Sharma-Mittal Entropy Properties on Generalized (k) Record Values

JERIN PAUL^a AND P. YAGEEN THOMAS^b



^aDepartment of Statistics, Vimala College (Autonomous), Thrissur, India

^bDepartment of Statistics, University of Kerala, Kraiavattom, Trivandrum, India

jerinstat@gmail.com & yageenthomas@gmail.com

Abstract

In this paper, we derive Sharma-Mittal entropy of generalized (k) record values and analyse some of its important properties. We establish some bounds for the Sharma-Mittal entropy of generalized (k) record values. We generate a characterization result based on the properties of Sharma-Mittal entropy of generalized (k) record values for the exponential distribution. We further establish some distribution-free properties of Sharma-Mittal divergence information between the distribution of a generalized (k) record value and the parent distribution. We extend the concept of Sharma-Mittal entropy to the concomitants of generalized (k) record values arising from a Farlie-Gumbel-Morgenstern (FGM) bivariate distribution. Also, we consider residual Sharma-Mittal Entropy and used it to describe some properties of generalized (k) record values.

Keywords: Generalized (k) record values, Sharma-Mittal entropy, Maximum entropy principle, Characterization, Concomitants of generalized (k) record values, Residual Sharma-Mittal entropy.

1. INTRODUCTION

In equilibrium thermodynamics, physicists originally developed the notion of entropy, which was later extended through the development of statistical mechanics. Shannon [30] introduced a generalization of Boltzmann-Gibbs entropy, and later it was known as Shannon entropy or Shannon information measure. Shannon entropy represents an absolute limit on any communication's best possible lossless compression. More generally, the concept of entropy is a measure of uncertainty associated with a random variable. For a continuous random variable X with probability density function (pdf) f , the Shannon entropy is defined by

$$H(X) = - \int_0^{\infty} f(x) \log f(x) dx. \quad (1)$$

In the continuous case, $H(X)$ is also referred to as the differential entropy. It is known that $H(X)$ measures the uniformity of f . When $H(X_1) > H(X_2)$, for any two random variables with pdf f_1 and f_2 respectively, then we conclude that it is more difficult to predict outcomes of X_1 , as compared with predicting outcomes of X_2 [see, 37]. One main drawback of $H(X)$ is that for some probability distributions, it may be negative and then it is no longer an uncertainty measure. This drawback is removed in the generalized entropies like Rényi entropy [29], Tsallis entropy [36] and so on.

Subsequently Sharma-Mittal entropy [31] was introduced as a two parameter measure $H_{\alpha, \beta}(X)$

of a random variable X with pdf f as

$$H_{\alpha,\beta}(X) = \frac{1}{1-\beta} \left\{ \left(\int_{-\infty}^{\infty} \{f(x)\}^{\alpha} dx \right)^{\frac{1-\beta}{1-\alpha}} - 1 \right\}, \quad (2)$$

with $\alpha, \beta > 0, \alpha \neq 1 \neq \beta$ and $\alpha \neq \beta$. It is clear to be note that if we take limit $\beta \rightarrow 1$ in (2) then Sharma-Mittal entropy becomes Rényi entropy [29] which is given by

$$H_{\alpha,1}(X) = \frac{1}{1-\alpha} \log \int \{f(x)\}^{\alpha} dx. \quad (3)$$

If we take limit as $\beta \rightarrow \alpha$, in (2), then the resulting expression is Tsallis entropy [36] and is given by

$$H_{\alpha,\alpha}(X) = \frac{1}{1-\alpha} \left\{ \int_{-\infty}^{\infty} \{f(x)\}^{\alpha} dx - 1 \right\}. \quad (4)$$

In the limiting case when both parameters approach 1, we recover the ordinary Shannon entropy [30] as given in (1).

One may observe several applications of Sharma-Mittal entropy from the available literature. Frank and Daffertshofer [10] have established the relation between anomalous diffusion process and Sharma-Mittal entropy. Masi [17] explained how this entropy measure unifies Rényi and Tsallis entropies. For more details on the applications of this entropy see, Aktürk et al. [4] and Kosztołowicz and Lewandowska [14]. Nielsen and Nock [21] obtained a closed-form formula for the Sharma-Mittal entropy of any distribution belonging to the exponential family of distributions.

Successive extremes occurring in a sequence of Independent and identically distributed (*iid*) random variables have been called by Chandler [8] as the record values of the sequence. Properties of record statistics arising from a distribution help to understand the intrinsic properties of the parent distribution as well. A limitation that one encounters in dealing with statistical inference problems based on classical record values is about their limited occurrence, as the expected value of inter arrival times of records is infinite [see, 11]. Also the occurrence of an outlier in a sequence of random variables arrests the subsequent realization of record values. However one may observe that generally the k th record values as introduced by Dziubdziela and Kopocinski [9] occur more frequently than those of the classical records. The reason for this is that the generation of the sequence of upper (k) records makes $k - 1$ of the upper extreme values (outliers) of the sequence incapacitated from their occurrence in the constructed record sequence. Similar property holds with the generated sequence of lower (k) record values as well. Suppose $\{X_n\}$ is a sequence of *iid* random variables. Then for a positive integer $k \geq 1$, the sequence of upper k th record times $\{T_{U(n,k)}, n \geq 1\}$ is defined as [see, 20, p. 82]:-

$$T_{U(1,k)} = k,$$

and, for $n \geq 1$

$$T_{U(n+1,k)} = \min\{j : j > T_{U(n,k)}, X_j > X_{T_{U(n,k)} - k + 1 : T_{U(n,k)}}\},$$

where $X_{i:m}$ denotes the i -th order statistic in a sample of size m . Now if we write

$$X_{U(n,k)} = X_{T_{U(n,k)} - k + 1 : T_{U(n,k)}}, \text{ for } n = 1, 2, \dots$$

then $\{X_{U(n,k)}\}$ is known as the sequence of the k th upper record values. In a similar manner we can define the sequence $\{X_{L(n,k)}\}$ of k th lower record values as well. It is to be noted that k th member of sequence of the classical record values is also called as k th record value. This contradicts with the k th record values as defined in [9]. Pointing out this conflict in the usage of k th record values of Dziubdziela and Kopocinski [9], and as it generates the classical record values for $k = 1$, Minimol and Thomas [18, 19], Paul [22], Paul and Thomas [23, 24, 25] and Thomas and

Paul [34, 35] have called the k th record values as defined in Dziubdziela and Kopocinski [9] as the generalized (k) record values. Agreeing with the contention of above authors, we also call the k th record values of [9] as generalized(k)record values all through this paper.

Suppose $\{X_i, i \geq 1\}$ is a sequence of random variables with absolutely continuous cdf $F(x)$ and pdf $f(x)$. Let $\{X_{U(n,k)}\}$ be the sequence of GURV's generated from the sequence $\{X_i\}$. Then the pdf $f_{X_{U(n,k)}}(x)$ of $X_{U(n,k)}$ is given by [see, 6]

$$f_{X_{U(n,k)}}(x) = \frac{k^n}{\Gamma(n)} [-\ln \{1 - F(x)\}]^{n-1} [1 - F(x)]^{k-1} f(x), -\infty < x < \infty, n = 1, 2, \dots \quad (5)$$

for $n \geq 2$. In a similar manner we can define generalized lower (k) record values (GLRV's) as well. If we write $X_{L(n,k)}$ to denote the n th GLRV, then the pdf $f_{X_{L(n,k)}}(x)$ of $X_{L(n,k)}$ is given by [see, 28]

$$f_{X_{L(n,k)}}(x) = \frac{k^n}{\Gamma(n)} [-\ln \{F(x)\}]^{n-1} [F(x)]^{k-1} f(x), -\infty < x < \infty, n = 1, 2, \dots \quad (6)$$

Generalized (k) record values arise naturally in problems such as industrial stress testing, meteorological analysis, hydrology, sporting, stock markets, athletic events and seismology. Anderson et al. [5] have attributed some connection between record statistics and the strain released in quakes. Majumdar and Ziff [16] have enlisted the detailed involvement of record theory in its multiple applications in spin glasses, adaptive process, evolutionary models of a biological population. See also Sibani and Henrik [33] for some record dynamics arising in some physical systems. For more details on applications of record, values see, Arnold et al. [6], Nevzorov [20] and the references therein.

Of late several articles have been published on various information measures associated with record values. [7] studied some information properties of records based on Shannon entropy. Abbasnejad and Arghami [1] studied the Rényi entropy properties of records and compared the same information with that of the *iid* observations. Baratpour et al. [7], Ahmadi and Fashandi [2] and Paul and Thomas [23, 24, 26, 27] have obtained some characterization results based on Shannon, Rényi, Tsallis and Mathai-Haubold entropies of record values. Shannon information in k -records was studied by Madadi and Tata [15].

The rest of this paper is organized as follows. In section 2, we express the Sharma-Mittal entropy of n th generalized upper (k) record arising from an arbitrary distribution in terms of Sharma-Mittal entropy of n th generalized upper (k) record arising from a standard exponential distribution. Section 3 provides bounds for Sharma-Mittal entropy of generalized (k) records. Section 4 characterizes exponential distribution by maximizing Sharma-Mittal entropy of generalized (k) record values arising from a specified class of distributions. Section 5 contains expressions for some measures associated with Sharma-Mittal entropy on generalized (k) records and concomitants of generalized (k) records. In subsection 5.1, it is shown that the Sharma-Mittal divergence information between generalized (k) record value and the parent distribution is distribution-free. Section 5.2 contains the representation of Sharma-Mittal entropy of concomitants of generalized (k) record values arising from the FGM family of bivariate distributions. In section 5.3, we provide an expression for the residual Sharma-Mittal entropy of n th generalized upper (k) record arising from an arbitrary distribution in terms of the corresponding expressions for the n th generalized upper (k) record arising from a standard uniform distribution.

2. SHARMA-MITTAL ENTROPY OF GENERALIZED (K) RECORD VALUES

In this section, we describe some properties of Sharma-Mittal entropy of generalized(k)record values. In the following theorem, we express Sharma-Mittal entropy of n th generalized upper (k) record arising from an arbitrary distribution in terms of Sharma-Mittal entropy of n th generalized upper (k) record arising from standard exponential distribution. In the theorem and in the remaining part of this paper we use the notation $G(a, b)$ to denote the well known gamma

distribution with pdf

$$g_{a,b}(x) = \frac{a^b}{\Gamma(b)} e^{-ax} x^{b-1}, \quad a > 0, b > 0, x > 0.$$

Theorem 1. Let $\{X_i, i \geq 1\}$ be a sequence of iid continuous random variables from a distribution with cdf $F(x)$, pdf $f(x)$ and quantile function $F^{-1}(\cdot)$. Let $\{X_{U(n,k)}\}$ be the associated sequence of generalized upper (k) record values. Then the Sharma-Mittal entropy of $X_{U(n,k)}$ can be expressed as

$$H_{\alpha,\beta}(X_{U(n)}) = \frac{1}{1-\beta} \left\{ \left(\frac{k^{n\alpha} \Gamma((n-1)\alpha + 1)}{\{\Gamma(n)\}^\alpha [(k-1)\alpha + 1]^{(n-1)\alpha + 1}} \right. \right. \\ \left. \left. \times E_{g_{(k-1)\alpha+1, (n-1)\alpha+1}} \left[\left\{ f \left(F^{-1}(1 - e^{-U}) \right) \right\}^{\alpha-1} \right] \right)^{\frac{1-\beta}{1-\alpha}} - 1 \right\}, \quad (7)$$

where U is a random variable, with $G((k-1)\alpha + 1, (n-1)\alpha + 1)$ distribution.

Proof. The Sharma-Mittal entropy of n th generalized upper (k) record value is given by

$$H_{\alpha,\beta}(X_{U(n,k)}) = \frac{1}{1-\beta} \left\{ \left(\int_{-\infty}^{\infty} \left[\frac{k^n \{-\log(1 - F(x))\}^{n-1} [1 - F(x)]^{k-1}}{(n-1)!} f(x) \right]^\alpha dx \right)^{\frac{1-\beta}{1-\alpha}} - 1 \right\}.$$

On putting $u = -\log[1 - F(x)]$, $x = [F^{-1}(1 - e^{-u})]$ and $du = \frac{f(x)}{1-F(x)} dx$ we get

$$H_{\alpha,\beta}(X_{U(n,k)}) = \frac{1}{1-\beta} \left\{ \left(\int_0^\infty \frac{k^{n\alpha} e^{-u[(k-1)\alpha+1]} u^{(n-1)\alpha}}{[(n-1)!]^\alpha} \left\{ f \left(F^{-1}(1 - e^{-U}) \right) \right\}^{\alpha-1} du \right)^{\frac{1-\beta}{1-\alpha}} - 1 \right\} \\ = \frac{1}{1-\beta} \left\{ \left(\frac{k^{n\alpha} \Gamma((n-1)\alpha + 1)}{[(k-1)\alpha + 1]^{(n-1)\alpha} \{\Gamma(n)\}^\alpha} \int_0^\infty \frac{[(k-1)\alpha + 1]^{(n-1)\alpha}}{\Gamma((n-1)\alpha + 1)} \right. \right. \\ \left. \left. \times e^{-u[(k-1)\alpha+1]} u^{(n-1)\alpha} \left\{ f \left(F^{-1}(1 - e^{-U}) \right) \right\}^{\alpha-1} du \right)^{\frac{1-\beta}{1-\alpha}} - 1 \right\} \\ = \frac{1}{1-\beta} \left\{ \left(\frac{k^{n\alpha} \Gamma((n-1)\alpha + 1)}{[(k-1)\alpha + 1]^{(n-1)\alpha + 1} \{\Gamma(n)\}^\alpha} \right. \right. \\ \left. \left. \times E_{g_{(k-1)\alpha+1, (n-1)\alpha+1}} \left[\left\{ f \left(F^{-1}(1 - e^{-U}) \right) \right\}^{\alpha-1} \right] \right)^{\frac{1-\beta}{1-\alpha}} - 1 \right\}. \quad (8)$$

■

Now we state the following theorem without proof as the proof is just similar to the proof of theorem 1.

Theorem 2. Let $\{X_i, i \geq 1\}$ be a sequence of iid continuous random variables with common cdf $F(x)$, pdf $f(x)$ and quantile function $F^{-1}(\cdot)$. Let $\{X_{L(n,k)}\}$ be the associated sequence of generalized lower (k) record values. Then the Sharma-Mittal entropy of $X_{L(n,k)}$ can be expressed as

$$H_{\alpha,\beta}(X_{L(n,k)}) = \frac{1}{1-\beta} \left\{ \left(\frac{k^{n\alpha} \Gamma((n-1)\alpha + 1)}{[(k-1)\alpha + 1]^{(n-1)\alpha + 1} \{\Gamma(n)\}^\alpha} E_{g_{(k-1)\alpha+1, (n-1)\alpha+1}} \left[\left\{ f \left(F^{-1}(e^{-U}) \right) \right\}^{\alpha-1} \right] \right)^{\frac{1-\beta}{1-\alpha}} - 1 \right\}, \quad (9)$$

where U is a random variable with $G(1, (n-1)\alpha + 1)$ distribution.

The following is a corollary to theorem 1.

Corollary 1. Let $\{X_i, i \geq 1\}$ be a sequence of iid continuous random variables arising from standard exponential distribution. Let $\{X_{U(n,k)}^*\}$ be the associated sequence of generalized upper (k) record values. Then the Sharma-Mittal entropy of $X_{U(n,k)}$ can be expressed as

$$H_{\alpha,\beta}(X_{U(n,k)}^*) = \frac{1}{1-\beta} \left\{ \left(\frac{k^{n\alpha} \Gamma((n-1)\alpha + 1)}{\{\Gamma(n)\}^\alpha [k\alpha]^{(n-1)\alpha + 1}} \right)^{\frac{1-\beta}{1-\alpha}} - 1 \right\}. \quad (10)$$

The following theorem follows from theorems 1 and 2 as a consequence of corollary 1.

Theorem 3. Let $\{X_i, i \geq 1\}$ be a sequence of iid continuous random variables having a common cdf $F(x)$, pdf $f(x)$ and quantile function $F^{-1}(\cdot)$. Let $\{X_{U(n,k)}\}$ and $\{X_{L(n,k)}\}$ be the associated sequences of generalized upper and lower(k)record values respectively. Then the Sharma-Mittal entropy of $X_{U(n,k)}$ and $X_{L(n,k)}$ can be expressed as

$$H_{\alpha,\beta}(X_{U(n,k)}) = \left(H_{\alpha,\beta}(X_{U(n,k)}^*) + \frac{1}{1-\beta} \right) \left(\left[\frac{k\alpha}{(k-1)\alpha + 1} \right]^{(n-1)\alpha + 1} \times E_{g_{1,(n-1)\alpha + 1}} \left[\left\{ f \left(F^{-1}(1 - e^{-U}) \right) \right\}^{\alpha - 1} \right]^{\frac{1-\beta}{1-\alpha}} - \frac{1}{1-\beta} \right) \quad (11)$$

$$H_{\alpha,\beta}(X_{L(n,k)}) = \left(H_{\alpha,\beta}(X_{U(n,k)}^*) + \frac{1}{1-\beta} \right) \left(\left[\frac{k\alpha}{(k-1)\alpha + 1} \right]^{(n-1)\alpha + 1} \times E_{g_{1,(n-1)\alpha + 1}} \left[\left\{ f \left(F^{-1}(e^{-U}) \right) \right\}^{\alpha - 1} \right]^{\frac{1-\beta}{1-\alpha}} - \frac{1}{1-\beta} \right), \quad (12)$$

where $X_{U(n,k)}^*$ denotes the n th generalized upper (k) record value arising from the standard exponential distribution and U is a random variable, with $G((k-1)\alpha + 1, (n-1)\alpha + 1)$ distribution.

3. BOUNDS FOR SHARMA-MITTAL ENTROPY OF GENERALIZED (K) RECORD VALUES

Baratpour et al. [7] and [1] have obtained bounds for Shannon entropy of records and Rényi entropy of records respectively. In this section, we use the relation (7) for deriving some bounds on Sharma-Mittal entropy of generalized upper (k) record values.

Theorem 4. If X has pdf $f(x)$ and the Sharma-Mittal entropy $H_{\alpha,\beta}(X_{U(n,k)})$ of $X_{U(n,k)}$ arising from $f(x)$ is such that $H_{\alpha,\beta}(X_{U(n,k)}) < \infty$ then we have

(a) for all $\alpha > 1$ and $0 < \beta < 1$, $H_{\alpha,\beta}(X_{U(n,k)}) \leq \left(H_{\alpha,\beta}(X_{U(n,k)}^*) + \frac{1}{1-\beta} \right) \times \left(\left[\frac{k\alpha}{(k-1)\alpha + 1} \right]^{(n-1)\alpha + 1} B_n S_{\alpha,\beta}(f) \right)^{\frac{1-\beta}{1-\alpha}} - \frac{1}{1-\beta}$, and

(b) for $0 < \alpha < 1$ and $\beta > 1$, $H_{\alpha,\beta}(X_{U(n,k)}) \geq \left(H_{\alpha,\beta}(X_{U(n,k)}^*) + \frac{1}{1-\beta} \right) \times \left(\left[\frac{k\alpha}{(k-1)\alpha + 1} \right]^{(n-1)\alpha + 1} B_n S_{\alpha,\beta}(f) \right)^{\frac{1-\beta}{1-\alpha}} - \frac{1}{1-\beta}$, where,

(i) $X_{U(n,k)}^*$ denotes the n th generalized upper (k) record value arising from the standard exponential distribution

(ii) $B_n = \frac{e^{-((n-1)\alpha)\{(n-1)\alpha\}^{(n-1)\alpha}}}{\Gamma((n-1)\alpha + 1)}$ and

(iii) $S_\alpha(f) = \int_{-\infty}^{\infty} \lambda_F(x) \{f(x)\}^{\alpha-1} dx$, where $\lambda_F(x)$ is the hazard function of X .

Proof. The Sharma-Mittal entropy of n th generalized upper (k) record value is given by

$$H_{\alpha, \beta}(X_{U(n,k)}) = \left(H_{\alpha, \beta}(X_{U(n,k)}^*) + \frac{1}{1 - \beta} \right) \left(\left[\frac{k\alpha}{(k-1)\alpha + 1} \right]^{(n-1)\alpha+1} \right. \\ \left. \times E_{g_{(k-1)\alpha+1, (n-1)\alpha+1}} \left[\left\{ f \left(F^{-1}(1 - e^{-U}) \right) \right\}^{\alpha-1} \right]^{\frac{1-\beta}{1-\alpha}} - \frac{1}{1 - \beta} \right'$$

where $g_{(k-1)\alpha+1, (n-1)\alpha+1}$ is the pdf corresponding to the $G((k-1)\alpha + 1, (n-1)\alpha + 1)$ distribution. Since the mode of the distribution with pdf $g_{(k-1)\alpha+1, (n-1)\alpha+1}$ is $m_n = \frac{(n-1)\alpha}{(k-1)\alpha+1}$ we have

$$g_{(k-1)\alpha+1, (n-1)\alpha+1}(m_n) = \frac{e^{-(n-1)\alpha} [(n-1)\alpha]^{(n-1)\alpha}}{\Gamma((n-1)\alpha + 1)} = B_n.$$

Hence we have $g_{(k-1)\alpha+1, (n-1)\alpha+1}(u) \leq B_n$. Now for $\alpha > 1$ and $0 < \beta < 1$ the entropy is

$$H_{\alpha, \beta}(X_{U(n,k)}) = \left(H_{\alpha, \beta}(X_{U(n,k)}^*) + \frac{1}{1 - \beta} \right) \left(\left[\frac{k\alpha}{(k-1)\alpha + 1} \right]^{(n-1)\alpha+1} \right. \\ \left. \times \int_0^\infty g_{(k-1)\alpha+1, (n-1)\alpha+1}(u) \left\{ f \left(F^{-1}(1 - e^{-U}) \right) \right\}^{\alpha-1} du \right)^{\frac{1-\beta}{1-\alpha}} - \frac{1}{1 - \beta} \\ \leq \left(H_{\alpha, \beta}(X_{U(n,k)}^*) + \frac{1}{1 - \beta} \right) \left(\left[\frac{k\alpha}{(k-1)\alpha + 1} \right]^{(n-1)\alpha+1} B_n \right. \\ \left. \times \int_0^\infty \left\{ f \left(F^{-1}(1 - e^{-U}) \right) \right\}^{\alpha-1} du \right)^{\frac{1-\beta}{1-\alpha}} - \frac{1}{1 - \beta} \\ = \left(H_{\alpha, \beta}(X_{U(n,k)}^*) + \frac{1}{1 - \beta} \right) \left(\left[\frac{k\alpha}{(k-1)\alpha + 1} \right]^{(n-1)\alpha+1} B_n \right. \\ \left. \times \int_{-\infty}^\infty \lambda_F(y) \left\{ f(y) \right\}^{\alpha-1} dy \right)^{\frac{1-\beta}{1-\alpha}} - \frac{1}{1 - \beta} \\ = \left(H_{\alpha, \beta}(X_{U(n,k)}^*) + \frac{1}{1 - \beta} \right) \left(\left[\frac{k\alpha}{(k-1)\alpha + 1} \right]^{(n-1)\alpha+1} B_n S_\alpha(f) \right)^{\frac{1-\beta}{1-\alpha}} - \frac{1}{1 - \beta}.$$

For $0 < \alpha < 1$ and $\beta > 1$ the proof is similar. ■

4. CHARACTERIZATION PROPERTY BY THE SHARMA-MITTAL ENTROPY OF GENERALIZED (K) RECORD VALUES

Sometimes we may observe the uncertainty prevailing in the system under study as so large that we are curious to know the type of distribution which governs the system. That is, in such a system, we look for a distribution that is capable of possessing maximum entropy as suggested in Jaynes [12]. This section derives exponential distribution as the distribution that maximizes the Sharma-Mittal entropy of record values under some information constraints. Let C be a class of all distributions with cdf $F(x)$ over the support set \mathbb{R}^+ with $F(0) = 0$ such that

- (i) $\lambda_F(x, \theta) = a(\theta)b(x)$
- (ii) $b(x) \leq M$, where M is a positive real constant with $b(x) = B'(x)$ such that $b(x)$ and $a(\theta)$ are non-negative functions of x and θ respectively.

Now we prove the following theorem.

Theorem 5. Under the conditions described above Sharma-Mittal entropy $H_{\alpha, \beta}(X_{U(n,k)})$ arising from the distribution $F(x)$ is maximum in C , if and only if $F(x; \theta) = 1 - e^{-Ma(\theta)x}$.

Proof. Let $X_{U(n,k)}$ be the n th generalized upper (k) record value arising from the cdf $F(x; \theta) \in C$. Then by (7) we have

$$\begin{aligned}
 H_{\alpha, \beta}(X_{U(n,k)}) &= \left(H_{\alpha, \beta}(X_{U(n,k)}^*) + \frac{1}{1 - \beta} \right) \left(\left[\frac{k\alpha}{(k-1)\alpha + 1} \right]^{(n-1)\alpha + 1} \right. \\
 &\quad \times E_{g_{(k-1)\alpha + 1, (n-1)\alpha + 1}} \left[\left\{ f \left(F^{-1}(1 - e^{-U}) \right) \right\}^{\alpha - 1} \right] \left. \right)^{\frac{1-\beta}{1-\alpha}} - \frac{1}{1 - \beta} \\
 &= \left(H_{\alpha, \beta}(X_{U(n,k)}^*) + \frac{1}{1 - \beta} \right) \left(\left[\frac{k\alpha}{(k-1)\alpha + 1} \right]^{(n-1)\alpha + 1} \frac{[(k-1)\alpha + 1]^{(n-1)\alpha + 1}}{\Gamma((n-1)\alpha + 1)} \right. \\
 &\quad \times \int_0^\infty e^{-u[(k-1)\alpha + 1]} u^{(n-1)\alpha} \left\{ f \left(F^{-1}(1 - e^{-U}) \right) \right\}^{\alpha - 1} du \left. \right)^{\frac{1-\beta}{1-\alpha}} - \frac{1}{1 - \beta} \\
 &= \left(H_{\alpha, \beta}(X_{U(n,k)}^*) + \frac{1}{1 - \beta} \right) \left(\left[\frac{k\alpha}{(k-1)\alpha + 1} \right]^{(n-1)\alpha + 1} \frac{[(k-1)\alpha + 1]^{(n-1)\alpha + 1}}{\Gamma((n-1)\alpha + 1)} \right. \\
 &\quad \times \int_0^\infty e^{-u[(k-1)\alpha + 1]} u^{(n-1)\alpha} \left\{ a(\theta)b \left[B^{-1} \left\{ \frac{u}{a(\theta)} \right\} \right] e^{-a(\theta)B \left[B^{-1} \left\{ \frac{u}{a(\theta)} \right\} \right]} \right\}^{\alpha - 1} du \left. \right)^{\frac{1-\beta}{1-\alpha}} \\
 &\quad - \frac{1}{1 - \beta} \\
 &= \left(H_{\alpha, \beta}(X_{U(n,k)}^*) + \frac{1}{1 - \beta} \right) \left(\left[\frac{k\alpha}{(k-1)\alpha + 1} \right]^{(n-1)\alpha + 1} \frac{[(k-1)\alpha + 1]^{(n-1)\alpha + 1}}{\Gamma((n-1)\alpha + 1)} \right. \\
 &\quad \times \int_0^\infty e^{-uk\alpha} u^{(n-1)\alpha} [a(\theta)]^{\alpha - 1} b^{\alpha - 1} \left[B^{-1} \left\{ \frac{u}{a(\theta)} \right\} \right] du \left. \right)^{\frac{1-\beta}{1-\alpha}} - \frac{1}{1 - \beta}. \tag{13}
 \end{aligned}$$

Noting that $b(x) \leq M$ we have

$$\begin{aligned}
 H_{\alpha, \beta}(X_{U(n,k)}) &\leq \left(H_{\alpha, \beta}(X_{U(n,k)}^*) + \frac{1}{1 - \beta} \right) \left(\frac{[a(\theta)M]^{\alpha - 1} [k\alpha]^{(n-1)\alpha + 1}}{\Gamma((n-1)\alpha + 1)} \int_0^\infty e^{-uk\alpha} u^{(n-1)\alpha} du \right)^{\frac{1-\beta}{1-\alpha}} \\
 &\quad - \frac{1}{1 - \beta} \\
 &\leq \left(H_{\alpha, \beta}(X_{U(n,k)}^*) + \frac{1}{1 - \beta} \right) \left\{ [a(\theta)]^{\alpha - 1} M^{\alpha - 1} \right\}^{\frac{1-\beta}{1-\alpha}} - \frac{1}{1 - \beta}. \tag{14}
 \end{aligned}$$

Then clearly

$$\begin{aligned}
 H_{\alpha, \beta}(X_{U(n,k)}) &\leq \frac{1}{1 - \beta} \left(\frac{k^{n\alpha} \Gamma((n-1)\alpha + 1)}{\{\Gamma(n)\}^\alpha [k\alpha]^{(n-1)\alpha + 1}} \{[a(\theta)] M\}^{\alpha - 1} \right)^{\frac{1-\beta}{1-\alpha}} - \frac{1}{1 - \beta} \\
 &\leq \frac{1}{1 - \beta} \left\{ \left(\frac{k^{n\alpha} \Gamma((n-1)\alpha + 1)}{\{\Gamma(n)\}^\alpha [k\alpha]^{(n-1)\alpha + 1}} \{[a(\theta)] M\}^{\alpha - 1} \right)^{\frac{1-\beta}{1-\alpha}} - 1 \right\}. \tag{15}
 \end{aligned}$$

This proves the necessary part of the theorem.

On the other hand, suppose the n th generalized upper (k) record value arising from $F(x; \theta) = 1 - e^{-Ma(\theta)x}$ has maximum Sharma-Mittal entropy in class C. Then we have

$$H_{\alpha, \beta}(X_{U(n,k)}) = \frac{1}{1 - \beta} \left\{ \left(\frac{k^{n\alpha} \Gamma((n-1)\alpha + 1)}{\{\Gamma(n)\}^\alpha [k\alpha]^{(n-1)\alpha + 1}} \{[a(\theta)] M\}^{\alpha-1} \right)^{\frac{1-\beta}{1-\alpha}} - 1 \right\}. \quad (16)$$

It is clear to be note that the maximum entropy of n th generalized upper (k) record value ($X_{U(n,k)}$) arising from any arbitrary distribution under conditions (i) and (ii) will holds the inequality (15). As (16) is the expression on the right side of (15), it then follows that exponential distribution attains the maximum Sharma-Mittal entropy in the class C. ■

5. SOME PROPERTIES OF SHARMA-MITTAL ENTROPY ON GENERALIZED (K) RECORD VALUES

This section provides exact expressions for the Sharma-Mittal divergence measure on generalized (k) record values. Further in this section, we derive expressions for Sharma-Mittal entropy of concomitants of generalized upper and lower (k) record values arising from the Farlie-Gumbel-Morgenstern family. In the last part of this section, we derive an expression for residual Sharma-Mittal entropy of generalized upper (k) record values arising from an arbitrary distribution.

5.1. Sharma-Mittal Divergence Measure on Generalized(k)Record Values

Sharma and Mittal in 1977 introduced a two parameter divergent measure viz. Shrma-Mittal divergence measure denoted by $D_{\alpha, \beta}(f : g)$, between two distributions $f(x)$ and $g(x)$ and is defined by

$$D_{\alpha, \beta}(f : g) = \frac{1}{\beta - 1} \left\{ \left(\int_{-\infty}^{\infty} \left(\frac{f(x)}{g(x)} \right)^{\alpha-1} f(x) dx \right)^{\frac{1-\beta}{1-\alpha}} - 1 \right\}, \quad \forall \alpha > 0, \alpha \neq 1 \neq \beta. \quad (17)$$

[3] shown that, most of the widely used divergence measures such as Rényi, Tsallis, Bhattacharya and Kullback-Liabler divergences are special cases of Sharma-Mittal divergence measure.

In this section we study the Sharma-Mittal divergence between the probability distribution of n th generalized upper (k) record value and the parent distribution from which it arises.

Theorem 6. The Sharma-Mittal divergence between the n th generalized upper (k) record and the parent distribution is given by the following representation

$$D_{\alpha, \beta}(f_{U(n,k)}, f) = \frac{1}{\beta - 1} \left\{ \left(\frac{\Gamma((n-1)\alpha + 1)}{(\Gamma(n))^\alpha} \right)^{\frac{1-\beta}{1-\alpha}} - 1 \right\}. \quad (18)$$

Proof. The Sharma-Mittal information between the n th generalized upper (k) record and the parent distribution is given by

$$D_{\alpha, \beta}(f_{U(n,k)}, f) = \frac{1}{\beta - 1} \left\{ \left(\int_{-\infty}^{\infty} \frac{[k^n \{-\log[1 - F(x)]\}]^{n-1} [1 - F(x)]^{k-1}}{((n-1)!)^\alpha} f(x) dx \right)^{\frac{1-\beta}{1-\alpha}} - 1 \right\}.$$

On putting $u = -\log[1 - F(x)]$, we get $x = [F^{-1}(1 - e^{-u})]$, $du = \frac{f(x)}{1-F(x)} dx$ and hence we have

$$\begin{aligned}
 D_{\alpha, \beta}(f_{U(n,k)}, f) &= \frac{1}{\beta - 1} \left\{ \left(\int_0^\infty \frac{k^{n\alpha} e^{-u[(k-1)\alpha+1]} u^{(n-1)\alpha}}{((n-1)!)^\alpha} du \right)^{\frac{1-\beta}{1-\alpha}} - 1 \right\} \\
 &= \frac{1}{\beta - 1} \left\{ \left(\frac{k^{n\alpha} \Gamma((n-1)\alpha + 1)}{(\Gamma(n))^\alpha [(k-1)\alpha + 1]^{(n-1)\alpha+1}} \right)^{\frac{1-\beta}{1-\alpha}} - 1 \right\}.
 \end{aligned} \tag{19}$$

Hence the theorem. ■

Note 1. The Sharma-Mittal divergence between the n th upper record and the parent distribution can also be represented as

$$D_{\alpha, \beta}(f_{U(n)}, f) = \left\{ H_{\alpha, \beta}(X_{U(n,k)}^*) + \frac{1}{\beta - 1} \right\} \left[\frac{k\alpha}{(k-1)\alpha + 1} \right]^{\frac{((n-1)\alpha+1)(1-\beta)}{1-\alpha}} - \frac{1}{\beta - 1} \tag{20}$$

where, $X_{U(n,k)}^*$ denotes the n th generalized upper (k) record value arising from the standard exponential distribution.

Remark 1. The Sharma-Mittal information between the n th generalized upper (k) record value $X_{U(n,k)}$ and the parent distribution as given by 18 and 20 establishes that this information is a distribution free information measure.

5.2. Sharma-Mittal Entropy of Concomitants of Generalized (k) Records from Farlie-Gumbel-Morgenstern (FGM) family of Distributions

Let X and Y be two random variables with cdf's given by $F_X(x)$ and $F_Y(y)$ respectively with corresponding pdf's $f_X(x)$ and $f_Y(y)$ and jointly distributed with cdf $F(x, y)$ given by, [see, 13].

$$F(x, y) = F_X(x)F_Y(y) \{1 + \gamma(1 - F_X(x))(1 - F_Y(y))\}, \quad -1 \leq \gamma \leq 1, \tag{21}$$

where γ is known as association parameter. Then the family of distributions having the above form of cdf's is called Farlie-Gumbel-Morgenstern (FGM) family of distributions. It is obvious that (21) includes the case of independence as well when $\gamma = 0$. The joint pdf corresponding to the cdf defined in (21) is given by,

$$f(x, y) = f_X(x)f_Y(y) \{1 + \gamma(1 - 2F_X(x))(1 - 2F_Y(y))\}, \quad -1 \leq \gamma \leq 1. \tag{22}$$

Let $(X_1, Y_1), (X_2, Y_2), \dots, (X_n, Y_n)$ be two-dimensional random vectors with the common bivariate distribution function $F(x, y)$ as given in (21). If we construct the sequence of GURV's $\{X_{U(n,k)}\}$ from the marginal sequence $\{X_i\}$, then the Y value occurring in an ordered pair with X observations equal to $X_{U(n,k)}$ is called the concomitant of the n th generalized upper(k)record value. We write $Y_{U[n,k]}$ to denote concomitant of n th GURV $X_{U(n,k)}$. Similarly the concomitant of n th GLRV, $X_{L(n,k)}$ as well can be defined and we denote it by $Y_{L[n,k]}$. Then the pdf of $Y_{U[n,k]}$ is denoted by $f_{Y_{U[n,k]}}$ and is given by

$$f_{Y_{U[n,k]}}(y) = \int f_{Y|X}(y|x) f_{X_{U(n,k)}}(x) dx = f_Y(y) \{1 - \gamma_n(1 - 2F_Y(y))\}, \tag{23}$$

where $\gamma_n = \left(1 - 2 \left\{ \frac{k}{k+1} \right\}^n\right) \gamma$. Using (2) and (23) we can represent the Sharma-Mittal entropy of concomitant of n th generalized upper (k) record value as follows:

$$\begin{aligned}
 H_{\alpha, \beta}(Y_{U[n,k]}) &= \frac{1}{1 - \beta} \left\{ \left(\int_{-\infty}^\infty (f_Y(y) \{1 - \gamma_n(1 - 2F_Y(y))\})^\alpha dy \right)^{\frac{1-\beta}{1-\alpha}} - 1 \right\} \\
 &= \frac{1}{1 - \beta} \left\{ \left(\int_{-\infty}^\infty \{f_Y(y)\}^\alpha (\{1 - \gamma_n(1 - 2F_Y(y))\})^\alpha dy \right)^{\frac{1-\beta}{1-\alpha}} - 1 \right\}.
 \end{aligned}$$

On putting $F_Y(y) = u, y = F_y^{-1}(u)$ and $f_y(y)dy = du$, we get

$$\begin{aligned} H_{\alpha, \beta}(Y_{U[n,k]}) &= \frac{1}{1-\beta} \left\{ \left(\int_0^1 \{f_Y(F_y^{-1}(u))\}^{\alpha-1} \{1 - \gamma_n(1-2u)\}^\alpha du \right)^{\frac{1-\beta}{1-\alpha}} - 1 \right\} \\ &= \frac{1}{1-\beta} \left\{ \left(E_U \left[\{f_Y(F_y^{-1}(U))\}^{\alpha-1} \{1 - \gamma_n(1-2U)\}^\alpha \right] \right)^{\frac{1-\beta}{1-\alpha}} - 1 \right\}, \end{aligned}$$

where U is a uniformly distributed random variable over $(0,1)$. Similarly the Sharma-Mittal entropy of concomitant of n th generalized lower(k)record can be represented by

$$H_{\alpha, \beta}(Y_{L[n,k]}) = \frac{1}{1-\beta} \left\{ \left(E_U \left[\{f_Y(F_y^{-1}(1-U))\}^{\alpha-1} \{1 + \gamma_n(1-2U)\}^\alpha \right] \right)^{\frac{1-\beta}{1-\alpha}} - 1 \right\}.$$

5.3. The Residual Sharma-Mittal Entropy of Generalized (k) Record Values

Suppose X represents the lifetime of a unit with pdf $f(\cdot)$, then $H_{\alpha, \beta}(X)$ as defined in (2) is useful for measuring the associated uncertainty. Suppose a component is known to have survived up to an age t . In that case, information about the remaining lifetime is an important characteristic required for data analysis arising from areas such as reliability, survival studies, economics, business etc. However, for the analysis of uncertainty about the remaining life time of the unit, we will consider residual Sharma-Mittal entropy and is defined by

$$H_{\alpha, \beta}(X;t) = \frac{1}{1-\beta} \left\{ \left(\int_t^\infty \left\{ \frac{f(x)}{\bar{F}(t)} \right\}^\alpha dx \right)^{\frac{1-\beta}{1-\alpha}} - 1 \right\}, \tag{24}$$

where $H_{\alpha, \beta}(X;t)$ measures the expected uncertainty contained in the conditional density of $X - t$ given $X > t$ and $\bar{F}(t) = 1 - F(t)$. In this section we derive a closed form representation for the residual Sharma-Mittal entropy of record values in terms of residual Sharma-Mittal entropy of uniform distribution over $[0,1]$. The survival function of the n th generalized(k)upper record, denoted by $\bar{F}_{X_{U(n,k)}}(x)$, is given by

$$\bar{F}_{X_{U(n,k)}}(x) = \sum_{j=1}^n \frac{[-k \log \bar{F}(x)]^j}{j!} \bar{F}(x)^k = \frac{\Gamma(n+1; -k \log \bar{F}(x))}{\Gamma(n+1)}, \tag{25}$$

where $\Gamma(a; x)$ denotes the incomplete Gamma function and is defined by

$$\Gamma(a; x) = \int_x^\infty e^{-u} u^{a-1} du, \quad a, x > 0.$$

Lemma 1. Let $Z_{U(n,k)}$ denote the n th generalized upper (k) record value from a sequence of observations from $U(0,1)$. Then

$$H_{\alpha, \beta}(Z_{U(n,k)}; t) = \frac{1}{1-\beta} \left\{ \left(\frac{k^{n\alpha} \Gamma((n-1)\alpha + 1; -[(k-1)\alpha + 1] \log(1-t))}{[(k-1)\alpha + 1]^{(n-1)\alpha + 1} \{\Gamma(n; -k \log(1-t))\}^\alpha} \right)^{\frac{1-\beta}{1-\alpha}} - 1 \right\}. \tag{26}$$

Proof. By considering (5), (24) and (25), the residual Sharma-Mittal entropy of $Z_{U(n,k)}$ is given by

$$H_{\alpha, \beta}(Z_{U(n,k)}; t) = \frac{1}{1-\beta} \left\{ \left(\int_t^\infty \frac{k^\alpha [-k \log(1-x)]^{(n-1)\alpha} [1-x]^{(k-1)\alpha}}{\{\Gamma(n; -k \log(1-t))\}^\alpha} dx \right)^{\frac{1-\beta}{1-\alpha}} - 1 \right\}.$$

On putting $-k \log(1 - x) = u$, $x = 1 - e^{-\frac{u}{k}}$ and $kdx = e^{-\frac{u}{k}} du$.

$$H_{\alpha, \beta}(Z_{U(n,k)}; t) = \frac{1}{1 - \beta} \left\{ \left(k^{\alpha-1} \int_{-k \log(1-t)}^{\infty} \frac{u^{(n-1)\alpha} e^{-\frac{u}{k}[(k-1)\alpha+1]}}{\{\Gamma(n; -k \log(1-t))\}^\alpha} du \right)^{\frac{1-\beta}{1-\alpha}} - 1 \right\}.$$

Now we consider the transformation $\frac{u}{k}[(k-1)(2-\alpha)+1] = v$, $u = \frac{vk}{(k-1)(2-\alpha)+1}$ and $du = \frac{k}{(k-1)(2-\alpha)+1} dv$.

$$\begin{aligned} H_{\alpha, \beta}(Z_{U(n,k)}; t) &= \frac{1}{1 - \beta} \left\{ \left(\int_{-[(k-1)(2-\alpha)+1] \log(1-t)}^{\infty} \frac{k^{n\alpha}}{[(k-1)\alpha+1]^{(n-1)\alpha+1}} \right. \right. \\ &\quad \left. \left. \times \frac{u^{(n-1)\alpha} e^{-v}}{\{\Gamma(n; -k \log(1-t))\}^\alpha} dv \right)^{\frac{1-\beta}{1-\alpha}} - 1 \right\} \\ &= \frac{1}{1 - \beta} \left\{ \left(\frac{k^{n\alpha} \Gamma((n-1)\alpha+1; -[(k-1)\alpha+1] \log(1-t))}{[(k-1)\alpha+1]^{(n-1)\alpha+1} \{\Gamma(n; -k \log(1-t))\}^\alpha} \right)^{\frac{1-\beta}{1-\alpha}} - 1 \right\}. \end{aligned} \tag{27}$$

Hence the lemma. ■

Theorem 7. The residual Sharma-Mittal entropy of $X_{U(n,k)}$ arising from an arbitrary distribution can be written in terms of the residual Sharma-Mittal entropy of $Z_{U(n,k)}$ as follows

$$H_{\alpha, \beta}(X_{U(n,k)}; t) = \left\{ H_{\alpha, \beta}(Z_{U(n,k)}; F(t)) + \frac{1}{1 - \beta} \right\} \left(E_V \left[\left\{ f \left(F^{-1} \left(1 - e^{-\frac{v}{(k-1)(2-\alpha)+1}} \right) \right) \right\}^{\alpha-1} \right] \right)^{\frac{1-\beta}{1-\alpha}} - \frac{1}{1 - \beta}. \tag{28}$$

where $V \sim \Gamma_{-[(k-1)\alpha+1] \log(1-F(t))}((n-1)\alpha+1; 1)$.

Proof. The residual Sharma-Mittal entropy of $X_{U(n)}$ is given by

$$H_{\alpha, \beta}(X_{U(n,k)}; t) = \frac{1}{1 - \beta} \left\{ \left(\int_t^\infty \frac{k^\alpha [-k \log(1 - F(x))]^{(n-1)\alpha} [1 - F(x)]^{(k-1)\alpha}}{\{\Gamma(n; -k \log(1 - F(t)))\}^\alpha} dx \right)^{\frac{1-\beta}{1-\alpha}} - 1 \right\}.$$

On putting $u = -k \log[1 - F(x)]$, $x = [F^{-1}(1 - e^{-\frac{u}{k}})]$ and $kdx = e^{-\frac{u}{k}} du$ we get

$$\begin{aligned} H_{\alpha, \beta}(X_{U(n,k)}; t) &= \frac{1}{1 - \beta} \left\{ \left(\int_{-k \log(1-F(t))}^{\infty} \frac{k^{\alpha-1} u^{(n-1)\alpha} e^{-\frac{u}{k}[(k-1)\alpha+1]}}{\{\Gamma(n; -k \log(1 - F(t)))\}^\alpha} \right. \right. \\ &\quad \left. \left. \{f(F^{-1}(1 - e^{-\frac{u}{k}}))\}^{\alpha-1} du \right)^{\frac{1-\beta}{1-\alpha}} - 1 \right\} \end{aligned}$$

Now we consider the transformation $\frac{u}{k} [(k-1)(2-\alpha) + 1] = v$, $u = \frac{vk}{(k-1)(2-\alpha)+1}$ and $du = \frac{k}{(k-1)(2-\alpha)+1} dv$.

$$\begin{aligned}
 H_{\alpha, \beta}(X_{U(n,k)}; t) &= \frac{1}{1-\beta} \left\{ \left(\int_{-[(k-1)\alpha+1]\log(1-F(t))}^{\infty} \frac{k^{n\alpha}}{[(k-1)\alpha+1]^{(n-1)\alpha+1}} \right. \right. \\
 &\quad \left. \left. \times \frac{e^{-v} v^{(n-1)\alpha}}{\{\Gamma(n; -k \log(1-F(t)))\}^\alpha} \left\{ f \left(F^{-1} \left(1 - e^{-\frac{v}{(k-1)(2-\alpha)+1}} \right) \right) \right\}^{\alpha-1} dv \right)^{\frac{1-\beta}{1-\alpha}} - 1 \right\} \\
 &= \frac{1}{1-\beta} \left\{ \left(\frac{k^{n\alpha} \Gamma((n-1)\alpha+1; -[(k-1)\alpha+1]\log(1-F(t)))}{[(k-1)\alpha+1]^{(n-1)\alpha+1} \{\Gamma(n; -k \log(1-F(t)))\}^\alpha} \right. \right. \\
 &\quad \left. \left. \times E_V \left\{ f \left(F^{-1} \left(1 - e^{-\frac{v}{(k-1)(2-\alpha)+1}} \right) \right) \right\}^{\alpha-1} \right)^{\frac{1-\beta}{1-\alpha}} - 1 \right\} \\
 &= \left\{ H_{\alpha, \beta}(Z_{U(n,k)}; F(t)) + \frac{1}{1-\beta} \right\} \left(E_V \left[\left\{ f \left(F^{-1} \left(1 - e^{-\frac{v}{(k-1)(2-\alpha)+1}} \right) \right) \right\}^{\alpha-1} \right] \right)^{\frac{1-\beta}{1-\alpha}} \\
 &\quad - \frac{1}{1-\beta}. \tag{29}
 \end{aligned}$$

Hence the theorem. ■

REFERENCES

- [1] Abbasnejad, M. and Arghami, N. R. (2011). Rényi entropy properties of records. *Journal of Statistical Planning and Inference*, 141:2312–2320.
- [2] Ahmadi, J. and Fashandi, M. (2012). Characterizations of symmetric distributions based on Rényi entropy. *Statistics & Probability Letters*, 82:798–804.
- [3] Aktürk, E., Bağcı, G., and Sever, R. (2007). Is Sharma-Mittal entropy really a step beyond Tsallis and Rényi entropies? *arXiv preprint cond-mat/0703277*.
- [4] Aktürk, O. Ü., Aktürk, E., and Tomak, M. (2008). Can Sobolev inequality be written for Sharma-Mittal entropy? *International Journal of Theoretical Physics*, 47:3310–3320.
- [5] Anderson, P. E., Jensen, H. P., Oliveira, L. P., and Sibani, P. (2004). Evolution in complex systems. *COMPLEXITY*, 10:49–56.
- [6] Arnold, B. C., Balakrishnan, N., and Nagaraja, H. N. (1998). *Records*. John Wiley and Sons, New York.
- [7] Baratpour, S., Ahmadi, J., and Arghami, N. R. (2007). Entropy properties of record statistics. *Statistical Papers*, 48:197–213.
- [8] Chandler, K. N. (1952). The distribution and frequency of record values. *Journal of the Royal Statistical Society. Series B*, 14:220–228.
- [9] Dziubdziela, W. and Kopocinski, B. (1976). Limiting properties of the k th record values. *Zastos. Mat.*, 15:187–190.
- [10] Frank, T. and Daffertshofer, A. (2000). Exact time-dependent solutions of the Rényi Fokker-Planck equation and the Fokker-Planck equations related to the entropies proposed by Sharma and Mittal. *Physica A: Statistical Mechanics and its Applications*, 285:351–366.
- [11] Glick, N. (1978). Breaking records and breaking boards. *American Mathematical Monthly*, 85:2–26.
- [12] Jaynes, E. T. (1957). Information theory and statistical mechanics II. *Physical review*, 108:171.
- [13] Johnson, N. L., Kotz, S., and Balakrishnan, N. (2002). *Continuous Multivariate Distributions, Models and Applications*, volume 1. John Wiley & Sons, New York.
- [14] Kosztołowicz, T. and Lewandowska, K. D. (2012). First-passage time for subdiffusion: The nonadditive entropy approach versus the fractional model. *Physical Review E*, 86:021108.

- [15] Madadi, M. and Tata, M. (2014). Shannon information in k-records. *Communications in Statistics-Theory and Methods*, 43:3286–3301.
- [16] Majumdar, S. N. and Ziff, R. M. (2008). Universal record statistics of random walks and Lévy flights. *Physical review letters*, 101:050601.
- [17] Masi, M. (2005). A step beyond Tsallis and Rényi entropies. *Physics Letters A*, 338:217–224.
- [18] Minimol, S. and Thomas, P. Y. (2013). On some properties of Makeham distribution using generalized record values and its characterizations. *Brazilian Journal of Probability and Statistics*, 27:487–501.
- [19] Minimol, S. and Thomas, P. Y. (2014). On characterization of Gompertz distribution by generalized record values. *Journal of Statistical Theory and Applications*, 13:38–45.
- [20] Nevzorov, V. B. (2001). *Records: Mathematical Theory. Translation of Mathematical Monographs, vol. 194*. American Mathematical Society, Providence, RI, USA.
- [21] Nielsen, F. and Nock, R. (2012). A closed-form expression for the Sharma-Mittal entropy of exponential families. *Journal of Physics A: Mathematical and Theoretical*, 45:1–8.
- [22] Paul, J. (2014). On generalized lower(k)record values arising from power function distribution. *Journal of the Kerala Statistical Association*, 25:49–64.
- [23] Paul, J. and Thomas, P. Y. (2013). On a property of generalized record values arising from exponential distribution. *Indian Association for Productivity, Quality and Reliability Transactions*, 38:19–27.
- [24] Paul, J. and Thomas, P. Y. (2014). On Tsallis entropy of generalized(k)record values. In *Proceedings of seminar on Process Capability Studies With Special Emphasis on Computational Techniques & Recent Trends in Statistics*, pages 1–14. Nirmala Academic and Research Publications (NARP).
- [25] Paul, J. and Thomas, P. Y. (2015a). On generalized upper(k)record values from Weibull distribution. *Statistica*, 75:313–330.
- [26] Paul, J. and Thomas, P. Y. (2015b). Tsallis entropy properties of record values. *Calcutta Statistical Association Bulletin*, 67:47–60.
- [27] Paul, J. and Thomas, P. Y. (2019). On some properties of mathai–haubold entropy of record values. *Journal of the Indian Society for Probability and Statistics*, 20(1):31–49.
- [28] Pawlas, P. and Szyndal, D. (1998). Relations for single and product moment of k – th record values from exponential and gumbel distribution. *J. Appl. Statist. Sci*, 7:53–62.
- [29] Rényi, A. (1961). On measures of entropy and information. In *Proceedings of Fourth Berkeley Symposium on Mathematics, Statistics and Probability 1960*, pages 547–561, University of California Press, Berkeley.
- [30] Shannon, C. E. (1948). A mathematical theory of communication. *Bell System Technical Journal*, 27:379–423.
- [31] Sharma, B. D. and Mittal, D. P. (1975). New nonadditive measures of entropy for discrete probability distributions. *J. Math. Sci*, 10:28–40.
- [32] Sharma, B. D. and Mittal, D. P. (1977). New non-additive measures of relative information. *Journal of Combinatorics Information & System Sciences*, 2:122–132.
- [33] Sibani, P. and Henrik, J. J. (2009). Record statistics and dynamics. In Meyers, R. A., editor, *Encyclopaedia of Complexity and Systems Science*, pages 7583–7591. Springer Science+Business Media, LLC., New York, USA.
- [34] Thomas, P. Y. and Paul, J. (2014). On generalized lower (k) record values from the Fréchet distribution. *Journal of the Japan Statistical Society*, 44:157–178.
- [35] Thomas, P. Y. and Paul, J. (2019). On diagnostic devices for proposing half-logistic and inverse half-logistic models using generalized (k) record values. *Communications in Statistics-Theory and Methods*, 48(5):1073–1091.
- [36] Tsallis, C. (1988). Possible generalization of Boltzmann-Gibbs statistics. *Journal of statistical physics*, 52:479–487.
- [37] Zarezadeh, S. and Asadi, M. (2010). Results on residual Rényi entropy of order statistics and record values. *Information Sciences*, 180:4195–4206.

The New Mixed Erlang Distribution: A Flexible Distribution for Modeling Lifetime Data

THERRAR KADRI¹, SOUAD KADRI², SEIFEDINE KADRY^{3*}, AND KHALED SMAILI⁴

•

Department of Education, Lebanese University, Beirut, Lebanon¹

Department of Mathematics and Physics, Lebanese International University, Khyara, Lebanon^{1,2}

Department of Applied Data Science, Noroff University College, Norway³

Department of Applied Mathematics, Faculty of Sciences, Lebanese University, Zahle, Lebanon⁴

*Corresponding author

Abstract

We introduce a new mixed distribution of the Erlang distribution that is generated from the convolution of the Extension Exponential distribution denoted by the Mixed Erlang distribution (ME). We derive an exact closed expression of the probability density function which is used to obtain closed expressions of the cumulative function, reliability function, hazard function, moment generating function and k th moment. The method of maximum likelihood and method of moments is used for estimating the model parameters. Two applications to real data sets are given to illustrate the potentiality of this distribution.

Keywords: Erlang Distribution, Extension Exponential Distribution, Probability Density Function, Maximum likelihood estimation, Moments, Akaike Information Criterion

1. INTRODUCTION

Numerous classical distributions have been extensively used over the past decades for modeling data in many applied areas such as lifetime analysis, finance and insurance, as the Exponential distribution and its alternatives the Erlang and Gamma distribution, see [1] and [2]. There is a clear need for extended forms of these distributions. In recent statistical literature modified extensions of the Exponential distributions have been proposed to give more flexibility to model real data. For example, Gupta and Kundu [6] introduced an extension of the Exponential distribution typically called the generalized exponential (GE) distribution and Mudholkar et al. [9] introduced the exponentiated Weibull (EW) distribution as another extension. Gómez et al. [5] introduced a new extension of the Exponential distribution denoted as the Extended Exponential (EE) distribution of two positive parameters.

On the other hand, the sum of independent random variables, the convolution of random variables, also plays a significant role in modeling many events in most domains of science, as communications, computer science, and teletraffic engineering (Trivedi [12]; Jasiulewicz and Kordecki [7]), Markov process, reliability and performance evaluation (Kadri et al. [8]; Smaili et al. [10]). A comprehensive study of these distributions is needed for modeling and the importance of providing closed and exact forms of probability density function (PDF), cumulative distribution function (CDF), reliability and hazard functions, moment generating function (MGF), and k^{th} moments...

The main aim of this paper is to study a new distribution generated from the convolution of the Extension Exponential distribution which is observed to have the form of a mixed distribution of the Erlang distribution. We denote this distribution by the Mixed Erlang Distribution (ME). We provide a comprehensive account of the mathematical properties of this new distribution

by deriving closed and exact forms of PDF, CDF, reliability and hazard functions, MGF, and k^{th} moments. Moreover, we propose that our distribution is quite flexible, evidence by its closed and simple expressions. Also, this distribution can be used quite effectively in analyzing positive data in place of proposed distribution in the literature, which indicates that the ME distribution is a serious competitor to the others. Thus, we perform a parameter estimation of the model by the method of maximum likelihood and the method of moment. Next, we fit the new distribution to two real data sets to examine the performance of the new model and compare it to lately new distributions proposed in the statistical literature.

2. SOME PRELIMINARIES

2.1. Erlang Distribution

Erlang distribution is a two-parameter continuous probability distribution with shape integer parameter n and scale parameter $\alpha > 0$. It is considered as the sum of n independent identical Exponential distributions of parameter α , so for $n = 1$ the Erlang distribution is simplified to the Exponential distribution. Erlang distribution like Exponential is widely used in life time analysis, see [4].

Let $Y \sim Erl(n, \alpha)$. The PDF of Y is given as:

$$f_Y(t) = \frac{(\alpha t)^{n-1} \alpha e^{-\alpha t}}{(n-1)!}, t > 0 \tag{1}$$

and CDF of Y is

$$F_Y(t) = 1 - \frac{\Gamma(n, \alpha t)}{(n-1)!} \tag{2}$$

where $\Gamma(\cdot, \cdot)$ is the incomplete Gamma function. Also the MGF of Y is

$$\phi_Y(t) = \left(\frac{\alpha}{\alpha - t} \right)^n, t < \alpha \tag{3}$$

and the moment of order k of Y is

$$E[Y^k] = \frac{\Gamma(n+k)}{\alpha^k \Gamma(n)} \tag{4}$$

2.2. Extension Exponential Distribution

Gómez et al. [5], introduced a new extension of the Exponential distribution denoted as the Extended Exponential (EE) distribution of two positive parameters, denoted by $EE(\alpha, \beta)$. They characterized this distribution having $X \sim EE(\alpha, \beta)$ with PDF

$$f_X(t) = \frac{\alpha^2(1 + \beta t)e^{-\alpha t}}{\alpha + \beta} \quad \alpha, \beta, t > 0$$

where α is a scale parameter and β is a shape parameter.

The EE distribution is considered as a mixed distribution of the Exponential distribution, $E(\alpha)$, and Erlang distribution $Erl(2, \alpha)$, i.e.

$$f_X(t) = \frac{\alpha}{\alpha + \beta} f_{E(\alpha)}(t) + \frac{\beta}{\alpha + \beta} f_{Erl(2, \alpha)}(t) \tag{5}$$

For further use, we have the Laplace transform of $f_X(t)$ as

$$\mathcal{L}\{f_X(t)\} = \frac{\alpha^2(t + \alpha + \beta)}{(\alpha + \beta)(t + \alpha)^2} \tag{6}$$

Other properties of EE distribution can be found in [5].

3. MIXED ERLANG DISTRIBUTION

Let $X_j, j = 1, 2, \dots, n$ be n identical independent (iid) random variables that follow Extension Exponential distribution i.e. $X_j \sim EE(\alpha, \beta)$ and let $S_n = \sum_{j=1}^n X_j$. We denote $S_n \sim ME(\alpha, \beta, n)$ to be the Mixed Erlang distribution for $\alpha > 0, \beta > 0$ and $n \in \mathbb{N}^*$. This name is derived from the obtained expressions of this distribution in this section, which has the form of a mixed Erlang (ME) distribution. We start by deriving the PDF of this new distribution in an exact closed form. The obtained simple form will help us to derive the other mathematical functions to characterize the ME distribution.

3.1. PDF of the ME distribution

It is known that the sum of independent distributions is the convolution random variable and its PDF can be determined by the n convolution of the PDF of the summands X_j , which is an approach used. Here we take the advantage of Laplace transform over convolution to obtain our expression.

Theorem 1. Let $S_n \sim ME(\alpha, \beta, n), \alpha > 0, \beta > 0$ and $n \in \mathbb{N}^*$. Then the PDF of S_n is given by

$$f_{S_n}(t) = \sum_{i=0}^n A_i f_{Y_i}(t)$$

where

$$A_i = \frac{\binom{n}{i} \alpha^{n-i} \beta^i}{(\alpha + \beta)^n} \text{ and } Y_i \sim \text{Erl}(n + i, \alpha) \tag{7}$$

Proof. Let $X_j \sim EE(\alpha, \beta), j = 1, 2, \dots, n$ be n iid distributions and let $S_n = \sum_{j=1}^n X_j \sim ME(\alpha, \beta, n)$.

We have $f_{S_n}(t)$ is the convolution of the PDF of X_j . Thus the Laplace transform of $f_{S_n}(t)$ is the product of identical distribution of EE and we get

$$\mathcal{L}\{f_{S_n}(t)\} = [\mathcal{L}\{f_{X_i}(t)\}]^n$$

From Equation (6) $\mathcal{L}\{f_{X_i}(t)\} = \frac{\alpha^2(\alpha + \beta + t)}{(\alpha + \beta)(t + \alpha)^2}$. We get

$$\mathcal{L}\{f_{S_n}(t)\} = \frac{\alpha^{2n}(\alpha + \beta + t)^n}{(\alpha + \beta)^n(t + \alpha)^{2n}}$$

and

$$\begin{aligned} f_{S_n}(t) &= \mathcal{L}^{-1} \left\{ \frac{\alpha^{2n}(\alpha + \beta + t)^n}{(\alpha + \beta)^n(t + \alpha)^{2n}} \right\} = \frac{\alpha^{2n}}{(\alpha + \beta)^n} \mathcal{L}^{-1} \left\{ \frac{(\alpha + \beta + t)^n}{(t + \alpha)^{2n}} \right\} \\ &= \frac{\alpha^{2n} e^{-\alpha t}}{(\alpha + \beta)^n} \mathcal{L}^{-1} \left\{ \frac{(\beta + t)^n}{t^{2n}} \right\} \end{aligned}$$

However, $(\beta + t)^n = \sum_{i=0}^n \binom{n}{i} \beta^i t^{n-i}$, then $\frac{(\beta + t)^n}{t^{2n}} = \sum_{i=0}^n \binom{n}{i} \beta^i t^{-n-i}$. Also $\mathcal{L}^{-1}\{t^{-n-i}\} = \frac{t^{i+n-1}}{(i+n-1)!}$.

Thus we conclude that

$$f_{S_n}(t) = \frac{\alpha^{2n} e^{-\alpha t}}{(\alpha + \beta)^n} \sum_{i=0}^n \binom{n}{i} \beta^i \frac{t^{i+n-1}}{(i+n-1)!}. \text{ Next, we rearrange the sum to pull out the closest PDF which}$$

is a Erlang distribution of the form $\frac{\alpha^{n+i} t^{(n+i-1)} e^{-\alpha t}}{(n+i-1)!} = f_{Y_i}(t)$, where $Y_i \sim \text{Erl}(n + i, \alpha)$. So we can rewrite

$$\begin{aligned} f_{S_n}(t) &= \sum_{i=0}^n \frac{\binom{n}{i} \beta^i \alpha^{n-i}}{(\alpha + \beta)^n} \times \frac{\alpha^{n+i} t^{(n+i-1)} e^{-\alpha t}}{(n+i-1)!} \\ &= \sum_{i=0}^n A_i f_{Y_i}(t) \end{aligned}$$

where $A_i = \frac{\binom{n}{i} \alpha^{n-i} \beta^i}{(\alpha + \beta)^n}$.

In the following, we give another proof of the previous theorem by using the approach of convolution of PDF of independent random variables instead of the Laplace inverse approach.

Proof. [Alternate Proof] Let $X_j \sim EE(\alpha, \beta)$, $j = 1, 2, \dots, n$ and S_n is the convolution random variable of EE. Then

$$f_{S_n}(t) = (f_{X_1} * f_{X_2} * \dots * f_{X_n})(t) \tag{8}$$

However, from Equation (5), the PDF of EE can be expressed as

$$f_{X_j}(t) = \frac{\alpha}{\alpha + \beta} f_{E(\alpha)}(t) + \frac{\beta}{\alpha + \beta} f_{Erl(2, \alpha)}(t)$$

Substitute $f_{X_j}(t)$ in 8 to obtain

$$f_{S_n}(t) = \overset{n}{\otimes} \left(\frac{1}{\alpha + \beta} (\alpha f_{E(\alpha)} + \beta f_{Erl(2, \alpha)}) \right) (t)$$

where $\overset{n}{\otimes}(g)$ means that the expression is convoluted n times by itself. Furthermore, convolution is associative with scalar multiplication, thus

$$f_{S_n}(t) = \frac{1}{(\alpha + \beta)^n} \overset{n}{\otimes} (\alpha f_{E(\alpha)} + \beta f_{Erl(2, \alpha)}) (t)$$

Now, using the generalized binomial expansion over the convolution operation, we obtain

$$\begin{aligned} f_{S_n}(t) &= \frac{1}{(\alpha + \beta)^n} \sum_{i=0}^n \binom{n}{i} \overset{n-i}{\otimes} \alpha f_{E(\alpha)}(t) * \overset{i}{\otimes} \beta f_{Erl(2, \alpha)}(t) \\ &= \frac{1}{(\alpha + \beta)^n} \sum_{i=0}^n \binom{n}{i} \alpha^{n-i} \beta^i \left(\overset{n-i}{\otimes} f_{E(\alpha)} * \overset{i}{\otimes} f_{Erl(2, \alpha)} \right) (t) \end{aligned}$$

Also the convolution of $n - i$ identical Exponential distribution is the Erlang distribution $Erl(n - i, \alpha)$ or $\overset{n-i}{\otimes} f_{E(\alpha)} = f_{Erl(n-i, \alpha)}$ and the convolution of i Erlang distributions $Erl(2, \alpha)$ is the Erlang distribution $Erl(2i, \alpha)$ or $\overset{i}{\otimes} f_{Erl(2, \alpha)} = f_{Erl(2i, \alpha)}$. Thus, we get

$$f_{S_n}(t) = \frac{1}{(\alpha + \beta)^n} \sum_{i=0}^n \binom{n}{i} \alpha^{n-i} \beta^i (f_{Erl(n-i, \alpha)} * f_{Erl(2i, \alpha)}) (t).$$

On the other hand $Erl(n - i, \alpha) * Erl(2i, \alpha) = Erl(n + i, \alpha)$ and thus

$$\begin{aligned} f_{S_n}(t) &= \sum_{i=0}^n \frac{\binom{n}{i} \alpha^{n-i} \beta^i}{(\alpha + \beta)^n} f_{Erl(n+i, \alpha)}(t) \\ &= \sum_{i=0}^n A_i f_{Y_i}(t) \end{aligned}$$

where $A_i = \frac{\binom{n}{i} \alpha^{n-i} \beta^i}{(\alpha + \beta)^n}$ and $Y_i \sim Erl(n + i, \alpha)$.

In the following corollary, we give the PDF of ME in one expression, related to regularized confluent hypergeometric function.

Corollary 1. Let $S_n \sim ME(\alpha, \beta, n)$, $\alpha > 0$, $\beta > 0$ and $n \in \mathbb{N}^*$. Then the PDF of S_n is given by

$$f_{S_n}(t) = \frac{\alpha^{2n} t^{n-1} e^{-\alpha t}}{(\alpha + \beta)^n} {}_1\tilde{F}_1(-n; n, -t\beta)$$

where ${}_1\tilde{F}_1(a; b; x)$ is the regularized confluent hypergeometric function.

Proof. From Theorem 1 we have $f_{S_n}(t) = \sum_{i=0}^n A_i f_{Y_i}(t)$ with $A_i = \frac{\binom{n}{i} \alpha^{n-i} \beta^i}{(\alpha + \beta)^n}$ and $Y_i \sim \text{Erl}(n + i, \alpha)$.

However, the PDF of Y_i from Equation (1) is given by $f_{Y_i}(t) = \frac{(\alpha t)^{n+i-1} \alpha e^{-\alpha t}}{(n+i-1)!} I_{(0,\infty)}(t)$. Thus

$$\begin{aligned} f_{S_n}(t) &= \sum_{i=0}^n \frac{\binom{n}{i} \alpha^{n-i} \beta^i}{(\alpha + \beta)^n} \times \frac{(\alpha t)^{n+i-1} \alpha e^{-\alpha t}}{(n+i-1)!} \\ &= \frac{\alpha^{2n} e^{-\alpha t}}{(\alpha + \beta)^n} \sum_{i=0}^n \frac{\frac{n!}{(n-i)!} \beta^i}{(n+i-1)!} t^{n+i-1} \\ &= \frac{\alpha^{2n} t^{n-1} e^{-\alpha t}}{(\alpha + \beta)^n} {}_1\tilde{F}_1(-n; n, -t\beta) \end{aligned}$$

where $\sum_{i=0}^n \frac{\frac{n!}{(n-i)!} (t\beta)^i}{(n+i-1)!} = {}_1\tilde{F}_1(-n; n, -t\beta)$ is the regularized confluent hypergeometric function which is defined as ${}_1\tilde{F}_1(a; b, x) = \frac{{}_1F_1(a; b, x)}{\Gamma(b)}$ having ${}_1F_1(a; b, x)$ be the Kummer confluent hypergeometric function. ■

3.2. CDF, MGF and other functions for ME distribution

In Theorem 1, we found a closed expression of the PDF for sum of identical EE random variables and we gave the PDF expression as $\sum_{i=0}^n A_i f_{Y_i}(t)$. This expression shows that our distribution is also a mixed distribution of the Erlang distribution. We take an advantage of this expression to find the other statistical characterization as CDF, MGF, moment of order k , reliability and hazard functions for ME distribution. Next, we derive exact closed expressions of these functions.

Theorem 2. Let $S_n \sim ME(\alpha, \beta, n)$, $\alpha > 0$, $\beta > 0$ and $n \in \mathbb{N}^*$. Then the CDF of S_n is given by

$$F_{S_n}(t) = \sum_{i=0}^n A_i F_{Y_i}(t)$$

where A_i is defined in Equation (7) and F_{Y_i} is the CDF of $Y_i \sim \text{Erl}(n + i, \alpha)$.

Proof. From Theorem 1, the PDF of S_n is $f_{S_n}(t) = \sum_{i=0}^n A_i f_{Y_i}(t)$. The CDF of S_n is defined as

$$F_{S_n}(t) = \int_0^t f_{S_n}(x) dx = \int_0^t \sum_{i=0}^n A_i f_{Y_i}(x) dx = \sum_{i=0}^n A_i \int_0^t f_{Y_i}(x) dx = \sum_{i=0}^n A_i F_{Y_i}(t).$$

Lemma 1. $\sum_{i=0}^n A_i = 1$. ■

Proof. Let $F_{Y_i}(t)$ and $F_{S_n}(t)$ be the CDF of Y_i and S_n respectively. However, the limit at infinity of any CDF is 1. Starting from the expression of the CDF in Theorem 2, $F_{S_n}(t) = \sum_{i=0}^n A_i F_{Y_i}(t)$, we have $\lim_{t \rightarrow \infty} F_{S_n}(t) = \lim_{t \rightarrow \infty} \sum_{i=0}^n A_i F_{Y_i}(t)$, thus $\sum_{i=0}^n A_i = 1$. ■

Next, we give another expression for the CDF of S_n .

Corollary 2. Let $S_n \sim ME(\alpha, \beta, n)$, $\alpha > 0$, $\beta > 0$ and $n \in \mathbb{N}^*$. Then the CDF of S_n is

$$F_{S_n}(t) = 1 - \frac{\alpha^n}{(\alpha + \beta)^n} \sum_{i=0}^n \frac{\binom{n}{i} \beta^i \Gamma(n + i, \alpha t)}{\alpha^i (n + i - 1)!}$$

where $\Gamma(\cdot, \cdot)$ is the upper incomplete gamma function.

Proof. From Theorem 2, the CDF of S_n is $F_{S_n}(t) = \sum_{i=0}^n A_i F_{Y_i}(t)$. However, from Equation (2) we have $F_{Y_i}(t) = 1 - \frac{\Gamma(n+i, \alpha t)}{(n+i-1)!}$. Therefore,

$$F_{S_n}(t) = \sum_{i=0}^n \left(A_i - A_i \frac{\Gamma(n+i, \alpha t)}{(n+i-1)!} \right),$$

but from Lemma 1, $\sum_{i=0}^n A_i = 1$ This leads to $F_{S_n}(t) = 1 - \sum_{i=0}^n A_i \frac{\Gamma(n+i, \alpha t)}{(n+i-1)!}$. Moreover, from Equation (7) $A_i = \frac{\binom{n}{i} \alpha^{n-i} \beta^i}{(\alpha + \beta)^n}$ and we get

$$\begin{aligned} F_{S_n}(t) &= 1 - \sum_{i=0}^n A_i \frac{\Gamma(n+i, \alpha t)}{(n+i-1)!} \\ &= 1 - \frac{\alpha^n}{(\alpha + \beta)^n} \sum_{i=0}^n \frac{\binom{n}{i} \beta^i \Gamma(n+i, \alpha t)}{\alpha^i (n+i-1)!} \end{aligned}$$

■

Theorem 3. Let $S_n \sim ME(\alpha, \beta, n)$, $\alpha > 0$, $\beta > 0$ and $n \in \mathbb{N}^*$. Then the MGF of S_n is

$$\phi_{S_n}(t) = \sum_{i=0}^n A_i \phi_{Y_i}(t)$$

where A_i is defined in Equation (7) and ϕ_{Y_i} is the MGF of $Y_i \sim Erl(n+i, \alpha)$.

Proof. Referring to Theorem 1 the PDF of S_n is $f_{S_n} = \sum_{i=0}^n A_i f_{Y_i}(t)$. Thus,

$$\begin{aligned} \phi_{S_n}(t) &= \int_{-\infty}^{+\infty} e^{tx} f_{S_n}(x) dx = \int_{-\infty}^{+\infty} e^{tx} \left(\sum_{i=0}^n A_i f_{Y_i}(x) \right) dx = \sum_{i=0}^n A_i \int_{-\infty}^{+\infty} e^{tx} f_{Y_i}(x) dx \\ &\text{but } \int_{-\infty}^{+\infty} e^{tx} f_{Y_i}(x) dx = \phi_{Y_i}(t), \text{ thus } \phi_{S_n}(t) = \sum_{i=0}^n A_i \phi_{Y_i}(t). \end{aligned}$$

■

Corollary 3. Let $S_n \sim ME(\alpha, \beta, n)$, $\alpha > 0$, $\beta > 0$ and $n \in \mathbb{N}^*$. Then the MGF of S_n is

$$\phi_{S_n}(t) = \frac{\alpha^{2n}}{(\alpha + \beta)^n} \sum_{i=0}^n \frac{\binom{n}{i} \beta^i}{(\alpha - t)^{n+i}}$$

Proof. From Theorem 3 $\phi_{S_n}(t) = \sum_{i=0}^n A_i \phi_{Y_i}(t)$ and the MGF of Erlang distribution Y_i is given in Equation (3) as $\phi_{Y_i}(t) = \left(\frac{\alpha}{\alpha-t}\right)^{n+i}$ which leads to $\phi_{S_n}(t) = \sum_{i=0}^n A_i \left(\frac{\alpha}{\alpha-t}\right)^{n+i}$. Moreover, from Equation (7) $A_i = \frac{\binom{n}{i} \alpha^{n-i} \beta^i}{(\alpha + \beta)^n}$ then

$$\begin{aligned} \phi_{S_n}(t) &= \sum_{i=0}^n \frac{\binom{n}{i} \alpha^{n-i} \beta^i}{(\alpha + \beta)^n} \left(\frac{\alpha}{\alpha - t} \right)^{n+i} \\ &= \frac{\alpha^{2n}}{(\alpha + \beta)^n} \sum_{i=0}^n \frac{\binom{n}{i} \beta^i}{(\alpha - t)^{n+i}} \end{aligned}$$

■

Theorem 4. Let $S_n \sim ME(\alpha, \beta, n)$, $\alpha > 0, \beta > 0$ and $n \in \mathbb{N}^*$. Then the reliability function of S_n is

$$R_{S_n}(t) = \sum_{i=0}^n A_i R_{Y_i}(t)$$

and the hazard function of S_n is given as

$$h_{S_n}(t) = \frac{\sum_{i=0}^n A_i h_i(t) R_{Y_i}(t)}{\sum_{i=0}^n A_i R_{Y_i}(t)}$$

where $h_{Y_i}(t)$ and $R_{Y_i}(t)$ are the hazard and reliability functions of $Y_i \sim Erl(n + i, \alpha)$ respectively, and A_i is defined in Equation (7).

Proof. $R_{S_n}(t) = 1 - F_{S_n}(t)$, and from Theorem 2 we have $F_{S_n}(t) = \sum_{i=0}^n A_i F_{Y_i}(t)$

$$R_{S_n}(t) = 1 - \sum_{i=0}^n A_i F_{Y_i}(t),$$

but $F_{Y_i}(t) = 1 - R_{Y_i}(t)$, and from Lemma 1, we have $\sum_{i=0}^n A_i = 1$, thus $R_{S_n}(t) = \sum_{i=0}^n A_i R_{Y_i}(t)$.

On the other hand, the expression of hazard function is given by

$$h_{S_n}(t) = \frac{f_{S_n}(t)}{R_{S_n}(t)} = \frac{\sum_{i=0}^n A_i f_{Y_i}(t)}{\sum_{i=0}^n A_i R_{Y_i}(t)}$$

however, $f_{Y_i}(t) = h_i(t) R_{Y_i}(t)$, then

$$h_{S_n}(t) = \frac{\sum_{i=0}^n A_i h_i(t) R_{Y_i}(t)}{\sum_{i=0}^n A_i R_{Y_i}(t)}.$$

■

Theorem 5. Let $S_n \sim ME(\alpha, \beta, n)$, $\alpha > 0, \beta > 0$ and $n \in \mathbb{N}^*$. Then the moment of order k of S_n is

$$E[S_n^k] = \sum_{i=0}^n A_i E[Y_i^k] = \frac{k! \alpha^{n-k}}{(\alpha + \beta)^n} \sum_{i=0}^n \frac{\beta^i}{\alpha^i} \binom{n}{i} \binom{n+i+k}{n+i}$$

where $Y_i \sim Erl(n + i, \alpha)$, and A_i is defined in Equation (7).

Proof. From Theorem 3, we have $\phi_{S_n}(t) = \sum_{i=0}^n A_i \phi_{Y_i}(t)$. Now the moment of S_n of order k is given by $E[S_n^k] = \left. \frac{d^k \phi_{S_n}(t)}{dt^k} \right|_{t=0} = \sum_{i=0}^n A_i \left. \frac{d^k \phi_{Y_i}(t)}{dt^k} \right|_{t=0} = \sum_{i=0}^n A_i E[Y_i^k]$. Moreover, $E[Y_i^k] = \frac{\Gamma(n+i+k)}{\alpha^k \Gamma(n+i)}$ and from Equation (7) $A_i = \frac{\binom{n}{i} \alpha^{n-i} \beta^i}{(\alpha + \beta)^n}$ then

$$\begin{aligned} E[S_n^k] &= \sum_{i=0}^n \frac{\binom{n}{i} \alpha^{n-i} \beta^i}{(\alpha + \beta)^n} \frac{\Gamma(n+i+k)}{\alpha^k \Gamma(n+i)} \\ &= \frac{\alpha^{n-k}}{(\alpha + \beta)^n} \sum_{i=0}^n \frac{\beta^i}{\alpha^i} \frac{\binom{n}{i} \Gamma(n+i+k)}{\Gamma(n+i)} \\ &= \frac{k! \alpha^{n-k}}{(\alpha + \beta)^n} \sum_{i=0}^n \frac{\beta^i}{\alpha^i} \binom{n}{i} \binom{n+i+k}{n+i} \end{aligned}$$

as

$$\frac{\binom{n}{i} \Gamma(n+i+k)}{\Gamma(n+i)} = \frac{\frac{n!}{(n-i)! i!} k! (n+i+k-1)!}{(n+i-1)! k!} = k! \binom{n}{i} \binom{n+i+k}{n+i}$$

■

We end this part to point out the importance of writing the PDF of our ME distribution as linear combination PDF of the known Erlang distribution. This expression facilitates in determining the other statistical expressions as CDF, reliability and hazard functions, moment generating function (MGF), and k^{th} moments. This procedure was adopted by Smaili et al. [10] and [11]. Later, these expressions are used to give an estimated model for a real-life data.

4. REAL LIFE DATA

To illustrate the new results presented in this paper, we fit the ME distribution to two examples of real data. The MLE and MME approaches are employed to estimate the parameters of the real-life data and MATHEMATICA software is used. We analyze real data sets to show that the ME distribution can be a better model than other existing distributions. We consider the distributions in recent papers that proposed their distribution to fit the model data. For each data set, we compare the fitted distributions using the three criteria: *AIC* (Akaike Information Criterion), *AICC* (Akaike Information Criterion Corrected) and *BIC* (Bayesian Information Criterion). Let us be precise that $\log(L)$ is the log-likelihood taking with the estimate values, $AIC = 2k - 2\log(L)$, $AICC = AIC + \frac{2k(k+1)}{n-k-1}$ and $BIC = -2\log(L) + k\log(n)$, where k denotes the number of estimated parameters and n denotes the sample size. The best fitted distribution corresponds to lower *AIC*, *AICC* and *BIC*. Also the histogram and the estimated PDFs and CDFs for the best fitted models to the two data are displayed in Figures 1 and 2, respectively.

Data set 1: The data set contains $n = 63$ measures related to the strength of 1.5cm glass bers. It is reported in Smith and Naylor (1987): 0.55, 0.93, 1.25, 1.36, 1.49, 1.52, 1.58, 1.61, 1.64, 1.68, 1.73, 1.81, 2, 0.74, 1.04, 1.27, 1.39, 1.49, 1.53, 1.59, 1.61, 1.66, 1.68, 1.76, 1.82, 2.01, 0.77, 1.11, 1.28, 1.42, 1.5, 1.54, 1.6, 1.62, 1.66, 1.69, 1.76, 1.84, 2.24, 0.81, 1.13, 1.29, 1.48, 1.5, 1.55, 1.61, 1.62, 1.66, 1.7, 1.77, 1.84, 0.84, 1.24, 1.3, 1.48, 1.51, 1.55, 1.61, 1.63, 1.67, 1.7, 1.78, 1.89.

We chose the analysis done by Chesneau in [3] for this data. Chesneau compared the Lindley, Exponential, Exponentiated Exponential (EExp), and Exponential Hypoexponential distribution (EHypo). The corresponding PDF of EExp and EHypo are given by

$$f_{EExp}(x) = \lambda \alpha e^{-\lambda x} (1 - e^{-\lambda x})^{\alpha-1}$$

$$f_{EHypo}(x) = \lambda \alpha (1 + 10\alpha) e^{-\lambda x} (1 - e^{-\lambda x})^{\alpha-1} \left(1 - (1 - e^{-\lambda x})^{0.1}\right)$$

respectively. We derive two estimated distributions of the ME distribution using MLE and MME and used as a competitive distribution of the previous ones. See Table 1. This table shows that the ME model gives a better fit to this data than the other distributions. The plots in Figures 1 also indicate the same thing. So, the ME model could be chosen as the best model.

Table 1: MLE and MME of ME Distribution with MLEs of competitor distributions and AIC, AICC and BIC of data set 1

Model	Estimated Parameters	AIC	AICC	BIC
ME(MLE)	$\hat{n} = 13, \hat{\alpha} = 13.771948428082293, \hat{\beta} = 20.34250599538599$	50.547	50.747	63.1195
ME(MME)	$\hat{n} = 15, \hat{\alpha} = 16.653713280301165, \hat{\beta} = 25.644927330965096$	53.678	53.8784	66.251
Lindley	$\hat{\theta} = 0.996116$	164.56	164.62	166.70
Exponential	$\hat{\lambda} = 0.663647$	179.66	179.73	181.80
EExp	$\hat{\alpha} = 31.3489, \hat{\lambda} = 2.61157$	66.76	66.96	71.05
EHypo	$\hat{\alpha} = 24.0816, \hat{\lambda} = 1.83894$	59.67	59.87	63.96

Data set 2: The data consist of 101 observations. The data was presented in Birnbaum & Saunders (1969) and correspond to the fatigue time of 101 6061-T6 aluminum coupons cut parallel to the direction of rolling and oscillated at 18 cycles per second (cps). The data are: 70, 90, 96, 97, 99, 100, 103, 104, 104, 105, 107, 108, 108, 108, 109, 109, 112, 112, 113, 114, 114, 114, 116, 119, 120, 120, 120, 121, 121, 123, 124, 124, 124, 124, 124, 128, 128, 129, 129, 130, 130, 130, 131, 131, 131, 131, 131, 132, 132, 132, 133, 134, 134, 134, 134, 134, 136, 136, 137, 138, 138, 138, 138, 139, 139, 141, 141, 142, 142, 142, 142, 142, 144, 144, 145, 146, 148, 148, 149, 151, 151, 152, 155, 156, 157, 157, 157, 157, 158, 159, 162, 163, 163, 164, 166, 166, 168, 170, 174, 196, 212.

We chose the analysis done by Yousof et al. in [13] for this data. They compared the Weibull, Wei-Weibull (WW) and their Weibull-Weibull logarithmic (WWL) distribution to fit this data. The

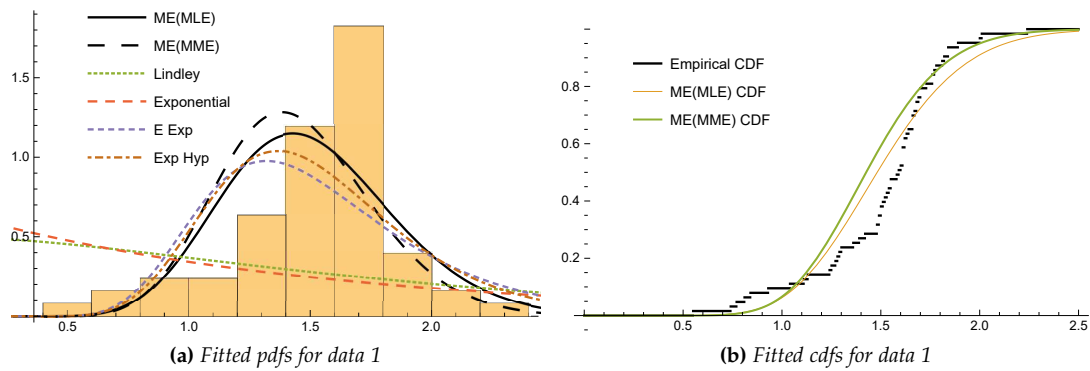


Figure 1: The two figures show a best fitting for the EE distribution

CDF of WW and WWL distribution are given by

$$F_{WW}(x; \alpha, \beta, \lambda, \gamma) = 1 - e^{-\alpha(e^{\lambda x^\gamma} - 1)^\beta}$$

$$F_{WWL}(x; \alpha, \beta, \lambda, \gamma, p) = \frac{p\alpha\beta\gamma\lambda x^{\gamma-1} (e^{\lambda x^\gamma} - 1)^{\beta-1} \left(e^{(\lambda x^{\gamma-1} - \alpha(e^{\lambda x^\gamma} - 1)^\beta)} \right)}{\left(p \left(1 - e^{-\alpha(e^{\lambda x^\gamma} - 1)^\beta} \right) - 1 \right) \ln(1 - p)}$$

respectively for $\alpha, \beta, \lambda, \gamma > 0$ and $0 < p < 1$. We derive two estimated distributions of the ME distribution using MLE and MME and used as a competitive distribution of the previous ones, see Table 2. This table shows that the ME model gives a better fit to this data than the other distributions. The plots in Figure 2 also indicate the same thing. So, the ME model for the second time could be chosen as the best model.

Table 2: MLE and MME of ME Distribution with MLEs of competitor distributions and AIC, AICC and BIC of data set 2

Model	Estimated Parameters	AIC	AICC	BIC
ME(MLE)	$\hat{n} = 32, \hat{\alpha} = 0.31305352844373824, \hat{\beta} = 0.13952982315141454$	916.557	916.679	931.018
ME(MME)	$\hat{n} = 28, \hat{\alpha} = 0.3149943298488485, \hat{\beta} = 0.27793752048684467$	918.586	933.047	918.709
Weibull	$\hat{\lambda} = 0.0036, \hat{\gamma} = 1.1516$	1167.38	1167.5	1172.61
WW	$\hat{\lambda} = 0.0036, \hat{\gamma} = 1.1516$	1167.38	1167.5	1172.61
WWL	$\hat{\alpha} = 0.0060, \hat{\beta} = 3.1600, \hat{\lambda} = 0.0873, \hat{\gamma} = 0.6264, \hat{p} = 0.8732$	948.49	948.91	961.56

We see in Tables 1 and 2 that the ME distribution has the smallest AIC, AICC and BIC for the two data sets, compared with lately proposed distributions, indicating that the ME distribution is a serious competitor to the other considered distributions.

5. CONCLUSION

A new distribution, Mixed Erlang (ME) distribution, has been proposed and its properties are studied. We derived exact closed expressions of the PDF, CDF, reliability function, hazard function, MGF, and k^{th} moments. We have studied the maximum likelihood estimators and method of moments estimators and the parameters estimation is carried out in the presence of real data. We presented two real life data sets, and our ME distribution was compared with lately proposed distributions and showed that the ME distribution is a serious competitor to the others.

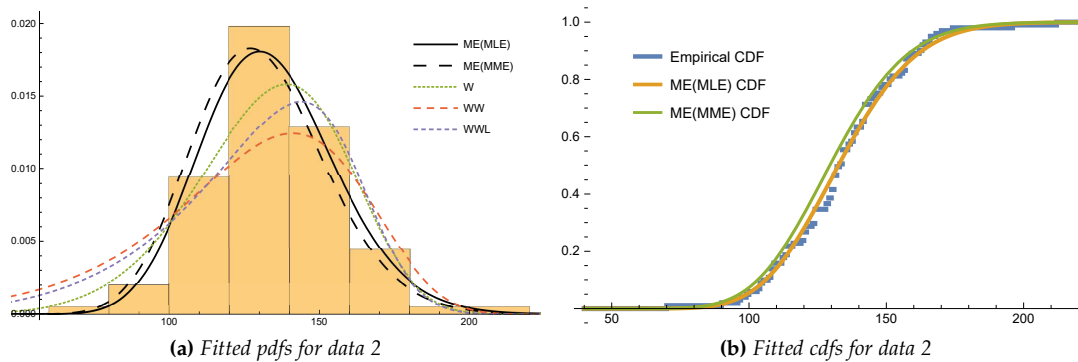


Figure 2: The two figures show a best fitting for the EE distribution

REFERENCES

- [1] Abdelkader, Y.H.: Erlang distributed activity times in stochastic activity networks. *Kybernetika*. 39(3), 347–358 (2003)
- [2] Bocharov, P.P., D’Apice, C., Pechinkin, A.V.: *Queueing theory*. Walter de Gruyter. (2011)
- [3] Chesneau, C.: A new family of distributions based on the hypoexponential distribution with fitting reliability data. *Statistica*. 78(2), 127–147 (2018)
- [4] Forbes, C., Evans, M., Hastings, N., Peacock, B.: *Statistical distributions*. John Wiley & Sons (2011)
- [5] Gómez, Y.M., Bolfarine, H., Gómez, H.W.: A new extension of the exponential distribution. *Revista Colombiana de Estadística*. 37(1), 25–34 (2014)
- [6] Gupta, R.D., Kundu, D.: Exponentiated exponential family: An alternative to Gamma and Weibull distribution’. *Biometrical Journal*. 43(1), 117–130 (2001)
- [7] Jasiulewicz, H., Kordecki, W.: Convolutions of Erlang and of Pascal distributions with applications to reliability. *Demonstr. Math.* 36(1), 231–238 (2003)
- [8] Kadri, T., Smaili, K., Kadry, S. In: *Markov modeling for reliability analysis using Hypoexponential distribution*. In *Numerical Methods for Reliability and Safety Assessment*, pp. 599–620. Springer, Cham (2015)
- [9] Mudholkar, G.S., Srivastava, D.K.: Exponentiated Weibull family for analysing bathtub failure data. *IEEE Trans. Reliability*. 42, 299–302 (1993)
- [10] Smaili, K., Kadri, T., Kadry, S.: A modified-form expressions for the hypoexponential distribution. *British Journal of Mathematics & Computer Science*. 4(3), 322–332 (2014)
- [11] Smaili, K., Kadri, T., Kadry, S.: Finding the PDF of the hypoexponential random variable using the Kad matrix similar to the general Vandermonde matrix. *Comm. Statist. Theory Methods*. 45(5), 1542–1549 (2016)
- [12] Trivedi, K.S.: *Probability & statistics with reliability, queuing and computer science applications*. John Wiley & Sons (2008)
- [13] Yousof, H.M., Rasekhi, M., Afify, A.Z., Alizadeh, M., Ghosh, I. and Hamedani, G.G.: The Beta Weibull-G Family of Distributions: Theory, Characterizations and Applications. *Pakistan Journal of Statistics*. 33, 95–116 (2017)

CONSTRUCTION OF LIFE TEST SAMPLING INSPECTION PLANS BY ATTRIBUTES BASED ON MARSHALL - OLKIN EXTENDED EXPONENTIAL DISTRIBUTION

R. Vijayaraghavan¹, A. Pavithra²

•

Department of Statistics, Bharathiar University, Coimbatore 641 046, Tamil Nadu, INDIA

¹vijaystatbu@gmail.com, ²pavistat95@gmail.com

Abstract

A life test is a random experiment conducted on the manufactured items such as electrical and electronic components for estimating their life time based on the inspection of randomly sampled items. Life time of the items is a random variable which follows a specific continuous-type distribution, called the lifetime distribution. Reliability sampling, which is one among the classifications of product control, deals with inspection procedures for sentencing one or more lots or batches of items submitted for inspection. In this paper, the concept of sampling plans for life tests involving two samples is introduced under the assumption that the life time random variable is modeled by Marshall - Olkin extended exponential distribution. A procedure is developed for designing the optimum plan with minimum sample sizes when two points on the desired operating characteristic curve are prescribed to ensure protection to the producer and the consumer.

Keywords: Life Test Sampling Plan, producer's risk, Marshall Olkin Extended Exponential Distribution, Consumers risk, OC function, Reliability sampling.

1. Introduction

Reliability sampling is the methodology that deals with sampling inspection procedures, called life test or reliability sampling plans essentially adopted in the industrial processes for taking decisions on the disposition of the lot(s) of items such as electric or electronic components based on the assessment of quality utilizing lifetimes of the items as the quality characteristics. A life test sampling plan is employed by drawing a random sample of test units, which are subjected to a set of test procedures, from the lot and inspecting the units for deciding whether the lot is accepted or rejected based on the information provided by the test results. A specific sampling plan focuses on the objective of determining whether the lifetimes of items reach the specified standard or not based on the observations made from the sampled lifetime data. Such sampling plans can be developed considering the lifetime of the products as the quality characteristic as well as the random variable, which is appropriately modeled by a probability distribution, like exponential, Weibull, lognormal, or gamma distribution rather than the normal distribution.

The literature in product control provides adequate references on the applications of many continuous-type probability distributions in the studies concerned with the development of sampling inspection plans for life tests. The earlier works, which laid the foundation for the expansion of various types of sampling plans, would include the theory of reliability sampling proposed and developed in [1], [2], [3], [4], [5], [6], [7] and [8]. Significant contributions in the development of life test sampling plans employing exponential, Weibull, lognormal and gamma distributions as well as

several compound distributions for modeling lifetime data have also been made in the past four decades. A detailed account of such plans was provided in [9]. Recent advances in the theory of life test sampling plans are provided in [10 – 25].

Marshall – Olkin extended exponential distribution (MOEED), introduced in [26] as a generalization of the exponential distribution, exhibits the property of monotone failure rate. In some applications of biological, agricultural and entomological studies, the failure rate function of the underlying distribution may be inverted bathtub – shaped hazard function or unimodal. When a probability distribution for life-time variable has a failure rate function that takes various shapes, it is the natural choice to adopt the distribution in practice. Further, MOEED has the failure rate that decreases with time, fairly constant failure rate and failure rate that increases with time, indicative of infantile or early-failures, useful life or random failures and wear-out failures, respectively.

Due to the possibility of various shapes of failure rate function, which is the case similar to gamma and Weibull distribution, MOEED is especially suitable for modeling life time of an item and is used commonly for the inferential aspect of utilizing life information. Hence, as a member of the lifetime continuous distributions, MOEED can be considered as an apt probability model to adopt in real life situations and may be used as an alternative to the gamma, Weibull and other exponentiated family of distributions. Considering its importance in reliability studies, Different criteria for designing life test sampling plans are discussed in [27] under the condition that the life test is evaluated in terms of mean life, hazard life and reliability life under the conditions for the application of MOEED.

In this paper, a special type of sampling plans which involves two random samples and allows a maximum of one failure in the combined samples for life tests is introduced under the assumption that the lifetime quality characteristic is modeled by MOEED. The method of designing optimum sampling plans indexed by two prescribed points on the operating characteristic curve, namely acceptable mean life and unacceptable mean life, associated with the producer's risk and the consumer's risk, respectively, is discussed with illustrations under the conditions for application of MOEED for desired degree of discrimination which would ensure protection to the producer and consumer.

2. Special Type of Sampling Plans for Life Tests

A special type of sampling plan, devised and discussed in [28 - 29], is a lot-by-lot sampling plan by attributes in which provisions are made to utilize only small acceptance numbers such as 0 or 1, and to inspect the submitted lot by drawing a second random sample even if the first random sample contains zero nonconforming (defective) items. A special feature of this plan is that the operating characteristics of the plan lies between those of $c = 0$ and $c = 1$ single sampling plans, and thus provides better discrimination over the single sampling plans with wide range of operating ratios. Consider the following conditions:

- (a) Sampling plans for life tests are required to be set up for product characteristics that involve costly or destructive testing.
- (b) Situations warrant small samples to be drawn from the lot.

In such conditions, a sampling plan with zero or fewer failures in the samples is quite reasonable to employ for the disposition of the lot. But, as demonstrated in [29] and [30], under sampling inspection by attributes, single sampling plans for life tests with zero failures or zero acceptance number, designated by $SSP - (n, 0)$, are unattractive as they fail to provide protection to the producer against the acceptable mean life of the product. The operating characteristic curves of such

sampling plans having zero failures are quite often in undesirable shapes and hence, they seldom ensures protection to producers, but ensures protection to consumers against unacceptable mean life of the product.

It can be demonstrated that single sampling plans admitting one or more failures in a sample of items improve upon the undesirable characteristics of $SSP - (n, 0)$, but may require larger sample sizes. In order to overcome this shortcoming, the special type of sampling plans can be adopted for life tests allowing a maximum of one failure in the random samples drawn from the submitted lot.

Most often, situations involving small samples may warrant the use of single sampling plans with a fewer number of failures such as $c = 0$ and $c = 1$. But, the OC curves of $c = 0$ and $c = 1$ plans would indicate that there will be a conflicting interest between the producer and the consumer as $c = 0$ plans always provide protection to the consumer with smaller risk of accepting the lot having unacceptable mean life of the product while $c = 1$ plans favor the producer with smaller risk of rejecting the lot having acceptable mean life. This situation of conflict can be annulled if a suitable life test plan having its OC curve lying between the OC curves of $c = 0$ and $c = 1$ plans is designed. While introducing the special type of sampling plan, it was shown in [28] that there is a wide gap between the OC curves of $c = 0$ and $c = 1$ plans and established that the OC curves of the special plan lie between the OC curves of $c = 0$ and $c = 1$ plans. He also advocated that the sampling plans of similar kind could be used effectively in such situations. Hence, the special type of sampling plans could be the natural choice and could be considered as an alternative to single sampling plans having zero or fewer failures, such as $c = 0$ or $c = 1$.

Before discussing the procedure for the selection of an optimum special type of sampling plan for life tests with the objective of providing protection to the producer and consumer against rejection of the lot for the specified acceptable mean life and against acceptance of the lot for the specified unacceptable mean life, the operating procedure of the plan is now described as given below:

A sample of n_1 items is taken from a given lot and inspected. If one or more failures are found, i.e., $m_1 \geq 1$, while inspecting n_1 items, then the lot is rejected; if no failure is found, i.e., $m_1 = 0$, a second sample of n_2 items is taken and the number of failures, m_2 , is observed. If zero or one failure is found, i.e., $m_2 \leq 1$, while inspecting n_2 items, then the lot is accepted; if two or more failures are found, i.e., $m_2 > 1$, then the lot is rejected.

Thus, the special type of the sampling plans for life tests is specified by two parameters n_1 and n_2 , which are the number of items in the first and second random samples, respectively.

3. Marshall - Olkin Extended Exponential Distribution

Let T be a random variable representing the lifetime of the components. Assume that T follows Marshall – Olkin extended exponential distribution (MOEED). The probability density function and the cumulative distribution function of T are, respectively, defined by

$$f(t; \gamma, \theta) = \frac{\gamma e^{-t/\theta}}{\theta(1 - \gamma e^{-t/\theta})^2}, t, \gamma, \theta > 0 \tag{1}$$

and

$$F(t; \gamma, \theta) = \frac{1 - e^{-t/\theta}}{1 - \gamma e^{-t/\theta}}, t, \gamma, \theta > 0, \tag{2}$$

where $\bar{\gamma} = 1 - \gamma$, γ is the shape parameter and θ is the scale parameter.

The mean life time, the reliability function and hazard function for specified time t under MOEED are, respectively, given by

$$\mu = E(T) = -\frac{\gamma\theta \log \gamma}{1 - \gamma}, \tag{3}$$

$$R(t; \theta, \gamma) = \frac{\gamma}{e^{t/\theta} - \bar{\gamma}}, t \geq 0 \tag{4}$$

and $Z(t; \theta, \gamma) = \frac{e^{t/\theta}}{\theta(e^{t/\theta} - \bar{\gamma})}, t \geq 0. \tag{5}$

The reliable life is the life beyond which some specified proportion of items in the lot will survive. The reliable life associated with MOEED is defined and denoted by

$$\rho = \theta \log \left(\frac{\gamma + \bar{\gamma}R}{R} \right), \tag{6}$$

where R is the proportion of items surviving beyond life ρ .

The proportion, p , of product failing before time t , is defined by the cumulative probability distribution of T and is expressed by

$$p = P(T \leq t) = F(t; \gamma, \theta). \tag{7}$$

4. Operating Characteristic Function of Life Test Sampling Plans

Associated with the special of type of sampling plans are the performance measures, such as operating characteristic function and average sample number function, which are, respectively, expressed by

$$P_a(p) = f(0 | n_1, p)[f(0 | n_2, p) + f(1 | n_2, p)] \tag{8}$$

and $ASN(p) = n_1 + n_2 f(0 | n_1, p), \tag{9}$

where p is the proportion of product failing before time t , and $f(0 | n_1, p)$, $f(0 | n_2, p)$ and $f(1 | n_1, p)$ are defined either from the binomial distribution or from the Poisson distribution. Under the conditions for application of Poisson model for the OC curve, the OC and ASN functions will have the following forms:

$$P_a(p) = e^{-n_1 p} (e^{-n_2 p} + n_2 p e^{-n_2 p}) \tag{10}$$

and $ASN(p) = n_1 + n_2 e^{-n_1 p} \tag{11}$

When the Binomial model is used, the OC and ASN functions are respectively given by

$$P_a(p) = (1 - p)^{n_1} \left((1 - p)^{n_2} + n_2 p (1 - p)^{n_2 - 1} \right) \tag{12}$$

and $ASN(p) = n_1 + n_2 (1 - p)^{n_1} \tag{13}$

In the context of sampling plans for life tests, it is to be observed that the failure probability, p , is defined by the proportion of product failing before time t , and hence, the expression for p is defined by the cumulative probability distribution of T given as (7). Associated with a specific value of p , there exists a unique value of t/μ , which is derived using (2), (3) and (7) as $t/\mu = -\left(\frac{t}{\theta}\right)\left(\frac{1-\gamma}{\gamma \log \gamma}\right)$.

In a similar way, for a specified value of t/μ , the value of p could be obtained. As the value of p is associated with t/μ , the operating characteristic function of a life test sampling plan can be considered as a function of t/μ , rather than p , and hence, the OC curve of the plan could be obtained by plotting the acceptance probabilities against the values of t/μ .

5. Procedure for the Selection of Life Test Sampling Plans

It can be observed that when the life time random variable follows a Marshall – Olkin extended exponential distribution, a life test sampling plan would be designated by the parameters, such as sample size(s) and acceptance number(s) of the sampling plan and the parameters of the distribution, like γ and θ (or μ). Hence, under MOEED, a specific life test sampling plan can be determined by specifying the requirements that the OC curve should pass through two prescribed points, namely, (μ_0, α) and (μ_1, β) , where μ_0 and μ_1 are the acceptable and unacceptable mean life, respectively, which are associated with the risks α and β .

Corresponding to μ_0 and μ_1 , one may define p_0 and p_1 as the acceptable and unacceptable proportions of the lot failing before time, t , respectively. Here, p_0 and p_1 may be considered as the producer's quality level and consumer's quality level with α and β as the associated producer's and consumer's risks, respectively.

Further, associated with p_0 and p_1 are the ratios t/μ_0 and t/μ_1 , respectively. The specification of these quality levels would ensure protection to the producer against rejection of satisfactory lots as well as the consumer against acceptance of unsatisfactory lots, and would be considered to fix the OC curve in accordance with a desired degree of discrimination. An optimum life test sampling plan for specified points $(p_0, 1 - \alpha)$ and (p_1, β) can be determined by satisfying the following two conditions so that the maximum producer's and consumer's risks will be fixed at α and β , respectively:

$$P_a(p_0) \geq 1 - \alpha \tag{14}$$

$$\text{and } P_a(p_1) \leq \beta \tag{15}$$

It may be noted that the specification of $(p_0, 1 - \alpha)$ and (p_1, β) is equivalent to the specification of the points $(\mu_0, 1 - \alpha)$ and (μ_1, β) or $(t/\mu_0, 1 - \alpha)$ and $(t/\mu_1, \beta)$. The following integrated approach can be used to determine a life test sampling plan that meets the specified requirements under the conditions of MOEED and its implementation:

Step 1: Specify the value of the shape parameter γ or its estimate.

Step 2: Specify the values of t/μ_0 and t/μ_1 with $\alpha = 0.05$ and $\beta = 0.10$, respectively.

Step 3: Find p_0 and p_1 corresponding to t/μ_0 and t/μ_1 based on the procedure described in the previous section.

Step 4: Find the optimum values of n_1 and n_2 for the specified strength $(p_0, \alpha, p_1, \beta)$ satisfying the conditions (14) and (15), utilizing the expressions either (10) or (12).

Step 5: Draw randomly a set of n_1 items from the submitted lot.

Step 6: Conduct the life test considering t_0 as the test termination time and μ as the expected mean life. Observe the number, m , of failures.

Step 7: Terminate the life test if either time t_0 is reached or the condition $m \geq 1$ occurs before time t_0 .

Step 8: Reject the lot if $m \geq 1$ at time t_0 ; If $m = 0$, draw a random sample of n_2 items from the remainder of the lot and observed the number of failures. If there is one or zero failure before time t_0 , accept the lot; otherwise reject the lot..

5.1. Numerical Illustration

Assume that the lifetime random variable follows MOEED defined with the shape parameter γ and the shape parameter is estimated from the past history as $\gamma = 1.5$, it is desired to institute a life test sampling plan when the acceptable mean life and unacceptable mean life are prescribed as 75000 hours and 4285 hours, respectively. The producer's and consumer's risks are specified as $\alpha = 0.05$ and $\beta = 0.10$. The experimenter wishes to terminate the life test at $t = 150$ hours. For the given requirements, the values of t/μ_0 and t/μ_1 are obtained as 0.002 and 0.035, respectively. Based on the procedure described earlier, the parameters of the special type of sampling plan are determined as $n_1 = 23$ and $n_2 = 109$. Thus, the life test plan for the given conditions is implemented as given below:

1. Select a random sample of 23 items from a lot, conduct the life test on each of the sampled item and observe the number of failures while inspecting 23 items before reaching the termination time fixed as $t = 150$ hours.
2. Terminate the life test once the termination time, $t_0 = 150$ hours is reached or when the number of failures is 1 or more before reaching the termination time.
3. Reject the lot if the observed number of failures is one or more; if no failure is observed in 23 items before reaching the test termination time, select a random sample of $n_2 = 109$ items and conduct the life test on each of the sampled item. If the observed number of failures is one or less, accept the lot; otherwise reject the lot.
4. Treat the items which survive beyond time $t_0 = 150$ hours as passed.

5.2. Numerical Illustration

Suppose that an experimenter is interested to implement a life test sampling inspection plan for taking a decision about the disposition of a submitted lot of manufactured products whose life time follows MOEED. The value of γ , the shape parameter, is estimated as 2.5. It is assumed that the life test will be terminated at $t = 18$ hours. The acceptable and unacceptable proportions of the lot failing before time, t , are respectively prescribed as $p_0 = 0.001$ and $p_1 = 0.018$ with the associated risks fixed at the levels $\alpha = 0.05$ and $\beta = 0.10$. The values of t/μ corresponding to $p_0 = 0.001$ and $p_1 = 0.018$ are determined as $t/\mu_0 = 0.00175$ and $t/\mu_1 = 0.03$. Thus, optimum sample sizes for the special type of sampling plan for life tests satisfying the conditions (14) and (15),

corresponding to $t/\mu_0 = 0.00175$ and $t/\mu_1 = 0.03$, are obtained as $n_1 = 34$ and $n_2 = 168$. The acceptable mean life and unacceptable mean life are also obtained as $\mu_0 = t/0.00175 = 10285$ hours and $\mu_1 = t/0.03 = 600$ hours, respectively.

6. Conclusion

A special type of sampling inspection plans for life-tests which involve two samples and allows a maximum of one failure is proposed when the lifetime quality characteristic is modeled by a Marshall – Olkin extended exponential distribution. A procedure for the selection of the proposed plan is discussed through numerical illustrations. The life test sampling plans which could be derived by the procedure discussed in this paper will ensure protection to the producer and consumer as the plans are indexed by acceptable and unacceptable proportion of product failing before the specified time, t . The practitioners can generate the required sampling plans for various choices of γ adopting the procedure.

7. Acknowledgments

The authors are grateful to Bharathiar University, Coimbatore for providing necessary facilities to carry out this research work. The second author is indebted to the Department of Science and Technology, India for awarding the DST-INSPIRE Fellowship under which the present research has been carried out.

References

- [1] Epstein, B. (1960a). Tests for the Validity of the Assumption that the Underlying Distribution of Life is Exponential, Part I, *Technometrics*, 2, pp. 83 - 101.
- [2] Epstein, B. (1960b). Tests for the Validity of the Assumption that the Underlying Distribution of Life is Exponential, Part II, *Technometrics*, 2, pp. 167 - 183.
- [3] Handbook H-108. (1960). Sampling Procedures and Tables for Life and Reliability Testing, Quality Control and Reliability, Office of the Assistant Secretary of Defense, US Department of Defense, Washington, D.C.
- [4] Goode, H. P., and Kao, J. H. K. (1961). Sampling Plans Based on the Weibull Distribution, *Proceedings of the Seventh National Symposium on Reliability and Quality Control*, Philadelphia, PA, pp. 24 - 40.
- [5] Goode, H. P., and Kao, J. H. K. (1962). Sampling Procedures and Tables for Life and Reliability Testing Based on the Weibull Distribution (Hazard Rate Criterion), *Proceedings of the Eight National Symposium on Reliability and Quality Control*, Washington, DC, pp. 37 - 58.
- [6] Goode, H. P., and Kao, J. H. K. (1964). Hazard Rate Sampling Plans for the Weibull Distribution, *Industrial Quality Control*, 20, pp. 30 - 39.
- [7] Gupta, S.S. and Groll, P. A. (1961). Gamma Distribution in Acceptance Sampling Based on Life Tests, *Journal of the American Statistical Association*, 56, pp. 942 – 970.
- [8] Gupta, S. S. (1962). Life Test Sampling Plans for Normal and Lognormal Distributions, *Technometrics*, 4, pp. 151 - 175.

- [9] Schilling, E. G., and Neubauer, D. V. (2009). *Acceptance Sampling in Quality Control*, Chapman and Hall, New York, NY.
- [10] Wu, J. W., and Tsai, W. L. (2000). Failure Censored Sampling Plan for the Weibull Distribution, *Information and Management Sciences*, 11, pp. 13 - 25.
- [11] Wu, J. W., Tsai, T. R., and Ouyang, L. Y. (2001). Limited Failure-Censored Life Test for the Weibull Distribution", *IEEE Transactions on Reliability*, 50, pp. 197 - 111.
- [12] Kantam, R.R.L., Rosaiah, K., and Rao, G.S. (2001). Acceptance Sampling Based on Life Tests: Log-Logistic Models, *Journal of Applied Statistics*, 28, pp. 121 - 128.
- [13] Jun, C.-H., Balamurali, S., and Lee, S.-H. (2006). Variables Sampling Plans for Weibull Distributed Lifetimes under Sudden Death Testing, *IEEE Transactions on Reliability*, 55, pp. 53 - 58.
- [14] Tsai, T.-R., and Wu, S.-J. (2006). Acceptance Sampling Based on Truncated Life-tests for Generalized Rayleigh Distribution, *Journal of Applied Statistics*, 33, pp. 595 - 600.
- [15] Balakrishnan, N., Leiva, V., and Lopez, J. (2007). Acceptance Sampling Plans from Truncated Life-test Based on the Generalized Birnbaum - Saunders Distribution, *Communications in Statistics - Simulation and Computation*, 36, pp. 643 - 656.
- [16] Aslam, M., and Jun, C.-H. (2009a). A Group Acceptance Sampling Plan for Truncated Life Test having Weibull Distribution, *Journal of Applied Statistics*, 39, pp. 1021 - 1027.
- [17] Aslam, M., and Jun, C.-H. (2009b). Group Acceptance Sampling Plans for Truncated Life Tests Based on the Inverse Rayleigh Distribution and Log-logistic Distribution, *Pakistan Journal of Statistics*, 25, pp. 107 - 119.
- [18] Aslam, M., Kundu, D., Jun, C.-H., and Ahmad, M. (2011). Time Truncated Group Acceptance Sampling Plans for Generalized Exponential Distribution, *Journal of Testing and Evaluation*, 39, pp. 968 - 976.
- [19] Kalaiselvi, S., and Vijayaraghavan, R. (2010). Designing of Bayesian Single Sampling Plans for Weibull-Inverted Gamma Distribution, *Recent Trends in Statistical Research*, Publication Division, M. S. University, Tirunelveli, pp. 123 - 132.
- [20] Kalaiselvi, S., Loganathan, A., and Vijayaraghavan, R. (2011). Reliability Sampling Plans under the Conditions of Rayleigh – Maxwell Distribution – A Bayesian Approach, *Recent Advances in Statistics and Computer Applications*, Bharathiar University, Coimbatore, pp. 280 - 283.
- [21] Loganathan, A., Vijayaraghavan, R., and Kalaiselvi, S. (2012). Recent Developments in Designing Bayesian Reliability Sampling Plans – An Overview, *New Methodologies in Statistical Research*, Publication Division, M. S. University, Tirunelveli, pp. 61 - 68.
- [22] Hong, C. W., Lee, W. C., and Wu, J. W. (2013). Computational Procedure of Performance Assessment of Life-time Index of Products for the Weibull Distribution with the Progressive First-failure Censored Sampling Plan, *Journal of Applied Mathematics*, Article ID 717184, 2012, pp. 1 - 13.
- [23] Vijayaraghavan, R., Chandrasekar, K., and Uma, S. (2012). Selection of sampling inspection plans for life test based on Weibull-Poisson Mixed Distribution, *Proceedings of the International Conference on Frontiers of Statistics and its Applications*, Coimbatore, pp. 225 - 232.
- [24] Vijayaraghavan, R., and Uma, S. (2012). Evaluation of Sampling Inspection Plans for Life Test Based on Exponential-Poisson Mixed Distribution, *Proceedings of the International Conference on Frontiers of Statistics and its Applications*, Coimbatore, pp. 233 - 240.

- [25] Vijayaraghavan, R., and Uma, S. (2016). Selection of Sampling Inspection Plans for Life Tests Based on Lognormal Distribution, *Journal of Testing and Evaluation*, 44, pp. 1960 - 1969.
- [26] Marshall, A.W., and Olkin, I. (1997). A New Method for Adding a Parameter to a Family of Distributions with Application to the Exponential and Weibull Families, *Biometrika*, 84, pp. 641 - 652.
- [27] Vijayaraghavan, R., and Saranya., Sathya Narayana Sharma, K. (2019). Life Test Sampling Plans Based on Marshall – Olkin Extended Exponential Distribution, *International Journal of Scientific Research in Mathematical and Statistical Sciences*, 6, pp.131-139.
- [28] Govindaraju, K. (1984). *Contributions to the Study of Certain Special Purpose Plans*, Ph.D., Thesis. Coimbatore, India: Department of Statistics, Bharathiar University.
- [29] Govindaraju, K. (1991). Fractional acceptance number single sampling plan. *Communications in Statistics – Simulation and Computation*, 20, pp. 173–190.
- [30] Vijayaraghavan, R. (2007). Minimum Size Double Sampling Plans for Large Isolated Lots, *Journal of Applied Statistics*, 34, 799-806.

A Comparative study of outlier detection of Yamuna River Delhi India by Classical Statistics and Statistical Quality Control

^{1,*}Mohammad Ahmad, ²Ahteshamul Haq, ³Abdul Kalam and ⁴Sayed Kifayat Shah

•

^{1,3}Faculty of Science, Beijing University of Technology, China

²Department of Statistics & Operations Research Aligarh Muslim University, Aligarh-202002, India

⁴College of Economics and Management, Beijing University of Technology, Beijing China

^{1,*}mahmador@gmail.com, ²a.haq@myamu.ac.in, ³faisal.stats@gmail.com, ⁴skifss_20@qq.com

*Corresponding author

Abstract

Water quality control aids in preventing pollution, public health, and the preservation and improvement of the biological integrity of water bodies. Water quality involves many variables and observations, some of which are outside of the acceptable range. An observation that apart from the rest of the data or looks diverge from other observation of the sample in which it occurs. In this paper, we proposed two methodologies for detecting outliers for the Yamuna River water quality data with three variables Chemical Oxygen Demand (COD), Bio-chemical Demand Oxygen (BOD) and PH, at three different locations did comparison of these two methodologies. These two methodologies are based on Descriptive Statistics and Statistical Process Control (SPC). A few outliers are present in the data. The outcome shows how far the outlier detection method has progressed and better knowledge of the various outlier methodologies and provide a clear path for future outlier detection methods for researchers.

Keywords: Classical Statistical Analysis, Statistical Process Control, Outlier, Yamuna Water Quality

I. Introduction

The Great Ganga plain is home to around 0.5 Billion population due to the sufficient freshwater availability (Misra [1]). The River Yamuna, its largest tributary, has around 1370 kilometres and originates from the Yamunotri Glacier of Uttar Kashi in Uttar Pradesh (Agarwal et al. [2]). It has several tributaries (Tons, Giri river), which provides fresh water to the mountainous regions. Whereas the Yamuna River flows through the densely populated regions of the plain, including Delhi, Haryana and Uttar Pradesh. While traversing around the megacity of Delhi, which is one of the highly polluted cities (Anand et al. [3]), it covers around 22 km of stretch and receives large quantities (3000 MLD) of partially treated and untreated industrial and domestic waste through twenty-two major drains. The important pollution monitoring stations are located in Kudesi, Nizamuddin and ITO, where three water pollution parameters are constantly monitored: COD, BOD and Negative logarithm of Hydrogen ion concentration (PH). Various wastewater treatment plants are constructed using these parameters; despite this, a significant amount of the untreated water (~1341 MLD) is discharged into the Yamuna River (CPCB, 2004-05). These data mainly indicate the point source, i.e. industrial pollution, although the diffusive sources such as the domestic wastewater supply (washing, cattle wading, cooking, defecation etc.) contribute significant yet unaccounted pollutants to the Yamuna River.

Apart from the source dependency, the levels of the contaminants in the Yamuna River also rely

on the climatic/weather fluctuations such as monsoon rainfall and surface water temperatures. During the heavy rainfalls, the levels dilute, whereas hot summers restrict the vertical water mixing in the river and thus induce the contaminants' spike. The climatic conditions and human-induced pollution thus affect the overall water quality of the Yamuna River and adjoining water reservoirs which are the primary source of drinking water for a significant number of the population living under poverty in and near the Delhi region (Sharma et al. [4]; Bhargava [5]). There might also be information on irregular processes, such as emissions in observations that are not excessively high but deviate from surrounding values. Outliers may merely be noisy observations or, instead, they would suggest atypical activity in the system. These abnormal values are significant and can lead to helpful knowledge or important results and selecting the most effective mitigation techniques or steps. SPC is a process that must work around the goal or nominal dimensions of the quality features with little variability. SPC is a powerful set of problem-solving methods that are useful in achieving process reliability and improving capacity by reducing variability. It is essential to develop and maintain a normal variation pattern through continuous process monitoring. A disturbance has occurred if there is a divergence from the usual fluctuation, and the process must be adjusted. Statistical process control provides data collection, measurement, recording, analysis, and decision making methods. The process is statistically controlled when all disturbances or specific causes of variance are removed. The SPC concept determines the central line, upper control limit, and lower control limit. The process is out of control if the point is above the upper control limit (UCL) or below the lower control limit (LCL) (Torres et al. [6]; Kamalov and Leung [7]). They provide a unique outlier identification method based on principal component analysis and kernel density estimation. The suggested technique is designed to solve the problems associated with high-dimensional data by projecting the original data into a smaller area and calculating anomaly scores for each data point based on the data's intrinsic structure. (Muniz et al. [8]) The study uses oxygen and turbidity as indicator variables to develop a new method for spotting outliers in water quality monitoring metrics. Until now, techniques relied on treating the various parameters as a vector with concentration values as its components. Horn et al. [9] proposed a physician-determined healthy sample, improvement in reference interval estimation utilizing a new outlier identification technique is investigated. The impact of incorporating non-healthy individuals in the sample as determined by a physician is assessed.

Singh et al. [10] sought to bring together an organized and generic overview of several outlier detection strategies. Sim et al. [11] concentrate on spotting potential outliers using the commonly known boxplot software. Outliers are subsets of observations inconsistent with the rest of the observations in a data collection. They find outliers by building a box plot with a lower fence (LF) and an upper fence (UF) (UF). Chakraborti et al. [12] presented phase I parametric control charts for univariate variables. Akarupu et al. [13] conducted a study on five aspects of water quality utilizing Statistical Quality Control methodologies applied to real 2014 data gathered for a water treatment facility in the United States. Fu and Wang [14] introduced several statistical approaches for evaluating water quality data. Three common graphs, boxplots, Q-Q plots, and scatter plots, which provide relevant summary information about datasets, are employed to give insight into datasets. Grubbs [15] study was mainly written as an explanatory and instructive essay on the difficulty of finding outlier observations in an extensive experimental effort. In this work, they solely look at tests of significance. Wang et al. [16] gave a thorough and structured overview of the advancement of outlier identification algorithms from 2000 to 2019. Martinez and colleagues [17] offered the one-class peeling (OCP) approach, a customizable framework for detecting numerous outliers in multivariate data that integrates statistical and machine learning methodologies (Di et al. [18]).

This work presents a novel technique for detecting outliers in water quality monitoring parameters by employing turbidity, conductivity, and ammonium as indicator variables.

II. Methodology

A collection of systems, such as water quality measurements, are available to analyze environmental data. These systems may discover unusual data items using classical analysis, patterns, differences between neighbouring network stations, and predicted values concerning the sampling position. For classical analysis, the data is only statistically evaluated. Today, automated analysis techniques are needed for the amount of data that has been accumulated in environmental databases. The study technique presented here is focused on knowledge discovery of information in databases (KDD) (Chan et al. [19]), which provides a complete data extraction procedure as well as a transparent methodology for preparing data and evaluating the findings produced. The knowledge discovery database provides an iterative and collaborative way of looking for models, patterns, and parameters that are beneficial for outlier detection, categorization, and/or prediction to create information and aid decision-making. We apply statistical techniques to detect the outliers; classical statistical analysis and SPC.

I. Classical Statistical Analysis

Individual time series, descriptive statistics, box plots, and so forth, the classical statistical analysis tracks water quality, decides the importance if any of them falls beyond the limits: quartiles, interquartile range, and evaluate the trend. In general, traditional statistical techniques explain the measurable property distribution (descriptive statistics) and assess the reliability of the sample drawn from the starting population (inferential statistics). Thus, classical analysis is based on continually measuring the characteristics of an item and attempting to forecast the frequency with which the measurement process is repeated stochastically or randomly with a certain conclusion. Properties may be evaluated repeatedly for the same object or only once per object. The classical statistical analysis seeks to assess the empirical frequency distribution that yields the absolute or relative frequency of occurrence of each of the numerous potential outcomes of repeated measurement of an object's property (discrete case) or object class (Torres et al. [6]). If the distribution function is employed in the event of an indefinitely repeated and arbitrarily reliable computation and each outcome is different, then the relative frequency of a particular occurrence will not be very informative.

II. Statistical Process Control

Outliers can be identified by using SPC to monitor the system. The analysis concentrates on significantly low and high readings even if the results do not meet the set limit. These techniques can examine individual or average maps to study individual observation. The dataset should be divided into reasonable subgroups (Shewart [20]). It is important to form rational subgroups because variation can be clustered, and variability can be easily detected in the presence of special causes. Unless it is impractical to utilize the rational subgroups, for instance, when a measurement repeatedly occurs in the same way, it differs only by laboratory or analytical error.

The method of gathering the data is the rational subgroup and generally be collected so that each one demonstrates the only intrinsic variety, which is the natural process of (common cause variation). It allows an additional source of variation (unique cause variation) to be established, which may affect the subgroups imperfectly where possible, to avoid unique cause variation. Moreover, if the mechanism is too violated, the limit of the control chart that defines the border is determined by the variability within each subgroup. For this reason, only subgroups that duplicate the common cause variation in the process should be gathered (Torres et al. [6]).

If the data is appropriately organized, a normality test must be performed. If the normality hypothesis is rejected, there are two possible ways to normalize the data. The first one is to use the modified techniques for non-normal distribution to convert in normality form or transform the data to normalize the data set (Chen [21]). The second technique is used for the transformation is Box-Cox transformation (Box and Cox [22]) is given as follows:

$$X_j^\omega = \begin{cases} X_j^\omega, & \omega \neq 0 \\ \log(X_j), & \omega = 0 \end{cases}$$

Where ω denotes the maximizes the profile likelihood function of the data X_j

It is possible to divide a classical process analysis into two stages, the first stage when a test has been conducted to remove normality and atypical measurement from the results, and the stage is the control stage, when the pattern is evaluated and when conditions outside of control are encountered. The first level specifies the central line (CL), UCL, and LCL. The control sample accurately defines the centre line, reflecting the objective value. Furthermore, the warning limit is placed at a distance of $\pm 2\sigma$ from it and is the operation's standard deviation (Leavenworth and Grant [23]).

For SPC, the control chart of Shewart is most frequently used for its substantial success in detecting the significant changes in a process. It is more accurate to suggest that the control chart is a monitoring system for graphical statistical processes. In most cases, conventional control charts are designed to track process parameters when the underlying form of the distribution of processes is known. Despite these charts using the most recent samples, the minor or progressive improvement in the process is not established. There is a need for complementary rules; different rules have been established by different authors to identify particular deviations (Champ and Woodal [24]; Zhang et al. [25]) and to complement the initial rules. Using these supplementary rules (Western [26]) makes the control charts of Shewart more alert and contributes to a substantial capacity for a non-random sample to be detected.

III. Results and Discussion

In this document, the results of the two approaches are shown below. R and Minitab 16 were used to create all of the figures.

I. Classical Analysis

The traditional statistical method on water quality, time series, descriptive statistics, and box plot analysis was used to see if the value was outside the limit. The table displays the dataset's descriptive statistical parameters. Data is taken from ENVIS Centre on Hygiene, Sanitation, Sewage Treatment Systems and Technology sponsored by the Ministry of Environment, Forest and Climate Change Govt. of India [27].

Table 1: Summary of descriptive statistics of Yamuna river water quality analysis

Variable	N	N*	Mean	SE Mean	StDev	Minimum	Q1	Median	Q3	Maximum	Range	IQR	Skewness	Kurtosis
KudesiCOD	12	0	72.50	6.20	21.48	28.0	65.00	78.00	86.0	106.00	78.00	21.00	-0.81	0.79
KudesipH	12	0	7.625	0.112	0.386	7.00	7.275	7.700	7.90	8.10	1.100	0.625	-0.57	-0.83
KudesiBOD	12	0	22.77	2.06	7.14	7.60	20.50	24.00	28.0	32.0	24.40	7.50	-1.03	0.82
NizamuddinpH	12	0	7.600	0.0728	0.2523	7.00	7.50	7.60	7.70	8.00	1.00	0.20	-0.90	2.40
NizamuddinCOD	12	0	66.33	2.85	9.87	48.0	58.00	68.00	75.00	80.0	32.00	17.00	-0.64	-0.37
NizamuddinBOD	12	0	21.17	1.54	5.34	14.0	16.75	21.00	23.75	32.0	18.00	7.00	0.53	0.24
ITOpH	12	0	7.733	0.1	0.347	7.00	7.525	7.800	8.00	8.10	1.100	0.475	-0.87	0.08
ITOCOD	12	0	71.33	4.97	17.21	40.0	57.00	72.00	85.0	96.0	56.00	28.00	-0.18	-0.45
ITOBOD	12	0	22.96	1.78	6.18	11.0	17.38	24.50	28.0	32.0	21.00	10.63	-0.55	-0.45

The statistical parameter in table 1 shows the limits and not more than the decided limit. The following step in classical data analysis is to present a time series of monthly data of water quality from 2019 to 2020 (one year) (Fig. 1) ranging of Kudesi COD (28.00,106.00), Kudesi PH(7.00,8.100),

Kudesi BOD(7.60,32.00), Nizamuddin COD(48.00,80.00), Nizamuddin PH(7.00,8.00), Nizamuddin BOD(14.00,32.00), ITO COD(40.00,96.00), ITO PH(7.00,8.10), ITO BOD(11.00,32.00).

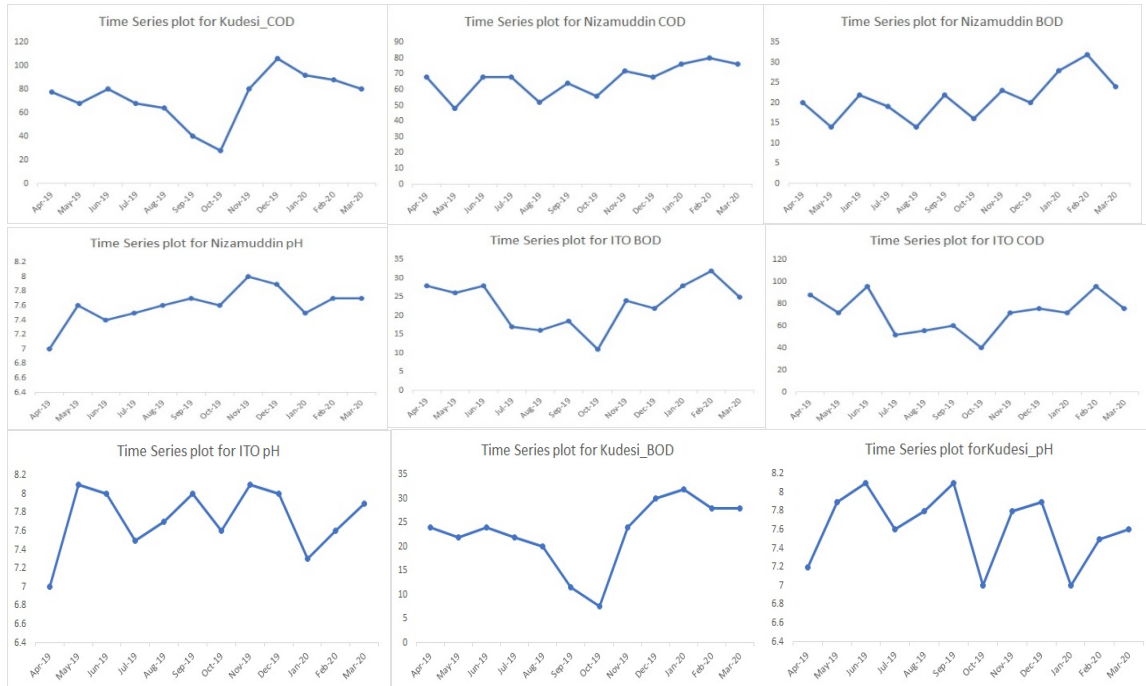


Figure1: Time series plot for Kudesi, Nizamuddin, ITO (COD, BOD and PH)

Figure 2 is a boxplot that graphically depicts COD, BOD, and PH data at various locations concentrated by quartiles. In the below fig., there are no outliers detected in the data except Kudesi COD, BOD and Nizamuddin PH.

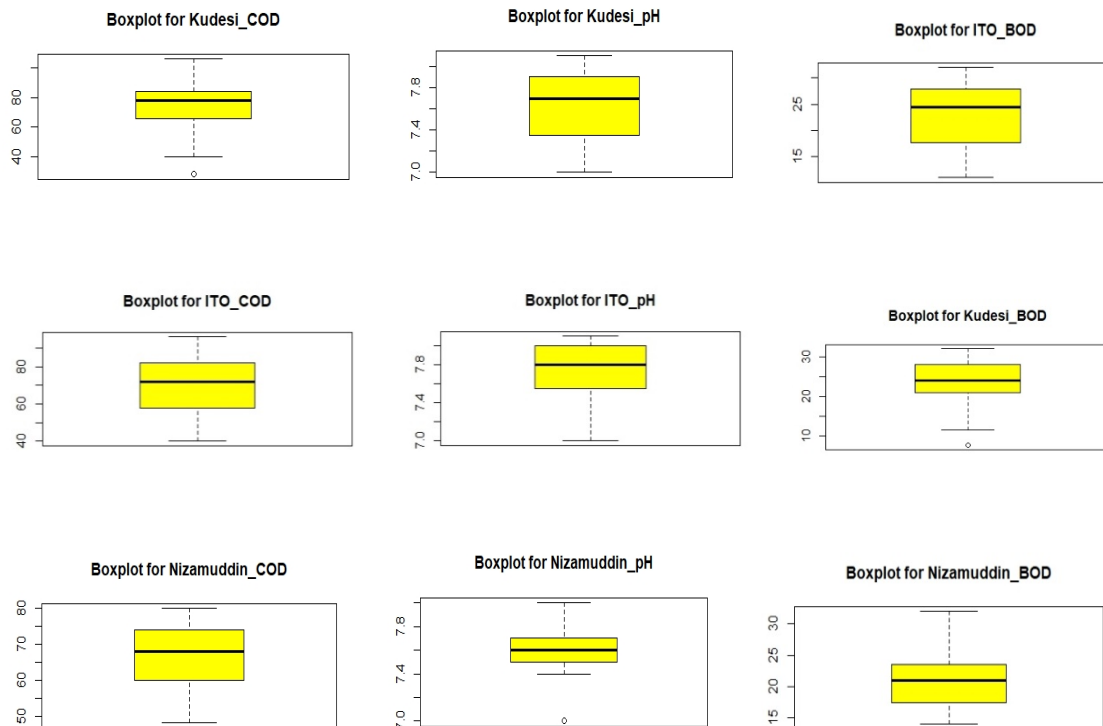


Figure 2: Box plot for Kudesi, Nizamuddin and ITO (COD, BOD, PH)

II. SQC Analysis

Individuals' IMR charts show each observation or measurement as a distinct data point that stands independently (subgroup size = 1). The analysis of the findings given in Fig. 3 reveals that few have a false alarm, i.e. outlier.

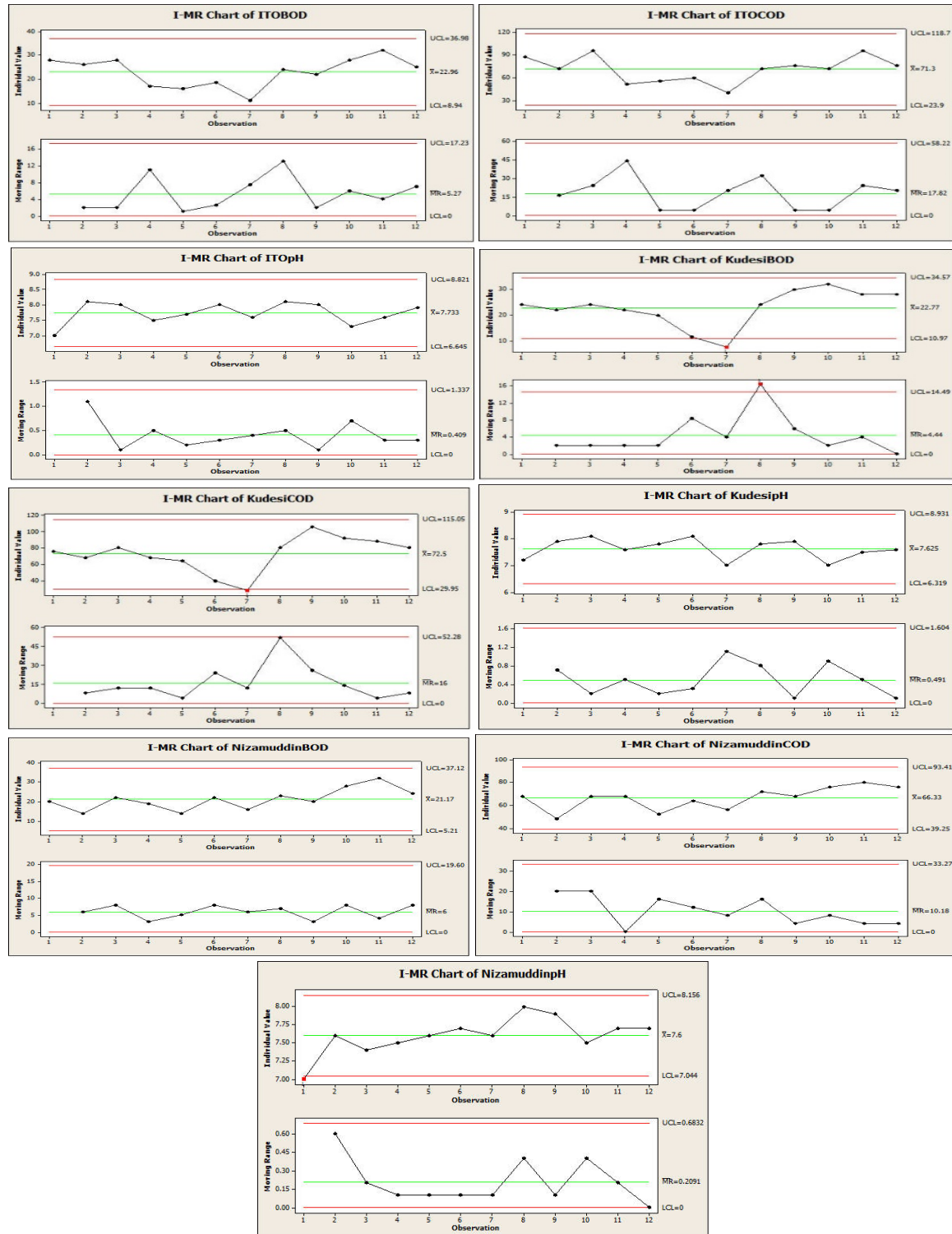


Figure 3: Individual moving range chart for Kudesi, Nizamuddin and ITO(COD, BOD, PH).

The Xbar chart of each observation or measurement of each data point is displayed in fig. 4. In this examination, we observed an outlier detected in the Kudesi COD at sample 7, Kudesi BOD and Nizamuddin PH.

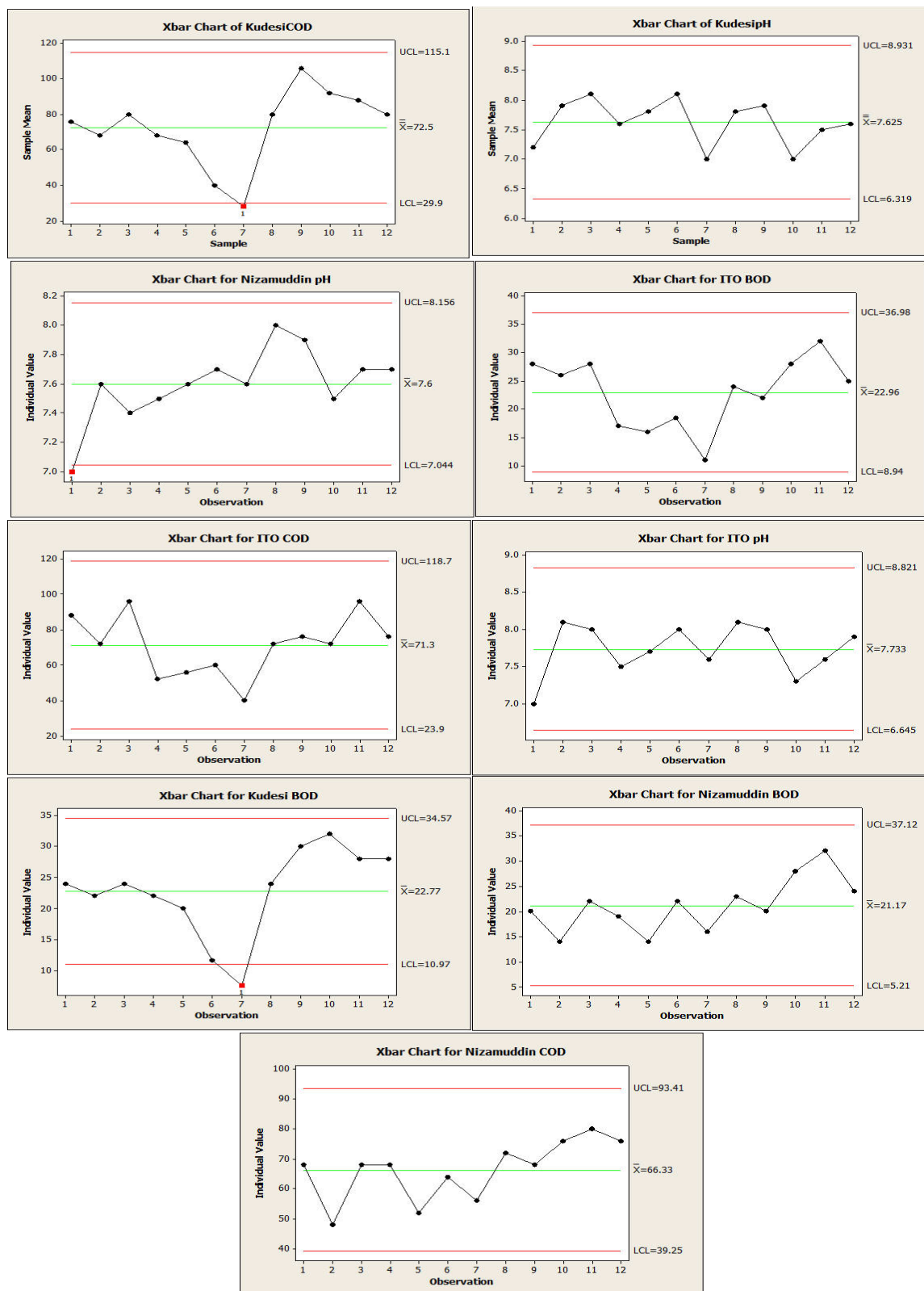


Figure 4: Xbar chart for Kudesi, Nizamuddin, ITO (COD, BOD, PH).

IV. Conclusion

We employed two approaches to analyze water pollution and outliers' data from the urban river Yamuna at three different locations, Kudesi, Nizamuddin, and ITO, using COD, BOD, and PH in Delhi, India. The data were collected monthly from April 2019 to March 2020 with monthly measurements. Firstly, we applied a classical approach by analyzing the data with descriptive statistics such as mean, range, Q1, Q2, Q3 and IQR, time series, and box plot. Secondly, adopted an SPC to learn the approximately normal data, gathered by month with different control charts such as IMR and Xbar chart. A novel method and set of instruments to efficiently access resident water pollution are necessary to effectively enable water pollution abatement and give genuine water quality circumstances. The classical approach is oversimplified despite giving helpful decision-making information. It has many flaws in the data's time correlation structure, including failing to find true outliers months with behaviour deviating from the norm simply because the points do not exceed the bound values. As a result, more complex and modern methodologies can better understand water pollution incidents. SPC is an advanced methodology for identifying outliers in pollution episodes. We create a model and graph it, and this method marks them as outliers. It only works with discrete explanations and cannot extract data in a continuous format. This document outlines a simpler method for environmentalists to discover outliers. We can include it in this functional outlier identification technique for future use. In general, as compared to traditional statistical analysis, SPC is the most effective method for detecting outliers.

References

- [1] Misra, A. K. (2010). A river about to die: Yamuna. *Journal of water resource and protection*, 2(5), 489.
- [2] Agarwal, T., Khillare, P. S., & Shridhar, V. (2006). PAHs contamination in bank sediment of the Yamuna River, Delhi, India. *Environmental monitoring and assessment*, 123(1), 151-166.
- [3] Anand, C., Akolkar, P., & Chakrabarti, R. (2006). Bacteriological water quality status of river Yamuna in Delhi. *Journal of environmental biology*, 27(1), 97-101.
- [4] Sharma, M. P., Singal, S. K., & Patra, S. (2008). Water quality profile of Yamuna river, India. *Hydro Nepal: Journal of Water, Energy and Environment*, 3, 19-24.
- [5] Bhargava, D. S. (1985). Water quality variations and control technology of Yamuna river. *Environmental Pollution Series A, Ecological and Biological*, 37(4), 355-376.
- [6] Martínez Torres, J., Pastor Pérez, J., Sancho Val, J., McNabola, A., Martinez Comesana, M., & Gallagher, J. (2020). A functional data analysis approach for the detection of air pollution episodes and outliers: A case study in Dublin, Ireland. *Mathematics*, 8(2), 225.
- [7] Kamalov, F., & Leung, H. H. (2020). Outlier detection in high dimensional data. *Journal of Information & Knowledge Management*, 19(01), 2040013.
- [8] Muñoz, C. D., Nieto, P. G., Fernández, J. A., Torres, J. M., & Taboada, J. (2012). Detection of outliers in water quality monitoring samples using functional data analysis in San Esteban estuary (Northern Spain). *Science of the Total Environment*, 439, 54-61.
- [9] Horn, P. S., Feng, L., Li, Y., & Pesce, A. J. (2001). Effect of outliers and non-healthy individuals on reference interval estimation. *Clinical chemistry*, 47(12), 2137-2145.
- [10] Singh, K., & Upadhyaya, S. (2012). Outlier detection: applications and techniques. *International Journal of Computer Science Issues (IJCSI)*, 9(1), 307.
- [11] Sim, C. H., Gan, F. F., & Chang, T. C. (2005). Outlier labeling with boxplot procedures. *Journal of the American Statistical Association*, 100(470), 642-652.
- [12] Chakraborti, S., Human, S. W., & Graham, M. A. (2008). Phase I statistical process control charts: an overview and some results. *Quality Engineering*, 21(1), 52-62.
- [13] AKARUPU, V., GUNKALA, S., PATTIGADAPA, S., PATTIGADAPPA, B. K., PONNAPALLI, S., & SEGALL, R. S. (2016). Statistical Quality Control and Improvement of Waste Water Treatment Plant. In *Proceedings of The 20th World Multi-Conference on Systemics, Cybernet and*

Informatics.

[14] Fu, L., & Wang, Y. G. (2012). Statistical tools for analyzing water quality data. *Water quality monitoring and assessment*, 1, 143-68.

[15] Grubbs, F. E. (1969). Procedures for detecting outlying observations in samples. *Technometrics*, 11(1), 1-21.

[16] Wang, H., Bah, M. J., & Hammad, M. (2019). Progress in outlier detection techniques: A survey. *Ieee Access*, 7, 107964-108000.

[17] Martinez, W. G., Weese, M. L., & Jones-Farmer, L. A. (2020). A one-class peeling method for multivariate outlier detection with applications in phase I SPC. *Quality and Reliability Engineering International*, 36(4), 1272-1295.

[18] Di Blasi, J. P., Torres, J. M., Nieto, P. G., Fernández, J. A., Muñiz, C. D., & Taboada, J. (2013). Analysis and detection of outliers in water quality parameters from different automated monitoring stations in the Miño river basin (NW Spain). *Ecological engineering*, 60, 60-66.

[19] Chan, K. C. C., Wong, A. K. C., Piatetsky-Shapiro, G., & Frawley, W. J. (1991). Knowledge Discovery in Databases.

[20] Shewhart, W. A. (1931). "Economic control of quality of manufactured product". Macmillan And Co Ltd, London.

[21] Chen, Y. K. (2003). "An evolutionary economic-statistical design for VSI X control charts under non-normality". *The International Journal of Advanced Manufacturing Technology*, 22(7), 602-610.

[22] Box, G. E., & Cox, D. R. (1964). "An analysis of transformations". *Journal of the Royal Statistical Society: Series B (Methodological)*, 26(2), 211-243.

[23] Leavenworth, R. S., & Grant, E. L. (2000). "Statistical quality control". Tata McGraw-Hill Education.

[24] Champ, C. W., & Woodall, W. H. (1987). "Exact results for Shewhart control charts with supplementary runs rules". *Technometrics*, 29(4), 393-399.

[25] Zhang, M. H., Lin, W. Y., Klein, S. A., Bacmeister, J. T., Bony, S., Cederwall, R. T., & Zhang, J. H. (2005). "Comparing clouds and their seasonal variations in 10 atmospheric general circulation models with satellite measurements". *Journal of Geophysical Research: Atmospheres*, 110(D15).

[26] Western Electric, C. (1956). "Statistical quality control handbook".

[27] Water quality Status of River Yamuna Water quality available online: [Water Quality Status of River Yamuna \(sulabhenvi.nic.in\)](http://WaterQualityStatusofRiverYamuna.sulabhenvi.nic.in) (accessed on March 2021).

